CHAPTER ONE

1.0 INTRODUCTION

1.1 Peptic Ulcer Disease

Ulcer is a loss of mucosal covering or excavation of a tissue surface as a result of disintegration of tissue necrosis (Yuan *et al.,* 2006). It is a painful sore formed at the stomach coating, esophagus, or the part of small intestine, duodenum. This is caused by disruptions of stomach resistance and restoration system. The gastric region is usually characterised by mucosal injury minor to secretion of pepsin and gastric acid. Pepsin is the main enzyme in the digestive system which breaks down proteins into peptides. Peptic Ulcer Disease occurs less commonly in the lower esophagus but usually takes place in the stomach and duodenum. Peptic ulcers also arise due to excess acid secretion than required and could take place due to inequality among the digestive fluid utilised by the gastric mucosa for food digestion and several other factors which protect the stomach (and duodenum) coating (Talia and Kevin, 2018). Peptic ulcer formation is connected to *Helicobacter pylori*, a bacterium generally found in the stomach and also connected to Non steroidal anti-inflammatory drugs (NSAIDs). These two factors account for 50% of patients (Laine *et al*., 2010), while the rest of 50% lies under unidentified causes. There is a difference between peptic ulcer and erosion in that peptic ulcer expands deep into the esophagus, stomach, or duodenum coatings, also raises additional provocative response from the worsened tissues. Approximately 500,000 cases of PUD are recorded in United States every year where ages 25 and 64 years account for about 70% of all patients (Thorsen *et al.,* 2013). Figure 1.1 showed the pictorial representation of the stomach mucosal defense according to Laine *et al.,* 2008. This consists mucus and bicarbonate, surface epithelial cells, cell renewal, micro circulation and the sensory nerves.

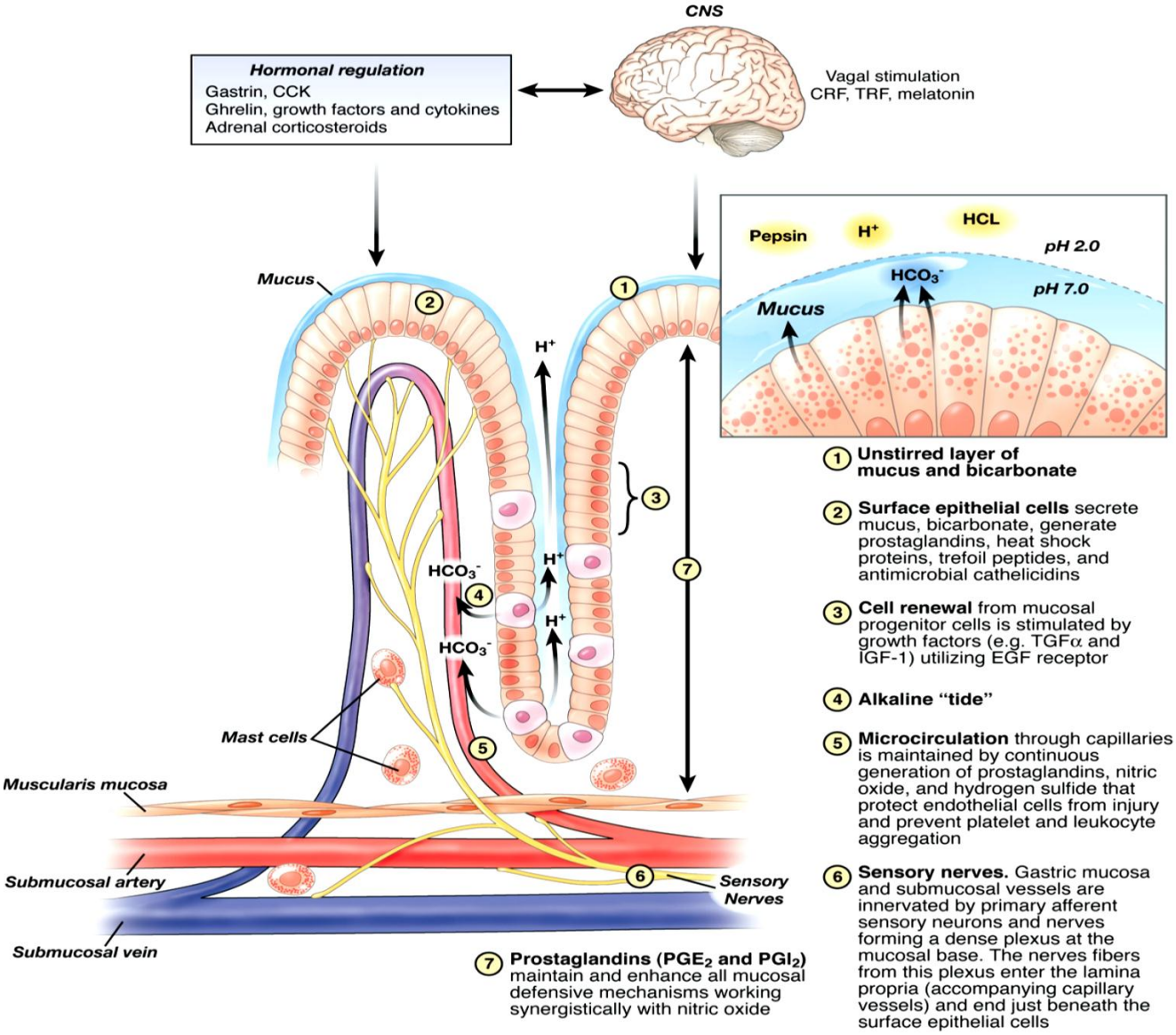

Figure 1.1: Pictorial representation of the gastric mucosal defense

(Laine *et al.*, 2008)

1.2 Peptic Ulcer Disease Pathophysiology

The pathogenesis includes an imbalance between damaging factors and defending factors. Defending factors are prostaglandins, mucus gel layer, mucosal blood flow, epithelial cells and mucosal cell renewal, while damaging factors include pepsin, HCl, alcohol, bile salts, drugs **(**Yandrapu and Sarosiek, 2015).

1.3 Gastric Mucosal Defense

Prostaglandin

This protects the gastric mucosa from various forms of injury. Prostaglandins are groups of ubiquitous long chain fatty acids with broad and enormously strong roles (Kvietys *et al*., 2014).

Mucus Gel Layer

This shelters gastric mucosal surface from the stomach to the colon; this defines the location of the leading line of protection against luminal attackers. This layer serves as barrier against harmful agents, captures micro-organisms, and improves the chyme impulsion down the gastrointestinal channel (Kemmerly and Kaunitz, 2014).

Mucosal Blood Flow: One of the requirements for preserving gastric integrity is adequate gastric blood flow. It has various defensive mechanisms which are essential factors for back-diffusing acid dilution, washing and cellular waste products. Maintenance of metabolic and rapid repair processes requires suitable oxygen and nutrient distribution (Kvietys *et al*., 2014).

Epithelial Cells

These cells are involved in mucus and bicarbonate secretion, they also produce prostaglandins and cathelicidins. These surface epithelial cells are hydrophobic, which resists acid and water –soluble harmful agents, because of phospholipids occurrence on their exterior (Kemmerly and Kaunitz, 2014).

Mucosal Cell Renewal

Structural integrity of the mucosa is preserved by constant cell regeneration from stomach progenitor cells. There is continual renewal of epithelium by well-organised and measured multiplying cells which permit extra injured/mature surface epithelial cells. It requires months to replace the glandular cells while whole replacement of stomach surface epithelium typically takes only 3 – 7 days (Laine *et al.,* 2008).

1.4 Signs and Symptoms of Gastric Ulcer

Most ulcers lack any signs thus are sometimes referred to as "silent ulcers". Symptoms in ulcer patients include: Superior stomach ache or distress, feeling full rapidly while eating, stomach pain, burping, or feeling swollen after eating, acid reflux or heartburn, nausea, vomiting (having blood in the vomit in severe cases), and blood in the stools. Acid-reducing medication is likely to relieve symptoms in most cases (Talia and Kevin, 2018).

1.5 Diagnosis of Peptic Ulcer

Two major methods are employed in the diagnosis of ulcer: Barium Upper Gastrointestinal X – ray and Upper Gastrointestinal Endoscopy.

In barium upper gastrointestinal X – ray, a chalky material (barium) is swallowed. The barium is observable on X – rays and allows the gastric summary to be visible on X – rays. This method is considered less accurate as it may slip ulcers up to 20 percent of the time. However, the risk is minimal (exposure to radiation) and easy to perform (Talia and Kevin, 2018).

Upper GI endoscopy in addition to ulcer detection also senses abnormalities of the upper GI series such as tumors, pouches, stricture, swallowing problem, inflammation, among others. This method is more accurate than barium upper GI X-ray. The endoscope is a lengthy thin elastic tube having an attachment of small camera and light which enables the specialist to view inside images of the patient's gut on a video screen. This instrument views the inside coating of esophagus, stomach, and duodenum when patients have GI tract problems. This method has the ability of taking out small tissue biopsies for *Helicobacter pylori* infection test. These tissues are similarly observed below microscope in order to eliminate any ulcer. Gastric ulcers can sometimes be cancerous while almost all duodenal ulcers are benign, thus biopsies are usually carried out on gastric ulcer to eliminate cancer (Talia and Kevin, 2018).

Recently produced extreme thin endoscopes with a tip of 5 mm width are also used to improve the patient's tolerance and lessen sedation necessity. Though, unsedated transnasal endoscopy has not been broadly accepted in western countries (Meves *et al.*, 2013).

1.6 Types of Peptic Ulcer Disease

1.6.1 Gastric ulcer

Ulcer that occurs in the stomach region is often known as stomach ulcer. This arises due to excess acid secretion than required and could take place when defensive stomach coating is washed away by the stomach juices (Bandyopadhyay *et al.*, 2001). The mucous layer, which coats the duodenum and stomach, acts as defense against acid and pepsin. Bicarbonate is also secreted by the body into the mucous layer, thereby neutralising the acid. Inadequate blood movement to the stomach has a contribution to ulcer formation. The stomach coating may be attacked by acid and pepsin thereby triggering an ulcer if any of the listed defense mechanisms are altered.

1.6.2 Duodenal ulcer

A peptic ulcer in the upper segment of the small intestine is the duodenal ulcer. Acid secretion in excess large amounts occurs in Zollinger-Ellison Syndrome, in which huge sums of secretion are stimulated by tumours positioned in the duodenum or pancreas (Tetsuhide *et al.,* 2013). The mucous cover which coats the stomach and duodenum acts as defense against acid pepsin and acid. A sore that develops in the duodenum results into duodenal ulcer.

1.6.3 Esophageal ulcer

This type of ulcer also causes upper gastrointestinal bleeding occasionally. It is defined as distinct disruption in esophageal having clearly confined margin. Most common occurrence of esophageal ulcers is the effect of gastroesophageal reflux disease (GERD) with stated incidence of 2% to 7% (Scida *et al*., 2018; Splechler, 2019; Sasaki *et al*., 2019). The stomach and gastric glands secret hydrochloric acid with an array of enzymes, which include pepsin that is involved in the breakdown and digestion of food. The stomach should be guarded from these acid and enzymes, or else it can also be assaulted by the gastric juices. Gastro-oesophageal reflux could occur when acid passes into the lower part of the esophagus, as a result of some fault in the mechanism of the normal sphincter which stops such reflux that causes indigestion regularly after meals. It frequently arises when there is surplus intra-abdominal pressure like straining or lifting weights, and after meals. It is commonly found at the lower end of a patient's esophagus. Esophageal ulcers including other types of ulcers are triggered by the harmful bacteria (Maesaka *et al*., 2018).

1.7 Common causes of peptic ulcer disease

1.7.1 *Helicobacter pylori* infection

Extensive information about peptic ulcer was derived through identification and isolation of *Helicobacter pylori* (Marshall and Warren, 1984). It is a bacterium accountable for maximum and persistent bacterial infection in the world. In developing countries, the incidence of infection is alarming (up to 90 percent), while in developed countries excluding Japan, the incidence is less than 40 percent. Overall, its contagion disturbs almost 50% of the universe (Tonkic *et al.*, 2012).

According to Bytzer and O'Morain (2005), *H. pylori* treatment employs threefold therapy, which includes proton pump inhibitor mixture with two antibiotics. Nevertheless, treatment is still less effective in clinical practice, since misuse of antibacterial drugs has occasioned the development of antibiotic-resistant strains. Antibiotic resistance is the foremost treatment failure caused by misuse of antibiotics aside the side effects (Bytzer and O'Morain 2005; Narayanan *et al*., 2018).

1.7.2 Use of non-steroidal anti-inflammatory drugs (NSAIDs)

These drugs are used majorly for management of slight pain, treatment of tissue damage as an outcome of arthritis, and for edema management. Few of the properties of these drugs include anti-inflammatory, analgesic, and treatment of fever. The mechanism of action of most NSAIDs includes prostaglandin inhibition which performs the role of gastric and bicarbonate secretion. The NSAIDs precisely inhibit cyclooxygenases (COXs), the enzymes involved in the production of prostaglandins (DeRuiter, 2002). Few examples of this class of medications include Diclofenac, Ibuprofen, Indomethacin, Aspirin, Naproxen, among others. There is an annual risk of life-threatening ulcer-related complication up to 4% in patients who use NSAIDs on a long-term basis, having elderly patients as the major risk (Graham, 1996). Proton pump inhibitors and misoprostol (Cytotec) are drugs that reduce the ulcerogenic potential of NSAIDs and decrease NSAID-related ulcer relapse.

1.7.3 Lifestyle risk factors

Other risk factors that contribute to formation of ulcer include the following:

Stress

Peptic ulcer may be caused by stress that arises as a result of serious health issues such as the ones that require intensive care treatment. This type of peptic ulcers is called stress ulcer (Steinberg, 2002).

Diet

Caffeinated drinks, coffee, and spice consumption have been confirmed to have a minor role in gastric ulcer formation, but not completely (Fink, 2011). This condition often occurs when meals are skipped. This ulcer causes stomach pain which worsen when meals are taken.

Alcohol and Smoking

Chronic alcohol interrupts the stomach mucosal barrier by inhibiting COX 1 receptor proteins, which in turn lowers cytoprotective prostaglandin output. Cigarette smoking leads to reduced epidermal growth and increased production of free radicals in stomach mucosa (Ko *et.al.,* 2000).

1.8 Urease and *Helicobacter pylori* bacteria

Urease is a major enzyme promoting *H. pylori* bacteria by ensuring its survival in the stomach acidic environment thereby causing gastrointestinal diseases, especially Peptic Ulcer Disease (PUD) and gastric cancer (Graham and Miftahussurur, 2018). Evidence showed that urease deficiency efficiently jeopardies *H. pylori* existence (Michetti, 1998).

Urease enzyme possesses buffering activity that changes the stomach medium to a tolerable environment for *H. pylori* through neutralising stomach acid *via* urea hydrolysis to form carbondioxide (CO_2) and ammonia (NH_3). Plants, bacteria, fungi, and yeast produce urease. The activity of this enzyme leads to numerous implications which include urinary stones, pyelonephritis, hepatic coma, ammonia encephalopathy (Upadhyay, 2012). Acetohydroxamic acid has been accepted for *Helicobacter pylori* infection treatment through urease inhibition. Their side effects, however, such as musculo-integumentary, psycho-neurological and other symptoms, have led to their restricted use (Jain *et al*., 2016).

Synthetic drug resistance in treating peptic ulcer paved way to medicinal plants as alternative use. *Helicobacter pylori* fall into gastric ulcer that are resistant to synthetic medication.

The search for new anti-*H. pylori* therapy has driven exploration in the field of medicinal plants. Natural products exhibit their own anti-*H. pylori* actions *via* different mechanisms. Many natural products have anti-*H.pylori* potentials. The mechanisms of such potentials include urease inhibition, DNA damage, protein synthesis inhibition, and anti-inflammatory effects (Baker, 2020).

1.9 Justification

Accurate data collection on medicinal plants for drug discovery is an essential part of pharmacognosy. However, scanty information is available on ethnomedicine used to treat gastric ulcer in terms of indigenous knowledge of the inhabitants, prevalence, and local names due to lack of documentation. It is therefore important to preserve the traditional knowledge for future reference. There is need to justify the medicinal claim of some selected plants as having anti-ulcerogenic activity as herbal medicine is a main therapeutic remedy for treating numerous diseases including gastric ulcer in many developing countries. This will ensure efficacy and safety as the method of plant identification still relies on traditional knowledge acquired over the years. Few currently used anti-ulcer drugs have side effects such as male infertility, central nervous system disorder and depression. This necessitated a search for more potent and safer anti-ulcer compounds from natural sources.

It is also important to possibly isolate bioactive compounds from the plants that could be used as drugs or lead compounds in the discovery of anti-ulcer drugs.

1.10 Research Hypothesis

Curculigo pilosa and *Sphenocentrum jollyanum* used traditionally in the treatment of gastric ulcer possess bioactive constituents that are responsible for their anti-ulcer activity.

1.11 Major aim

This research is aimed to evaluate the anti-ulcer activities of some selected Nigerian medicinal plants, isolating and characterising their bioactive compounds.

1.12 Specific objectives

The specific objectives are:

1. To carry out an ethno botanical survey of medicinal plants with anti-ulcer activities in some local government areas of Ibadan, Nigeria.
2. To screen the selected plants for anti-ulcer activity *in vivo* using Wistar rats.
3. To evaluate the antioxidant, antacid, and urease inhibitory activities of these selected plants.
4. To isolate and characterise anti-ulcer compounds using different chromatographic and spectroscopic techniques.

CHAPTER TWO

2.0 Literature review

2.1 Classes of anti-ulcer drugs

Anti-ulcer drugs are classified according to Tripathy (2004) as proton pump inhibitors (Figure 2.1), H_2 histamines (Figure 2.2), anti-*Helicobacter pylori* drugs, antacids, among others.

2.1.1 Proton pump inhibitors

This class of drugs reduces acid production and relief heartburn that are not resolved by H_2 blockers or antacids significantly. They function primarily by blocking the gastric H^+/K^+ ATPase activated by parietal cells of the stomach (Shah and Gossman, 2020). Reduction of the symptoms usually takes more time in proton pump inhibitor than an H_2 blocker, but relief remained longer. Proton pump inhibitors are most effective for people suffering from heartburn for more than 2 days weekly. The common proton pump inhibitors that are available orally are Omeprazole (1), Lansoprazole (2), Pantoprazole (3), Esomeprazole (4), Rabeprazole (5), and Dexlansoprazole (6) **(**Shin and Sachs, 2008). Proton pump inhibitors (Figure 2.1) are replaced by benzimidazole derivatives with better inhibition effects on stomach acid secretion.

Omeprazole Magnesium, Lansoprazole, Dexlansoprazole, Esomeprazole, and Pantoprazole: These proton pump inhibitor (PPI) drugs are used majorly for treatment of certain esophagus problems (such as acid reflux, ulcers) and stomach problems. They decrease the excess acid amount in the stomach and relieve symptoms of swallowing difficulty, heartburn, ulcers, and help to stop cancer of the esophagus. All the mentioned drugs are closely related thus having the same healing effects of preventing acid secretion completely. These PPIs have substituted H_2 blockers in several medical practices due to their more efficacy and greater prompt action. Omeprazole 20 mg daily can be administered for a period of 4 weeks for uncomplicated duodenal ulcers. Patients undergoing serious fundamental illness are to be treated with increased doses of Omeprazole 40 mg or Dexlansoprazole 60 mg once in a day. Gastric ulcer patients need treatment for 6 to 8 weeks whereas Gastritis needs 8-12 weeks treatment but long-term continuation is necessary for GERD patients.

Preliminary treatment with pantoprazole is eight weeks after which additional eight-week course of treatment might be continued if required. There is a direct link between scientific response of acidity treatment and the level of restraint of acid secretion achieved. Frequent liver enzymes check is essential if there are severe liver problem, especially when Pantoprazole is taken for a long time.

It is important to note that prolongation of proton pump inhibitor in the treatment of gastric ulcer may bring about cell hyperplasia where there isbunusual upsurge in amount of tissue or growth of new normal cells. Development of malabsorption of vitamin B_{12} may also occur (Ochoa *et al*., 2020; Shah and Gossman, 2020).

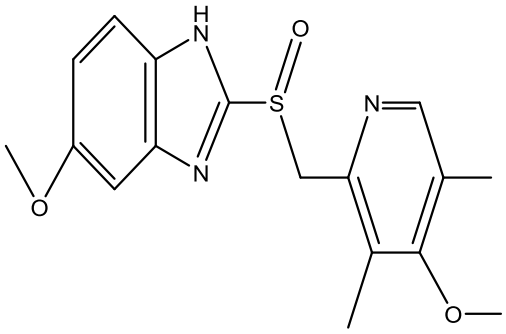

Omeprazole (1)
(Shin and Sachs, 2008)

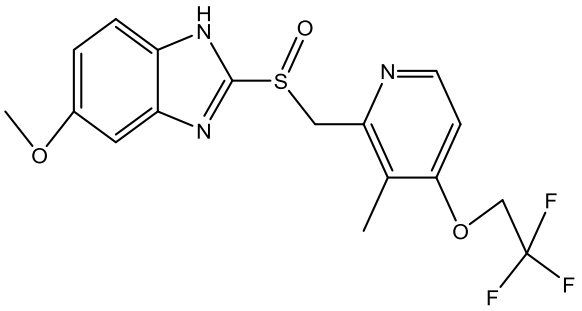

Lansoprazole (2)
(Shin and Sachs, 2008)

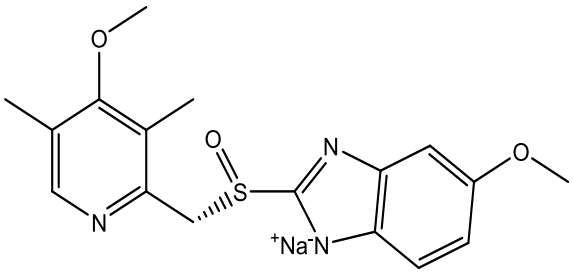

Pantoprazole (3)
(Shin and Sachs, 2008)

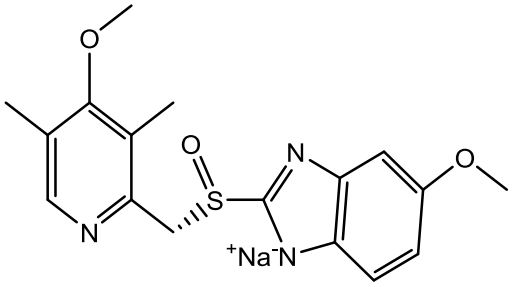

Esomeprazole (4)
(Shin and Sachs, 2008)

Figure 2.1: Chemical structures of proton pump inhibitors

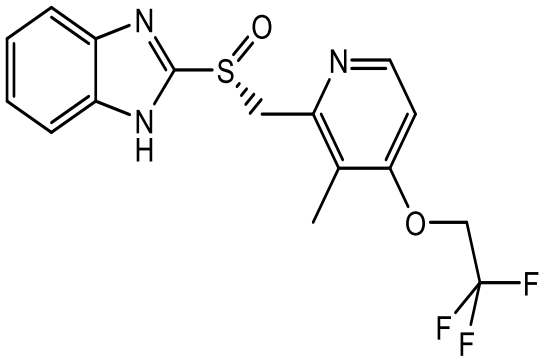

Rabeprazole (5)
(Shin and Sachs, 2008)

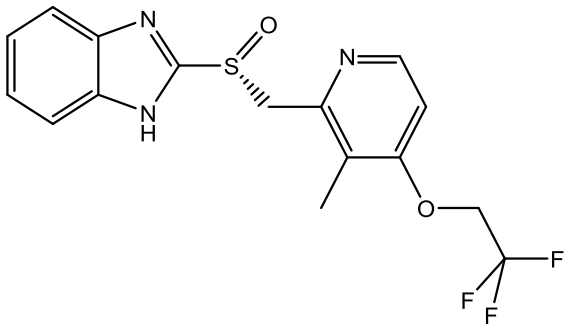

Dexlansoprazole (6)
(Shin and Sachs, 2008)

Figure 2.1: Chemical structures of proton pump inhibitors

2.1.2 Histamine blockers: Histamine H_2 blockers reduce the amount of stomach acid by reducing stimulating effect of gastrin and Adrenocorticotropic hormone (ACE). Histamine blockers relieve symptoms for a longer period of time than antacids though they do not relieve symptoms instantly. These drugs include Cimetidine (7), Famotidine (8), Nizatidine (9)**,** and Ranitidine (10) (Stojkovic *et al*., 2015) which are available orally without prescription and are ready for action to inhibit histamine (H_2 receptor). Cimetidine possesses slight anti-androgen effects which are expressed as overdevelopment of the male breast, rarely erectile dysfunction with continued usage. All H_2 blockers (Figure 2.2) usually show up signs like fever, diarrhoea, and hypotension, usually in less than 1 % of treated patients but regularly in ageing patients after rapid intravenous administrations.

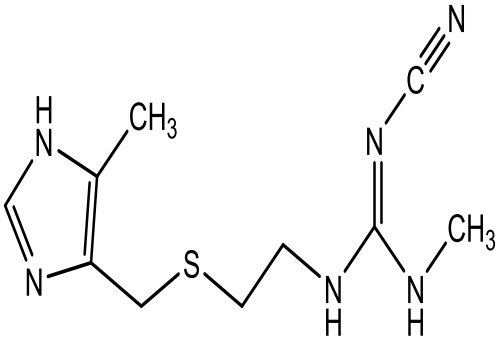

Cimetidine (7)
(Stojkovic *et al.*, 2015)

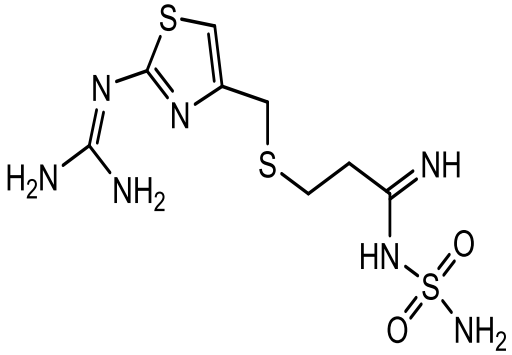

Famotidine (8)
(Stojkovic *et al.*, 2015)

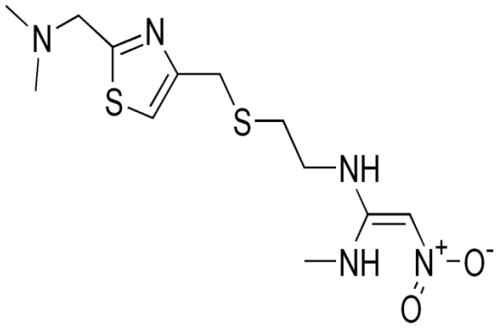

Nizatidine (9)
(Stojkovic *et al.*, 2015)

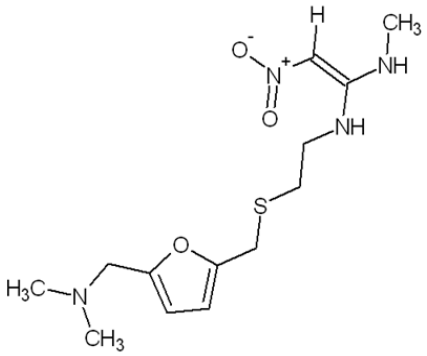

Ranitidine (10)
(Stojkovic *et al.*, 2015)

Figure 2.2: H_2 Histamine blockers

2.1.3 Antacids

Antacids are drugs that reduce stomach acidity by increasing the pH of the stomach and duodenum (Mandel *et al*., 2000). Antacids can provide nearly immediate relief for many stomach distresses such as indigestion. On the other hand, additional treatments are required if there are more serious problems. They act against acidity of the stomach by neutralising stomach HCl or averting acid secretion. These drugs are taken orally in capsule or liquid form, for treating heartburn and signs of acid reflux. Interference of antacids with absorption of other drugs (e.g. Tetracycline, Digoxin) may occur. Antacids can interact with Tetracyclines and Amphetamines. Antacids are known to relieve symptoms and promote healing of ulcer. They are comparatively cheaper than PPIs. The best treatment is 15-30 mL liquid or 2 -3 capsule antacids 1 hour and 3 hours after each meal and also at bedtime (Mbatchou *et al*., 2017). Usually, there are 2 types of antacids which are absorbable and non-absorbable. Absorbable antacids give thorough and prompt neutralisation but should only be used temporarily (1 or 2 days) because it may cause alkalosis. Examples include Calcium carbonate and sodium bicarbonate. Non absorbable antacids have lesser systemic adverse effects, are preferred. Examples include aluminum or Magnesium hydroxide.

2.1.4 Digestive enzymes oral: Digestive enzymes are essential for breakdown and digestion of food by the body and offer benefit in digestion disorders (Roxas, 2008). It is used when the pancreas is unable to release sufficient digestive enzymes into the gut for food digestion. These drugs are used for indigestion, replacement or supplement treatment in cystic fibrosis, and cancer of the pancreas depending on amount of enzymes in the product. They also play the roles of stomach acid neutralisation and pepsin acid reduction.

2.1.5 Prostaglandins: Prostaglandins hinder acid secretion and increase mucosal defense. Misoprostol is a synthetic analogue of natural prostaglandin E1. It produces a dose-related inhibition of gastric acid and pepsin secretion and enhances mucosal resistance to injury (Kvietys *et al*., 2014). Prostaglandins side effects include diarrhea and abdominal cramping, which occur in nearly 30% of patients. Misoprostol; a potent abortifacient is categorically contraindicated in pregnant women.

2.1.6 Sucralfate: Sucralfate is sucrose - aluminium complex drug which separates in gastric acid and forms a physical block over an inflamed region, defending it from acid, bile salts and pepsin. This drug also hinders pepsin-substrate interface, binds bile salts, and stimulates mucosal prostaglandin production (Candelli *et al*., 2000). It requires no effect on gastrin secretion or acid output. Constipation arises in 3 to 5 % of patients. Sucralfate may interfere with other drugs

absorption by binding to them. Furthermore, consumption of foods requires timing, for example, breakfast must be taken around 7 am to 8 am, lunch must be taken around 12 noon to 1:00 pm and dinner should be taken around 7 pm. Consistent walking can lessen the health problems and acidity.

2.2 Gastroprotection and ulcer healing models

Gastric ulcers induction may be achieved by pharmacological, physiological, or clinical handling in numerous animal organisms. Nevertheless, laboratory rodents are mostly used *in vivo* experimental models (Adinortey *et al*., 2013). It is the frequently used experimental models to investigate the gastroprotective effects of plants, and their fundamental mechanisms of action are described below.

2.2.1 Ethanol-induced stomach injury: Gastric mucosal damage usually occurs when resistance devices are reduced by harmful substances like gastric acid and HCl are administered into the animals (Defoneska, 2010). Ethanol promotes stomach injuries development by exposing the mucosa to the proteolytic and hydrolytic activities of pepsin and HCl. The damaging effects exhibited by ethanol prompted its use as ethanol induced gastric ulcer model for testing various medicinal plants for their gastroprotective activities.

2.2.2 Hydrochloric acid/ethanol (EtOH) induced gastric injury: This model is an advanced model of absolute ethanol induced gastric injury. Hydrochloric acid and ethanol combination is used for ulcer induction instead of ethanol only. This combination is considered to hasten the ulcerogenesis progress and increase stomach damage.

2.2.3 Water-immersion stress ulcer

These models are similar to human gastric ulcers, both wholly and in histopathology. These models are facilitated principally by histamine release that results in improved acid secretion, pancreatic juice reflux, reduced mucus production, and deprived stomach blood flow. Generation of reactive oxygen species and inhibition of prostaglandin synthesis also stimulate development of stress induced ulcers (Tamashiro *et al.,* 2012). These models are used extensively in assessing the gastroprotective effects of numerous medicinal floras.

2.2.4 Non-steroidal anti-inflammatory Drugs induced mucosal damage

The NSAIDs are well-known cause of stomach ulcers particularly when abused. These include aspirin, indomethacin, diclofenac and ibuprofen (Shekelle *et al*., 2017). These drugs have been used in developing stomach ulcer models in experimental rats. It is significant in exploring possible efficacy of cytoprotective and anti-secretory mediators as the fundamental pathophysiology includes

gastric acid secretion and synthesis of prostaglandin mucosa. In gastroprotection research, the NSAIDs induced gastric ulcer is considered to be the most accepted ulcer model. The incidence of use may be because peptic ulcers caused by NSAID are, apart from those instigated by *H. pylori* the second most prevalent etiology of PUD (Hayllar *et al*., 1992). The NSAIDs cause ulcers by hindering prostaglandin synthase in the cyclooxygenase pathway. Prostaglandins play a key role in stimulating bicarbonate and mucus secretion, and maintenance of mucosal blood motion, and regulating and repairing mucosal cell turnover (Hayllar *et al.,* 1992). These prostaglandins are found in the stomach and many tissues. As a result, interruption of prostaglandin synthesis by NSAIDs results in enhanced exposure to mucosal damage resulting in ulceration of stomach. Indomethacin and aspirin are mostly used for this model. Induction of ulcer is performed via a suitable means after fasting animals for 24 h. Aspirin dosage is usually administered in the range of 125 – 150 $mgkg^{-}$ *b.w.,* and the rats' euthanised 4 h later. For indomethacin, the dose is usually 40 mg/kg *b.w.,* and the ulcers graded after 4 – 8 h. Ibuprofen-induced ulcer model involves administering 400 $mgkg^{-}$ *b.w.* dosage of ibuprofen to rats, which are euthanised 5 h after administration (Repetto and Llesuy, 2002.).

2.3 Antioxidants and free radical scavenging activity

Antioxidants have free radical chain reaction breaking property. They guard against harmful oxidative reaction effects formed by reactive oxygen species (ROS) in a living system thereby acting as resistance mechanism (Jayachitra *et al.,* 2010). These ROS are formed naturally in cells and also produced by bacteria, alcohol, smoking, and psychological stress. Inadequate antioxidants lead to pathogenesis and problems of disease like arthritis, neurodegenerative and Alzheimer's disease, cancer, and ageing (Patel *et al.,* 2010). They are known to be the principal line of protection against free radical damage, thus crucial in preserving most favorable health and wellbeing. Numerous medicinal plants comprise chemical constituents that exhibit antioxidant activities. Medicinal plants encompass several molecules that display substantial antioxidant activity; such as the capacity to prevent, reduce or stop oxidative damage to diverse cellular constituents, which include nucleic acids, lipids, and proteins (Sousa *et al.,* 2014). More focus has been on phenolic compounds among these molecules which have been confirmed to be the principal sources of antioxidant property exhibited by medicinal plants. Antioxidants present in biological system are classified as enzymatic or nonenzymatic. The enzymatic are superoxide dismutase (SOD), catalase (CAT), and glutathione (GSH) while non-enzymatic comprise ascorbic acid, vitamin E, polyphenols, and selenium. Onoja *et*

al. (2014) evaluated the antioxidant activity of methanol extract of *Aframomum melegueta* Schum (Zingiberaceae) using *in vivo* and *in vitro* methods. *In vivo* superoxide dismutase and serum catalase were used, while the DPPH assay was used *in vitro*. The sample showed a significant increase ($P<0.05$) in superoxide dismutase and serum catalase at 400 mg / kg when compared to the control group.

2.4 Medicinal plants

Medicinal plants remain the significant basis of traditional medicine for the populace. About 80% of people worldwide depend mostly on traditional, mainly herbal medicines for their main healthcare needs (Pei, 2001). Unfortunately, there have been records of numerous cases of unsustainable collection of several therapeutic floras in diverse groups in the world, including Africa (Sonibare and Abegunde, 2012a). Traditional use of plants for managing numerous diseases remains an essential part of traditions of majority of the populace. Furthermore, affordability, availability, and accessibility of medicinal plants are important factors that led to the great request and practice. Plants producing secondary metabolites such as tannins, saponins, essential oils, alkaloids, flavonoids offer protection mechanisms which are involved in the healing properties of several medicinal floras (Ghribia, *et al.*, 2014).

2.5 Research plants

Fourteen plants were selected based on the result of ethnobotanical survey conducted. *Entada gigas* (L.) Fawc., family Leguminosae, commonly called monkey-ladder tree. Ogungbenle *et al.* (2015) confirmed the plant as source of nutrients and the cultivation is encouraged. *Vitellaria paradoxa* C.F. Gaertn., family Sapotaceae is known as shea tree and indigenous to Africa. Oyetoro and Sonibare (2015) reported the wound healing activity of *Vitellaria paradoxa* stem bark. Compounds such as (+) – catechin (11), (-) epicatechin (12), Butulinic acid (13), Bassic acid (14), and Vitellaric acid (15) were previously isolated from *Vitellaria paradoxa* as shown in Figure 2.3 (Talla *et al*., 2016). *Alstonia congensis* Engl., family Apocynaceae is locally known as Ahun in southwestern Nigeria. It is locally utilised in the managemet of malaria in Nigeria. *Uvaria chamae* P. Beauv., family Annonaceae originated from tropical forests in Central and West Africa and grows in humid and dry land. It has an edible fruits and its roots show boundless interest all over the world. Uvaretin (16), Diuvaretin (17), Chamanetin (18), Isochamanetin (19), Uvangoletin (20), and Dichamanetin (21) were previously isolated from *Uvaria chamae* as shown in Figure 2.4 (Kuodokpon *et al*., 2018).

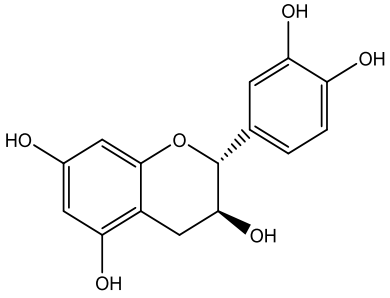

(+) - Catechin (11)
(Talla *et al*., 2016)

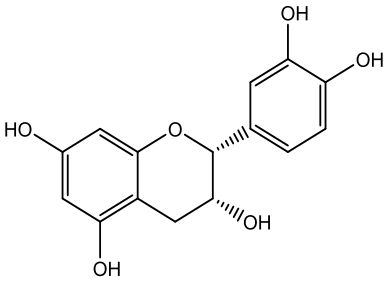

(-) epicatechin (12)
(Talla *et al*., 2016)

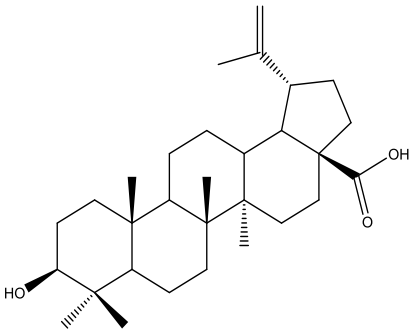

Betulinic acid (13)
(Talla *et al*., 2016)

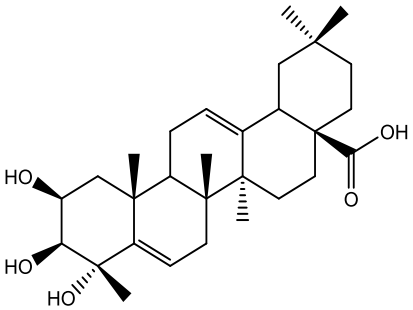

Bassic acid (14)
(Talla *et al*., 2016)

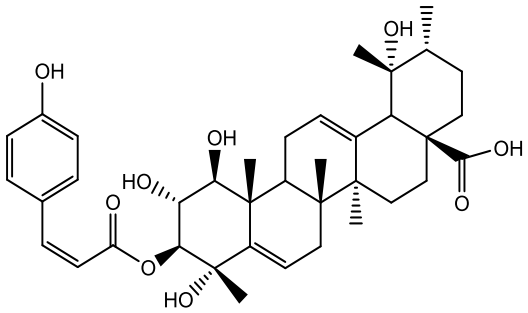

Vitellaric acid (15)
(Talla *et al*., 2016)

Figure 2.3: Isolated compounds from *Vitellaria paradoxa*

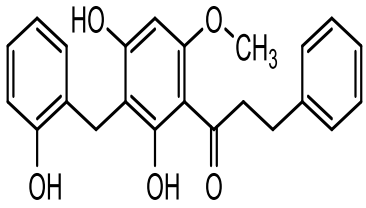

Uvaretin (16)
(Koudokpon *et al*., 2018)

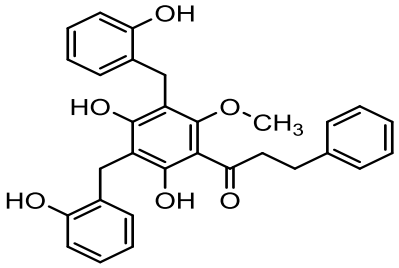

Diuvaretin (17)
(Koudokpon *et al*., 2018)

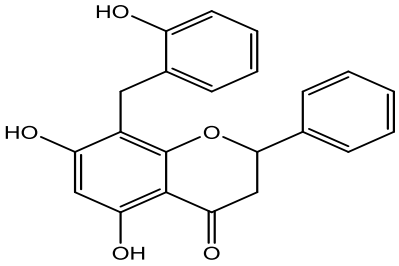

Chamanetin (18)
(Koudokpon *et al*., 2018)

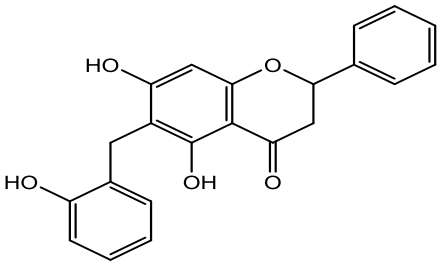

Isochamanetin (19)
(Koudokpon *et al*., 2018)

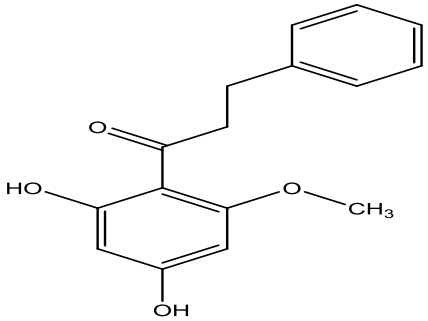

Uvangoletin (20)
(Koudokpon *et al*., 2018)

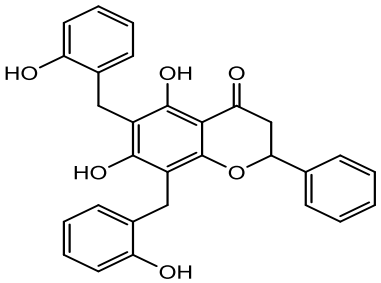

Dichamanetin (21)
(Koudokpon *et al*., 2018)

Figure 2.4: Isolated compounds from *Uvaria chamae*

Uvaria afzelii Scott – Elliot, Annonaceae family, is broadly distributed in the southern and eastern areas of Nigeria and locally called Yoruba's "gbogbonishe" (Odugbemi, 2006). It is used locally for vaginal tumor management, cough, swollen feet and hands, diabetes, leucorrhoea and gonorrhea (Kayode *et al.*, 2009). It was utilised for the management of bronchitis, jaundice, and malaria fever in traditional medicine (Ofeimum *et al.*, 2013). Afzeliindanone (22), syncarpic acid (23), uvafzelic acid (24), and syncarpurea (25) were previously isolated from *Uvaria afzelii* as shown in Figure 2.5 (Okpekon *et al*., 2001). *Ageratum conyzoides* L., family Compositae is found in the tropics. This plant is very prominent in West Africa, some parts of South America and Asia. The genus *Ageratum* comprises about 30 species. *Ageratum conyzoides* is identified majorly for its healing potentials and has been utilised locally in many parts of Africa for treating variety of ailments. It has been used as antibacterial and antidiarrheal (Ukwe *et al*., 2010). Phat and Ngoan, (2016) isolated –O-methyl apigenin (26), sinensetin (27) and scutellarein (28), while Moreira *et al*. (2007) isolated coumarin (29), 5, 6, 7, 8, 3, 4, 5 – heptamethoxyflavone (30) and 5, 6, 7, 8, 3 – pentamethoxy-4, 5-methylenedioxyflavone (31) from the aerial part of this plant (Figure 2.6).

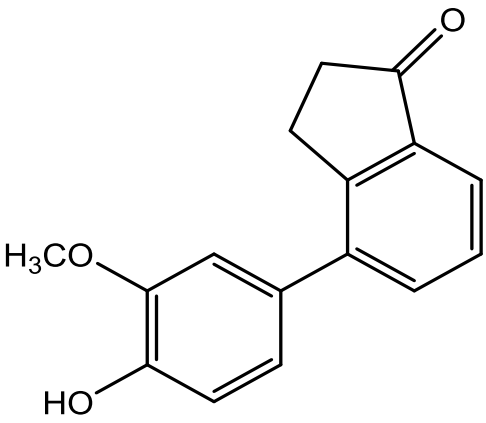

Afzeliindanone (22)
(Okpekon *et al*., 2001)

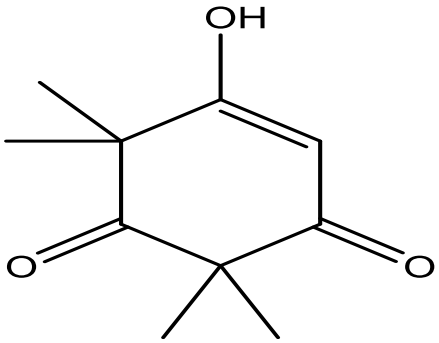

Syncarpic acid (23)
(Okpekon *et al*., 2001)

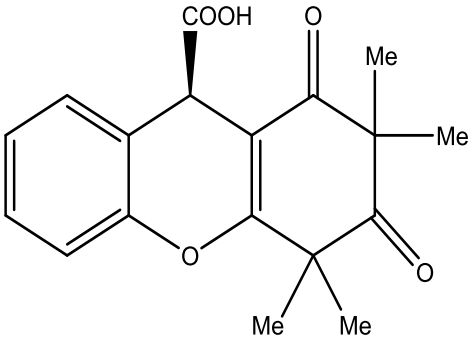

Uvafzelic acid (24)
(Okpekon *et al*., 2001)

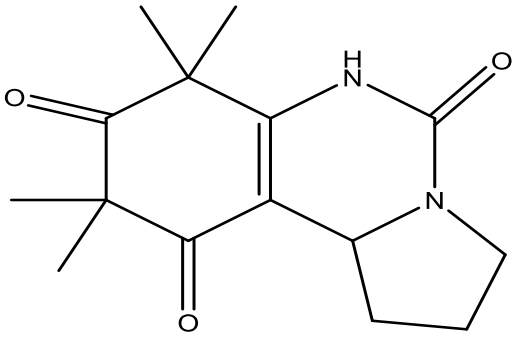

Syncarpurea (25)
(Okpekon *et al*., 2001)

Figure 2.5: Isolated compounds from *Uvaria afzelii*

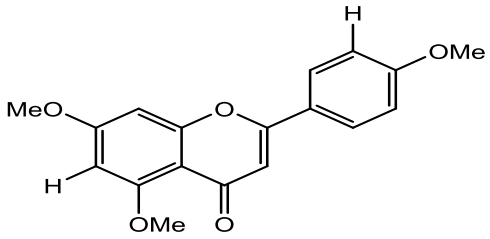

O – methyl apigenin (26)
(Phat *et al*., 2016)

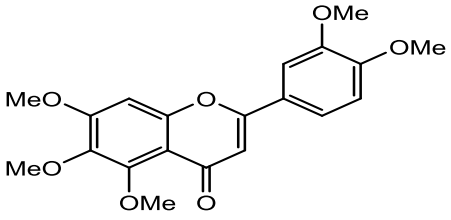

Sinensetin (27)
(Phat *et al*., 2016)

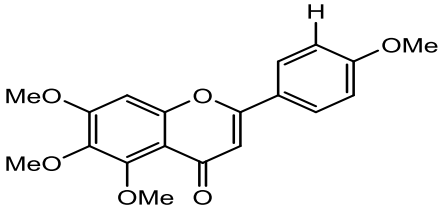

Scutellarein (28)
(Phat *et al*., 2016)

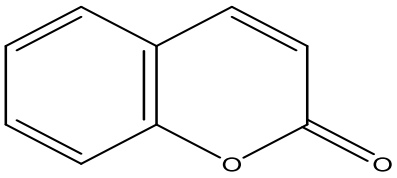

Coumarin (29)
(Moreira *et al*., 2007)

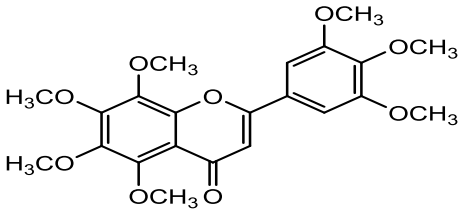

5, 6, 7, 8, 3, 4, 5 – heptamethoxyflavone (30)
(Moreira *et al*., 2007)

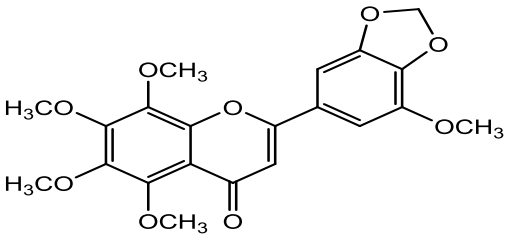

5, 6, 7, 8, 3 – pentamethoxy - 4
, 5-methylenedioxyflavone (31)
(Moreira *et al*., 2007)

Figure 2.6: Isolated compounds from *Ageratum conyzoides*

Vernonia amygdalina Del., family Compositae is cultivated in Africa. It is locally used for treating diabetis mellitus and malaria fever. Vernolepin (32), Vernodalin (33), Vernomelin (34), Vernodalol (35), Vernomygdin (36) and 4, 15- dihydrovernedalin (37) and many more were isolated from the leaves of *Vernonia amygdalina* as shown in Figure 2.7 (Alara *et al*., 2017). *Kigelia africana* (Lam.) Benth., Bignoniaceae family is frequently referred to as the sausage tree and is common in various areas of Africa. *Kigelia* fruits are the most prevalently used plant part in herbal medicine (Houghton, 2002). The fruit has been utilised in traditional medicine for skin illnesses, reproductive disorders, tumors, topical application for wound healing, male infertility, (Agyare *et al.*, 2013), bacterial infections. Sidjui *et al*. (2015) isolated lupeol (38), β – sitosterol (39), β- Sitosteryl β-D- glucoside (40), Canophyllol (41), Pomolic acid (42), Hydroxy-pomolic acid (43) from the leaves and fruits of *Kigelia africana* (Figure 2.8).

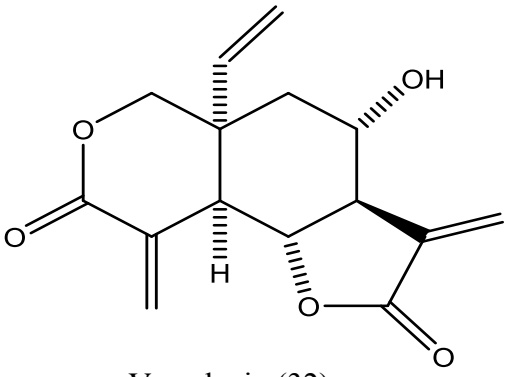

Vernolepin (32)
(Alara *et al*., 2017)

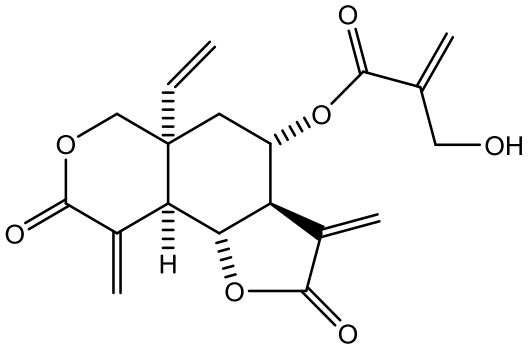

Vernodalin (33)
(Alara *et al*., 2017)

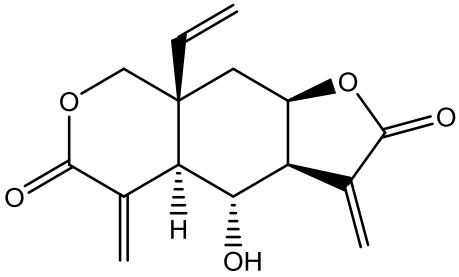

Vernomelin (34)
(Alara *et al*., 2017)

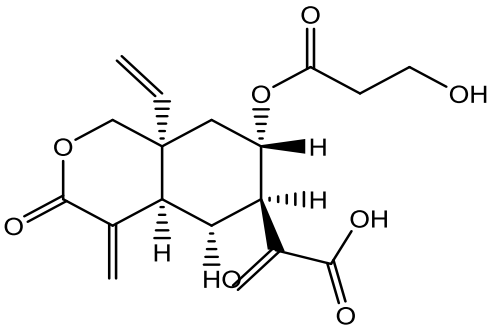

Vernodalol (35)
(Alara *et al*., 2017)

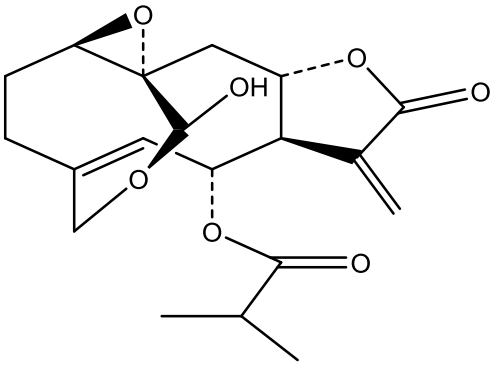

Vernomygdin (36)
(Alara *et al*., 2017)

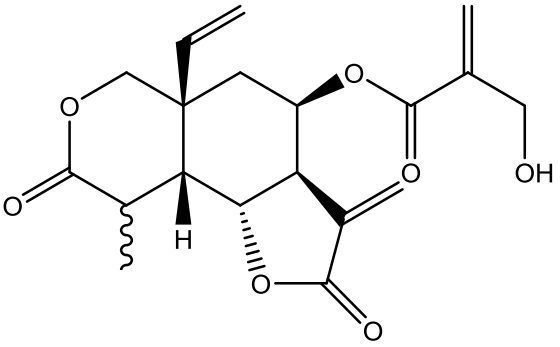

4,15-dihydrovernodalin (37)
(Alara *et al*., 2017)

Figure 2.7: Isolated compounds from *Vernonia amygdalina*

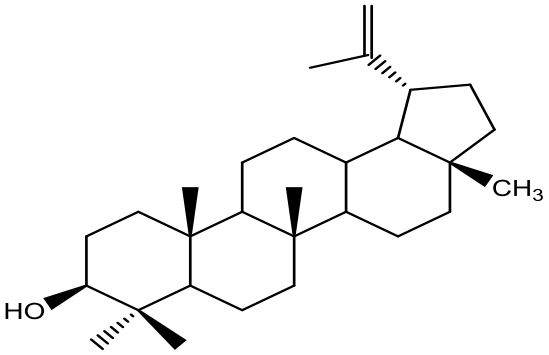

Lupeol (38)
(Sidjui *et al*., 2015)

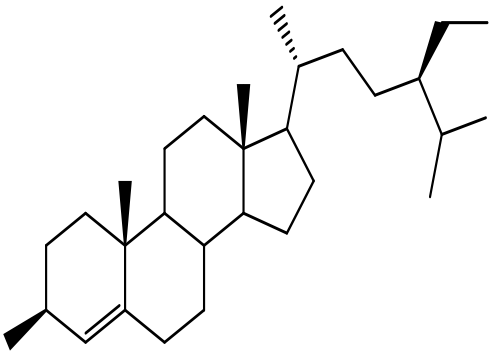

β – sitosterol (39)
(Sidjui *et al*., 2015)

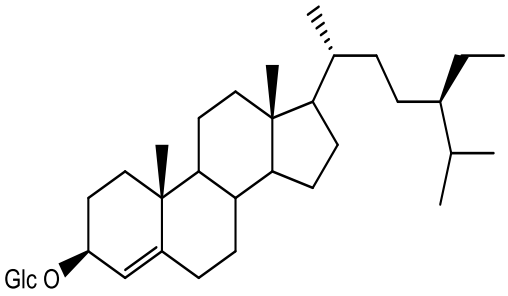

β- Sitosteryl *β*-D- glucoside (40)
(Sidjui *et al*., 2015)

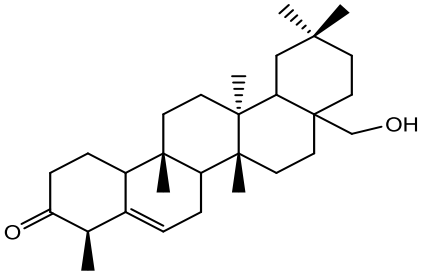

Canophyllol (41)
(Sidjui *et al*., 2015)

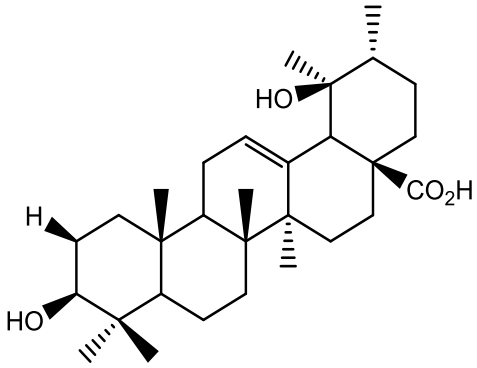

Pomolic acid (42)
(Sidjui *et al*., 2015)

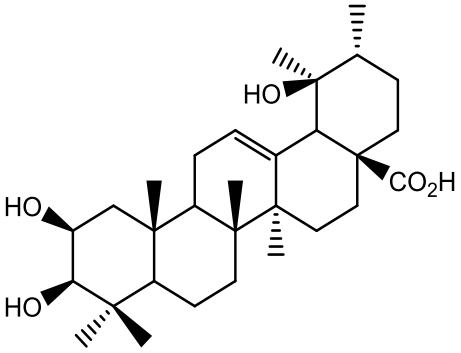

Hydroxy-pomolic acid (43)
(Sidjui *et al*., 2015)

Figure 2.8: Isolated compounds from *Kigelia africana*

Euadenia trifoliolata (Schum. & Thonn.) Oliv., family Capparaceae originated from the thick forest in Nigeria, Ghana, Cameroon, and Gabon (Burkill, 1995). The decoction of leaves is taken as anti-anaemic and tonic. It is also used in managing chronic wound. *Khaya ivorensis* A. Chev., family Meliaceae is a common medicinal plant indigenous to Africa and is also planted in southern China (Zhang *et al.*, 2009). It is abundant in West Africa and southern Nigeria. Locally, the bark is used as a natural cough medicine. The combination of the bark is used as a beverage or bath for spinal pain relief and rheumatism lotion. Studies of stem bark extract showed anti-inflammatory and anti-malarial activities (Agbedahunsi *et al.,* 2004). Earlier chemical study of *K. ivorensis* also showed that it was a good source of limonoids (Abdelgaleil *et al.,* 2005). Seneganolide (44), 3-deacetyl-7-oxokhivorin (45), 1, 3 – dideacetylkhivorin (46) and 1-deacetylkhivorin (47) were isolated from *Khaya ivorensis* as shown in Figure 2.9 (Ji *et al*., 2014). *Philenoptera cyanescens* Schumach. & Thonn. (formerly called *Lonchocarpus cyanescens* Benth), family Leguminosae is native to Africa. It has anti-arthritis, antipsychotic and ulcer treatment (Sonibare *et al*., 2012b; Arowona *et al*., 2014). Triterpenoids and oils such as Phytol (48), 1 – tridecene (49), hexadecanoic acid (50), Heneicosane (51) were previously isolated from the leaves and stems of *Philenoptera cyanescens* as shown in Figure 2.10 (Moronkola and Oladosu, 2013).

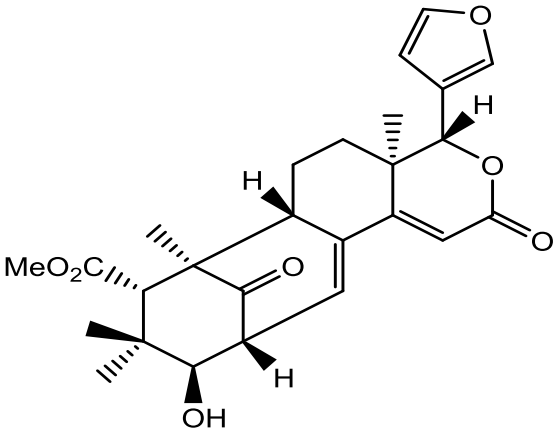

Seneganolide (44)
(Ji *et al*., 2014)

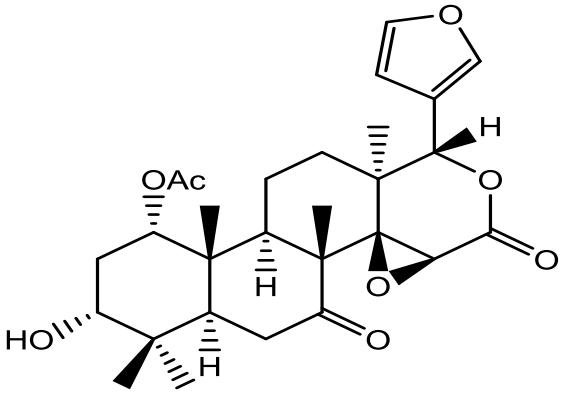

3-deacetyl-7-oxokhivorin (45)
(Ji *et al*., 2014)

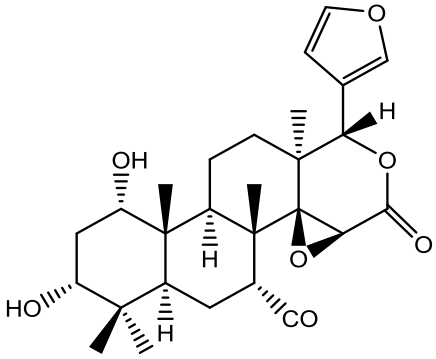

1, 3 – dideacetylkhivorin (46)
(Ji *et al*., 2014)

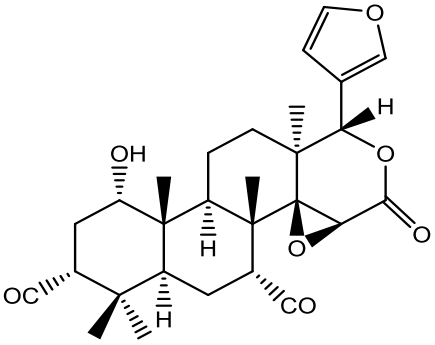

1-deacetylkhivorin (47)
(Ji *et al*., 2014)

Figure 2.9: Isolated compounds from *Khaya ivorensis*

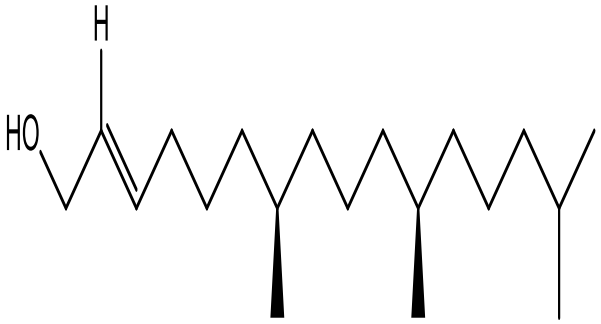

Phytol (48)
Moronkola and Oladosu, 2013

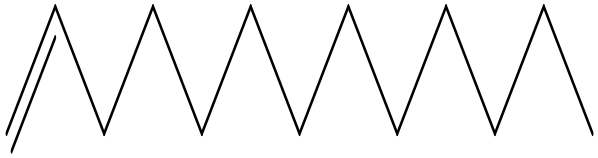

1 – tridecene (49)
Moronkola and Oladosu, 2013

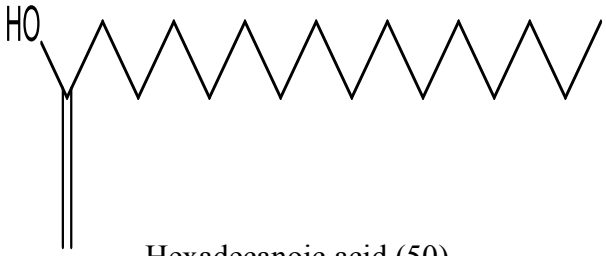

Hexadecanoic acid (50)
Moronkola and Oladosu, 2013

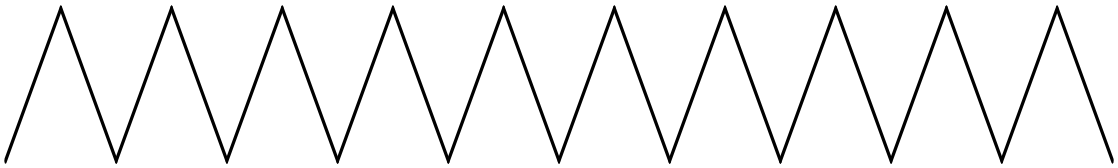

Heneicosane (51)
Moronkola and Oladosu, 2013

Figure 2.10: Isolated compounds from *Philenoptera cyanescens*

Pseudocedrella kotschyii Harms, family Meliaceae and locally termed emigbebi' or 'emigbegbe' in Yoruba languages. The leaf decoction treats several diseases and health conditions which include diabetes, fever, pains, and convulsion in Nigeria (Akuodor *et al.*, 2013). Hay *et al*. (2007) previously isolated 7- deacetylgedunin (52), 7 - deacetyl-7-oxogedunin (53) and Cubebol (54) from *Pseudocedrella kotschyii* (Figure 2.11).

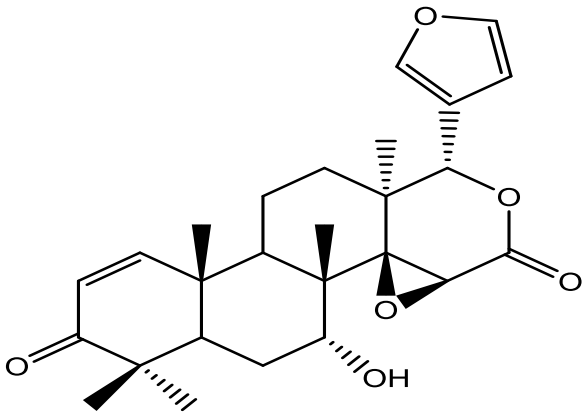

7- deacetylgedunin (52)
(Hay *et al*., 2007)

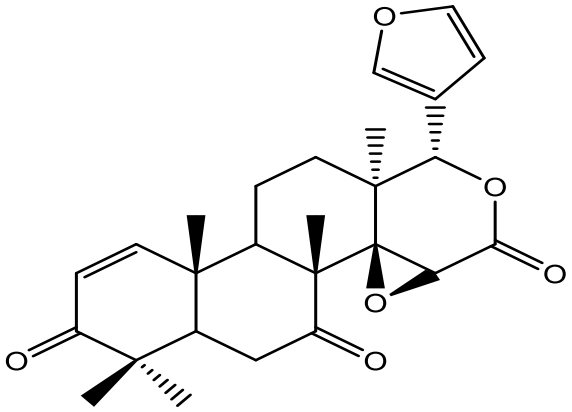

7 - deacetyl-7-oxogedunin (53)
(Hay *et al*., 2007)

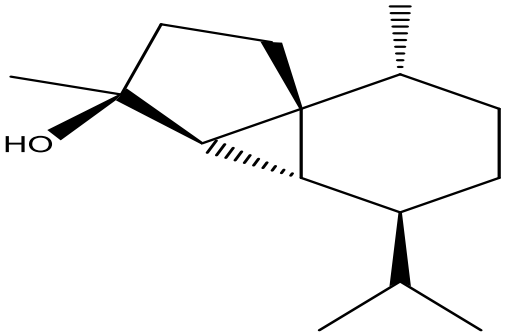

Cubebol (54)
(Hay *et al*., 2007)

Figure 2.11: Isolated compounds from *Pseudocedrella kotschyii*

2.6 Selected plants

2.6.1 *Sphenocentrum jollyanum*

2.6.1.1 Description

Sphenocentrum jollyanum Pierre (Menispermaceae) is a perennial plant growing to a height of 15 m, frequently found in regions with 1800 mm of frequent annual rain (Iwu, 1993). The leaves are wedge-shaped and smooth on both sides with a small arrow apex (Iwu, 1993). The habitat photograph and seeds are shown in Figures 2.12a and 2.12b.

Figure 2.12a: Habitat photograph of *Sphenocentrum jollyanum*

Source: Odo-ona, Ibadan, Nigeria

Figure 2.12b: Seeds of *Sphenocentrum jollyanum*

Source: Odo-ona, Ibadan, Nigeria

2.6.1.2 Origin and geographical distribution

Sphenocentrum jollyanum is a shrub native to West African tropical forest areas and widely distributed throughout Nigeria, Sierra Leone, Ghana, Cameroon and the Ivory Coast (Hutchinson and Dalziel, 1954; Hutchinson *et al*., 1958; Nia *et al*., 2004).

2.6.1.3 Reported ethnomedicinal uses of various parts of *Sphenocentrum jollyanum*

Sphenocentrum jollyanum, is locally known as "Akerejupon" in Yoruba, southwestern Nigeria (Burkill, 1995). *Sphenocentrum jollyanum* is recognised for numerous biological activities and generally used in traditional medicine for treating several ailments. The traditional medical practitioners use different plant parts in folkloric medicine. The root is extensively used as aphrodisiac by men. It is extracted with alcohol for few days and the extract is afterward taken to fortify male erection (Burkill, 1995). The pulverised root when dried is also used as remedy for muscular pains and fever when mixed with some anti-malarial plants. The aerial part is mixed with *Piper guineense* Schumach. & Thonn., family Piperaceae and lime juice for treating coughs, chronic injuries, and fever (Abbiw, 1990). In Nigeria, the roots of *S. jollyanum* once chewed stimulate appetite, relieve constipation, and improve food digestion. The morphological organs of the plant also constitute important components for treatment of sickle cell disease (Abbiw, 1990). The roots are also used for managing hypertension, irregular menstrual flow, breast tumor, and diabetes mellitus in herbal medicine of Ghana and Cote d Ivoire (Odugbemi, 2006; Kayode *et al*., 2009).

2.6.1.4 Biological and pharmacological activity

Antidiabetic activity

Various extracts of *S. jollyanum* morphological organs were studied which was shown in the blood glucose level usng oral glucose tolerant test (OGTT) and diabetic rabbits induced by alloxan. The petroleum ether seed extract (1 gkg^{-} *b.w.*) reduced blood glycemic level by 20% compared with control. A separate study observed a reduction in plasma glucose level from third to the ninth day. Antidiabetic study of *S. jollyanum* leaf ethanol extract at concentrations of 5, 100 and 200 $mgkg^{-}$ *b.w.* showed a significant ($P<0.05$) reduction in blood glycemic index of alloxan induced diabetic rabbits with plasma glucose level of 200.2 $mg100\ mL^{-}$ (42.8%) at 200 $mgkg^{-}$ (Mbaka *et al*., 2010).

Antioxidant activity

The antioxidant activity of *S. jollyanum* (morphological organs) extract was evaluated using DPPH (Nia *et al*., 2004). The methanol stem extract was screened for superoxide and hydrogen peroxide scavenging potential. The study showed antioxidant activity (IC_{50} 13.11 μgmL^{-1} and 30.0 μgmL^{-1}) respectively. The leaf extract gave a weak activity (IC_{50} 4.35 μgmL^{-1}) followed by the root bark (3.50 μgmL^{-1}). The most active was the chloroform fraction of the stem bark (IC_{50} 1.54 μgmL^{-1}). The antioxidant (*in vitro*) activity of *S. jollyanum* stem extract was also assessed with radical scavenging of superoxide and hydrogen peroxide (H_2O_2) which displayed significant antioxidant activity (Olorunnisola *et al*., 2011).

Hepatoprotective activity

The methanol crude extracts; 50, 100 and 200 mgkg $^{-}$ were given orally to wistar rats and the hepatotoxicity induced by 30%, 1.0 $mLkg^{-1}$ CCl_4. The extract displayed a good hepatoprotective activity against CCl_4 – induced total protein and antioxidant markers depletion in liver. The extract returned the activity of the marker enzymes to almost normal. The research revealed that *S. jollyanum* extract had excellent hepatoprotective activity with liver damage caused by CCl_4. The strong antioxidant property may be responsible for this activity (Olorunnisola *et al*., 2011).

Anti-inflammatory activity

Moody *et al.* (2005) researched the *in vivo* anti-inflammatory activity of *S. jollyanum* methanol crude extracts using carrageenan-induced hind paw oedema of orally administered albino rats. In healthy adult wistar rats, the methanol fruit extract gave a higher activity (79.58% inhibition) at a concentration of 200 $mgkg^{-1}$ when compared with root extracts which gave 53.75% inhibition at 200 $mgkg^{-1}$. The reference drug acetylsalicylic acid gave percentage inhibition of 72.5% at 100 $mgkg^{-1}$. The fruit methanol extract was the most active and further purified to give three clerodane diterpenoids; columbin, isocolumbin, fibleucin, which were also screened for anti-inflammatory activity. Out of the three isolated compounds, columbin was found active with 67.08% inhibition at 20 $mgkg^{-1}$ ($P<0.05$).

Anti-malarial activity

The anti-plasmodial activity of *S. jollyanum* leaf and root methanol extracts was reported by Olorunnisola and Afolayan (2011). Anti-plasmodial activity of the methanol extract was assessed *in vitro* using Swiss albino mice inoculated with chloroquine-resistant Plasmodium berghei NK67 strain. The two extracts showed considerable dose-dependent antiplasmodial activity in isolation as well as in combination with elevated average survival time in the four-day curative standard test. The standard drug; Arthemeter-Lumefartrin gave the maximum antimalarial activity with 81.4% inhibition; the leaf extracts gave 74.4%, while the root extracts gave 54.1%. The two extracts also had a beneficial impact on the weight of treated animals and hematology values. The promising antiplasmodial activity displayed by the plant extract could be due to the plant's phytochemicals. The research also found that the leaf and root of *Sphenocentrum jollyanum* have efficient anti-malarial activity against chloroquine-resistant strain. This confirmed the traditional claim that *Sphenocentrum jollyanum* extract was used in malaria management.

Anti-allergy activity

The hyper-sensitivity of immune system to non-infectious stimulation in the environment is characteristic of allergic disorder which could be detrimental reactions to the host. Allergic disorders include eczema, bronchial asthma, inflammatory bowel disease, allergic rhinitis. Over 300 million people are affected by these illnesses and 1 in every 250 fatalities worldwide. The anti-allergic activity of *S. jollyanum* fruit extracts was evaluated in milk induced eosinophilia and leukocytosis mice. The considerable ($P<0.05$) dose-dependent decrease in eosinophilis and leukocytosis wistar mice proposed *S. jollyanum* fruit extract to show anti-allergy activity (Olorunnisola *et al*., 2017).

Antidepressant activity

The ethanol extracts of *S. jollyanum* roots were studied for antidepressant activity. Two depression animal models; forced swimming test (FST) and tail suspension test (TST) were recorded. The immobility duration in both FST (ED_{50} 296.20±53.97 mgkg $^{-1}$) and TST (203.90±39.01 mgkg $^{-1}$) was reduced dose dependently by the extract at 100-1000 mgkg $^{-1}$. Two standards; imipramime and fluocetin were used. The plant extract's effect was 20-50 times less active than the standards. The result implies that *S. jollyanum* is an effective antidepressant drug which can be further purified to serve as drug discovery (Woode *et al*., 2009).

Haematological activity

Sphenocentrum jollyanum methanol extracts (leaf and root) were tested with chloroquine-resistant *Plasmodium berghei* NK 67 for haematological activity using wistar mice. The extracts were given to the mice for 7 days in a row. The outcome acquired showed an increase in the pack cell volume (PCV) and mean corpuscular volume (MCV). Except for neutrophils and monocytes, the red and white blood cells also increased. Therefore, the study indicates that the extract stimulated hematopoietic stem cells (Mbaka *et al*., 2010)

2.6.1.5 Phytochemistry

Phytochemical screening of *Sphenocentrum jollyanum* showed the presence of terpenes, saponins, alkaloids and tannins in the various fractions of the stem bark methanol extract (Nia *et al*., 2004). The essential oil of *S. jollyanum* root was analysed by Aboaba and Ekundayo (2010) using Gas chromatography-Mass spectrometry (GC-MS) analysis. In total, 19 compounds were obtained, including camphene (55), d3-carene (56), globulol (57), 5-Guaiene-11-ol (58), p-cymene (59), α Eudesmol (60), β pinene (61) (Figure 2.13). The proximate seed extract analysis gave the content of crude protein, moisture, carbohydrates, ash, crude fat and fiber as 48.09, 16.70, 48.09, 16.79, 9.65, and 5.51 percent respectively, with an energy value of 1460 kcal/100 kg. The isolated compounds comprise monoterpenoids (33.5%) and sesquiterpenoids (56.3%), while the remaining 10.2% were unknown.

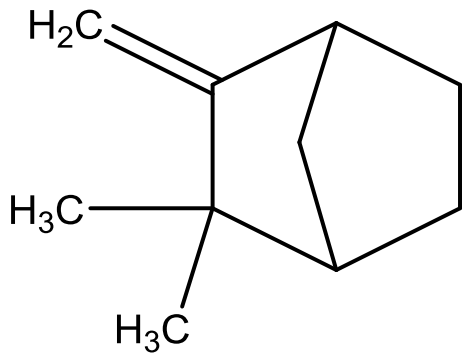

Camphene (55)
Aboaba and Ekundayo, 2010

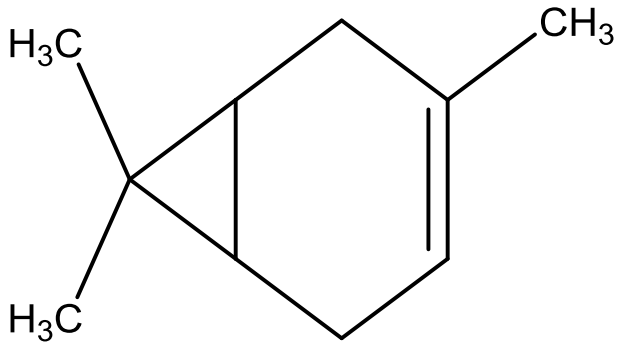

d3-carene (56)
Aboaba and Ekundayo, 2010

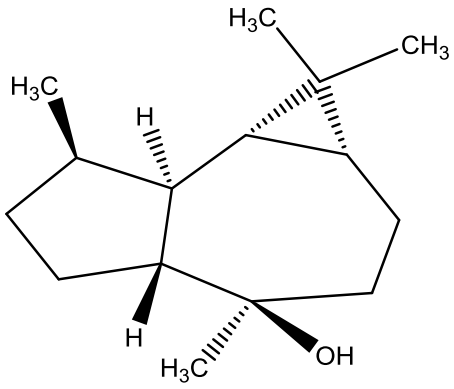

Globulol (57)
Aboaba and Ekunday, 2010

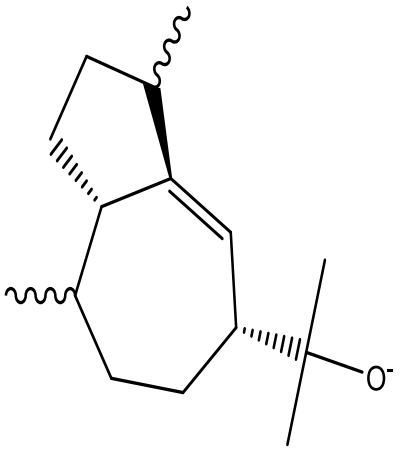

5 - Guaiene-11-ol (58)
Aboaba and Ekundayo, 2010

Figure 2.13: Isolated compounds from the essential oil of *Sphenocentrum jollyanum*

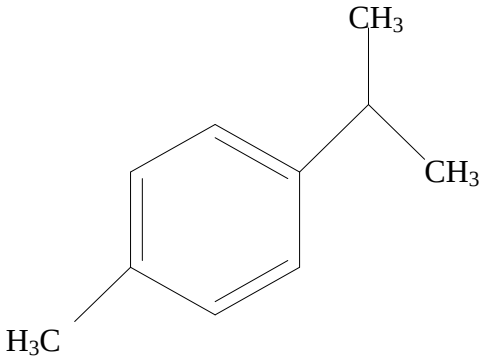

P-cymene (59)
Aboaba and Ekundayo, 2010

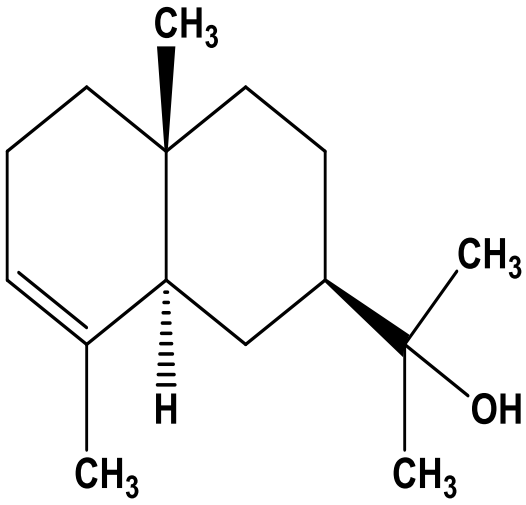

α Eudesmol (60)
Aboaba and Ekundayo, 2010

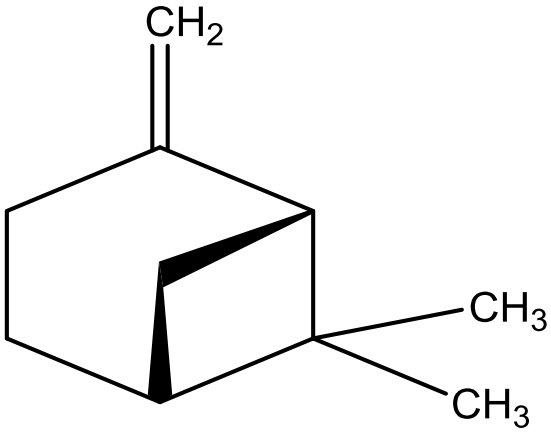

β pinene (61)
Aboaba and Ekundayo, 2010

Figure 2.13: Isolated compounds from the essential oil of *Sphenocentrum jollyanum*

Moody *et al*. (2005) isolated three furanoditerpenes; columbin (62), isocolumbin (63), and fibleucin (64) from the seeds of *S. jollyanum* (Figure 2.14). The isolated compounds displayed anti-inflammatory activity. Biological activities of clerodane diterpenes include insect antifeedant activity, antifungal, antitumor, antibiotics, anti-ulcer, hypoglycemic, antiplasmodial, hypolipidemic, and antithrombin inhibitory activities. Clerodane diterpenes are well known for insect antifeeding and insecticidal features that emphasise the safety of life related to fish and mammals of such natural insect antifeedants. Over 400 natural and semi-synthetic clerodanes were evaluated using various laboratory experiments to produce several compounds with strong antifeedant activity against numerous classes of insects (Li *et al*., 2016). Camphene is a bicyclic monoterpene and a major component of plant-based essential oil. It is used for fragrance preparation and as artificial flavoring food additives. It is also used in camphor and insecticides manufacturing. It has also been shown to have a protective impact against oxidative stress (Tiwari and Kakkar, 2009).

Essential oils generally function as antibacterial agents against a broad variety of pathogenic bacterial strains such as *Listeria innocua*, *Listeria monocytogenes*, *Bacillus cereus*, *Staphylococcus aureus*, etc. In addition to the use of essential oils as natural sanitising agents in the food industry, antimicrobial activity such as minimal inhibitory concentration (MIC), mycelial growth inhibition and minimum fungicidal concentration (MFC) of six essential oils against *Penicillium chrysogenum*, *Aspergillus terreus*, *Aspergillus niger*, *Chaetomium globosum*, *Penicillium pinophilum*, *Trichoderma viride* and *Trichoderma harzianum* was also evaluated (Angelini *et al*., 2008)**.** The antimicrobial activity was monitored using microdilution method and a wide spectrum of antimicrobial activities was exhibited in the essential oil. Essential oils are also rich in phenolic compounds thus attracting scientists to evaluate their antioxidant activity.

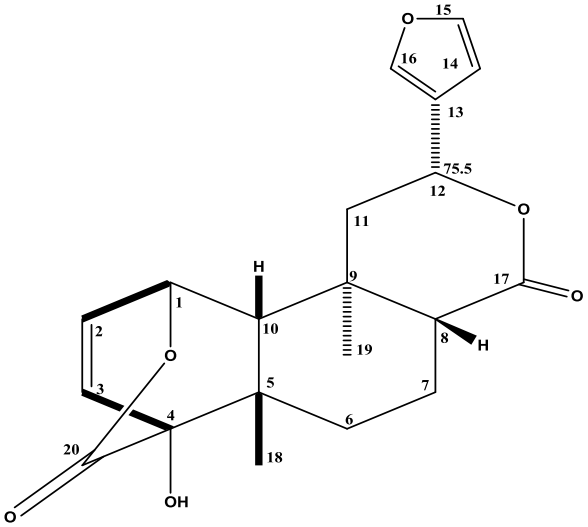

Columbin (62)
(Moody *et al*., 2005)

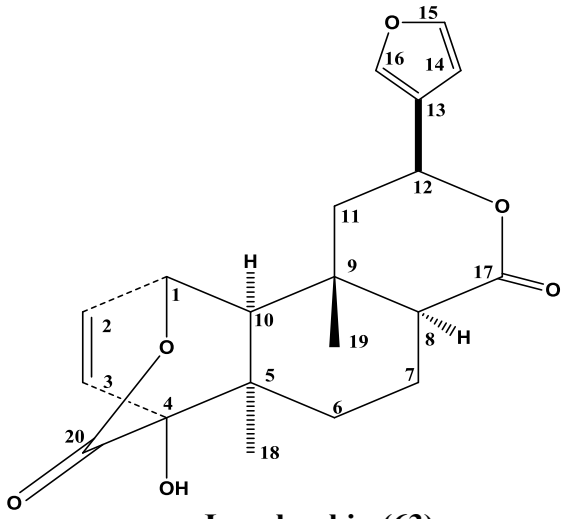

Isocolumbin (63)
(Moody *et al*., 2005)

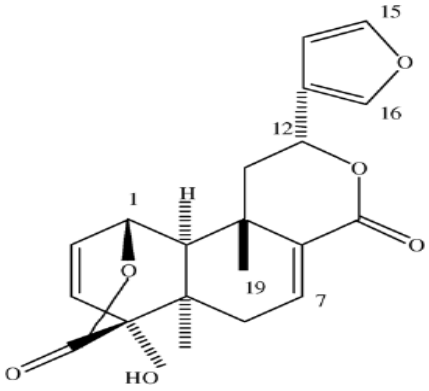

Fibleucin (64)
(Moody *et al*., 2005)

Figure 2.14: Isolated compounds from *Sphenocentrum jollyanum* seeds

2.6.2 *Curculigo pilosa* (Schumach. & Thonn.) Engl. family Hypoxidaceae, is an African plant with an erect rhizome. It is a perennial herb, often with tuberous rhizome with sessile, basal or petiolate leaf types with racemose inflorecenses. The flowers are unisexual or bisexual with an often yellow perianth spreading, subequal, and sometimes basically tubelike (Flora of China, 2006). The habitat photograph and rhizomes of *C.pilosa* are shown in Figures 2.15a and 2.15b respectively.

Figure 2.15a: Habitat photograph of *Curculigo pilosa*

Source: Itoku, Abeokuta

Figure 2.15b: Rhizomes of *Curculigo pilosa*

Source: Itoku, Abeokuta

2.6.2.1 Reported ethnomedicinal uses of various parts of *Curculigo pilosa*

The rhizome is used in folk medicine for the management of heart and gastrointestinal illness (Dicko *et al*., 1999). It is conventionally used in the southwestern Nigeria for treatment of infertility, sexually communicable infections, especially gonorrhea, and as purgative for the treatment of hemia. It is also used in sterility, epilepsy, meteorism, and drepanocytosis therapy in Africa (Dicko *et al*., 1999). It is locally used for the manufacturing of sorghum beer and baby food in West Africa. This is because of elevated amylolytic activity in the plant extract. *Curculigo pilosa* is used as a laxative in southern Nigeria and in Congo Brazaville for hemia therapy. The root is applied topically to swellings when reduced to a pulp in the Central African Republic (Burkill, 1995).

2.6.2.2 Pharmacological Activities of Genus Curculigo

Antioxidant activity of *Curculigo pilosa*

Antioxidant activities of *Curculigo pilosa* methanol extracts and *Gladilous psittascinus* Hook. f., family Iridaceae, were evaluated using 2, 2, diphenyl-1-picrylhydrazyl (DPPH) scavenging assay, total antioxidant capacity (TAC) reducing power, total phenolics and total flavonoid content (Karigidi *et al*., 2019). Healthy Wistar albino rats were used for *in vivo* while sodium nitroprusside was used to induce lipid peroxidation in the liver and heart of the animals. The peroxidation was observed by the malondialdehyde content where the obtained result showed that *C. pilosa* possessed higher total antioxidant capacity, total phenolic, total flavonoidand DPPH scavenging and reducing power activity than *G. psittascinus*. *Curculigo pilosa* also inhibited malondialdehyde production in sodium nitroprusside-incubated liver and heart homogenates (Karigidi *et al*., 2019).

Vasoconstrictor activity of *Curculigo pilosa*

For vasoconstrictor activity, *C. pilosa* methanol extract, *n* Butanol fraction, and the isolated nyasicoside curculigine, pilosidine and norlignan glucosides were assessed. They all facilitated the contraction of rabbit aorta strips induced by adrenaline. This contraction could be reversed by prior nifedipine administration (Palazzino *et al*., 2000).

Antimicrobial and cytotoxic activities of *Curculigo pilosa*

Shaba *et al.* (2014) revealed antimicrobial and cytotoxic activity of *Curculigo pilosa* methanol extract and partitioned fractions. Except for *n* hexane fraction, the antimicrobial activity of the tested solvent fractions appears to have potential with a minimum inhibitory concentration (MIC) range of 0.09-6.25 $mgmL^{-1}$. However, the *n* Butanol and ethyl acetate fractions showed antibacterial activity

against highest number of bacterial strains. In summary, the outcome of antimicrobial activity acquired showed that the crude extract was more active than the fractions and weak cytotoxic activity of *Curculigo pilosa*'s crude methanol extract as established by its 764.07 μgmL $^{-1}$ LC_{50} value.

Adaptive activity of *Curculigo orchioides*

The adaptive activity of *C. orchioides* have been evaluated which showed enhanced effects of the plant. The extract could improve elevated temperature and hypoxia tolerance, it increased immunological activity in mice, had a sedative and anticonvulsant effect (Chen *et al*., 1989).

Immunostimulatory effect of *Curculigo orchioides*

The immunostimulatory effect of *C. orchioides* methanol extract was studied. The extract was found to increase the white blood cell count. The result revealed that *C. orchioides* methanol extract exerted an immunostimulatory outcome through humoral antibodies and mediating cells (Bafna and Mishra, 2006).

2.6.2.3 Phytochemistry

Due to their various medicinal properties, several phytochemical studies have been performed on the genus, *Curculigo*. These include alkaloids, triterpenes and triterpenoid glycosides (Zuo *et al*., 2012), Lignans and Lignan glycosides, Phenols and phenolic glycosides and other components. Triterpenoids and Norlignans are observed as the main constituents and may possibly be responsible for majority of the activities found in the plants of this genus (Nie *et al*., 2013). According to Flora of China (2006), the genus *Curculigo* is categorised into two sections; Section Curculigo and Section Molineria. Section Curculigo incudes *Curculigo orchoides* Gaertn and *Curculigo glabrescens* (Ridl.) Merr., while Section Molineria (colla) includes *Curculigo pecurvata* Dryand, *Curculigo pilosa* (Schumach. and Thonn.) Engl., *Curculigo sinensis* S. C. Chen and *Curculigo breviscapa* S. C. Chen. Lignans and lignin glycosides are typical components of the flora of Section Molineria, triterpenes and triterpenoid glycosides are majorly found in Section Curculigo plants; while phenols and phenolic glycosides are present in both sections (Nie *et al*., 2013). Palazzino *et al.* (2000) previously isolated Curculigine (65), Pilosidine (66), and Piloside A (67) from *Curculigo pilosa*. Other isolated compounds from genus Curculigo include Curculigoside A (68), Curculigoside B (69), Curculigoside C (70), and Curculigoside D (71) isolated by Valls *et al*., 2006. Figure 2.16 shows the isolated compounds from *C. pilosa* while Figure 2.17 shows the isolated compounds and their structures from Genus Curculigo.

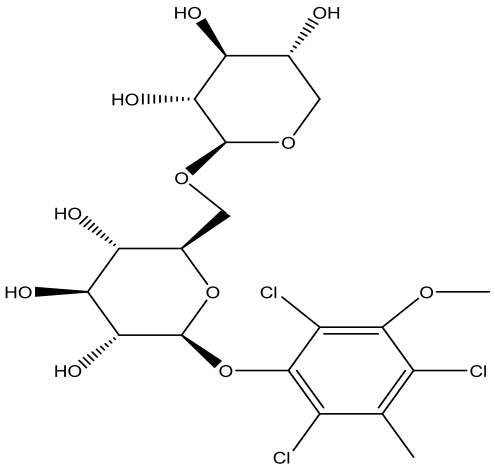

Curculigine C (65)
(Palazzino *et al*., 2000)

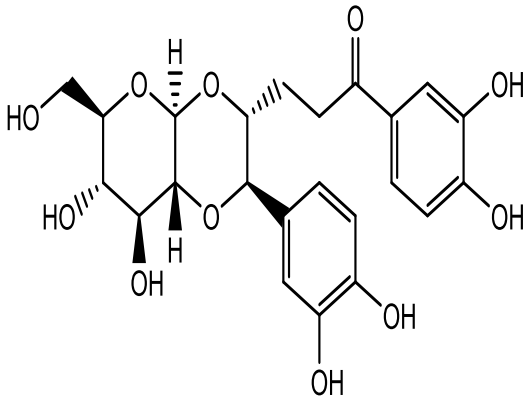

Pilosidine (66)
(Palazzino *et al*., 2000)

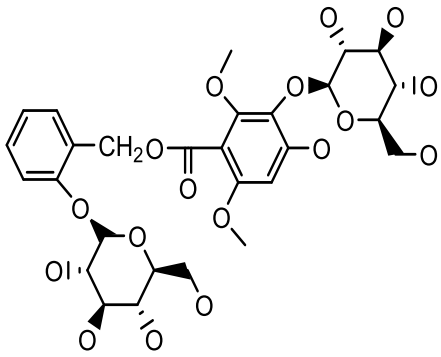

Piloside A (67)
(Palazzino *et al*., 2000)

Figure 2.16: Isolated compounds from Curculigo *pilosa*

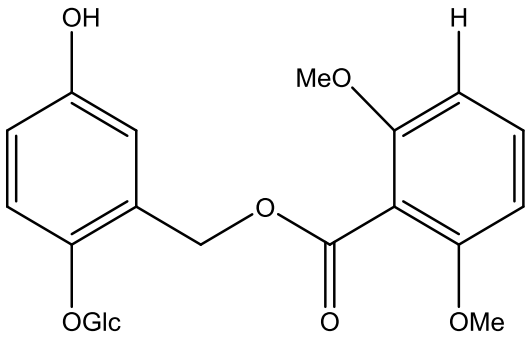

Curculigoside A (68)
Valls *et al*., 2006

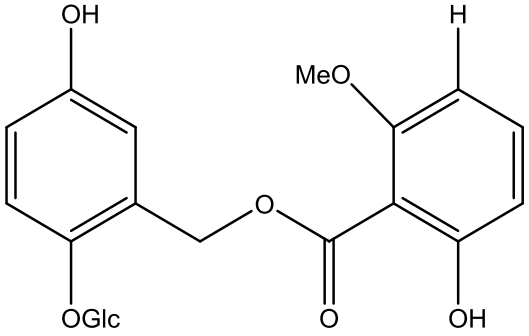

Curculigoside B (69)
Valls *et al*., 2006

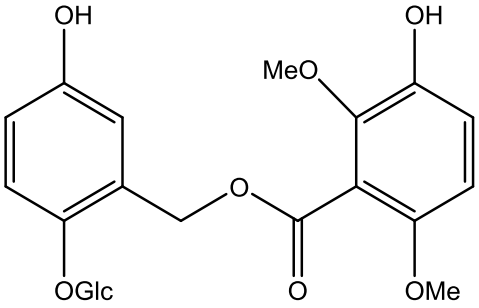

Curculigoside C (70)
Valls *et al*., 2006

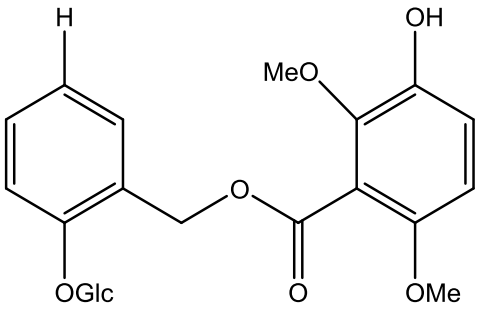

Curculigoside D (71)
Valls *et al*., 2006

Figure 2.17: Isolated compounds from Genus Curculigo

Li *et al*. (2005) also isolated two eudesmanes named Capitulatin A (72) and Capitulatin B (73) from *Curculigo capitulata* (Lour) O. Ktze (Figure 2.18). Also, two flavones namely 5,7-dimethoxmyricetin-3-O-α-L-xylopyranosyl-(4-1)-β-D-glucopyranoside (74) and 3',4',5'-trimthoxy-6,7-methylenedioxyflavone (75) were isolated from *Curculigo orchiodes* Gaertn (Tiwari and Mishra, 1976) as shown in Figure 2.19.

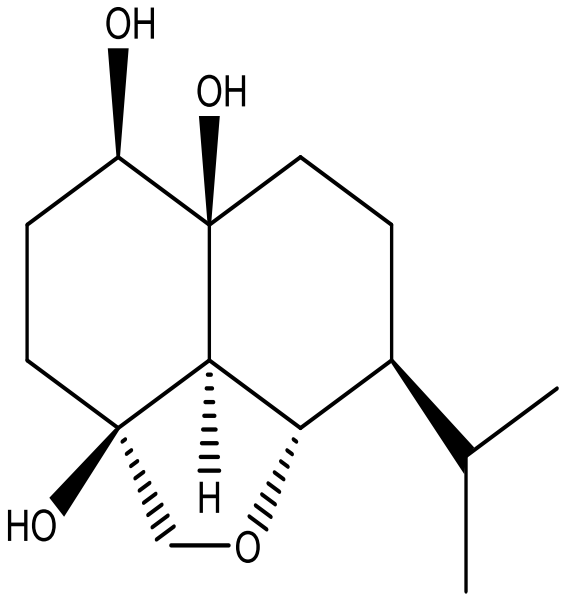

Capitulatin A (72)
Li *et al*., 2005

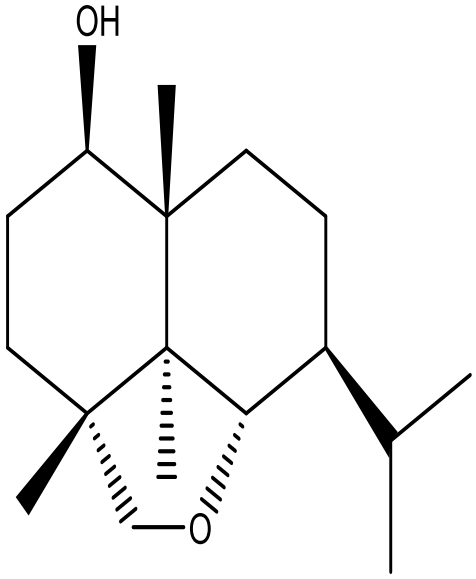

Capitulatin B (73)
Li *et al*., 2005

Figure 2.18: Eudesmanes isolated from *Curculigo capitulata*

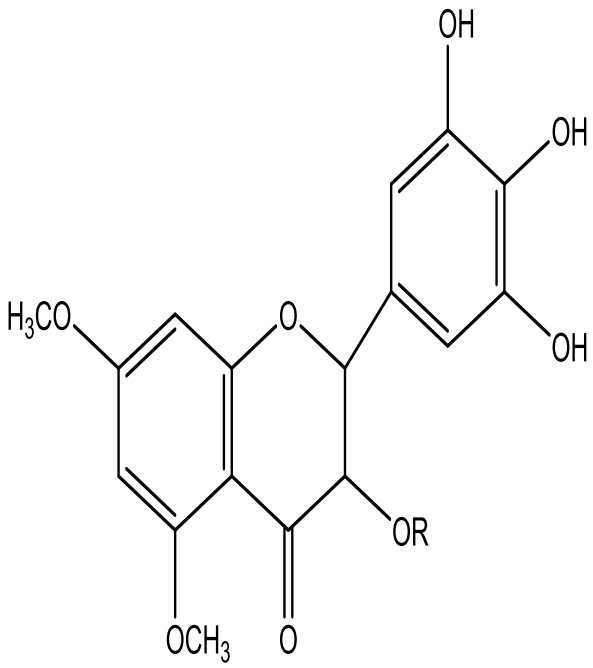

R = α - L - Xyl - (4-1) - β – D - Glc

5, 7-dimethoxmyricetin-3-O-α-L-xylopyranosyl - (4-1)-β-D-glucopyranoside (74) Tiwari and Misra, 1976

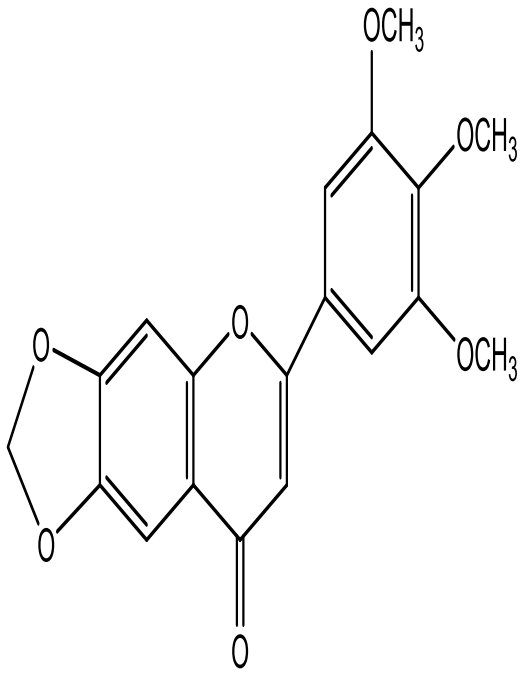

3', 4', 5'-trimthoxy-6, 7-methylenedioxyflavone (75) Tiwari and Misra, 1976

Figure 2.19: Flavones isolated from *Curculigo orchioides*

CHAPTER 3

3.0 MATERIALS AND METHODS

3.1 Chemicals and reagents

Absolute Methanol (MeOH), *n* Hexane, Dichloromethane (DCM), Ethyl acetate (EtOAc), *n* Butanol, Acetic acid, Acetone, Ammonia, Ammonium hydroxide, Benedict's solution (BDH Laboratory Supplies, Poole, England), Cimetidine tablet (Rx Nigeria), Indomethacin tablet, Pepsin enzymes (HI Media Lab PVT Ltd, Hyderabad, India), Sodium carbonate, Aluminium chloride, Potassium acetate, Distilled water, Deionized water, Gallic acid, Quercetin, Ascorbic acid, DPPH, Rutin, Folin Ciocalteu, Dragendorff's reagents, Meyer's reagents, Wagner's reagents, Normal saline, Sodium hydroxide, Vanillin H_2SO_4, Hand Gloves, Methylated spirit, 10% (v/v) HCl, 1% Ferric chloride ($FeCl_3$) reagent, Dilute NaOH, Conc. HCl, Lead acetate solution, Glacial acetic acid, 3, 5 – dinitrobenzoic acid, Conc. Sulphuric acid, 10% H_2SO_4, p-anisaldehyde, Cerric sulphate, Pepsin enzyme (BDH Laboratory Supplies, Poole, England). Analytical grade/HPLC grade: *n* hexane, EtOAc, Methanol, Silica gel (Merck, 70–230 mesh size), precoated silica gel TLC plates (Merck, F-254, 20 cm by 20 cm.

3.2 Apparatus and animals

Cages, Cotton wool, Syringes and needles, Oral cannula, Dissecting set (Needle holders, scalpel, holders, Thumb forceps, toothed forceps, Mayo scissors, Artery forceps), Albino rats (130 - 150 g), Retort stand, Rotary evaporator, Separating funnel (Pyrex), Water bath (Bibby), Weighing scale (Acculab L. series).

3.3 Equipment

Hitachi U-3200 UV-Visible spectrophotometer Japan, Shimadzu 8900 FTIR spectrophotometer Japan, Buchi-535 melting apparatus. Bruker Avance-400, 500, 600 and 800 NMR spectrophotometers, JEOL JMS- 600H mass spectrometer, Agilent 1100 liquid chromatograph

Model LC – 908W - 060 equipped with a Phenomena Luna 5µ C18(2) 100 A column (250mm 20 mm, 4 µm), UV lamp (254 and 366 nm), Chromatographic columns, Chromatographic tanks, Separating funnel, Glass wares, Rotary evaporator (Bibby Scientific Limited, Stone Staffordshire ST15 OSA, UK), Beaker, Conical flask.

3.4 Research design

3.5 Ethnobotanical survey

3.5.1 Study area

Ethnobotanical survey was conducted in five local government areas of Ibadan, southwestern Nigeria. These local government areas include: Oluyole, Ibadan South/West, Akinyele, Ibadan North East, and Egbeda LGAs as shown in the locality map (Figure 3.1). The areas constitute traditional medical practitioners, herb sellers, and elderly who are versatile and experienced in the local treatment of gastric ulcer. There is high incidence rate of gastric ulcer treatment due to high ulcer rate.

The five LGAs are part of the 11 LGAs of Ibadan, Oyo State with latitude 7°22′N and longitude 3°55′E. The region, being South West has tropical climate with two distinct seasons: dry and wet. The dry season is usually between November and February. Rainfall occurs throughout the year with an average annual rainfall of 250 cm^3 while dry season is usually between November and February. The areas still have villages with little or no access to modern health care and thereby rely on traditionalists and TMPs for solutions to their health challenges. Most of the natives interviewed are Yoruba and their occupations include herb selling and trading. Some of the places are rural areas which are not well developed, while some of the areas are moderately urbanized.

Oluyole LGA comprises Idi Ayunre and CRIN (Cocoa Research Institute of Nigeria), Ibadan South/West comprises Molete and Bode market, Akinyele LGA comprises Ojoo, Idi-ose, Moniya, and Ajibode, Ibadan North-East LGA includes Oje market while Egbeda LGA includes Gbagi market and Alakia market.

3.5.2 Informed consent

The respondents included Herb Sellers, Traditional Medicine Practitioners (TMP) and elderly with indigenous knowledge of medicinal plant used for treating numerous diseases, including

gastric ulcer. Informed consent was obtained verbally from all participants before the commencement of the interview.

3.5.3 Data collection

The ethno botanical study was conducted between August, 2015 and February, 2016. Herb sellers, Traditional Medicine Practitioners (TMPs), and elderly were categories of people interviewed. The TMPs were interviewed at Oluyole local government, the association of TMPs at Oluyole Local Government of Ibadan comprises both males and females; twelve members were present on the day of the interview. Herb markets were mostly visited at the remaining four local governments where fifty herb sellers were interviewed. Ten elderly were also interviewed at the four local governments. According to them, most of their knowledge was inherited from ancestors. Their ages ranged between 30 and 70 years. The interview was granted after seeking consent orally from all the participants. Detailed information was obtained through the use of semi-structured questionnaire and oral interview. Questions such as: the name and part of the medicinal plant used for treatment of gastric ulcer, side effects of the mentioned plant, the mode of preparation, method of administration of the plant, dosage during treatment, time of collection of the mentioned plants, other method of treatment apart from herbs, among others. The sample of the questionnaire is shown in Appendix 1. The local plant names were provided in all cases because most of the respondents were not educated; journals, textbooks, and plant databases were consulted to confirm the botanical names.

3.6 Collection, identification and authentication of plant material

The ethnobotanical survey carried out in five local government areas: Ibadan South/West LGA, Akinyele LGA, Oluyole LGA, Ibadan North East LGA, and Egbeda LGA led to plant selection based on Use Mention Index (UMi). The fourteen selected plants were collected at different places in southwestern Nigeria in June 2016. Identification and authentication of the most mentioned plants was done by Mr. Tope Soyewo of Forest Herbarium, Ibadan, located at Forestry Research Institute of Nigeria, where voucher specimens were deposited. The various selected plants' parts were shade dried for three weeks and pulverised.

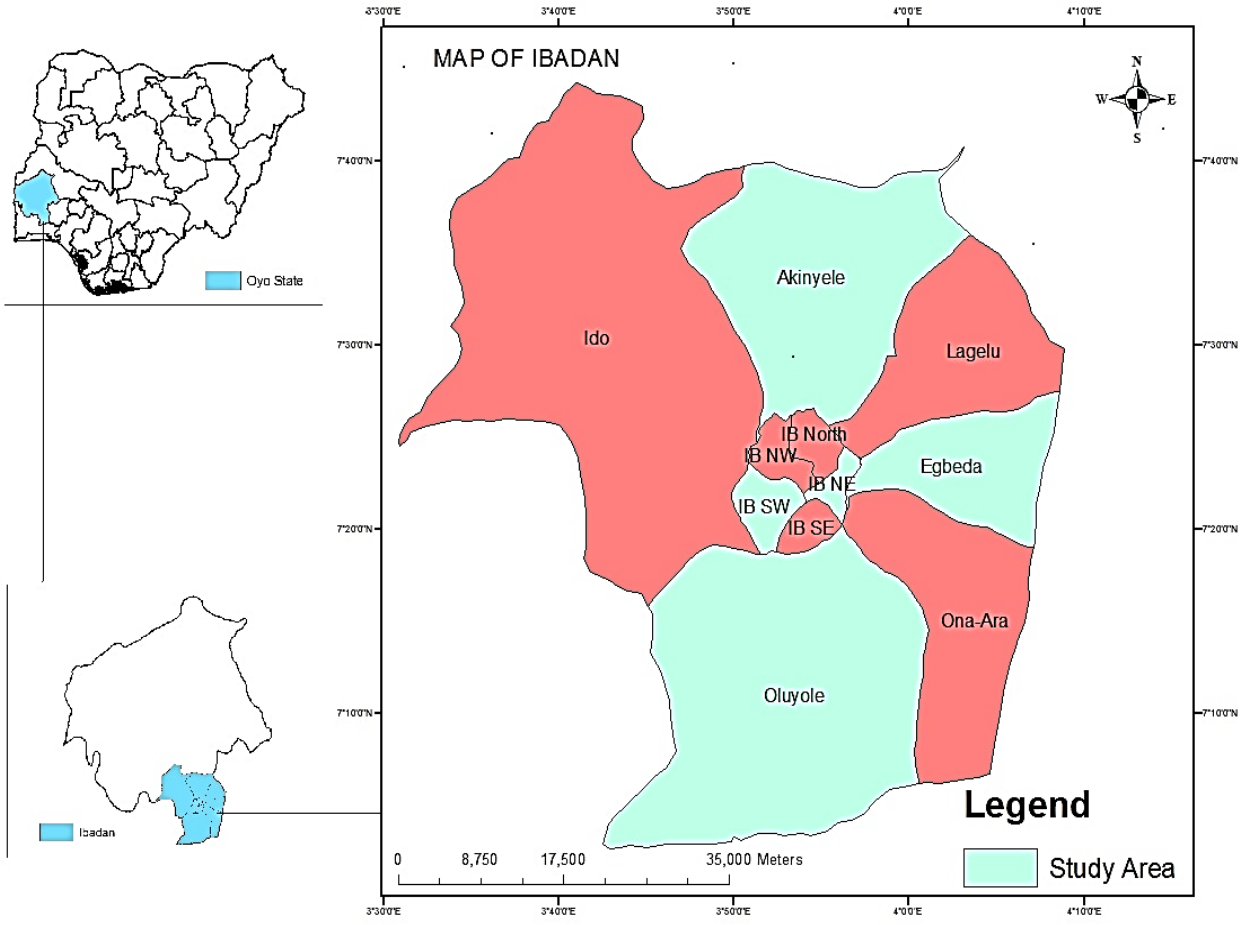

Figure 3.1: Map of Ibadan showing the local government areas visited for the survey.

3.7 Extraction of plant material

Three hundred grams of each of the fourteen powdered samples and 2.5 kg each of the two selected plants were macerated with 100% methanol for 120 h stirring daily with a glass rod. Maceration was carried out three times using fresh solvent for exhaustive extraction. The filtrates were pooled, evaporated *in vacuo* at 30°C, and kept at 4^{o}C for biological assays.

3.7.1 Yield of extracts

This was calculated by dividing the weight of the extract by the corresponding weight of the powdered plant part multiplied by 100%.

3.8 Preliminary phytochemical screening

The selected plants were screened for the presence of secondary metabolites such as tannins, saponins, flavonoids, alkaloids, cardiac glycosides and anthraquinones using standard methods (Sofowora, 1993; Trease and Evans, 2002).

3.9 Preliminary biological activity of extracts

The summary of this study is shown in the flow chart of general experimental procedure (Figure 3.2)

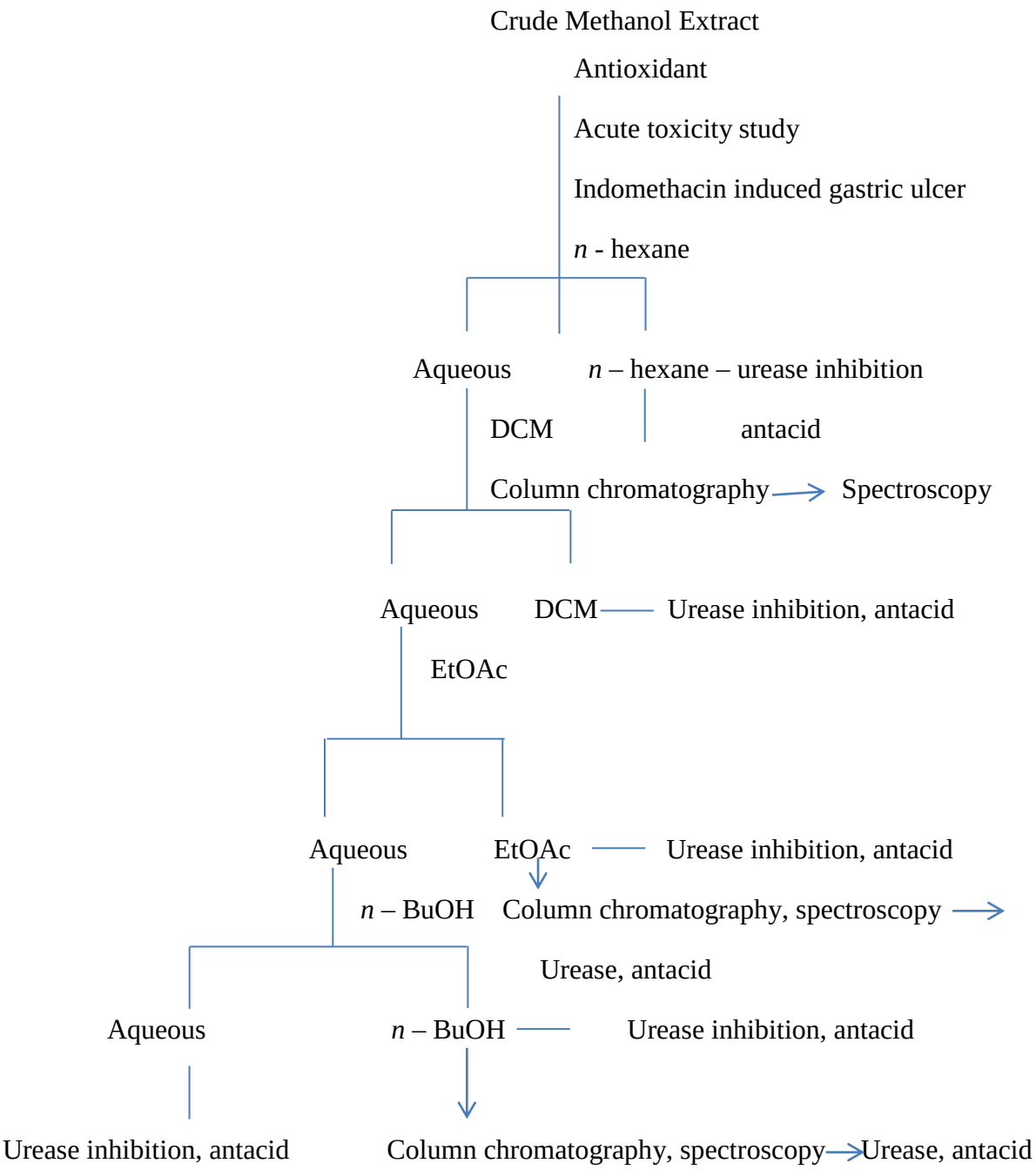

Figure 3.2: Workflow chart showing general experimental procedures

3.9.1 Estimation of total phenolic content (TPC)

The selected plant crude extracts were screened for TPC using the Khatoon *et al.* (2013) method. The TPC of the crude extracts were measured using a gallic acid calibration curve prepared by mixing 0.5 mL aliquots of 12.5, 25, 50, 100, and 200 μgmL^{-1} methanol gallic acid solutions with 2.5 mL Folin-Ciocalteu reagent (diluted ten-fold) and 2.0 mL (75 g/L) sodium carbonate. This mixture was then incubated at room temperature for 30 min and UV / visible spectrophotometer (752 spectrum lab UV) was used to determine the quantitative phenolic estimate at 765 nm. A graph of absorbance against concentration is shown in the calibration curve. For crude extracts (200 μgmL^{-1}) the same procedure was repeated. The studies were carried out in triplicates and total phenolic content was expressed as gallic acid equivalent milligrams per gram of extract ($mgGAEg^{-1}$).

3.9.2 Estimation of total flavonoid content

Aluminum chloride was used to determine total flavonoid content according to Ebrahimzadeh *et al.* (2009) method. The sample (0.5 mL of 200 μgmL^{-1}) in methanol was mixed with 1.5 mL methanol, 0.1 mL 10% aluminium chloride, 0.1 mL 1 M potassium acetate, and 2.8 mL of distilled water. The extract was kept for 30 min at room temperature (28 ^{o}C – 30 ^{o}C); the absorbance of the reaction mixture was evaluated at 415 nm with a laboratory UV / Visible spectrophotometer (double beam spectrum 752s). The calibration curve was prepared by preparing quercetin solutions at levels of 12.5 to 200 μmL^{-1} in methanol. All experiments were done in triplicate and total flavonoid content expressed as milligrams of quercetin equivalent per gram of extract ($mgQEg^{-1}$).

3.9.3 The DPPH free radical scavenging assay

This assay was measured using ascorbic acid as standard in terms of hydrogen donating or radical – scavenging ability using the stable radical 2, 2 – diphenyl-1-picrylhydrazyl (DPPH) according to the method described by Susanti *et al.* (2007) with some modifications. Extract as well as the control (2 mL) at various concentrations (100, 50, 25, 12.5, 6.25, 3.125, and 1.625 μgmL^{-1}) were added to 3 mL of freshly prepared DPPH solution (0.1 Mm) in methanol. At room temperature, the mixture was incubated in the dark for 30 min and the absorbance was measured at 517 nm using UV / Visible spectrophotometer (752s spectrum lab UV). All experiments were repeated three times independently. The degree of decolorisation of DPPH from purple to yellow indicates the

scavenging efficiency of the extract. The percentage inhibition of DPPH free radical scavenging activity was calculated using the following equation:

% inhibition = [(absorbance of control – absorbance of test sample)/absorbance of control] x 100%. The antioxidant activity of each sample was described in terms of IC_{50} (micromolar concentration required to inhibit DPPH radical formation by 50%), which was calculated from the linear regression curve.

3.10 Ethical approval

This experiment was approved by the institutional Animal Care and Use Research Ethics Committee with UI-ACUREC/19/0018.

3.11 Experimental animals

For both assays (acute toxicity study and indomethacin-induced gastric ulcer) a total of seventy-seven healthy male Wistar rats (120 – 150 g) were used; thirty-two animals for acute toxicity study and forty-five animals for indomethacin induced gastric ulcer. The animals were obtained from the central animal house, College of Medicine, University of Ibadan. Acclimatisation was done for two weeks while maintaining standard conditions (12 h light and 12 h dark), fed with Ladokun commercial rat diet Nigeria (standard rat diet feed) and given access to clean water *ad. libitum*. The guidelines of National Institute of Health (NIH publication 85-23) for laboratory animal care and use were followed in the management and treatment of the rat. This experiment was approved by the institutional Animal Care and Use Research Ethics Committee with UI-ACUREC/19/0018.

3.12 Toxicity study

Acute toxicity and lethality studies were carried out using Lorke (1983) method to determine the safe effective dose. Twelve Wistar rats were randomly divided into four groups (n=3) and orally administered 10, 100, 1000 mgkg $^{-1}$ *b.w.*of *S. jollyanum* or *C. pilosa* methanol extracts, respectively while the fourth group was the control. Since no mortality was recorded, higher doses of 1600 mgkg $^{-1}$, 2900 mgkg $^{-1}$, and 5000 mgkg $^{-1}$ doses were administered to a new group of Wistar rats at one rat per dose, taking the last rat as control to determine lethality. The animals were closely observed 1h, 2h, 4h, 6h, 8h, 12h, and 24h for signs and symptoms of toxicity and death (Lorke, 1983). The surviving animals were closely observed for 14 days and euthanised. Histopathological assessment was performed on liver, heart, and kidney to determine the level of toxicity damage.

3.13.0 Gastroprotection methodology

3.13.1 Indomethacin induced gastric ulcer

Forty-five healthy male Wistar rats were divided randomly into 9 groups having 5 animals per group (n = 5). Group A (Cimetidine group), group B (ulcer untreated), groups C, D, and E: (*C. pilosa* methanol extracts 50, 100, and 200 mgkg $^{-1}$), groups F, G, and H (*S. jollyanum* methanol extracts 50, 100, and 200 mgkg $^{-1}$), and group I (normal control). Animals were pretreated with cimetidine (100 mgkg $^{-1}$), *C. pilosa* and *S. jollyanum* at varied doses (50, 100, and 200 mgkg $^{-1}$ *b.w.*) orally for 7 uninterrupted days. Slightly modified method of Akpamu *et al.* (2013) was used for gastric ulcer induction where 40 mgkg $^{-1}$ *b.w.* indomethacin was administered to the animals; 1 h after cimetidine or extract dosing. The ulcer untreated group (group B) received indomethacin only in the last day, while the group I animals (normal control) were not administered either drug or indomethacin. Animals were fasted 24 h before the experiment. Euthanasia by cervical dislocation was carried out and their stomachs removed 4 h after gastric ulcer induction. The stomachs were washed off any food residues by gently washing in cold phosphate buffer solution, and carefully spread on a waxed paper. Gastric ulcer index (UI) was calculated using Lee *et al*. (2005) method. Gastric ulcer index of each animal was calculated as average of ulcers in each group using Lee *et al.* (2005) method with slight modifications:

No lesion – 0, Bleeding and Slight lesions (0.5 – 1.0) mm = 1, Moderate Lesions (1.0 – 1.5) mm = 2, severe lesions (1.5 – 2.5) mm = 3, and perforated ulcers (2.5 – 3.5) mm = 4.

Percentage inhibition was calculated using:

$$\% \text{ Inhibition} = \frac{^{UI}\text{ ulcer untreated} - ^{UI}\text{ treated}}{^{UI}\text{ ulcer untreated}} \times 100$$

(Kayode *et al.*, 2009).

A segment of the gastric tissue was cut and fixed in formalin (10%) for histological assessment.

3.13.2 Histological assessment

The stomach samples in 10% formalin were processed and fixed in paraffin wax. Section (5 µm) was prepared and stained with Haematoxylin and Eosin (H&E). Histopathological changes were observed and photographed using digital camera.

3.13.3 Biochemical assays

3.13.3.1 Gastric nitric oxide (NO)

The method of Miranda *et al.* (2001) was used for this assay.

3.13.3.2 Analysis of gastric antioxidant

Superoxide dismutase (SOD), Catalase (CAT), Glutathione (GSH) reductase and Malondialdehyde (MDA) were quantified using Marklund and Marklund (1974); Aebi (1984); Sedlak and Lindsay, (1968) and Ohkawa *et al.* (1979) methods respectively.

3.14 Antacid activity

3.14.1 Preparation of samples

The 50 mg and 100 mg of crude extracts and partitioned fractions (*n* hexane, DCM, EtOAc, *n* Butanol, and Aqueous) each were weighed and dissolved in 5 mL methanol and each made up to 250 mL with distilled water (Sandhya *et al*., 2012).

3.14.2 Preparation of artificial gastric juice

Pepsin enzymes (3.2 mg) and NaCl (2 g) were dissolved in 500 mL of water. To this mixture, hydrochloric acid (7.0 mL) and adequate water were added to make a 1000 mL solution of the artificial gastric acid at pH 1.20 (Sandhya *et al*., 2012).

3.14.3 pH of extracts and fractions

The pH of extracts, fractions, and control were determined using a pH meter at temperature ranging from 25-37^{o}C. The pH values of the control solution were also determined.

3.14.4 Determination of the neutralising effects on artificial gastric acid

About 90 mL of test solution was added to 100 mL artificial gastric juices at pH 1.2. The neutralising effect was observed by determining the pH values (Sandhya *et al*., 2012).

3.14.5 *In vitro* titration Method of Fordtran's model for determination of neutralisation capacity

Test sample (90 mL) was put in a 250 mL beaker and heated to 37^{o}C and aeration was given to mimic peristaltic movements at 136 air bubbles per minute. The samples were then titrated to an endpoint of pH 3 with artificial gastric juice. The consumed volume (V) of artificial gastric juice was observed and noted. The total consumed hydrogen ion (m mol) was measured and calculated as 0.06309 x V (mL).

3.15 Urease Inhibition

The crude extracts and partitioned fractions (*n* hexane, DCM, EtOAc, *n* Butanol, and Aqueous) from *C. pilosa* and *S. jollyanum* were screened for urease inhibition. In 96-well plates, reaction mixtures containing 25 µL of enzyme (jack bean urease) solution and 55 µL of buffer containing 100 mM urea were incubated at 30°C with 5 µL of extract/compound (0.5 mM). Briefly, 45 µL of each phenol reagent (1% (w / v) phenol and 0.005% (w / v) sodium nitroprussside) and 70 µL of alkali reagent (0.5% (w / v) NaOH and 0.1% active chloride, NaOCl) were added to each well (Weatherburn, 1967). A microplate reader (Molecular Devices, Sunnyvale, CA, USA) was used to measure the increasing absorbance after 50 min at 630 nm. All reactions were performed in triplicate in a final volume of 200 µL. The results (change in absorbance per min) were processed using SoftMax Pro software Molecular Devices. The assay was performed at pH 6.8. Percentage inhibitions were measured from the formula 100 – (ODtestwell / ODcontrol) X 100 where OD = Optical Density. Acetohydroxamic acid was used as reference drug while methanol served as the control.

3.16.1 Solvent-solvent partition of *Curculigo pilosa* rhizome extract

The crude methanol extract (250 g) obtained from maceration of *C. pilosa* was further separated by solvent partitioning using the following procedure. The extract was divided into two (125 g each) and partitioning was carried out twice where 125 g of extract was dissolved in 1000 mL MeOH: H_2O (3:1) and poured into separating funnel. This was first partitioned with aliquots of *n*-hexane until exhausted, the resulting fractions were pooled. The mother liquor was re-extracted with aliquots of Dichloromethane until exhausted and pooled. The mother liquor was again re-extracted with aliquots volume of ethyl acetate until exhausted and also pooled. The mother liquor was finally re-extracted with aliquots volume of *n* butanol until exhausted and also pooled (Figure 3.4). All the fractions were concentrated on rotary evaporator and reserved for *in vitro* assays.

3.16.2 Solvent-solvent partition of *Sphenocentrum jollyanum* seed extract

The crude methanol extract (300 g) obtained from maceration of *S. jollyanum* was further separated by solvent partitioning using the following procedure. The extract was divided into two (150 g each) and partitioning was carried out twice where 150 g of extract was dissolved in 1000 mL MeOH: H_2O (3:1) and poured into separating funnel. This was first partitioned with aliquots of *n*-hexane until

exhausted, the resulting fractions were pooled. The mother liquor was re-extracted with aliquots of Dichloromethane until exhausted and pooled. The mother liquor was again re-extracted with aliquots volume of ethyl acetate until exhausted and also pooled. The mother liquor was finally re-extracted with aliquots volume of *n* butanol until exhausted and also pooled (Figure 3.5). All the fractions were concentrated on rotary evaporator and reserved for *in vitro* assays

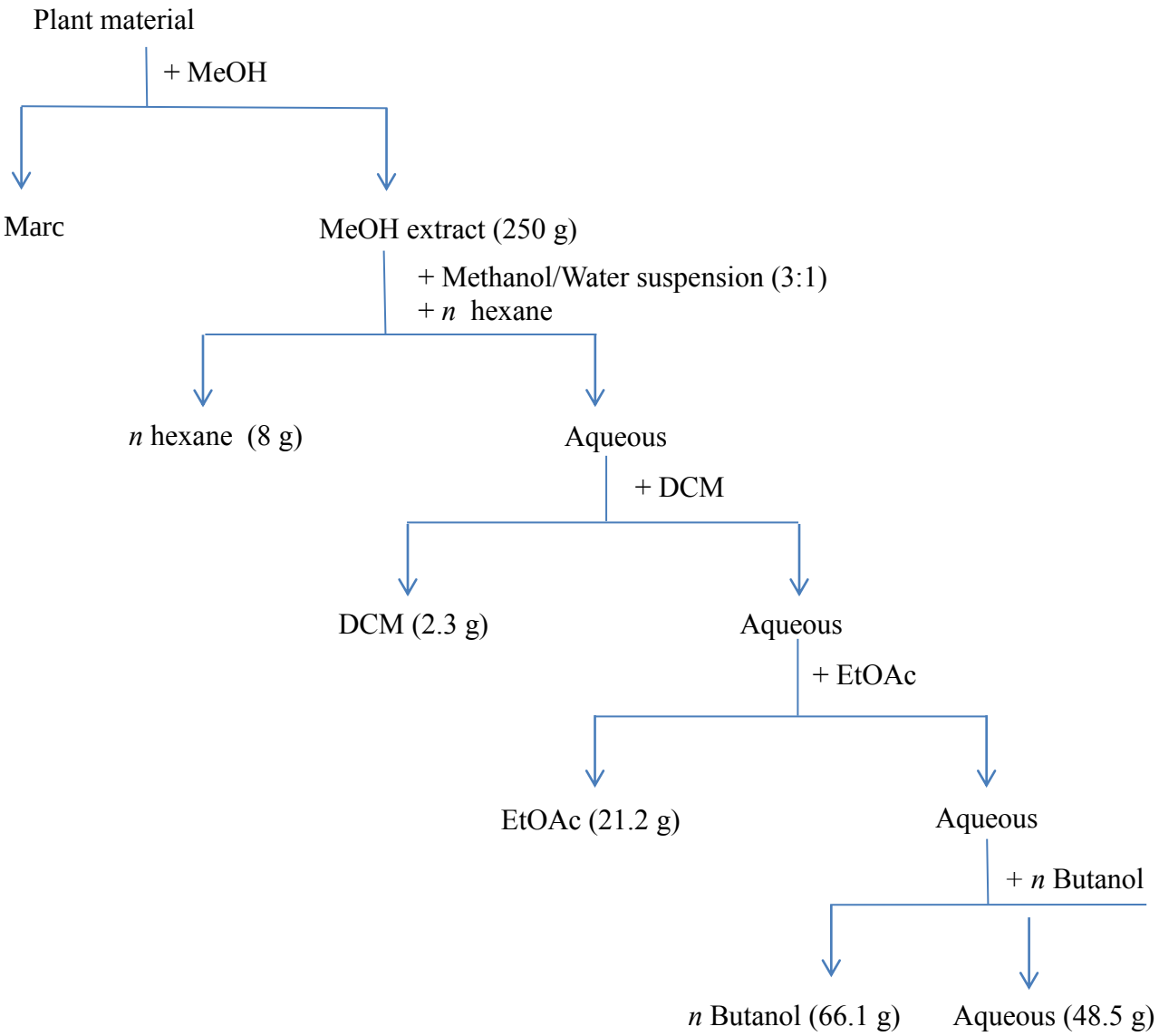

Figure 3.4: Solvent-solvent partitioning of *Curculigo pilosa* crude extract

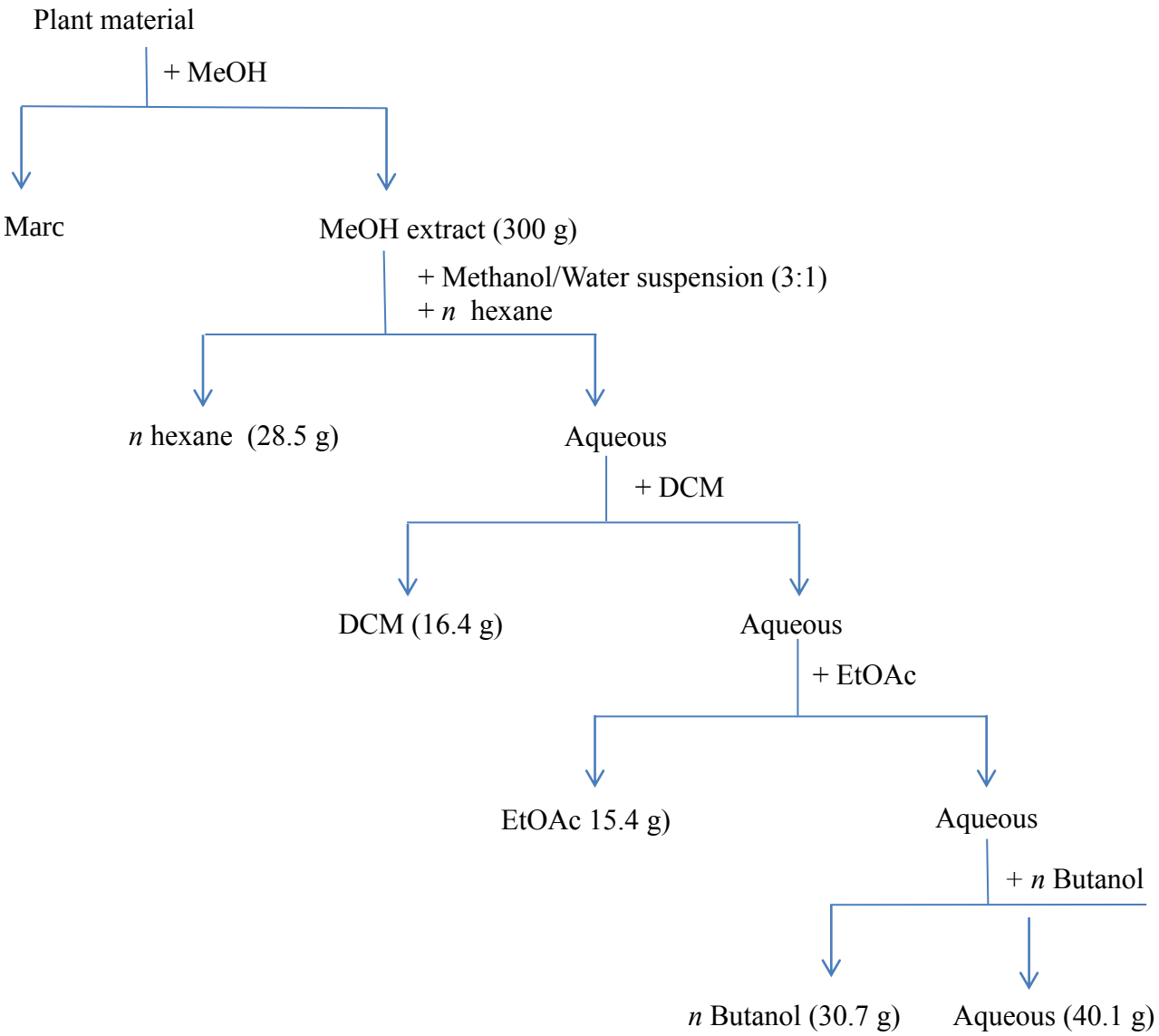

Figure 3.5: Solvent-solvent partitioning of *Sphenocentrum jollyanum* crude extract

3.17 Isolation of compounds from *Sphenocentrum jollyanum* EtOAc fraction

3.17.1 Column chromatography

The choice of ethyl acetate fraction of *Sphenocentrum jollyanum* for column chromatography was based on its antacid activity. The column chromatography was carried out on *S. jollyanum* ethyl acetate fraction using silica gel (Merck; Germany 70–230 mesh size) and successively eluted with increasing solvent polarities starting from *n* Hexane to DCM to MeOH. The columns used include: (Column 1: length 75 cm, internal diameter: 17 cm, column 2: length 76 cm, internal diameter 11 cm, column 3: length 77 cm, internal diameter 9.5 cm). A clean defatted cotton wool was placed into the bottom of the chromatographic column using a clean rod. A volume of *n* hexane, (500 mL) was poured into the chromatographic glass column (length = 75 cm Internal diameter = 17 cm). The tap was opened to allow the *n* hexane to flow through for some time and later closed. The sample (15 g) was pre-adsorbed in Silica gel and allowed to dry. Column grade silica gel 200-400 mesh (450 g) was mixed with small volume of hexane to form slurry and gently packed into the column that was already well plugged with cotton wool. The dried pre adsorbed sample was introduced into the column and the solvent mixtures of increasing polarity starting from *n* hexane (non-polar) to DCM (medium polar) to methanol (polar) was used for the elution. Two hundred and ninety fractions of 100 mL each were collected and spotted on thin layer chromatographic plates using appropriate solvent systems (*n* Hexane: EtOAc, DCM: MeOH, *n* Hexane: EtOAc: MeOH) with the flow rate of 2 drops per seconds. Similar fractions were pooled based on TLC profile to give twenty-eight sub-fractions and coded. Sub-fractions coded SJE-19-23, SJE-24-28 and SJE-12-16 were taken to micro column chromatography. Sub-fraction coded SJE-24-28 subjected to micro column chromatography with solvent systems *n* Hexane: DCM: MeOH afforded 110 fractions.

Sub-fraction 9-11 (2 g) was subjected to preparative Normal phase-high performance liquid chromatography using solvent mixtures of *n* Hexane: Ethyl acetate (70: 30) to afford two compounds: SJE-10B and SJE-10C at the retention times of 12 minutes and 24 minutes respectively. The flow rate was 3 mL/min with 3.0 mL injection volume and 254 nm detection wavelength. Sub-fraction 20-23 (1 g) was further purified using preparative TLC. The glass silica plate was developed in a solvent system *n* Hexane: Choroform: MeOH, in a ratio 5: 4: 1 to afford compound SJE-23D, while sub-fraction 24-28 (1.5 g) from micro column chromatography eluted SJE-28B as pure compound at 10% MeOH in DCM (Figure 3.6).

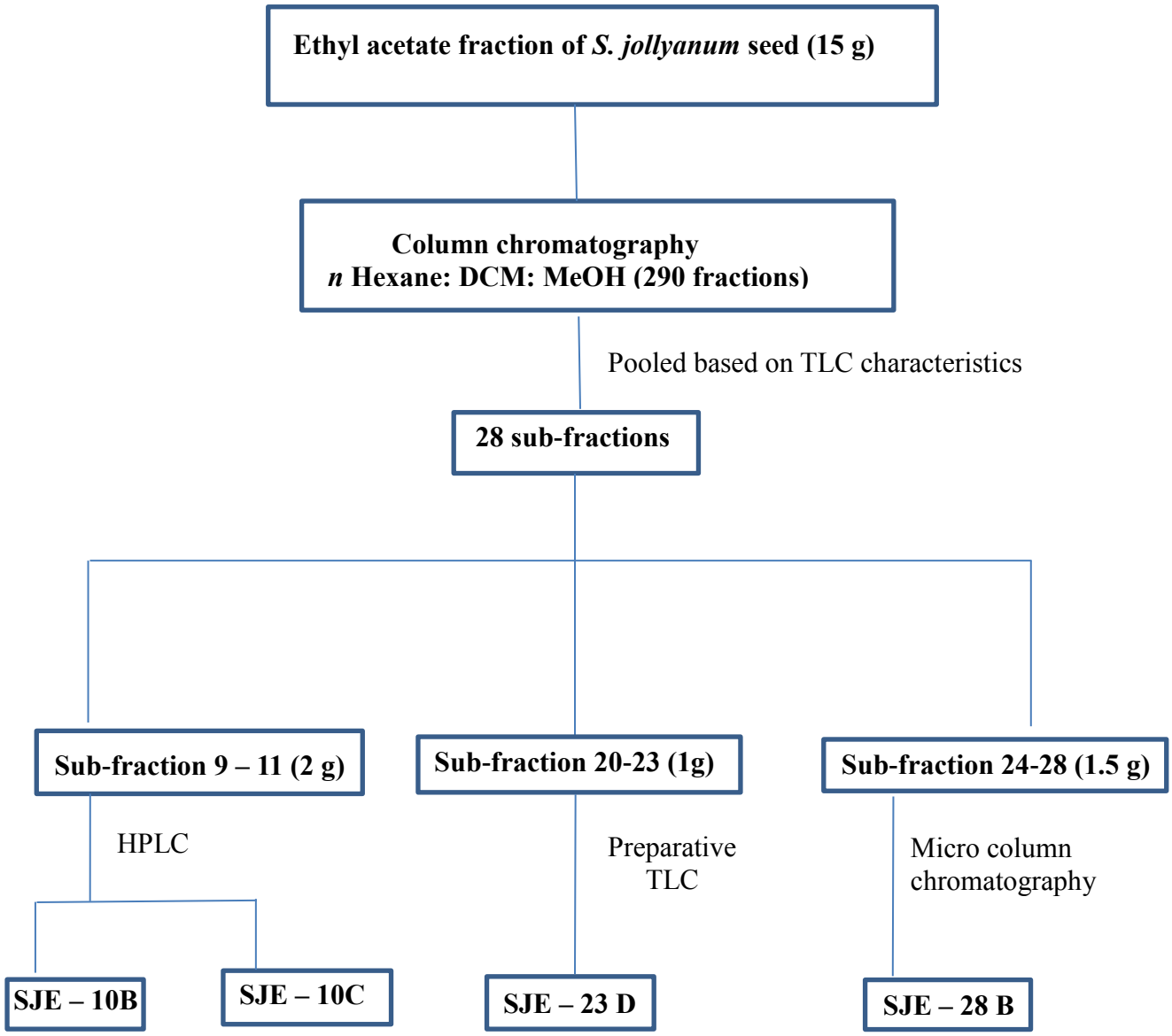

Figure 3.6: Isolation of compounds from ethyl acetate fraction of *S. jollyanum* seed

3.18 Isolation of compounds from *Curculigo pilosa* EtOAc fraction

3.18.1 Column chromatography

The choice of ethyl acetate fraction of *Curculigo pilosa* for column chromatography was also based on its antacid activity. The same procedure of column packing was done during isolation of *C. pilosa* ethyl acetate fraction. Chromatographic glass column (length = 75 cm Internal diameter = 17 cm) was used and sample (15 g) was pre-adsorbed on Silica gel and allowed to dry. Column grade silica gel 200 - 400 mesh (450 g) was mixed with small volume of *n* hexane to form slurry and gently packed into the column that was already well plugged with cotton wool. The dried pre adsorbed sample was introduced into the column and the solvent mixtures of increasing polarity starting from *n* hexane (non-polar) to DCM (medium polar) to methanol (polar) was used for the elution. One hundred and sixty-three fractions of 100 mL each were collected and spotted on thin layer chromatographic plates using appropriate solvent systems (*n* Hexane: DCM: MeOH, *n* Hexane: EtOAc) with the flow rate of 2 drops per seconds. Similar fractions were pooled based on TLC profile to give thirteen sub-fractions. Sub-fractions 10-12 (500 mg) and 43-46 (400 mg) were further purified using preparative RP-HPLC with solvent system of MeOH: H_2O (70: 30). The flow rate was 3 mL/min with 3.0 mL injection volume and 254 nm detection wavelength. This afforded CPE-10A (retention time of 30 minutes) and CPE-43A (retention time of 10 minutes), respectively (Figure 3.7).

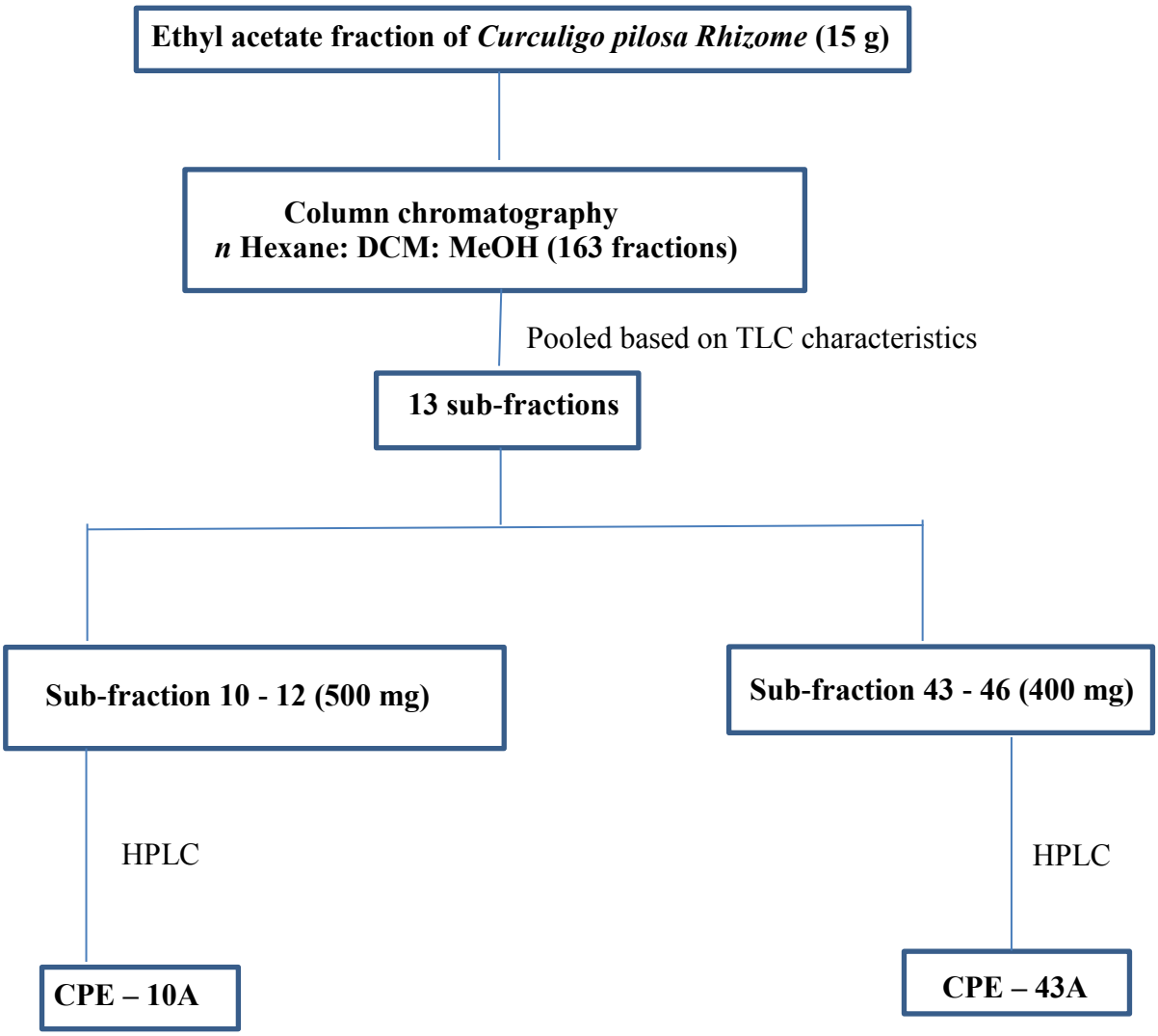

Figure 3.7: Isolation of compounds from ethyl acetate fraction of *C. pilosa* rhizomes

3.19 Isolation of compounds from *Sphenocentrum jollyanum n* butanol fraction

3.19.1 Column chromatography

The *n* butanol fraction of *S. jollyanum* was selected based on its urease inhibition. The same procedure of column packing was carried out where chromatographic glass column (length = 75 cm Internal diameter = 17 cm) was used and sample (15 g) was pre-adsorbed on silica gel and allowed to dry. Column grade silica gel 200 - 400 mesh (450 g) was packed with *n* Hexane and DCM (50: 50) to form slurry and gently packed into the column that was already well plugged with cotton wool. The dried pre-adsorbed sample was introduced into the column and the solvent mixtures of increasing polarity starting from *n* Hexane: DCM (30: 70) to EtOAc to 100% Methanol was used for the elution. The elution afforded 170 fractions of 100 mL each. All fractions were spotted on TLC plates (silica) using appropriate solvent systems (*n* Hexane: Chloroform: MeOH, *n* Hexane: EtOAc: MeOH) and comparable fractions were pooled based on TLC profile to give twenty-eight sub-fractions. The flow rate of the column was 2 drops per seconds Sub-fraction 12-15 (800 mg) was subjected to preparative RP-HPLC using Methanol: Water (70: 30) as solvent systems. The flow rate was 3 mL/min with 3.0 mL injection volume and 254 nm detection wavelength. This afforded two compounds; SJB-12 and SJB-12B at the retention times of 12 minutes and 16 minutes respectively. Sub-fraction 26-28 (500 mg) was also separated from its impurities and probably other constituents using semi-preparative RP-HPLC using Methanol: Water (70: 30) as solvent systems. The flow rate was 3 mL/min with 3.0 mL injection volume and 254 nm detection wavelength. This afforded compound SJB-26A with a retention time of 12 minutes (Figure 3.8).

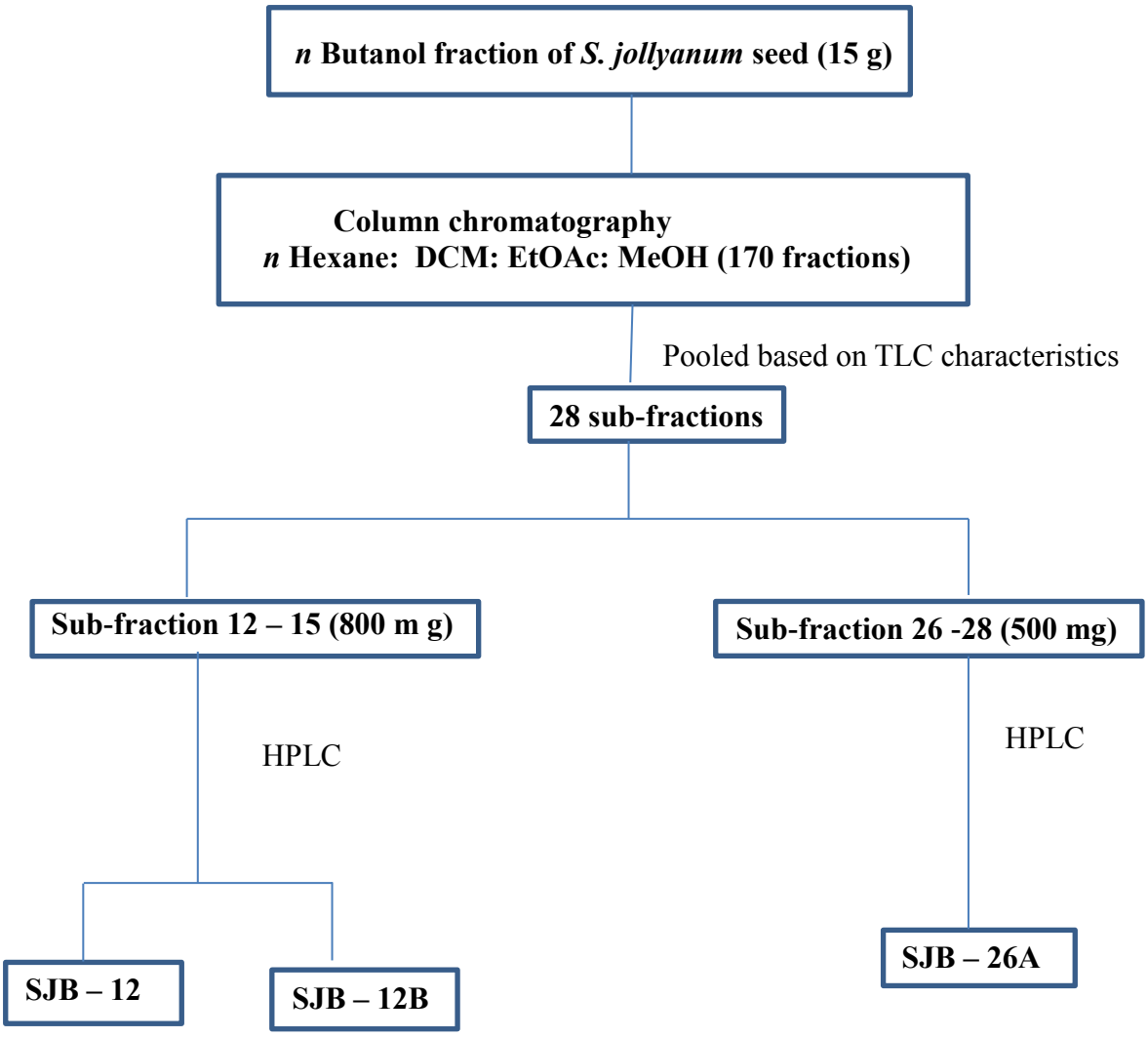

Figure 3.8: Isolation of compounds from *n* butanol fraction of *S. jollyanum* seed

3.20 Isolation of compounds from *Sphenocentrum jollyanum n* Hexane fraction

3.20.1 Column chromatography

The selection of *Sphenocentrum jollyanum*'s *n* Hexane fraction for column chromatography was based on its urease inhibition. Similar procedure of column packing was done during isolation of *S. jollyanum n* hexane fraction. Chromatographic glass column (length = 75 cm Internal diameter = 17 cm) was used and sample (15 g) was pre-adsorbed in Silica gel and allowed to dry. Column grade silica gel 200 – 400 mesh (450 g) was packed with small volume of *n* Hexane to form slurry and gently packed into the column that was already well plugged with cotton wool. The dried pre adsorbed sample was loaded into the column and the solvent mixtures of increasing polarity starting from *n* Hexane 100% to EtOAc: MeOH: 90: 10 was used for the elution. Seventy-two fractions of 100 mL each were collected with the flow rate of 2 drops per seconds. All fractions were spotted using suitable solvent systems (*n* Hexane: EtOAc) on thin layer chromatographic plates (silica) and similar fractions were pooled to give nine sub-fractions based on the TLC profile. Sub-fraction 28 (900 mg) was purified using preparative Normal phase HPLC with solvent mixtures of *n* Hexane: Ethyl acetate (70: 30). The flow rate was 3 mL/min with 3.0 mL injection volume and 254 nm detection wavelength. This yielded pure compounds coded SJH-28A and SJH-28B at the retention times of 50 minutes and 72 minutes respectively. Sub-fraction 34 (500 mg) was also purified by using preparative Normal phase HPLC (solvent mixtures: *n* Hexane: Ethyl acetate (70: 30); flow rate: 3 mL/min; injection volume: 3.0 mL; detection wavelength: 254 nm) to yield pure compound coded SJH-34B at the retention time of 30 minutes (Figure 3.9).

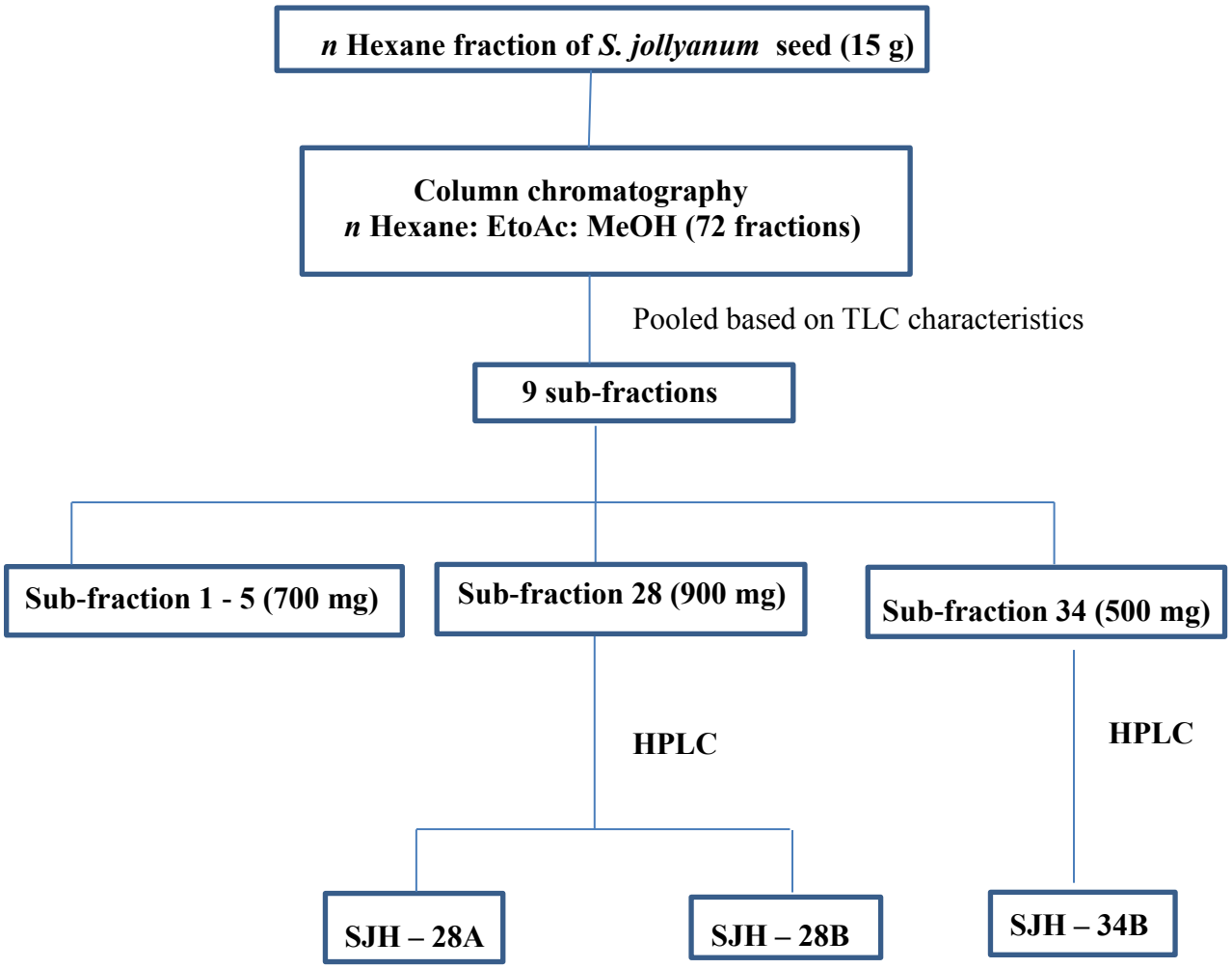

Figure 3.9: Isolation of compounds from *n* Hexane fraction of *S. jollyanum* seed

3.21 Semi-preparative high performance liquid chromatography

Semi-preparative HPLC was carried out using an Agilent 1100 fluid chromatograph Model LC – 908W – 060 (Figure 3.10) equipped with a Phenomena Luna 5μ C18(2) 100 A column (250 mm 20 mm, 4 μm). The mobile phases were determined by Thin Layer Chromatography and analytical HPLC using solvent mixtures of *n* Hexane: Ethyl acetate (70: 30) for normal phase and Methanol: Water (70: 30) for reversed phase. The flow rate was 3 mL/min with 3.0 mL injection volume and 254 nm detection wavelength.

3.22 Identification of isolated compounds using NMR, EI-MS, FAB-MS, FT-IR and UV-VIS spectroscropies

The isolated compounds from *Curculigo pilosa* ethyl acetate fraction were structurally identified using ESI-HR and 1-D NMR spectroscopies. Compounds from *Sphenocentrum jollyanum n* Hexane, EtOAc, and *n* Butanol fractions were structurally identified using Nuclear Magnetic Resonance (NMR), EI-MS, FAB-MS, FT-IR and UV-VIS Spectroscopies. The NMR spectra were recorded in deuterated solvents such as $CDCl_3$, CD_3OD, and C_5D_5N with internal standard of TMS at different frequencies such as: 300, 400, 500 and 600 MHz on Bruker Avance-400, Avance-500, Avance-600, Avance-800 instruments and 500 MHz for ^{1}H-NMR and 100, 125, 150 and 200 MHz for ^{13}C-NMR respectively. Compounds SJE-10B, SJE-10C, SJE-23D, SJE-28B, CPE-10A and CPE-43A were dissolved with methanol (CD_3OD). Compounds SJB-12, SJB-12B and SJB-26A were dissolved in pyridine (C_5D_5N), while Compounds SJH-28A, SJH-28B and SJH-34B were dissolved in chloroform ($CDCl_3$). The choice of solvent was based on absolute dissolution of compound in it. The chemical shift (δ) was expressed in parts per million (ppm). The JEOL JMS-600H mass spectrometer was used to obtain the EI-MS and FAB-MS. The IR spectra were obtained on a Shimadzu 8900 FTIR spectrophotometer using KBr pellet sample preparation method. A Buchi-535 melting unit was used to perform the IR melting point. The UV spectra were obtained on the spectrophotometer of Hitachi U-3200.

3.23 Statistical analysis

Data were expressed as Mean ± SEM, analysed using one-way ANOVA and Dunnet multiple comparison test. Statistical difference was significant at $p=0.05$.

CHAPTER FOUR

4.0 RESULTS

4.1 Ethnobotanical survey

4.1.1 Demographic data

The ethnomedicines used to treat gastric ulcer in southwestern Nigeria were documented. Five local government areas (LGAs) were visited; Ibadan South/West, Akinyele, Oluyole, Ibadan North East, and Egbeda LGAs. Seventy-two respondents participated in the survey and were not secretive about their knowledge on the medicinal properties of the plant species. The responses were encouraging throughout the survey. The types of respondents include Herb sellers (72.3%), TMPs (16.6%), and 11.1% elderly (Figure 4.1.1). Women were the majority of the participants (69.4%) while the remaining 30.6% constitute the men (Figure 4.1.2). Their ages were between 25 and 70 years with age group 41-60 having the highest percentage of 50% (Figure 4.1.3). All respondents were Nigerians from the Yoruba ethnic group with 23.7% practicing Christianity, 34.7% practicing traditional religion, and 41.6% practicing Islamic religion (Figure 4.1.4).

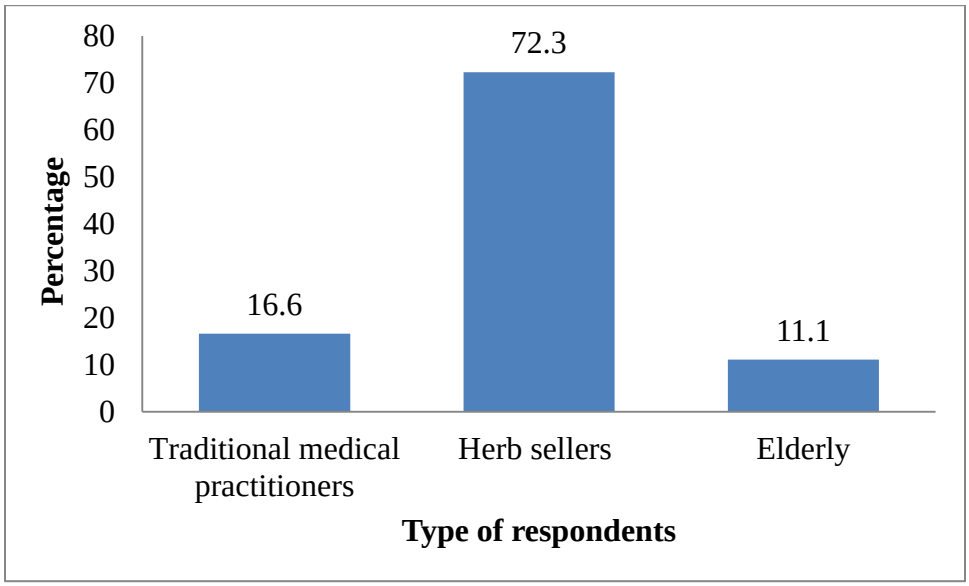

Figure 4.1.1: Type of respondents (%)

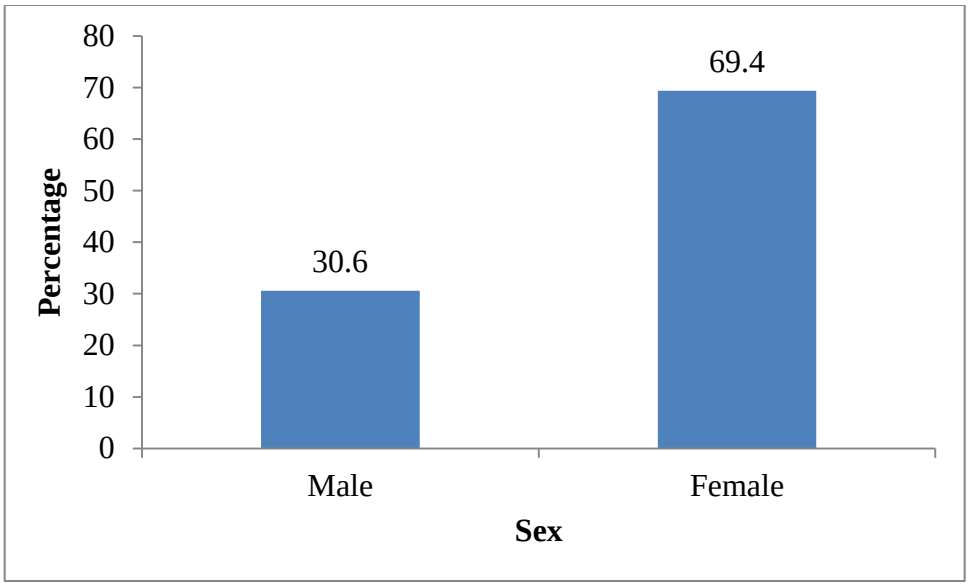

Figure 4.1.2: Sex of respondents (%)

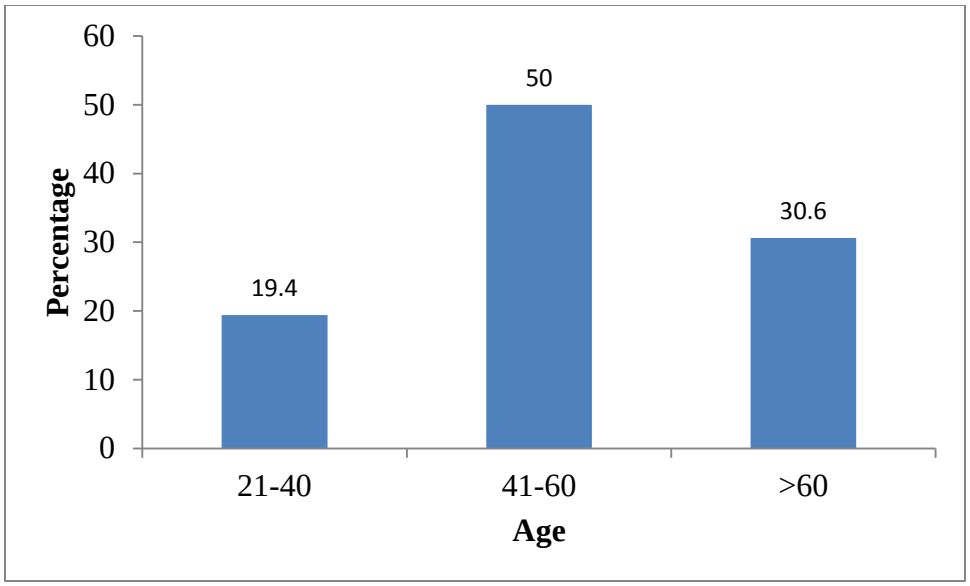

Figure 4.1.3: Age of Respondents (%)

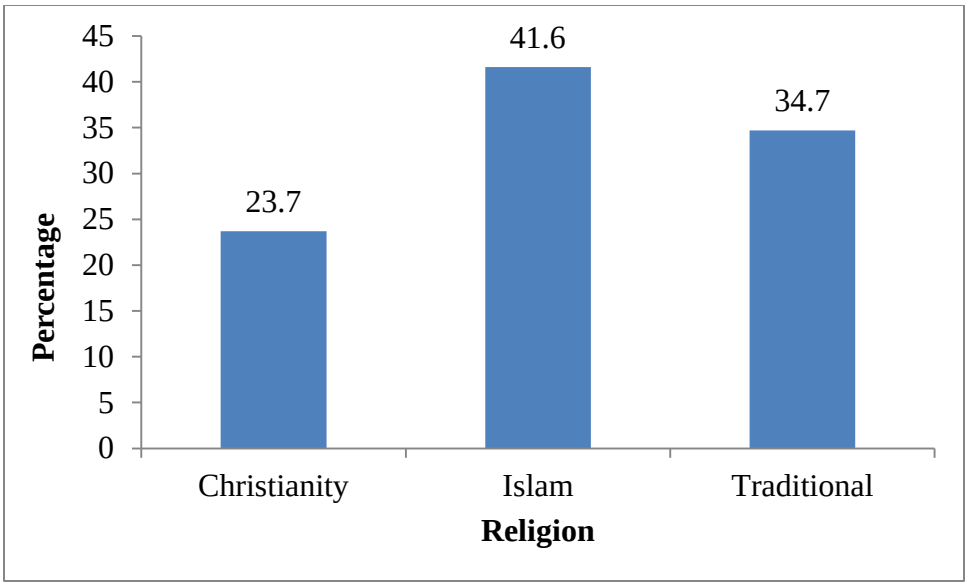

Figure 4.1.4: Religion of respondents (%)

4.1.2 Plant information and their families

Ninety-two plant species belonging to seventy-eight genera and forty-five different families were identified (Table 4.1.2.1) having their local names, parts used, occurrence frequency and fidelity level. Apocynaceae, Fabaceae, and Loranthaceae and Lamiaceae recorded the highest number of species with ten, seven, and six species respectively. Other plant families include Lamiaceae, Compositae and Moraceae with four species each. Many of these plant species are also used for wound healing and diabetes. There is regular supply of the plant remedies from the forest as confirmed by most respondents. The respondents revealed that knowledge of herbal treatment was mostly inherited while few of them were trained. Some of the mentioned plants include *Alstonia boonei* (L.) R. Br., *Artocarpus integrifolius* L. F. , *Ageratum conyzoides* L., *Aloe barbadensis* Miller, *Artocarpus altilis* (Parkinson ex F. A. Zonn), *Aspilia africana* (Persoon) C.D. Adams, *Bacopa monnieri* (L.) Pennell, *Benincasa hispida* (Thunb.) Cogn., *Carica papaya* L., *Ceiba pentandra* (L.) Gaertn., *Centella asiatica* (L.) Urb., *Clitandra cymulosa* Benth., *Citrus aurantium* L. among others (Table 4.1.2.1). Many of these plants are obtained from the forest, while few are collected in the garden around the house.

Table 4.1.2.1: Medicinal plants used for the treatment of gastric ulcer

S/N	Botanical names	Family	Local names	Part(s) used	Frequency of Occurrence	Fidelity Level (%)
1	*Ageratum conyzoides* L.	Compositae	Imi-esu	Leaf	4	5.6
2	*Aloe barbadensis* Miller	Asphodelaceae	Eti-erin	Root	5	6.9
3	*Aloe barteri* L.	Asphodelaceae	Eti-erin	Leaf	5	6.9
4	*Alstonia congensis* Engl.	Apocynaceae	Ahun	Whole plant	6	8.3
5	*Ananas comosus* (L.) Merr.	Bromeliaceae	Penapu ibile	Fruit	1	1.4
6	*Artocarpus altilis* (Parkinson ex F. A. Zonn) Fosberg	Moraceae	Berefuutu	Leaf	2	2.8
7	*Artocarpus integrifolius* L. F.	Moraceae	Tapoun	Root	2	2.8
8	*Asparagus racemosus* Willd.	Asparagaceae	Aluki	Root	4	5.6
9	*Aspilia africana* (Persoon) C.D. Adams	Compositae	Yonyon-agbute	Leaf	1	1.4
10	*Bacopa monnieri* (L.) Pennell	Plantaginaceae	Awenu	Fruit	1	1.4
11	*Benincasa hispida* (Thunb.) Cogn.	Cucurbitaceae	Abua	Fruit	1	1.4
12	*Kalanchoe pinnata* (Lam.) Pers.	Crassulaceae	Abamoda	Leaf	1	1.4
13	*Byrsocarpus coccineus* Thonn. ex Schumach.	Connaraceae	Amuje	Stem bark	3	4.2
14	*Carica papaya* L.	Caricaceae	Ibepe	Seed, fruit	5	6.9
15	*Ceiba pentandra* (L.) Gaertn.	Bombacaceae	Araba	Leaf	5	6.9
16	*Centella asiatica* (L.) Urb.	Apiaceae	Tutugbo	Fruit	1	1.4
17	*Clitandra cymulosa* Benth.	Mimosaceae	Aagba	Root	1	1.4
18	*Citrus aurantium* L.	Rutaceae	Jaganyin	Leaf	4	5.6
19	*Citrus medica* L.	Rutaceae	Osan wewe	Leaf, Root	6	8.3
20	*Citrus sinensis* (L.) Osbeck	Rutaceae	Jaganyin	Leaf, Root	6	8.3

Table 4.1.2.1 contd.

S/N	Botanical names	Family	Local names	Part(s) used	Frequency of Occurrence	Fidelity Level (%)
21	*Clitandra orientalis* K. Schum.	Apocynaceae	Aagba	Root	4	5.6
22	*Clitandra togolana* (Hall. f) Stapf.	Apocynaceae	Aagba	Root	3	4.2
23	*Cocos nucifera* L.	Arecaceae		Fruit	2	2.8
24	*Cruda klainei* Pierre ex De Wild.	Caesalpinaceae	Afomo	Leaf	6	8.3
25	*Curculigo pilosa* (Schumach. & Thonn.) Engl.	Hypoxidaceae	Epakun	Seed	25	34.7
26	*Dalbergia lactea* Vatke.	Fabaceae	Ojiji	Root	8	11.1
27	*Desmodium gangeticum* (L.) DC.	Fabaceae	Emo	Root	12	16.7
28	*Detarium microcarpum* Guill. & Perr.	Fabaceae	Arira	Stem bark	12	16.7
29	*Phyllanthus emblica* L.	Phyllanthaceae	Ojiji	Leaf	8	11.1
30	*Englerina gabonensis* (Engl.) Balle	Loranthaceae	Afomo	Leaf	12	16.7
31	*Englerina lecardii* (Engl.) Balle	Loranthaceae	Afomo	Leaf	9	12.5
32	*Entada gigas* L.	Fabaceae	Aagba	Root	28	38.9
33	*Euadenia trifoliolata* (Schumach. &Thonn.) Oliv.	Capparaceae	Logbokiya	Leaf	26	36.1
34	*Ficus arnottiana* (Miq.) Miq	Moraceae	Obata	Fruit	7	9.7
35	*Ficus exasperata* Vahl	Moraceae	Ipin	Root	7	9.7
36	*Floscopa africana* (P. Beauv.) C.B. Clarke	Commelinaceae	Toronini	Root	11	15.3
37	*Fluerya aestuans* (L.) Gaudich	Urticaceae	Iranje	Leaf	12	16.7
38	*Garcinia cambogia* L.	Cluciaceae	Okuta	Fruit	10	13.9
39	*Globimetula braunii* (Engl.) Danser	Loranthaceae	Afomo	Leaf	12	16.7
40	*Hedranthera barteri* (Hook. F.) Pichon	Apocynaceae	Oko aja	Root	6	8.3

Table 4.1.2.1 contd.

S/N	Botanical names	Family	Local names	Part(s) used	Frequency of Occurrence	Fidelity Level (%)
41	*Hemidesmus indicus* (L.) R. Br.	Apocynaceae	Ogbe akuko	Root, leaf	7	9.7
42	*Hoslundia opposita* Vahl	Lamiaceae	Efinrin odan	Leaf	9	12.5
43	*Hunteria umbellata* (K. Schum.) Hallier f.	Apocynaceae	Erin	Root	12	16.7
44	*Khaya ivorensis* A. Chev.	Meliaceae	Ogano	Stem bark	28	38.9
45	*Kielmeyera coriaceae* Mart. & Zucc.	Calophyllaceae	Emo	Stem bark	9	12.5
46	*Kigelia africana* (Lam.) Benth.	Bignoniaceae	Pandoro	Root, stem bark, fruit	26	36.1
47	*Lagenaria siceraria* (Molina) Standl.	Cucurbitaceae	Igba	Stem bark	3	4.2
48	*Lonchocarpus cyanescens* (Schumach. & Thonn.) Benth.	Fabaceae	Elu	Leaf	22	30.6
49	*Macaranga barteri* Mull. Arg.	Euphorbiaceae	Agbaasa	Root	10	13.9
50	*Markhamia tomentosa* (Benth.) K. Schum. ex Engl.	Bignoniaceae	Oruru	Root, Bark	9	12.5
51	*Microdesmis puberula* Hook. F. ex Planch.	Pandaceae	Aringo	Leaf	12	6.7
52	*Morinda citrifolia* L.	Rubiaceae	Oruwo	Fruit, Root	18	25.0
53	*Motandra guineensis* (Thonn.) A.D.C.	Apocynaceae	Aagba	Root	21	29.2
54	*Musa paradisiaca* L.	Musaceae	Ogede agbagba	Fruit	23	31.9
55	*Musa sapientum* L.	Musaceae	Omini	Fruit	21	29.2
56	*Ocimum basilicum* L.	Lamiaceae	Efinrin aja	Leaf	18	25
57	*Ocimum sanctum* L.	Lamiaceae	Efinrin aja	All parts	16	22.2
58	*Oxytenanthera abyssinica* (A. Rich.) Munro	Poaceae	Aparun	Root	13	18.1
59	*Parkia biglobosa* (Jacque) R. Br. ex G. Don	Fabaceae	Igba	Stem bark	22	30.6
60	*Parquetina nigrescens* (Afzel.) Bullock	Apocynaceae	Ogbo	Root, Leaf	18	25

Table 4.1.2.1 contd.

S/N	Botanical names	Family	Local names	Part(s) used	Frequency of Occurrence	Fidelity Level (%)
61	*Peperomia pellucida* (L.) Kunth	Piperaceae	Erin	Root	12	16.7
62	*Persea americana* Mill.	Lauraceae	Oguro	Leaf	12	16.7
63	*Phragmanthera capitata* (Sprengel) S. Balle	Loranthaceae	Afomo	Leaf	5	6.9
64	*Phragmanthera kamerunensis* (Engl.) Balle	Loranthaceae	Afomo	Leaf	7	9.7
65	*Picralima nitida* (Stapf) T. Durand & H Durand	Apocynaceae	Erin	Root	9	12.5
66	*Piper guineense* Schumach. & Thonn.	Piperaceae	Iyere	Root	11	15.3
67	*Piper nigrum* L.	Piperaceae	Iyere	Fruit	12	16.7
68	*Plectranthus amboinicus* (Lour.) Spreng	Lamiaceae	Aringo	Whole plant	6	8.3
69	*Plumbago zeylanica* L.	Plumbaginaceae	Inabiri	Root	7	9.7
70	*Pseudocedrela kotschyi* (Schweinf.) Harms	Meliaceae	Emigbegiri	Stem bark	29	40.3
71	*Pycnanthus cingolensis* (Welw.) Warb.	Myristicaceae	Akomu	Stem bark	12	16.7
72	*Pyrus communis* L.	Rosaceae		Leaf	5	6.9
73	*Rauvolfia vomitoria* Afzel.	Apocynaceae	Asofeyeje	Root, leaf	4	5.6
74	*Ricinodendron heudelotii* (Baill.) Heckel	Euphorbiaceae	Erinmodo	Stem bark	7	9.7
75	*Ritchiea capparoides* (Andrews) Britten	Capparaceae	Capparaceae	Leaf	6	8.3
76	*Sarcocephalus latifolius* (Sm.). E. A. Bruce	Rubiaceae	Egbesi	Stem bark, root	5	6.9
77	*Securidaca longepedunculata* Fres.	Polygalaceae	Ipeta	Root	14	19.4
78	*Spathodea campanulata* Beauv.	Bignoniaceae	Ruuru	Root, stem bark	3	4.2
79	*Spondias mombin* L.	Anacardiaceae	Iyeye	Stem bark	14	9.4
80	*Sphenocentrum jollyanum* Pierre	Menispermaceae	Akerejupon	Root, fruit	30	41.7

Table 4.1.2.1 contd.

S/N	Botanical names	Family	Local names	Part(s) used	Frequency of Occurrence	Fidelity level (%)
81	*Staudtia stipitata* Warb.	Myristicaceae	Amuje	Stem bark	4	5.6
82	*Talinum triangulare* (Jacq.) Willd	Talinaceae	Gbure	Leaf	8	11.1
83	*Tapinanthus buntingii* (Sprague) Danser	Loranthaceae	Afomo	Leaf	7	9.7
84	*Terminalia pallida* Brandis	Combretaceae	Idi	Whole plant	14	19.4
85	*Terminalia superba* Engl. & Diels	Combretaceae	Afara	Stem bark	12	16.7
86	*Urena lobata* L.	Malvaceae	Efore loka	Leaf	15	20.8
87	*Uvaria afzelii* Sc. Elliot	Annonaceae	Gbogbonise	Root	30	41.7
88	*Uvaria chamae* P. Beauv	Annonaceae	Eruju	Root	30	41.7
89	*Vernonia amygdalina* Delile	Compositae	Ewuro jije	Root	18	25
90	*Vernonia odoensis* Delile	Compositae	Ewuro oko	Root	12	16.7
91	*Vitellaria paradoxa* C.F Gaertn.	Sapotaceae	Emiyemi	Stem bark	16	22.2
92	*Zingiber officinale* Rosc.	Zingerberaceae	Atale	Leaf	14	19.4

The ethnobotanical survey result showed that majority of the plant families have prospects for drug development. The prominent plant families include Apocynaceae with 28.5% species, Fabaceae with 20% species, Loranthaceae with 17.1% species and Lamiaceae with 11.4% species (Figure 4.1.2.1). The high occurrence of family Apocynaceae in the list showed that the plant family may contain useful species that can be further explored as sources of anti-ulcer drugs. The plants' roots are mostly used for treating gastric ulcer (37%), followed by the leaf (30%). The plants' seeds are least used (Figure 4.1.2.2).

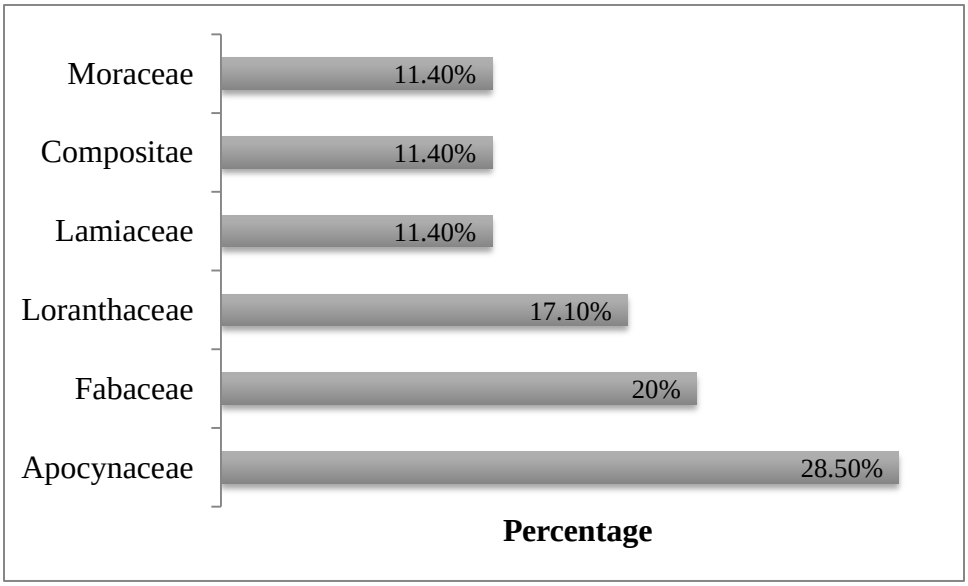

Figure 4.1.2.1: Prominent plant families of medicinal plants used in treating gastric ulcer (%).

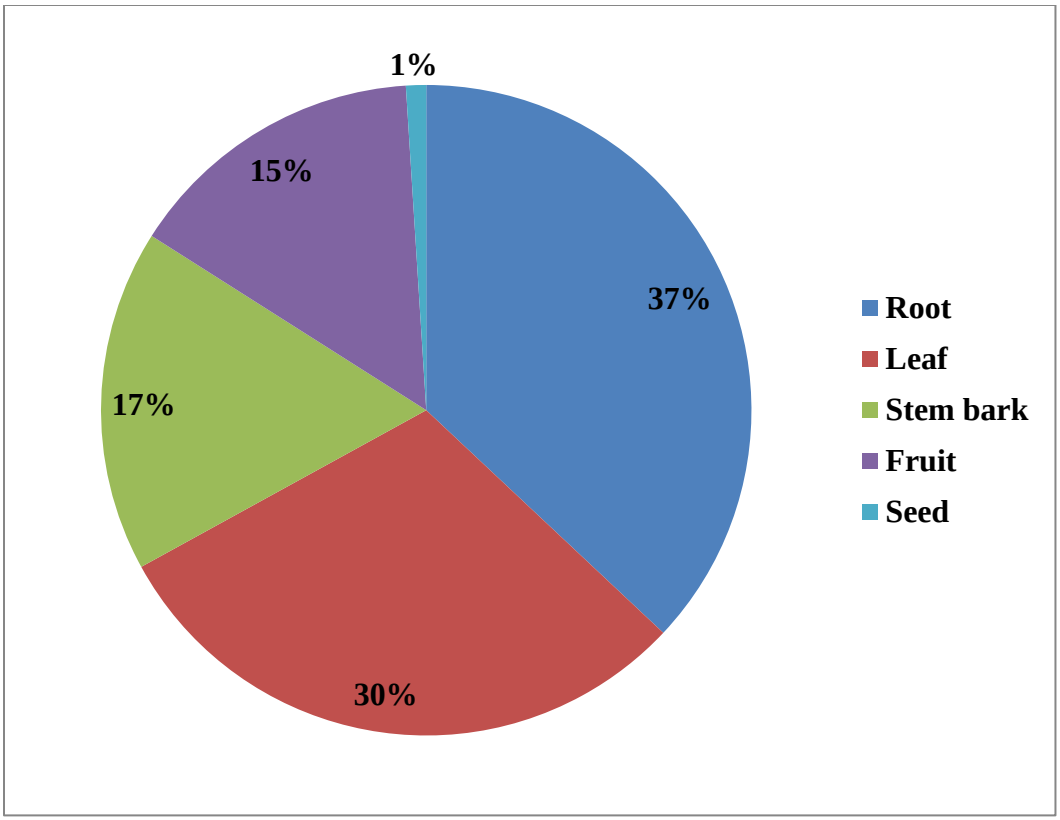

Figure 4.1.2.2: Plant parts used in the treatment of gastric Ulcer (%)

The results also revealed that most respondents are acquainted with the use of certain species such as *Curculigo pilosa, Entada gigas, Euadenia trifoliolata, Kigelia africana, Sphenocentrum jollyanum, Uvaria chamae,* and *Vitellaria paradoxa* in the treatment of gastric ulcer. This was inferred from the frequency of occurrence and fidelity level of the plant species. Fourteen plants were selected based on the use mention index for preliminary *in vitro* screening (Table 4.1.2.2).

Table 4.1.2.2: List of collected plants for preliminary screening

S/N	Botanical name	Family	Part (s)	Local name
1	*Ageratum conyzoides* L.	Compositae	Leaf	Imi-esu
2	*Alstonia congensis* Engl.	Apocynaceae	Whole plant	Ahun
3	*Curculigo pilosa* (Schumach. & Thonn.) Engl.	Hypoxidaceae	Rhizome	Epa-ikun
4	*Entada gigas* Gaertn	Fabaceae	Root	Aagba
5	*Euadenia trifoliolata* (Schumach. &Thonn.) Oliv.	Capparaceae	Leaf	Logbokiya
6	*Khaya ivorensis* A. Chev.	Meliaceae	Stem bark	Oganwo
7	*Kigelia africana* (Lam.) Benth.	Bignoniaceae	stem bark	Pandoro
8	*Philenoptera cyanescens cyanescens* Benth	Fabaceae	Leaf	Elu
9	*Pseudocedrella kotschyi* (Schweinf.) Harms	Meliaceae	Stem bark	Emigbegiri
10	*Sphenocentrum jollyanum* Pierre	Menispermaceae	Root, seed	Akerejupon
11	*Uvaria afzelii* Sc. Elliot	Annonaceae	Root	Gbogbonise
12	*Uvaria chamae* P. Beauv	Annonaceae	Root	Eruju
13	*Vitellaria paradoxa* C.F. Gaertn	Sapotaceae	Stem bark	Emiyemi
14	*Vernonia amygdalina* Delile	Compositae	Leaf	Ewuro jije

4.1.3 Method of preparation

The medicinal plants surveyed can be prepared either by using freshly collected samples from the forest or from dry plants from markets or households. Though, the respondents confirmed that the use of fresh samples and dry plants are both effective in the preparation except in few cases where fresh samples are chosen. Decoction in 100% water (boiling in water) method is mostly used for preparation of herbal remedies while infusion (in 100% water) and concoction are less used. There is variation in the time required for boiling which depends on plant parts or standardisation. The preparation must be taken orally 100% in all cases.

4.1.4 Enumeration of Species

Some plants were reported to be prepared as concoction;

1. *Citrus medica* leaves and roots, *Citrus sinensis* leaves and roots, *Citrus medica* var. *acida* leaves and roots are prepared together in water as concoction.
2. The fruit and root of *Sphenocentrum jollyanum* should be pulverised and swallowed with pap or water.
3. The root of *Vernonia amygdalina* should be cooked in water (decoction) and allowed to cool before drinking.
4. *Ananas comosus* fruit, *Uvaria afzelii* root and stem bark of *Parkia biglobosa* are mixed with honey and raw egg, boiled together with water and taken orally on a daily basis.
5. Stem bark of *Vitellaria paradoxa*, *Khaya ivorensis*, and *Pseudocederella kotchyii* fruits and roots of *Morinda citrifolia*, roots and fruits of *Sphenocentrum jollyanum*, stem barks of *Detarium microcarpum*, *Staudtia stipitata*, *Kigelia africana*, and *Sarcocephalus latifolius* are used in combination when boiled with water.
6. Stem barks of *Peperoma pellucida* and *Picralima nitida* are also cooked with water and taken orally, the patients are advised to take less salt and avoid peppery food during usage.

4.2 Identification and authentication of most mentioned plants

The voucher specimens of the most mentioned plants with their respective FHI numbers are presented in Table 4.2.1.

4.3 Percentage yield of samples

The percentage yield of screened samples showed that *Vernonia amygdalina* leaf extract and *Uvaria afzelii* root extract gave the highest yield of 14.3% and 13.5% respectively (Table 4.3.1). The yields obtained from methanol extraction of *C. pilosa* and *S. jollyanum* plants were 11.3% and 14.3% respectively (Table 4.3.2). The *n* Butanol and aqueous fractions of *C. pilosa* gave the highest percentage yield of 26.4% and 19.4% respectively (Table 4.3.3). *Vernonia amygdalina* leaf and *Uvaria afzelii* root gave high percentage yields of 14.3% and 13.5% respectively.

Table 4.2.1: Authentication of most mentioned Plants

Plant Samples	Voucher Specimen no.
Curculigo pilosa	FHI 109816
Entada gigas	FHI 110507
Euadenia trifoliolata	FHI 110522
Kigelia africana	FHI 110520
Sphenocentrum jollyanum	FHI 110510
Uvaria chamae	FHI 110508
Vitellaria paradoxa	FHI 109816

Table 4.3.1: Percentage yield of screened samples

Plant Sample	Weight of Extract (g)	Percentage Yield (%)
Ageratum conyzoides leaf	11.5	3.8
Alstonia congensis stem bark	6.7	0.2
Alstonia congensis root	2.3	0.8
Curculugo pilosa seed	17.7	5.9
Entada gigas leaf	2.3	0.8
Entada gigas root	1.4	0.5
Euadenia trifoliolata leaf	15.7	5.2
Khaya ivorensis stem bark	4.4	1.5
Kigelia africana stem bark	5.1	1.7
Lonchocarpus cyanescens leaf	16.4	5.5
Pseudocedrella kotschyii stem bark	7.1	2.4
Sphenocentrum jollyanum seed	5.7	1.9
Sphenocentrum jollyanum root	4.9	1.6
Uvaria afzelii root	40.5	13.5
Uvaria chamae root	11.5	3.8
Vernonia amygdalina leaf	42.8	14.3
Vitellaria paradoxa stem bark	12.8	4.3

Table 4.3.2: Percentage yield of *Curculigo pilosa* and *Sphenocentrum jollyanum* crude extracts

Extract	Weight (g)	Percentage Yield (%)
C. pilosa	282.0	11.3
S. jollyanum	358.4	14.3

Table 4.3.3: Percentage yield of *Curculigo pilosa* and *Sphenocentrum jollyanum* partitioned fractions

Fraction	Weight (g)	Percentage Yield (%)
C. pilosa n hexane	8.0	3.2
C. pilosa Dichloromethane	2.3	0.9
C. pilosa Ethyl acetate	21.2	8.5
C. pilosa n Butanol	66.1	26.4
C. pilosa Aqueous	48.5	19.4
S. jollyanum n Hexane	28.5	9.5
S. jollyanum Dicloromethane	16.4	5.5
S. jollyanum Ethyl acetate	15.4	5.1
S. jollyanum n Butanol	30.7	10.2
S. jollyanum Aqueous	40.1	13.4

4.4 Preliminary phytochemical screening

The result of preliminary phytochemical screening of *Curculigo pilosa* and *Sphenocentrum jollyanum* revealed the presence of saponins, tannins, flavonoids, and cardiac glycosides while alkaloid and anthraquinones were absent in both plants (Table 4.4.1). The screened plants revealed the presence of tannins, saponins, alkaloids, flavonoids and cardiac glycosides in *Vitellaria paradoxa* and *Vernonia amygdalina* while anthraquinone was absent. Tannins, saponins, flavonoids and cardiac glycosides were present in *Lonchocarpus cyanescens*, *Uvaria chamae*, and *Khaya ivorensis*, while alkaloid was absent. Tannins, saponins, alkaloids and cardiac glycosides were present in *Pseudocedrella kotschyii* and *Kigelia africana*, while flavonoid was absent. Saponins, alkaloids and cardiac glycosides were present in *Euadenia trifoliolata* while tannins, flavonoids, and anthraquinones were absent. Saponins, flavonoids and cardiac glycosides were present *Alstonia congensis* while tannins, alkaloids, and anthraquinones were absent. *Entada gigas* showed the presence of tannins, saponins, anthraquinones, and cardiac glycosides while alkaloid and flavonoid were absent (Table 4.4.1).

Table 4.4.1: Preliminary phytochemical screening of selected plants

Plant samples	Tannins	Saponins	Alkaloids	Flavonoids	Cardiac glycosides	Anthraquinones
Curculigo pilosa	++	++	-	++	++	-
Sphenocentrum jollyanum	++	++	-	++	++	-
Entada gigas	++	++	-	-	++	++
Vitellaria paradoxa	++	++	++	++	++	-
Alstonia congensis	-	++	-	++	++	-
Lonchocarpus cyanescens	++	++	-	++	++	-
Uvaria chamae	++	++	-	++	++	++
Vernonia amygdalina	++	++	-	++	++	-
Pseudocederella kotchyii	++	++	++	-	++	++
Kigelia africana	++	++	++	-	++	-
Euadenia trifoliolata	-	++	++	-	++	-
Khaya ivorensis	++	++		++	++	++

Key:

++: Abundantly present

-: Absent

4.5 Total phenolic content (TPC)

The TPC of the screened sample showed the highest value in *Pseudocedrella kotschyii* stem bark (560.50 mgGAEg $^{-1}$), followed by *Uvaria chamae* root (338.40 mgGAEg $^{-1}$) and *Uvaria afzelii* root; 265.91 mgGAEg $^{-1}$ (Figure 4.5).

4.6 Total flavonoid content (TFC)

The highest TFC was observed in *Ageratum conyzoides* (236.80 mgQg $^{-1}$) followed by *Vernonia amygdalina* leaf (126.40 mgQg $^{-1}$) and *Euadenia trifoliolata* leaf (122.9 mgQg $^{-1}$) (Figure 4.6).

4.7 Free radical scavenging activity by DPPH of screened extracts

The obtained DPPH result summarized in Table 4.7 showed the lowest IC_{50} value observed in *Pseudocedrella kotschyii* (2.74 ± 0.00 µgmL $^{-1}$) corresponding to the most active extract which is comparable to the standard drugs; Ascorbic acid and Rutin with IC_{50} values 2.76 ± 0.01 µgmL $^{-1}$ and 20.60 ± 9.26 µgmL $^{-1}$, respectively. *Kigelia africana* stem bark, *Uvaria afzelii* root, *Khaya ivorensis* stem bark and *Curculigo pilosa* seed gave IC_{50} values of 11.30 ± 0.02 µgmL $^{-1}$, 11.58 ± 0.01 µgmL $^{-1}$, 11.89 ± 2.49 µgmL $^{-1}$, and 36.68 ± 0.74 µgmL $^{-1}$ respectively (Table 4.7).

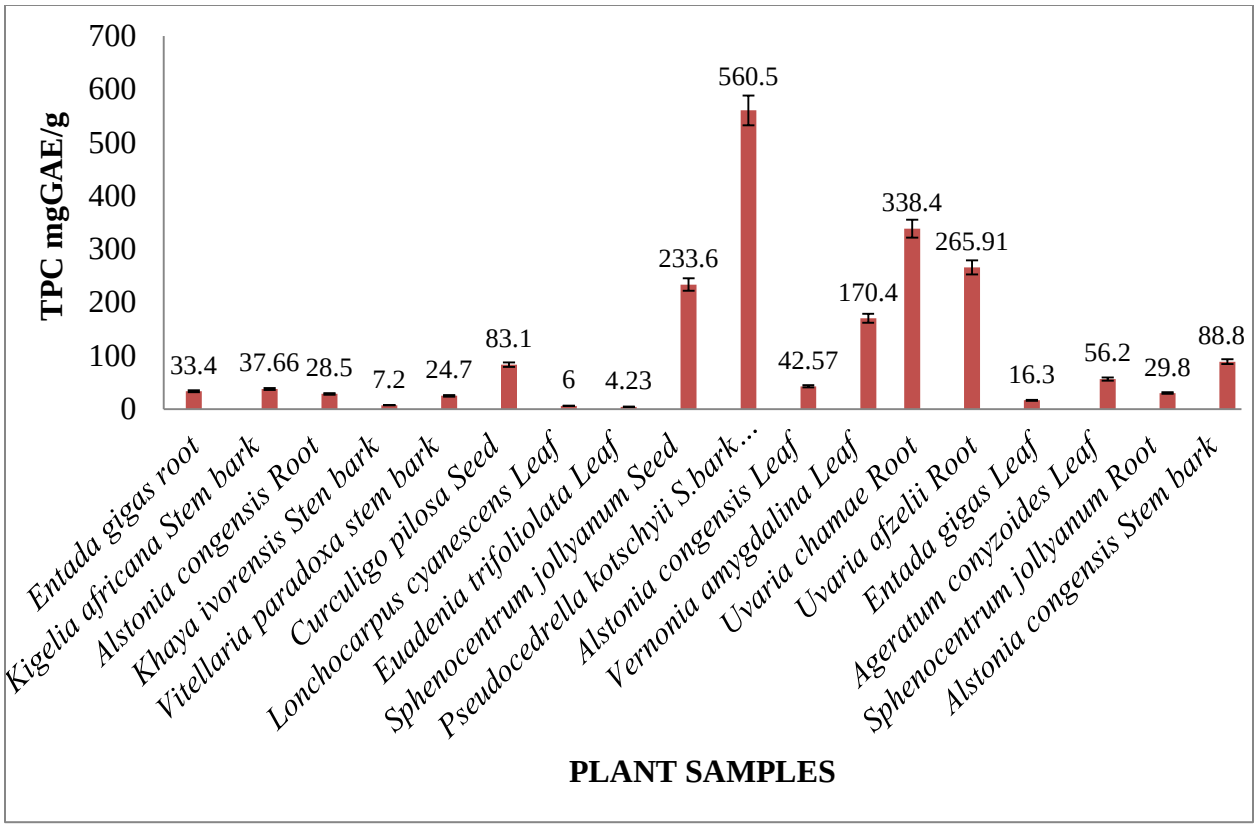

Figure 4.5: Total phenolic content of samples

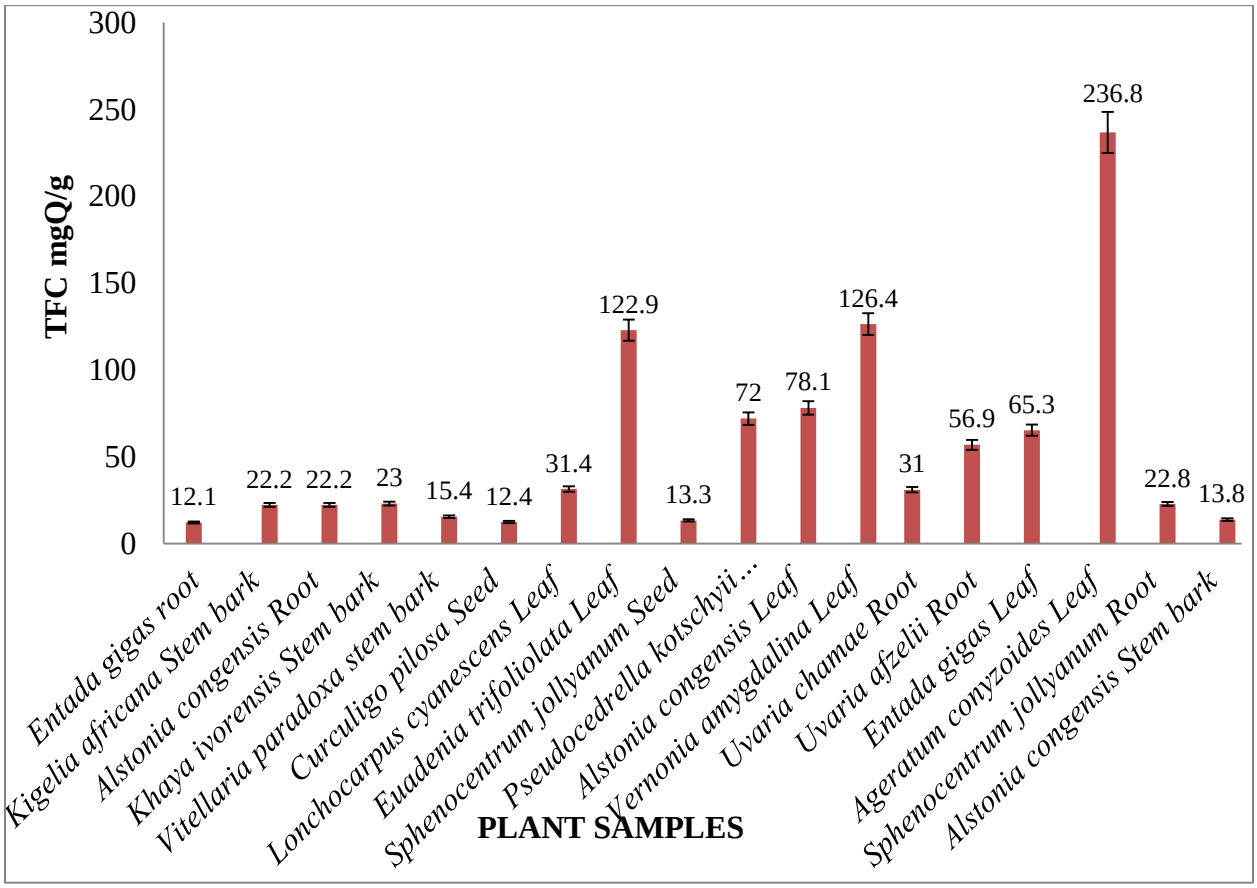

Figure 4.6: Total flavonoid content of samples

Table 4.7: DPPH antioxidant activity

Samples	IC_{50} ± SEM (µgmL $^{-1}$)
Ascorbic acid	2.76 ± 0.01 [a]
Rutin	20.60 ± 9.26 [c]
Ageratum conyzoides leaf	281.06 ± 11.22
Alstonia congensis leaf	228.40 ± 2.84
Alstonia congensis stem bark	5518.34 ± 9.45
Alstonia congensis root	218.65 ± 0.56
Curculigo pilosa seed	36.68 ± 0.74
Entada gigas leaf	169.00 ± 8.95
Entada gigas root	832.89 ± 4.77
Euadenia trifoliolata leaf	972.71 ± 186.12
Khaya ivorensis stem bark	11.89 ± 2.49 [b]
Kigelia africana stem bark	11.30 ± 0.02 [b]
Lonchocarpus cyanescens leaf	179.39 ± 1.66
Pseudocedrella kotschyii stem bark	2.74 ± 0.00 [a]
Sphenocentrum jollyanum root	102.57 ± 11.16
Sphenocentrum jollyanum seed	239.61 ± 18.61
Uvaria chamae root	36.93 ± 2.30
Uvaria afzelii root	11.58 ± 0.01 [b]
Vernonia amygdalina leaf	200.28 ± 14.34
Vitellaria paradoxa stem bark	24.80 ± 1.33 [c]

4.8 Acute toxicity study

Single dose oral administration of 10, 100, and 1000 $mgkg^{-1}$ *b.w.* of *C. pilosa* and *S. jollyanum* crude extracts seemed to be safe visually as no death or obvious toxicity signs were observed in treated animals for the first 24 h and by the end of 48 h observation (Tables 4.8.1 and 4.8.2). No late toxicological effect was observed up to 14 days after treatment. Consequently, the LD_{50} of the extract is > 5000 $mgkg^{-1}$. The effect of *C. pilosa* and *S. jollyanum* plant extracts was observed on kidney, liver, and heart to note the severity of damage and establish a safety profile for these plants.

4.8.1 Effects of *C. pilosa* seed extract on the kidney, heart and liver

The kidney of the control animals (A) 10 $mgkg^{-1}$ (B), and 100 $mgkg^{-1}$ (C) showed no visible lesion. However, slight diffuse tubular renewal and glomeruli shrinkage was observed in animals administered with 1000 $mgkg^{-1}$ (D), 1600 $mgkg^{-1}$ (E) and 2900 $mgkg^{-1}$ (F) which became more severe at 5000 $mgkg^{-1}$ (G) treated animals (Figure 4.8.1.1). Photomicrograph of heart of control animals, 10, 100, 1000, 1600, 2900, up to 5000 $mgkg^{-1}$ extracts treated animals presented no visible lesion (Figure 4.8.1.2). Photomicrograph of a section of liver tissues exhibited no visible lesions in the control animals up to 1000 $mgkg^{-1}$ treated animals. However, severe portal congestion, diffuse vacuolar degeneration of hepatocytes were observed in 1,600 $mgkg^{-1}$, 2900 $mgkg^{-1}$, and 5000 $mgkg^{-1}$ treated animals (Figure 4.8.1.3).

4.8.2 Effects of *S. jollyanum* seed extract on the kidney, heart, and liver

The kidney of control animals (A), 10 $mgkg^{-1}$ (B), 100 $mgkg^{-1}$ (C), up to 1000 $mgkg^{-1}$ treated animals showed no observable lesion. However, mild diffuse tubular regeneration was noticed in high dosages of 1600 $mgkg^{-1}$, 2900 $mgkg^{-1}$ and 5000 $mgkg^{-1}$ treated animals (Figure 4.8.2.1). Photomicrograph of heart tissue section in control animals, 10 $mgkg^{-1}$, 100 $mgkg^{-1}$, up to 1000 $mgkg^{-1}$ presented no visible lesions but doses at 1600 $mgkg^{-1}$, 2900 $mgkg^{-1}$, and 5000 $mgkg^{-1}$ treated animals revealed several foci of perivascular cellular infiltration, the affected vessels are moderately to severely congested (Figure 4.8.2.2). Liver tissues of normal control, animals treated with 10 $mgkg^{-1}$, 100 $mgkg^{-1}$, and 1000 $mgkg^{-1}$ showed no observable damage while slight portal and central venous congestion, with moderate periportal cellular infiltration were observed in the liver tissues of 1600 $mgkg^{-1}$, 2900 $mgkg^{-1}$, and 5000 $mgkg^{-1}$ treated animals (Figure 4.8.2.3).

Table 4.8.1: Acute toxicity (LD_{50}) of *Curculigo pilosa* rhizome

Dosage ($mgkg^{-1}$ *b.w.*)	Observation(s)	
	24 h	48 h
10	0/3	0/3
100	0/3	0/3
1000	0/3	0/3
1600	0/3	0/3
2900	0/3	0/3
5000	0/3	0/3

Table 4.8.2: Acute toxicity (LD_{50}) of *Sphenocentrum jollyanum* seed

Dosage ($mgkg^{-1}$ *b.w.*)	Observation(s)	
	24 h	48 h
10	0/3	0/3
100	0/3	0/3
1000	0/3	0/3
1600	0/3	0/3
2900	0/3	0/3
5000	0/3	0/3

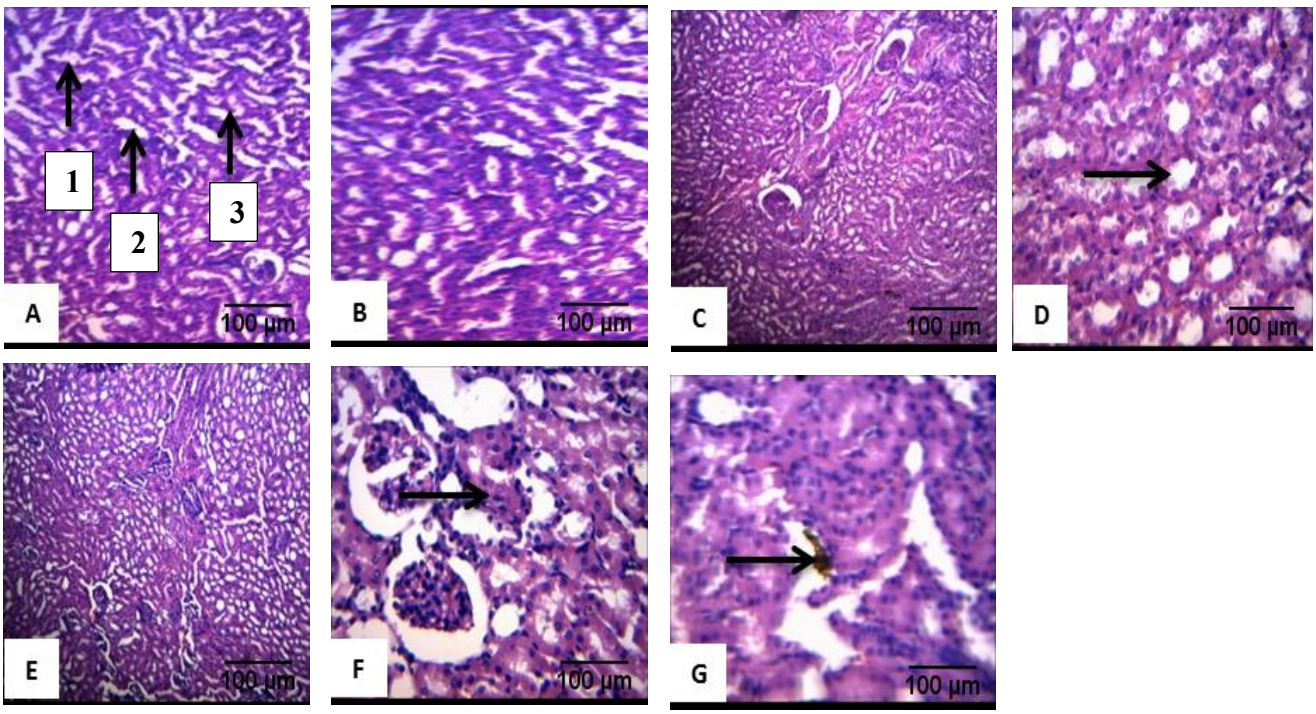

Figure 4.8.1.1: Photomicrograph of kidney of animals administered with *C. pilosa* extract, Magnification X 400

(A) Control animals: 1: Glomerulus, 2: Bowman's capsule, 3: Renal tubules (B) 10 mg/kg

(C) 100 $mgkg^{-1}$ (D) 1000 $mgkg^{-1}$ (E) 1600 $mgkg^{-1}$ (F) 2900 $mgkg^{-1}$ (G) 5000 $mgkg^{-1}$

Black arrows in D, F and G signify diffuse tubular renewal and glomeruli shrinkage

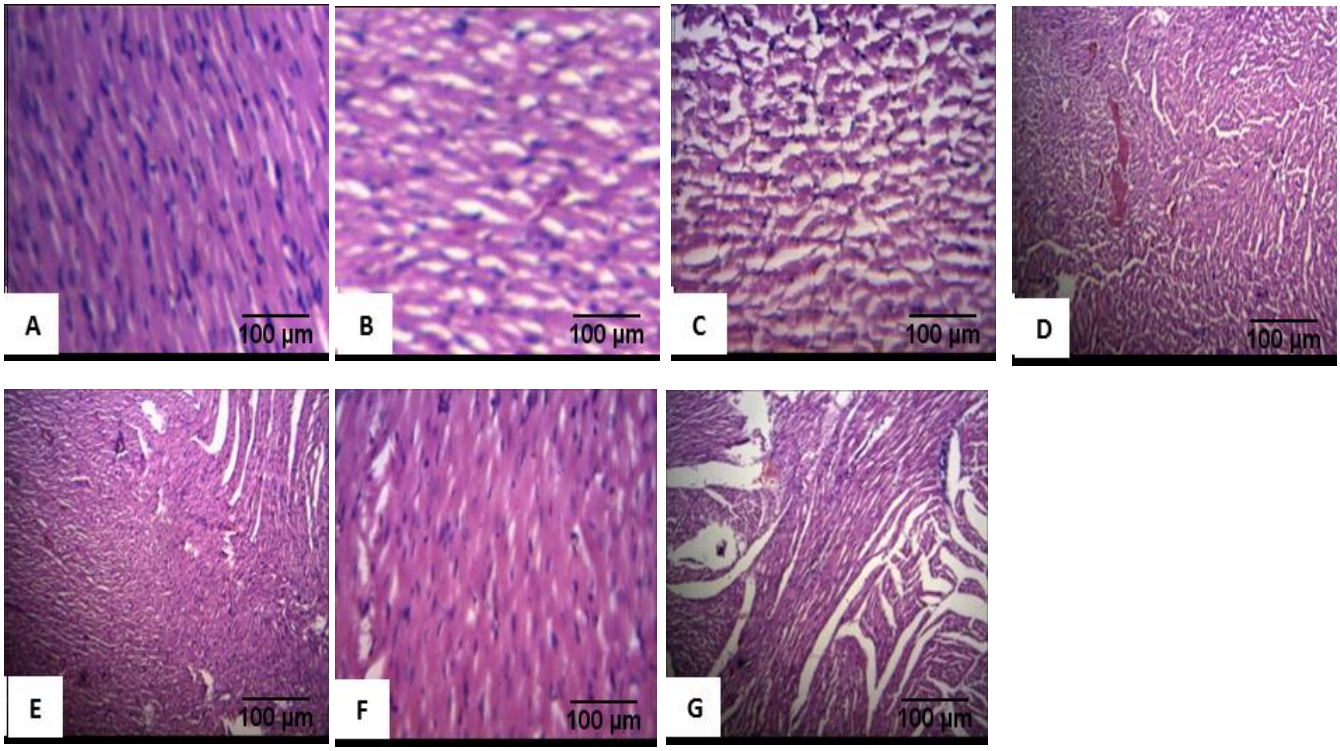

Figure 4.8.1.2: Photomicrograph of heart of animals administered with *C. pilosa* extract, Magnification X 400 (A) Control animals (B) 10 $mgkg^{-1}$ (C) 100 $mgkg^{-1}$ (D) 1000 $mgkg^{-1}$ (E) 16000 $mgkg^{-1}$ (F) 2900 $mgkg^{-1}$ (G) 5000 $mgkg^{-1}$

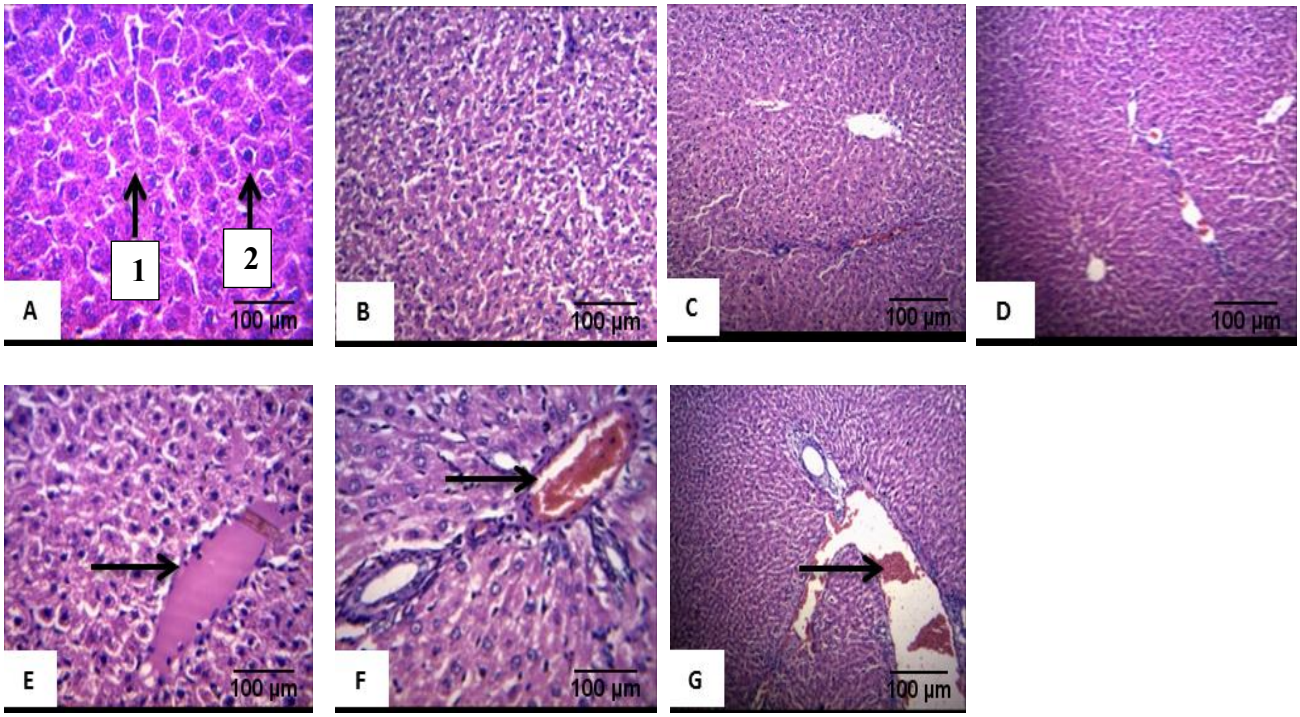

Figure 4.8.1.3: Photomicrograph of liver of animals administered with *C. pilosa* extract, Magnification X 400

(A) Control animals: 1: Normal hepatocytes, 2: Interstitial spaces (B) 10 $mgkg^{-1}$ (C) 100 $mgkg^{-1}$ (D) 1000 $mgkg^{-1}$ (E) 1600 $mgkg^{-1}$ (F) 2900 $mgkg^{-1}$ (G) 5000 $mgkg^{-1}$

Black arrows in E, F and G signify severe portal congestion and diffuse vacuolar degeneration of hepatocytes

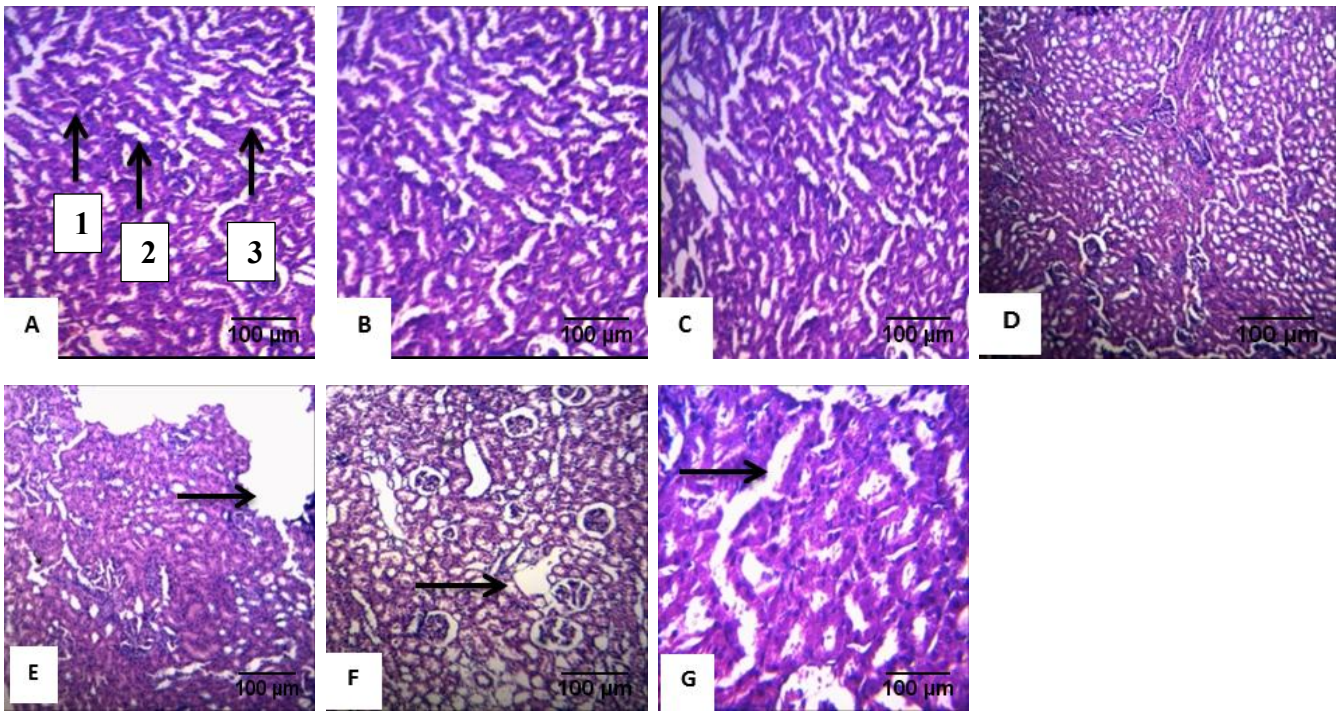

Figure 4.8.2.1: Photomicrograph of Kidney of animals administered with *S. jollyanum* extract, Magnification X 400

(A) Control animals: 1: Glomerulus, 2: Bowman's capsule, 3: Renal tubules (B) 10 $mgkg^{-1}$ (C) 100 $mgkg^{-1}$ (D) 1000 $mgkg^{-1}$ (E) 1600 $mgkg^{-1}$ (F) 2900 $mgkg^{-1}$ (G) 5000 $mgkg^{-1}$

Black arrows in E, F and G signify mild diffuse tubular regeneration

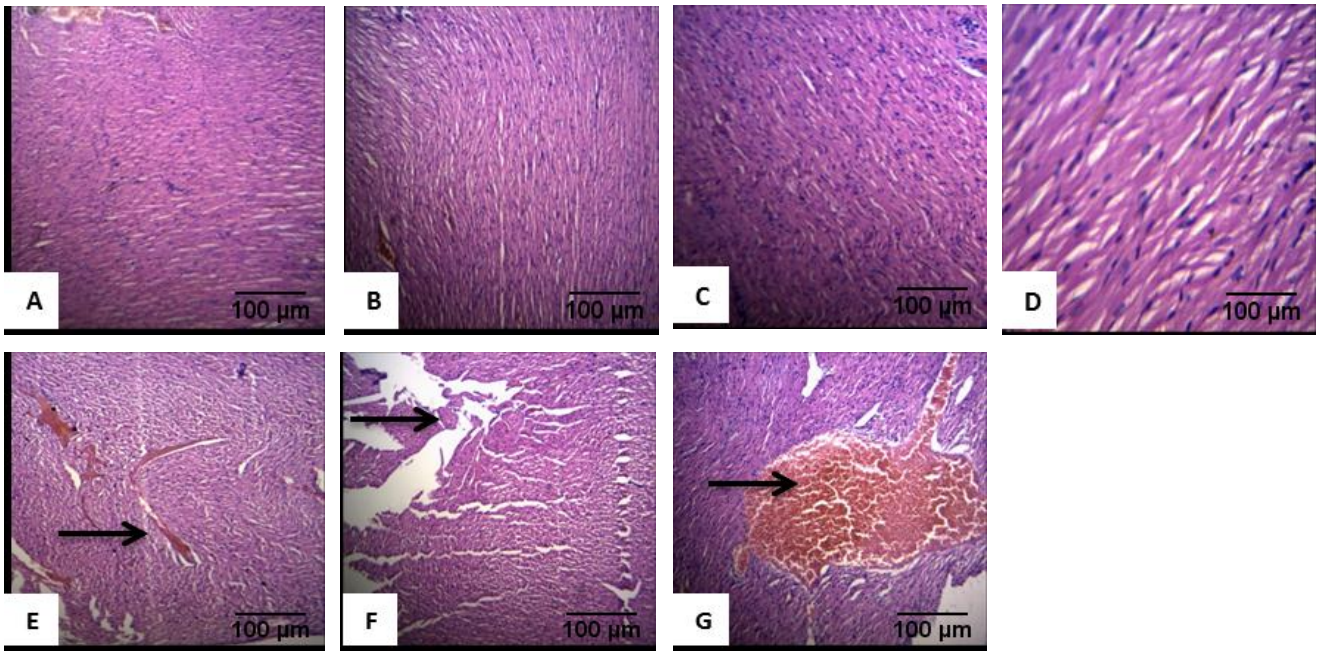

Figure 4.8.2.2: Photomicrograph of heart of animals administered with *S. jollyanum* extract, Magnification X 400 (A) Control animal (B) 10 $mgkg^{-1}$ (C) 100 $mgkg^{-1}$ (D) 1000 $mgkg^{-1}$ (E) 1600 $mgkg^{-1}$ (F) 2900 $mgkg^{-1}$ (G) 5000 $mgkg^{-1}$.

Black arrows in E, F and G signify several foci of perivascular cellular infiltration

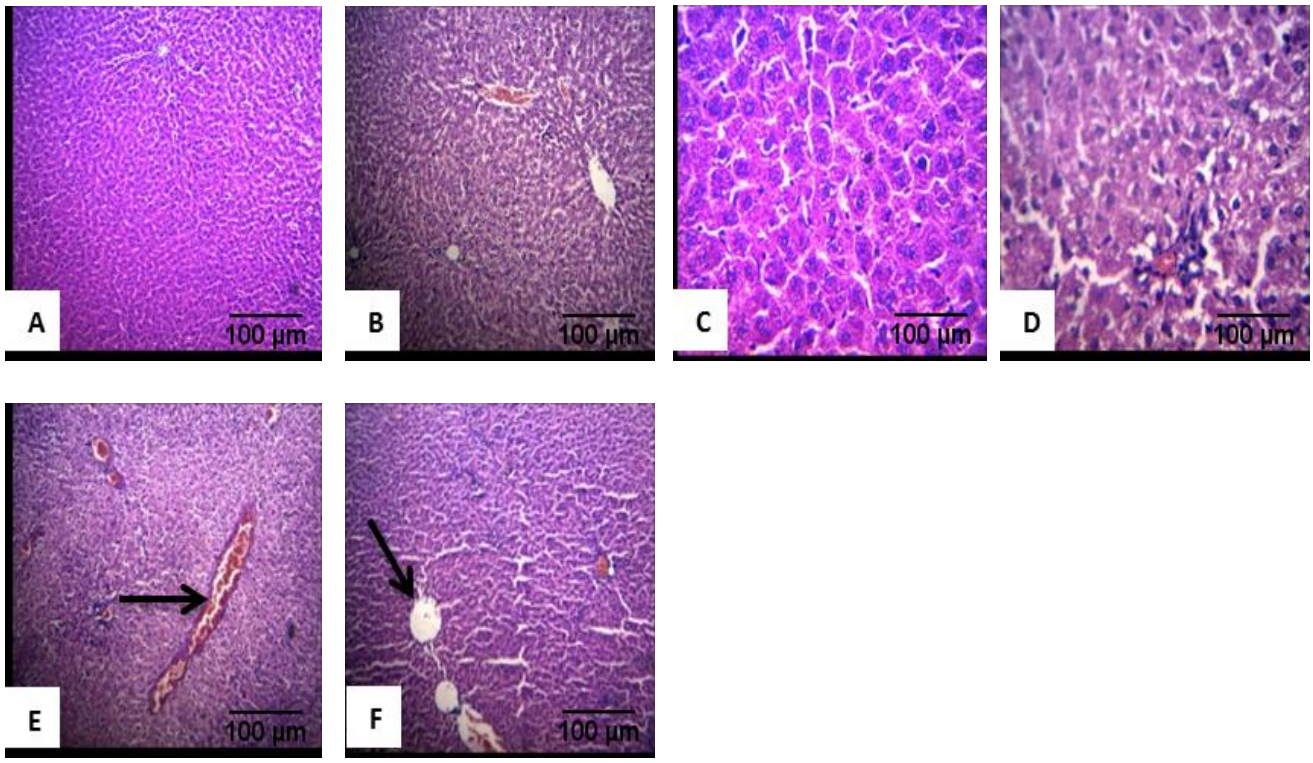

Figure 4.8.2.3: Photomicrograph of liver of animals administered with *S. jollyanum* extract, Magnification X 400 (A) Control animals: 1: Normal hepatocytes, 2: Interstitial spaces (B) 10 $mgkg^{-1}$ (C) 100 $mgkg^{-1}$ (D) 1000 $mgkg^{-1}$ (E) 1600 $mgkg^{-1}$ (F) 2900 $mgkg^{-1}$ (G) 5000 $mgkg^{-1}$
Black arrows in E and F signify slight portal and central venous congestion, with moderate periportal cellular infiltration

4.9 Indomethacin induced gastric ulcer

4.9.1 Effect of methanol extracts of *C. pilosa* rhizomes and *S. jollyanum* seeds on body weight change

The body weights of the treated groups significantly increased compared with ulcer untreated group after 8 days of treatment (Figure 4.9).

4.10.1 Reduction in severity of lesions caused by indomethacin induced gastric ulcer

Three treatment doses: 50 mg, 100 mg, and 200 $mgkg^{-1}$ *b.w.* of extracts were used. The standard (cimetidine) treated group significantly reduced the gastric ulcer index from 8.00 ± 2.72 in the ulcer untreated group to 0.20 ± 0.20, while the *Curculigo pilosa* 50 mg treated group significantly reduced the ulcer index from 8.00 ± 2.72 to 1.17 ± 0.83. *Sphenocentrum jollyanum* 200 mg treated group also showed significant reduction in gastric ulcer index from 8.00 ± 2.72 to 2.20 ± 1.24. *Curculigo pilosa* 100 mg and 200 mg treated groups significantly reduced the gastric ulcer index from 8.0 ± 2.72 to 5.17 ± 1.99, and 3.80 ± 1.46, respectively, while 50 mg/kg *b.w.* and 100 $mgkg^{-1}$ *b.w. S. jollyanum* extracts caused a significant reduction of gastric ulcer index from 8.0 ± 2.72 to 5.60 ± 0.92 and 3.60 ± 1.14, respectively. *Curculigo pilosa* extract at 50 mg exhibited the highest activity among the extracts (Table 4.10.1). Percentage inhibition of indomethacin induced gastric mucosal damage for all the groups pre-treated with cimetidine and extracts revealed 97.5% inhibition in the cimetidine treated group. This study also revealed that *C. pilosa* at 50 mg, 100 mg, and 200 mg gave percentage inhibitions of 85.4, 35.4, and 52.5%, respectively, while *S. jollyanum* at 50 mg, 100 mg, and 200 mg gave percentage inhibitions of 30.0, 55.0, and 72.5%, respectively. Cimetidine 100 mg gave the highest percentage inhibition followed by *C. pilosa* 50 mg extract, which gave 85.4% inhibition (Table 4.10.1). The result revealed that *C. pilosa* at 50 $mgkg^{-1}$ has the capacity of reducing gastric injury induced by indomethacin, while *S. jollyanum* at 200 $mgkg^{-1}$ showed a reduction in gastric damage. This implies that the seeds of *S. jollyanum* and rhizomes of *C. pilosa* showed anti-ulcer activity indicated by lowering ulcer index or increasing percentage inhibition.

4.10.2 Macroscopic picture of stomach

The macroscopic picture of the stomach shows the gross appearance of the stomach. The indomethacin induced section (ulcer untreated) shows the ulcerated parts in black spots (Figure 4.10.2).

Table 4.10.1: Reduction in the severity of lesions caused by indomethacin induced gastric ulcer

Groups	Ulcer index (mean) ± SEM	Inhibition (%)
A – Cimetidine 100 mg	**0.20 ± 0.20 [a]**	**97.5**
B – Ulcer untreated	8.00 ± 2.72	0
C – *C. pilosa* 50 mg	**1.17± 0.83 [ab]**	**85.4**
D – *C. pilosa* 100 mg	5.17 ± 1.99	35.4
E – *C. pilosa* 200 mg	3.80 ± 1.46 [b]	52.5
I – *S. jollyanum* 50 mg	5.60 ± 0.92	30.0
J - *S. jollyanum* 100 mg	3.60 ± 1.14 [b]	55.0
K – *S. jollyanum* 200 mg	**2.20 ± 1.24 [ab]**	**72.5**
L – Normal Control	0.00 ± 0.00 [a]	100

[a] $p < 0.05$ when compared with normal control,

[b] $p < 0.05$ when compared with ulcer untreated,

[c] p when compared with cimetidine

4.10.3 Histology of the stomach

The ulcer untreated group showed necrosis and congestion in blood vessels while the cimetidine and *C. pilosa* treated groups revealed abundant parietal and mucosal cells with mild hemorrhagic lesion. Abundance of parietal and mucosal cells with no significant lesion was also observed in *S. jollyanum* treated groups and normal control (Figure 4.10.3). Abundance of parietal and mucosal cells with mild hemorrhagic lesion was observed in cimetidine and *C. pilosa* treated groups. This suggests that both plants possess gastroprotective properties comparable to the standard drug.

4.11 Effect of test drugs on stomach weight

The stomach weight of treated and untreated groups on day 8 of the experiment did not differ significantly (Table 4.11).

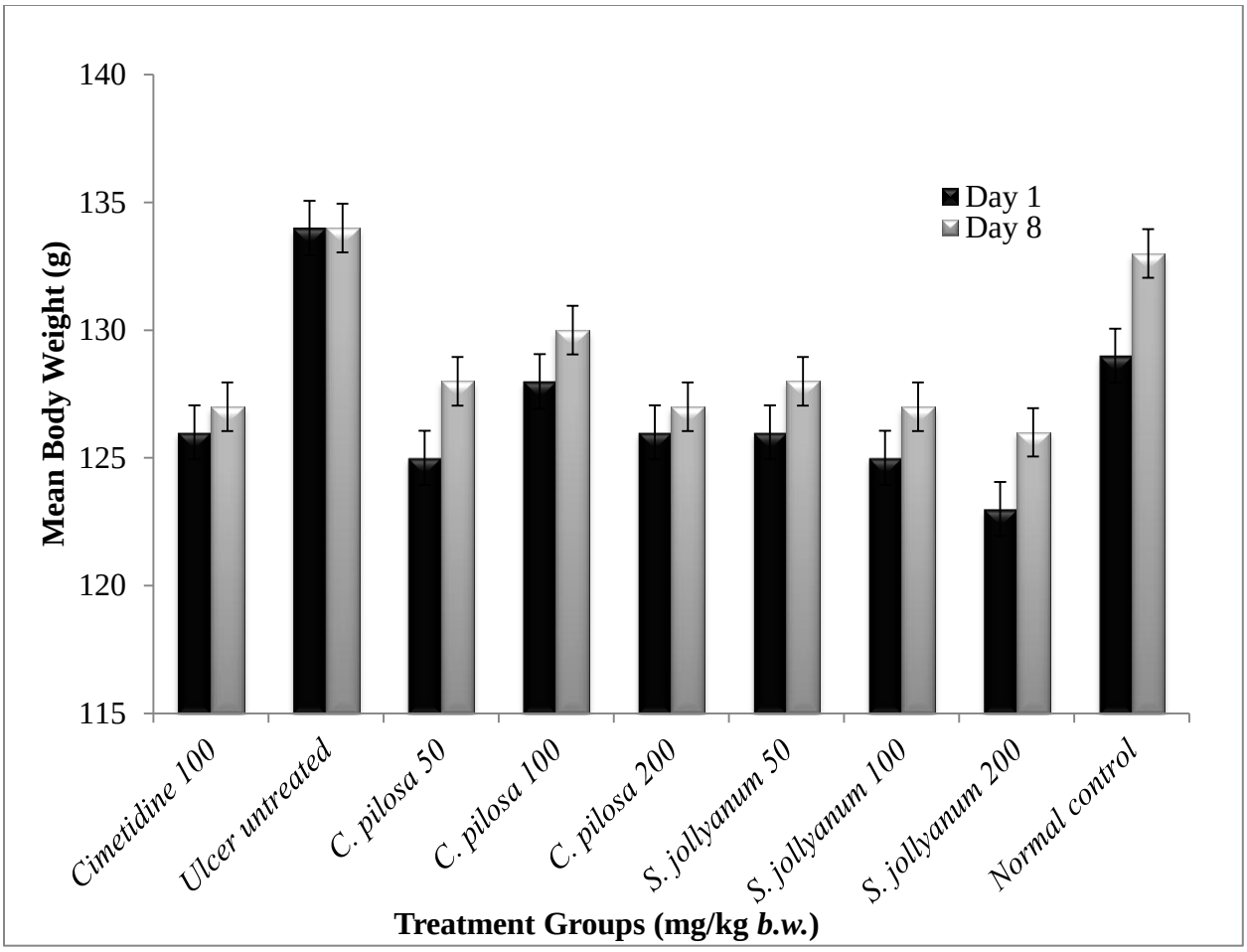

Figure 4.9: Body weight of animals. Each vertical bar represents Mean ± SEM of five rats per group.

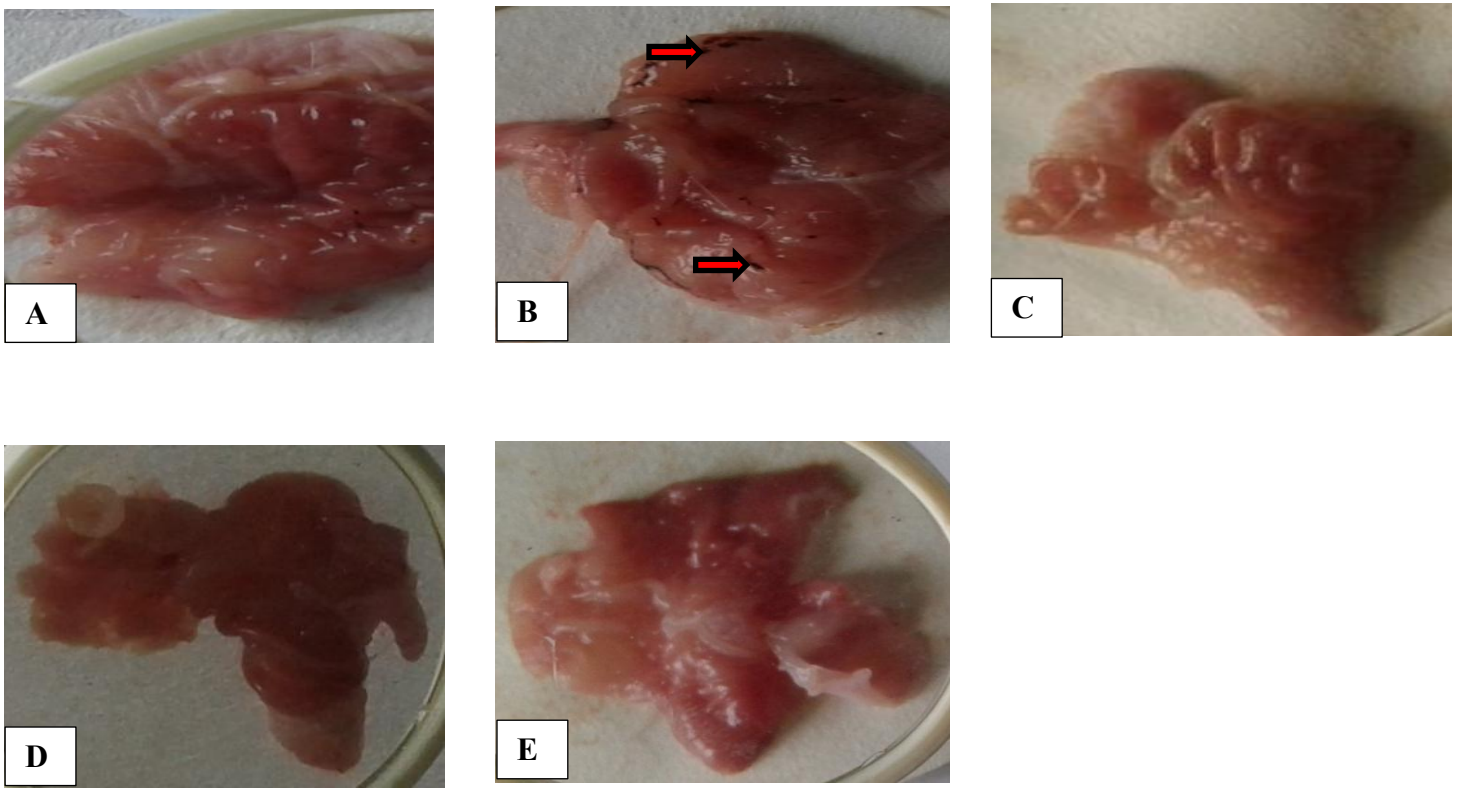

Figure 4.10.2: Gross appearance of stomach;

A: Cimetidine treated section (100 mgkg $^{-1}$)

B: Indomethacin induced section

C: *Sphenocentrum jollyanum* treated section (200 mgkg $^{-1}$)

D: *Curculigo pilosa* treated section (50 mgkg $^{-1}$)

E: Normal Control.

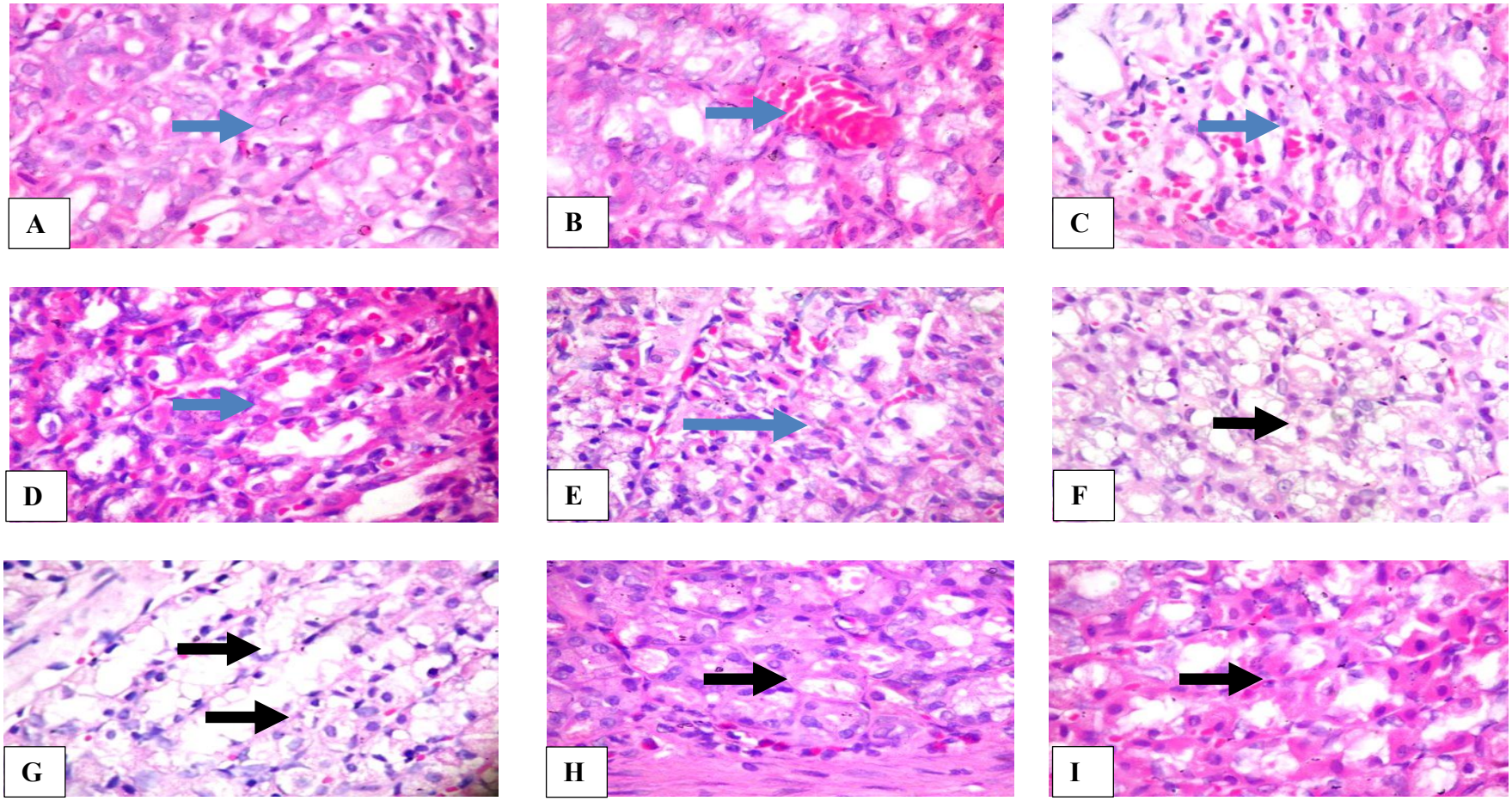

Figure 4.10.3: Histopathology of stomach Magnification X 400

A: Cimetidine treated group, B: Ulcer untreated group, C: *C. pilosa* 50 mgkg^{-1} *b.w.*, D: *C. pilosa* 100 mgkg^{-1} *b.w.*, E: *C. pilosa* 200 mgkg^{-1} *b.w.*, F: *S. jollyanum* 50 mgkg^{-1} *b.w,* G: *S. jollyanum* 100 mgkg^{-1} *b.w.*, H: *S. jollyanum* 200 mgkg^{-1} *b.w.*, I: Normal control. Blue arrow in B signifies necrosis and blood vessels congestion, blue arrows in A, C, D and E signify abundant parietal and mucosal cells, black arrows in F, G, H, and I signify no significant lesion with abundant parietal and mucosal cells.

Table 4.11: Effect of *C. pilosa* and *S. jollyanum* methanol extracts on mean stomach weight

Groups (mgkg^{-1} *b.w.*)	**Mean Stomach Weight (g)**
A – Cimetidine	0.92 ± 0.03
B – Ulcer untreated	0.84 ± 0.02
C – *C. pilosa* 50	0.81 ± 0.04
D – *C. pilosa* 100	0.84 ± 0.02
E – *C. pilosa* 200	0.87 ± 0.03
F – *S. jollyanum* 50	0.93 ± 0.03
G- *S. jollyanum* 100	0.87 ± 0.01
H- *S. jollyanum* 200	0.84 ± 0.01
I – Normal control	0.94 ± 0.04

4.12 Biochemical assays

4.12.1 Effect of *C. pilosa* and *S. jollyanum* methanol extracts on total gastric protein, catalase (CAT), and superoxide Dismutase (SOD)

The total gastric protein increased significantly in the *C. pilosa* 50 and 100 $mgkg^{-1}$ *b.w.* (0.26 ± 0.00 U/mg, 0.27 ± 0.00 U/mg) groups when compared with ulcer untreated (0.23 ± 0.00 U/mg) group. The *C. pilosa* treated groups showed a decrease in CAT (33.10 ± 1.33 mmol/min / mg, 31.48 ± 0.83 mmol / min / mg, 38.79 ± 2.04 mmol/min/mg), *S. jollyanum* treated groups at 50, 100 and 200 $mgkg^{-1}$ *b.w.* (31.23 ± 0.51 mmol/min/mg, 30.79 ± 1.08 mmol/min/mg, 37.41 ± 2.47 mmol/min/mg), and ulcer untreated group (36.79 ± 3.91 mmol/min/mg) compared with normal control (45.04 ± 5.15 mmol/min/mg). There was a significant increase in SOD level in groups treated with *S. jollyanum*, *C. pilosa* and cimetidine compared to ulcer untreated group (Table 4.12.1).

4.12.2 Effect of methanol extracts of *C. pilosa* and *S. jollyanum* on nitric oxide (NO) level

There was a significant increase in the NO level of all treated groups compared to the ulcer-untreated group. The NO level of *C. pilosa* 100 $mgkg^{-1}$ *b.w.* was significantly higher compared to all the treated groups (Figure 4.12.2).

4.12.3 Effect of *C. pilosa* and *S. jollyanum* methanol extracts on glutathione

A significant increase was observed in the Glutathione levels in *S. jollyanum* 100 $mgkg^{-1}$ *b.w.* treated group (73.62 µg/g) and *C. pilosa* 50 $mgkg^{-1}$ *b.w.*treated group (66.5 µg/g) compared with cimetidine 100 $mgkg^{-1}$ *b.w.* treated groups (62.67 µg/g) as shown in Figure 4.12.3.

4.12.4 Effect of *C. pilosa* and *S. jollyanum* methanol extracts on malondialdehyde (MDA) level

A significant reduction was observed in the MDA level in *C. pilosa* and *S. jollyanum* treated groups when compared with ulcer untreated group (Figure 4.12.4).

Table 4.12.1: Effect of *C. pilosa* and *S. jollyanum* methanol extracts on total gastric protein, catalase, and superoxide dismutase

Groups ($mgkg^{-1}$)	Total Gastric Protein (U/mg)	Catalase (CAT) (mmol/ min/ mg)	Superoxide Dismutase (SOD) U/mg
A – Cimetidine	0.25 ± 0.00^{c}	37.85 ± 3.18	31.24 ± 0.25^{b}
B – Ulcer untreated	0.23 ± 0.00	36.79 ± 3.91	25.10 ± 2.12
C – *C. pilosa* 50	0.26 ± 0.00^{b}	33.10 ± 1.33	34.33 ± 0.12^{b}
D – *C. pilosa* 100	0.27 ± 0.00^{b}	31.48 ± 0.83	32.96 ± 0.91^{b}
E – *C. pilosa* 200	0.24 ± 0.01	38.79 ± 2.04	32.72 ± 0.10^{b}
F – *S. jollyanum* 50	0.16 ± 0.02	31.23 ± 0.51	45.86 ± 2.12^{a}
G- *S. jollyanum* 100	0.19 ± 0.02	30.79 ± 1.08	44.39 ± 0.90^{a}
H- *S. jollyanum* 200	0.16 ± 0.00	37.41 ± 2.47	47.61 ± 1.36^{a}
I – Normal control	0.23 ± 0.03	45.04 ± 5.15	36.37 ± 0.65^{b}

Values are expressed as Mean ± SEM. [a] $p < 0.05$ when compared with normal control, [b] $p < 0.05$ when compared with ulcer untreated, [c] p when compared with cimetidine

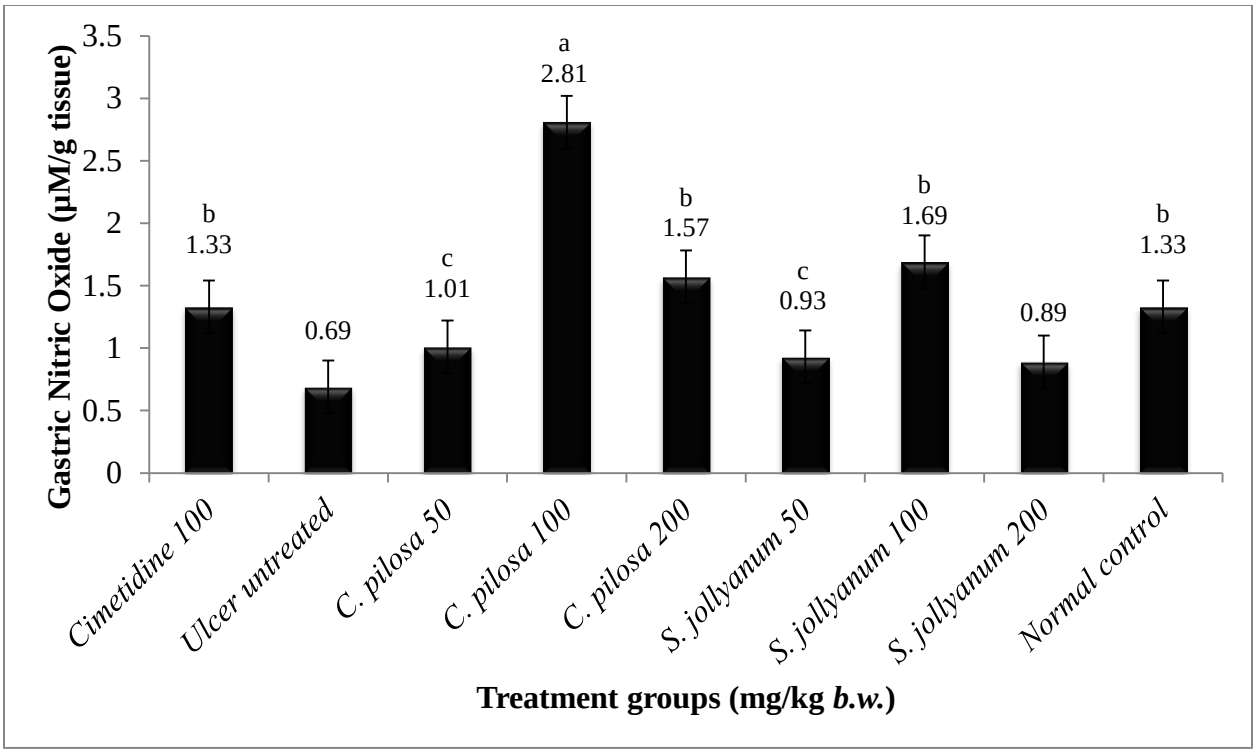

Figure 4.12.2: Gastric nitric oxide

[a] $p < 0.05$ when compared with normal control, [b] $p < 0.05$ when compared with ulcer untreated, [c] p when compared with cimetidine

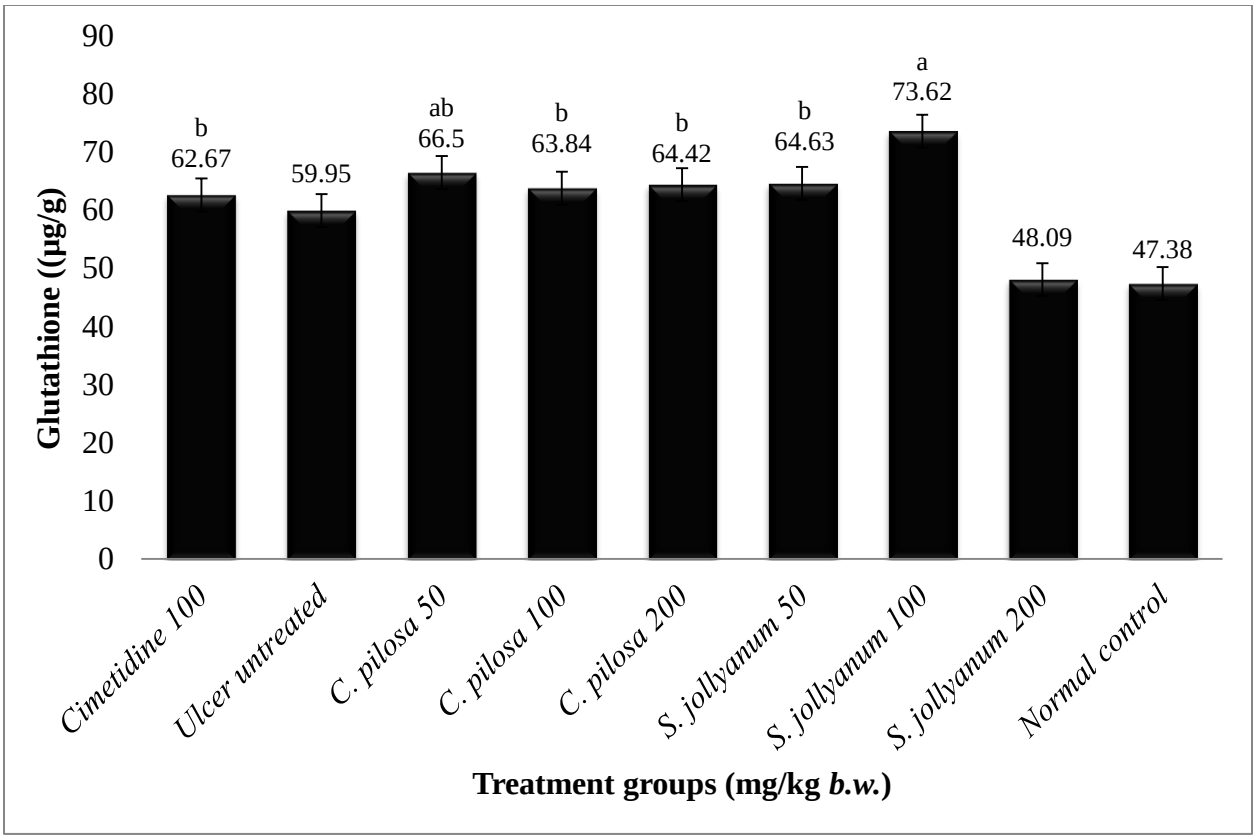

Figure 4.12.3: Glutathione

Each vertical bars represents Mean ± SEM. Values are significant when $P < 0.05$

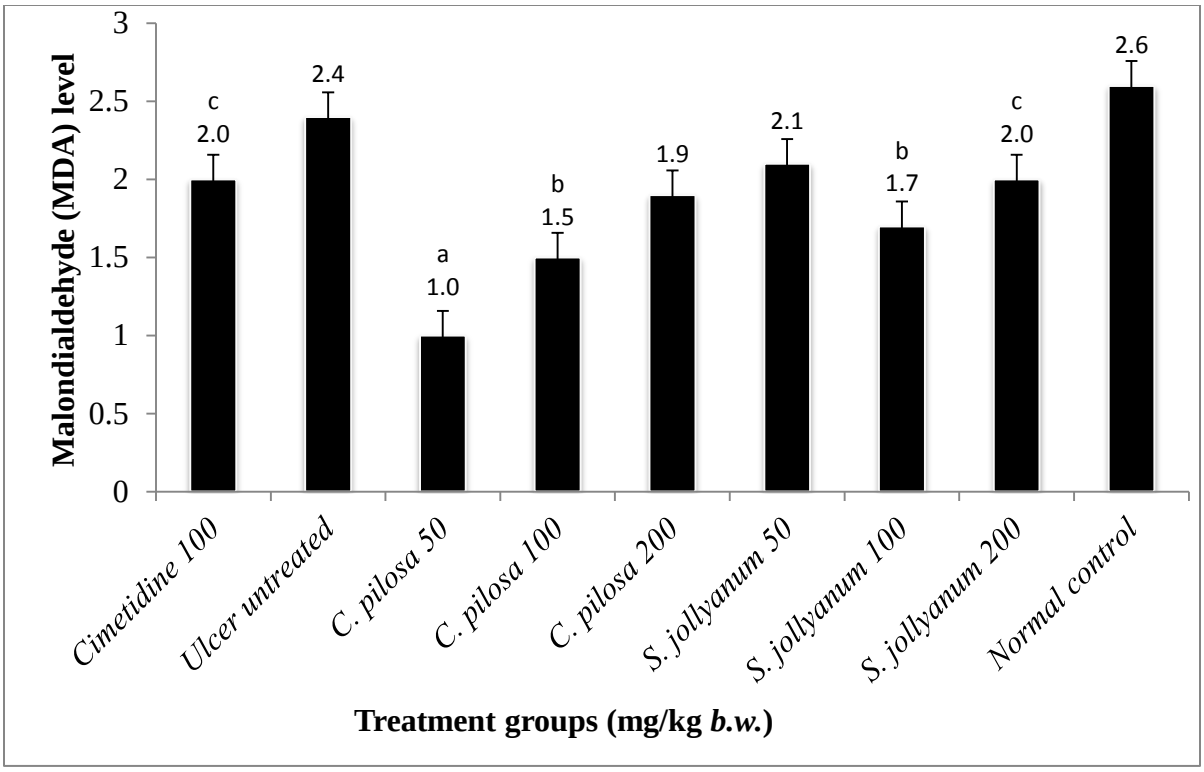

Figure 4.12.4: Lipid peroxidation (MDA) level

[a] $p < 0.05$ when compared with normal control, [b] $p < 0.05$ when compared with ulcer untreated, [c] $p < 0.05$ when compared with cimetidine

4.13 Antacid activity of *C. pilosa* and *S. jollyanum* Extracts and Fractions

Neutralising Effect of *C. pilosa* and *S. jollyanum* Extracts and Fractions

The neutralising effects of *C. pilosa* and *S. jollyanum* methanol extracts and fractions were studied for the two concentrations of extracts, fractions, and standard sodium bicarbonate. All the obtained values were compared with the standard and the control. The result showed that aqueous fraction of *C. pilosa* at 50 mg and 100 mg showed outstanding neutralising effect by increasing the pH of the artificial gastric juice from baseline pH 1.2 to 1.86±0.0033 and 2.03±0.0033, respectively. This result showed that *C. pilosa* aqueous fraction has a better neutralising effect than the standard sodium bicarbonate at 50 mg and 100 mg which gave a final pH of 1.53±0.0033 and 1.47±0.0033 respectively. *C. pilosa n* butanol fraction, *C. pilosa* ethyl acetate fraction, and *S. jollyanum* ethyl acetate fraction at 50 mg and 100 mg concentrations increased the pH to 1.82±0.0000 and 1.85±0.0066, 1.78±0.0033 and 1.82±0.0057, 1.61±0.0033 and 1.53±0.0033, respectively, which are also considered good response since the neutralising effect is greater than the standard, sodium bicarbonate (Table 4.13).

Neutralising Capacity of *C. pilosa* and *S. jollyanum* Extracts and Fractions

The amount of artificial gastric juice consumed to pH 3 showed that *S. jollyanum* ethyl acetate fraction at 50 mg and 100 mg were able to consume 14.01±0.0066 mL and 16.02±0.0115 mL of the artificial gastric juice whereas sodium bicarbonate consumed 19.01±0.0057 and 28.49±0.0066 mL respectively. *Sphenocentrum jollyanum n* Hexane fraction and *C. pilosa* aqueous fraction at 50 mg and 100 mg were able to consume 11.02±0.1155, 12.51±0.0088 and 10.03±0.0333, 11.03±0.0881, respectively, which were lower than the standard.

The amount of H^+ ions consumed by 50 mg and 100 mg *S. jollyanum* ethyl acetate were 0.88±0.0033 and 1.01±0.0000 mmoles, whereas 1.20±0.0000 and 1.80±0.0000 mmoles were consumed by sodium bicarbonate at the same levels. For *S. jollyanum n* Hexane and *C. pilosa* aqueous fractions, the no of H^+ ions consumed at 50 mg and 100 mg were observed to be 0.70±0.0033, 0.79±0.0000 and 0.63±0.0033, 0.70±0.0066 (Table 4.14). The higher the volume of artificial gastric juice consumed, the higher the antacid activity.

4.14 Urease inhibition of *C. pilosa* and *S. jollyanum* extracts and fractions

The *in vitro* urease inhibitory activity of *C. pilosa* and *S. jollyanum* extracts and fractions were compared to that of acetohydroxamic acid; a well known urease inhibitor. *C. pilosa* aqueous fraction

gave an IC_{50} of 20.2±0.96 μM which is comparable to the standard, acetohydroxamic acid with an IC_{50} of 19.6±0.34 μM. *Sphenocentrum jollyanum* aqueous fraction, *C. pilosa n* Hexane, and *S. jollyanum n* Hexane fractions gave promising urease inhibitory activity with IC_{50} values of 22.7±0.36 μM, 24.3±0.33 μM, and 25.4±3.02 μM respectively (Table 4.14).

Table 4.13: *In vitro* antacid activity of *Curculigo pilosa* and *Sphenocentrum jollyanum* extracts and fractions

S/No	Extract	Concentration mg/250 mL	pH	Neutralisation Efficiency	Action efficiency (Amount of AGJ consumed mL)	No of H^+ ion consumed
1	$NaHCO_3$	50	8.11	1.53 ± 0.0033	19. 01 ±0.0057 [b]	1.20 ± 0.0000 [a]
		100	8.48	1.47 ± 0.0033	28. 49 ±0.0066 [a]	1.80 ± 0.0000 [a]
2	Water	100	6.19	1.30 ± 0.0033	3.01 ± 0.0057	0.19 ± 0.0000
3	C. *pilosa*	50	6.50	1.47 ± 0.0066	11.10 ± 0.0577 [b]	0.70 ± 0.0057 [b]
	Methanol	100	5.53	1.47 ± 0.0033	9.02 ± 0.0115	0.57 ± 0.0000
4	*S. jollyanum*	50	7.42	1.46 ± 0.0033	6.52 ± 0.0088	0.41 ± 0.0000
	Methanol	100	7.12	1.36 ± 0.0088	8.50 ± 0.0033	0.54 ± 0.0000
5	*C. pilosa*	50	6.88	1.61 ± 0.0033	9.03 ± 0.0033	0.56 ± 0.0021
	Hexane	100	7. 01	1.68 ± 0.0033	9.50 ± 0.0000	0.60 ± 0.0000
6	*C. pilosa*	50	7. 08	1.68 ± 0.0000	10.17 ± 0.8819	0.64 ± 0.035
	DCM	100	6.95	1.74 ± 0.0057	9.50 ± 0.3333	0.60 ± 0.0000
7	*C. pilosa*	50	6.43	1.78 ± 0.0033	11.17 ± 0.8819 [b]	0.70 ± 0.0000 [b]
	Ethyl acetate	100	6.45	1.82 ± 0.0057	9.67 ± 0.8819	0.60 ± 0.0000
8	*C. pilosa*	50	6.74	1.82 ± 0.0000	9.53 ± 0.3333	0.60 ± 0.0577
	Butanol	100	6.85	1.85 ± 0.0066	10. 20 ±0.1155	0.64 ± 0.0088
9	*C. pilosa*	50	6.83	1.86 ± 0.0033	10. 03 ±0.0333	0.63 ± 0.0033
	Aqueous	100	6.92	2.03 ± 0.0033	11. 03 ±0.0881 [b]	0.70 ± 0.0066 [b]
10	*S. jollyanum*	50	7. 00	1.42 ± 0.0088	11.02 ± 0.1155 [b]	0.70 ± 0.0033 [b]
	Hexane	100	7. 02	1. 40 ± 0.0066	12.51 ± 0.0088 [b]	0.79 ± 0.0000 [b]
11	*S. jollyanum*	50	6. 90	1.39 ± 0.0033	10.52 ± 0.0115	0.66 ± 0. 0033
	DCM	100	6.93	1.61 ± 0.0033	10.00 ± 0.0033	0.63 ± 0.0000
12	*S. jollyanum*	50	7.16	1.61 ± 0.0033	14.01 ± 0.0066 [b]	0.88 ± 0.0033 [b]
	Ethyl acetate	100	7.26	1.53 ± 0.0033	16.02 ± 0.0115 [b]	1.01 ± 0.0000 [b]
13	*S. jollyanum*	50	7.45	1.51 ± 0.0033	5.10 ± 0.0577	0.32 ± 0.0033
	Butanol	100	7.45	1.50 ± 0.0033	9. 10 ± 0.0577	0.57 ± 0.0033
14	*S. jollyanum*	50	7.45	1.50 ± 0.0033	9. 08 ± 0.0611	0.57 ± 0.0033
	Aqueous	100	7.49	1.50 ± 0.0057	9. 01 ±0.0057	0.57 0.0000

[a] $p < 0.05$ when compared with control, [b] $p < 0.05$ when compared with standard

Table 4.14: Urease inhibition (IC_{50}) of *Curculigo pilosa* and *Sphenocentrum jollyanum* extracts and fractions

Sample	Concentration (mM)	IC_{50} ± SEM (μM)
S. jollyanum MeOH	0.5	40.0 ± 0.92
S. jollyanum n Hexane	0.5	25.4 ± 3.02
S. jollyanum Dichloromethane	0.5	------
S. jollyanum Ethyl acetate	0.5	------
S. jollyanum n Butanol	0.5	28.6 ± 0.41
S. jollyanum Aqueous	0.5	22.7 ± 0.36
C. pilosa MeOH	0.5	-------
C. pilosa n Hexane	0.5	24.3 ± 0.33
C. pilosa Dichloromethane	0.5	-------
C. pilosa Ethyl acetate	0.5	-------
C. pilosa n Butanol	0.5	-------
C. pilosa Aqueous	0.5	20.2 ± 0.96
Acetohydroxamic acid	0.5	19.6 ± 0.34

Footnote: ------: Fraction is inactive at 0.5 mg concentration

4.15 Column chromatography of *Sphenocentrum jollyanum* ethyl acetate fraction

The column chromatography of *Sphenocentrum jollyanum* ethyl acetate fraction which was selected based on its antacid activity yielded 290 fractions of 100 mL each (Table 4.15a) which were spotted on TLC plate using different solvent systems (*n* Hexane: EtOAc, DCM: MeOH, *n* Hexane: EtOAc: MeOH) and pooled based on the TLC profile to afford 28 sub-fractions with codes SJE-1 to SJE-28 (Table 4.15b).

4.16 Column chromatography of *Curculigo pilosa* ethyl acetate fraction

The column chromatography of *C. pilosa* ethyl acetate fraction which was selected based on its antacid activity yielded 163 fractions of 100 mL each (Table 4.16) which were spotted on TLC plate using different solvent systems (*n* Hexane: DCM: MeOH) and pooled to afford 13 sub-fractions based on the TLC profile.

4.17 Column chromatography of *Sphenocentrum jollyanum n* Butanol fraction

The *S. jollyanum n* Butanol fraction which was selected based on its urease inhibitory activity yielded 170 fractions of 100 mL each (Table 4.17) which were spotted on TLC plate using different solvent systems (*n* Hexane: Chloroform: MeOH) and pooled to afford 15 sub-fractions based on the TLC profile.

4.18 Column chromatography of *Sphenocentrum jollyanum n* Hexane fraction

The column chromatography of *S. jollyanum* ethyl acetate fraction which was selected based on its urease inhibitory activity yielded 72 fractions of 100 mL each (Table 4.18) which were spotted on TLC plate using different solvent systems (*n* Hexane: EtOAc) and pooled to afford 9 sub-fractions based on the TLC profile.

Table 4.15a: Column chromatography of *Sphenocentrum jollyanum* ethyl acetate fraction

Fractions	Solvent mixture	Ratio (%)	Colour under UV (254 nm)	Colour under UV (366 nm)
1	*n* Hexane	100	-	-
2	*n* Hexane	100	-	-
3	*n* Hexane	100	-	-
4	*n* Hexane	100	-	-
5	*n* Hexane	100	-	-
6	*n* Hexane: Dichloromethane	90: 10	-	-
7	*n* Hexane: Dichloromethane	90: 10	-	-
8	*n* Hexane: Dichloromethane	90: 10	-	-
9	*n* Hexane: Dichloromethane	90: 10	-	-
10	*n* Hexane: Dichloromethane	90: 10	-	-
11	*n* Hexane: Dichloromethane	80: 20	-	-
12	*n* Hexane: Dichloromethane	80: 20	-	-
13	*n* Hexane: Dichloromethane	80: 20	-	-
14	*n* Hexane: Dichloromethane	80: 20	-	-
15	*n* Hexane: Dichloromethane	80: 20	-	-
16	*n* Hexane: Dichloromethane	80: 20	-	-
17	*n* Hexane: Dichloromethane	80: 20	-	-
18	*n* Hexane: Dichloromethane	50: 50	brown	-
19	*n* Hexane: Dichloromethane	50: 50	brown	-
20	*n* Hexane: Dichloromethane	50: 50	brown	-
21	*n* Hexane: Dichloromethane	50: 50	brown	-
22	*n* Hexane: Dichloromethane	50: 50	brown	-
23	*n* Hexane: Dichloromethane	50: 50	brown	-
24	*n* Hexane: Dichloromethane	50: 50	brown	-
25	*n* Hexane: Dichloromethane	50: 50	brown	-
26	*n* Hexane: Dichloromethane	50: 50	brown	-
27	*n* Hexane: Dichloromethane	50: 50	brown	-
28	*n* Hexane: Dichloromethane	50: 50	brown	-
29	*n* Hexane: Dichloromethane	50: 50	brown	-
30	*n* Hexane: Dichloromethane	50: 50	brown	-
31	*n* Hexane: Dichloromethane	50: 50	brown	-
32	*n* Hexane: Dichloromethane	50: 50	brown	-
33	*n* Hexane: Dichloromethane	50: 50	brown	-
34	*n* Hexane: Dichloromethane	50: 50	brown	-
35	*n* Hexane: Dichloromethane	50: 50	brown	-
36	*n* Hexane: Dichloromethane	50: 50	brown	-

Table 4.15a contd.

Fractions	Solvent mixture	Ratio (%)	Colour under UV (254 nm)	Colour under UV (366 nm)
37	*n* Hexane: Dichloromethane	50: 50	brown	-
38	*n* Hexane: Dichloromethane	50: 50	brown	-
39	*n* Hexane: Dichloromethane	50: 50	brown	-
40	*n* Hexane: Dichloromethane	50: 50	brown	-
41	*n* Hexane: Dichloromethane	50: 50	brown	-
42	*n* Hexane: Dichloromethane	50: 50	brown	-
43	*n* Hexane: Dichloromethane	50: 50	brown	-
44	*n* Hexane: Dichloromethane	50: 50	brown	-
45	*n* Hexane: Dichloromethane	50: 50	brown	-
46	*n* Hexane: Dichloromethane	30: 70	-	-
47	*n* Hexane: Dichloromethane	30: 70	-	-
48	*n* Hexane: Dichloromethane	30: 70	-	-
49	*n* Hexane: Dichloromethane	30: 70	-	-
50	*n* Hexane: Dichloromethane	30: 70	-	-
51	*n* Hexane: Dichloromethane	30: 70	-	-
52	*n* Hexane: Dichloromethane	30: 70	-	-
53	*n* Hexane: Dichloromethane	30: 70	-	-
54	*n* Hexane: Dichloromethane	30: 70	-	-
55	*n* Hexane: Dichloromethane	30: 70	-	-
56	*n* Hexane: Dichloromethane	30: 70	-	-
57	*n* Hexane: Dichloromethane	30: 70	-	-
58	*n* Hexane: Dichloromethane	30: 70	-	-
59	*n* Hexane: Dichloromethane	30: 70	-	-
60	*n* Hexane: Dichloromethane	20:80	brown	-
61	*n* Hexane: Dichloromethane	20:80	brown	-
62	*n* Hexane: Dichloromethane	20:80	brown	-
63	*n* Hexane: Dichloromethane	20:80	brown	-
64	*n* Hexane: Dichloromethane	20:80	brown	-
65	*n* Hexane: Dichloromethane	20:80	brown	-
66	*n* Hexane: Dichloromethane	20:80	brown	-
67	*n* Hexane: Dichloromethane	20:80	brown	-
68	*n* Hexane: Dichloromethane	20:80	brown	-
69	*n* Hexane: Dichloromethane	20:80	brown	-
70	*n* Hexane: Dichloromethane	20:80	brown	-
71	*n* Hexane: Dichloromethane	20:80	brown	-
72	*n* Hexane: Dichloromethane	20:80	brown	-

Table 4.15a contd.

Fractions	Solvent mixture	Ratio (%)	Colour under UV (254 nm)	Colour under UV (366 nm)
73	*n* Hexane: Dichloromethane	10: 90	brown	-
74	*n* Hexane: Dichloromethane	10: 90	brown	-
75	*n* Hexane: Dichloromethane	10: 90	brown	-
76	*n* Hexane: Dichloromethane	10: 90	brown	-
77	*n* Hexane: Dichloromethane	10: 90	brown	-
78	*n* Hexane: Dichloromethane	10: 90	brown	-
79	*n* Hexane: Dichloromethane	10: 90	brown	-
80	*n* Hexane: Dichloromethane	10: 90	brown	-
81	Dichloromethane	100	brown	-
82	Dichloromethane	100	brown	-
83	Dichloromethane	100	brown	-
84	Dichloromethane	100	brown	-
85	Dichloromethane	100	brown	-
86	Dichloromethane	100	brown	-
87	Dichloromethane	100	brown	-
88	Dichloromethane	100	brown	-
89	Dichloromethane	100	-	-
90	Dichloromethane	100	-	-
91	Dichloromethane	100	-	-
92	Dichloromethane	100	-	-
93	Dichloromethane	100	-	-
94	Dichloromethane	100	-	-
95	Dichloromethane	100	-	-
96	Dichloromethane: MeOH	99.5: 0.5	-	-
97	Dichloromethane: MeOH	99.5: 0.5	-	-
98	Dichloromethane: MeOH	99.5: 0.5	-	-
99	Dichloromethane: MeOH	99.5: 0.5	-	-
100	Dichloromethane: MeOH	99.5: 0.5	-	-
101	Dichloromethane: MeOH	99.5: 0.5	-	-
102	Dichloromethane: MeOH	99.5: 0.5	-	-
103	Dichloromethane: MeOH	99: 1	brown	-
104	Dichloromethane: MeOH	99: 1	brown	-
105	Dichloromethane: MeOH	99: 1	brown	-
106	Dichloromethane: MeOH	99: 1	brown	-
107	Dichloromethane: MeOH	99: 1	brown	-
108	Dichloromethane: MeOH	99: 1	brown	-

Table 4.15a contd.

Fractions	Solvent mixture	Ratio (%)	Colour under UV (254 nm)	Colour under UV (366 nm)
109	Dichloromethane: MeOH	99: 1	brown	-
110	Dichloromethane: MeOH	99: 1	brown	-
111	Dichloromethane: MeOH	99: 1	brown	-
112	Dichloromethane: MeOH	99: 1	brown	-
113	Dichloromethane: MeOH	99: 1	brown	-
114	Dichloromethane: MeOH	99: 1	brown	-
115	Dichloromethane: MeOH	99: 1	brown	-
116	Dichloromethane: MeOH	99: 1	brown	-
117	Dichloromethane: MeOH	99: 1	brown	-
118	Dichloromethane: MeOH	99: 1	brown	-
119	Dichloromethane: MeOH	99: 1	brown	-
120	Dichloromethane: MeOH	99: 1	brown	-
121	Dichloromethane: MeOH	99: 1	brown	-
122	Dichloromethane: MeOH	99: 1	brown	-
123	Dichloromethane: MeOH	99: 1	brown	-
124	Dichloromethane: MeOH	98: 2	brown	-
125	Dichloromethane: MeOH	98: 2	brown	-
126	Dichloromethane: MeOH	98: 2	brown	-
127	Dichloromethane: MeOH	98: 2	brown	-
128	Dichloromethane: MeOH	98: 2	brown	-
129	Dichloromethane: MeOH	98: 2	brown	-
130	Dichloromethane: MeOH	98: 2	brown	-
131	Dichloromethane: MeOH	95: 5	brown	-
132	Dichloromethane: MeOH	95: 5	brown	-
133	Dichloromethane: MeOH	95: 5	brown	-
134	Dichloromethane: MeOH	95: 5	brown	-
135	Dichloromethane: MeOH	95: 5	brown	-
136	Dichloromethane: MeOH	95: 5	brown	-
137	Dichloromethane: MeOH	95: 5	brown	-
138	Dichloromethane: MeOH	95: 5	brown	-
139	Dichloromethane: MeOH	95: 5	brown	-
140	Dichloromethane: MeOH	95: 5	brown	-
141	Dichloromethane: MeOH	95: 5	brown	-
142	Dichloromethane: MeOH	95: 5	brown	-
143	Dichloromethane: MeOH	95: 5	brown	-
144	Dichloromethane: MeOH	95: 5	brown	-

Table 4.15a contd.

Fractions	Solvent mixture	Ratio (%)	Colour under UV (254 nm)	Colour under UV (366 nm)
145	Dichloromethane: MeOH	95: 5	brown	-
146	Dichloromethane: MeOH	95: 5	brown	-
147	Dichloromethane: MeOH	95: 5	brown	-
148	Dichloromethane: MeOH	95: 5	brown	-
149	Dichloromethane: MeOH	95: 5	brown	-
150	Dichloromethane: MeOH	95: 5	brown	-
151	Dichloromethane: MeOH	95: 5	brown	-
152	Dichloromethane: MeOH	95: 5	brown	-
153	Dichloromethane: MeOH	95: 5	brown	-
154	Dichloromethane: MeOH	95: 5	brown	-
155	Dichloromethane: MeOH	95: 5	-	-
156	Dichloromethane: MeOH	95: 5	-	-
157	Dichloromethane: MeOH	95: 5	-	-
158	Dichloromethane: MeOH	95: 5	-	-
159	Dichloromethane: MeOH	95: 5	-	-
160	Dichloromethane: MeOH	95: 5	-	-
161	Dichloromethane: MeOH	95: 5	-	-
162	Dichloromethane: MeOH	95: 5	-	-
163	Dichloromethane: MeOH	95: 5	-	-
164	Dichloromethane: MeOH	95: 5	-	-
165	Dichloromethane: MeOH	95: 5	-	-
166	Dichloromethane: MeOH	95: 5	-	-
167	Dichloromethane: MeOH	95: 5	-	-
168	Dichloromethane: MeOH	95: 5	-	-
169	Dichloromethane: MeOH	95: 5	-	-
170	Dichloromethane: MeOH	95: 5	-	-
171	Dichloromethane: MeOH	95: 5	-	-
172	Dichloromethane: MeOH	95: 5	-	-
173	Dichloromethane: MeOH	95: 5	-	-
174	Dichloromethane: MeOH	95: 5	-	-
175	Dichloromethane: MeOH	95: 5	-	-
176	Dichloromethane: MeOH	95: 5	-	-
177	Dichloromethane: MeOH	95: 5	-	-
178	Dichloromethane: MeOH	95: 5	-	-
179	Dichloromethane: MeOH	95: 5	-	-
180	Dichloromethane: MeOH	95: 5	-	-

Table 4.15a contd.

Fractions	Solvent mixture	Ratio (%)	Colour under UV (254 nm)	Colour under UV (366 nm)
181	Dichloromethane: MeOH	95: 5	brown	-
182	Dichloromethane: MeOH	95: 5	brown	-
183	Dichloromethane: MeOH	95: 5	brown	-
184	Dichloromethane: MeOH	95: 5	brown	-
185	Dichloromethane: MeOH	95: 5	brown	-
186	Dichloromethane: MeOH	95: 5	brown	-
187	Dichloromethane: MeOH	95: 5	brown	-
188	Dichloromethane: MeOH	95: 5	brown	-
189	Dichloromethane: MeOH	95: 5	brown	-
190	Dichloromethane: MeOH	93: 7	brown	-
191	Dichloromethane: MeOH	93: 7	brown	-
192	Dichloromethane: MeOH	93: 7	brown	-
193	Dichloromethane: MeOH	93: 7	brown	-
194	Dichloromethane: MeOH	93: 7	brown	-
195	Dichloromethane: MeOH	93: 7	brown	-
196	Dichloromethane: MeOH	93: 7	brown	-
197	Dichloromethane: MeOH	93: 7	-	-
198	Dichloromethane: MeOH	93: 7	-	-
199	Dichloromethane: MeOH	93: 7	-	-
200	Dichloromethane: MeOH	93: 7	-	-
201	Dichloromethane: MeOH	93: 7	-	-
202	Dichloromethane: MeOH	93: 7	-	-
203	Dichloromethane: MeOH	93: 7	-	-
204	Dichloromethane: MeOH	93: 7	-	-
205	Dichloromethane: MeOH	93: 7	-	-
206	Dichloromethane: MeOH	93: 7	-	-
207	Dichloromethane: MeOH	93: 7	-	-
208	Dichloromethane: MeOH	93: 7	-	-
209	Dichloromethane: MeOH	93: 7	-	-
210	Dichloromethane: MeOH	93: 7	brown	-
211	Dichloromethane: MeOH	93: 7	brown	-
212	Dichloromethane: MeOH	93: 7	brown	-
213	Dichloromethane: MeOH	93: 7	brown	-
214	Dichloromethane: MeOH	93: 7	brown	-
215	Dichloromethane: MeOH	93: 7	brown	-
216	Dichloromethane: MeOH	93: 7	brown	-

Table 4.15a contd.

Fractions	Solvent mixture	Ratio (%)	Colour under UV (254 nm)	Colour under UV (366 nm)
217	Dichloromethane: MeOH	93: 7	brown	-
218	Dichloromethane: MeOH	93: 7	brown	-
219	Dichloromethane: MeOH	93: 7	brown	-
220	Dichloromethane: MeOH	93: 7	-	-
221	Dichloromethane: MeOH	93: 7	-	-
222	Dichloromethane: MeOH	93: 7	-	-
223	Dichloromethane: MeOH	93: 7	-	-
224	Dichloromethane: MeOH	93: 7	-	-
225	Dichloromethane: MeOH	93: 7	-	-
226	Dichloromethane: MeOH	93: 7	brown	-
227	Dichloromethane: MeOH	93: 7	brown	-
228	Dichloromethane: MeOH	90: 10	brown	-
229	Dichloromethane: MeOH	90: 10	brown	-
230	Dichloromethane: MeOH	90: 10	brown	-
231	Dichloromethane: MeOH	90: 10	brown	-
232	Dichloromethane: MeOH	90: 10	brown	-
233	Dichloromethane: MeOH	90: 10	-	-
234	Dichloromethane: MeOH	90: 10	-	-
235	Dichloromethane: MeOH	90: 10	-	-
236	Dichloromethane: MeOH	90: 10	-	-
237	Dichloromethane: MeOH	90: 10	-	-
238	Dichloromethane: MeOH	90: 10	-	-
239	Dichloromethane: MeOH	90: 10	-	-
240	Dichloromethane: MeOH	90: 10	-	-
241	Dichloromethane: MeOH	90: 10	-	-
242	Dichloromethane: MeOH	90: 10	-	-
243	Dichloromethane: MeOH	90: 10	-	-
244	Dichloromethane: MeOH	90: 10	-	-
245	Dichloromethane: MeOH	90: 10	-	-
246	Dichloromethane: MeOH	90: 10	-	-
247	Dichloromethane: MeOH	90: 10	-	-
248	Dichloromethane: MeOH	90: 10	-	-
249	Dichloromethane: MeOH	90: 10	-	-
250	Dichloromethane: MeOH	80: 20	-	-
251	Dichloromethane: MeOH	80: 20	-	-
252	Dichloromethane: MeOH	80: 20	-	-

Table 4.15a contd.

Fractions	Solvent mixture	Ratio (%)	Colour under UV (254 nm)	Colour under UV (366 nm)
253	Dichloromethane: MeOH	80: 20	-	-
254	Dichloromethane: MeOH	80: 20	-	-
255	Dichloromethane: MeOH	80: 20	-	-
256	Dichloromethane: MeOH	80: 20	-	-
257	Dichloromethane: MeOH	80: 20	-	-
258	Dichloromethane: MeOH	80: 20	-	-
259	Dichloromethane: MeOH	80: 20	-	-
260	Dichloromethane: MeOH	80: 20	-	-
261	Dichloromethane: MeOH	80: 20	-	-
262	Dichloromethane: MeOH	80: 20	brown	-
263	Dichloromethane: MeOH	80: 20	brown	-
264	Dichloromethane: MeOH	80: 20	brown	-
265	Dichloromethane: MeOH	80: 20	brown	-
266	Dichloromethane: MeOH	80: 20	brown	-
267	Dichloromethane: MeOH	80: 20	brown	-
268	Dichloromethane: MeOH	70: 30	brown	-
269	Dichloromethane: MeOH	70: 30	-	-
270	Dichloromethane: MeOH	70: 30	-	-
271	Dichloromethane: MeOH	70: 30	-	-
272	Dichloromethane: MeOH	70: 30	-	-
273	Dichloromethane: MeOH	70: 30	-	-
274	Dichloromethane: MeOH	70: 30	-	-
275	Dichloromethane: MeOH	70: 30	-	-
276	Dichloromethane: MeOH	70: 30	-	-
277	Dichloromethane: MeOH	70: 30	-	-
278	Dichloromethane: MeOH	70: 30	-	-
279	Dichloromethane: MeOH	70: 30	-	-
280	Dichloromethane: MeOH	70: 30	-	-
281	Dichloromethane: MeOH	70: 30	-	-
282	Dichloromethane: MeOH	70: 30	-	-
283	Dichloromethane: MeOH	70: 30	-	-
284	Dichloromethane: MeOH	70: 30	-	-
285	Dichloromethane: MeOH	50: 50	-	-
286	Dichloromethane: MeOH	50: 50	-	-
287	Dichloromethane: MeOH	50: 50	-	-
288	Dichloromethane: MeOH	50: 50	-	-
289	Dichloromethane: MeOH	50: 50	-	-
290	Dichloromethane: MeOH	50: 50	-	-

Table 4.15b: The TLC profile of pooled fractions and their respective codes

Code	Pooled fractions	Number of spots	Weight (g)	TLC Solvent systems
SJE-1	1-3	-	0.12	*n* Hexane: DCM: MeOH
SJE-2	4-6	-	0.09	*n* Hexane: DCM: MeOH
SJE-3	7-10	-	0.10	*n* Hexane: DCM: MeOH
SJE-4	11-17	4	0.31	*n* Hexane: DCM: MeOH
SJE-5	18-37	4	0.30	*n* Hexane: DCM: MeOH
SJE-6	38-45	4	0.30	*n* Hexane: DCM: MeOH
SJE-7	46-59	4	0.28	*n* Hexane: DCM: MeOH
SJE-8	60-72	3	0.39	*n* Hexane: DCM: MeOH
SJE-9	73-80	3	0.56	*n* Hexane: DCM: MeOH
SJE-10	81-88	2	1.02	*n* Hexane: DCM: MeOH
SJE-11	81-95	2	0.48	DCM: MeOH
SJE-12	96-102	2	0.48	DCM: MeOH
SJE-13	103-123	4	0.39	DCM: MeOH
SJE-14	124-130	4	0.07	DCM: MeOH
SJE-15	131-135	6	0.82	DCM: MeOH
SJE-16	136-140	6	0.36	DCM: MeOH
SJE-17	141-145	5	0.61	DCM: MeOH
SJE-18	146-154	5	0.47	DCM: MeOH
SJE-19	155-162	4	0.56	*n* Hexane: $CHCl_3$: MeOH
SJE-20	163-171	4	0.60	*n* Hexane: $CHCl_3$: MeOH
SJE-21	172-180	3	0.80	*n* Hexane: $CHCl_3$: MeOH
SJE-22	181-196	3	0.77	*n* Hexane: $CHCl_3$: MeOH
SJE-23	197-227	2	0.80	*n* Hexane: $CHCl_3$: MeOH
SJE-24	228-249	3	0.37	*n* Hexane: $CHCl_3$: MeOH
SJE-25	250-253	4	0.53	*n* Hexane: $CHCl_3$: MeOH
SJE-26	254-267	4	0.42	*n* Hexane: $CHCl_3$: MeOH
SJE-27	268-284	4	0.42	*n* Hexane: $CHCl_3$: MeOH
SJE-28	285-290	2	0.39	*n* Hexane: $CHCl_3$: MeOH

Table 4.16: Column chromatography of *Curculigo pilosa* ethyl acetate fraction

Fractions	Solvent mixture	Ratio (%)	Colour under UV (254 nm)	Colour under UV (366 nm)
1	*n* Hexane	100	-	-
2	*n* Hexane	100	-	-
3	*n* Hexane: Dichloromethane	50: 50	-	-
4	*n* Hexane: Dichloromethane	50: 50	-	-
5	*n* Hexane: Dichloromethane	50: 50	-	-
6	*n* Hexane: Dichloromethane	50: 50	-	-
7	*n* Hexane: Dichloromethane	30: 70	-	-
8	*n* Hexane: Dichloromethane	30: 70	-	-
9	*n* Hexane: Dichloromethane	30: 70	-	-
10	*n* Hexane: Dichloromethane	30: 70	-	-
11	*n* Hexane: Dichloromethane	20: 80	-	Sky blue
12	*n* Hexane: Dichloromethane	20: 80	-	Sky blue
13	*n* Hexane: Dichloromethane	20: 80	-	Sky blue
14	*n* Hexane: Dichloromethane	20: 80	-	Sky blue
15	*n* Hexane: Dichloromethane	20: 80	-	Sky blue
16	*n* Hexane: Dichloromethane	20: 80	-	Sky blue
17	*n* Hexane: Dichloromethane	20: 80	-	Sky blue
18	*n* Hexane: Dichloromethane	20: 80	-	Sky blue
19	Dichloromethane	100	-	-
20	Dichloromethane	100	-	-
21	Dichloromethane	100	-	-
22	Dichloromethane	100	-	-
23	Dichloromethane	100	-	-
24	Dichloromethane	100	-	-
25	Dichloromethane	100	-	-
26	Dichloromethane	100	-	-
27	Dichloromethane	100	-	-
28	Dichloromethane	100	-	-
29	Dichloromethane	100	-	-
30	Dichloromethane	100	-	-
31	Dichloromethane: MeOH	99: 1	-	-
32	Dichloromethane: MeOH	99: 1	-	-
33	Dichloromethane: MeOH	99: 1	-	-
34	Dichloromethane: MeOH	99: 1	-	-
35	Dichloromethane: MeOH	98: 2	Brown	-
36	Dichloromethane: MeOH	98: 2	Brown	-

Table 4.16 contd.

Fractions	Solvent mixture	Ratio (%)	Colour under UV (254 nm)	Colour under UV (366 nm)
37	Dichloromethane: MeOH	98: 2	Brown	-
38	Dichloromethane: MeOH	98: 2	Brown	-
39	Dichloromethane: MeOH	98: 2	Brown	-
40	Dichloromethane: MeOH	98: 2	Brown	-
41	Dichloromethane: MeOH	98: 2	Brown	-
42	Dichloromethane: MeOH	98: 2	Brown	-
43	Dichloromethane: MeOH	98: 2	Brown	-
44	Dichloromethane: MeOH	98: 2	Brown	-
45	Dichloromethane: MeOH	98: 2	Brown	-
46	Dichloromethane: MeOH	98: 2	Brown	-
47	Dichloromethane: MeOH	98: 2	Brown	-
48	Dichloromethane: MeOH	98: 2	Brown	-
49	Dichloromethane: MeOH	98: 2	Brown	-
50	Dichloromethane: MeOH	98: 2	Brown	-
51	Dichloromethane: MeOH	98: 2	Brown	-
52	Dichloromethane: MeOH	98: 2	Brown	-
53	Dichloromethane: MeOH	98: 2	Brown	-
54	Dichloromethane: MeOH	98: 2	Brown	-
55	Dichloromethane: MeOH	98: 2	Brown	-
56	Dichloromethane: MeOH	98: 2	Brown	-
57	Dichloromethane: MeOH	98: 2	Brown	-
58	Dichloromethane: MeOH	98: 2	Brown	-
59	Dichloromethane: MeOH	98: 2	Brown	-
60	Dichloromethane: MeOH	98: 2	Brown	-
61	Dichloromethane: MeOH	98: 2	Brown	-
62	Dichloromethane: MeOH	98: 2	Brown	-
63	Dichloromethane: MeOH	98: 2	Brown	-
64	Dichloromethane: MeOH	98: 2	Brown	-
65	Dichloromethane: MeOH	98: 2	Brown	-
66	Dichloromethane: MeOH	98: 2	Brown	-
67	Dichloromethane: MeOH	98: 2	Brown	-
68	Dichloromethane: MeOH	98: 2	Brown	-
69	Dichloromethane: MeOH	98: 2	Brown	-
70	Dichloromethane: MeOH	98: 2	Brown	-
71	Dichloromethane: MeOH	98: 2	Brown	-
72	Dichloromethane: MeOH	98: 2	Brown	-

Table 4.16 contd.

Fractions	Solvent mixture	Ratio (%)	Colour under UV (254 nm)	Colour under UV (366 nm)
73	Dichloromethane: MeOH	95: 5	Brown	-
74	Dichloromethane: MeOH	95: 5	Brown	-
75	Dichloromethane: MeOH	95: 5	Brown	-
76	Dichloromethane: MeOH	95: 5	Brown	-
77	Dichloromethane: MeOH	95: 5	Brown	-
78	Dichloromethane: MeOH	95: 5	Brown	-
79	Dichloromethane: MeOH	95: 5	Brown	-
80	Dichloromethane: MeOH	95: 5	Brown	-
81	Dichloromethane: MeOH	95: 5	Brown	-
82	Dichloromethane: MeOH	95: 5	Brown	-
83	Dichloromethane: MeOH	95: 5	Brown	-
84	Dichloromethane: MeOH	95: 5	Brown	-
85	Dichloromethane: MeOH	95: 5	Purple	-
86	Dichloromethane: MeOH	95: 5	Purple	-
87	Dichloromethane: MeOH	95: 5	Purple	-
88	Dichloromethane: MeOH	95: 5	Purple	-
89	Dichloromethane: MeOH	95: 5	Purple	-
90	Dichloromethane: MeOH	95: 5	Purple	-
91	Dichloromethane: MeOH	93: 7	-	-
92	Dichloromethane: MeOH	93: 7	-	-
93	Dichloromethane: MeOH	93: 7	-	-
94	Dichloromethane: MeOH	93: 7	-	-
95	Dichloromethane: MeOH	93: 7	-	-
96	Dichloromethane: MeOH	93: 7	-	-
97	Dichloromethane: MeOH	93: 7	-	-
98	Dichloromethane: MeOH	93: 7	-	-
99	Dichloromethane: MeOH	93: 7	-	-
100	Dichloromethane: MeOH	93: 7	-	-
101	Dichloromethane: MeOH	93: 7	-	-
102	Dichloromethane: MeOH	93: 7	-	-
103	Dichloromethane: MeOH	90: 10	-	-
104	Dichloromethane: MeOH	90: 10	-	-
105	Dichloromethane: MeOH	90: 10	-	-
106	Dichloromethane: MeOH	90: 10	-	-
107	Dichloromethane: MeOH	90: 10	-	-
108	Dichloromethane: MeOH	90: 10	-	-

Table 4.16 contd.

Fractions	Solvent mixture	Ratio (%)	Colour under UV (254 nm)	Colour under UV (366 nm)
109	Dichloromethane: MeOH	90: 10	Brown	-
110	Dichloromethane: MeOH	90: 10	Brown	-
111	Dichloromethane: MeOH	80: 20	Brown	-
112	Dichloromethane: MeOH	80: 20	Brown	-
113	Dichloromethane: MeOH	80: 20	Brown	-
114	Dichloromethane: MeOH	80: 20	Brown	-
115	Dichloromethane: MeOH	80: 20	Brown	-
116	Dichloromethane: MeOH	80: 20	Brown	-
117	Dichloromethane: MeOH	80: 20	Brown	-
118	Dichloromethane: MeOH	80: 20	Brown	-
119	Dichloromethane: MeOH	80: 20	Brown	-
120	Dichloromethane: MeOH	80: 20	Brown	-
121	Dichloromethane: MeOH	80: 20	Brown	-
122	Dichloromethane: MeOH	80: 20	Brown	-
123	Dichloromethane: MeOH	80: 20	Brown	-
124	Dichloromethane: MeOH	80: 20	Brown	-
125	Dichloromethane: MeOH	80: 20	Brown	-
126	Dichloromethane: MeOH	80: 20	Brown	-
127	Dichloromethane: MeOH	80: 20	Brown	-
128	Dichloromethane: MeOH	80: 20	Brown	-
129	Dichloromethane: MeOH	80: 20	Brown	-
130	Dichloromethane: MeOH	80: 20	Brown	-
131	Dichloromethane: MeOH	70: 30	Brown	-
132	Dichloromethane: MeOH	70: 30	Brown	-
133	Dichloromethane: MeOH	70: 30	Brown	-
134	Dichloromethane: MeOH	70: 30	Brown	-
135	Dichloromethane: MeOH	70: 30	Brown	-
136	Dichloromethane: MeOH	70: 30	Brown	-
137	Dichloromethane: MeOH	70: 30	Brown	-
138	Dichloromethane: MeOH	70: 30	Brown	-
139	Dichloromethane: MeOH	70: 30	Brown	-
140	Dichloromethane: MeOH	70: 30	Brown	-
141	Dichloromethane: MeOH	60: 40	Brown	-
142	Dichloromethane: MeOH	60: 40	Brown	-
143	Dichloromethane: MeOH	60: 40	Brown	-
144	Dichloromethane: MeOH	60: 40	Brown	-

Table 4.16 contd.

Fractions	Solvent mixture	Ratio (%)	Colour under UV (254 nm)	Colour under UV (366 nm)
145	Dichloromethane: MeOH	60: 40	Brown	-
146	Dichloromethane: MeOH	60: 40	Brown	-
147	Dichloromethane: MeOH	60: 40	Brown	-
148	Dichloromethane: MeOH	60: 40	Brown	-
149	Dichloromethane: MeOH	60: 40	Brown	-
150	Dichloromethane: MeOH	60: 40	Brown	-
151	Dichloromethane: MeOH	60: 40	Brown	-
152	Dichloromethane: MeOH	60: 40	Brown	-
153	Dichloromethane: MeOH	60: 40	Brown	-
154	Dichloromethane: MeOH	60: 40	Brown	-
155	Dichloromethane: MeOH	60: 40	Brown	-
156	Dichloromethane: MeOH	60: 40	Brown	-
157	Dichloromethane: MeOH	60: 40	Brown	-
158	Dichloromethane: MeOH	60: 40	Brown	-
159	Dichloromethane: MeOH	60: 40	Brown	-
160	Dichloromethane: MeOH	60: 40	Brown	-
161	Dichloromethane: MeOH	60: 40	Brown	-
162	Dichloromethane: MeOH	60: 40	Brown	-
163	Dichloromethane: MeOH	60: 40	Brown	-

Table 4.17: Column chromatography of *Sphenocentrum jollyanum n* Butanol fraction

Fractions	Solvent mixture	Ratio (%)	Colour under UV (254 nm)	Colour under UV (366 nm)
1	*n* Hexane: Dichloromethane	50: 50	-	-
2	*n* Hexane: Dichloromethane	50: 50	-	-
3	*n* Hexane: Dichloromethane	50: 50	-	-
4	*n* Hexane: Dichloromethane	30: 70	Purple	-
5	*n* Hexane: Dichloromethane	30: 70	Purple	-
6	*n* Hexane: Dichloromethane	30: 70	Purple	-
7	*n* Hexane: Dichloromethane	30: 70	Purple	-
8	*n* Hexane: Dichloromethane	30: 70	Purple	-
9	*n* Hexane: Dichloromethane	30: 70	Purple	-
10	*n* Hexane: Dichloromethane	30: 70	Purple	-
11	*n* Hexane: Dichloromethane	30: 70	Purple	-
12	*n* Hexane: Dichloromethane	30: 70	Purple	-
13	*n* Hexane: Dichloromethane	30: 70	Purple	-
14	*n* Hexane: Dichloromethane	30: 70	Purple	-
15	*n* Hexane: Dichloromethane	30: 70	Purple	-
16	*n* Hexane: Dichloromethane	30: 70	Purple	-
17	*n* Hexane: Dichloromethane	30: 70	Purple	-
18	*n* Hexane: Dichloromethane	30: 70	Purple	-
19	*n* Hexane: Dichloromethane	30: 70	Purple	-
20	*n* Hexane: Dichloromethane	30: 70	Purple	-
21	*n* Hexane: Dichloromethane	30: 70	Purple	-
22	*n* Hexane: Dichloromethane	30: 70	Purple	-
23	*n* Hexane: Dichloromethane	30: 70	Purple	-
24	*n* Hexane: Dichloromethane	30: 70	Purple	-
25	*n* Hexane: Dichloromethane	30: 70	Purple	-
26	*n* Hexane: Dichloromethane	30: 70	Purple	-
27	*n* Hexane: Dichloromethane	30: 70	Purple	-
28	*n* Hexane: Dichloromethane	30: 70	Purple	-
29	*n* Hexane: Dichloromethane	30: 70	Purple	-
30	*n* Hexane: Dichloromethane	30: 70	Purple	-
31	*n* Hexane: Dichloromethane	30: 70	Purple	-
32	*n* Hexane: Dichloromethane	30: 70	Purple	-
33	*n* Hexane: Dichloromethane	30: 70	Purple	-
34	*n* Hexane: Dichloromethane	30: 70	Purple	-
35	*n* Hexane: Dichloromethane	30: 70	Purple	-
36	*n* Hexane: Dichloromethane	30: 70	Purple	-

Table 4.17 contd.

Fractions	Solvent mixture	Ratio (%)	Colour under UV (254 nm)	Colour under UV (366 nm)
37	*n* Hexane: Dichloromethane	30: 70	-	-
38	*n* Hexane: Dichloromethane	10: 90	-	-
39	*n* Hexane: Dichloromethane	10: 90	-	-
40	*n* Hexane: Dichloromethane	10: 90	Yellow	-
41	*n* Hexane: Dichloromethane	10: 90	Yellow	-
42	*n* Hexane: Dichloromethane	10: 90	Yellow	-
43	*n* Hexane: Dichloromethane	10: 90	Yellow	-
44	*n* Hexane: Dichloromethane	10: 90	Yellow	-
45	*n* Hexane: Dichloromethane	10: 90	Yellow	-
46	*n* Hexane: Dichloromethane	10: 90	Yellow	-
47	*n* Hexane: Dichloromethane	10: 90	Yellow	-
48	*n* Hexane: Dichloromethane	10: 90	Yellow	-
49	*n* Hexane: Dichloromethane	10: 90	Yellow	-
50	*n* Hexane: Dichloromethane	10: 90	Yellow	-
51	Dichloromethane	100	-	Sky blue
52	Dichloromethane	100	-	Sky blue
53	Dichloromethane	100	-	Sky blue
54	Dichloromethane	100	-	Sky blue
55	Dichloromethane	100	-	Sky blue
56	Dichloromethane	100	-	Sky blue
57	Dichloromethane	100	-	Sky blue
58	Dichloromethane	100	-	Sky blue
59	Dichloromethane	100	-	Sky blue
60	Dichloromethane	100	-	Sky blue
61	Dichloromethane	100	-	Sky blue
62	Dichloromethane	100	-	Sky blue
63	Dichloromethane: EtOAc	95: 5	Yellow	-
64	Dichloromethane: EtOAc	95: 5	Yellow	-
65	Dichloromethane: EtOAc	95: 5	Yellow	-
66	Dichloromethane: EtOAc	95: 5	Yellow	-
67	Dichloromethane: EtOAc	95: 5	Yellow	-
68	Dichloromethane: EtOAc	90: 10	Yellow	-
69	Dichloromethane: EtOAc	90: 10	Yellow	-
70	Dichloromethane: EtOAc	90: 10	Yellow	-
71	Dichloromethane: EtOAc	90: 10	Yellow	-
72	Dichloromethane: EtOAc	90: 10	Yellow	-

Table 4.17 contd.

Fractions	Solvent mixture	Ratio (%)	Colour under UV (254 nm)	Colour under UV (366 nm)
73	Dichloromethane: EtOAc	90: 10	-	-
74	Dichloromethane: EtOAc	80: 20	-	-
75	Dichloromethane: EtOAc	80: 20	-	-
76	Dichloromethane: EtOAc	80: 20	-	-
77	Dichloromethane: EtOAc	80: 20	-	-
78	Dichloromethane: EtOAc	80: 20	-	-
79	Dichloromethane: EtOAc	80: 20	-	-
80	Dichloromethane: EtOAc	80: 20	-	-
81	Dichloromethane: EtOAc	70: 30	Yellow	-
82	Dichloromethane: EtOAc	70: 30	Yellow	-
83	Dichloromethane: EtOAc	70: 30	Yellow	-
84	Dichloromethane: EtOAc	70: 30	Yellow	-
85	Dichloromethane: EtOAc	70: 30	Yellow	-
86	Dichloromethane: EtOAc	50: 50	Yellow	-
87	Dichloromethane: EtOAc	50: 50	Yellow	-
88	Dichloromethane: EtOAc	50: 50	Yellow	-
89	Dichloromethane: EtOAc	50: 50	Yellow	-
90	Dichloromethane: EtOAc	50: 50	Yellow	-
91	Dichloromethane: EtOAc	50: 50	Yellow	-
92	Dichloromethane: EtOAc	50: 50	Yellow	-
93	Dichloromethane: EtOAc	50: 50	Yellow	-
94	Dichloromethane: EtOAc	50: 50	Yellow	-
95	Dichloromethane: EtOAc	30: 70	Light brown	-
96	Dichloromethane: EtOAc	30: 70	Light brown	-
97	Dichloromethane: EtOAc	30: 70	Light brown	-
98	Dichloromethane: EtOAc	30: 70	Light brown	-
99	Dichloromethane: EtOAc	30: 70	Light brown	-
100	Dichloromethane: EtOAc	30: 70	Light brown	-
101	Dichloromethane: EtOAc	30: 70	Light brown	-
102	Dichloromethane: EtOAc	30: 70	Light brown	-
103	EtOAc	100	Yellow	-
104	EtOAc	100	Yellow	-
105	EtOAc	100	Yellow	-
106	EtOAc	100	Yellow	-
107	EtOAc	100	Yellow	-
108	EtOAc	100	Yellow	-

Table 4.17 contd.

Fractions	Solvent mixture	Ratio (%)	Colour under UV (254 nm)	Colour under UV (366 nm)
109	EtOAc	100	Yellow	-
110	EtOAc	100	Yellow	-
111	EtOAc	100	Yellow	-
112	EtOAc	100	Yellow	-
113	EtOAc: MeOH	95: 5	Brown	-
114	EtOAc: MeOH	95: 5	Brown	-
115	EtOAc: MeOH	95: 5	Brown	-
116	EtOAc: MeOH	95: 5	Brown	-
117	EtOAc: MeOH	95: 5	Brown	-
118	EtOAc: MeOH	95: 5	Brown	-
119	EtOAc: MeOH	95: 5	Brown	-
120	EtOAc: MeOH	95: 5	Brown	-
121	EtOAc: MeOH	95: 5	Brown	-
122	EtOAc: MeOH	95: 5	Brown	-
123	EtOAc: MeOH	80: 20	Yellow	-
124	EtOAc: MeOH	80: 20	Yellow	-
125	EtOAc: MeOH	80: 20	Yellow	-
126	EtOAc: MeOH	80: 20	Yellow	-
127	EtOAc: MeOH	80: 20	Yellow	-
128	EtOAc: MeOH	80: 20	Yellow	-
129	EtOAc: MeOH	80: 20	Yellow	-
130	EtOAc: MeOH	80: 20	Yellow	-
131	EtOAc: MeOH	80: 20	Yellow	-
132	EtOAc: MeOH	80: 20	Yellow	-
133	EtOAc: MeOH	80: 20	Yellow	-
134	EtOAc: MeOH	70: 30	Yellow	-
135	EtOAc: MeOH	70: 30	Yellow	-
136	EtOAc: MeOH	70: 30	Yellow	-
137	EtOAc: MeOH	70: 30	Yellow	-
138	EtOAc: MeOH	70: 30	Yellow	-
139	EtOAc: MeOH	70: 30	Yellow	-
140	EtOAc: MeOH	70: 30	Yellow	-
141	EtOAc: MeOH	70: 30	Yellow	-
142	EtOAc: MeOH	70: 30	Yellow	-
143	EtOAc: MeOH	70: 30	Yellow	-
144	EtOAc: MeOH	70: 30	Yellow	-

Table 4.17 contd.

Fractions	Solvent mixture	Ratio (%)	Colour under UV (254 nm)	Colour under UV (366 nm)
145	EtOAc: MeOH	50: 50	Brown	-
146	EtOAc: MeOH	50: 50	Brown	-
147	EtOAc: MeOH	50: 50	Brown	-
148	EtOAc: MeOH	50: 50	Brown	-
149	EtOAc: MeOH	50: 50	Brown	-
150	EtOAc: MeOH	50: 50	Brown	-
151	EtOAc: MeOH	50: 50	Brown	-
152	EtOAc: MeOH	50: 50	Brown	-
153	EtOAc: MeOH	50: 50	Brown	-
154	EtOAc: MeOH	30: 70	Brown	-
155	EtOAc: MeOH	30: 70	Brown	-
156	EtOAc: MeOH	30: 70	Brown	-
157	EtOAc: MeOH	30: 70	Brown	-
158	EtOAc: MeOH	30: 70	Brown	-
159	EtOAc: MeOH	30: 70	Brown	-
160	EtOAc: MeOH	30: 70	Brown	-
161	EtOAc: MeOH	30: 70	Brown	-
162	EtOAc: MeOH	30: 70	Brown	-
163	EtOAc: MeOH	30: 70	Brown	-
164	MeOH	100	Brown	-
165	MeOH	100	Brown	-
166	MeOH	100	Brown	-
167	MeOH	100	-	-
168	MeOH	100	-	-
169	MeOH	100	-	-
170	MeOH	100	-	-

Table 4.18: Column chromatography of *Sphenocentrum jollyanum n* Hexane fraction

Fractions	Solvent mixture	Ratio (%)	Colour under UV (254 nm)	Colour under UV (366 nm)
1	*n* Hexane	100	-	-
2	*n* Hexane	100	-	-
3	*n* Hexane	100	-	-
4	*n* Hexane: EtOAc	90: 10	-	-
5	*n* Hexane: EtOAc	90: 10	-	-
6	*n* Hexane: EtOAc	90: 10	-	-
7	*n* Hexane: EtOAc	90: 10	Yellow	-
8	*n* Hexane: EtOAc	90: 10	Yellow	-
9	*n* Hexane: EtOAc	80: 20	Yellow	-
10	*n* Hexane: EtOAc	80: 20	Yellow	-
11	*n* Hexane: EtOAc	80: 20	Yellow	-
12	*n* Hexane: EtOAc	80: 20	Yellow	-
13	*n* Hexane: EtOAc	80: 20	Yellow	-
14	*n* Hexane: EtOAc	80: 20	Yellow	-
15	*n* Hexane: EtOAc	80: 20	Yellow	-
16	*n* Hexane: EtOAc	80: 20	Yellow	-
17	*n* Hexane: EtOAc	80: 20	Yellow	-
18	*n* Hexane: EtOAc	80: 20	Yellow	-
19	*n* Hexane: EtOAc	80: 20	Yellow	-
20	*n* Hexane: EtOAc	80: 20	Yellow	-
21	*n* Hexane: EtOAc	70: 30	Yellow	-
22	*n* Hexane: EtOAc	70: 30	Yellow	-
23	*n* Hexane: EtOAc	70: 30	Yellow	-
24	*n* Hexane: EtOAc	70: 30	Yellow	-
25	*n* Hexane: EtOAc	70: 30	Yellow	-
26	*n* Hexane: EtOAc	70: 30	Yellow	-
27	*n* Hexane: EtOAc	70: 30	Yellow	-
28	*n* Hexane: EtOAc	70: 30	Yellow	-
29	*n* Hexane: EtOAc	70: 30	Yellow	-
30	*n* Hexane: EtOAc	60: 40	Yellow	-
31	*n* Hexane: EtOAc	60: 40	Yellow	-
32	*n* Hexane: EtOAc	60: 40	Yellow	-
33	*n* Hexane: EtOAc	60: 40	Yellow	-
34	*n* Hexane: EtOAc	60: 40	Yellow	-
35	*n* Hexane: EtOAc	60: 40	Yellow	-
36	*n* Hexane: EtOAc	60: 40	Yellow	-

Table 4.18 contd.

Fractions	Solvent mixture	Ratio (%)	Colour under UV (254 nm)	Colour under UV (366 nm)
37	*n* Hexane: EtOAc	40: 60	Yellow	-
38	*n* Hexane: EtOAc	40: 60	-	-
39	*n* Hexane: EtOAc	40: 60	-	-
40	*n* Hexane: EtOAc	40: 60	-	-
41	*n* Hexane: EtOAc	40: 60	-	-
42	*n* Hexane: EtOAc	40: 60	-	-
43	*n* Hexane: EtOAc	40: 60	-	-
44	*n* Hexane: EtOAc	40: 60	-	-
45	*n* Hexane: EtOAc	40: 60	-	-
46	*n* Hexane: EtOAc	20: 80	Yellow	-
47	*n* Hexane: EtOAc	40: 60	Yellow	-
48	*n* Hexane: EtOAc	40: 60	Yellow	-
49	*n* Hexane: EtOAc	40: 60	Yellow	-
50	*n* Hexane: EtOAc	40: 60	Yellow	-
51	*n* Hexane: EtOAc	40: 60	Yellow	-
52	*n* Hexane: EtOAc	40: 60	Yellow	-
53	*n* Hexane: EtOAc	40: 60	Yellow	-
54	*n* Hexane: EtOAc	40: 60	Yellow	-
55	*n* Hexane: EtOAc	40: 60	Yellow	-
56	EtOAc	100	Yellow	-
57	EtOAc	100	Yellow	-
58	EtOAc	100	Yellow	-
59	EtOAc	100	Yellow	-
60	EtOAc	100	Yellow	-
61	EtOAc	100	Yellow	-
62	EtOAc	100	Yellow	-
63	EtOAc	100	Yellow	-
64	EtOAc	100	Yellow	-
65	EtOAc: MeOH	90: 10	Yellow	-
66	EtOAc: MeOH	90: 10	Yellow	-
67	EtOAc: MeOH	90: 10	Yellow	-
68	EtOAc: MeOH	90: 10	Yellow	-
69	EtOAc: MeOH	90: 10	Yellow	-
70	EtOAc: MeOH	90: 10	Yellow	-
71	EtOAc: MeOH	90: 10	Yellow	-
72	EtOAc: MeOH	90: 10	Yellow	-

4.19 Identification of compound SJE-10B using EI-MS, ^{1}H NMR, and ^{13}C NMR spectroscopies

Compound SJE-10B (10 mg), a colourless crystal with an R_f 0.47 on silica gel TLC plate (*n* Hexane: Ethyl acetate 6: 4) giving a pink colour with 20% H_2SO_4 reagent with melting point 182 ^{o}C. The ^{1}H NMR, UV, IR, and ^{13}C NMR are the same with columbin literature values (Figure 4.19) as shown in Tables 4.19.1 and 4.19.2. EI-MS, *m/z* (relat. intensity %): 359 (2.7, M^{+}+1), 358 (4.1,M^{+}), 314 (16.5), 247 (21.9), 246 (57.1), 231 (77), 204 (28), 190 (17.9), 161 (22.7), 153 (85.1), 152 (91.6), 108 (58.8), 107 (100), 93 (24.8). The EI-MS, ^{1}H NMR, and ^{13}C NMR spectra are shown in Appendix X.

4.20 Identification of compound SJE-10C using EI-MS, ^{1}H NMR, and ^{13}C NMR spectroscopies

Compound SJE-10C (10 mg) was isolated as a colourless crystal with an R_f of 0.42 on silica gel TLC plate (*n* Hexane: Ethyl acetate 6: 4) giving a pink colour with H_2SO_4 reagent, melting point 183 - 187 ^{o}C. The ^{1}H NMR, UV, IR, and ^{13}C NMR are the same with Isocolumbin literature values (Figure 4.20). The ^{13}C NMR and ^{1}H NMR spectra of the compound are shown in Tables 4.20.1 and 4.20.2.

EI-MS, *m/z* (relat. intensity %): 314 (53.3), 253 (11.5), 246 (26.6), 231 (29.2), 205 (76.8), 191 (13.7), 153 (71.3), 148 (22.8), 133 (44.4), 121 (73.6), 108 (85.1), 107 (100), 43 (56.5).

The EI-MS, ^{1}H NMR, and ^{13}C NMR spectra are shown in Appendix XI.

4.21 Identification of compound SJE-23D using EI-MS, ^{1}H NMR, and ^{13}C NMR spectroscopies

Compound SJE-23D (6 mg) was found as a white amorphous powder and named Atrotosterone A (Figure 4.21) when compared with literature. Composition $C_{28}H_{46}O_7$, Molecular weight: 494. EI-MS, *m/z* (relat. intensity %): 476 (10), 444 (3), 426 (21), 408 (10), 363 (15), 345 (76), 327 (58), 309 (30), 285 (63), 267 (41), 239 (21), 227 (34), 189 (30), 173 (41), 143 (42), 113 (78), 99 (100), 73 (94), 57 (43), 43 (97), 41 (30). FAB-MS (negative ion mode): 493$[M-1]^{+}$. The ^{13}C and ^{1}H NMR data are shown in Tables 4.21.1 and 4.21.2. The EI-MS, ^{1}H NMR, and ^{13}C NMR spectra are shown in Appendix XII while the FAB-MS is shown in Appendix XXI.

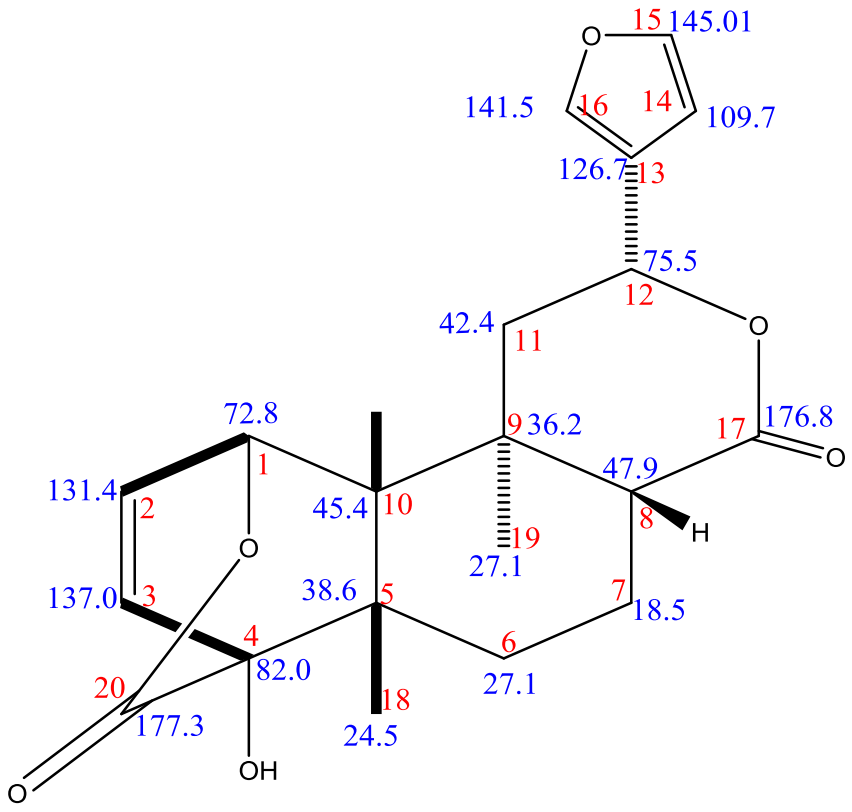

Figure 4.19: Columbin

Table 4.19.1: ^{13} C NMR chemical shifts assignment of Columbin (400 MHz)

Carbon	Observed (CD_3OD)	Reported 1	Reported 2
1	72.8	71.0	74.2
2	131.4	130.0	128.7
3	137.0	137.1	136.8
4	82.0	83.9	80.5
5	38.6	37.5	37.2
6	27.1	26.0	25.6
7	18.5	17.7	17.3
8	47.9	44.8	47.6
9	36.2	37.2	35.3
10	45.4	46.1	44.5
11	42.4	40.1	41.9
12	75.5	73.8	70.7
13	126.7	125.6	124.8
14	109.7	109.5	108.4
15	145.0	144.2	139.7
16	141.5	140.8	143.9
17	176.8	174.4	175.5
18	24.5	24.1	24.3
19	27.1	27.5	27.0
20	177.3	175.1	172.4

Reported 1 (Moody *et al*., 2005, $CDCl_3$), Reported 2 (Choudhury *et al*., 1997, $CDCl_3$)

Note: Assignments were based on ^{1}H-^{1}H-COSY, ^{1}H-^{13}C-HSQC, DEPT, NOESY, and HMBC experiments.

Table 4.19.2: ^{1}H NMR chemical shifts assignment of Columbin (400 MHz)

Carbon	Observed (CD_3OD)	J values (Hz)	Reported	J values
1	5.29 d	4.4	5.17 dd	5.1, 1.8
2	6.55 dd	8, 4.4	6.49 dd	7.9, 5.1
3	6.27 dd	1.6, 8	6.36 dd	7.7, 1.8
4			3.54 s	
5				
6	1.73 dd	14.8, 8	1.77 ddd	14.3, 8, 3, 1.5
	1.41 – 1.49 m		1.40 ddd	14.3, 11, 1, 8.5
7	2.05 – 2.12 m		2.07 dddd	15, 4, 11.1, 8.3, 2.0
	2.52 – 2.62 m		2.66 dddd	15.4, 11.8, 8.3, 1.5
8	2.55 dd	5.6, 2	2.42 dd	11.8, 2.0
9				
10	1.83 s		1.75 s	
11	1.94 dd	14.8, 4.4	2.28 dd	14.8, 4.3
	2.30 dd	12.9, 10	1.95 dd	14.8, 12.0
12	5.59 dd	12.4, 4.4	5.42 dd	12.0, 4.5
13				
14	6.54 dd	2.1, 1.8	6.45 dd	2.2, 1.8
15	7.51 d	2.5, 1.8	7.44 dd	2.7, 1.8
16	7.59 d	1.6, 1.6	7.49 dd	1.8, 1.8
17				
18	1.20 s		1.06 s	
19	0.99 s		1.25 s	
20				

Reported (Choudhury *et al*., 1997, $CDCl_3$)

s – singlet d – doublet dd – double doublet m – multiplet

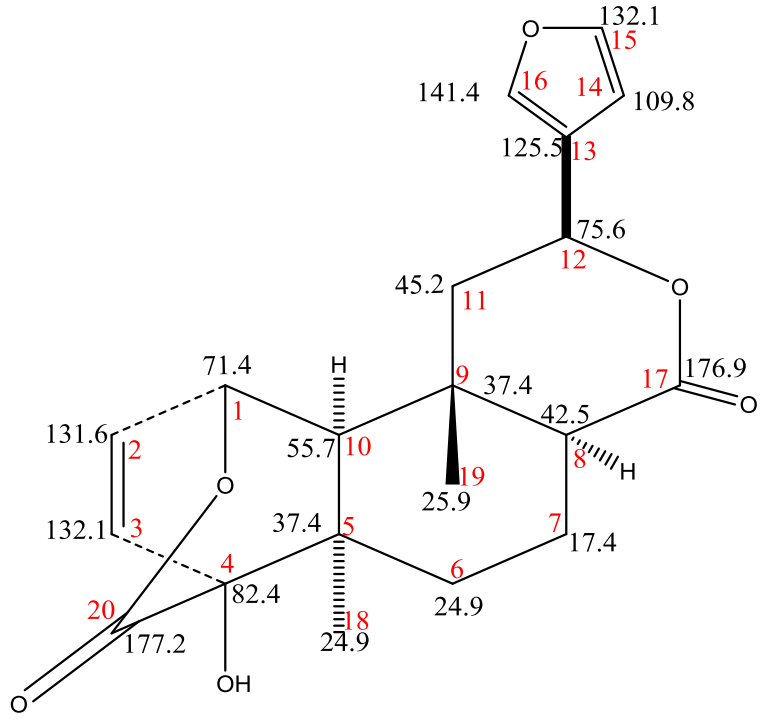

Figure 4.20: Isocolumbin

Table 4.20.1: ^{13}C NMR chemical shifts assignment of Isocolumbin (500 MHz)

Carbon	Observed (CD_3OD)	Reported
1	71.4	68.2
2	131.6	130.0
3	132.1	133.0
4	82.4	80.4
5	37.4	35.8
6	24.9	24.2
7	17.4	16.1
8	42.5	40.4
9	37.4	35.8
10	55.7	55.1
11	45.2	45.0
12	75.6	73.2
13	125.5	122.1
14	109.8	107.2
15	132.1	133.5
16	141.4	141.2
17	176.9	174.1
18	24.9	24.8
19	25.9	24.8
20	177.2	173.4

Reported (Moody *et al*., 2005, $CDCl_3$)

Note: Assignments were based on ^{1}H-^{1}H-COSY, ^{1}H-^{13}C-HSQC, DEPT, NOESY, and HMBC experiments.

Table 4.20.2: ^{1}H NMR chemical shifts assignment of Isocolumbin (500 MHz)

Carbon	Observed	Jvalues (Hz)	Reported	J values
1	5.25 d	5.0	5.17 dd	5.1, 1.8
2	6.54 m		6.49 dd	7.9, 5.1
3	6.20 dd	2.0, 8.0	6.36 dd	7.7, 1.8
4			3.54 s	
5				
6	1.73 dd	14.0, 4.5	1.77 ddd	14.3, 8, 3, 1.5
	1.41 m		1.40 ddd	14.3, 11, 1, 8.5
7	2.07 m		2.07 dddd	15, 4, 11.1, 8.3, 2.0
	1.84 m		2.66 dddd	15.4, 11.8, 8.3, 1.5
8	2.98 dd	10.5, 8.0	2.42 dd	11.8, 2.0
9				
10	1.86 s		1.75 s	
11	1.92 m		2.28 dd	14.8, 4.3
	2.38 dd	15, 4	1.95 dd	14.8, 12.0
12	5.59 dd	15.5, 3.5	5.42 dd	12.0, 4.5
13				
14	6.54 m		6.45 dd	2.2, 1.8
15	7.51 m		7.44 dd	2.7, 1.8
16	7.61 m		7.49 dd	1.8, 1.8
17				176.7
18	1.19 s		1.06 s	24.5
19	1.01 s		1.25 s	28.1
20				177.2

Reported (Choudhury *et al*., 1997, $CDCl_3$)

s – singlet d – doublet dd – double doublet m - multiplet

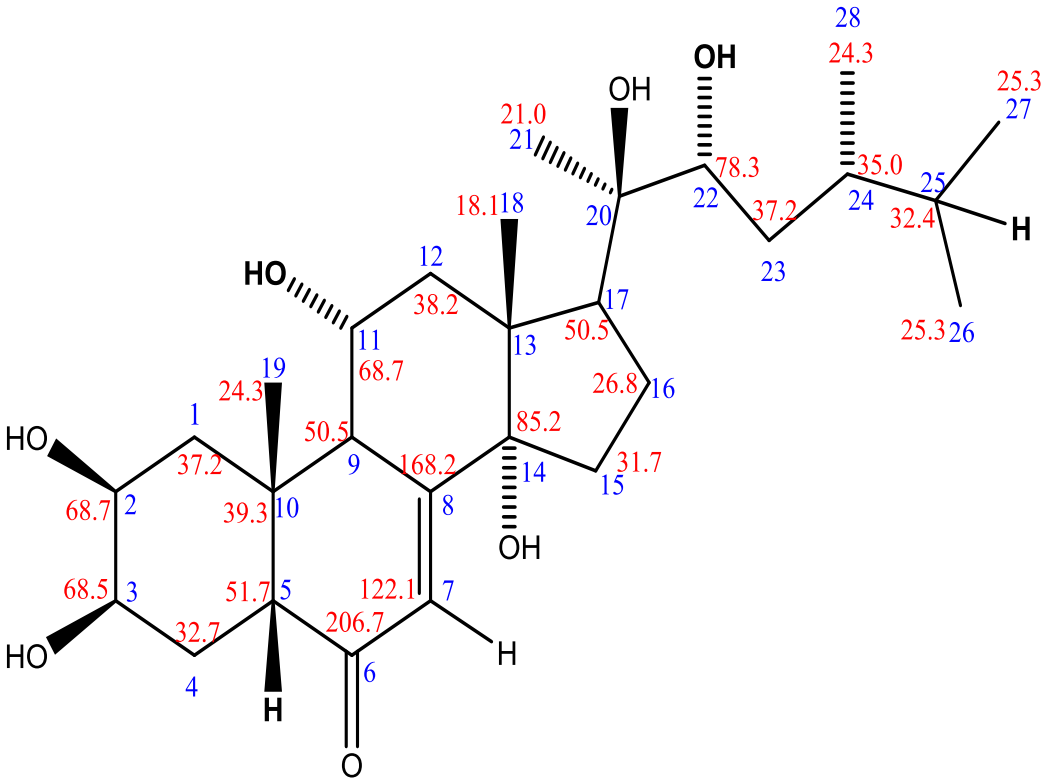

Figure 4.21: Atrotosterone A

Table 4.21.1: ^{13}C NMR assignment of Atrotosterone A (500 MHz)

Position	Observed (CD_3OD)	Reported
1	37.2	39.1
2	68.7	68.9
3	68.5	68.5
4	32.7	33.3
5	51.7	52.8
6	206.7	206.7
7	122.1	122.7
8	168.2	165.9
9	50.5	42.9
10	39.3	39.9
11	68.7	69.4
12	38.2	43.7
13	c	c
14	85.2	84.8
15	31.7	31.8
16	26.8	21.6
17	50.5	50.2
18	18.1	18.9
19	24.3	24.6
20	77.9	77.9
21	21.0	20.8
22	78.3	75.5
23	37.2	37.5
24	35.0	36.7
25	32.4	30.4
26	25.3	16.2
27	25.3	15.7
28	24.3	21.6

Reported (Vokac *et al*., 1999, CD_3OD)

Note: Assignments were based on ^{1}H-^{1}H-COSY, ^{1}H-^{13}C-HSQC, DEPT, NOESY, and HMBC experiments. [c] Overlapped signal in solvent.

Table 4.21.2: ^{1}H NMR assignment of Atrotosterone A (500 MHz)

S/N	Observed (CD_3OD)	Reported
1	1.76 - 1.81, m	2.59, dd (13.0, 4.2)
	1.39 – 1.45 m	1.38, dd (13.0, 12.0)
2	3.94 (m)	4.01, ddd (11.0, 4.2, 3.3)
3	3.82 – 3.86 (m)	3.95, q (2.8)
4	1.76 – 1.81	1.77, ddd (14.0, 13.0, 2.5)
		1.69, dt (14.0, 3.6, 3.6)
5	2.38 – 2.35 dd (*J* =5.0, 13.5)	2.33, dd (13.0, 4.0)
6		
7	5.81 (d, *J* = 2.5)	5.80, dd, (2.1, 1.0)
8		
9	2.38 – 2.35 (dd, *J* = 5.0, 13.5)	3.16, dd (9.0, 2.7)
10		
11	3.94, m	4.10, ddd (10.6, 9.0, 6.0)
12	1.39-1.49, m	2.21, dd (12.1, 10.0)
		2.15, dd (12.1, 6.0)
13		
14		
15	1.59 (d, *J* = 9.0)	1.95
		1.58
16	1.59 (d, *J* = 9.0)	2.01
		2.01
17	2.38 (dd, *J* = 5.0, 13.5)	2.42 dd (9.5, 8.5)
18	0.87 (s)	
19	0.95 (s)	
20		
21	1.18 (s)	
22	3.34 (m)	3.45, dd (10.5, 1.7)
23	1.39-1.45 (m)	1.53
	1.76-1.81 (m)	1.09 ddd (14.1, 10.0, 4.0)
24	3.15, m	
25	1.39-1.45, m	
	1.76-1.81, m	
26	1.16 (d, *J* = 3.5)	
27	1.17 (d, *J* = 3.5	
28	1.18 (d, *J* = 8.5)	

s – singlet d – doublet dd – double doublet m – multiplet

Reported (Vokac *et al*., 1999, CD_3OD)

4.22 Identification of Compound SJE-28B using EI-MS, ^{1}H NMR, and ^{13}C NMR spectroscopies

Compound SJE-28B (8 mg) was obtained as a white amorphous powder with an R_f of 0.54 on silica gel TLC plate (*n* Hexane: Chloroform: Methanol 3: 5: 2) giving a brown colour under UV wavelength 254 nm and a deep brown colour when sprayed with H_2SO_4 reagent. Melting point 243-245 ^{o}C. The ^{1}H NMR, UV, IR, and ^{13}C NMR data (Tables 4.22.1 and 4.22.2) are identical with literature values for Pinnatasterone (Figure 4.22). The EI-MS, ^{1}H NMR, and ^{13}C NMR spectra are shown in Appendix XIII.

4.23 Identification of Compound CPE-10A using ^{1}H NMR and HR-MS spectroscopies

Compound CPE-10A (Palmatine) is a white powder (7 mg). Composition: $C_{21}H_{22}NO_4^+$: 352. The HR ESI-MS shows the molecular ion peak at m/z: 352 [M] $^+$. The ESI-MS was consistent with molecular formula for ($C_{21}H_{22}NO_4^+$). The EI-MS shows fragmentation at m/z (rel. int. %): 353 [100, M^+ +1], 352 [83], 338 [50], 322 [19], 294 [20], 239 [20], 185 [19], 152 [25], 129 [25], 119 [50], 97 [40], 85 [35], 57 [75], 43 [62]. The structure of Palmatine is shown in Figure 4.23 while Table 4.23 showed the reported and observed ^{1}H NMR data. The HR-MS and ^{1}H NMR spectra are shown in Appendix IX.

4.24 Identification of Compound CPE-43A using EI-MS, ^{1}H NMR, and ^{13}C NMR spectroscopies

Compound CPE-43A (7 mg) was obtained as a brown oil; R_f = 0.47 on silica gel TLC plate (*n* Hexane: Ethyl acetate 5: 5) active on UV 254 nm wavelength. The ^{13}C and ^{1}H NMR values (Tables 4.24.1 and 4.24.2) are identical with literature values for 5-Hydroxymethyl-2-furancarbaldehyde (Figure 4.24). Composition $C_6H_6O_3$ with molecular weight: 126**.** The EI-MS, ^{1}H NMR, and ^{13}C NMR spectra are shown in Appendix V and the IR spectra in Appendix II.

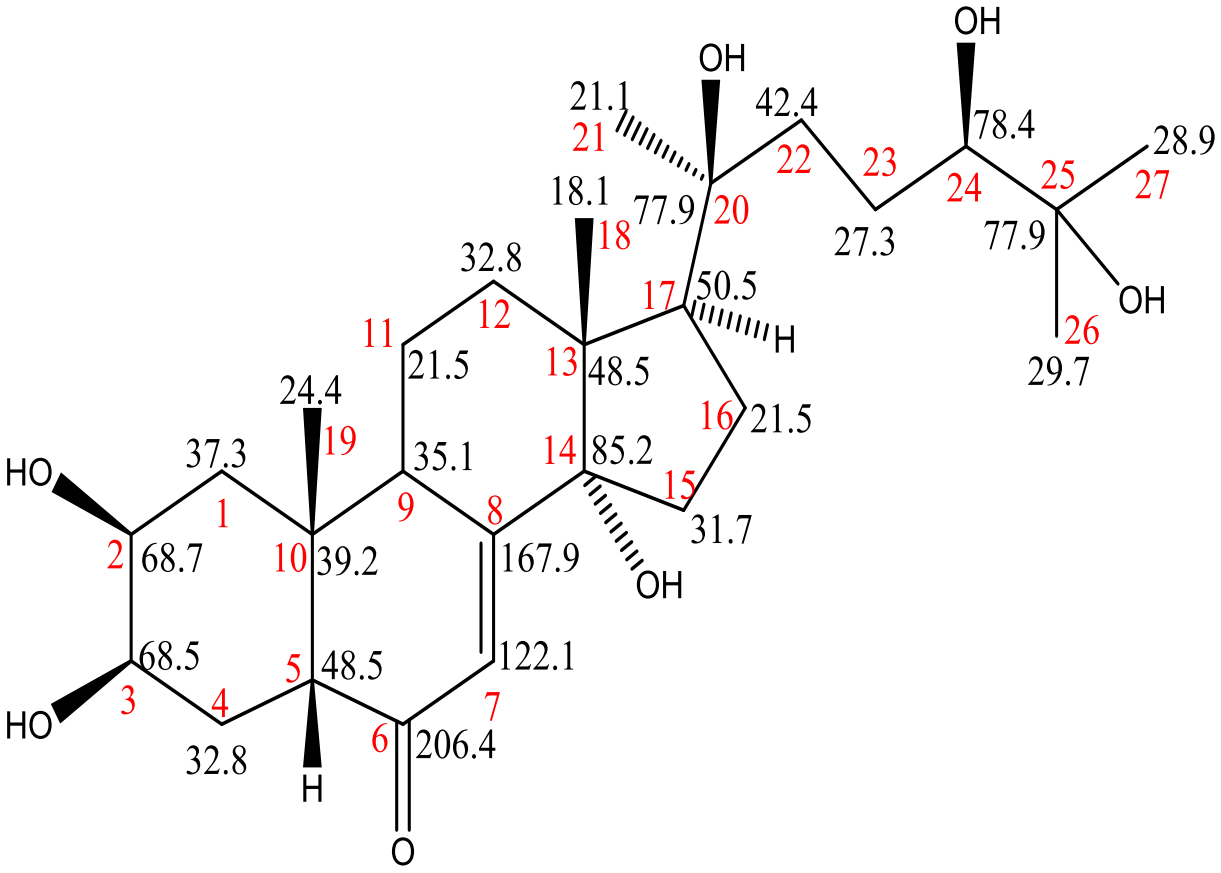

Figure 4.22: Pinnatasterone

Table 4.22.1: ^{13}C NMR assignment of Pinnatasterone (600 MHz)

Position	Observed (CD_3OD)	Reported
1	37.3	37.6
2	68.7	68.0
3	68.5	67.9
4	32.8	32.3
5	48.5	51.2
6	206.4	203.5
7	122.1	121.5
8	167.9	166.3
9	35.1	34.2
10	39.2	38.8
11	21.5	20.9
12	32.8	31.7
13	48.5	47.4
14	85.2	84.3
15	31.7	31.4
16	21.5	21.9
17	50.5	53.6
18	18.1	17.8
19	24.4	24.3
20	77.9	74.2
21	21.1	27.0
22	42.4	42.3
23	27.3	26.6
24	78.4	79.8
25	77.9	72.7
26	29.7	25.9
27	28.9	25.8

Reported (Filho *et al*., 2008, C_5D_5N)

Note: Assignments were based on ^{1}H-^{1}H-COSY, ^{1}H-^{13}C-HSQC, DEPT, NOESY, and HMBC experiments.

Table 4.22.2: ^{1}H NMR assignment of Pinnatasterone (600 MHz)

S/N	Observed (CD_3OD)	Reported
1	1.39 – 1.45, m	
	1.76 – 1.82, m	
2	3.80 – 3.84 (m)	4.19
3	3.94 (d, 2.5)	4.26
4	1.85 (dd, 3, 13)	
5	2.35 – 2.40 (m)	3.04 (dd, 13, 4)
6		
7	5.80 (d, 2.0)	6.26 (d, 2.5)
8		
9	3.12 (m)	3.61 (1 H, m)
10		
11	1.19 – 2.01 (m)	
12	2.09 – 2.15, m	
	1.85 – 1.88, m	
13		
14		
15	1.56 (m)	
	1.91 (m)	
16	1.91 – 2.01 (m)	
	1.76 – 1.82 (m)	
17	2.35 – 2.40 (m)	2.93 (t, 9)
18	0.88 (s)	1.17 (s)
19	0.95 (s)	1.09 (s)
20		
21	1.19 (s)	1.61 (s)
22	1.39 – 1.45 (m)	
	1.76 – 1.82 (m)	
23	1.23 (m)	
	1.62 (m)	
24	3.30 (m)	3.76 (1 H, br. d, J = 8.8 Hz)
25		
26	1.19 (s)	1.47 (s)
27	1.18 (s)	1.51 (s)

s – singlet d – doublet dd – double doublet m – multiplet

Reported (Suksamrarn *et al*., 1995, C_5D_5N)

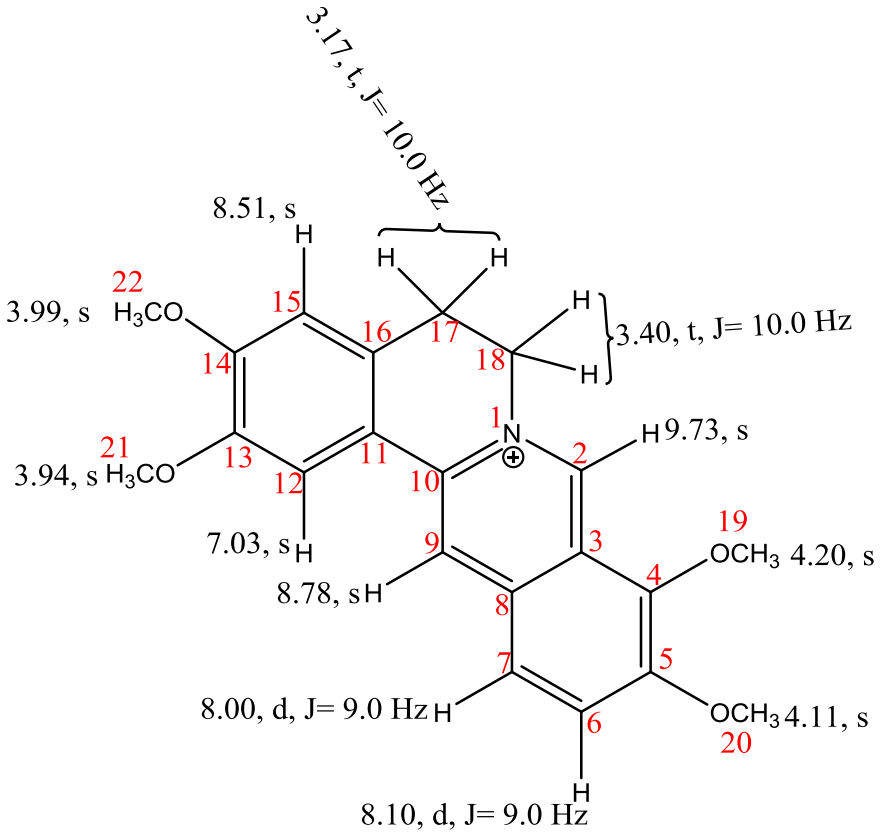

Figure 4.23: Palmatine

Table 4.23: ^{1}H NMR spectroscopic data of Palmatine (400 MHz)

Position	Observed (CD_5OD)	Reported
1	--	
2	9.72 (s, 1H)	9.04 (s, 1H)
3	--	
4	--	
5	--	
6	8.10 (d, *J* = 9.0 Hz, 1H)	8.02 (d, *J* = 8.4)
7	8.00 (d, *J* = 9.0 Hz, 1H)	8.22 (d, *J* = 8.4)
8	--	
9	8.78 (s, 1H)	7.72 (s, 1H)
10	--	
11	--	
12	7.03 (s, 1H)	7.09 (s, 1H)
13	--	
14	--	
15	8.51 (s, 1H)	4.95 (t, J = 5.4, 2H)
16	--	
17	3.17 (d, J = 10.0, 2H)	3.24 (t, J = 5.4, 2H)
18	3.18 (d, J = 10.0, 2H)	4.95 (t, J = 5.4)
19	4.20 - OCH_3	4.12 - oMe
20	4.11 - OCH_3	4.07 - oMe
21	3.94 - OCH_3	3.87 - oMe
22	3.99 – OCH_3	3.96 - oMe

Reported (Zhu *et al*., 2016, DMSO-d_6)

s – singlet d – doublet dd – double doublet m - multiplet

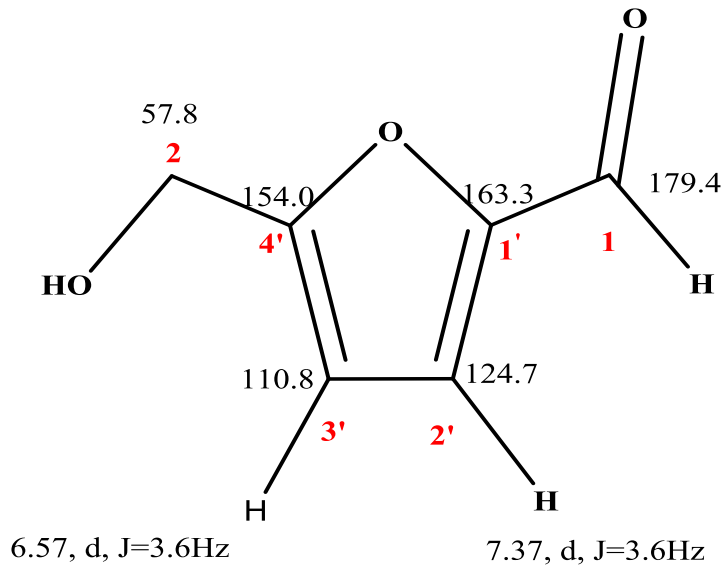

Figure 4.24: 5-Hydroxymethyl-2-furancarbaldehyde

Table 4.24.1: ^{13}C NMR chemical shifts assignment of 5 – (hydroxymethyl) furan – 2-carbaldehyde (400 MHz)

Carbon	Observed (CD_3OD)	Reported
1	179.4	179.5
2	57.8	57.7
1^1	163.3	163.3
2^1	124.7	123.6
3^1	110.8	110.9
4^1	154.0	154.0

Reported (Zuo *et al*., 2014, CD_3OD)

Table 4.24.2: ^{1}H NMR chemical shifts assignment of 5 – (hydroxymethyl) furan – 2-carbaldehyde (400 MHz)

Carbon	Observed (CD_3OD)	Reported
1	9.52	9.53, s
2	4.60, s	4.61, s
1^1		
2^1	7.37 (d, J=3.6)	7.38, (d, J=3.6)
3^1	6.57 (d, J=3.6)	6.58, (d, J=3.6)
4^1		

Reported (Zuo *et al*., 2014, CD_5OD)

s – singlet d – doublet dd – double doublet m - multiplet

4.25 Identification of Compound SJB-12 using EI-MS, ^{13}C NMR, ^{1}H NMR, FAB-MS, IR and UV spectroscopies

Compound SJB-12 (8 mg) was found as a white amorphous powder with an R_f of 0.72 on silica gel TLC plate (*n* Hexane: Chloroform: Methanol 4: 5: 1) giving a brown colour under UV wavelength 254 nm and not visible at 365 nm wavelength. It has a deep brown colour when sprayed with H_2SO_4 reagent and a melting point of 252-253 ^{o}C. The ^{13}C, ^{1}H NMR, IR and UV data are identical with literature values for Polypodine B (Figure 4.21). The ^{13}C and ^{1}H NMR data are shown in Tables 4.21.1 and 4.21.2. The EI-MS, ^{1}H NMR, and ^{13}C NMR spectra are shown in Appendix III while the FAB-MS is shown in Appendix XVIII.

4.26 Identification of Compound SJB-12B using EI-MS, ^{13}C NMR, ^{1}H NMR, IR and UV spectroscopies

Compound SJB-12B (10 mg) was found as a white amorphous powder with an R_f of 0.5 on silica gel TLC plate (*n* Hexane: Chloroform: Methanol 3: 5: 2) giving a brown colour under UV wavelength 254 nm and a deep brown colour when sprayed with H_2SO_4 reagent and a melting point of 241-242 ^{o}C. The ^{1}H NMR, and ^{13}C NMR are identical with literature values for 20-hydroxyecdysone (Figure 4.22)**.** The ^{13}C and ^{1}H NMR data are shown in Tables 4.22.1 and 4.22.2. The EI-MS, ^{1}H NMR, and ^{13}C NMR spectra are shown in Appendix IV, the IR spectrum is shown in Appendix XIV, while the FAB-MS is shown in Appendix XIX.

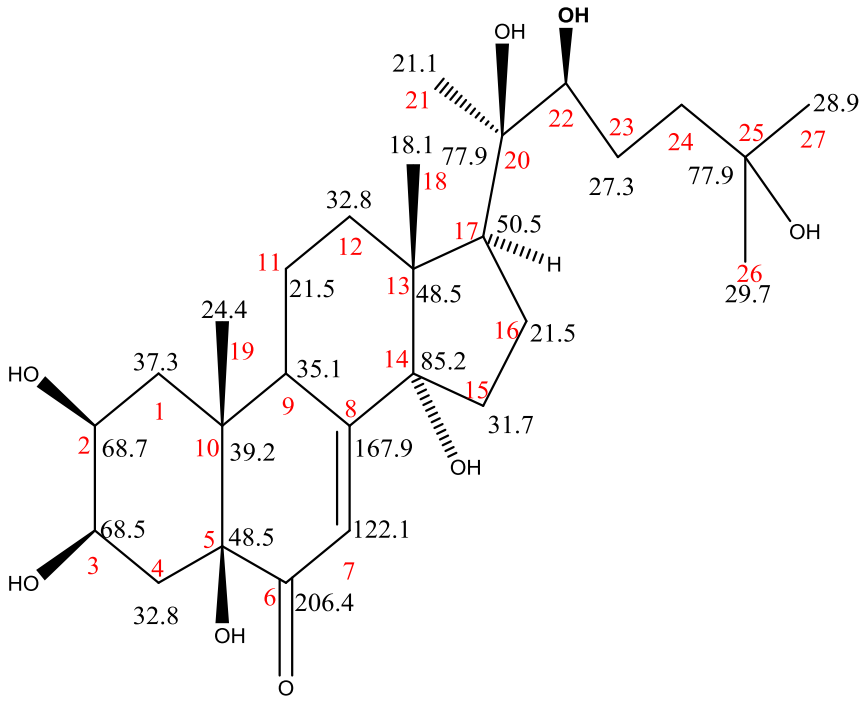

Figure 4.25: Polypodine B

Table 4.25.1: ^{13}C NMR chemical shifts assignment of Polypodine B (600 MHz)

Position	Observed (C_5D_5N)	Reported
1	34.8	34.8
2	67.9	67.9
3	69.8	69.8
4	36.0	35.9
5	79.8	79.8
6	200.9	200.9
7	119.8	119.9
8	166.8	166.7
9	38.2	38.2
10	44.7	44.7
11	22.0	22.0
12	31.6	31.9
13	48.1	48.1
14	84.0	83.9
15	32.0	31.6
16	21.4	21.3
17	49.9	59.9
18	17.8	17.8
19	17.1	17.1
20	76.8	76.7
21	21.6	21.6
22	77.5	77.5
23	27.5	27.4
24	42.6	42.6
25	69.5	69.5
26	30.0	29.9
27	30.1	30.1

Reported (Coll *et al*., 1994, C_5D_5N)

Note: Assignments were based on ^{1}H-^{1}H-COSY, ^{1}H-^{13}C-HSQC, DEPT, NOESY, and HMBC experiments.

[c] Overlapped signal in solvent.

Table 4.25.2: ^{1}H NMR chemical shifts assignment of Polypodine B (600 MHz)

S/N	Observed (C_5D_5N)	Reported
1	2.07 – 2.15, m	1.82, m
	2.16 – 2.3, m	1.92, m
2	4.26 (m)	4.26, m
3	4.16 (d, 4.0 Hz)	4.15, br. s
4	1.97 – 2.03 (m)	2.08, dd, J =14.9,
	1.97 – 2.03 (m)	3.0
5		
6		
7	6.27 (d, 2.4 Hz)	6.25, d, J=2.2
8		
9	3.65 (m)	3.62, m
10		
11	1.85 – 1,94 (m)	1.92, m
	1.15, s	
12	2.42 – 2.60 (m)	2.54, m
	2.42 – 2.60 (m)	
13		
14		
15	1.97 – 2.03 (m)	1.89, m
	1.97 – 2.03 (m)	
16	2.42 – 2.60 (m)	2.43, q, J=10.2
	2.42 – 2.60 (m)	
17	3.01 (t, 9.2 Hz)	2.96, (t, 9.0Hz)
18	1.21 (s)	1.19, s
19	1.15 (s)	1.19, s
20		
21	1.58 (s)	1.57, s
22	3.87 (d, 1.2 Hz)	3.84, br d, J=9.2Hz)
23	2.07 – 2.15 (m)	
	1.85 – 1.94 (m)	
24	2.16 – 2.30, m	
	1.75 – 1.83 (m)	
25		
26	1.36 (s)	1.36, s
27	1.36 (s)	1.36, s

Reported (Coll *et al*., 1994, C_5D_5N)

s – singlet d – doublet dd – double doublet m - multiplet

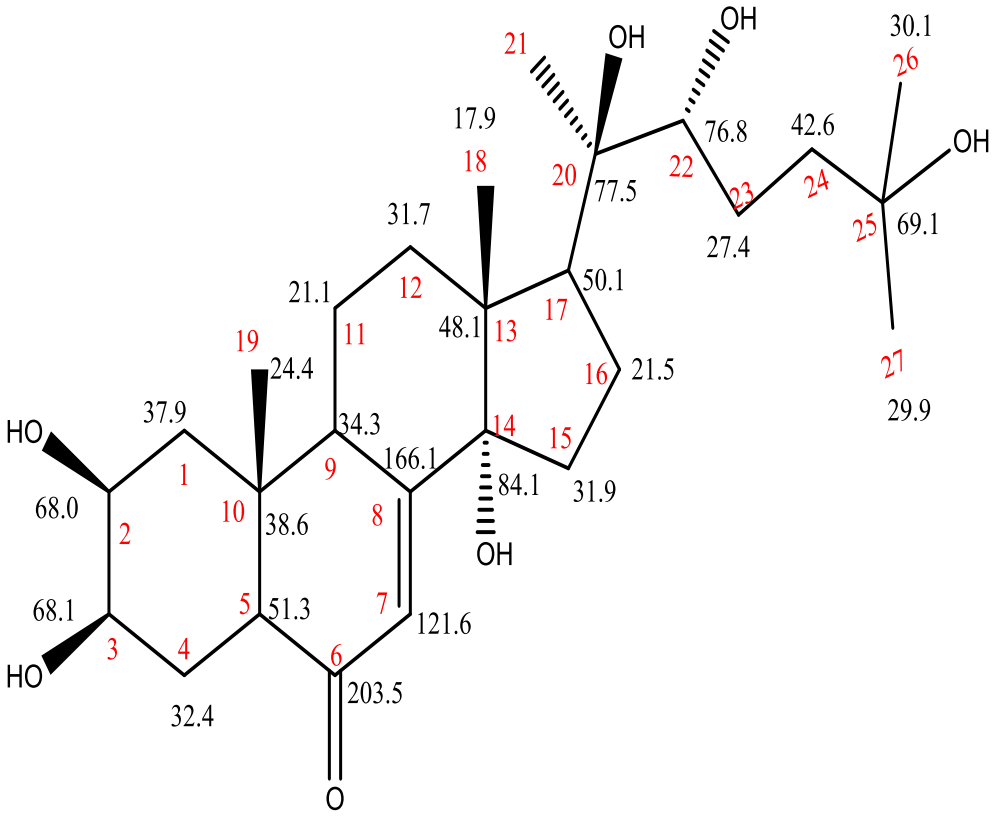

Figure 4.26: 20-hydroxyecdysone

Table 4.26.1: ^{13}C NMR chemical shifts assignment of 20-hydroxyecdysone (600 MHz)

Position	Observed (C_5D_5N)	Reported
1	37.9	38.09
2	68.0	68.33
3	68.1	68.23
4	32.4	32.53
5	51.3	51.48
6	203.5	203.56
7	121.6	121.79
8	166.1	166.11
9	34.3	34.67
10	38.6	38.80
11	21.1	21.29
12	31.7	32.19
13	48.1	48.27
14	84.1	84.42
15	31.9	31.88
16	21.5	21.61
17	50.1	50.28
18	17.9	17.99
19	24.4	24.55
20	77.5	77.09
21	21.6	21.77
22	76.8	77.75
23	27.4	27.59
24	42.6	42.64
25	69.1	69.86
26	30.1	30.10
27	29.9	30.15

Reported (Bandara *et al*., 1989, C_5D_5N)

Note: Assignments were based on ^{1}H-^{1}H-COSY, ^{1}H-^{13}C-HSQC, DEPT, NOESY, and HMBC experiments.

Table 4.26.2: ^{1}H NMR chemical shifts assignment of 20-hydroxyecdysone (600 MHz)

S/N	Observed (C_5D_5N)	Reported
1	1.86 – 1.97, m	
	2.15 – 2.22, m	
2	4.19 – 4.24 (m)	
3	4.19 – 4.24 (m)	
4	2.03 – 2.13 (m)	
	1.73 – 1.84 (m)	
5	3.01 – 3.04 (m)	
6		
7	6.26 (br. s)	6.24 d
8		
9	3.59 – 3.62 (m)	
10		
11	1.73 (m)	
	1.84 (m)	
	1.15, s	
12	2.03 – 2.14 (m)	
	2.56 – 2.63 (m)	
13		
14		
15	2.15 – 2.22 (m)	
	2.15 – 2.22 (m)	
16	2.03 – 2.13 (m)	
	2.45 – 2.50 (m)	
17	3.01 – 3.04 (m)	
18	1.24 (s)	1.23 (s)
19	1.09 (s)	1.06 (s)
20		
21	1.61 (s)	1.59 (s)
22	3.90 (d, 9.6 Hz)	3.88 (m)
23	2.15 (m)	2.15 (m)
	1.83 (m)	1.83 (m)
24	1.73 – 1.84, m	
	2.28 – 2.32 (m)	
25		
26	1.39 (s)	1.39 (s)
27	1.39 (s)	1.39 (s)

Reported (Bandara *et al*., 1989, C_5D_5N)

s – singlet d – doublet dd – double doublet m – multiplet

4.27 Identification of Compound SJB-26A using ^{13}C NMR, ^{1}H NMR, EI-MS, UV and IR spectroscopies

Compound SJB-26A (5 mg) was obtained as amorphous yellow powder with an R_f of 0.6 on silica gel TLC plate (*n* Hexane: Chloroform: Methanol 3: 5: 2) giving a brown colour under UV wavelength 254 nm and a deep brown colour when sprayed with H_2SO_4 reagent and a melting point of 240-244 ^{o}C. The ^{1}H NMR, UV, IR, and ^{13}C NMR (Tables 4.27.1 and 4.27.2) are identical with literature values for 20, 26-dihydroxyecdysone (Figure 4.27)**.** The EI-MS, ^{1}H NMR, and ^{13}C NMR spectra are shown in Appendix V; the IR spectrum is shown in Appendix XV while the FAB-MS is shown in Appendix XX.

4.28 Identification of Compound SJH-28A using EI-MS, ^{1}H NMR and ^{13}C NMR spectroscopies

Compound SJH-28A (6 mg) was obtained as a colorless crystal, named Tehuanin A (Figure 4.28) with melting point 240-242^{o}C, R_f of 0.68 on silica gel TLC plate (*n* Hexane: Ethyl acetate 1: 1), UV inactive with a light brown colour when sprayed with H_2SO_4 reagent. The ^{13}C and ^{1}H-NMR values (Tables 4.28.1 and 4.28.2) are identical with literature (Bautista, 2012). The EI-MS, ^{1}H NMR, and ^{13}C NMR spectra are shown in Appendix VI and the IR spectra in Appendix XVI.

4.29 Identification of Compound SJH-28B using EI-MS, ^{1}H NMR and ^{13}C NMR spectroscopies

Compound SJH-28B (30 mg) was obtained as light-yellow oil with an R_f of 0.56 on silica gel TLC plate (*n* Hexane: Ethyl acetate 1: 1), UV inactive with a light brown colour when sprayed with H_2SO_4 reagent. The compound is named 2, 3-dihydroxypropyl-octadec-5-enoate (Figure 4.29) with the ^{13}C and ^{1}H NMR data shown in Table 4.29. The EI-MS, ^{1}H NMR, and ^{13}C NMR spectra are shown in Appendix VII and the IR spectra in Appendix XVII.

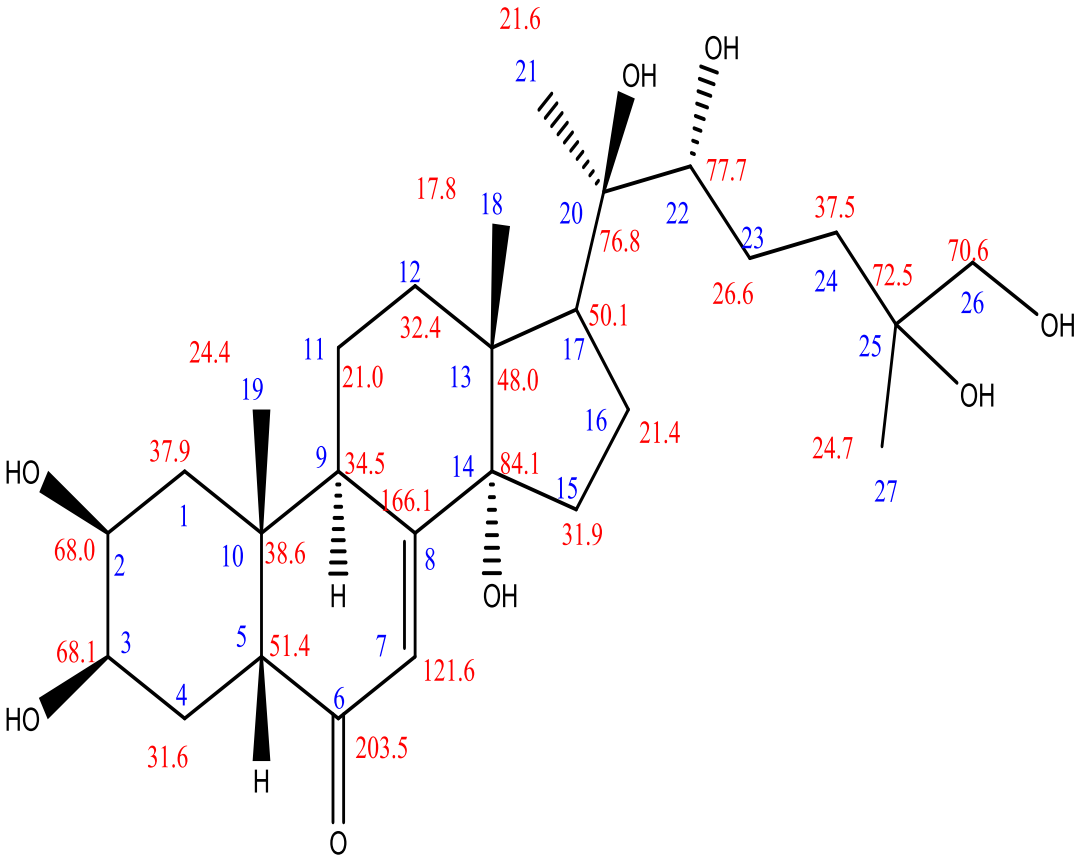

Figure 4.27: 20, 26 – dihydroxyecdysone

Table 4.27.1: ^{13}C NMR chemical shifts assignment of 20, 26-dihydroxyecdysone (600 MHz)

Position	Observed (C_5D_5N)	Reported
1	37.9	38.0
2	68.0	68.0
3	68.1	68.1
4	31.6	31.7
5	51.4	51.4
6	203.5	203.5
7	121.6	121.6
8	166.1	166.1
9	34.5	34.4
10	38.6	38.6
11	21.0	21.1
12	32.4	31.9
13	48.0	48.1
14	84.1	84.1
15	31.9	31.7
16	21.4	21.4
17	50.1	50.1
18	17.8	17.9
19	24.4	24.4
20	76.8	76.8
21	21.6	21.7
22	77.7	77.6
23	26.6	26.8
24	37.5	37.6
25	72.5	72.6
26	70.6	70.9
27	24.7	24.5

Reported (Zhu *et al*., 2001, C_5D_5N)

Table 4.27.2: ^{1}H NMR chemical shifts assignment of 20, 26-dihydroxyecdysone (600 MHz)

S/N	Observed (C_5D_5N)	Reported
1	1.86 – 1.92, m	
	2.13 – 2.22, m	
2	4.19 – 4.23 (m)	4.18, m
3	4.19 – 4.23 (m)	4.20, m
4	2.00 – 2.11 (m)	
	1.73 – 1.84 (m)	
5	3.01 – 3.03 (m)	
6		
7	6.24 (d, J=2.0)	6.24 d (d, J=2.0)
8		
9	3.60, s	
10		
11	1.70 – 1.82 (m)	
	1.86 – 1.92 (m)	
12	2.00 – 2.11 (m)	
	2.55 – 2.60 (m)	
13		
14		
15	2.15 – 2.22 (m)	
	2.15 – 2.22 (m)	
16	2.00 – 2.11 (m)	
	2.45 – 2.50 (m)	
17	3.01 – 3.03 (m)	
18	1.22 (s)	1.20 (s)
19	1.08 (s)	1.05 (s)
20		
21	1.59 (s)	1.58 (s)
22	3.90 (d, 9.6 Hz)	3.91 (br. d, J=11.0)
23	2.17 – 2.22 (m)	2.15 (m)
	1.94 – 1.99 (m)	1.83 (m)
24	2.43 – 2.54, m	
	1.86 – 1.92 (m)	
25		
26	3.87 – 3.91, m	3.86, m
27	1.49 (s)	1.47 (s)

Reported (Zhu *et al.*, 2001, C_5D_5N)

s – singlet d – doublet dd – double doublet m – multiplet

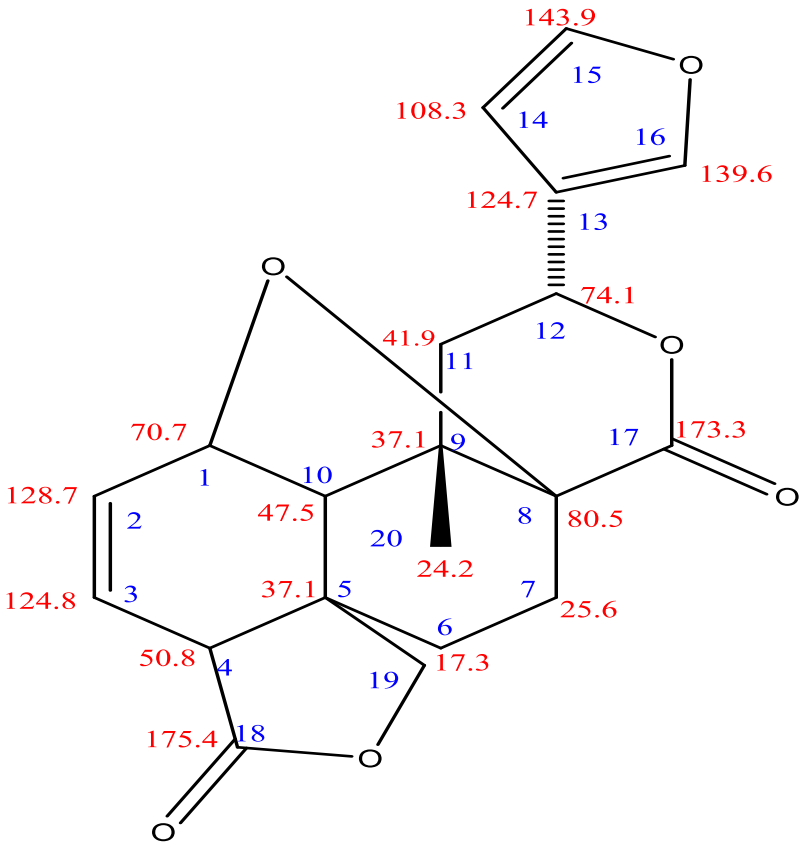

Figure 4.28: Tehuanin A

Table 4.28.1: ^{13}C NMR chemical shifts assignment of Tehuanin A (600 MHz)

S/N	Observed ($CDCl_3$)	Reported
1	70.7	71.6
2	128.7	126.6
3	124.8	122.9
4	50.8	49.2
5	37.1	40.3
6	17.3	25.3
7	25.6	25.4
8	80.5	82.4
9	37.1	44.8
10	47.5	46.6
11	41.9	43.2
12	74.1	71.8
13	124.7	123.7
14	108.3	107.8
15	143.9	143.1
16	139.6	139.2
17	173.3	168.9
18	175.4	172.8
19	c	76.3
20	24.2	23.6

Reported (Bautista, 2012, $CDCl_3$)

Note: Assignments were based on ^{1}H-^{1}H-COSY, ^{1}H-^{13}C-HSQC, DEPT, NOESY, and HMBC experiments.

[c] Overlapped signal in solvent.

Table 4.28.2: ^{1}H NMR chemical shifts assignment of Tehuanin A (600 MHz)

S/N	Observed Reported ($CDCl_3$)	Reported
1	5.39, dd, *J* = 4.0Hz, 11.5Hz	4.55 ddd (8.0, 4.0, 1.0)
2	6.44, m	3.08 ddd (21.0, 8.0, 6.0)
		2.78 ddd(21.0, 2.5, 1.0)
3	6.35, dd (1.5, 8.0)	6.88 dd (6.0, 2.5)
4	3.45, s	
5		
6	2.03, m	2.02 m
		1.67 dddd (14.5, 12.0, 8.0,
		1.0)
7	1.75, d (8.5)	1.91, m
		2.21 dd (14.5, 8.0)
8		
9		
10	1.91 (m)	1.91 d (4.0)
11	1.73 (t, *J* = 9.5 Hz)	2.02, m
		2.02, m
12	5.13, dd, *J* = 4.5Hz, 9Hz	5.78 dd (12.0, 4.5)
13		
14	6.42, d, *J* = 6.0Hz	6.44 dd (2.0. 1.0)
15	7.42, d, *J* = 22.0	7.43 t (2.0)
16	7.46, s	7.49 m
17		
18		
19		4.50 d (9.5)
		4.24, dd (9.5, 1.0)
20	1.05, s	1.21 s

Reported (Bautista, 2012, $CDCl_3$)

s – singlet d – doublet dd – double doublet m - multiplet

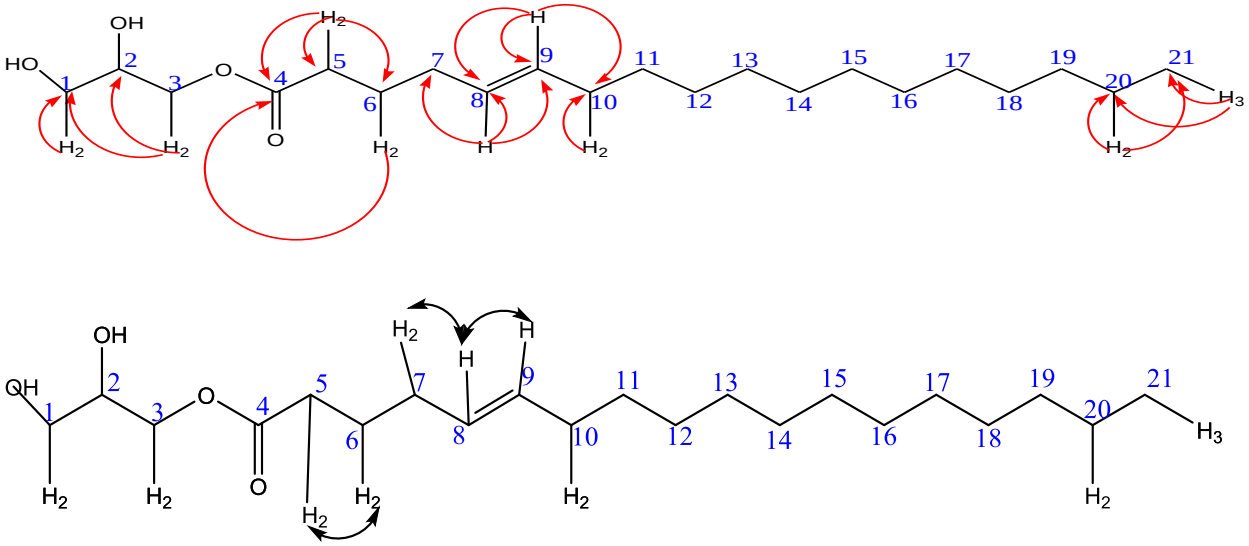

Figure 4.29: Key ^{13}C-^{1}H HMBC and ^{1}H-^{1}H COSY correlations of 2, 3-dihydroxypropyl-octadec-5-enoate

Table 4.29: ^{13}C NMR and ^{1}H NMR chemical shifts assignment of 2, 3-dihydroxypropyl-octadec-5-enoate (400 MHz) in $CDCl_3$

S/N	^{13}C ($CDCl_3$) 600 MHz	^{1}H values
1	63.3	3.67, dd, J = 4.2 Hz, 12 Hz
		3.57, dd, J = 5.4 Hz, 10.8 Hz
2	70.2	3.90 m
3	65.2	4.19, dd, J = 4.8 Hz, 12 Hz
		4.13, dd, J = 6.0 Hz, 11.4 Hz
4	174.1	
5	33.5	2.34, t, J = 7.8 Hz
		2.34, t, J = 7.8 Hz
6	24.9	1.67, m
		1.67, m
7	26.5	2.05, m
		2.05, m
8	128.0	5.28, m
9	131.3	5.39 m
10	27.2	1.97, m
11	29.3	1.28 m, 1.28 m
12	29.5	1.28 m
13	29.6	1.28 m
14	24.8	1.28 m
15	29.7	1.28 m
16	29.3	1.28 m
17	31.9	1.28 m
18	22.7	1.28 m
19	31.9	1.28 m
20	22.6	1.26, m
		1.26, m
21	14.1	0.86, t, J = 7.2 Hz
		0.86, t, J = 7.2 Hz
		0.86, t, J = 7.2 Hz

s – singlet d – doublet dd – double doublet m - multiplet

4.30 Identification of compound SJH-34B using EI-MS, ^{1}H NMR and ^{13}C NMR spectroscopies

Compound SJH-34B (4 mg) was isolated as colorless solid (R_f 0.42) on silica gel TLC plate (*n* Hexane: Ethyl acetate 1: 1), UV inactive with a brown colour when sprayed with H_2SO_4 reagent. It has the molecular formula $C_{20}H_{20}O_6$, as confirmed by FAB-MS from the 357 $[M + 1]^+$. The ^{13}C and ^{1}H data are shown in Tables 4.30.1 and 4.30.2 and the structure is named Tinospin E (Figure 4.30). The EI-MS, ^{1}H NMR, and ^{13}C NMR spectra are shown in Appendix VIII.

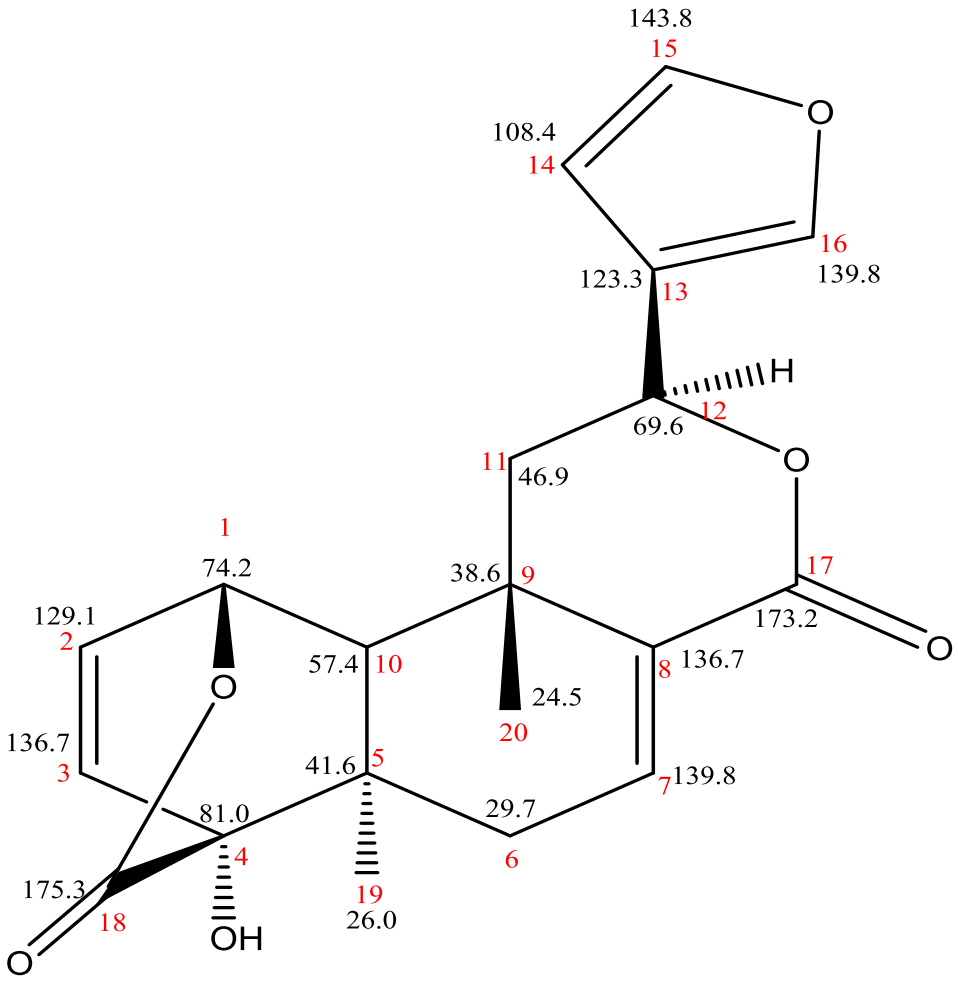

Figure 4.30: Tinospin E

Table 4.30.1: ^{13}C NMR chemical shifts assignment of Tinospin E (600 MHz)

Carbon	Observed (CD_3Cl_3)	Reported
1	74.2	74.6
2	129.1	130.7
3	136.7	138.6
4	81.0	81.3
5	41.6	43.2
6	29.7	31.7
7	139.8	141.3
8	136.7	137.9
9	38.6	37.2
10	57.4	54.9
11	46.9	44.4
12	69.6	70.2
13	123.3	124.6
14	108.4	109.5
15	143.8	144.1
16	139.8	140.8
17	173.2	166.8
18	175.3	175.3
19	26.0	26.5
20	24.5	25.5

Reported (Huang *et al*., 2012, C_5D_5N)

Note: Assignments were based on ^{1}H-^{1}H-COSY, ^{1}H-^{13}C-HSQC, DEPT, NOESY, and HMBC experiments.

Table 4.30.2: ^{1}H NMR chemical shifts assignment of Tinospin E (600 MHz)

Carbon	Observed ($CDCl_3$)	J values (Hz)	Reported	J values
1	5.13 d	4.8	5.41 d	5.0
2	6.54 m		6.43 dd	7.8, 5.0
3	6.33 dd	3.6, 12.0	6.53 dd	7.8, 1.4
4				
5				
6	1.29		2.74 dd	15.8, 8.1
	1.24 s		2.35 dd	15.8, 3.5
7	7.42 d	1.8	7.27 dd	8.1, 3.5
8				
9				
10	2.66 dd		2.08 s	
11	1.94 m		2.41 d	14.7
	1.94 m		2.13 dd	14.7, 11.5
12	5.33 dd	3.6, 12.0	5.35 d	11.5
13				
14	6.44 m		6.72 t	0.9
15	7.42 d	1.8	7.65 t	1.6
16	7.47 s		7.78 dd	1.3, 0.7
17				
18				
19	1.19 s		1.23 s	
20	1.01 s		1.24 s	

Reported (Huang *et al*., 2012, C_5D_5N)

s – singlet d – doublet dd – double doublet m - multiplet

4.31 Summary of isolated compounds

In summary, twelve compounds were isolated from both *Curculigo pilosa* rhizomes and *Sphenocentrum jollyanum* seeds. The names, eluting solvents, colour and weight are shown in Table 4.31.

4.32 Antacid activity of isolated compounds

The neutralising effects of isolated compounds were studied using 0.5 mg of each compound and standard. The obtained result showed that Columbin and isocolumbin showed the highest neutralising effect among the compounds by increasing the artificial gastric juice from baseline pH 1.2 to 1.85±0.0000 and 1.80±0.0000 (Table 4.32) respectively. The amount of artificial gastric juice consumed to pH 3 showed that columbin and isocolumbin were able to consume 17.59±0.0000 mL and 15.52±0.0000 mL of the artificial gastric juice. Polypodine B and pinnatasterone also showed a strong neutralising effect among the compounds by increasing the artificial gastric juice from pH 1.2 to 1.78±0.01 and 1.65±0.00, respectively (Table 4.32). The volume of artificial gastric juice consumed to reach pH 3 showed that polypodine B and pinnatasterone were able to consume 7.26±0.01 mL and 7.04±0.00 mL of the artificial gastric juice.

4.33 Urease inhibition of isolated compounds

The isolated compounds showed the best activity in Polypodine B with an IC_{50} of 7.0±0.56 µM, this compound was found to be active than the standard acetohydroxamic acid with an IC_{50} of 20.3±0.43 µM. Other isolated compounds with higher activity compared to standard drug include: Pinnatasterone with an IC_{50} of 14.1±0.59 µM, 20-hydroxyecdysone with an IC_{50} of 13.8±0.49 µM. Tehuanin A and 2, 3 – dihydroxypropyl (E) – octadec – 5 – enoate gave IC_{50} of 23.9±1.02 µM and 23.4±0.43 µM respectively. Columbin and isocolumbin also gave IC_{50} of 24.1±1.10 µM and 37.5±2.70 µM respectively (Table 4.33).

Table 4.31: Summary of isolated compounds

S/No	Code	Name	Eluting Solvent	Colour	Weight (mg)
1	SJE - 10B	Columbin	DCM 100 %	White crystals	10
2	SJE - 10C	Isocolumbin	DCM 100 %	White crystals	10
3	CPE - 10A	Palmatine	DCM + 5% MeOH	White powder	4
4	CPE - 43A	5-(hydroxymethyl) furan-2-carbaldehyde	DCM + 2% MeOH	Brown oil	7
5	SJE - 23D	Atrotosterone A	DCM 100%	White powder	6
6	SJE - 28B	Pinnatasterone	DCM + 10% MeOH	Off white powder	8
7	SJB - 12	Polypodine B	H: DCM 30 : 70	White powder	8
8	SJB - 12B	20-Hydroxyecdysone	H: DCM 30 : 70	White powder	10
9	SJB - 26A	20, 26 – dihydroxyecdysone	H: DCM 30 : 70	Yellow powder	6
10	SJH - 28A	Tehuanin A	H: EtoAc 70 : 30	White crystals	6
11	SJH - 28B	2, 3 – dihydroxypropyl (E) – octadec – 5 - enoate	H: EtoAc 70 : 30	Light yellow oil	30
12	SJH – 34B	Tinospin E	H: EtoAc 60: 40	Colourless solid	4

Table 4.32: *In vitro* antacid activity of isolated compounds

S/No	Compounds	Concentration mg/250 mL	pH	Neutralisation Efficiency	Action efficiency (Amount of AGJ consumed mL)	No of H^+ ion consumed
1	$NaHCO_3$	0.5	8.11	1.53 ± 0.0033	19. 01 ±0.0057 [a]	1.20 ± 0.0000
2	Water	0.5	6.19	1.30 ± 0.0033	3.01 ± 0.0057 [c]	0.19 ± 0.0000
3	Columbin	0.5	6.34	1.85 ± 0.0000	17.59 ± 0.0000	1.11 ± 0.0000
4	Isocolumbin	0.5	5.42	1.80 ± 0.0000	15.52 ± 0.0000	0.98 ± 0.0000
5	Atrotosterone A	0.5	6.78	1.43 ± 0.0011	7.22 ± 0.0100 [b]	0.52 ± 0.011
6	5-(hydroxymethyl) furan-2-carbaldehyde	0.5	6.42	1.72± 0.0100	7.02 ± 0.0100 [b]	0.44 ± 0.0100
7	Pinnatasterone	0.5	7.22	1.65 ± 0.0000	7.04 ± 0.0000 [b]	0.44 ± 0.033
8	Polypodine B	0.5	6.87	1.78 ± 0.0100	7.26 ± 0.0100 [b]	0.45 ± 0.0012
9	20-Hydroxyecdysone	0.5	7.00	1.49 ± 0.0023	8.82 ± 0.0022 [b]	0.56 ± 0.0003
10	20, 26 – dihydroxyecdysone	0.5	6.82	1.47 ± 0.0033	8.22 ± 0.0100 [b]	0.52 ± 0.011
11	Tehuanin A	0.5	6.78	1.54 ± 0.0012	6.84 ± 0.0100 [b]	0.43 ± 0.0100
12	2,3– dihydroxypropyl (E) – octadec – 5 -enoate	0.5	6.54	1.68 ±0.0100 [b]	7.26 ± 0.0033 [b]	0.45 ± 0.0033 [b]

Table 4.33: Urease inhibition of isolated compounds

S/N	Sample	Concentration (mM)	IC_{50} ± SEM (µM)
1	SJE – 10B: Columbin	0.5	24.1 ± 1.10
2	SJE – 10C: Isocolumbin	0.5	37.5 ± 2.70
3	SJE – 23D: Atrotosterone A	0.5	24.1± 1.21
4	CPE – 43A: 5- (hydroxymethyl) furan-2-carbaldehyde	0.5	55.8 ± 2.16
5	SJE – 28B: Pinnatasterone	0.5	14.1 ± 0.59
6	SJB – 12: Polypodine B	0.5	7.0 ± 0.56
7	SJB -12B: 20-hydroxyecdysone	0.5	13.8 ± 0.49
8	SJB – 26A: 20, 26 – dihydroxyecdsone	0.5	29.3 ± 1.45
9	SJH – 28A: Tehuanin A	0.5	23.9 ± 1.02
10	SJH 28B: 2, 3 – dihydroxypropyl (E) – octadec – 5 – enoate	0.5	23.4 ± 0.43
11	Acetohydroxamic acid	0.5	20.3 ± 0.43

CHAPTER FIVE

DISCUSSION AND CONCLUSION

5.1 Ethnobotanical study and ethnopharmacological data

The study revealed that most of the plant species used for treating gastric ulcer are obtained from the wild. A report showed that though, medicinal plants are essential in primary health care, conservation practices are yet to be in place as most of these natural resources are not documented and their importance are not taken into cognizant due to uncontrolled and incessant plant harvesting from the natural habitat. This practice is quite enormous in different communities in Africa and other continents of the world (Soladoye *et al*., 2005). Traditional medicine is described as the overall understanding, abilities and methods native to diverse cultures used for maintenance and improvement of human health and also for prevention, diagnosis and treatment of mental and physical ailments (WHO, 2008). It is of great importance to document medicinal plants used by indigenous people from different parts of the world. However, indigenous plant knowledge used for treatment of human ailments is gradually going into extinction as this information is transmitted verbally without documentation from one generation to the other. This is because many traditional medical practitioners are not educated and have inadequate written documents where it exists. It is therefore essential to document the data obtained from traditional medical practitioners, herb sellers and elderly people in order to serve as a future reference for scientists, students and appropriate stakeholders. The documentation will also preserve the use of traditional medicinal products, find new drugs and may discover enhanced implementation of traditional medicine. It will also help conserve the cultural heritage of indigenous people for future generations. Ethnobotany is regarded as an efficient method for finding new medicinal plants to extract and isolate valuable bioactive compounds (Thirumalai *et al*., 2009).

The plants' roots and leaves are mostly used for herb preparation while the seeds are least used.
The results also showed that majority of the respondents are familiar with the use of certain species such as *Entada gigas, Kigelia africana, Curculigo pilosa, Khaya ivorensis, Lonchocarpus cyanescens*, *Parkia biglobosa, Sphenocentrum jollyanum*, *Musa sapientum*, *Uvaria chamae*, *Uvaria afzelii*, *Pseudocedrella kotschyi,* and *Euadenia trifoliolata* in the treatment of gastric ulcer. This was inferred from the frequency of occurrence and fidelity level of the plant species. This result also revealed that various parts of the plants especially the leaves, stem bark, roots, and fruits but rarely the whole plants have been used in the treatment of the disease. Investigations on the plant parts used and the mode of preparation and administration revealed that water was the main medium for all the medicinal preparations irrespective of the plant part(s) or combinations used. The drug was administered along with honey or hot pap. Most of the respondents claimed there are usually no side effects in the use of the medicinal plants.

This study has recognised important medicinal plants used for treating gastric ulcer by traditional medical practitioners in southwestern Nigeria. This offers a basis for future pharmacological and phytochemical research into the useful medicinal properties of the plants being documented.

5.2 Phytochemical analysis

The phytochemical screening of seeds of *Sphenocentrum jollyanum* established the presence of saponins, tannins, flavonoids and cardiac glycosides while alkaloid and anthraquinones were absent. This result supports the previous report of Ojelere, (2016). Tannins have been reported to speed up the wound healing process and/or swollen mucous membrane possibly by tanning the membrane surface thereby acting as a defensive covering against aggressive substances. Tannins might have been responsible for mucosal surface covering thus reducing lipid peroxidation. Flavonoids are a diverse class of secondary metabolites with useful health properties widely distributed in plants (Zayachkivska *et al.,* 2005). They possess antioxidant, cytoprotective, and anti-secretory activities. They also act as gastroprotective and ulcer healing agents which can be new alternatives for subduing peptic ulcer diseases related to *Helicobacter pylori* (Zayachkivska *et al*., 2005). Flavonoids also have certain defensive actions against free radicals, microbes, ulcers, viruses, allergies, inflammation, and tumors (Salami *et al.,* 2017). They are capable of activating the mucosal defense system by stimulating gastric mucus secretion and scavenge for the reactive oxygen species and free radicals. Flavonoids were observed to scavenge free radicals and might have been

responsible for the reduced oxidative reactions in gastroprotection study. Saponins are involved in the stimulation of mucous membrane defensive factors by exerting its defensive activities in gastric ulceration (Choudhary *et al.*, 2013).

Curculigo pilosa rhizome has phytochemicals such as saponins, tannins, flavonoids, and cardiac glycosides which also confirm the previous result of Gbadamosi and Egunyomi, (2009).

5.3 Total phenolic content, total flavonoid content and DPPH radical scavenging activity

The highest Total phenolic content was noted in *Pseudocedrella kotschyi* stem bark (560.5 mg GAE/g). *Uvaria chamae* root also gave high value of 338.4 mg GAE/g, followed by *Uvaria afzelii* root (265.91 mg GAE/g). *Ageratum conyzoides* had the highest Total flavonoid content (236.8 mg QE/g), followed by *Vernonia amygdalina* and *Euadenia trifoliolata* leaves with values 126.4 and 122.9 respectively. *Pseudocedrella kotschyi* stem bark (IC_{50} 2.74 µg / mL) gave the smallest IC_{50} value corresponding to the highest scavenging activity. This value was comparable to the reference drug; Ascorbic acid (2.76 µg/mL). *Uvaria afzelii* root and *Khaya ivorensis* stem barks also gave promising results (IC_{50} 11.58 µg/mL and 11.89 µg/mL respectively). Ascorbic acid and Rutin used as standards had IC_{50} of 2.76 µg/mL and 20.6 µg/mL respectively. It has been noted that polyphenolic compounds play a useful role in gastric ulcers. Phenols have been suggested to boost the development of prostaglandin (Alanko *et al.*, 1999). The status of different oxidative stress biomarkers is clearly improved by polyphenols. The action mechanism of these potential impacts was ascribed to their antioxidant characteristics through numerous probable mechanisms including their capacity to break radical chain reactions, scavenge free radicals, reduce peroxides and stimulate antioxidant defense enzyme activity.

5.4 Toxicity study of *Curculigo pilosa* and *Sphenocentrum jollyanum* extracts

The acute toxicity study carried out on the plant extracts showed that the extracts seemed to be safe visually as no death or obvious toxicity signs were observed in treated animals for the first 24 h and by the end of 48 h observation. However, slight diffuse tubular glomeruli shrinkage was observed in the kidney of animals administered with high doses (1600 $mgkg^{-1}$, 2900 $mgkg^{-1}$, and 5000 $mgkg^{-1}$) of the two extracts. Also, *S. jollyanum* treated animals revealed several foci of perivascular cellular infiltration in the heart of the animals administered with high doses (1600 $mgkg^{-1}$, 2900 $mgkg^{-1}$, and 5000 $mgkg^{-1}$). In the liver of high-dose animals (1600 $mgkg^{-1}$, 2900 $mgkg^{-1}$, and 5000 $mgkg^{-1}$) of the two extracts, severe portal congestion, and diffuse vacuolar degeneration of hepatocytes were also

observed. The present study supports the report of Mbaka *et al*. (2010) where acute toxicity study of *S. jollyanum* leaf extract displayed no toxicity when administered up to 11 g/kg *b.w.* orally. Acute toxicity study of *C. pilosa* is reported for the first time. Toxicity studies are crucial in setting safety limits for potential drugs and are also frequently used to assess potential health hazards from plant extracts (Klassen and Eaton, 1991).

5.5 Reduction in severity of lesions caused by indomethacin induced gastric ulcer and stomach histology

The research was aimed at evaluating the anti-ulcer activity of *Curculigo pilosa* rhizomes and *Sphenocentrum jollyanum* seeds methanol extracts so as to validate the traditional claim as anti-ulcerogenic plants.

The standard (cimetidine) and *Curculigo pilosa* 50 mg treated groups significantly reduced the gastric ulcer index from 8.00 ± 2.72 in the ulcer untreated group to 0.20 ± 0.20 and 1.17 ± 0.83 respectively. *Sphenocentrum jollyanum* 200 mg treated group also showed significant reduction in gastric ulcer index from 8.00 ± 2.72 to 2.20 ± 1.24. Cimetidine, *C. pilosa* 50 mg, and *S. jollyanum* 200 mg treated groups gave percentage inhibitions of 97.6%, 82.9% and 73.2%, respectively. This suggests that the plants displayed anti-ulcer activity indicated by lowering ulcer index or increasing percentage inhibition. Numerous medicinal values are associated with *Curculigo pilosa* and *Sphenocentrum jollyanum* plant extracts with reported pharmacological activities. Several drugs are marketed for gastric ulcer therapy including antacids, proton pump inhibitors, antihistamines, and anticholinergic. Many of these drugs possess severe side effects, such as altered bowel function when antacids are used (Sandhya *et al.*, 2012), toxicity of the liver and kidney in the case of anti-histamines (Fisher and Le-Couteur, 2012).

Indomethacin is a well-known NSAID used for treating pain, joint stiffness caused by arthritis, and fever. Inhibition of prostaglandin is the mechanism of action (Wallace, 2001). Roles of endogenous prostaglandin involve maintaining mucosal integrity and protecting stomach against toxic agents (Wallace, 2001). Therefore, indomethacin and other NSAIDs act on stomach tissue to interrupt the defensive covering of the mucus layer. Indomethacin possesses higher ulcerogenic potential than other NSAIDs therefore the choice in the gastric ulcer experiment (Sigthorsson *et al*., 2000). The present study showed erosion of mucus layer, necrosis, and congestion in the blood vessels of ulcer untreated group by action of indomethacin. This is comparable to earlier results of Adewoye and Salami (2013), and Boeing *et al*. (2016) whereby NSAIDs inhibited the mucus layer and

prostaglandin when assessing the anti-ulcer mechanism of magnesium and *Vernonia condensata* Baker, respectively.

5.6 Effects of antioxidant parameters in gastroprotection

5.6.1 Effects of total gastric protein and nitric oxide in gastroprotection

The increased total gastric protein, nitric oxide, and antioxidant parameters observed might have assisted in the neutralisation, reduction, or prevention of some damages caused by free radicals. Nitric oxide prevents gastric secretion by suppressing histamine release from enterochromaffin-like cells (Freitas *et al*., 2004). The moderated nitric oxide levels observed in *C. pilosa* and *S. jollyanum* treated groups could be another mechanism by which the plants enhance gastroprotection by possibly increasing blood flow, oxygen and nutrients to the stomach injury site. Total gastric protein assists in repair of worn out tissues at the ulcer site.

5.6.2 Effects of superoxide dismutase (SOD) and catalase (CAT) in gastroprotection

Evidence showed that oxygen derived free radicals play a major part in the pathogenesis of numerous diseases, including peptic ulcer disease with antioxidant being actively involved in the protection of gastric mucosa against several necrotic mediators (Dhasan *et al*., 2010). This could be the reason for increase in antioxidant markers such as SOD and CAT. The observed increase in SOD and CAT of *C. pilosa* and *S. jollyanum* treated groups could have contributed to gastroprotection activity. Many drugs with strong antioxidant activity are efficient in healing experimentally induced gastric ulcers (Dhuley, 1999).

5.6.3 Effect of *C. pilosa* and *S. jollyanum* methanol extracts on glutathione

Gastric wall has an elevated GSH concentration providing protection against oxidative damage caused by necrotising agent such as indomethacin. When the GSH in gastric tissue is depleted, there is an enhanced danger of gastric injury. The augmented GSH observed in *C. pilosa* and *S. jollyanum* treated groups might have aided in the neutralisation, reduction, or prevention of some damages caused by free radicals. The observed increase in GSH supports the report of Dhuley (1999) who reported the *in vivo* antioxidant effect of *Cinnamomum verum* Fresl. (Lauraceae) stem bark in rats where the GSH content was restored in rats administered with the extract. This research also supports Nahla *et al*. (2016) earlier report on the gastroprotective effect of garlic in gastric ulcer induced by indomethacin. Garlic extracts pretreated groups, when compared to the control group, adjusted gastric MDA and partly GSH concentrations in rats.

5.6.4 Effect of *C. pilosa* and *S. jollyanum* methanol extracts on malondialdehyde (MDA) level

The inflammatory response produced by indomethacin could be facilitated by oxidative stress induction. This is consistent with the present study as indomethacin induction caused a rise in gastric MDA. The estimated MDA concentration is an important oxidative stress marker within the biological system (Thorpe and Baynes, 2003). *Curculigo pilosa* and *Sphenocentrum jollyanum* reduced the MDA levels, meaning they helped control the amount of MDA thereby reducing the free radicals generated at the ulcer site. The lipid peroxidation decrease might also have been an outcome of the synergistic action of phytochemical constituents present in the plants.

5.7 Antacid activity of *Curculigo pilosa* and *Sphenocentrum jollyanum* extracts and fractions

The obtained result showed that *S. jollyanum* ethyl acetate fraction, *C. pilosa* ethyl acetate, *n* butanol, and aqueous fractions at 50 mg and 100 mg concentrations had good neutralising capacities greater than the standard drug, sodium bicarbonate. The antacid activity exhibited by the fractions was also higher than that of crude extracts. In terms of neutralising capacity, *S. jollyanum* ethyl acetate fraction at 50 mg and 100 mg concentrations was able to consume 14.01 mL and 16.02 mL of artificial gastric juice, whereas sodium bicarbonate was able to consume 19.01 mL and 28.49 mL respectively. Antacids have been widely used in gastric ulcer treatment. They act chemically to neutralise existing amounts of stomach acid, but have no immediate impact on their production (Sandhya *et al*., 2012). Efficient antacid treatment has prevalent side effects, mainly altered bowel movement. Magnessium salts cause diarrhea, aluminum salts can cause constipation, while sodium bicarbonate includes large quantities of sodium that can change the pH of the system. Antacids also possess significant clinical interaction with tetracycline, ferrous sulfate and quinolone antibiotics (Wu *et al.,* 2010). There is therefore need for alternatives from medicinal plants. The antacid result obtained revealed that the highest neutralising effect was observed in *C. pilosa* aqueous fraction, which was discovered to be greater than the sodium bicarbonate standard. It appears that the antacid activity is attributed to the polar solvent extracts than the non-polar solvent extracts, which suggests the fact that polar compounds gave better antacid activity than non-polar compounds (Sandhya *et al*., 2012). The antacid activity exhibited by *C. pilosa* and *S. jollyanum* could be as a result of the flavonoids in the plants. The inhibitory effect of flavonoids mediated by the alpha adrenergic and calcium system on the gastric secretions has been discovered to be useful in ulcer therapy (Raj *et al*., 2001).

5.8 Urease inhibition of *Curculigo pilosa* and *Sphenocentrum jollyanum* extracts and fractions

The urease inhibition showed that *C. pilosa n* hexane fraction, *S. jollyanum n* hexane, *n* butanol and aqueous fractions showed good results with IC_{50} values of 24.3 µM, 25.4 µM, 28.6 µM and 22.7 µM respectively, which were comparable with the standard; acetohydroxamic acid (IC_{50} value 20.3 µM). *Sphenocentrum jollyanum* crude extract gave IC_{50} of 40.0 µM while *Curculigo pilosa* crude extract was considered inactive at 0.5 mg concentration.

Medicinal plants and natural compounds isolated from higher plants are commonly used for treatment of many diseases as natural compounds provide a useful model for new drugs (Khan *et al*., 2015). Synthetic compounds such as imidazoles, hydroxamic acids, and phosphazenes are effective urease inhibitors. However, few natural product studies have been reported (Rahman and Choudhary, 2001). Urease is one of the major causes of pathologies induced by *Helicobacter pylori* thus allowing the *H. pylori* to survive at the acidic medium of the stomach.

This study suggests that *C. pilosa* and *S. jollyanum* fractions and isolated compounds can be used as urease inhibitor for the treatment of gastrointestinal tract ailments.

5.9 Identification of Compound SJE-10B using EI-MS, ^{1}H NMR and ^{13}C NMR spectroscopies

The ^{13}C NMR information (Table 4.16.1) revealed twenty carbons with six quaternary carbons, nine methine carbons, three methylene carbons, and two methyl carbons. Composition $C_{20}H_{22}O_6$, Molecular weight: 358. EI-MS, *m/z* (relat. intensity %): 358 (M^+, 7), 246 (45), 231 (44), 190 (12), 152 (86), 134 (16), 121 (41), 107 (100). FAB-MS (negative ion mode): 359 [M-1] $^+$. The NMR values of ^{13}C and ^{1}H were consistent with the literature (Moody *et al*., 2005). Details of EI-MS, ^{1}H NMR and ^{13}C NMR spectra are presented in Appendix XI. There is correlation of δ_H 1.20 (H-18) with δ_C 18.4 (C-7)/ δ_C 38.5 (C-5) and this suggests the presence of a methyl at position C-18. The HMBC correlations of δ_H 0.99 (H-19) with δ_C 28.1 (C-19)/ δ_C 38.5 (C-5)/ δ_C 57.6 (C-8)/ δ_C 75.5 (C-12) also suggests a methyl present between C-19. There are also correlations of δ_H 1.73 (H-6) with δ_C 24.4 (C-18)/ δ_C 38.5 (C-5)/ δ_C 42.4 (C-10) which suggest the presence of a methylene carbon at C-6. There are also correlations of δ_H 6.27 (H-3) with δ_C 71.6 (C-1)/ δ_C 137.2 (C-2) which suggest the presence of a double bond C-2 and C-3. Correlation also exist between δ_H 6.54 (H-14) and δ_C 75.5 (C-12) / δ_C 135.2 (C-13) and a correlations of δ_H 7.51 (H-15) with δ_C 135.2 (C-13)/ δ_C 141.4

(C-16)/ δ_C 144.9 (C-15) which confirms the presence of the furan ring in the structure. The observed data supports the report of Moody *et al*. (2005) in the elucidation of columbin. The key ^{1}H-^{1}H-COSY correlations of SJE-10B shows the following. The proton H-14 (δ_H 6.54) correlates with δ_H 7.51 (^{1}H-15). Also δ_H 6.55 (H-2) with δ_H 6.27 (H-3), δ_H 5.29 (H-1) with δ_H 6.55 (H-2), δ_H 5.59 (H-12) with δ_H 2.30 (H-11) show the vicinal couplings at H-14 with H-15, H-2 with H-3, H-1 with H-2, and H-12 with H-11. ^{1}H-^{1}H-NOESY correlation shows a correlation of δ_H 7.59 (H-16) with δ_H 6.54 (H-14). The assignment of carbon to proton was done using DEPT/HSQC (Moody *et al*., 2005).

5.10 Identification of Compound SJE-10C using EI-MS, ^{1}H NMR and ^{13}C NMR spectroscopies

The ^{13}C NMR of isocolumbin showed the presence of twenty carbons comprising six quatenary carbons, nine methine carbons, three methylene carbons, and two methyl carbons (Moody *et al*., 2005). Composition $C_{20}H_{22}O_6$, Molecular weight: 358. EI-MS, *m/z* (relat. intensity %): 314 [M – CO_2]$^+$ (7), 247 (13), 246 (18), 231 (17), 153 (100), 122 (23), 121 (29), 112 (48), 108 (57), 107 (77). FAB-MS (negative ion mode): 359 [M-1] $^+$. The ^{13}C NMR and ^{1}H NMR spectra of the compound are justified by Moody *et al*. (2005). There is correlation of δ_H 6.54 (H-2) with δ_C 82.4 (C-4) also, δ_H 5.59 (H-12) with δ_C 109.7 (C-14)/ δ_C 125.4 (C-13)/ δ_C 142.8 (C-15), then δ_H 5.24 (H-1) with δ_C 137.2 (C-3)/ δ_C 131.5 (C-8)/ δ_C 177.4 (C-20) this indicates the presence of a carbonyl carbon at C-20. δ_H 1.01 (H-19) with δ_C 57.6 (C-10)/ δ_C 47.5 (C-11)/ δ_C 40.0 (C-9), this suggests a methyl at C-19. The HMBC correlations of δ_H 1.19 (H-18) with δ_C 25.9 (C-19)/ δ_C 57.6 (C-10)/ δ_C 82.4 (C-4) suggests an hydroxyl at C-4, a methyl at C-18. The observed data supports the report of Moody *et al*. (2005) in the elucidation of isocolumbin. The key ^{1}H-^{1}H-COSY correlations show δ_H 6.26 (H-3) with δ_H 6.54 (H-2), also δ_H 2.30 (H-11) with δ_H 1.86 (H-10). The assignment of carbon to proton was done using DEPT/HSQC (Moody *et al*., 2005).

5.11 Identification of Compound SJE-23D using EI-MS, ^{1}H NMR and ^{13}C NMR spectroscopies

Compound SJE-23D was identified as Atrotosterone A. The ^{1}H and ^{13}C NMR data (Tables 4.18.1 and 4.18.2) agree with the reported (Vokac *et al*., 1999). The IR spectrum [KBr, Vmax (cm^{-1})]: 3414 (O-H), 1640 (C=O), 1056 (C - O) cm^{-1}. The observed data supports the report of Vokac *et al*. (1999) in the elucidation of Atrotosterone A. This compound is an ecdysteroid, with 6-keto, 7-ene conjugated system. The five isolated ecdysteroids; Pinnatasterone, Polypodine B**,** 20-Hydroxyecdysone, 20, 26 – dihydroxyecdysone, and Atrotosterone A have 6-keto, 7-ene conjugated

system; all the compounds are similar in the steroidal part with exception of polypodine B with hydroxyl function at C-5 and Atrotosterone A with hydroxyl function at C-11. The major difference in the structure is in the side chain. The molecular mass of the compounds was confirmed using FAB-MS (Vokac *et al*., 1999).

5.12 Identification of Compound SJE-28B using EI-MS, ^{1}H NMR and ^{13}C NMR spectroscopies

Compound SJE-28B was identified as Pinnatasterone. Composition $C_{27}H_{44}O_{7.}2H_20$, Molecular weight: 480. EI-MS, *m/z* (relat. intensity %): 462 (1), 444 (2), 426 (9), 408 (5), 393 (2), 363 (60), 345 (100), 327 (20), 309 (17), 303 (22), 285 (20), 269 (18), 250 (9), 227 (13), 191 (9), 173 (12), 143 (12), 125 (10), 99 (32), 81 (10), 57 (6), 43 (19). FAB-MS (negative ion mode): 479 $[M-1]^{+}$, FAB-MS (positive ion mode): 481 $[M+1]^{+}$. The ^{13}C NMR and ^{1}H data are justified by Filho *et al*. (2008) and Suksamrarn *et al*. (1995) respectively. The key HMBC correlations of Pinnatasterone and 20, hydroxyecdysone showed Pinnatasterone having correlation between δ_H 5.80 (H-7) and δ_C 85.2 (C-14)/ δ_C 31.5 (C-9) δC 167.9 (C-8) and this suggests the presence of conjugated double bond at position C-7. The HMBC correlations of δ_H 0.95 (H-19) with δ_C 35.1 (C-9)/ δC 39.2 (C-10) suggests the presence of an angular methyl at C-19. There is also a correlation of δ_H 3.12 (H-9) with δ_C 206.4 (C-6)/ δ_C 122.1 (C-7) this suggests the presence of a carbonyl at C-6 and oleifinic signal at C-7. Also correlation of δ_H 3.80 (H-2) with δ_C 68.5 (C-3)/ δ_C 37.3 (C-1) suggests the presence of an hydroxyl at C-3. There is also a correlation of δ_H 3.30 (H-24) with δ_C 77.9 (C-24)/ δ_C 29.7 (C-26) which suggests the presence of an hydroxyl in the side chain at position C-25. There is a correlation of δ_H 1.19 (H-21) with δ_C 21.1 (C-21)/ δ_C 42.4 (C-22) also at the side chain. For 20-hydroxyecdysone, there is correlation of δ_H 3.01 (H-5) with δ_C 203.5 (C-6)/ δ_C 121.6 (C-7), this suggests the presence of a carbonyl at C-6 and a conjugated double bond system at C-7. The HMBC correlations of δ_H 2.03 (H-3) with δ_C 68.1 (C-3)/ δ_C 68.0 (C-2) suggests the presence of an hydroxyl at C-2 and C-3 respectively. There are also correlations of δ_H 1.39 (H-26) with δ_C 29.9 (C-27)/ δ_C 42.6 (C-24) on the side chain, also correlation of δ_H 1.24 (H-18) with δ_C 48.1 (C-13)/ δ_C 84.1 (C-14), this suggests the presence of an hydroxyl at C-14. The assignment of carbon to proton was done using DEPT/HSQC (Suksamrarn *et al*., 1995; Filho *et al*., 2008).

5.13 Identification of Compound CPE-10A using HR-MS and ^{1}H NMR spectroscopies

Compound CPE-10A (Palmatine) was determined using EI-MS and ^{1}H NMR as reported by Zhu *et al*. (2016). The ^{13}C NMR could not be determined due to paucity of sample. The HR ESI-MS was justified with molecular formula for ($C_{21}H_{22}NO_4^+$) at *m/z* (rel. int. %): 353 [100, M^+ +1], 352 [83], 338 [50], 322 [19], 294 [20], 239 [20], 185 [19], 152 [25], 129 [25], 119 [50], 97 [40], 85 [35], 57 [75], 43 [62]. ^{1}H-NMR of the compound showed six aromatic protons at δ, 9.72, (1H, s, H-2), 8.78, (1H, s, H-9), 8.51, (1H, s, H-15), 8.10 (1H, d, J = 9.0 Hz, H-6), 8.00 (1H, d, J = 9.0 Hz, H-7) and 7.03 (1H, s, H- 12), two methylene proton signals at δ 3.17 (1H, t, J = 10.0 Hz, H-17) and 3.40 (1H, t, J = 10.0 Hz, H-18) and four methoxy peaks at δ 4.20 (3H, s, 19-OMe), 4.11 (3H, s, 20-OMe), 3.99 (3H, s, 22-OMe) and 3.94 (3H, s, 21-OMe). This justifies the report of Zhu *et al*. (2016).

5.14 Identification of Compound CPE-43A using EI-MS, ^{1}H NMR, ^{13}C NMR spectroscopies

Compound CPE-43A (7 mg) was identified as 5-Hydroxymethyl-2-furancarbaldehyde with composition $C_6H_6O_3$, Molecular weight: 126 as previously reported by Zuo *et al*. (2014). EI-MS *m/z*: 126 (M, 64.3)$^+$, 123.1 (13), 97 (100), 84 (23), 69 (23), 53 (10), 41 (47). FAB-MS (positive ion mode): 127 (M + 1)$^+$. ^{1}H NMR (CD_3OD, 400 MHz): 9.52 (1H, s, H-1), 7.37 (1H, d, J = 3.6 Hz, H-2^1), 6.57 (1H, d, J = 3.6 Hz, H-3^1), 4.60 (2H, s, H-2); ^{13}C NMR (CD_3OD, 300 MHz): 179.5 (C-1), 163.3 (C-1^1), 154.0 (C-4^1), 124.7 (C-2^1), 110.9 (C-4), , 57.7 (C-7), this justifies Zuo *et al*. (2014) report. The key HMBC correlation of the compound revealed correlation of δ_H 9.52 (H-1) with δ_C 163.3 (C-1^1)/ δ_C 124.7 (C-2^1); this suggests the presence of double bond at position C-2^1. The HMBC correlations of δ_H 7.37 (H-2^1) with δ_C 163.3 (C-1^1)/ δ_C 179.4 (C-1)/ δ_C 110.8 (C-3^1)/ δ_C 154.0 (C-4^1)/ δ_C 57.8 (C-2) suggests the presence of an unsaturation at C-3^1 and at C-4^1. There is also correlation of δ_H 4.60 (H-2) with δ_C 154.0 (C-4^1)/ δ_C 110.8 (C-3^1), this suggests the presence of an hydroxyl at C-2. The assignment of carbon to proton was done using DEPT/HSQC. The ^{1}H-^{1}H COSY correlation shows a correlation of δ_H 7.37 (H-2^1) with δ_H 6.57 (H-3^1), which further confirms the structure of the compound (Zuo *et al*., 2014).

5.15 Identification of Compound SJB-12 using EI-MS, ^{1}H NMR, ^{13}C NMR, and IR spectroscopies

Compound SJB-12 (8 mg) was identified as Polypodine B (Figure 4.22). Composition $C_{27}H_{44}O_8$, Molecular weight: 496. EI-MS, *m/z* (relat. intensity %): 445 (5), 426 (4), 411 (7), 393 (4), 363 (72), 345 (100), 327 (18), 309 (20), 300 (26), 285 (22), 269 (39), 249 (11), 227 (13), 191 (13), 173 (24),

143 (19), 125 (14), 99 (85), 81 (38), 57 (12), 43 (56), 41 (11). FAB-MS (positive ion mode): 497$(M+1)^+$.

^{13}C NMR (600 MHz, C_5D_5N): 34.8 (C-1), 67.9 (C-2), 69.8 (C-3), 36.0 (C-4), 79.8 (C-5), 200.9 (C-6), 119.8 (C-7), 166.8 (C-8), 38.2 (C-9), 44.7 (C-10), 22.0 (C-11), 31.6 (C-12), 48.1 (C-13), 84.0 (C-14), 32.0 (C-15), 21.4 (C-16), 49.9 (C-17), 17.8 (C-18), 17.1 (C-19), 76.8 (C-20), 21.6 (C-21), 77.5 (C-22), 27.5 (C-23), 42.6 (C-24), 69.5 (C-25), 30.0 (C-26), 30.1 (C-27). The IR (KBr, cm^{-1}) spectrum shows: 3414 (OH), 1667 (-C=O, 6-keto-7-ene) and 1063 (C-O). The ^{13}C and ^{1}H NMR data (Tables 4.22.1 and 4.22.2) justify Nishimoto *et al*. 1987 and Coll *et al*., 1994 reports respectively.

5.16 Identification of Compound SJB-12B using EI-MS, ^{1}H NMR, ^{13}C NMR, and IR spectroscopies

Compound SJB-12B (10 mg) was identified as 20-hydroxyecdysone (Figure 4.23)**.** Composition $C_{27}H_{44}O_7$, Molecular weight: 480 justifies the previous report of Bandara *et al.* (1989). EI-MS, *m/z* (relat. intensity %): 445 (1), 426 (20), 411 (8), 393 (2), 363 (78), 345 (100), 327 (79), 309 (18), 300 (26), 285 (22), 269 (39), 249 (11), 227 (13), 191 (13), 173 (24), 143 (19), 125 (14), 99 (85), 81 (38), 57 (12), 43 (56), 41 (11). FAB-MS (positive ion mode): 481$(M+1)^+$.

^{13}C NMR (600 MHz, C_5D_5N): 37.9 (C-1), 68.0 (C-2), 68.1 (C-3), 32.4 (C-4), 51.3 (C-5), 203.5 (C-6), 121.6 (C-7), 166.1 (C-8), 34.3 (C-9), 38.6 (C-10), 21.1 (C-11), 31.7 (C-12), 48.1 (C-13), 84.1 (C-14), 31.9 (C-15), 21.5 (C-16), 50.1 (C-17), 17.9 (C-18), 24.4 (C-19), 77.5 (C-20), 21.6 (C-21), 76.8 (C-22), 27.4 (C-23), 42.6 (C-24), 69.1 (C-25), 30.1 (C-26), 29.9 (C-27).

The ^{13}C and ^{1}H NMR data agree with the reported (Bandara *et al*., 1989). The IR spectrum shows: 3021 (–C=C-) signifying the presence of double bond in the compound (Bandara *et al*., 1989).

5.17 Identification of Compound SJB-26A using EI-MS, ^{1}H NMR, ^{13}C NMR and IR spectroscopies

Compound SJB-26A (5 mg) was identified as 20, 26-dihydroxyecdysone with composition $C_{27}H_{44}O_8$ and molecular weight: 496. EI-MS, *m/z* (relat. intensity %): 345 (56), 327 (39), 309 (16), 300 (31), 285 (32), 267 (28), 253 (15), 241 (11), 227 (23), 209 (11), 189 (21), 173 (28), 155 (16), 141 (23), 129 (35), 115 (74), 91 (28), 83 (18), 71 (37), 55 (30), 43 (100), 41 (26). FAB-MS (negative ion mode): 495 $[M-1]^+$. The IR spectrum [KBr, Vmax (cm^{-1})]: 3021(–C=C-) (indicating the presence of –C=C- conjugated to the keto group), 1740 (-C=O, 6-keto-7-ene). The ^{13}C and ^{1}H NMR data (Tables 4.24.1 and 4.24.2) agree with the reported (Zhu *et al*., 2001).

5.18 Identification of Compound SJH-28A using EI-MS, ^{1}H NMR and ^{13}C NMR, spectroscopies

Compound SJH-28A (6 mg) was identified as Tehuanin A (Figure 4.25) with melting point 240-242^{o}C. Composition $C_{20}H_{21}O_6$, Molecular weight: 357 justify the previous report of Bautista (2012). EI-MS, *m/z* (relat. intensity %): 358 (M+1, 2.9) $^{+}$, 307 (14), 231 (64), 152 (54), 107 (100). The ^{13}C and ^{1}H-NMR values (Tables 4.25.1 and 4.25.2) justify Bautista (2012) report. The ^{13}C NMR spectrum shows 20 signals and the IR spectrum indicated the presence of lactones and a furan, also that the compound had a neo-clerodane skeleton. The 1H and ^{13}C NMR spectra showed the presence of a tertiary methyl (δ_H 1.05 s, δC 24.2, CH_3-20), a furan ring (δ_H 6.42, H-14; δ_H 7.42, H-15; δ_H 7.46, H-16), a 17, 18-γ- lactone (δ_C 173.3, C-18; δ_C 175.4 respectively). In the HMBC spectrum, the signal at δ_H 7.46 (H-16) correlated with δ_C 124.7 (C-13). There is correlation of δ_H 7.42 (H-15) with δ_C 143.9 (C-15)/ δ_C 139.6 (C-16) δ_C 108.3 (C-14) which suggests the presence of a furan skeleton in the structure. The HMBC correlations from δ_H 5.39 (H-1) to δ_C 47.5 (C-10). There is also a correlation from δ_H 1.05 (H-20) to δ_C 80.8 (C-8) which suggests the presence of an oxo-carbon bridge at C-1 and C-8. Also correlation from δ_H 3.45 (H-4) to δ_C 37.1 (C-9)/ δ_C 80.4 (C-8)/ δ_C 175.4 (C-18) suggests the presence of a carbonyl at C-18 and a cyclic ester (lactone) in the structure. The assignment of carbon to proton was done using DEPT/HSQC (Bautista, 2012).

5.19 Identification of Compound SJH-28B using EI-MS, ^{1}H NMR, ^{13}C NMR and IR spectroscopies

Compound SJH-28B (30 mg) was obtained as light-yellow oil. Composition $C_{21}H_{40}O_4$, Molecular weight: 356. FAB-MS (positive ion mode): 357 (M+1) $^{+}$. The compound (lipid-fatty acid methyl ester) is isolated for the first time and named 2, 3-dihydroxypropyl-octadec-5-enoate using ^{13}C and ^{1}H NMR data. The IR spectrum (KBr, Vmax (cm^{-1})): 3466 (OH), 3004 (=C-H $_{stretch}$), 2922 (-C-H $_{stretch}$), 1732 (-C=O) and 1060 (C-O). The IR absorption peak at 3466, which was broad represents hydrogen bonded alcohols at carbon 1 and 2, the peak 3004 (=C-H $_{stretch}$), shows the presence of double bond on C-8 and C-9 respectively. 2922 (-C-H $_{stretch}$), 1732 (-C=O), indicates the presence of a carbonyl group of an ester. The key HMBC correlation of the compound showed a correlation of δ_H 5.39 (H-9) with δ_C 128.0 (C-8)/ δ_C 27.2 (C-10) δ_C 131.3 (C-9) which suggests the presence of a double bond at position C-8. The HMBC correlations of δ_H 5.28 (H-8) with δ_C 26.4 (C-7)/ δ_C 128.0 (C-8)/ δ_C 131.3 (C-9) still suggests the presence of a double bond at C-8 and C-9. There is also a correlation of δ_H 4.19 (H-3) with δ_C 70.2 (C-2)/ δ_C 63.3 (C-1), this suggests the presence of an

hydroxyl at C-1 and C-2 respectively. Also correlation of δ_H 0.86 (H-21) with δ_C 14.1 (C-21)/ δ_C 22.6 (C-20) suggests the presence of a terminal methyl at C-21. There is also a correlation of δ_H 1.26 (H-20) with δ_C 14.1 (C-21)/ δ_C 22.6 (C-20), this suggests the presence of a straight chain continuous alkyl in the compound. The assignment of carbon to proton was done using DEPT/HSQC. The key ^{1}H-^{1}H -COSY correlations showed that the two protons, δ_H 5.28 (H-8) and δ_H 5.39 (H-9) has a vicinal coupling, one of the methylene protons at position 7, δ_H 2.05 (H-7) with δ_H 5.28 (H-8) and one of the methylene protons at position 5, δ_H 2.34 (H-5) with another methylene proton on δ_H 1.67 (C-6, H-6).

5.20 Identification of Compound SJH-34B using EI-MS, ^{1}H NMR, ^{13}C NMR, spectroscopies

Compound SJH-34B (4 mg) was identified as Tinospin E based on the previous report of Huang *et al*. (2012). It has the molecular formula $C_{20}H_{20}O_6$, as confirmed by FAB-MS from the 357 $(M + 1)^+$. The compound is a diterpenoid form of cis-clerodane which was indicated by the typical C-12 furan ring downfield resonances in the ^{1}H-NMR spectrum (Huang *et al*., 2012). A 12-oxymethine proton resonance at δH 5.33 was noted in the ^{1}H-NMR spectrum. ^{1}H -^{1}H COSY correlation was noted between δH 6.44 (H-2) and 6.33 (H-3), indicating the existence of C-2 and C-3 olefin motherhood. H-12 was noted in the ^{1}H –^{1}H COSY spectrum to correlate with one of the pairs of methylene-coupled proton resonances at δH 1.94 (H-11). A downfield olefin resonance proton at π-H 7.42 was assigned to be H-15 by the HMBC correlation to C-14, C-15/C 139.6, C-16, suggesting the existence of a furan ring system. There is a correlation of δ_H 7.47 (H-16) with δ_C 108.4 (C-14)/ δ_C 123.3 (C-13)/ δ_C 143.8 (C-15)/ δ_C 139.8 (C-16) which also suggests the existence of a furan ring system. H-2 with δ_C 74.2 (C-1)/ δ_C 81.0 (C-4)/ δ_C 175.3 (C-18), suggests the existence of a double bond at C-2 and a carbonyl carbon at C-18. In the HMBC spectrum, the signal at δ_H 1.07 (H-20) correlated with δ_C 38.6 (C-9)/ δ_C 41.6 (C-10) thereby suggesting a methyl at C-20. There is correlation of δ_H 2.66 (H-10) with δ_C 24.5 (C-20)/ δ_C 38.6 (C-9), which suggest a methyl at C-20. The HMBC correlations of δ_H 1.19 (H-19) with δ_C 81.0 (C-4)/ δ_C 38.6 (C-9)/ δ_C 24.5 (C-20) (Huang *et al*., 2012).

5.21 Biological activities of isolated compounds

The best urease inhibition was observed in Polypodine B, which was found active than the standard drug, acetohydroxamic acid. Polypodine B belongs to a class of compound known as ecdysteroids. Ecdysteroids are polar classes of steroids which are nearly soluble like sugar (Gilbert *et al*., 2002). Medicinal plants rich in plant ecdysteroids include; 20-hydroxyecdysone in *Spinacia oleraceae* L., (Chenopodiaceae), ajugasterone in *Ajuga reptans* L., (Lamiaceae), Leuzeasterone in *Leuzea*

carthamoides (syn. *Rhaponticum carthamoides* (Willd.) Iljin, (Compositae), 20-hydroxyecdysone in *Tinospora cordifolia* (Willd.) Miers, Menispermaceae (Song and Xu, 1991). The two prominent hormones present in insects are ecdysteroids and sesquiterpene (also known as juvenile hormone). These hormones are typically accompanied by small ecdysteroids. Biological activities of plant ecdysteroids include anabolic, antidiabetic and wound healing (Lafont and Dinan, 2009). For the first time, the anti-ulcer activity of the isolated ecdysteroids from *Sphenocentrum jollyanum* seeds is reported. The result obtained in this research also showed that in terms of neutralisation efficiency and neutralisation capacity, columbin and isocolumbin showed the highest antacid activity among the compounds. Columbin and isocolumbin; furanoditerpenoids belong to the class of compound called clerodane diterpenes. This furanolactone diterpenoid was isolated from many plants such as *Sphenocentrum jollyanum* (Moody *et al*., 2005) and *Jateorhiza malumba* Miers, (Menispermaceae) (Li *et al*., 2016). Biological activities include insect antifeedant effect (Klein *et al*., 2002) and anti-inflammatory (Moody *et al*., 2005).

5.22 Conclusion

Medicinal plants predominantly used to treat gastrointestinal ulcer in southwestern Nigeria have been documented from the ethnobotanical survey conducted in five local government areas of Ibadan, Nigeria. Some of the most frequently used medicinal plants mentioned by the respondents are: *Curculigo pilosa* (Schumach. & Thonn.) Engl., *Sphenocentrum jollyanum* Pierre, *Euadenia trifoliolata* (Sch. &Thon.) Oliv., *Khaya ivorensis* A. Chev., *Lonchocarpus cyanescens* Benth, and *Kigelia africana* (Lam.) Benth. The phytochemical screening showed the presence of tannins, saponins, flavonoid, and cardiac glycosides in all the screened plants. *Curculigo pilosa* and *Sphenocentrum jollyanum* crude extracts exerted high radical scavenging activity with IC_{50} value of 36.68±0.74 µg/mL and 2.76±0.01 µg/mL, respectively, compared with ascorbic acid (IC_{50} 2.76±0.01 µg/mL) and rutin (IC_{50} 20.6±9.26 µg/mL). The LD_{50} of the two plants are > 5000 $mgkg^{-1}$, however, the histopathology of organs revealed severe damages to the kidney, heart and liver at high concentrations (1600, 2900 and 5000 $mgkg^{-1}$ *b.w.*). *Curculigo pilosa* (50 $mgkg^{-1}$ *b.w.*) and *Sphenocentrum jollyanum* (200 $mgkg^{-1}$ *b.w.*) methanol extracts showed anti-ulcer activities similar to Cimetidine (100 $mgkg^{-1}$ *b.w.*). The reduction in gastric ulcer index and increased percentage inhibition showed the gastroprotection potential of the plants. The antacid activity exhibited by *C. pilosa* and *S. jollyanum* could be as a result of presence of flavonoids in the plants. The urease inhibition exhibited by the plants showed their potentials in eradicating *Helicobacter pylori.* These

medicinal plants can therefore be used for prevention and treatment of gastric ulcers. The compounds isolated from *Curculigo pilosa* include Palmatine and 5-(hydroxymethyl) furan-2-carbaldehyde. Columbin, isocolumbin, Atrotosterone A and Pinnatasterone were isolated from *Sphenocentrum jollyanum* ethyl acetate fraction. Polypodine B, 20-hydroxyecdysone and 20, 26–dihydroxyecdysone were isolated from *Sphenocentrum jollyanum n* Butanol fraction, while *n* hexane fraction of *Sphenocentrum jollyanum* afforded Tehuanin A, Tinospin E and a new 2, 3 – dihydroxypropyl (E) – octadec – 5 – enoate. The isolated compounds exhibited urease and antacid activities with polypodine B having the highest urease inhibition (IC_{50} 7.0±0.56 µM). The isolated ecdysteroids from *Sphenocentrum jollyanum* exhibited significant urease inhibitory activity, which could be linked to the anti-ulcerogenic property of the plants. These compounds could serve as leads in drug discovery for development of novel anti-ulcer drugs.

5.23 Contributions to knowledge

1. Documentation of medicinal plants used in some areas of southwestern Nigeria for the treatment of gastric ulcer.

2. The gastroprotection activity of *Curculigo pilosa* and *Sphenocentrum jollyanum* using indomethacin induced gastric ulcer was provided for the first time.

3. The urease inhibition and antacid of *C. pilosa* and *S. jollyanum* plant extracts, fractions and isolated compounds were described for the first time.

4. Palmatine, and 5 – (hydroxymethyl) furan-2-carbaldehyde were isolated from *C. pilosa* for the first time.

5. Five ecdysteroids; Atrotosterone A, Pinnatasterone, Polypodine B, 20-hydroxyecdysone and 20, 26, dihydroxyecdysone were isolated from *S. jollyanum* for the first time. The compounds were new to family menispermaceae except 20-hydroxyecdysone which was previously isolated from *Tinospora species*.

6. Two clerodane diterpenoids; Tehuanin A and Tinospin E were isolated from *S. jollyanum* for the first time.

7. A new lipid-fatty acid methyl ester; 2, 3-dihydroxypropyl-(E)-octadec-5-enoate was isolated from *n* Hexane fraction of *S. jollyanum*.

5.24 Recommendation

The following recommendations are provided based on the outcome of this research.

1. Considering the wide ethnomedicinal uses of the identified plants, it is suggested to properly document the medicinal plants used to treat different ailments. The research should not be limited to anti-ulcer plants.

2. Conservation of the plant is recommended to prevent them from being endangered and going into extinction.

3. Further exploration of documented plants for potential bioactive compounds is recommended.

REFERENCES

Abdelgaleil, S. A. M., Hashinaga, F. and Nakatani, M. 2005. Antifungal activity of limonoids from *Khaya ivorensis*. *Pest Management Science* 61: 186–190.

Abbiw, D. K. 1990. Useful Plants of Ghana. Inter. Tech. Pub. Royal Botanical Gardens: Kew, UK.

Aboaba, S. A. and Ekundayo, O. 2010. Constituents, antibacterial activities and toxicological assay of essential oils of *Artocarpus communis* Forst (Moraceae) and *Sphenocentrum jollyanum* (Menispermaceae). *International Journal of Biological and Chemical Sciences* 4: 1455–1461.

Adewoye, E. O. and Salami, A. T. 2013. Anti-ulcerogenic mechanism of Magnesium in Indomethacin Induced Gastric Ulcer in Rats. *Nigerian Journal of Physiological Science* 28: 193-199.

Adinortey, M., Ansah, C., Galyuon, I. K. A. and Nyarko, A. K. 2013. *In vivo* Models Used for Evaluation of Potential Antigastroduodenal Ulcer Agents. *Ulcers* 4: 1-12.

Aebi, H. 1974. Catalase Methods in enzymatic analysis. *Academic Press* 276-289.

Agbedahunsi, J., Fakoya, F. and Adesanya, S. 2004. Studies on the anti-inflammatory and toxic effects of the stem bark of *Khaya ivorensis* (Meliaceae) on rats. *Phytomedicine* 11: 504–508.

Agyare, C., Dwobeng, A. S., Agyepong, N., Boakye, Y. D., Mensah, K. B. and Ayande, P. G. 2013. Antimicrobial, antioxidant, and wound healing properties of *Kigelia africana* (Lam.) beneth. and *Strophanthus hispidus* DC. *Advances in Pharmacological Sciences* 692613.

Akpamu, U., Owoyele, V. B., Ozor, M. and Osifo, U. C. 2013. Indomethacin- induced gastric ulcer model in female Wistar rats. *International Journal of Innovative Research and Development* 2. 4: 78–84.

Akuodor, G. C., Essien, A. D., Essiet, G. A., Oku, D., Akpan, J. L. and Udoh, F. V. 2013. Evaluation of antipyretic potential of *Pseudocedrela kotschyi* Schweinf. Hams (Meliaceae). *European Journal of Medicinal Plants* 3.1: 105-113.

Alanko, J., Riutta, A., Holm, P., Mucha, I., Vapata, H. and Metsa‐Ketela, T. 1999. Modulation of arachidonic acid metabolism by phenols: Relation to their structure and antioxidant /prooxidant properties. *Free Radical Biology and Medicine* 26: 193−201.

Alara, O. R., Abdurahman, N. H., Mudalif, S. K. A. and Olalere, O. A. 2017. Phytochemical and Pharmacological properties of *Vernonia amygdalina*. A Review. *Journal of Chemical Engineering and Industrial Biotechnology* 2: 80-96.

Angelini, P., Pagiotti, R. and Granetti, B. 2008. Effect of antimicrobial activity of *Melaleuca alternifolia* essential oil on antagonistic potential of *Pleurotus* spp. against *Trichoderma harzianum* in dual culture. *World Journal of Microbiology and Biotechnology* 24: 197-202.

Arowona, I.T . Sonibare, M. A. and Umukoro, S. 2014. Antipsychotic property of solvent-partitioned fractions of *Lonchocarpus cyanescens* leaf extract in mice. *Journal of Basic and Clinical Physiology and Pharmacology* 25.2: 235-240.

Bafna, A. K. and Mishra, S. H. 2006. Immunostimulatory effect of methanol extract of *Curculigo orchioides* on immunosuppressed mice. *Journal of Ethnopharmacology* 104: 1–4.

Baker, D. A. 2020. Plants against *Helicobacter pylori* to combat resistance: An ethnopharmacological review. *Biotechnology Reports* 26: 1-15.

Bandara, B. M. R., Jayasinghe, L., Karunaratne, V., Wannigama, G. P., Bokel, M., Kraus, W. and Sotheeswaran, S. 1989. Ecdysterone from stem of *Diploclisia glaucescens*. *Phytochemistry* 28: 1073–5.

Bandyopadhyay, D., Biswas, K., Bhattacharyya, M., Reiter, R. J. and Banerjee, R. K. 2001. Gastric toxicity and mucosal ulceration induced by oxygen-derived reactive species, protection by melatonin. *Current Molecular Medicine* 1: 501-513.

Bautista, E. 2012. Elucidation and structural evaluation of activated biological diterpenoids from neo-clerodane from *Salvia herbacea, S. shannoni,* Y., *S. microphilla*. A PhD thesis submitted to the University of Mexico.

Boeing, T., Mota da Silver, L., Somensi, L. B., Cury, B. J., Costa, A. P. M., Petreanu, M., Niero, R. and Faloni de Andrade, S. 2016. Anti-ulcer mechanisms of *Vernonia condensata* Baker: A medicinal plant used in the treatment of gastritis and gastricula. *Journal of Ethnopharmacology* 184: 196-207.

Burkill, H. M. 1995. The Useful Plants of West Tropical Africa. 2nd Edition, Volume 1, Families A–D. Royal Botanic Gardens, Kew, Richmond, United Kingdom. pp. 21-25.

Bytzer, P. and O'Morain C. 2005. Treatment of *Helicobacter pylori*. *Helicobacter* 10.1: 40-46.

Candelli, M., Armuzzi, A. and Cammarota, G. 2000. Role of Sucralfate in gastrointestinal diseases. *Panminerva Medica* 42.1: 55-59.

Chen, Q.S., Chen, W.R. and Yang, S.Y. 1989. Pharmacologic study of *Curculigo orchioides* Gaertn. *Zhongguo Zhong Yao Za Zh* 14.10: 618-620.

Choudhary, M. K., Bodakhe, S. H. and Gupta, S. K. 2013. Assessment of the antiulcer potential of *Moringa oleifera* root-bark extract in rats. *Journal of Acupuncture and Meridian Studies* 6: 214–220.

Choudhury, M. K., Hruna, A. K., Johnson, E. C. and Houghton, P. J. 1997. Structural Elucidation of Columbin, A Diterpene isolated from the rhizomes of *Artistolochia albida*. *Indian Journal of Pharmaceutical Sciences* 59: 34-37.

Coll, J., Reixach, N., Sanchez-Baeza, F., Casas, J. and Camps, F. 1994. New Ecdysteroids from *Polypodium vulgare. Tetrahedron* 50.24: 1247-1252.

DeFoneska, A. and Kaunitz, J. D. 2010. Gastroduodenal mucosal defense. *Current Opinion in Gastroenterology* 26: 604-610.

DeRuiter, J. 2002. Non-Steroidal Anti-inflammatory Drugs (NSAIDs). *Principles of Drug Action* 2: 1-25.

Dhasan, P. B., Jegadeesan, M. and Kavimani, S. 2010. Antiulcer activity of aqueous extract of fruits of *Momordica cymbalaria* hook F. in Wistar rats. *Pharmaceutical Research* 2: 58–61

Dhuley, J. N. 1999. Protective effect of *Rhinax*, a herbal formulation against physical and Chemical factors induced gastric and duodenal ulcers in rats. *Indian Journal of Pharmacology* 31: 128–132.

Dicko, M. H., Searle-van Leeuwen, M. J. F., Beldman, G., Ouedraogo, O.G., Hilhorst, R. and Traore, A.S. 1999. Purification and characterisation of β-amylase from *Curculigo pilosa*. *Applied Microbiology and Biotechnology* 52: 802–805.

Ebrahimzadeh, M. A., Nabavi, S. M., Nabavi, S. F. and Eslami, B. 2009. Free radical scavenging ability of methanolic extract of *Hyoscyamus squarrosus* leaves. *Pharmacology online* 2: 796-802.

Editorial Committee of Flora of China, Chinese Academy of Sciences, 2006. Flora of China Science Press, Beijing, pp 35-37.

Filho, J. G. S., Duringer, J., Gabriela, L. A. Josean, M., Tavaresa, F., Xavierb, H. S., Sobral da Silvaa, M., Emdio, V., da-Cunhaa, L. and Barbosa-Filhoa, J. M., 2008. Ecdysteroids from *Vitex* species: Distribution and Compilation of Their ^{13}C-NMR Spectra Data. *Chemical biodiversity* 5: 707-713.

Fink, G. 2011. Stress Controversies: Post-Traumatic Stress Disorder, Hippocampal Volume, Gastroduodenal Ulceration. *Journal of Neuroendocrinology* 23.2: 107-17.

Fisher, A. A. and Le-Couteur, D. G. 2012. Nephrotoxicity and Hepatotoxicity of Histamine H_2 Recepteor Antagonists. *Drug safety* 24.1: 39-57.

Freitas, C. S., Baggio, C. H., Da Silva – Santos, J. E., Rieck, L., De Moraes Santos, C. A., Junior, C. C., Ming, L. C., Cortez, D. A . and Marques, M. C. 2004. Involvement of Nitric Oxide in the Gastroprotective Effects of an aqueous extract of *Pfaffia glomerata* (Spreng) Pedersen, Amaranthaceae in Rats. *Life Science* 74: 1167-1179.

Gbadamosi, I. T. and Egunyomi, A. 2009. Phytochemical Screening and *in vitro* anti candidal activity of extracts and essential oil of *Curculigo pilosa* (Schum and Thonn) Engl. Hypoxidaceae. *African Journal of Biotechnology* 9.8: 1236–1240.

Ghribia, L., Ghouilaa, H., Omrib, A., Besbesb, M. and Janneta, H.B. 2014. Antioxidant and anti-Acetylcholinesterase activities of extracts and secondary metabolites from *Acacia cyanophylla*. *Asian Pacific Journal of Tropical Biomedicine* 4: 417-23.

Gilbert, L. I, Rybczynski, R. and Warren, J. T 2002. Control and biochemical nature of the ectysteroidogenic pathway. *Annual Review of Entomology* 47: 883-916.

Graham, D. Y. 1996. Non-steroidal anti-inflammatory drugs, *Helicobacter pylori*, and ulcers: where we stand. *American Journal of Gastroenterology* 91: 2080-2086.

Graham, D. Y. and Miftahussurur, M. 2018. Helicobacter pylori urease for diagnosis of *Helicobacter pylori* infection: A mini review. *Journal of Advanced Research* 13: 51-57.

Hay, A. E., Ioset, J. R., Ahua, K. M., Diallo, D., Brun, R. and Hostettmann, K. 2007. Limonoid orthoacetates and Antiprotozoal compounds from the roots of *Pseudocedrela kotschyi*. *Journal of Natural Product* 70: 9-13.

Hayllar, J., Macpherson, A. and Bjarnason, I. 1992. Gastroprotection and non-steroidal anti-inflammatory drugs. *Drug Safety* 7: 86–105

Houghton, P. J. 2002. The sausage tree (*Kigelia pinnata*): Ethnobotany and recent scientific work. *South African Journal of Botany* 68: 14‑20.

Huang, W., Zhang, S., Qin, G., Wenquan, L. and Wu, J. 2012. Isolation and determination of major anthocyanin pigments in the pericarp of *P. communis* L. cv. 'Red Du Comices' and their association with antioxidant activity. *African Journal of Agricultural Research* 7.26: 3772-3780.

Hutchinson, J., Dalziel, J. M. and Keay, R. W. J. 1958. Floral of West Tropical Africa. Agents for Overseas Government and Administration, London, 531.

Hutchinson, J. and Dalziel, J. M. 1954. Flora of West Tropical Africa. Vol. I, Part 1, 2nd Edition, Crown Agents for Overseas Governments Administrations, London.

Iwu, M. M. 1993. Handbook of African Medicinal Plants; CRC Press: Boca Raton, FL, USA, p. 239.

Jain, S. K., Haider, T., Kumar, A. and Jain, A. 2016. Lectin-Conjugated Clarithromycin and Acetohydroxamic Acid-Loaded PLGA Nanoparticles: A Novel Approach for Effective Treatment of *Helicobacter pylori*. *Pharmaceutical Science Technology* 17: 1131–1140.

Jayachitra, A. and Krithiga, N. 2010. Study on antioxidant property in selected medicinal plant extract. *International Journal of Medicinal and Aromatic Plants* 2: 495–500.

Ji, K., Liao, S., Zheng, X., Na, Z., Hu, H., Zhang, R. and Xu, Y. 2014. Limonoids from the fruits of *Khaya ivorensis*. *Molecules* 19: 3004-3011.

Karigidi, K. O., Ojebode, M. E., Anjorin, O. J., Omiyale, B. O. and Olaiya, C. O. 2019.

Antioxidant activities of methanol extracts *Curculigo pilosa* rhizome and *Gladilous psittascinus* corm against lipid peroxidation in rat's liver and heart. *Journal of Herbs, Spices, and Medicinal plants* 25.1: 1-10.

Kayode, J., Ige, O. E., Adetogo, T. A. and Igbakin, A. P. 2009. Conservation and Bioderversity in Ondo State, Nigeria. Survey of plant barks used in native pharmaceutical extraction in Akoko region. *EthnoBotanical Leaflet* 13: 665–667.

Kayode, A. A. A., Kayode, O. T. and Odetola, A. A. 2009. Antiulcerogenic Activity of two extracts of *Parquetina nigrescens* and their Effects on Mucosal antioxidants Defense System on Ethanol-Induced Ulcer in Rats. *Journal of Medicinal Plants Research* 3: 102-108.

Kemmerly, T. and Kaunitz, J. 2014. Gastroduodenal Mucosal Defense. *Current Opinion in Gastroenterology* 30.6: 583-588.

Khan, M. A., Islam, M. K., Siraj, M. A., Saha, S., Barman, A. K. and Awang, K. 2015. Ethnomedicinal survey of various communities residing in Garo Hills of Durgapur, Bangladesh. *Journal of Ethnobiology and Ethnomedicine* 11: 44-55.

Khatoon, M., Islam, E., Islam, R., Rahman, A. A., Khurshid, A. H. M., Khondkan, P., Mamunur, R. and Parvin, S. 2013. Estimation of Total Phenol and *In vitro* antioxidant activity of *Albizia procera* leaves. *Springer* 3: 21-33.

Klassen, C. D. and Eaton, D. L. 1991. Principles of Toxicity in Casaret and Doull's toxicity - The basic science of poisons. Pergamon Elmsford Press 4: 12-50.

Klein, G. E. A., Jansen, B. J. M. and de Groot, A. 2002. Insect Antifeedant Activity of Clerodane Diterpenes and Related Model Compounds. *Phytochemistry* 61: 737-770.

Ko, J. K. and Cho, C. H. 2000. Alcohol drinking and Cigarette Smoking "A Partner for Gastric Ulceration". *Zhonghua Yi XueZa Zhi* 63.12: 845-54.

Koudokpon, H., Armstrong, N., Dougnan, T. V., Fah, L., Hounsa, E., Bankole, H. S., Loko, F., Chabriere, E. and Rolain, J. M. 2018. Antibacterial activity of Chalcone and dihydrochalcone compound from *Uvaria chamae* roots against multi-drug resistant bacteria. *Biomedicinal Research International* 1453173.

Kvietys, P.R., Yaqinuddin, A. and Al-Kattan, W. 2014. Gastrointestinal Mucosal Defense System. *Colloquium Series on Integrated Systems Physiology from Molecule to Function* 6.5: 1-172.

Lafont, R. and Dinan L. 2009. Innovative and future applications for ecdysteroids. In: Smagghe G, editor. Ecdysone: structures and functions. New York: Springer Science. p 551–578.

Laine, L., Curtis, S. P., Cryer, B., Kaur, A. and Cannon, C. P. 2010. Risk factors for NSAID-associated upper GI clinical events in a long-term prospective study of 34701 arthritis patients. *Aliment Pharmacological Therapy* 32.10: 1240-8.

Laine, L. 2008. Gastric mucosal defense and cytoprotection: bench to bedside. *Gastroenterology* 135: 41-60.

Lee, E. B., Kim, O. J., Kang, S. S., Jeong, C. 2005. Araloside A, An Anti-ulcer Constituent from the Root Bark of *Aralia* e*lata*. *Biological and Pharmaceutical Bulletin* 28: 523-426.

Li, R., Morris-Natschke, S. and Lee, K. H. 2016. Clerodane diterpenes: sources, structures and biological activities. *Natural Product Reports* 33.10: 1166.

Li, N., Chen, J. J. and Zhou, J. 2005. Capitulatin B, an eudesmane derivative from *Curculigo capitulata*, and revised assignment of ^{13}C NMR data of 6 alpha, 15 alpha – epoxy – 1 beta, 4 beta - dihydroxyeudesmane. *Journal of Asian Natural Products Research* 7: 279 – 282.

Lorke, D. 1983. A new approach to practical acute toxicity testing. *Archives of Toxicology* 54.4: 275-87.

Maesaka, K., Tsujii, Y., Shinzaki, S., Yoshii, S., Hayashi, Y., Iijima, H., Nakamoto, K., Ohtani, T., Sakata, Y. and Takehara, T. 2018. Successful treatment of drug-induced esophageal ulcer in a patient with chronic heart failure: A case report. Medicine 97.48: 13380.

Mandel, K. G., Daggy, V. P., Brodie, D.A. and Jacoby, H. I. 2000. Alginate-raft formulations in the treatment of heartburn and acid reflux. *Ailment Pharmacological Therapy* 14: 669-690.

Marklund, S. and Marklund, G. 1974. Involvement of the superoxide anion radical in the autooxidation of Pyrogallol and a convenient assay for Superoxide Dismutase. *European Journal of Biochemistry* 47: 469–474.

Marshall, B. J. and Warren, J. R. 1984. Unidentified curve bacilli the stomach of patients with gastritis and peptic ulceration. *Lancet* 1.8390: 1311-1315.

Mbaka, G. O., Adeyemi, O. O. and Oremosu, A. A. 2010. Acute and sub-chronic toxicity studies of the ethanol extract of the leaves of *Sphenocentrum jollyanum* (Menispermaceae). *Agriculture and Biology Journal of North America* 1: 265–272.

Mbatchou, V.C., Nabayire, K. O. and Akuoko, Y. 2017. *Vernonia amygdalina* leaf: unveiling its Antacid and carminative properties *in vitro*. *Critical Social Policy* 3.3: 148-155.

Meves, V. and Pohl, J . 2013. Upper GI Endoscopy: Exam Technique and Standard Findings. *Video Journal and Encyclopedia of GI endoscopy* 1.1: 202 – 203.

Michetti, K. 1998. Pathogenesis of *Helicobacter pylori* infection. *Current Opinion in Gastroenterology* 14: 57-63.

Miranda, K., Espey, M. G. and Wink, D. A. 2001. A rapid, simple spectrophotometric method for simultaneous detection of nitrate and nitrite. *Nitric Oxide* 5: 62–67.

Moody, J. O., Robert, V. A., Connolly, J. D. and Houghton, P. J. 2005. Anti-inflammatory activities of the methanol extracts and an isolated furanoditerpene constituent of *Sphenocentrum jollyanum* Pierre (Menispermaceae). *Journal of Ethnopharmacology* 104: 87–91.

Moreira, M. D., Picanco, M. C., Barbosa, L. C. A., Guedes, R. N. C., Barros, E. C. and Campos, M. R. 2007. Compounds from *Ageratum conyzoides*; isolation, structural elucidation, and insecticidal activity. *Pest management science* 63: 615-621.

Moronkola, D. O. and Oladosu, I. 2013. Chemical compositions of *Lonchocarpus cyanescens* Benth. (Fabaceae) – Case study of its Volatile Oils and Two triterpenoids . *American Journal of Plant sciences* 4.8: 1653-1659.

Nahla, E. E., Eman, G. K., Hoda, A. E. and Hend, M. S. 2016. Gastroprotective effect of Garlic in indomethacin induced Gastric ulcer in Rats. *Nutrition* 32: 849-854.

Narayanan, M., Reddy, K. M. and Marsicano E. 2018. Peptic Ulcer Disease and *Helicobacter pylori* infection. *Missouri Medicine* 115.3: 219-224.

Nia, R., Paper, D. H., Essien, E. E., Iyadi, K. C., Bassey, A. I. L., Antai, A. B. and Franz, G. 2004. Evaluation of the Antioxidant and Anti-Angiogenic Effects of *Sphenocentrum jollyanum* Pierre. *African Journal of Biomedical Research* 7: 129–132.

Nie, Y., Don, X., He, Y. and Yuan, T. 2013. Medicinal plants of genus *Curculigo*: Traditional uses and a phytochemical and ethnopharmacological review. *Journal of Ethnopharmacology* 147.3: 547-563.

Nishimoto, N., Shiobara, Y, Fujina, M., Fnoue, S., Takemoto, T., Oliviere, F., Akisue, G., Akisue, M. K., Hashimoto, G., Tanaka, O., Kasai, R. and Matsuura H. 1987. Ecdysteroids from *Pfaffia iresinoides* and reassignment of some ^{13}C NMR chemical shift. *Phytochemistry* 26.9: 2505-2507.

Ochoa, D., Roman, M., Cabaleiro, T., Saiz-Rodriguez, M., Mejia, G. and Abad-Santos, F. 2020. Effect of food on the pharmacokinetics of Omeprazole, pantoprazole and rabeprazole. *BMC Pharmacology and Toxicology* 21: 54.

Odugbemi, T. T. 2006. Outline and Pictures of Medicinal Plants from Nigeria. 1st ed. Nigeria: University of Lagos Press; 2006.

Ofeimun, J. O., Eze, G. I., Okirika, O. M. and Uanseoje, S. O. 2013. Evaluation of the hepatoprotective effect of the methanol extract of the root of *Uvaria afzelii* (Annonaceae). *Journal of Applied Pharmaceutical Science* 3: 125–129.

Ogungbenle, H. N. and Oyadipe, O. T. 2015. Compositional and Amino Acid Profile of Nicker Bean (*Entada gigas*) seeds. *British Biotechnology Journal* 6.2: 43 – 50.

Ohkawa, H., Ohishi, N. and Yagi, K. 1979. Assay for Lipid Peroxides in Animal Tissues by Thiobarbituric Acid Reaction. *Anals of Biochemistry* 9.5: 351–358.

Ojelere, O. 2016. Phytochemicals, Proximate, Mineral Element Composition and Antimicrobial Activity of Some Selected Medicinal Plant Seeds. *www.researchgate.net/publication*.

Okpekon, T., Millot, M., Champy, P., Gleye, C., Yolou, S. A., Bories, C., Loiseau, P., Laurens, A. and Hacquemiller, M. 2001. A novel 1 – indanone isolated from *Uvaria afzelii* roots. *Natural Product Research* 23.10: 909-915.

Olorunnisola, O.S., Adetutu, A. and Fadahunsi, O.S. 2017. Anti-allergy potential and possible modes of action of *Sphenocentrum jollyanum* Pierre fruit extracts. *The Journal of Phytopharmacology* 6.1: 20-26.

Olorunnisola, O. S. and Afolayan, A.J. 2011. *In vivo* anti-malaria activity of methanolic leaf and root extracts of *Sphenocentrum jollyanum* Pierre. *African Journal of Pharmacy and Pharmacology* 5.14: 1669-1673.

Olorunnisola, O. S., Akintola, A. A. and Afolayan, A. J. 2011. Hepatoprotective and antioxidant effect of *Sphenocentrum jollyanum* (Menispermaceae) stem bark extract against CCl4-induced oxidative stress in rats. *African Journal of Pharmacy and Pharmacology* 5: 1241–1246.

Onoja, S. O., Omeh, Y. N., Ezeja, M. I. and Chukwu, M. N. 2014. Evaluation of the *in vitro* and *in vivo* antioxidant potentials of *Aframomum melegueta* methanolic extract. *Journal of Tropical Medicine* 159343.

Oyetoro, I. A. and Sonibare, M. A. 2015. Preliminary Study on Wound Healing Activity of Ethanolic Extract of *Vitellaria paradoxa* C.F. Gaertn. in Rats. *Nigerian Journal of Pharmaceutical Research* 21: 89-93.

Palazzino, G., Galeffi, C., Federici, E., Monache, F., Cometa, M. F. and Palmery, M. 2000. Benzylbenzoate and norlignan glucosides from *Curculigo pilosa*: structural analysis and *in vitro* vascular activity. *Phytochemistry* 55: 411–417.

Patel, V. R., Patel, P. R. and Kajal, S. S. 2010. Antioxidant activity of some selected medicinal plants in western region India. *Advances in Biological Research* 4: 23–26.

Pei, S. 2001. Ethnobotanical approaches of traditional medicine studies. Some experiences from Asia. *Pharmaceutical Biology* 39.1: 74-79.

Phat, P. T. and Ngoan, L. H. 2016. Isolation of three polymethoxylated flavones from *Ageratum conyzoides* L. growing in Can Tho city. *Can Tho University Journal of Science* 4: 13-19.

Rahman, A. U. and Choudhary, M. I. 2001. Bioactive natural products as a potential source of new pharmacophores. A theory of memory. *Pure and Applied Chemistry* 73: 555–560.

Raj, N. K., Sripal, R. M. and Chaluvadi, M. R. 2001. Bioflavonoids classification, Pharmacological, Biochemical effects and therapeutic potential. *Indian Journal of Pharmacology* 33: 2-16.

Repetto, M.G. and Llesuy, S. F. 2002. Antioxidant properties of natural compounds used in popular medicine for gastric ulcers. *Brazilian Journal of Medical and Biological Research* 35.5: 523-534.

Roxax, M. 2008. The Role of Enzyme Supplementation in Digestive Disorders. *Alternative Medicine Review* 13: 4-11.

Salami, A. T., Odukanmi, O. A., Faniyan, O. F., Omayone, T. P. and Olaleye, S. B. 2017. Seeds of *Buchholzia coriaceae* in Diet Mitigate Ischemic Reperfusion – Induced Gastric Ulceration in Experimental Rats. *Journal of Dietary Supplements* 20: 1-18.

Sandhya, S., Venkuta, R. K., Vinod, K. R. and Chaitanya, R. 2012. Assessment of *in vitro* Antacid Activity of Different Root Extacts of *Tephrosa purpurea* (L) Pers. by Modified Artificial Stomach Model. *Asian Pacific Journal of Tropical Biomedicine* 1487–1492.

Sasaki, S., Nishikawa, J., Goto, A. and Sakaida, I. 2019. Dabigatran-induced Esophageal Ulcer at a Natural Constriction. *Internal Medicine* 58.5: 757-758.

Scida, S., Russo, M., Miraglia, C., Leandro, G., Franzoni, L., Meschi, T., De' Angelis, G. L. and Di-Mario, F. 2018. Relationship between *Helicobacter pylori* infection and GERD. *Acta Biomedica* 89.8: 40-43.

Sedlak, J. and Lindsay, R. H. 1968. Estimation of total protein-bound and nonprotein sulfhydryl groups in tissue with Ellman's reagent. *Anals of Biochemistry* 25.1: 192–205.

Shaba, E. Y., Mann, A. and Yisa, J. 2014. Antimicrobial and cytotoxic activities and GC-MS Analysis of phytocomponents of methanol extract of *Curculigo pilosa* (Schum and Thonn.) Engl. (Hypoxidaceae) rhizomes. *British Journal of Pharmaceutical Research* 4.12: 1552 – 1567.

Shah, N. and Gossman, W. 2020. Omeprazole. In StatPearls – Treasure Island: StatPearlsPublishing.

Shekelle, P. G., Newberry, S. J., FitzGerald, J. D., Motala, A., O'Hanlon, C. E., Tariq, A., Okunogbe, A., Han, D. and Shanman, R. 2017. Management of Gout: A systemic Review in support of an American College of Physicians Clinical Practice Guideline. *Annals of Internal Medicine* 166.1: 37-51.

Shin, J. M. and Sachs, G. 2008. Pharmacology of proton pump inhibitors. *Current Gastroenterology Reports* 10.6: 528-534.

Sidjui, L. S., Melong, R., Mahiou-Leddet, V., Herbette, G., Tchinda, A. T., Ollivier, E. and Folefoc, G. N. 2015. Triterpenes and Lignans from *Kigelia africana*. *Journal of Applied Pharmaceutical Science* 5: 001-006.

Sigthorsson, G. R., Crane, T., Simon, M., Hoover, H. and Quan, J. 2000. COX-2 inhibition with rofecoxib does not increase intestinal permeability in healthy subjects: a double blind crossover study comparing rofecoxib with placebo and indomethacin. *Gut* 47: 527–532.

Sofowora, A. 1993. Medicinal Plants and Traditional Medicine in Africa. 2nd Ed. Sunshine House, Ibadan, Nigeria: Spectrum Books Ltd; Screening Plants for Bioactive Agents: pp. 134-156.

Soladoye, M. O., Sonibare, M. A., Nadi, A. O. and Alabi, D. A. 2005. Indigenous angiosperm biodiversity of Olabisi Onabanjo University permanent site. *African Journal of Biotechnology* 4: 554–556.

Song, C. Q and Xu, R. S. 1991. Phytoecdysones from the roots of *Tinospora capillipes*. Chinese *Chemical Letters* 2.1: 13-14.

Sonibare, M. A. and Abegunde, R. B. 2012a. Ethnobotanical study of medicinal plants used by the Laniba village people in South Western Nigeria. *African Journal of Pharmacy and Pharmacology* 6.24: 1726-1732.

Sonibare, M. A., Umukoro, S. and Shonibare, E.T. 2012b. Antipsychotic property of aqueous and ethanolic extracts of *Lonchocarpus cyanescens* (Schumach and Thonn.) Benth. (Fabaceae) in rodents. *Journal of Natural Medicines* 66.1: 127-132.

Sousa, R. M. F., Lira, C. S., Rodrigues, A. O., Morais, S. A. L., Queiroz, C. R. and Chang, R. 2014. Atividade antioxidante de extratos de folhas de ora-pro-nóbis (*Pereskia aculeata* Mill.) usando métodos especométricos evoltamétricos. *Bioscience Journal* 30: 448-457.

Spechler, S. J. 2019. Proton Pump Inhibitors: What the Internist Needs to Know. *Medical and Clinical of North America* 103.1: 1-14.

Suksamrarn, A., Sommechai, C., Harulpong, P. and Chitkul, P. 1995. Ecdysteroids from *Vitex canescens. Phytochemistry* 38.2: 473-476.

Susanti, D., Ahmad, F., Ali, R. M. and Aimi, N. 2007. Antioxidant and cytotoxic flavonoids from the flowers of *Melastoma malabathricum* L. *Food chemistry* 103: 710-716.

Steinberg, K. P. 2002. Stress- Related Mucosal Disease in the Critically Ill Patient: Risk Factors and Strategies to Prevent Stress-Related Bleeding in the Intensive Care Unit. *Critical Care Medicine* 30: S362 - 4.

Stojkovic, N., Cekic, S., Ristov, M. and Ristic, M. 2015. Histamine and Antihistamine. *Scientific Journal of the Faculty of Medicine* 32.1: 7-22.

Talia, F. M. and Kevin, S. 2018. Peptic Ulcer Disease. NCBI Bookshelf. A service of the National Library of Medicine, National Institutes of Health.

Talla, E., Nyemb, J. N. and Elst, L. V. 2016. Antioxidant activity and a new ursane type triterpene from *Vitellaria paradoxa*. *European Journal of Medicinal Plants* 16.3: 1-20.

Tamashiro, F. P., Sikiru, O. B., Tavares de Almeida, D. A., Lima, J. C., Marson - Ascencio, P. G., Donizeti A. S. 2012. Evaluation of antiulcer activity and mechanism of action of methanol stem bark extract of *Lafoensia pacari* A. St.-Hil. (Lytraceae) in experimental animals. *Journal of Ethnopharmacology* 144: 497-505.

Tetsuhide I., Hisato I. and Robert T. J. 2013. Zollinger-Ellison syndrome: Recent advances and controversies. *Current Opinion in Gastroenterology* 29.6: 650-661.

Thirumalai, T., Kelumalai, E., Senthilkumar, B. and David, E. 2009. Ethnobotanical study of medicinal plants used by the local people in Vellore District, Tamilnadu, India. *Ethnobotanical leaflets* 13: 1302–1311.

Thorpe, S. R. and Baynes, J. W. 2003. Maillard reaction products in tissue proteins; new products and new perspectives. *Amino acids* 25: 275–281.

Thorsen, K., Sorede, J. A., Kvaloy, J. T., Glomsaker, T. and Soreide, K. 2013. Epidemiology of Perforated Peptic Ulcer; Age and gender – adjusted analysis of incidence and mortality. *World Journal of Gastroenterology* 19.3: 347 – 354.

Tiwari, M. and Kakkar, P. 2009. Plant derived antioxidants – Geraniol and camphene protect rat alveolar macrophages against E-BHP induced oxidative stress. *Toxicology in vitro* 23: 295-301.

Tiwari, R. D. and Misra, G. 1976. Strutural studies of the constitutents of the rhizomes of *Curculigo orchiodes*. *Planta Medica* 29: 291–294.

Trease, G.E., Evans, W.C. 2002. Pharmacognosy. 15th Ed. London: Saunders Publishers, pp. 42-44, 221-229, 246-249, 304-306, 331-332, 391-393.

Tripathy, K. D. 2004. Essentials of medical pharmacology; 5th Edition. Jaypee brothers publication, New Delhi 587-598.

Tonkic, A., Tonkic, M., Lehours, P. and Mégraud, F. 2012. Epidemiology and diagnosis of *Helicobacter pylori* infection. *Helicobacter* 17**.**1: 1-8.

Ukwe, V. C., Epueke, E. A., Ekwunife, O. I., Okoye, T. C., Akudor, G. C. and Ubaka, C. M. 2010. Antimalarial activity of aqueous extract and fractions of leaves of *Ageratum conyzoides* in mice infected with *Plasmodium berghei*. *International Journal Pharmaceutical Science* 2: 33-38.

Upadhyay, L. S. 2012. Urease inhibitors: A review. *Indian Journal of Biotechnology* 11: 381-388.

Valls, J., Richard, T., Laronde, F., Leblais, V., Muller, B., Delaunay, J. C., Monti, J. P., Ramawat, K. G. and Merillon, J. M. 2006. Two new benzylbenzoate glucosides from Capitulatin A and B from *Curculigo orchioides*. *Fitoterapia* 77: 416 – 419.

Vokac, K., Budesinsky, M., Harmatha, J. and Pis, J. 1999. New Ergostane Type Ecdysteroids from Fungi. Ecdysteroid Constituents of Mushroom *Paxillus atrotomentosus. Tetrahedron* 54: 1657-1666.

Wallace, J. L. 2001. Mechanisms of protection and healing: current knowledge and future research. *American Journal of Medicine* 110: 19S–22S.

Weatherburn, M. W. 1967. Phenolhypochlorite reaction for the determination of ammonia. *Analytical Chemistry* 3: 971–974.

Woode, E., Amidu, N., Owiredu, K., Boakye, G., Ansah, C. and Duweijua, M. 2009. Antidepressant–Like effects of an ethanol extract of Sphenocentrum jollyanum Pierre Roots in Mice. *International Journal of Pharmacology* 5: 22–29.

World Health Organization, 2008. Traditional medicine. Fact sheet No.134. December, 2008. http://www.who.int/mediacentre/factsheets/fs123/en/ (Accessed,06/03/2013).

Wu, T. H., Chen, I. C. and Chen, L. C. 2010. Antacid effects of Chinese herbal prescriptions assessed by a modified artificial stomach model. *World Journal of Gastroenterology* 16.35: 4455 – 4459.

Yandrapu, H. and Sarosiek, J. 2015. Protective Factors of the Gastric and Duodenal Mucosa: An Overview. *Current Gastroenterology Reports* 17.6: 452.

Yuan, Y., Padol, I. T. and Hunt, R. H. 2006. Peptic ulcer disease today. *Nature Clinical Practice Gastroenterology and Hepatology* 3: 80–89.

Zayachkivska, O. S., Konturek, S. J., Drozdowicz, D. and Konture, P. C. 2005. Gastroprotective Effects of Flavonoids in Plant Extracts. *Journal of Physiology and Pharmacology* 56.1: 219 – 231.

Zhang, B., Yang, S. P., Yin, S., Zhang, C. R., Wu, Y. and Yue, J. M. 2009. Limonoids from *Khaya ivorensis*. *Phytochemistry* 70: 1305-1308.

Zhu, H., Wang, D., Wen, L., Yu, J., Geng, Y., Zhao, H., Zhao, R. and Wang, X. 2016. Preparative separation of quartenary ammonium alkaloids from *Caulis mahoniae* by conventional and pH- zone refining counter-current chromatography. *Royal society of Chemistry* 6: 83343.

Zhu, N., Kikuzaki, H., Vastano, B. C., Nakatani, N., Karwe, M. V., Rosen, R. T. and Ho, C. T. 2001. Ecdysteroids of Quinoa Seeds (*Chenopodium quinoa* Willd.). *Journal of Agricultural and Food Chemistry* 49: 2576-2578.

Zuo, W. J., Jin, P. F., Dong, W. H., Dai, H. F. and Mei, W. L. 2014. Metabolites from the endophytic fungus hp-1 of chinese eaglewood zuo wen-jian# , jin peng-fei#. *Chinese Journal of Natural Medicines* 12.2: 01510153.

Zuo, A. X., Shen, Y., Jiang, Z. Y., Zhang, X. M., Jiang, Z. Y., Zhou, J., Lu, J. and Chen, J. J. 2012. Two new triterpenoid glycosides from *Curculigo orchioides*. *Journal of Asian Natural Products Research* 12: 43-50.

APPENDICES

Appendix I

Ethnobotanical Survey Questionnaire

The participants; herb sellers, traditional medical practitioners and some elders in these Local Government Areas were informed of the concept of surveying medicinal plants for therapy of gastric ulcer to achieve their readiness to engage in the study and approval.

Demographic characteristics

Tick option appropriately

1. Name of respondent……

2. Type of respondents:

a. Traditional Medical Practitioner b. Herb Seller

c. Elder d. Mothers e. Others

3. Age: ……years

4. Sex: 1. Male 2. Female

5. Religion 1. Christianity 2. Islam

3. Traditional Religion 4. Others (Specify)

6. Education: 1. None 2.Primary 3. Secondary

4. Post-secondary 5. Tertiary 6. Arabic school

7. Adult education. 8. Others (specify)

7. Occupation: ……..…..

8. Marital status: 1. never married 2. Married 3.seperated
4. Divorced 5. Widow

9. Personally what do you know about Gastric Ulcer?
……..……**……**
……..

10. Do you know any other types of Ulcer apart from Gastric Ulcer?

11. How often do you treat Gastric Ulcers?

12. Give local names of medicinal plants used for treating Gastric Ulcers.

PLANT USED	PLANT PART	SYNONYMS	SCIENTIFIC NAME

13. Which of the above-mentioned plants is the most used?

……....

14.What are the other most used plants ' medicinal uses?……
…….**.....**
.....

15. Do you combine more than one plants for treatment? If yes, which of the plants?

16. Do you have other methods of treatment apart from herbs?

17. If yes, name the method.

……

18. What are the side effects of the mentioned plants?

…….....

19. What is the method of administration of the plants?

…….....

20. What is the dosage during treatment?

……

21. What is the duration of the treatment?

…….....

22. What is the time of collection of the plants?

23. State the method of storage of the plants.

……

24. Are the plants readily available?.....

25. Are there other materials to apply with the plants for the treatment?.....

26. Are there any treated cases of Gastric Ulcers?.....

27. How often do you treat Gastric Ulcers using the mentioned plants?.....

28. What are the different plant locations in the study area?

……

29. Are there any special information on the plants?.....

30. What are your sources of herbal therapy knowledge?.....

31. Do you offer verbal therapy directions?.....

32. Where do you normally collect your plants?.....

33. How often do you go?.....

34. Mention the plants you often collect and their locations.

……

……

35. What are the medicinal uses of those plants?

……

…….....

36. Do you have suggestions on how the local drugs for treating Ulcers could be improved?

……

……

Thank you for the moment you spent answering this questionnaire.

Appendix II (a)

EI-MS, 1D and 2D NMR Spectra of CPE-43A

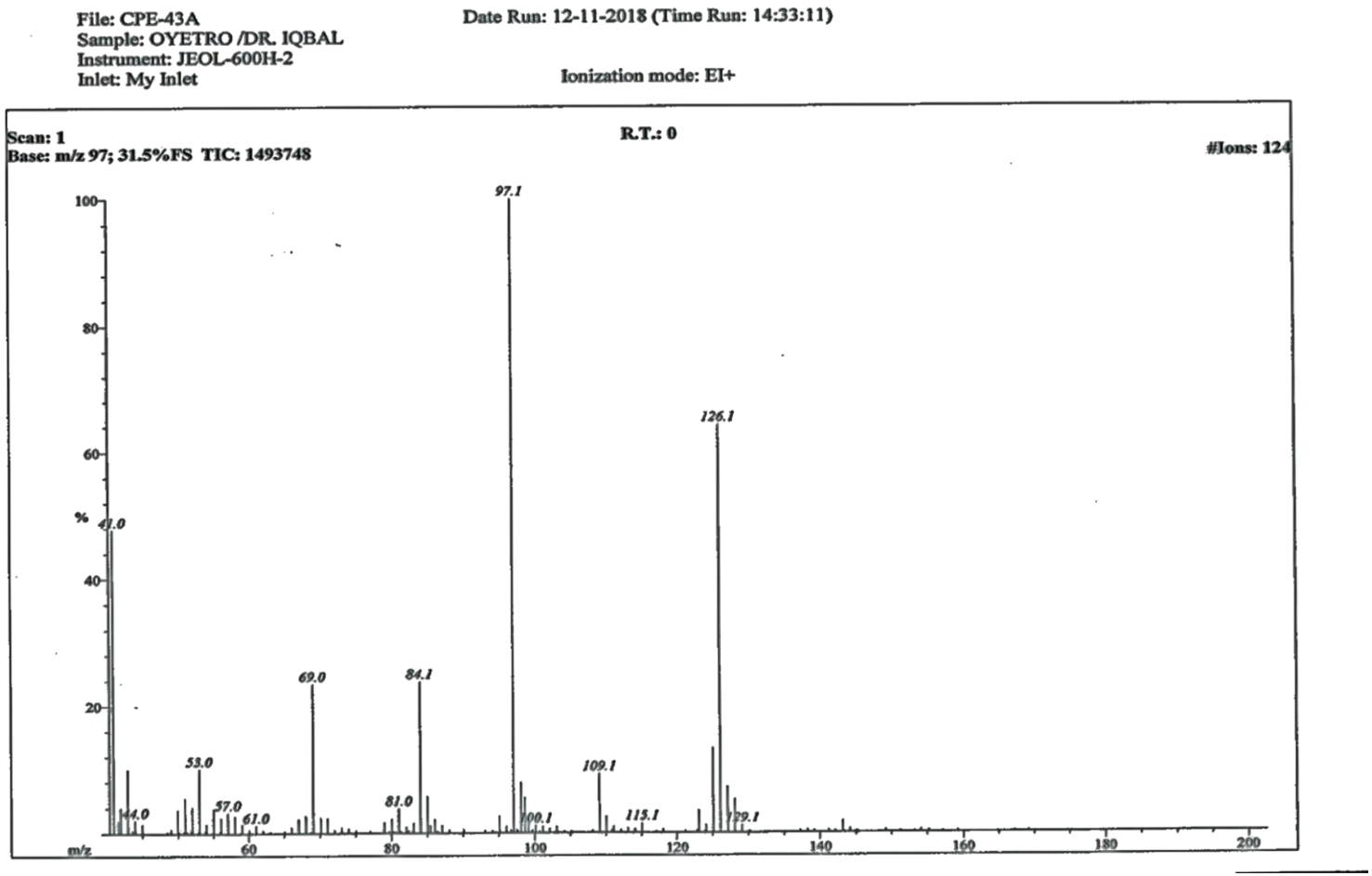

Appendix II (b)

File: CPE-43A
Sample: OYETRO /DR. IQBAL
Instrument: JEOL-600H-2
Inlet: My Inlet

Date Run: 12-11-2018 (Time Run: 14:33:11)

Ionization mode: EI+

Scan: 1
Base: m/z 97; 31.5%FS TIC: 1493748

R.T.: 0

#Ions: 124

Threshold: 2% of Base

Displayed TIC: 1493748

Mass	%Base	Mass	%Base	Mass	%Base	Mass	%Base	Mass	%Base	Mass	%Base
41.0004	47.8	52.0159	4.1	67.0351	2.2	81.0392	3.9	98.0876	7.9	125.1145	13.2
41.9882	4.0	53.0362	10.1	68.0362	2.8	84.0621	23.8	98.6308	5.6	126.1100	64.3
42.9877	10.0	55.0150	3.8	69.0443	23.5	85.0508	5.8	99.0947	2.6	127.1320	7.2
43.9853	2.1	56.0328	2.4	70.0766	2.5	86.0641	2.2	109.0869	9.3	128.1122	5.3
49.9898	3.7	57.0442	3.2	71.0652	2.4	95.0576	2.7	110.1018	2.6		
51.0052	5.5	58.0333	2.7	80.0559	2.2	97.0657	100.0	123.0899	3.5		

Appendix II (c)

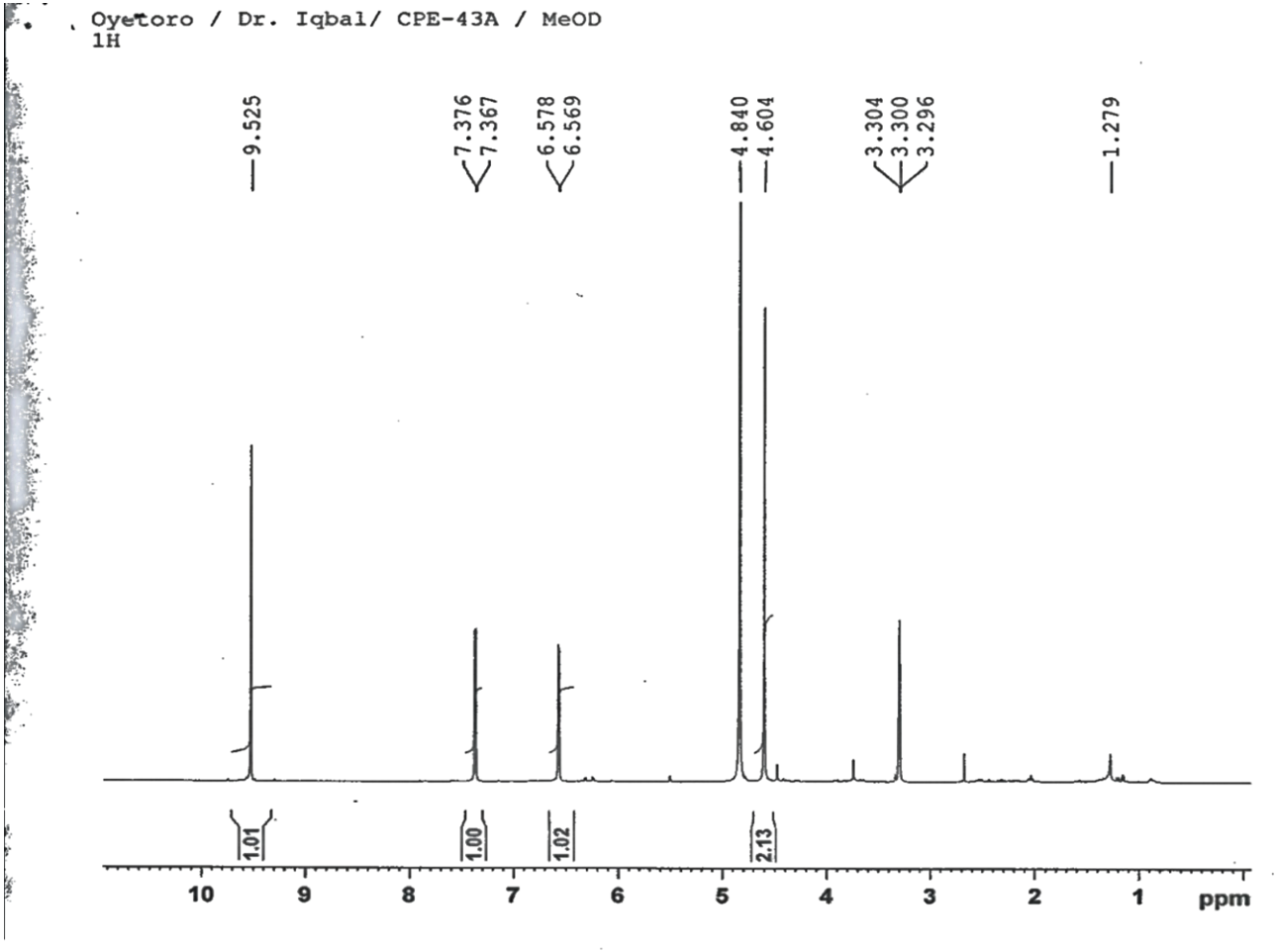

AVAVCE -III
AV-400 MHz (A)
LAB # 109

Current Data Parameters	
NAME	Dec05-18
EXPNO	3
PROCNO	1
F2 - Acquisition Parameters	
Date_	20181205
Time	12.18 h
INSTRUM	spect
PROBHD	Z116098_0090 (
PULPROG	zg30
TD	32768
SOLVENT	MeOD
NS	64
DS	0
SWH	8012.820 Hz
FIDRES	0.489064 Hz
AQ	2.0447233 sec
RG	176.53
DW	62.400 usec
DE	6.50 usec
TE	297.6 K
D1	1.00000000 sec
TD0	1
SFO1	400.2832022 MHz
NUC1	1H
P1	10.13 usec
PLW1	15.00000000 W
F2 - Processing parameters	
SI	32768
SF	400.2800116 MHz
WDW	EM
SSB	0
LB	0.30 Hz
GB	0
PC	1.00

Appendix II (d)

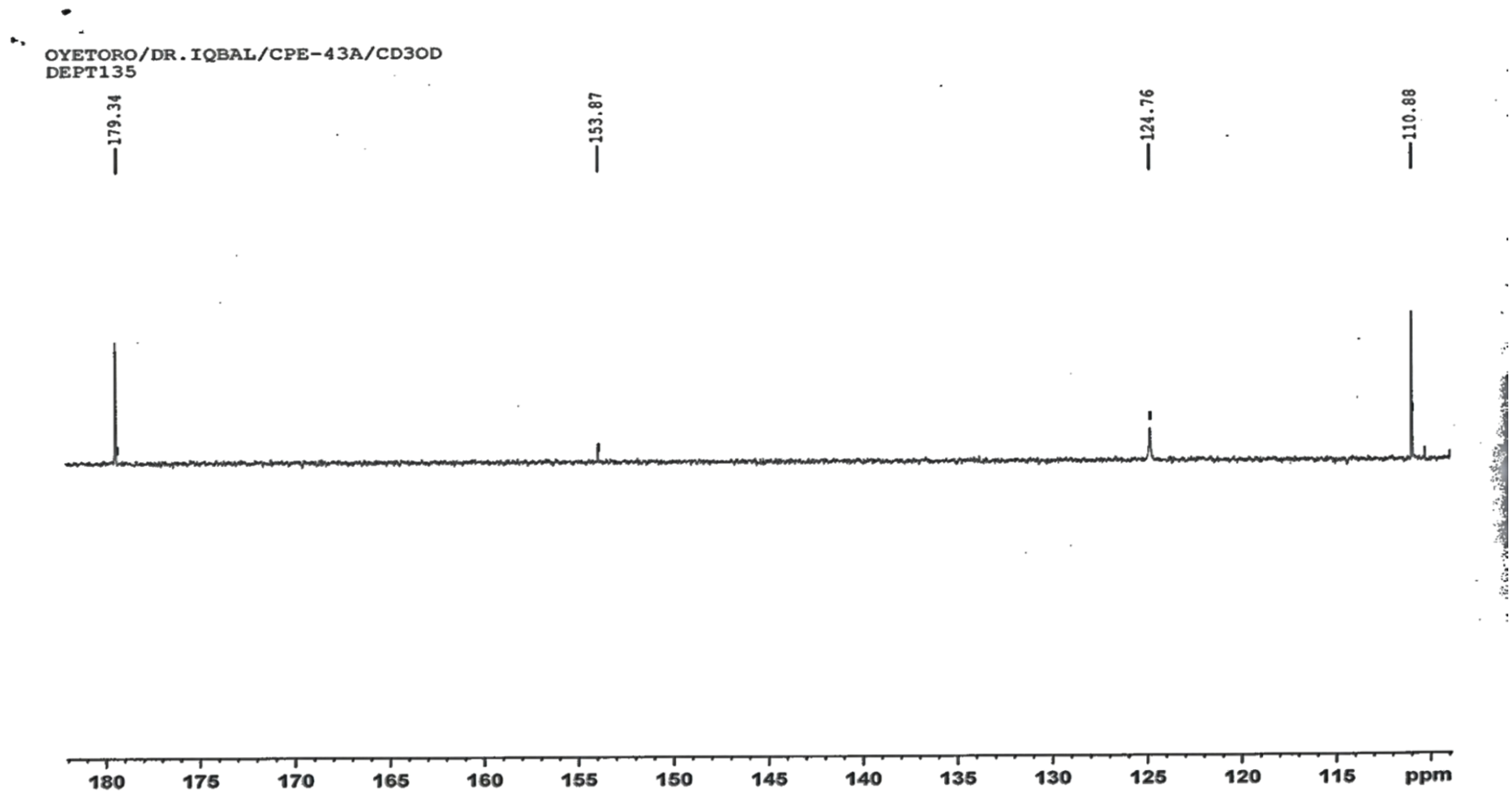

Appendix II (e)

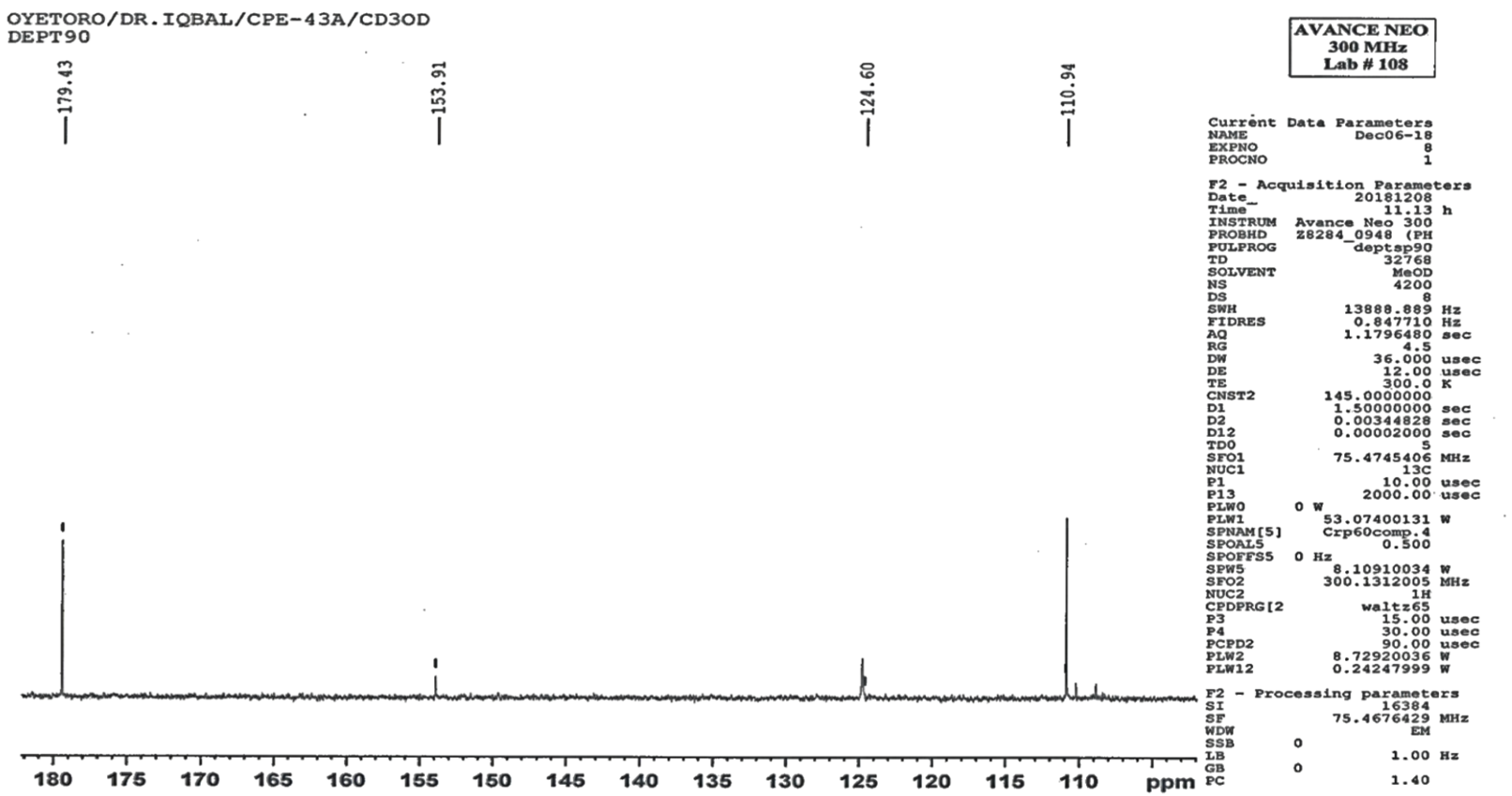

Appendix II (f)

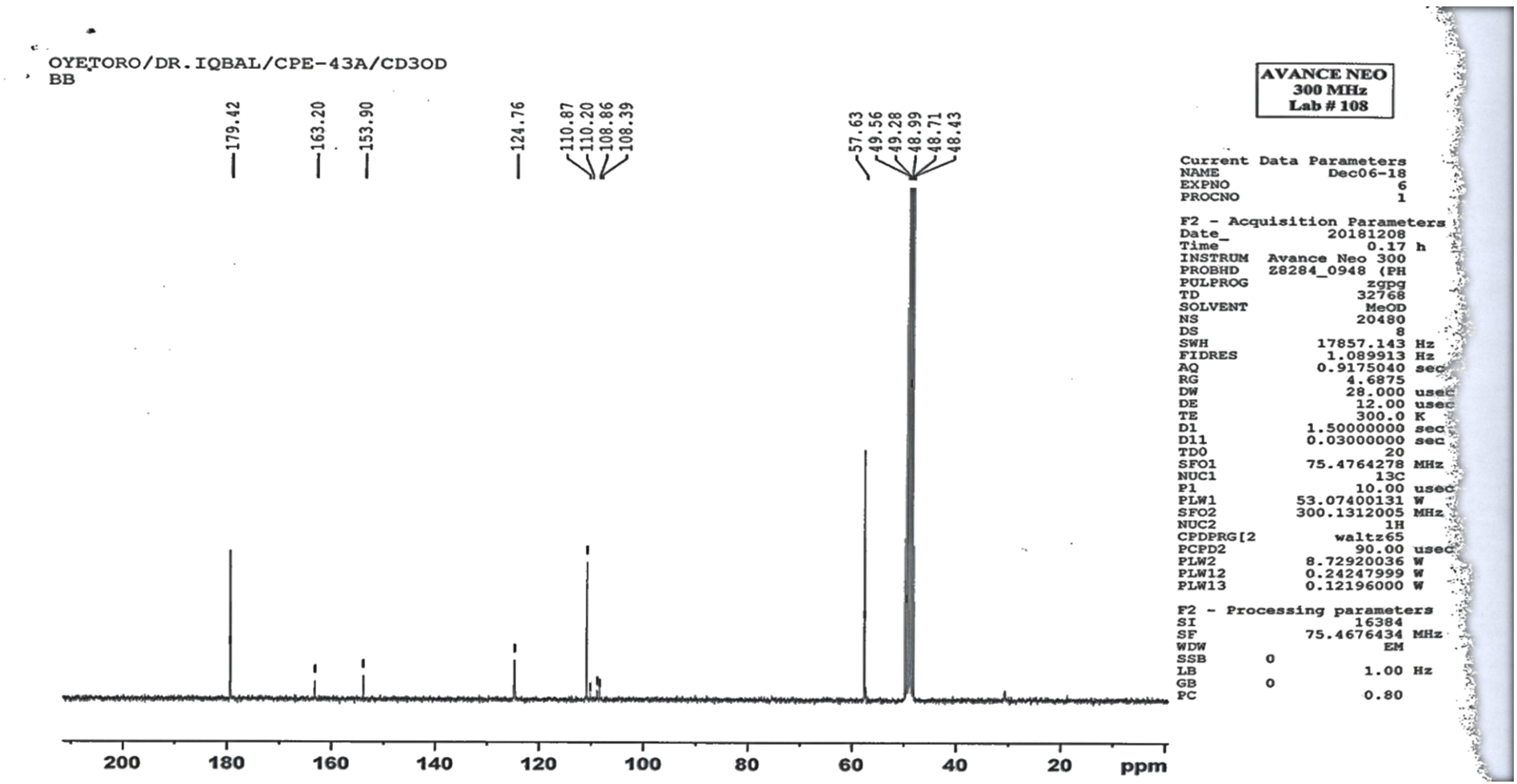

Appendix II (g)

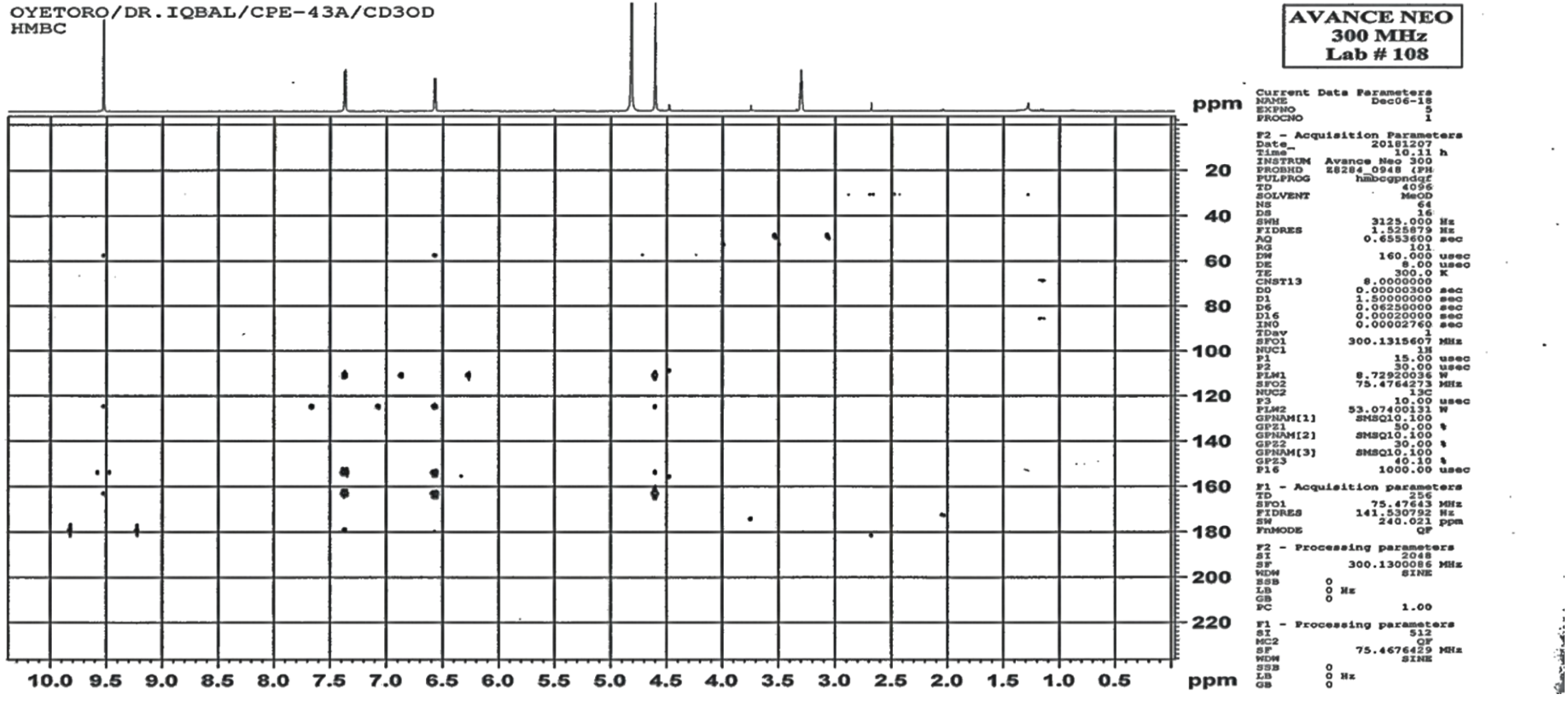

Appendix II (h)

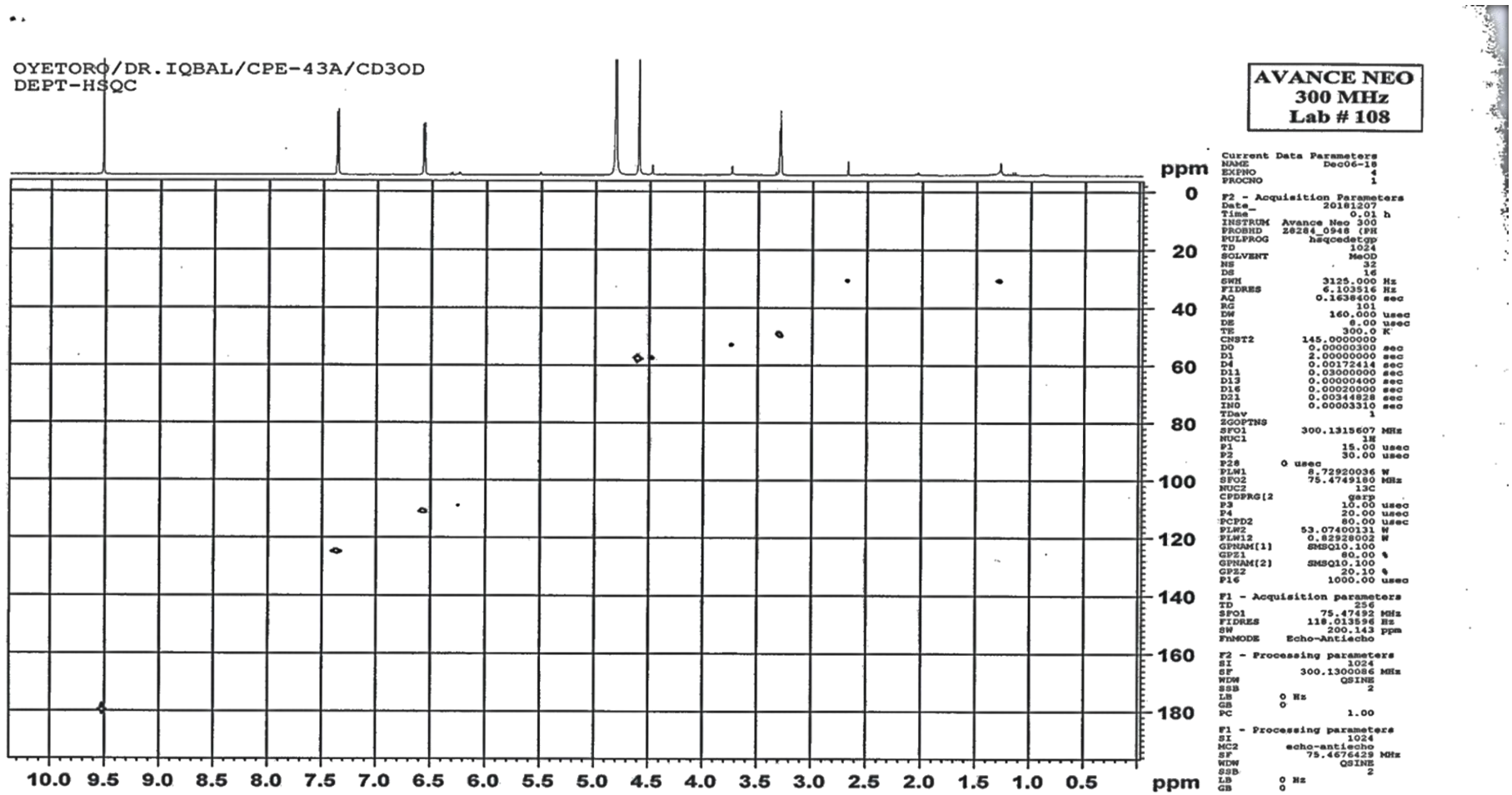

Appendix II (i)

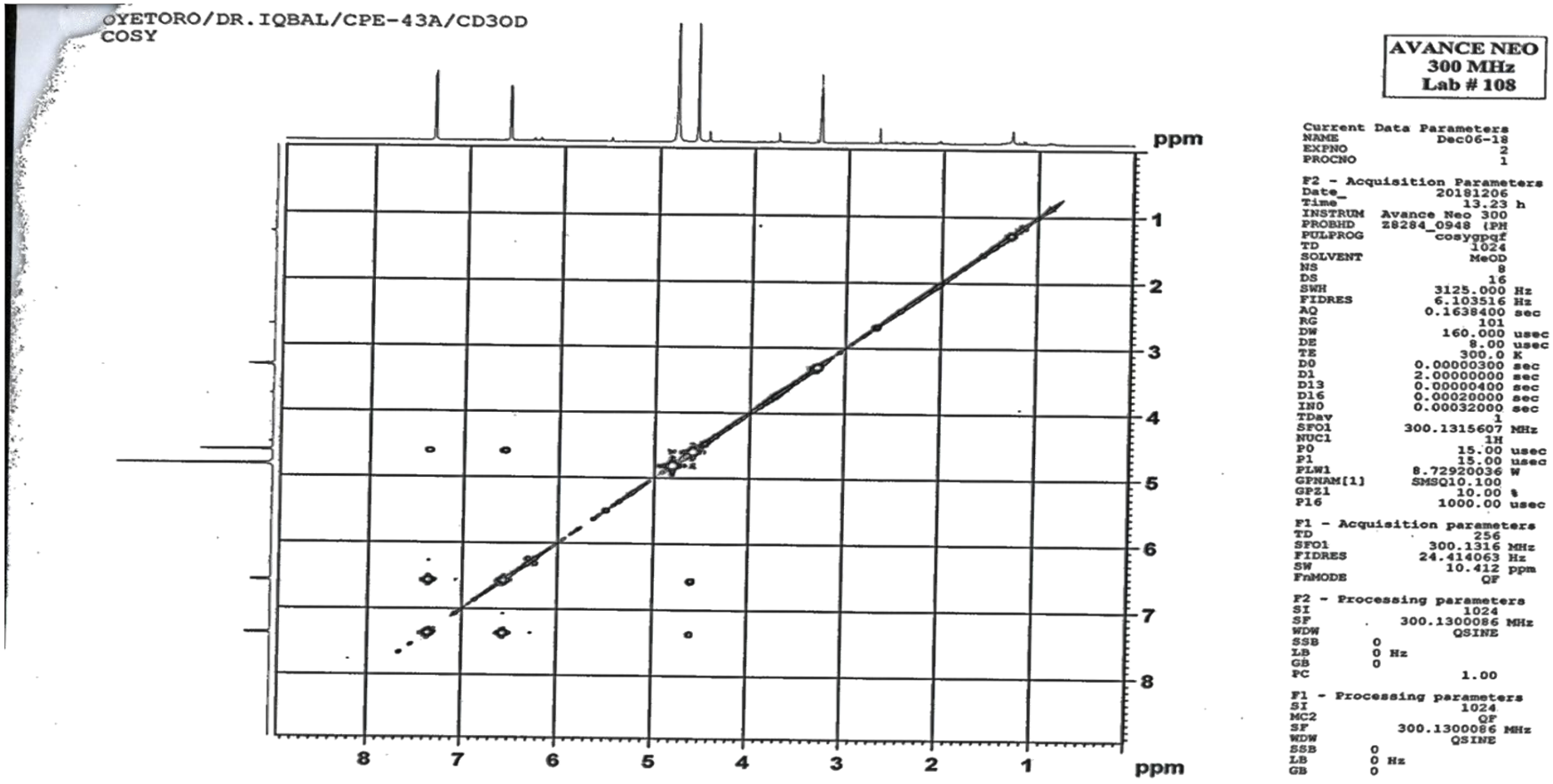

AVANCE NEO
300 MHz
Lab # 108

```
Current Data Parameters
NAME                  Dec06-18
EXPNO                        2
PROCNO                       1

F2 - Acquisition Parameters
Date_                 20181206
Time                     13.23 h
INSTRUM          Avance Neo 300
PROBHD           28284_0948 (PH
PULPROG               cosygpqf
TD                        1024
SOLVENT                   MeOD
NS                           8
DS                          16
SWH                  3125.000 Hz
FIDRES               6.103516 Hz
AQ                   0.1638400 sec
RG                         101
DW                   160.000 usec
DE                     8.00 usec
TE                     300.0 K
D0                0.00000300 sec
D1                2.00000000 sec
D13               0.00000400 sec
D16               0.00020000 sec
IN0               0.00032000 sec
TDav                         1
SFO1            300.1315607 MHz
NUC1                       1H
P0                    15.00 usec
P1                    15.00 usec
PLW1             8.72920036 W
GPNAM[1]         SMSQ10.100
GPZ1                  10.00 %
P16                 1000.00 usec

F1 - Acquisition parameters
TD                         256
SFO1            300.1316 MHz
FIDRES          24.414063 Hz
SW                    10.412 ppm
FnMODE                     QF

F2 - Processing parameters
SI                        1024
SF              300.1300086 MHz
WDW                     QSINE
SSB                  0
LB                   0 Hz
GB                   0
PC                        1.00

F1 - Processing parameters
SI                        1024
MC2                        QF
SF              300.1300086 MHz
WDW                     QSINE
SSB                  0
LB                   0 Hz
GB                   0
```

Appendix III (a)

EI-MS, 1D and 2D NMR spectra of SJB-12

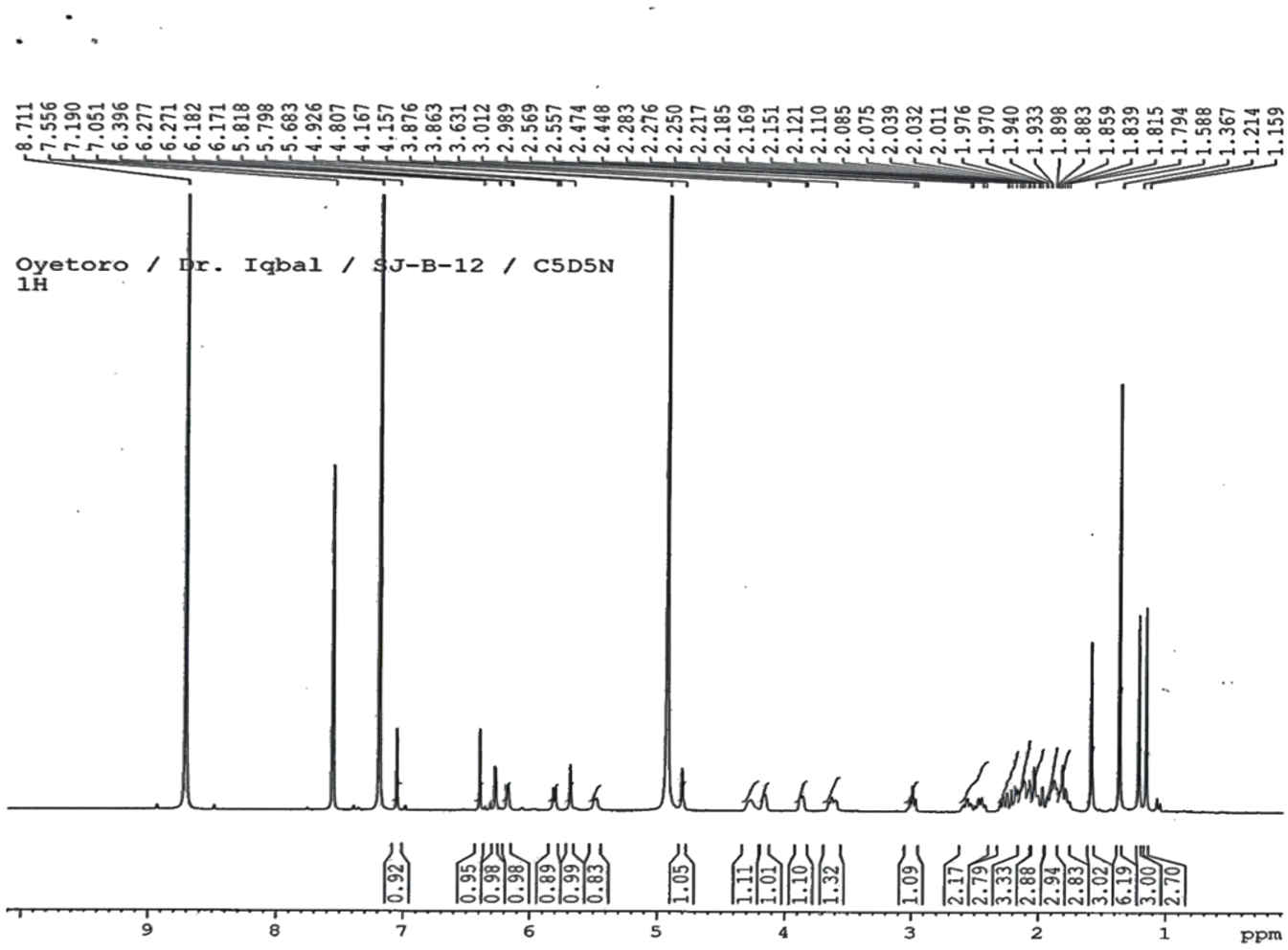

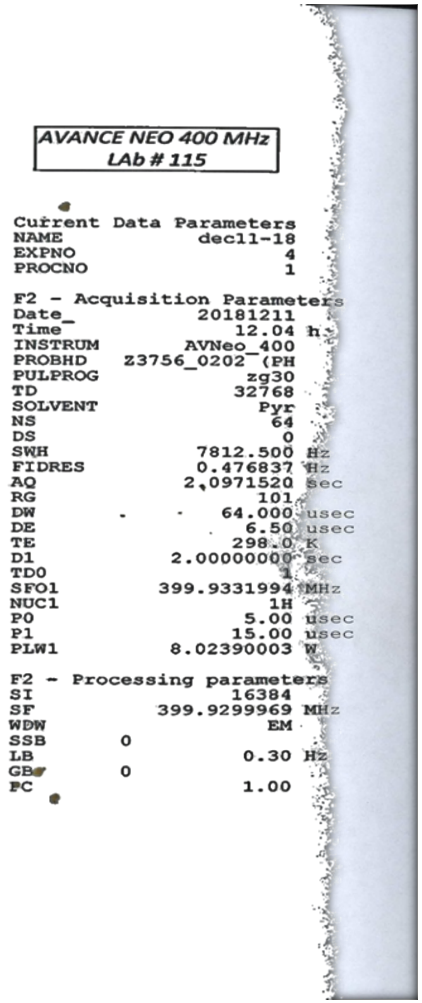

Appendix III (b)

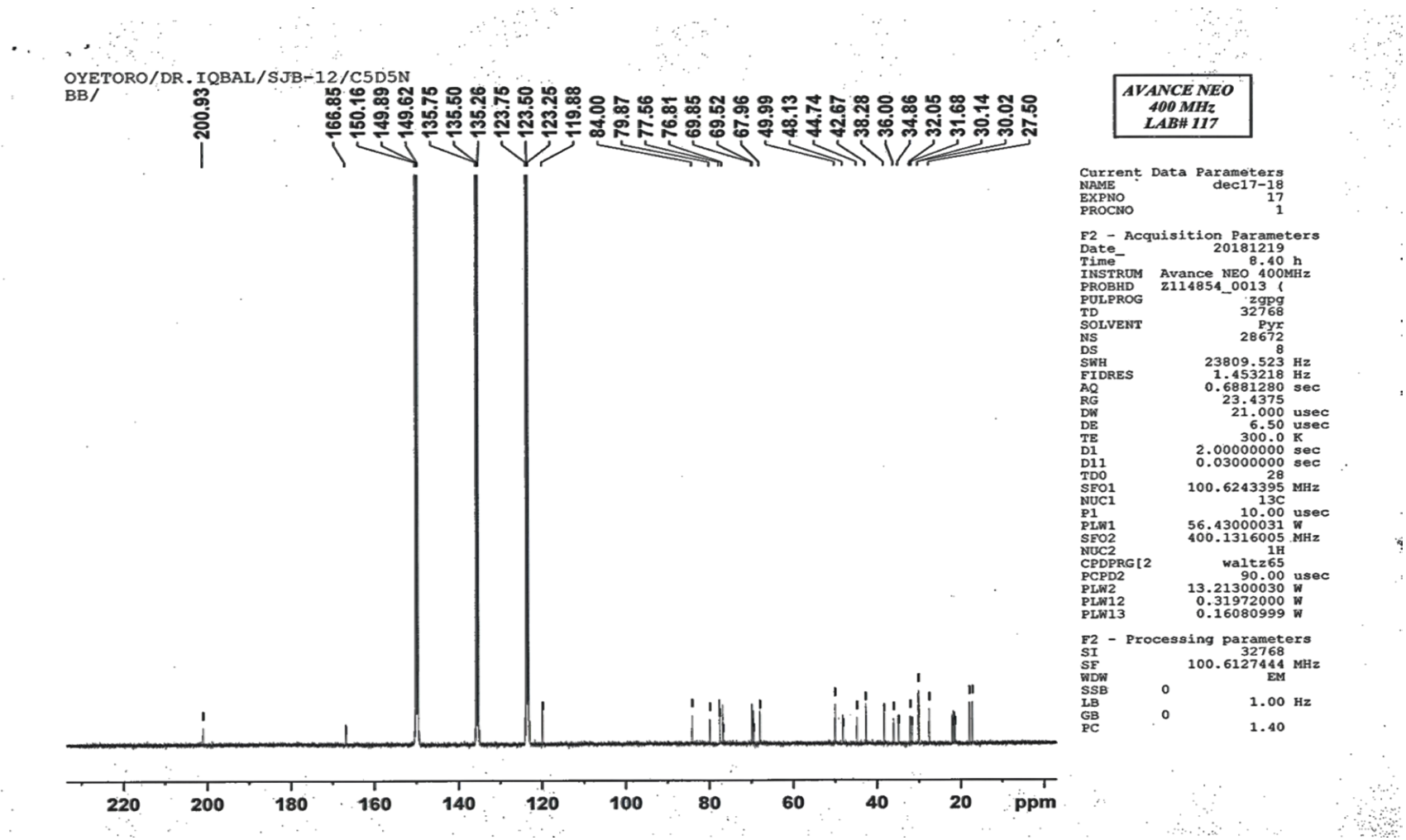

Appendix III (c)

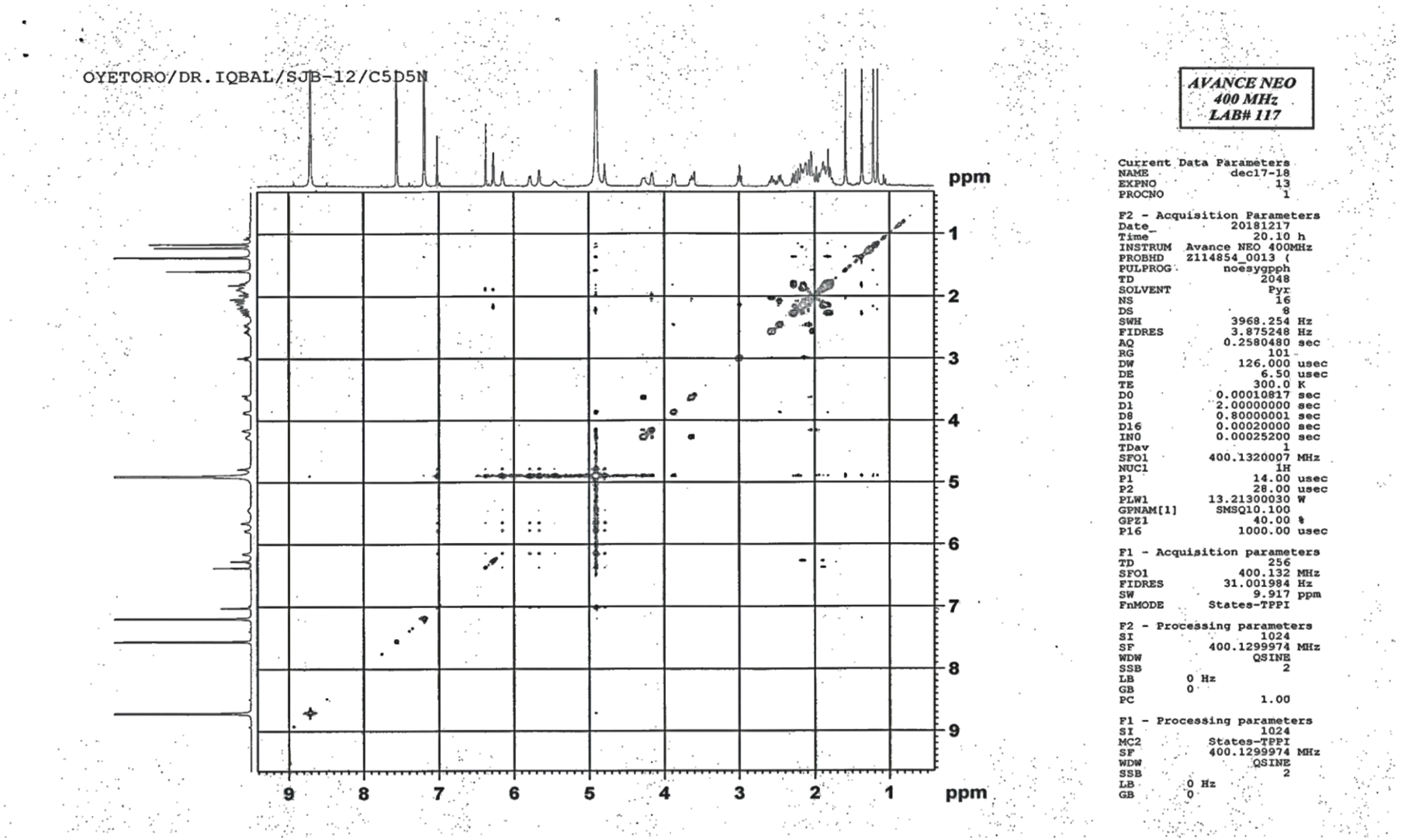

Appendix III (d)

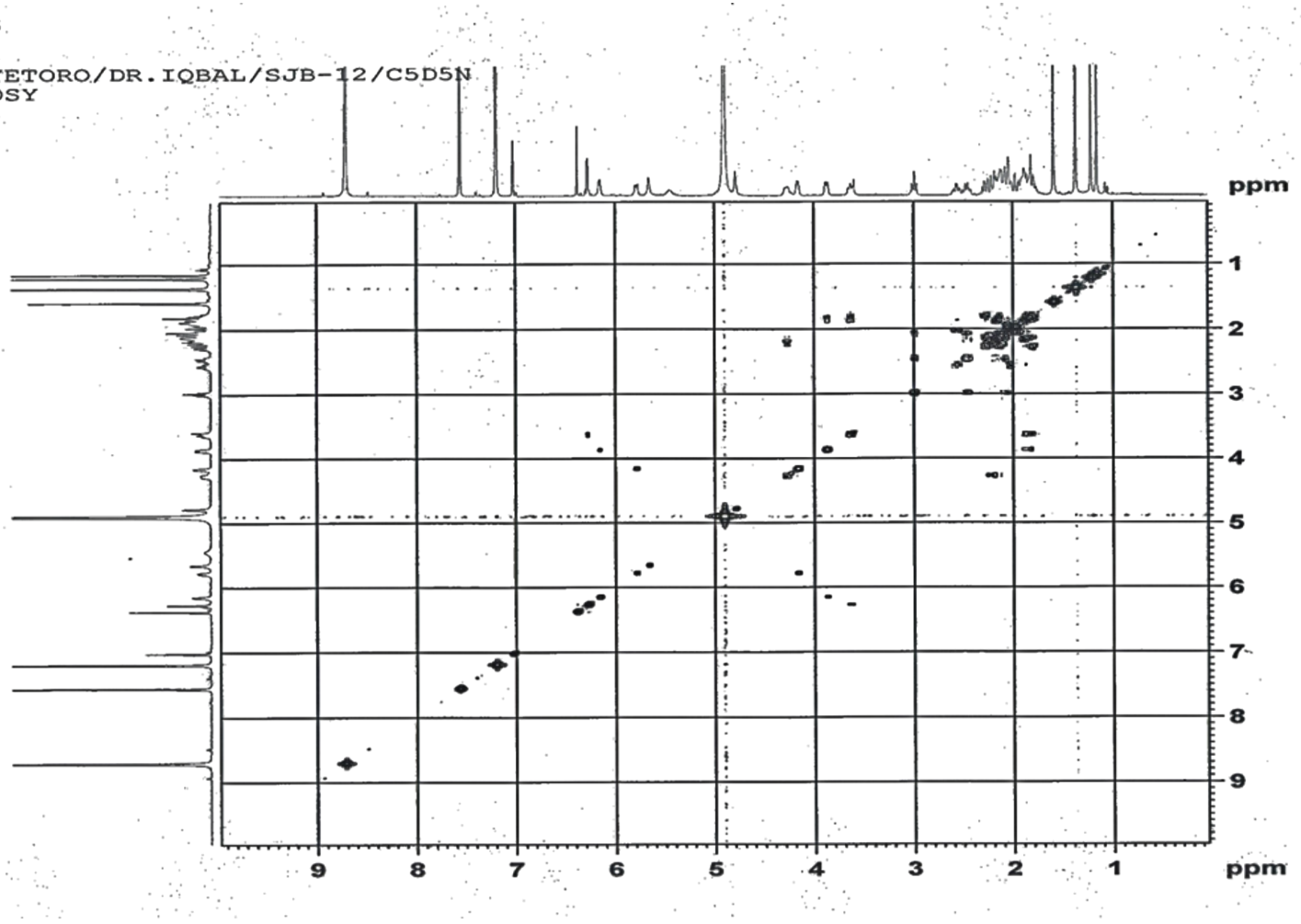

AVANCE NEO
400 MHz
LAB# 117

```
Current Data Parameters
NAME                  dec17-18
EXPNO                       12
PROCNO                       1

F2 - Acquisition Parameters
Date_               20181217
Time                    16.39 h
INSTRUM   Avance NEO 400MHz
PROBHD    Z114854_0013 (
PULPROG             cosygpqf
TD                      2048
SOLVENT                  Pyr
NS                         8
DS                         4
SWH                 3968.254 Hz
FIDRES              3.875248 Hz
AQ                0.2580480 sec
RG                       101
DW                  126.000 usec
DE                    6.50 usec
TE                   300.0 K
D0                0.00000300 sec
D1                1.50000000 sec
D13               0.00000400 sec
D16               0.00020000 sec
IN0               0.00025200 sec
TDav                       1
SFO1            400.1320007 MHz
NUC1                    1H
P0                    14.00 usec
P1                    14.00 usec
PLW1           13.21300030 W
GPNAM[1]        SMSQ10.100
GPZ1                  10.00 %
P16                 1000.00 usec

F1 - Acquisition parameters
TD                       256
SFO1                400.132 MHz
FIDRES             31.001984 Hz
SW                     9.917 ppm
FnMODE                    QF

F2 - Processing parameters
SI                       1024
SF              400.1299974 MHz
WDW                     SINE
SSB          0
LB           0 Hz
GB           0
PC                     1.00

F1 - Processing parameters
SI                       1024
MC2                       QF
SF              400.1299974 MHz
WDW                     SINE
SSB          0
LB           0 Hz
GB           0
```

Appendix III (e)

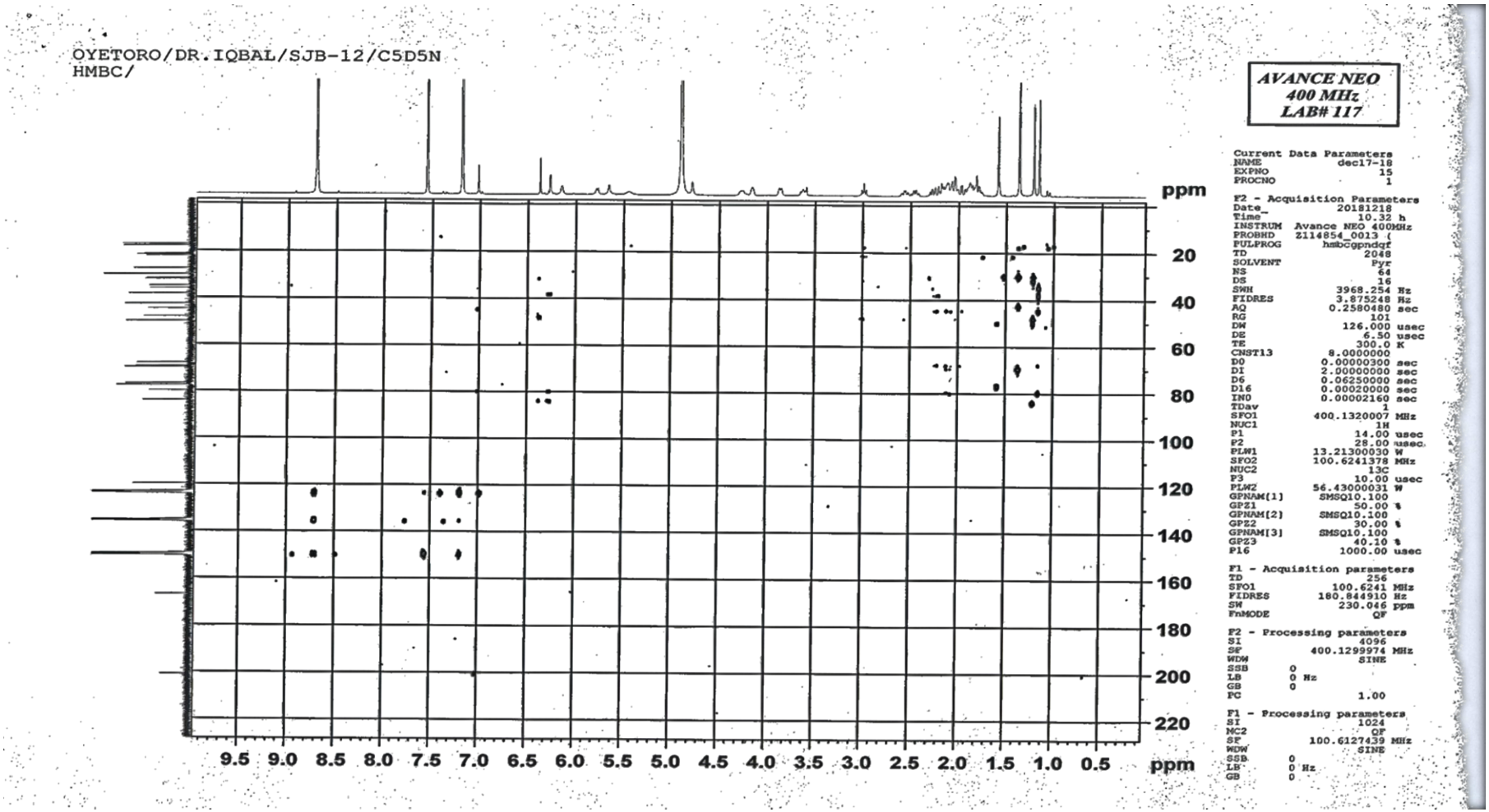

Appendix IV (a)

EI-MS, 1D and 2D NMR spectra of SJB-12B

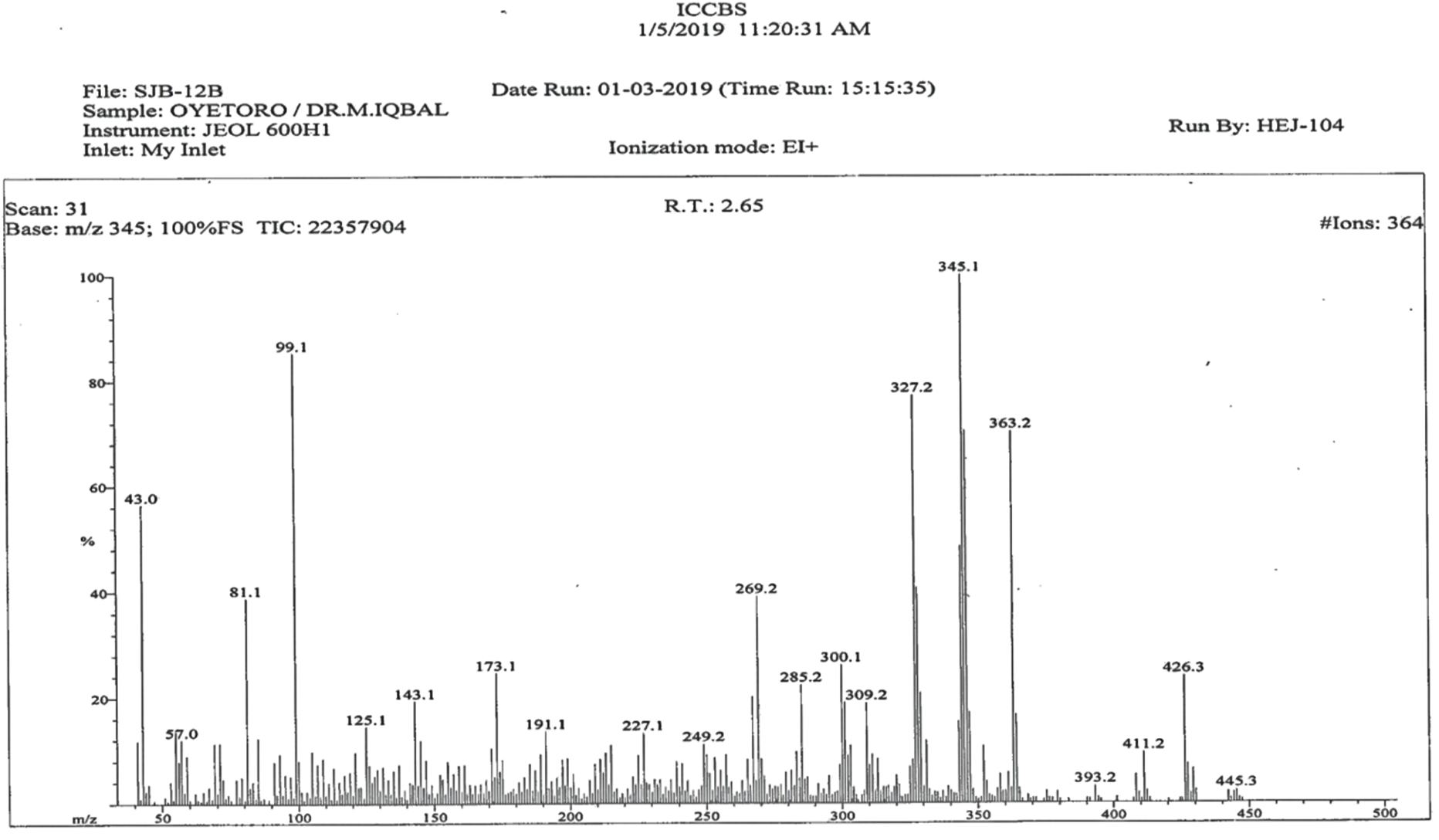

Appendix IV (b)

ICCBS
1/5/2019 11:27:04 AM

File: SJB-12B
Sample: OYETORO / DR.M.IQBAL
Instrument: JEOL 600H1
Inlet: My Inlet

Date Run: 01-03-2019 (Time Run: 15:15:35)

Ionization mode: EI+

Run By: HEJ-104

Scan: 31
Base: m/z 345; 100%FS TIC: 22357904

R.T.: 2.65

#Ions: 364

Threshold: 2.5% of Base

Displayed TIC: 22357904

Mass	%Base	Mass	%Base	Mass	%Base	Mass	%Base	Mass	%Base	Mass	%Base	Mass	%Base
41.0	11.9	99.1	85.3	139.1	2.6	172.1	5.0	203.1	2.9	237.1	4.5	269.2	39.1
43.0	56.5	100.1	8.1	141.0	4.0	173.1	24.7	207.1	4.3	239.1	7.9	270.1	8.4
45.0	3.7	105.0	9.8	142.0	3.6	174.1	6.0	209.1	7.4	240.2	3.1	271.1	5.3
53.0	4.2	107.0	7.5	143.1	19.4	175.1	8.2	210.1	2.6	241.1	7.5	273.1	3.4
55.0	13.7	109.0	8.5	144.1	3.5	179.0	2.8	211.1	8.4	243.1	4.3	274.1	2.6
56.0	8.0	111.0	3.9	145.0	11.9	181.1	4.0	212.1	5.8	247.1	2.5	275.1	3.2
57.0	12.1	113.0	6.8	146.0	3.1	183.1	5.0	213.1	9.5	248.1	3.2	276.2	3.0
59.0	9.1	115.0	4.1	147.1	8.2	184.1	2.8	214.1	3.5	249.2	11.2	277.2	3.5
67.1	3.2	117.0	5.4	149.1	3.6	185.1	7.5	215.1	11.0	250.2	9.2	279.1	5.8
69.1	11.4	119.0	6.0	152.1	5.5	186.1	2.5	217.1	2.8	251.1	5.7	281.2	6.2
71.1	11.4	121.1	9.7	153.0	4.7	187.1	6.3	221.1	2.8	253.1	8.6	282.3	3.3
72.1	4.7	122.0	3.1	155.0	7.9	189.1	9.3	223.1	5.0	254.1	3.1	283.2	9.7
77.0	4.7	123.0	3.2	156.1	3.1	191.1	13.6	224.1	3.6	255.1	6.2	284.2	4.7
79.0	5.1	125.1	14.6	157.1	5.7	192.1	2.8	225.1	9.1	256.1	3.2	285.2	22.4
81.1	38.8	126.1	7.3	158.0	2.6	193.1	4.2	226.1	3.5	257.2	9.1	286.2	4.5
82.1	3.1	127.1	4.1	159.1	7.2	195.1	4.8	227.1	13.3	258.1	3.1	287.2	4.9
83.1	4.1	128.1	5.2	161.1	7.3	196.1	3.1	228.1	3.9	259.1	4.0	291.2	3.7
85.0	12.4	129.1	6.4	163.1	3.7	197.1	8.2	229.1	3.6	263.1	4.3	293.1	2.7
91.0	7.9	131.1	6.9	165.0	3.5	198.1	3.4	231.1	4.5	265.1	8.3	295.2	5.2
93.1	9.3	133.1	4.6	167.1	3.8	199.1	8.5	232.1	3.5	266.1	3.4	299.2	7.2
95.0	5.5	135.1	6.2	169.1	4.5	200.1	3.0	233.1	4.5	267.1	20.2	300.1	26.2
97.0	5.2	137.1	7.3	171.1	10.4	201.1	5.5	235.1	3.0	268.1	4.3		

Appendix IV (c)

ICCBS
1/5/2019 11:27:39 AM

File: SJB-12B
Date Run: 01-03-2019 (Time Run: 15:15:35)
Sample: OYETORO / DR.M.IQBAL
Instrument: JEOL 600H1
Run By: HEJ-104
Inlet: My Inlet
Ionization mode: EI+

Scan: 31
R.T.: 2.65
Base: m/z 345; 100%FS TIC: 22357904
#Ions: 364

Threshold: .5% of Base
Displayed TIC: 22357904

Mass	%Base	Mass	%Base	Mass	%Base	Mass	%Base	Mass	%Base	Mass	%Base	Mass	%Base
302.2	9.0	315.5	.7	330.1	3.1	345.1	100.0	360.2	2.3	379.2	2.1	413.2	.9
303.2	10.9	316.2	3.0	331.2	11.8	346.2	70.5	361.2	5.7	380.2	.7	420.2	.6
303.6	.8	317.1	3.2	332.2	2.6	347.2	17.1	362.2	2.8	383.2	.7	424.3	.8
304.2	3.0	318.2	1.9	333.2	1.4	348.2	2.6	363.2	70.3	390.2	.9	425.2	.8
305.2	1.5	319.1	3.1	334.2	2.2	349.2	1.1	364.2	16.7	391.2	.8	426.3	24.0
305.8	.6	320.1	5.2	335.2	2.0	350.1	.7	365.2	2.8	393.2	3.1	427.3	7.4
307.2	1.5	321.1	3.5	336.2	.9	351.2	1.1	366.2	.7	394.3	1.1	428.3	1.9
308.1	2.4	322.1	1.2	337.1	2.2	352.2	10.7	368.3	1.5	395.3	.6	429.3	6.4
309.2	19.0	323.1	1.5	338.3	1.1	353.2	4.1	369.3	.7	401.2	1.1	430.3	2.5
310.1	7.2	324.1	1.6	339.2	3.2	354.2	1.5	370.3	1.0	407.3	.8	442.2	2.2
311.2	9.2	325.1	6.8	340.2	2.3	355.1	1.2	371.3	1.0	408.2	5.3	443.2	1.0
312.1	2.3	326.2	8.1	341.2	1.8	356.1	1.0	374.2	.7	409.3	1.9	444.3	2.0
313.1	8.3	327.2	77.2	342.2	1.7	357.2	2.7	375.2	2.3	410.4	.8	445.3	2.3
314.2	2.2	328.2	40.7	343.2	15.4	358.2	5.4	376.3	1.1	411.2	9.5	446.3	1.0
315.2	3.0	329.2	20.8	344.2	48.5	359.2	2.2	377.2	.9	412.2	2.3	447.3	.7

Appendix IV (d)

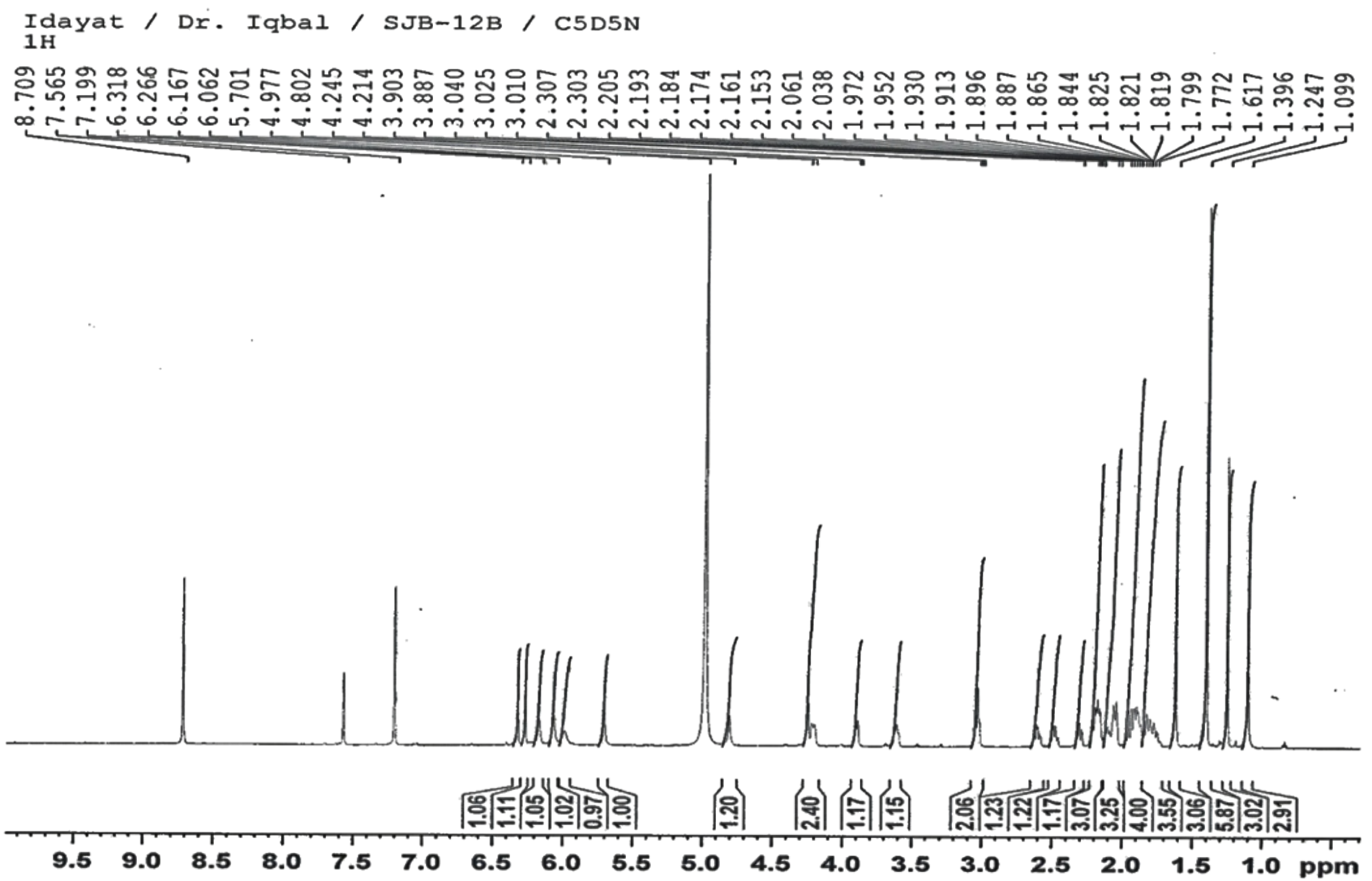

AVANCE NEO 600 MHz
Cryoprobe
Lab # 108

Current Data Parameters

NAME	Jan07-19
EXPNO	4
PROCNO	1

F2 - Acquisition Parameters

Date_	20190107
Time	12.25 h
INSTRUM	Avance NEO 600MHz
PROBHD	Z44896_0021 (C
PULPROG	zg30
TD	32768
SOLVENT	Pyr
NS	16
DS	0
SWH	14648.438 Hz
FIDRES	0.894070 Hz
AQ	1.1184810 sec
RG	10.6534
DW	34.133 usec
DE	15.36 usec
TE	298.0 K
D1	1.50000000 sec
TD0	1
SFO1	600.0342602 MHz
NUC1	1H
P0	3.33 usec
P1	10.00 usec
PLW1	4.25000000 W

F2 - Processing parameters

SI	16384
SF	600.0308926 MHz
WDW	EM
SSB	0
LB	0.30 Hz
GB	0
PC	1.00

Appendix IV (e)

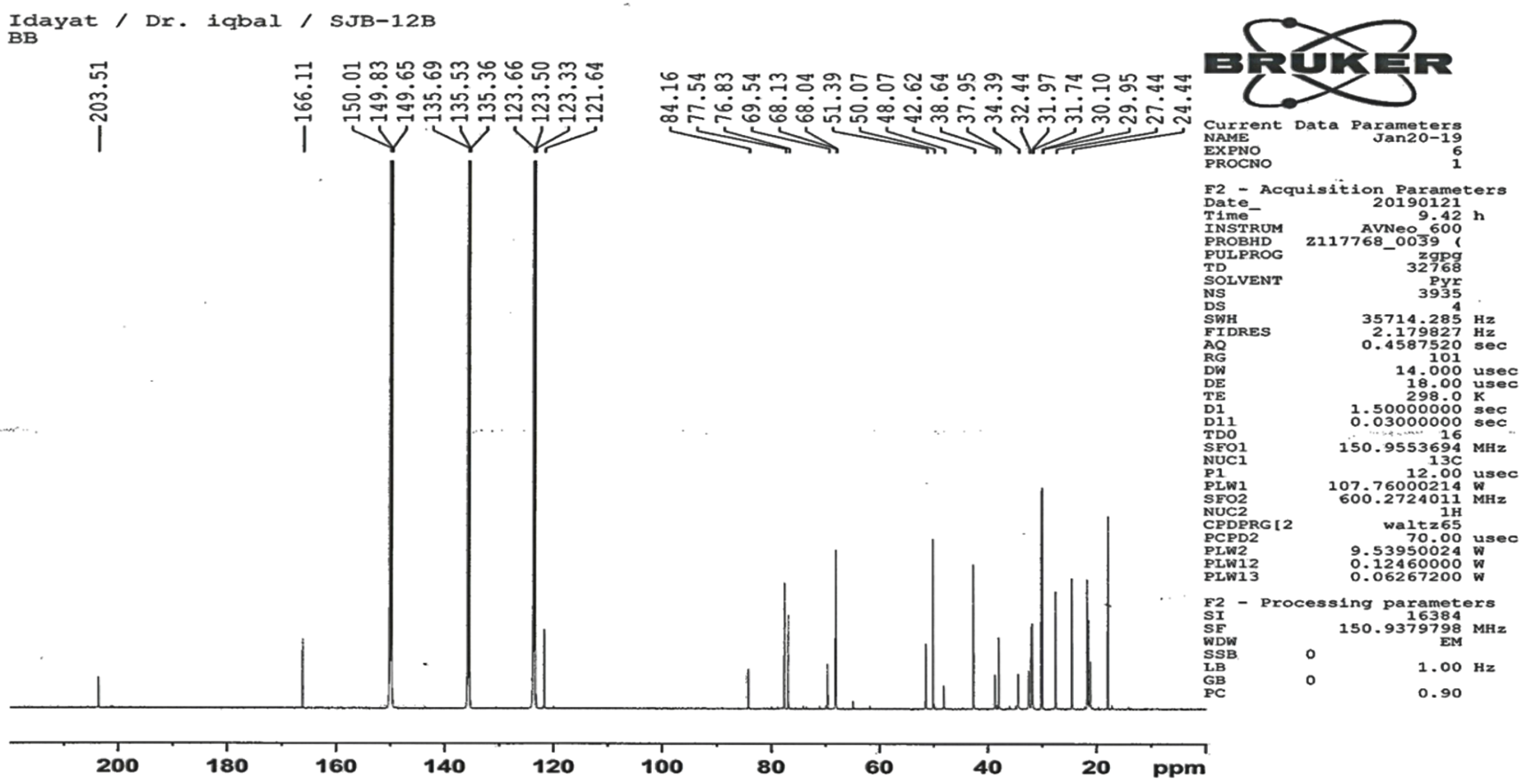

Appendix IV (f)

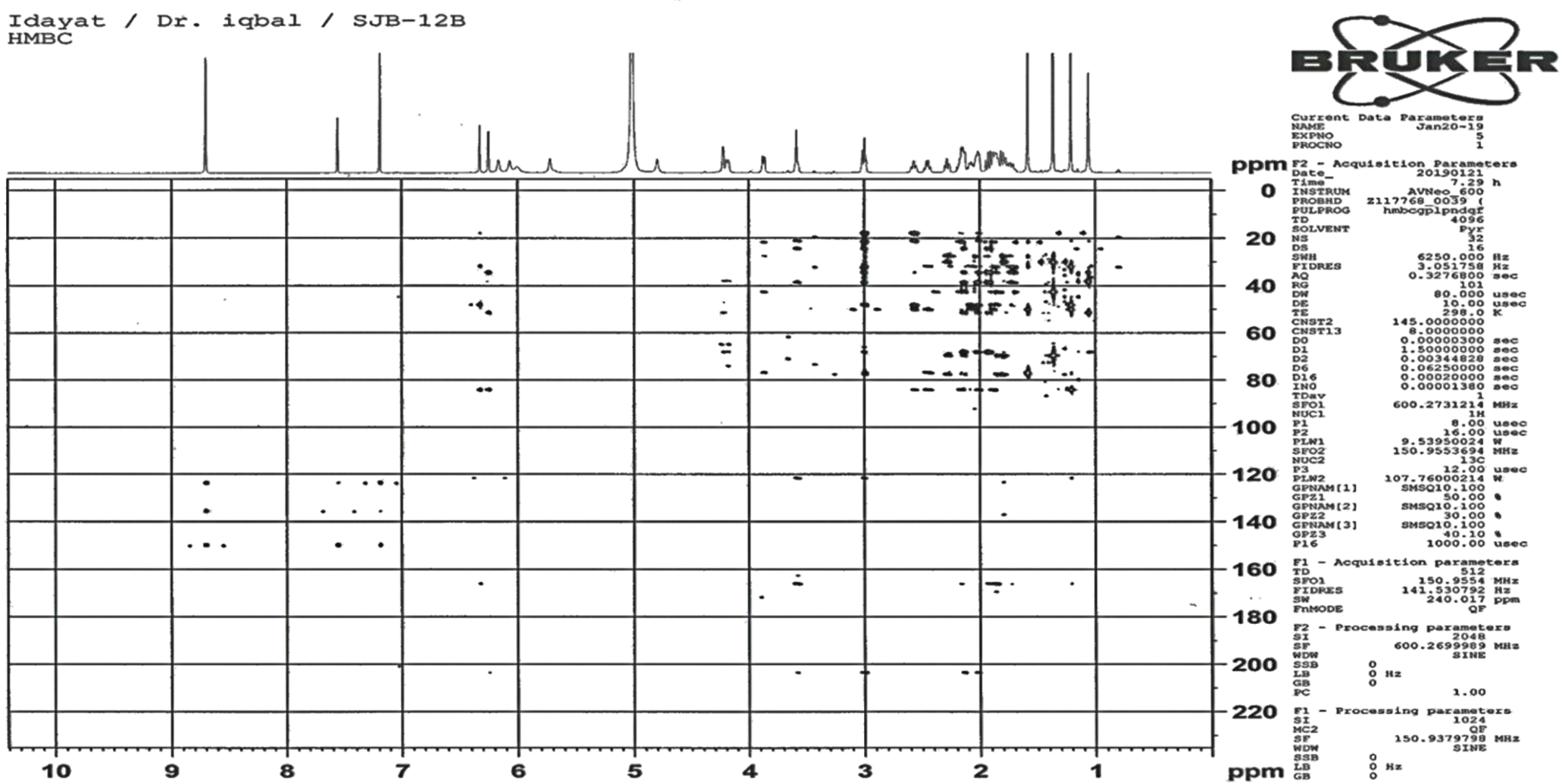

Appendix IV (g)

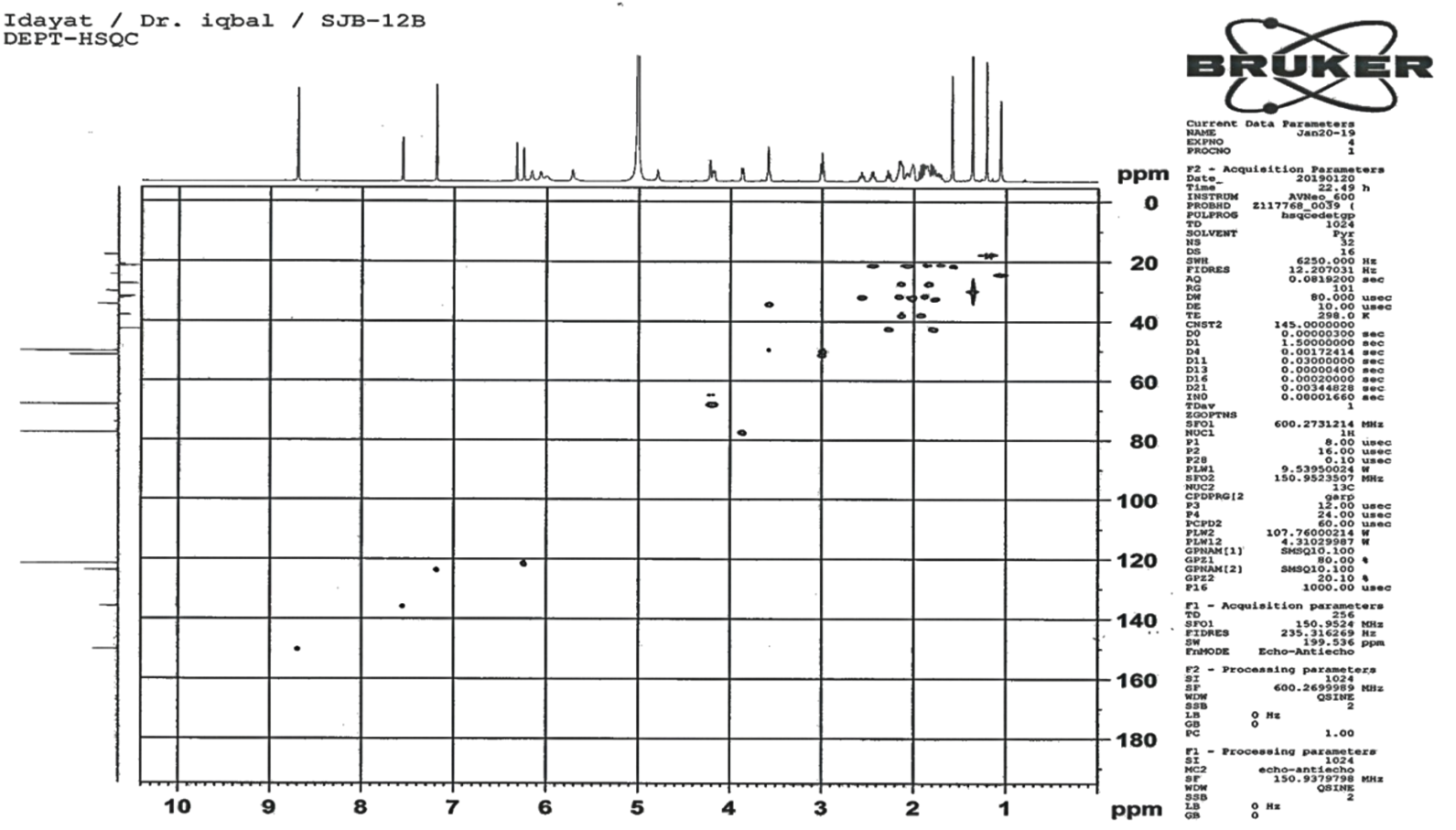

Appendix IV (h)

Idayat / Dr. iqbal / SJB-12B
DEPT-HSQC

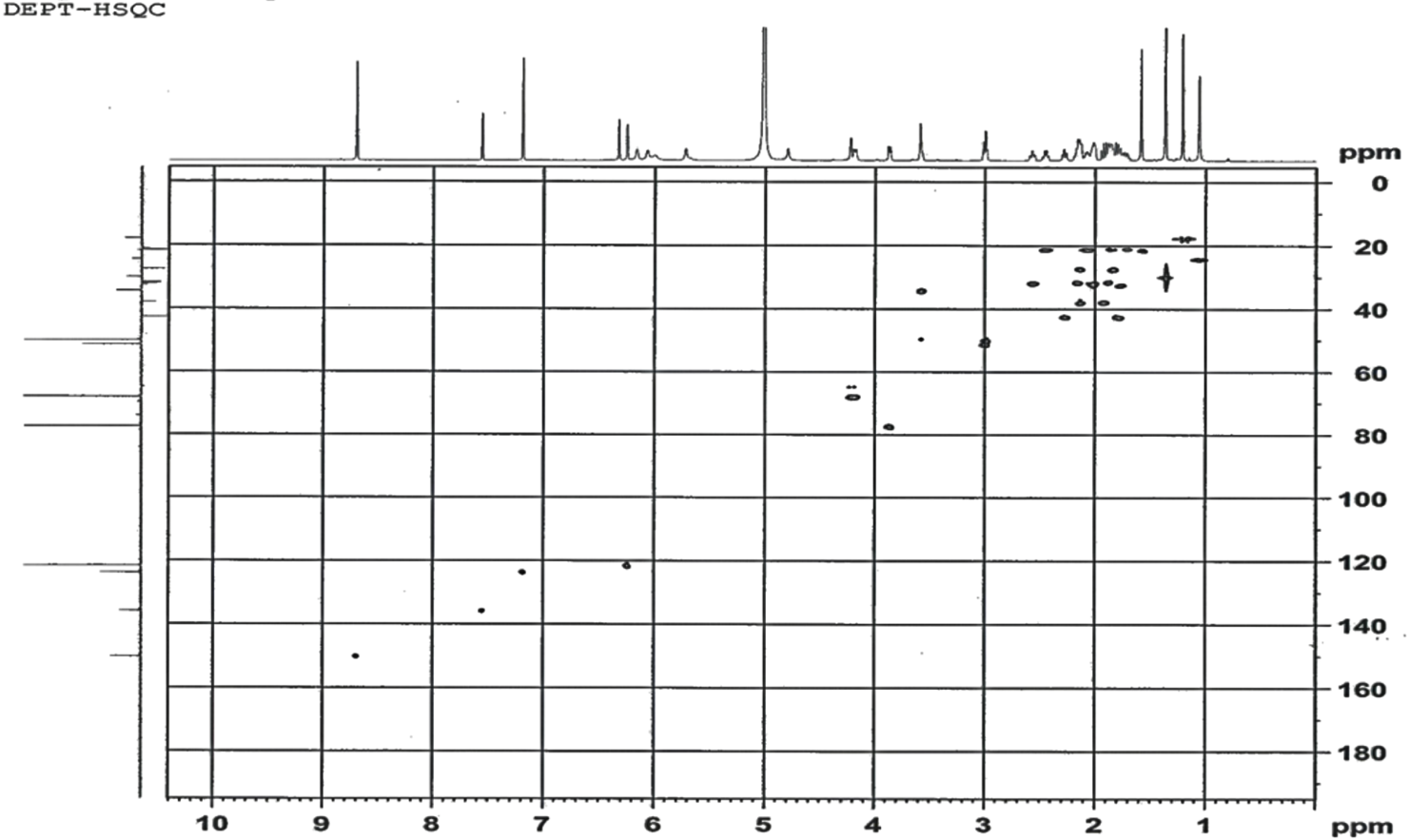

BRUKER

```
Current Data Parameters
NAME                  Jan20-19
EXPNO                        4
PROCNO                       1

F2 - Acquisition Parameters
Date_              20190120
Time                 22.49 h
INSTRUM            AVNeo 600
PROBHD     Z117768_0039 (
PULPROG          haqcedetgp
TD                     1024
SOLVENT                 Pyr
NS                       32
DS                       16
SWH                6250.000 Hz
FIDRES               12.207031 Hz
AQ                 0.0819200 sec
RG                       101
DW                    80.000 usec
DE                    10.00 usec
TE                   298.0 K
CNST2              145.0000000
D0                 0.00000300 sec
D1                 1.50000000 sec
D4                 0.00172414 sec
D11                0.03000000 sec
D13                0.00000400 sec
D16                0.00020000 sec
D21                0.00344828 sec
IN0                0.00001660 sec
TDav                         1
ZGOPTNS
SFO1               600.2731214 MHz
NUC1                       1H
P1                    8.00 usec
P2                   16.00 usec
P28                   0.10 usec
PLW1               9.53950024 W
SFO2               150.9523507 MHz
NUC2                      13C
CPDPRG[2                  garp
P3                   12.00 usec
P4                   24.00 usec
PCPD2                60.00 usec
PLW2              107.74000214 W
PLW12               4.31029987 W
GPNAM[1]          SMSQ10.100
GPZ1                 80.00 %
GPNAM[2]          SMSQ10.100
GPZ2                 20.10 %
P16                1000.00 usec

F1 - Acquisition parameters
TD                       256
SFO1               150.9524 MHz
FIDRES            235.316269 Hz
SW                 199.536 ppm
FnMODE     Echo-Antiecho

F2 - Processing parameters
SI                      1024
SF                600.2699989 MHz
WDW                     QSINE
SSB                         2
LB          0 Hz
GB          0
PC                      1.00

F1 - Processing parameters
SI                      1024
MC2           echo-antiecho
SF                150.9379798 MHz
WDW                     QSINE
SSB                         2
LB          0 Hz
GB          0
```

Appendix IV (i)

Idayat / Dr. iqbal / SJB-12B
NOESY

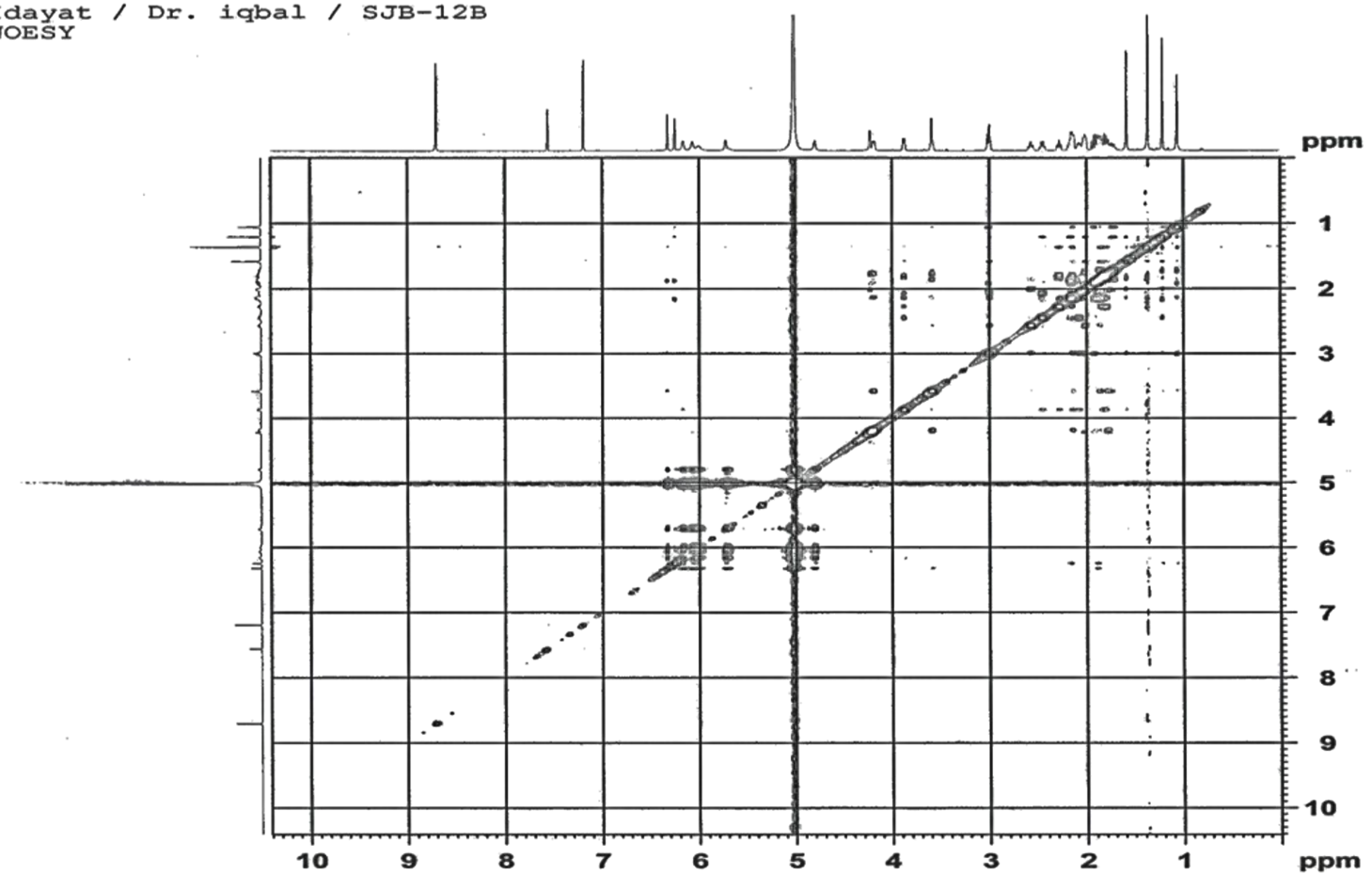

BRUKER

Current Data Parameters
NAME Jan20-19
EXPNO 3
PROCNO 1

F2 - Acquisition Parameters
Date_ 20190120
Time 19.10 h
INSTRUM AVNeo 600
PROBHD Z117768_0039 (
PULPROG noesygpph
TD 2048
SOLVENT Pyr
NS 16
DS 16
SWH 6250.000 Hz
FIDRES 6.103516 Hz
AQ 0.1638400 sec
RG 16.7411
DW 80.000 usec
DE 10.00 usec
TE 298.0 K
D0 0.00006981 sec
D1 1.50000000 sec
D8 0.80000001 sec
D16 0.00020000 sec
IN0 0.00016000 sec
TDav 1
SFO1 600.2731214 MHz
NUC1 1H
P1 8.00 usec
P2 16.00 usec
PLW1 9.53950024 W
GPNAM[1] SMSQ10.100
GPZ1 40.00 %
P16 1000.00 usec

F1 - Acquisition parameters
TD 256
SFO1 600.2731 MHz
FIDRES 48.828125 Hz
SW 10.412 ppm
FnMODE States-TPPI

F2 - Processing parameters
SI 1024
SF 600.2699989 MHz
WDW QSINE
SSB 2
LB 0 Hz
GB 0
PC 1.00

F1 - Processing parameters
SI 1024
MC2 States-TPPI
SF 600.2699989 MHz
WDW QSINE
SSB 2
LB 0 Hz
GB 0

Appendix IV (j)

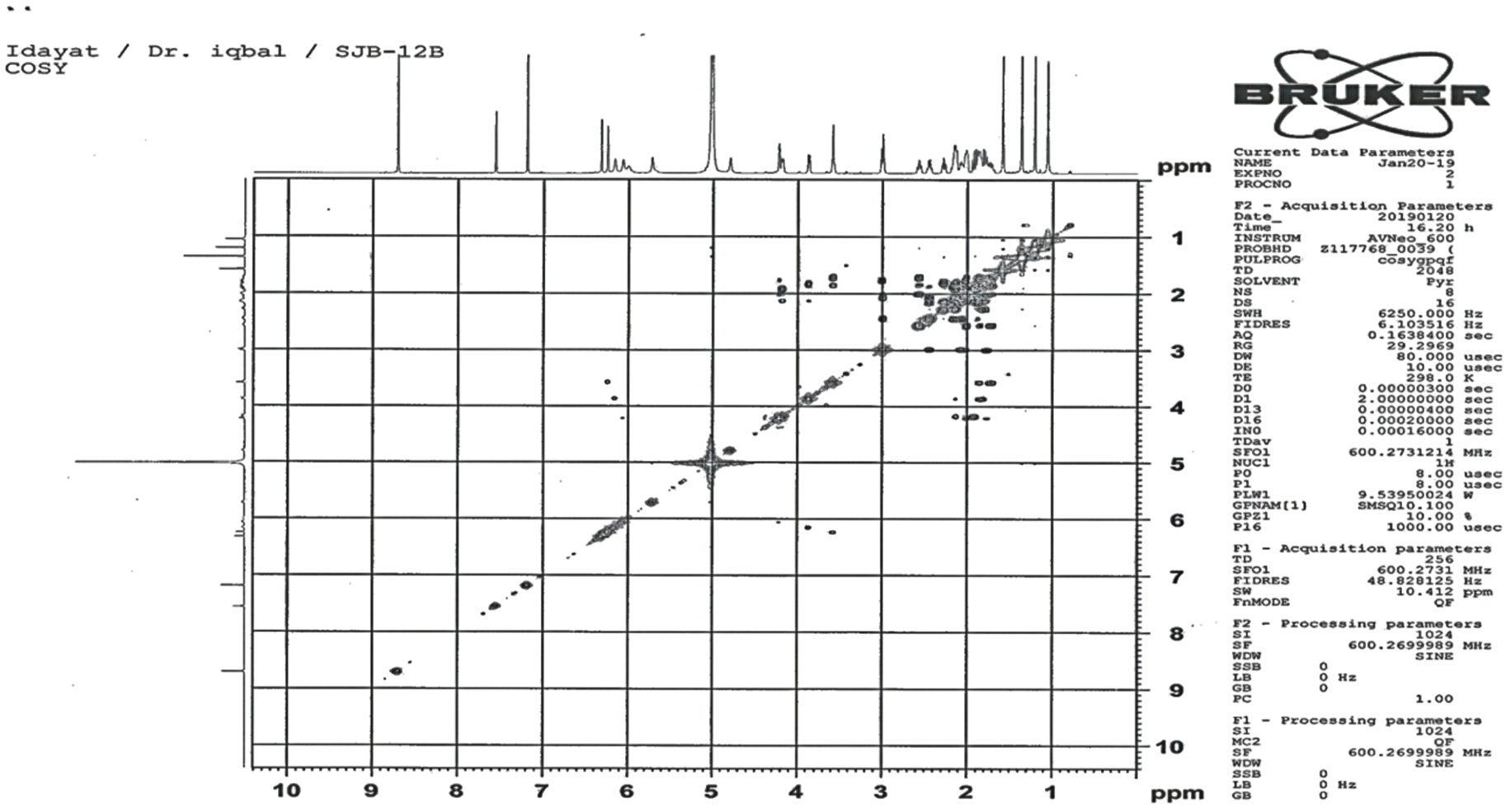

BRUKER

Current Data Parameters
NAME Jan20-19
EXPNO 2
PROCNO 1

F2 - Acquisition Parameters
Date_ 20190120
Time 16.20 h
INSTRUM AVNeo_600
PROBHD z117768_0039 (
PULPROG cosygpqf
TD 2048
SOLVENT Pyr
NS 8
DS 16
SWH 6250.000 Hz
FIDRES 6.103516 Hz
AQ 0.1638400 sec
RG 29.2969
DW 80.000 usec
DE 10.00 usec
TE 298.0 K
D0 0.00000300 sec
D1 2.00000000 sec
D13 0.00000400 sec
D16 0.00020000 sec
IN0 0.00016000 sec
TDav 1
SFO1 600.2731214 MHz
NUC1 1H
P0 8.00 usec
P1 8.00 usec
PLW1 9.53950024 W
GPNAM[1] SMSQ10.100
GPZ1 10.00 %
P16 1000.00 usec

F1 - Acquisition parameters
TD 256
SFO1 600.2731 MHz
FIDRES 48.828125 Hz
SW 10.412 ppm
FnMODE QF

F2 - Processing parameters
SI 1024
SF 600.2699989 MHz
WDW SINE
SSB 0
LB 0 Hz
GB 0
PC 1.00

F1 - Processing parameters
SI 1024
MC2 QF
SF 600.2699989 MHz
WDW SINE
SSB 0
LB 0 Hz
GB 0

Appendix IV (k)

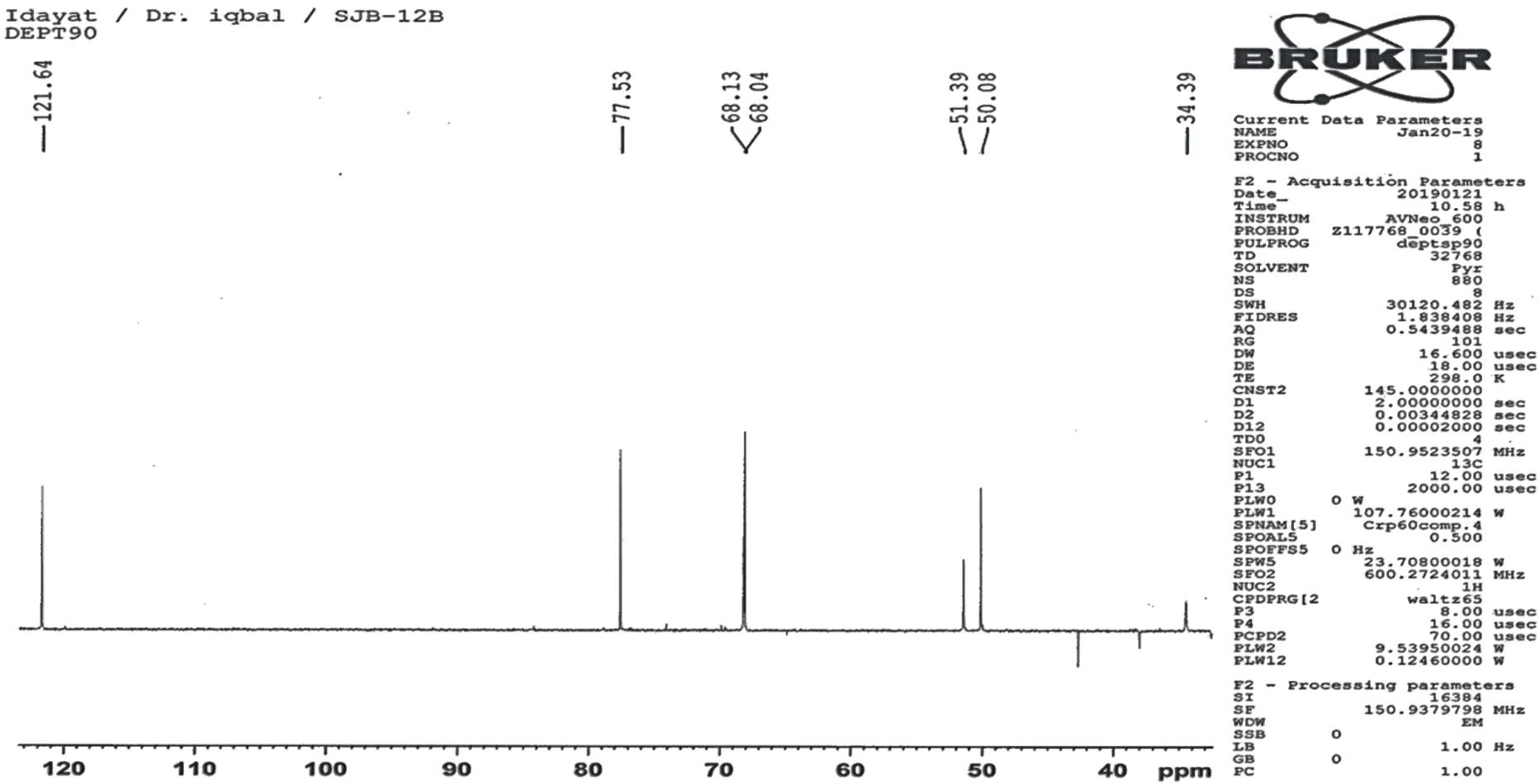

BRUKER

Current Data Parameters
NAME Jan20-19
EXPNO 8
PROCNO 1

F2 - Acquisition Parameters
Date_ 20190121
Time 10.58 h
INSTRUM AVNeo_600
PROBHD Z117768_0039 (
PULPROG deptsp90
TD 32768
SOLVENT Pyr
NS 880
DS 8
SWH 30120.482 Hz
FIDRES 1.838408 Hz
AQ 0.5439488 sec
RG 101
DW 16.600 usec
DE 18.00 usec
TE 298.0 K
CNST2 145.0000000
D1 2.00000000 sec
D2 0.00344828 sec
D12 0.00002000 sec
TD0 4
SFO1 150.9523507 MHz
NUC1 13C
P1 12.00 usec
P13 2000.00 usec
PLW0 0 W
PLW1 107.76000214 W
SPNAM[5] Crp60comp.4
SPOAL5 0.500
SPOFFS5 0 Hz
SPW5 23.70800018 W
SFO2 600.2724011 MHz
NUC2 1H
CPDPRG[2 waltz65
P3 8.00 usec
P4 16.00 usec
PCPD2 70.00 usec
PLW2 9.53950024 W
PLW12 0.12460000 W

F2 - Processing parameters
SI 16384
SF 150.9379798 MHz
WDW EM
SSB 0
LB 1.00 Hz
GB 0
PC 1.00

Appendix IV (l)

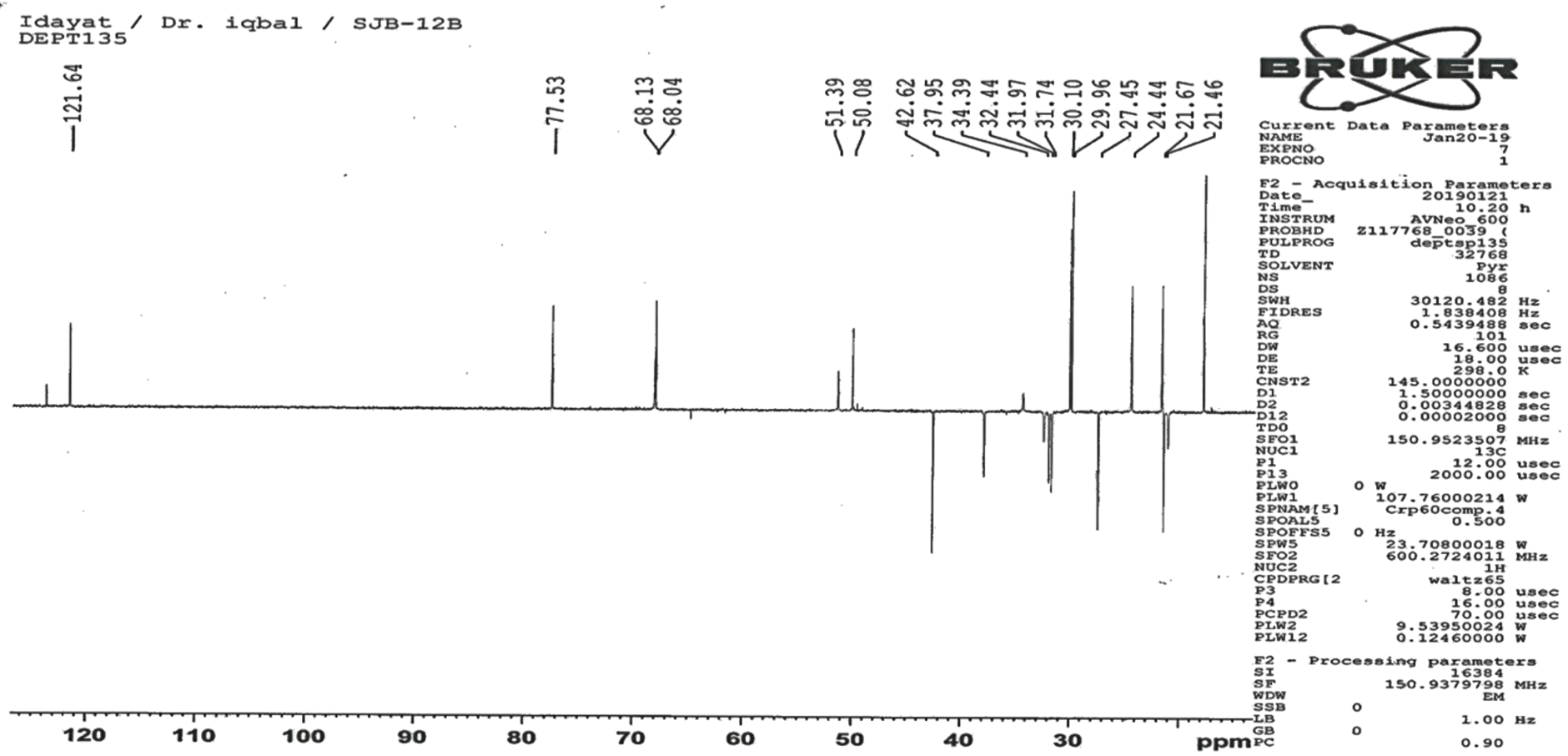

Appendix V (a)

EI-MS, 1D and 2D NMR spectra of SJB-26A

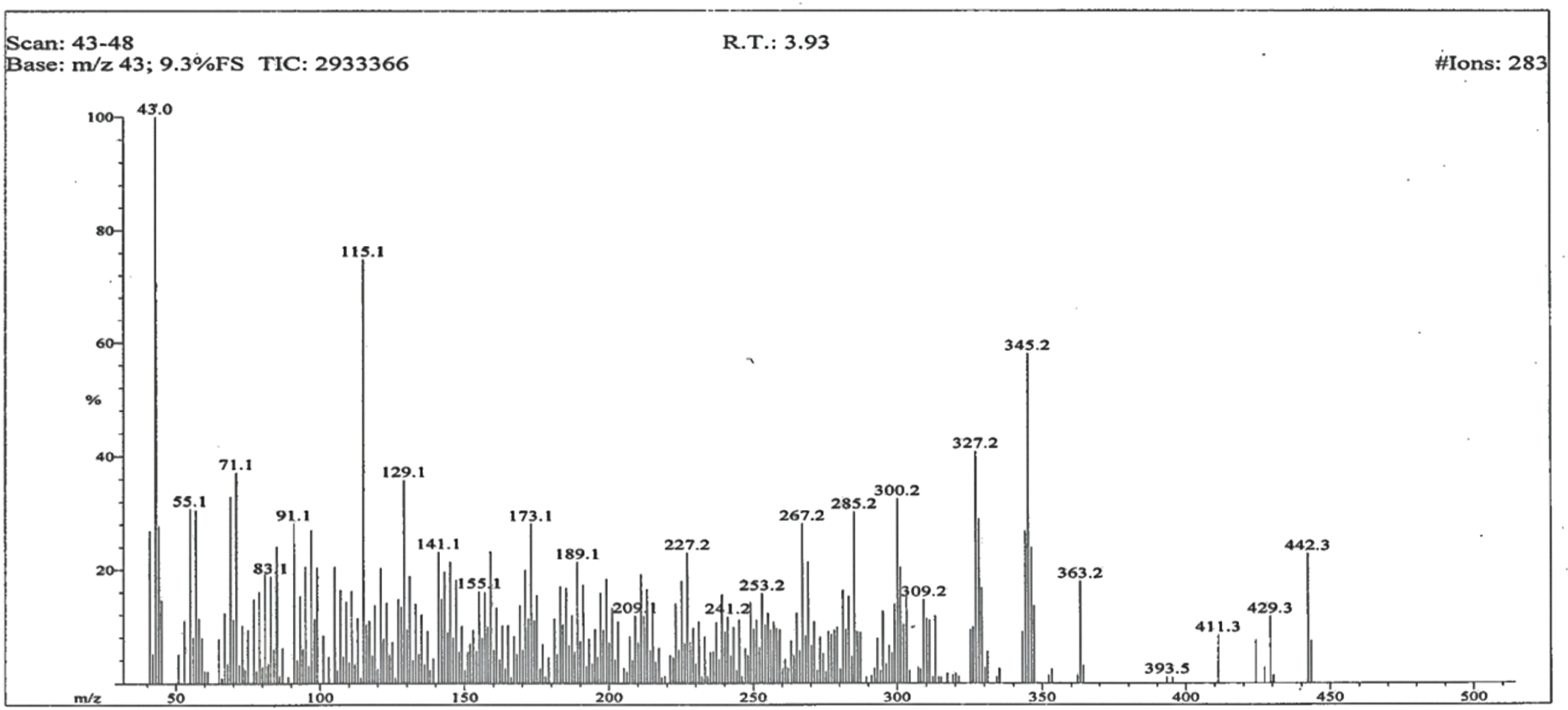

Appendix V (b)

ICCBS
1/4/2019 2:05:57 PM

File: SJ-B-26a
Sample: OYETORO / DR. M.IQBAL
Instrument: JEOL 600H1
Inlet: My Inlet

Date Run: 01-04-2019 (Time Run: 12:52:26)

Run By: HEJ-104

Ionization mode: EI+

Scan: 43-48
Base: m/z 43; 9.3%FS TIC: 2933366

R.T.: 3.93

#Ions: 283

Threshold: 2% of Base

Displayed TIC: 2933366

Mass	%Base	Mass	%Base	Mass	%Base	Mass	%Base	Mass	%Base	Mass	%Base	Mass	%Base
41.0	26.9	79.1	16.1	112.1	3.3	141.1	23.2	168.1	5.2	196.1	4.6	226.1	7.0
42.0	5.2	80.1	2.8	113.1	11.5	142.1	14.8	169.1	13.7	197.1	16.0	227.2	23.0
43.0	100.0	81.1	19.3	115.1	74.9	143.1	19.7	170.1	5.8	198.1	9.4	228.1	7.2
44.0	27.7	82.1	3.4	116.1	10.3	144.1	8.9	171.1	20.0	199.1	18.4	229.1	9.7
45.0	14.6	83.1	18.9	117.1	11.0	145.1	21.5	172.1	11.3	200.1	7.1	230.1	3.4
51.0	5.1	84.1	5.9	118.1	4.9	146.1	8.0	173.1	28.1	201.1	13.2	231.1	10.8
53.0	11.0	85.1	24.1	119.1	13.8	147.1	18.2	174.1	11.0	202.2	4.2	233.1	8.2
55.1	30.8	87.1	6.2	120.1	2.6	148.1	5.5	175.1	15.5	203.1	10.9	235.1	5.4
56.1	8.0	91.1	28.3	121.1	20.3	149.1	10.1	176.1	2.6	205.1	2.6	236.1	5.5
57.1	30.6	92.1	4.0	122.1	7.8	150.1	2.3	177.1	6.9	206.1	2.0	237.2	10.7
58.1	11.4	93.1	15.3	123.1	14.2	151.1	5.5	179.1	4.6	207.1	8.2	238.2	4.2
59.1	8.0	94.1	6.0	124.1	5.0	152.1	6.9	181.1	11.3	208.1	4.1	239.2	15.6
60.0	2.2	95.1	20.6	125.1	7.2	153.1	9.4	182.1	5.1	209.1	11.9	240.2	9.0
61.1	2.1	96.1	3.1	127.1	14.8	154.1	5.6	183.1	17.0	210.1	7.1	241.2	11.7
65.1	7.8	97.1	27.1	128.1	13.5	155.1	16.2	184.1	10.3	211.1	19.2	242.2	4.8
67.1	12.4	98.1	11.3	129.1	35.9	156.1	8.0	185.1	16.7	212.2	11.8	243.2	10.0
68.1	3.4	99.1	20.4	130.1	9.4	157.1	16.0	186.1	6.6	213.1	16.6	244.2	2.3
69.1	32.9	101.1	8.5	131.2	19.0	158.1	9.9	187.1	12.0	214.2	5.8	245.2	11.1
70.1	11.2	103.0	4.6	132.1	4.1	159.1	23.3	188.1	5.5	215.2	14.1	247.2	6.1
71.1	37.2	105.1	20.6	133.1	14.0	160.1	5.8	189.1	21.4	216.1	3.8	248.2	4.9
72.1	3.3	106.1	2.3	134.1	5.1	161.1	13.2	190.1	7.3	217.2	6.2	249.2	14.3
73.1	10.1	107.1	16.5	135.1	12.1	162.1	4.2	191.1	17.4	221.2	4.8	250.2	9.5
74.1	2.4	108.1	4.7	136.2	3.3	163.1	10.1	192.1	3.0	222.2	4.5	251.2	11.1
75.1	9.4	109.1	14.4	137.1	9.2	164.1	2.6	193.1	7.8	223.2	14.1	252.2	6.3
77.1	14.8	110.1	3.7	138.1	2.3	165.1	10.2	194.1	3.4	224.2	5.8	253.2	15.8
78.1	2.2	111.1	16.3	139.1	4.4	167.1	8.2	195.1	9.5	225.1	18.1	254.2	10.3

Appendix V (c)

ICCBS
1/4/2019 2:07:48 PM

File: SJ-B-26a
Sample: OYETORO / DR. M.IQBAL
Instrument: JEOL 600H1
Inlet: My Inlet

Date Run: 01-04-2019 (Time Run: 12:52:26)

Run By: HEJ-104

Ionization mode: EI+

Scan: 42-49
Base: m/z 43; 9.1%FS TIC: 2907192

R.T.: 3.93

#Ions: 290

Threshold: 1.5% of Base

Displayed TIC: 2907192

Mass	%Base	Mass	%Base	Mass	%Base	Mass	%Base	Mass	%Base	Mass	%Base	Mass	%Base
247.2	6.0	260.2	3.0	273.2	8.2	286.2	9.6	302.2	11.1	325.2	9.8	353.3	1.9
248.2	5.1	261.1	4.3	274.2	4.7	287.2	8.4	303.2	16.2	326.2	10.2	363.2	18.3
249.2	15.2	262.1	2.0	275.2	1.5	291.2	1.9	304.3	2.9	327.2	39.5	364.2	3.8
250.2	10.6	263.2	7.2	276.2	9.3	292.2	2.0	307.2	3.1	328.2	29.7	411.3	8.0
251.2	11.0	264.2	5.6	277.2	8.7	293.2	7.3	308.2	2.8	329.2	16.6	424.3	7.1
252.2	5.6	265.2	13.0	278.2	9.4	294.2	2.6	309.2	16.0	330.2	3.2	427.3	2.1
253.2	15.8	266.2	5.3	279.2	8.9	295.2	11.5	310.2	11.9	331.3	5.5	429.3	11.0
254.2	10.1	267.2	28.8	280.2	3.9	296.2	3.5	311.2	12.2	335.2	2.0	442.3	22.4
255.1	13.1	268.2	7.6	281.2	16.0	297.2	5.9	313.2	12.6	343.2	9.1	443.4	7.3
256.2	9.3	269.2	22.0	282.2	9.5	298.2	4.1	314.2	1.7	344.2	28.2		
257.2	12.7	270.2	7.2	283.2	16.0	299.2	14.2	317.2	2.4	345.2	56.9		
258.2	8.8	271.2	12.0	284.2	5.9	300.2	31.0	319.2	2.6	346.2	25.6		
259.2	10.1	272.2	2.5	285.2	32.0	301.2	19.6	320.2	2.4	347.2	13.9		

Appendix V (d)

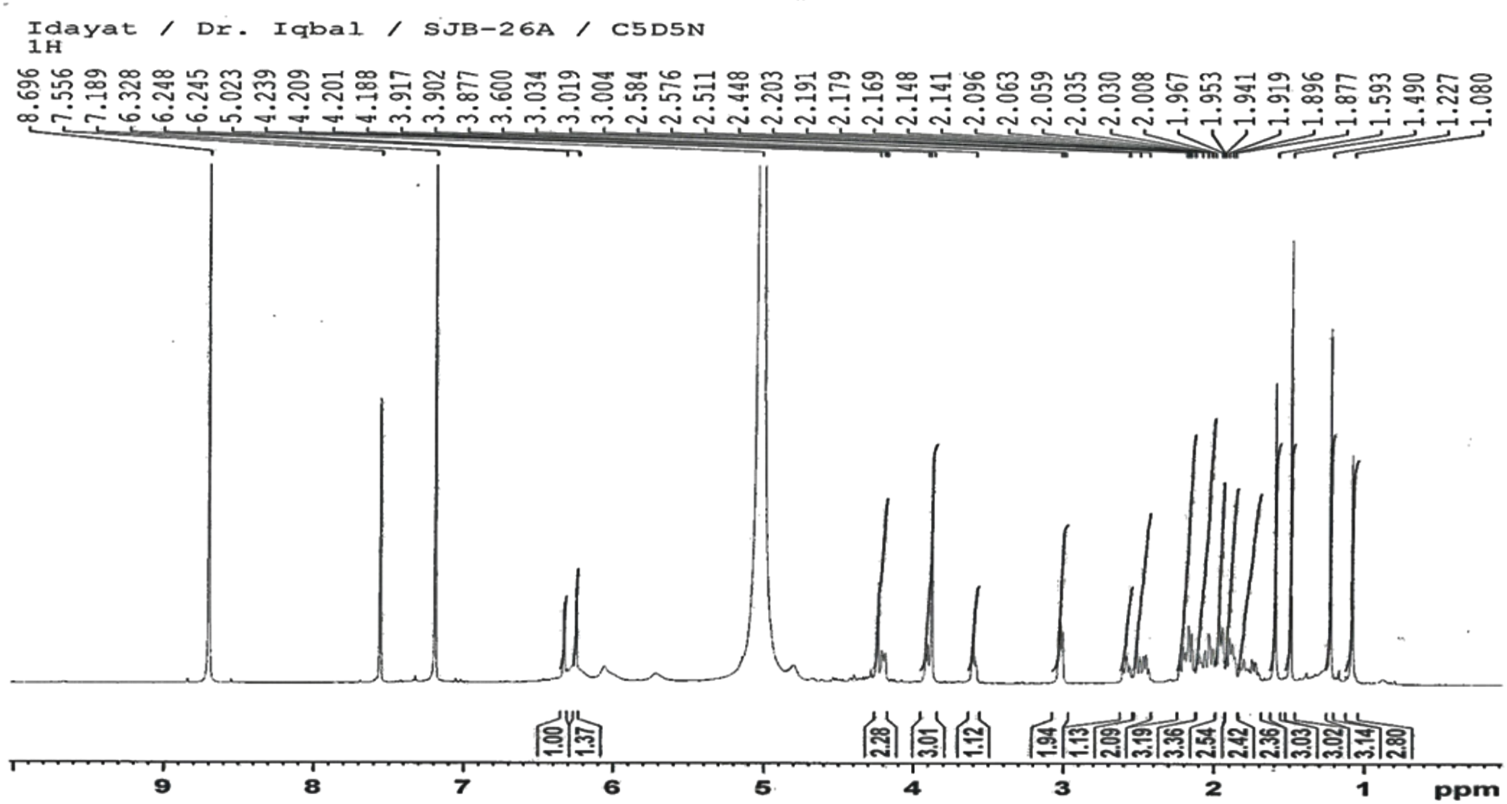

AVANCE NEO 600 MHz
Cryoprobe
Lab # 108

Current Data Parameters	
NAME	Jan07-19
EXPNO	6
PROCNO	1
F2 - Acquisition Parameters	
Date_	20190107
Time	14.35 h
INSTRUM	Avance NEO 600MHz
PROBHD	Z44896_0021 (C
PULPROG	zg30
TD	32768
SOLVENT	Pyr
NS	16
DS	0
SWH	14648.438 Hz
FIDRES	0.894070 Hz
AQ	1.1184810 sec
RG	10.6534
DW	34.133 usec
DE	15.36 usec
TE	298.0 K
D1	1.50000000 sec
TD0	1
SFO1	600.0342602 MHz
NUC1	1H
P0	3.33 usec
P1	10.00 usec
PLW1	4.25000000 W
F2 - Processing parameters	
SI	16384
SF	600.0299996 MHz
WDW	EM
SSB	0
LB	0.30 Hz
GB	0
PC	1.00

Appendix V (e)

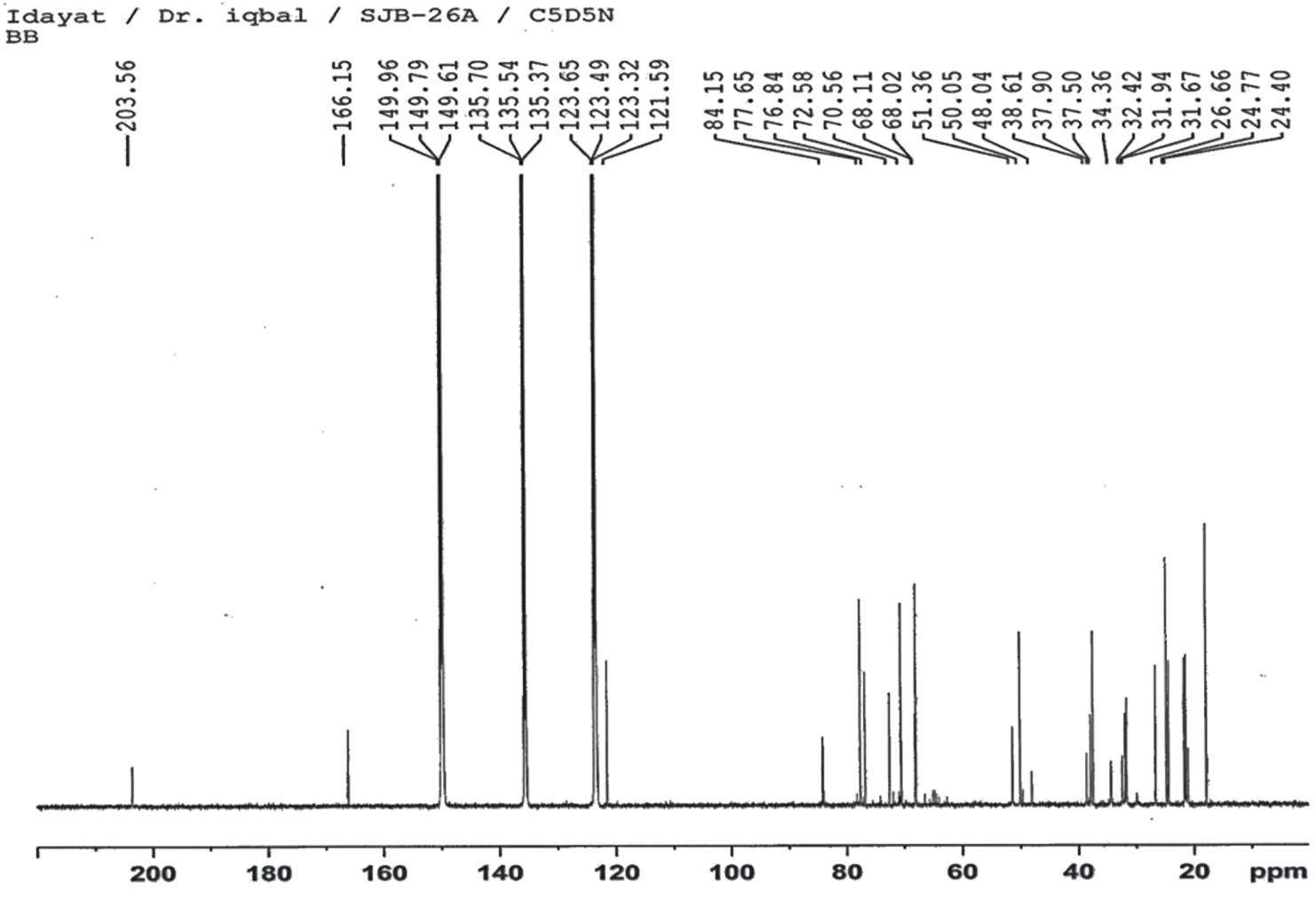

BRUKER

Current Data Parameters
NAME Jan21-19
EXPNO 7
PROCNO 1

F2 - Acquisition Parameters
Date_ 20190122
Time 10.20 h
INSTRUM AVNeo_600
PROBHD Z117768_0039 (
PULPROG zgpg
TD 32768
SOLVENT Pyr
NS 3454
DS 4
SWH 35714.285 Hz
FIDRES 2.179827 Hz
AQ 0.4587520 sec
RG 101
DW 14.000 usec
DE 18.00 usec
TE 298.0 K
D1 1.50000000 sec
D11 0.03000000 sec
TD0 16
SFO1 150.9553694 MHz
NUC1 13C
P1 12.00 usec
PLW1 107.76000214 W
SFO2 600.2724011 MHz
NUC2 1H
CPDPRG[2 waltz65
PCPD2 70.00 usec
PLW2 9.53950024 W
PLW12 0.12460000 W
PLW13 0.06267200 W

F2 - Processing parameters
SI 16384
SF 150.9379843 MHz
WDW EM
SSB 0
LB 1.00 Hz
GB 0
PC 0.90

Appendix V (f)

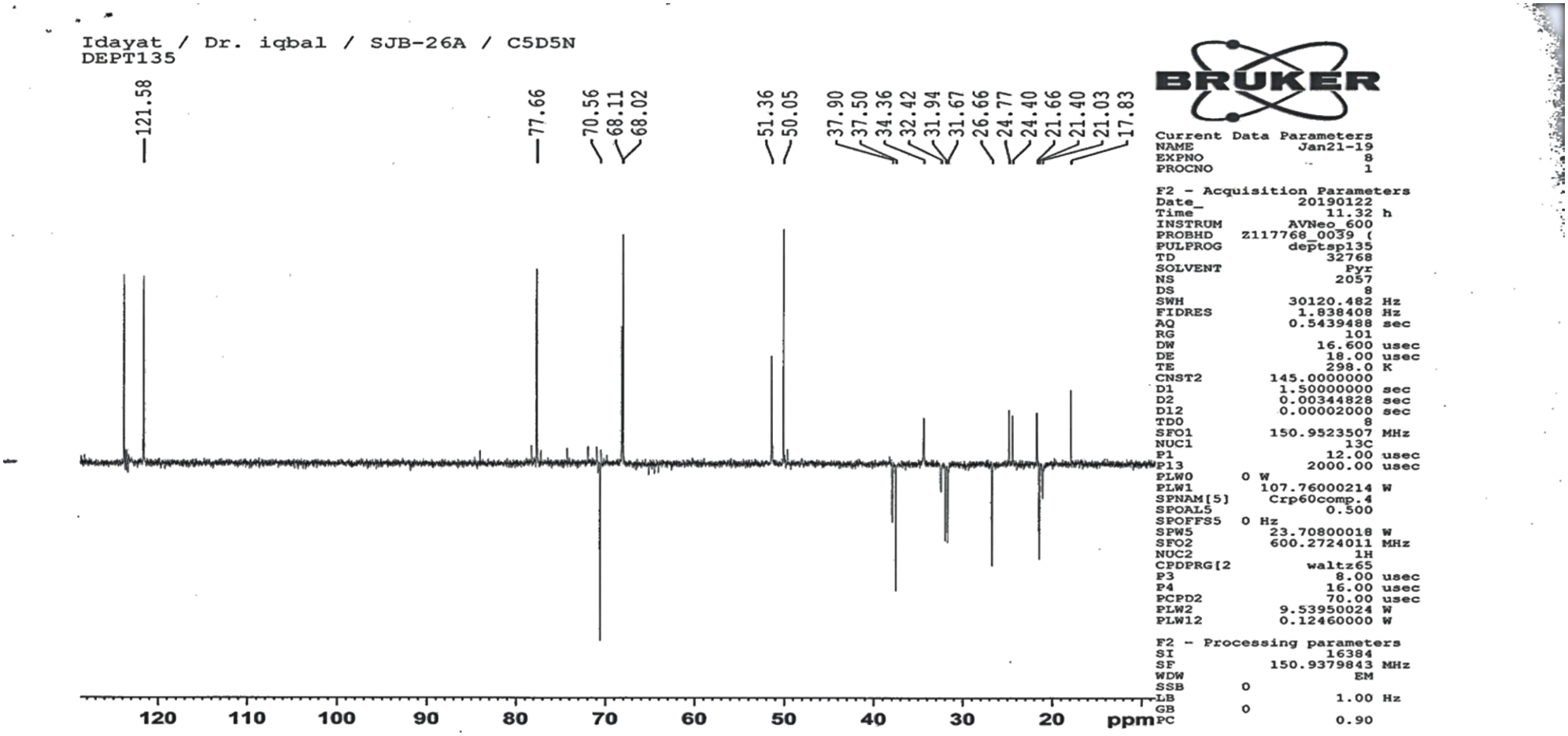
Idayat / Dr. iqbal / SJB-26A / C5D5N
DEPT135
121.58
77.66
70.56
68.11
68.02
51.36
50.05
37.90
37.50
34.36
32.42
31.94
31.67
26.66
24.77
24.40
21.66
21.40
21.03
17.83
120
110
100
90
80
70
60
50
40
30
20
ppm
BRUKER
Current Data Parameters
NAME Jan21-19
EXPNO 8
PROCNO 1
F2 - Acquisition Parameters
Date_ 20190122
Time 11.32 h
INSTRUM AVNeo_600
PROBHD Z117768_0039 (
PULPROG deptsp135
TD 32768
SOLVENT Pyr
NS 2057
DS 8
SWH 30120.482 Hz
FIDRES 1.838408 Hz
AQ 0.5439488 sec
RG 101
DW 16.600 usec
DE 18.00 usec
TE 298.0 K
CNST2 145.0000000
D1 1.50000000 sec
D2 0.00344828 sec
D12 0.00002000 sec
TD0 8
SFO1 150.9523507 MHz
NUC1 13C
P1 12.00 usec
P13 2000.00 usec
PLW0 0 W
PLW1 107.76000214 W
SPNAM[5] Crp60comp.4
SPOAL5 0.500
SPOFFS5 0 Hz
SPW5 23.70800018 W
SFO2 600.2724011 MHz
NUC2 1H
CPDPRG[2 waltz65
P3 8.00 usec
P4 16.00 usec
PCPD2 70.00 usec
PLW2 9.53950024 W
PLW12 0.12460000 W
F2 - Processing parameters
SI 16384
SF 150.9379843 MHz
WDW EM
SSB 0
LB 1.00 Hz
GB 0
PC 0.90

Appendix V (g)

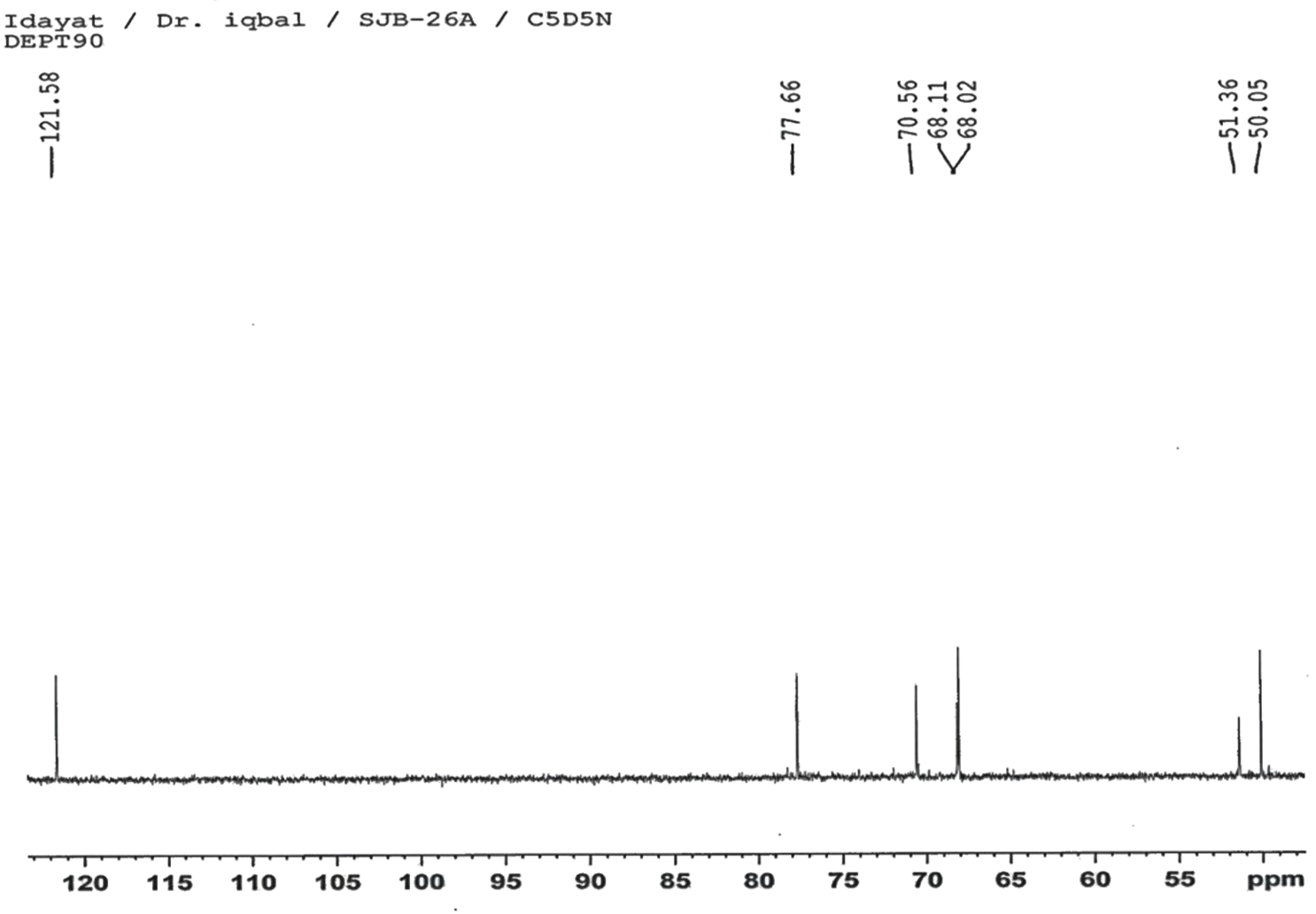

BRUKER

Current Data Parameters
NAME Jan21-19
EXPNO 9
PROCNO 1

F2 - Acquisition Parameters
Date_ 20190122
Time 11.54 h
INSTRUM AVNeo_600
PROBHD Z117768_0039 (
PULPROG deptsp90
TD 32768
SOLVENT Pyr
NS 500
DS 8
SWH 30120.482 Hz
FIDRES 1.838408 Hz
AQ 0.5439488 sec
RG 101
DW 16.600 usec
DE 18.00 usec
TE 298.0 K
CNST2 145.0000000
D1 2.00000000 sec
D2 0.00344828 sec
D12 0.00002000 sec
TD0 4
SFO1 150.9523507 MHz
NUC1 13C
P1 12.00 usec
P13 2000.00 usec
PLW0 0 W
PLW1 107.76000214 W
SPNAM[5] Crp60comp.4
SPOAL5 0.500
SPOFFS5 0 Hz
SPW5 23.70800018 W
SFO2 600.2724011 MHz
NUC2 1H
CPDPRG[2 waltz65
P3 8.00 usec
P4 16.00 usec
PCPD2 70.00 usec
PLW2 9.53950024 W
PLW12 0.12460000 W

F2 - Processing parameters
SI 16384
SF 150.9379843 MHz
WDW EM
SSB 0
LB 1.00 Hz
GB 0
PC 1.00

Appendix V (h)

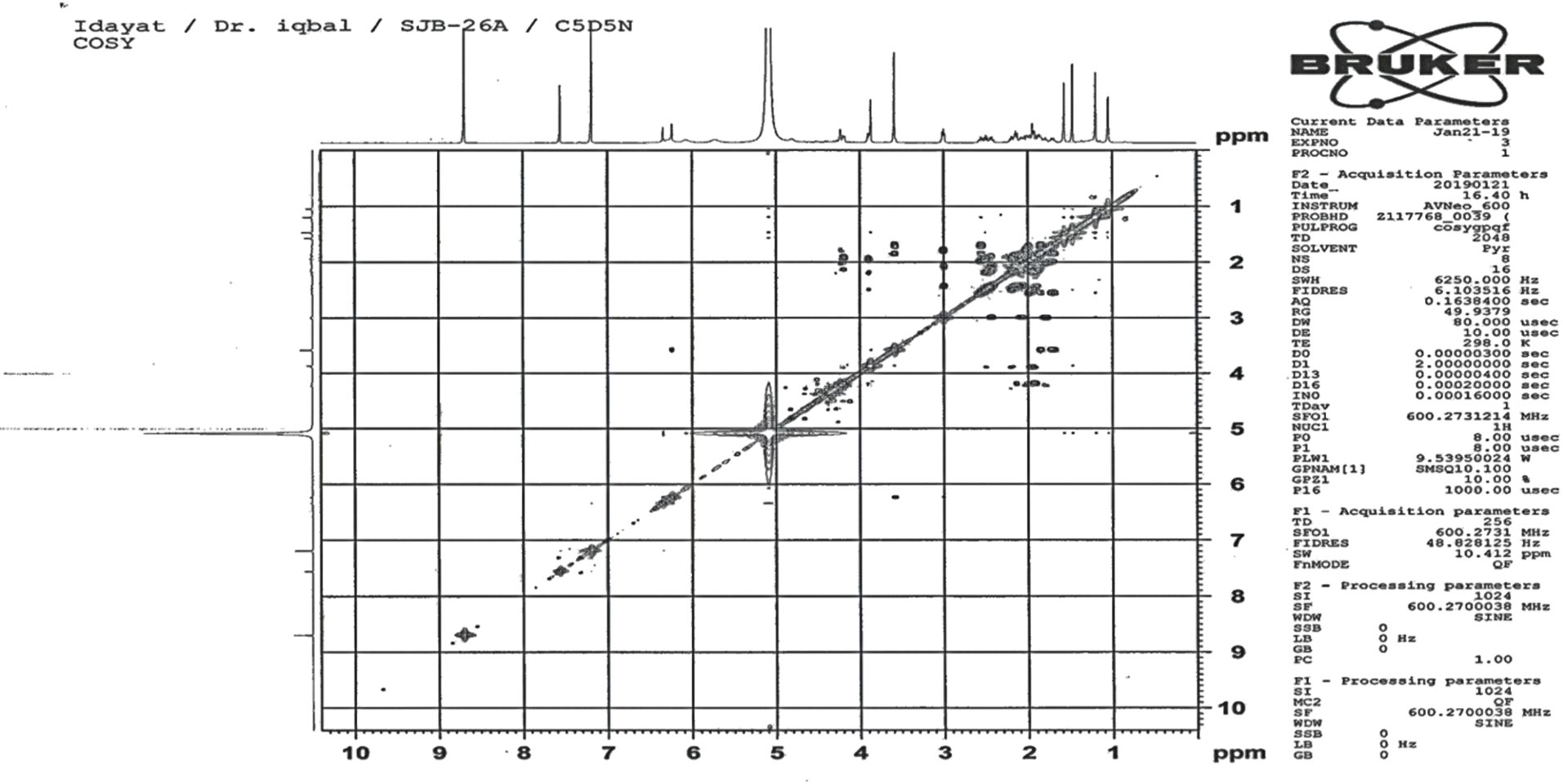

BRUKER

```
Current Data Parameters
NAME                  Jan21-19
EXPNO                        3
PROCNO                       1

F2 - Acquisition Parameters
Date_                 20190121
Time                     16.40 h
INSTRUM                AVNeo_600
PROBHD    Z117768_0039 (
PULPROG                cosygpqf
TD                         2048
SOLVENT                     Pyr
NS                            8
DS                           16
SWH                    6250.000 Hz
FIDRES                 6.103516 Hz
AQ                     0.1638400 sec
RG                        49.9379
DW                       80.000 usec
DE                       10.00 usec
TE                       298.0 K
D0                     0.00000300 sec
D1                     2.00000000 sec
D13                    0.00000400 sec
D16                    0.00020000 sec
IN0                    0.00016000 sec
TDav                          1
SFO1                600.2731214 MHz
NUC1                        1H
P0                       8.00 usec
P1                       8.00 usec
PLW1                9.53950024 W
GPNAM[1]            SMSQ10.100
GPZ1                    10.00 %
P16                   1000.00 usec

F1 - Acquisition parameters
TD                          256
SFO1                 600.2731 MHz
FIDRES                48.828125 Hz
SW                       10.412 ppm
FnMODE                       QF

F2 - Processing parameters
SI                          1024
SF                 600.2700038 MHz
WDW                       SINE
SSB          0
LB           0 Hz
GB           0
PC                        1.00

F1 - Processing parameters
SI                          1024
MC2                          QF
SF                 600.2700038 MHz
WDW                       SINE
SSB          0
LB           0 Hz
GB           0
```

Appendix V (i)

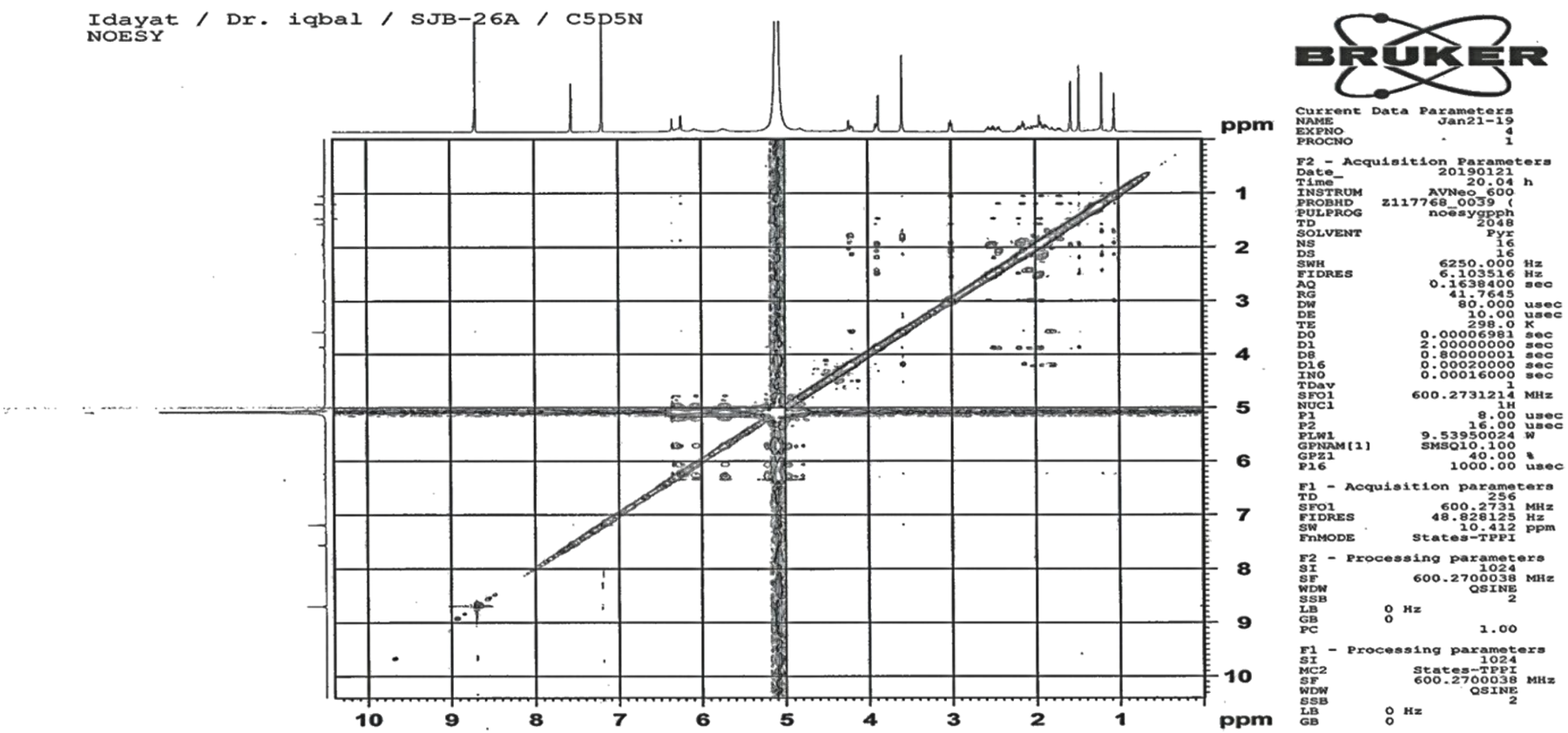

BRUKER

```
Current Data Parameters
NAME                  Jan21-19
EXPNO                        4
PROCNO                       1

F2 - Acquisition Parameters
Date_              20190121
Time                   20.04 h
INSTRUM            AVNeo_600
PROBHD     Z117768_0039 (
PULPROG            noesygpph
TD                      2048
SOLVENT                  Pyr
NS                        16
DS                        16
SWH                 6250.000 Hz
FIDRES              6.103516 Hz
AQ                  0.1638400 sec
RG                   41.7645
DW                    80.000 usec
DE                    10.00 usec
TE                    298.0 K
D0                  0.00006981 sec
D1                  2.00000000 sec
D8                  0.80000001 sec
D16                 0.00020000 sec
IN0                 0.00016000 sec
TDav                         1
SFO1               600.2731214 MHz
NUC1                      1H
P1                     8.00 usec
P2                    16.00 usec
PLW1               9.53950024 W
GPNAM[1]           SMSQ10.100
GPZ1                  40.00 %
P16                 1000.00 usec

F1 - Acquisition parameters
TD                       256
SFO1               600.2731 MHz
FIDRES             48.828125 Hz
SW                    10.412 ppm
FnMODE          States-TPPI

F2 - Processing parameters
SI                      1024
SF                 600.2700038 MHz
WDW                     QSINE
SSB                         2
LB          0 Hz
GB          0
PC                      1.00

F1 - Processing parameters
SI                      1024
MC2             States-TPPI
SF                 600.2700038 MHz
WDW                     QSINE
SSB                         2
LB          0 Hz
GB          0
```

Appendix V (j)

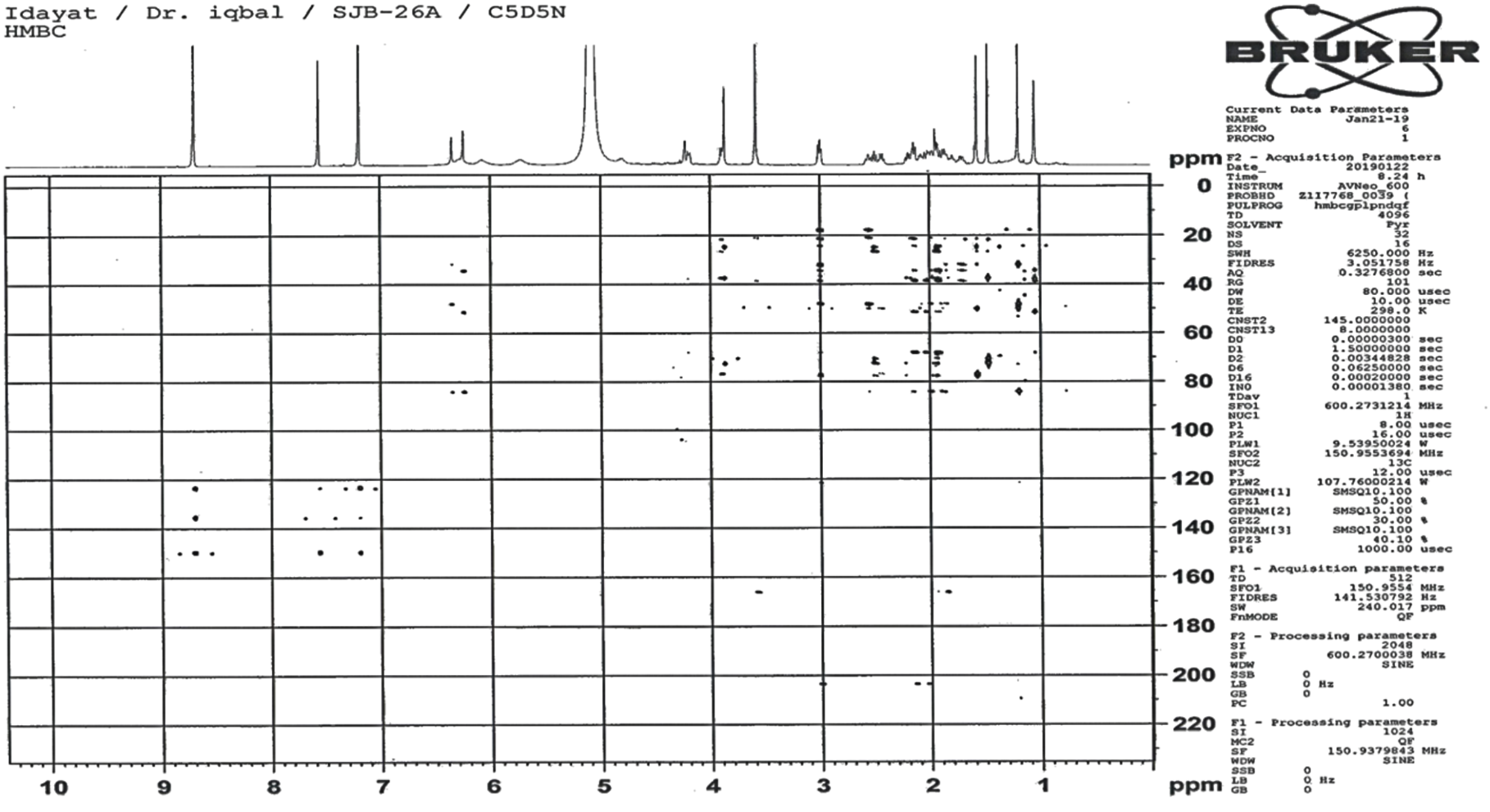
Idayat / Dr. iqbal / SJB-26A / C5D5N
HMBC
BRUKER
Current Data Parameters
NAME Jan21-19
EXPNO 6
PROCNO 1
F2 - Acquisition Parameters
Date_ 20190122
Time 8.24 h
INSTRUM AVNeo_600
PROBHD Z117768_0039 (
PULPROG hmbcgplpndqf
TD 4096
SOLVENT Pyr
NS 32
DS 16
SWH 6250.000 Hz
FIDRES 3.051758 Hz
AQ 0.3276800 sec
RG 101
DW 80.000 usec
DE 10.00 usec
TE 298.0 K
CNST2 145.0000000
CNST13 8.0000000
D0 0.00000300 sec
D1 1.50000000 sec
D2 0.00344828 sec
D6 0.06250000 sec
D16 0.00020000 sec
IN0 0.00001380 sec
TDav 1
SFO1 600.2731214 MHz
NUC1 1H
P1 8.00 usec
P2 16.00 usec
PLW1 9.53950024 W
SFO2 150.9553694 MHz
NUC2 13C
P3 12.00 usec
PLW2 107.76000214 W
GPNAM[1] SMSQ10.100
GPZ1 50.00 %
GPNAM[2] SMSQ10.100
GPZ2 30.00 %
GPNAM[3] SMSQ10.100
GPZ3 40.10 %
P16 1000.00 usec
F1 - Acquisition parameters
TD 512
SFO1 150.9554 MHz
FIDRES 141.530792 Hz
SW 240.017 ppm
FnMODE QF
F2 - Processing parameters
SI 2048
SF 600.2700038 MHz
WDW SINE
SSB 0
LB 0 Hz
GB 0
PC 1.00
F1 - Processing parameters
SI 1024
MC2 QF
SF 150.9379843 MHz
WDW SINE
SSB 0
LB 0 Hz
GB 0
ppm
0
20
40
60
80
100
120
140
160
180
200
220
10
9
8
7
6
5
4
3
2
1
ppm

Appendix V (k)

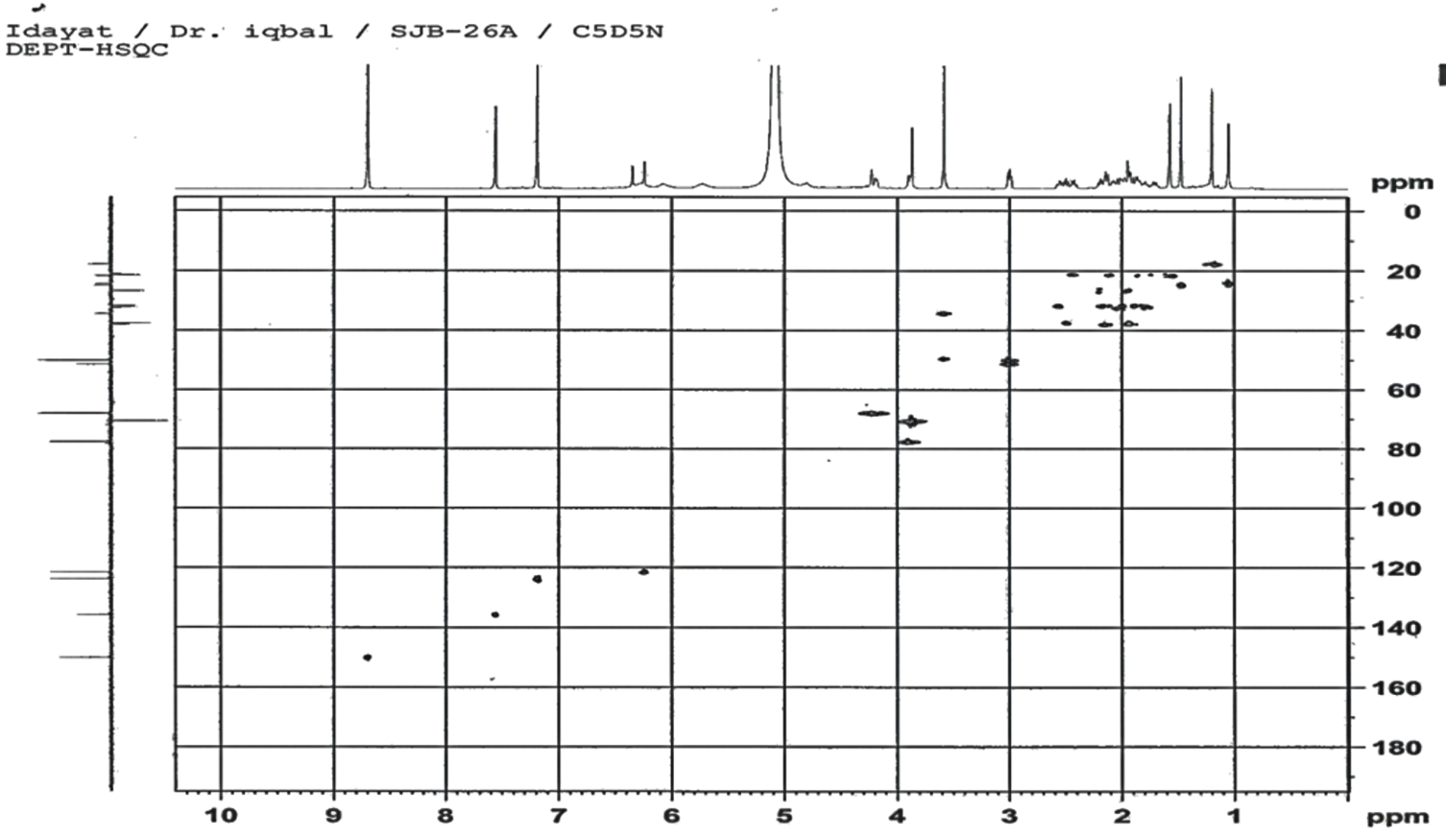

BRUKER

```
Current Data Parameters
NAME                  Jan21-19
EXPNO                        5
PROCNO                       1

F2 - Acquisition Parameters
Date_              20190121
Time_                23.43 h
INSTRUM            AVNeo_600
PROBHD     Z117768_0039 (
PULPROG            hsqcedetgp
TD                       1024
SOLVENT                   Pyr
NS                         32
DS                         16
SWH                  6250.000 Hz
FIDRES              12.207031 Hz
AQ                   0.0819200 sec
RG                         101
DW                    80.000 usec
DE                    10.00 usec
TE                    298.0 K
CNST2              145.00000000
D0                   0.00000300 sec
D1                   1.50000000 sec
D4                   0.00172414 sec
D11                  0.03000000 sec
D13                  0.00000400 sec
D16                  0.00020000 sec
D21                  0.00344828 sec
IN0                  0.00001660 sec
TDav                         1
ZGOPTNS
SFO1                600.2731214 MHz
NUC1                        1H
P1                       8.00 usec
P2                      16.00 usec
P28                      0.10 usec
PLW1                9.53950024 W
SFO2                150.9523507 MHz
NUC2                       13C
CPDPRG[2                 garp
P3                      12.00 usec
P4                      24.00 usec
PCPD2                   60.00 usec
PLW2               107.76000214 W
PLW12                4.31029987 W
GPNAM[1]           SMSQ10.100
GPZ1                    80.00 %
GPNAM[2]           SMSQ10.100
GPZ2                    20.10 %
P16                  1000.00 usec

F1 - Acquisition parameters
TD                        256
SFO1                150.9524 MHz
FIDRES              235.316269 Hz
SW                  199.536 ppm
FnMODE     Echo-Antiecho

F2 - Processing parameters
SI                       1024
SF                600.2700038 MHz
WDW                      QSINE
SSB                         2
LB          0 Hz
GB          0
PC                       1.00

F1 - Processing parameters
SI                       1024
MC2          echo-antiecho
SF                150.9379843 MHz
WDW                      QSINE
SSB                         2
LB          0 Hz
GB          0
```

Appendix VI (a)

EI-MS, 1D and 2D NMR spectra of SJH-28A

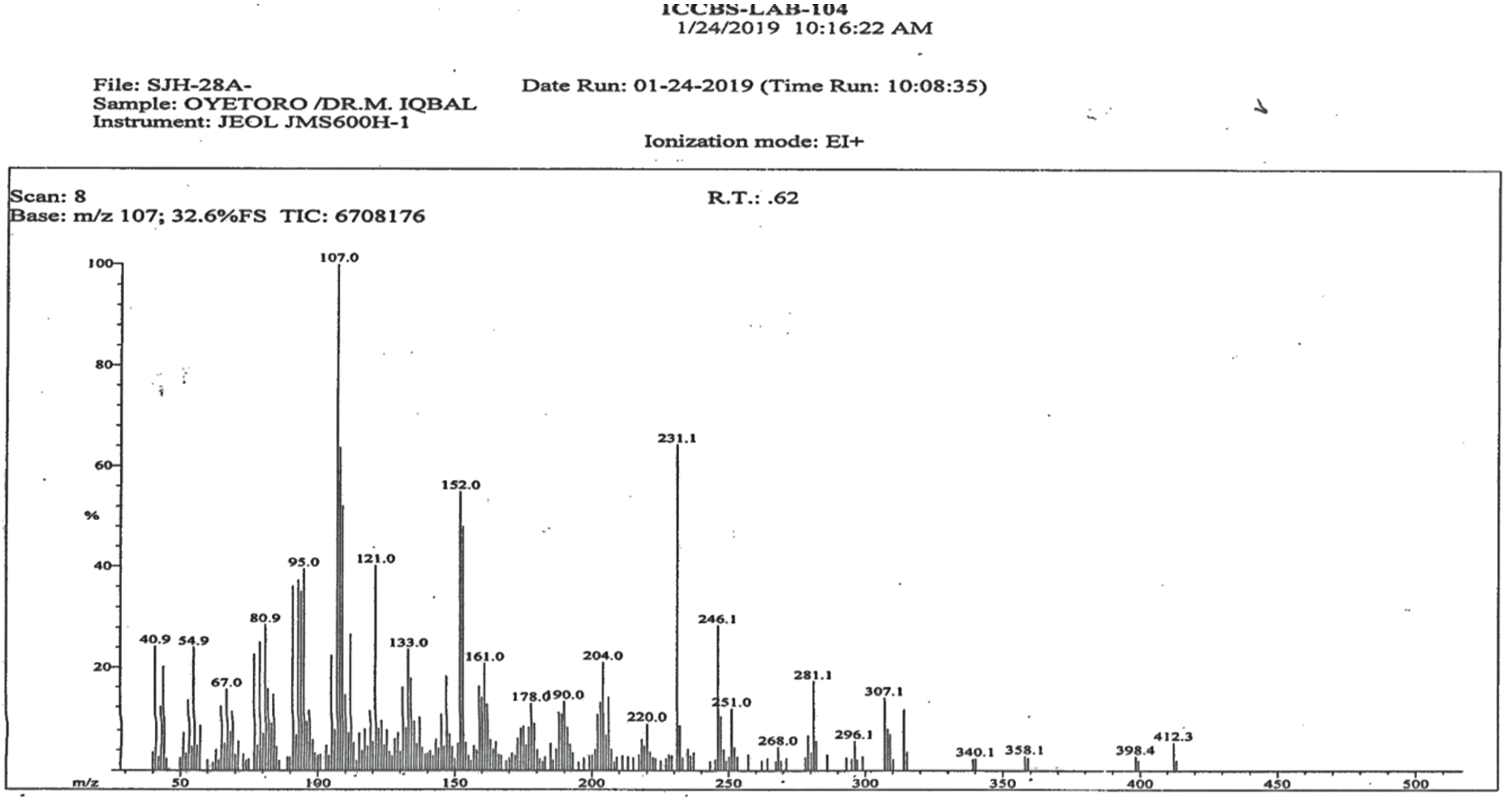

Appendix VI (b)

1/24/2019 10:17:13 AM

File: SJH-28A- Date Run: 01-24-2019 (Time Run: 10:08:35)
Sample: OYETORO /DR.M. IQBAL
Instrument: JEOL JMS600H-1

Ionization mode: EI+

Scan: 8 R.T.: .62
Base: m/z 107; 32.6%FS TIC: 6708176

Threshold: 2.6% of Base Displayed TIC: 6708176

Mass	%Base	Mass	%Base	Mass	%Base	Mass	%Base	Mass	%Base
39.9180	3.6	81.9547	15.7	112.9465	5.5	140.0303	3.4	171.0277	3.4
40.9354	24.3	82.9681	9.4	114.9714	7.5	141.0204	3.9	172.0175	3.0
41.9334	2.7	83.9421	14.6	115.9772	4.0	141.9846	2.9	173.0101	6.4
42.9108	12.1	84.9445	4.7	116.9873	8.2	143.0401	6.2	174.0376	8.4
43.8832	20.2	88.9424	2.7	117.9750	4.8	144.0108	4.4	175.0359	8.9
50.9277	7.6	90.9633	36.1	118.9935	11.5	145.0139	10.9	176.0047	5.1
51.9494	3.4	91.9583	7.0	119.9894	5.7	146.0202	4.8	176.9761	8.6
52.9440	13.4	92.9825	37.4	120.9894	40.3	147.0295	18.3	177.9827	12.9
53.9657	4.8	93.9641	35.1	121.9662	8.3	148.0719	7.2	178.9919	9.3
54.9409	24.1	94.9507	39.6	123.0289	9.9	148.9978	4.7	180.0367	4.1
55.9429	5.0	95.9663	9.7	123.9864	5.1	151.0381	5.3	183.0241	2.7
56.9910	8.9	96.9624	11.6	124.9750	8.1	152.0328	54.9	185.0072	5.4
62.9199	4.2	97.9875	6.1	125.9952	3.7	153.0305	48.0	187.0009	4.2
64.9457	12.3	98.9682	3.5	126.9639	2.9	154.0312	5.5	188.0018	11.3
65.9502	5.4	99.9777	3.0	127.9642	6.3	155.0653	2.9	188.9719	11.0
66.9623	15.7	100.9670	3.2	128.9962	7.6	157.0515	4.9	189.9780	13.3
67.9411	7.8	102.9850	5.0	130.0042	3.7	158.0338	4.0	191.0205	8.5
68.9476	11.4	103.9635	3.0	130.9879	16.1	159.0189	16.3	191.9983	5.3
69.9615	3.2	104.9718	22.5	131.9752	8.5	160.0069	14.1	193.0125	3.6
70.9827	5.8	105.9848	8.2	132.9944	23.8	161.0288	21.0	199.0158	3.0
72.9410	3.2	107.0025	100.0	134.0173	17.9	162.0226	12.7	200.0827	3.0
76.9364	22.7	107.9994	63.7	135.0155	9.7	162.9880	6.1	201.0833	4.2
77.9407	5.1	109.0007	52.1	136.0172	5.3	164.0186	4.2	202.0517	11.0
78.9515	25.2	109.9808	14.5	136.9936	10.5	165.0207	5.7	203.0571	13.1
79.9686	7.4	110.9910	7.5	138.0023	4.5	166.1199	3.1	204.0302	21.3
80.9475	28.6	111.9275	26.8	139.0435	3.2	167.0332	3.0	205.0055	7.0

Appendix VI (c)

ICCBS-LAB-104
1/24/2019 10:17:13 AM

File: SJH-28A-
Sample: OYETORO /DR.M. IQBAL
Instrument: JEOL JMS600H-1

Date Run: 01-24-2019 (Time Run: 10:08:35)

Ionization mode: EI+

Scan: 8
R.T.: .62 Base: m/z 107; 32.6%FS TIC: 6708176

(Continued)

Threshold: 2.6% of Base

Displayed TIC: 6708176

Mass	%Base	Mass	%Base	Mass	%Base	Mass	%Base	Mass	%Base
206.0173	14.1	221.0481	3.7	247.0687	10.6	280.0971	3.5	314.0986	11.9
207.0305	4.2	228.0455	3.2	248.0591	4.1	281.1061	17.4	315.0785	3.7
209.0618	2.6	229.0364	3.0	250.0840	2.7	282.0760	5.8	358.0927	2.9
211.0651	2.9	231.0585	64.3	251.0419	11.9	286.0531	3.1	398.3855	2.8
213.0060	2.8	232.0164	8.9	252.0784	4.6	296.1175	5.8	412.3000	5.6
217.0938	3.1	235.0115	4.2	253.1555	2.7	299.1087	2.8		
218.0601	6.2	235.9767	2.9	257.1729	3.1	307.0716	14.1		
219.0291	4.8	237.0554	3.5	268.0439	4.6	308.0834	8.3		
220.0011	9.2	246.0804	28.6	279.0483	6.9	309.0964	7.1		

Appendix VI (d)

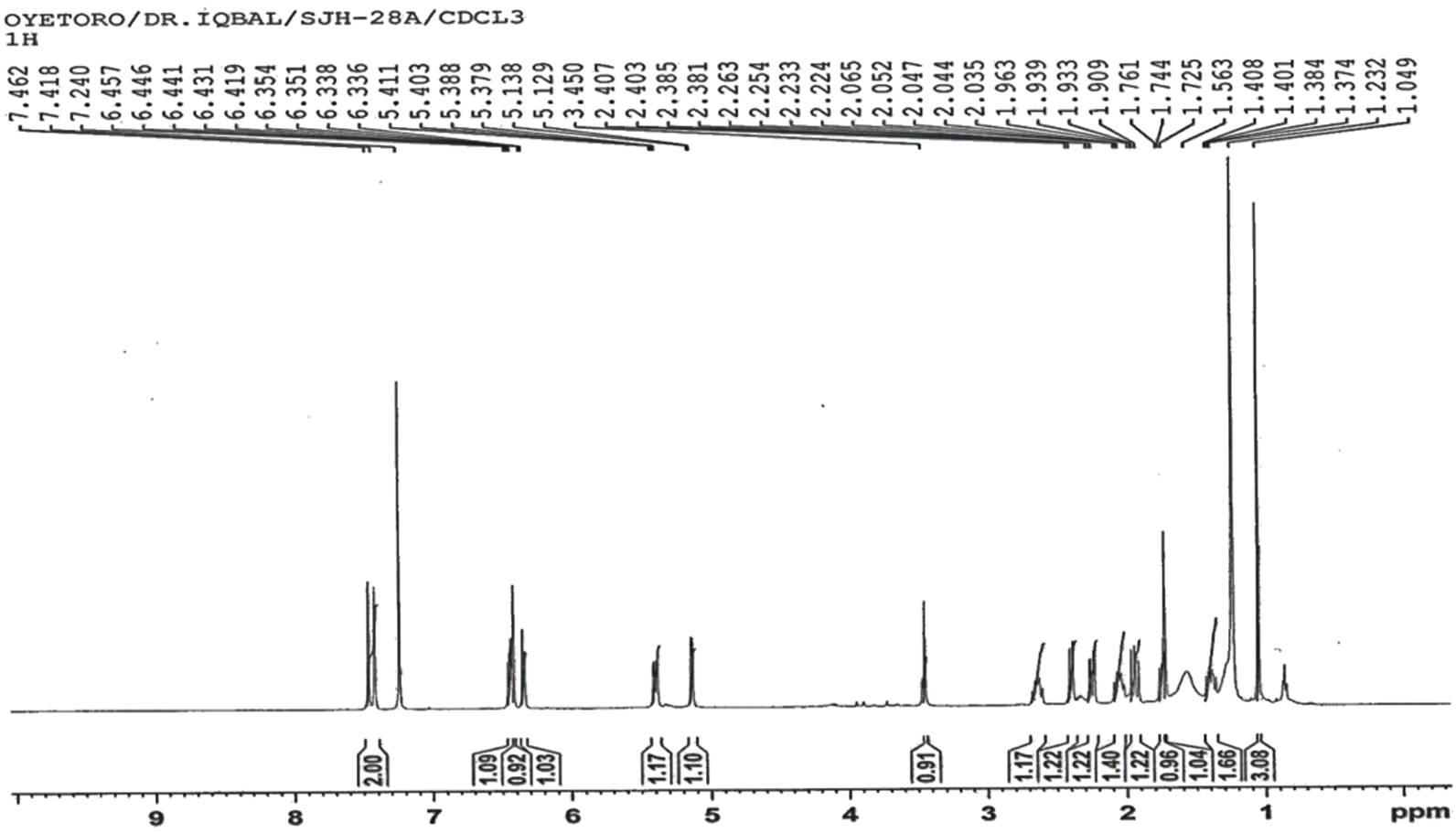

AVANCE NEO 500 MHz
Cryoprobe
Lab # 108

Current Data Parameters	
NAME	jan24-19
EXPNO	2
PROCNO	1
F2 - Acquisition Parameters	
Date_	20190124
Time	10.29 h
INSTRUM	Avance Neo 500
PROBHD	Z44862_0021 (C
PULPROG	zg30
TD	32768
SOLVENT	CDCl3
NS	64
DS	0
SWH	10000.000 Hz
FIDRES	0.610352 Hz
AQ	1.6384000 sec
RG	68.6646
DW	50.000 usec
DE	25.00 usec
TE	298.0 K
D1	1.50000000 sec
TD0	1
SFO1	500.3340026 MHz
NUC1	1H
P0	5.00 usec
P1	15.00 usec
PLW1	9.74149990 W
F2 - Processing parameters	
SI	32768
SF	500.3300222 MHz
WDW	EM
SSB	0
LB	0.30 Hz
GB	0
PC	1.00

Appendix VI (e)

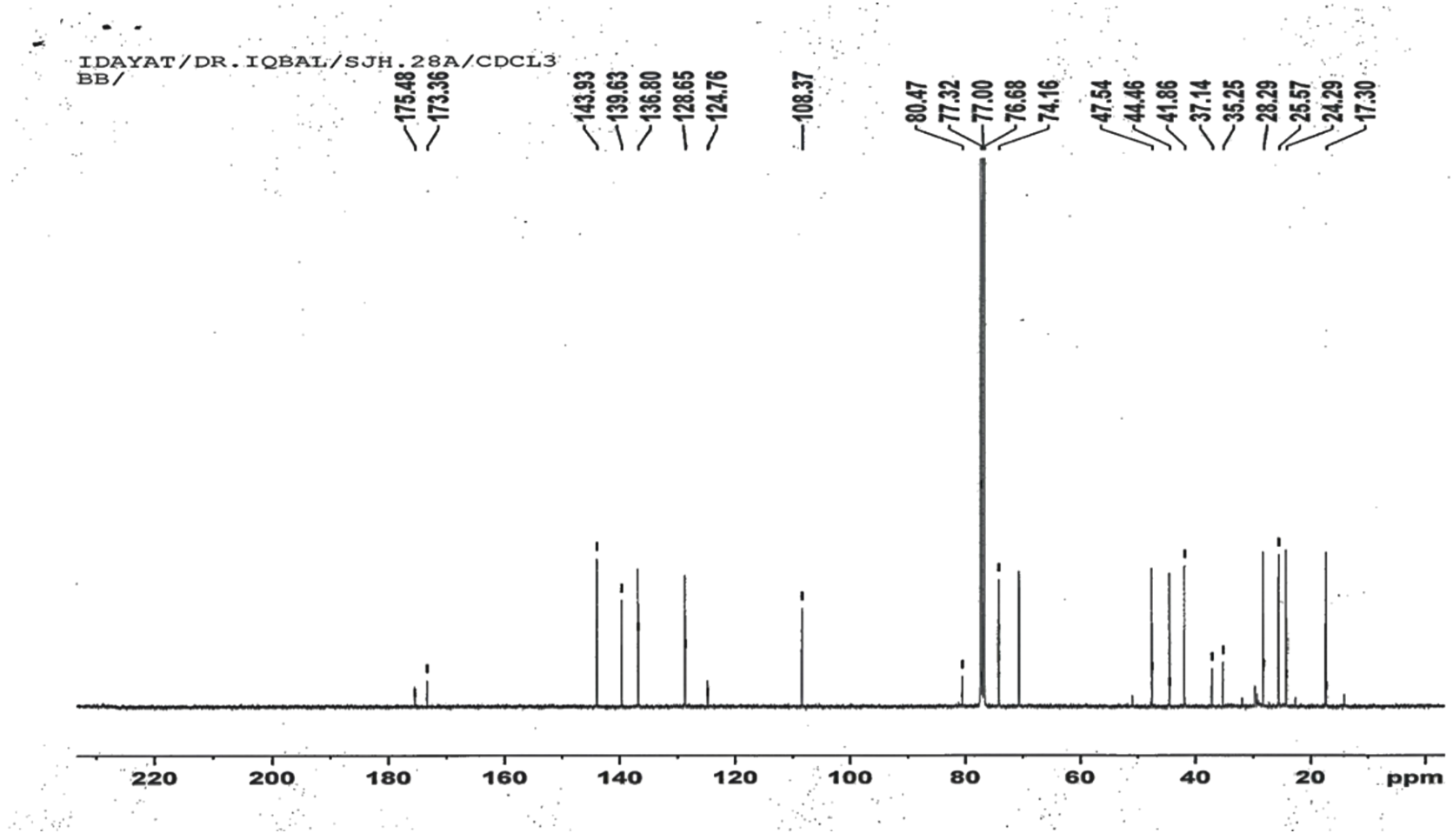

AVANCE NEO
400 MHz
LAB# 117

Current Data Parameters
NAME feb05-19
EXPNO 6
PROCNO 1

F2 - Acquisition Parameters
Date_ 20190207
Time 4.56 h
INSTRUM Avance NEO 400MHz
PROBHD Z114854_0013 (
PULPROG zgpg
TD 32768
SOLVENT CDCl3
NS 18432
DS 8
SWH 23809.523 Hz
FIDRES 1.453218 Hz
AQ 0.6881280 sec
RG 23.4375
DW 21.000 usec
DE 6.50 usec
TE 300.4 K
D1 2.00000000 sec
D11 0.03000000 sec
TD0 18
SFO1 100.6243395 MHz
NUC1 13C
P1 10.00 usec
PLW1 56.43000031 W
SFO2 400.1316005 MHz
NUC2 1H
CPDPRG[2 waltz65
PCPD2 90.00 usec
PLW2 13.21300030 W
PLW12 0.31972000 W
PLW13 0.16080999 W

F2 - Processing parameters
SI 32768
SF 100.6127700 MHz
WDW EM
SSB 0
LB 1.00 Hz
GB 0
PC 1.40

Appendix VI (f)

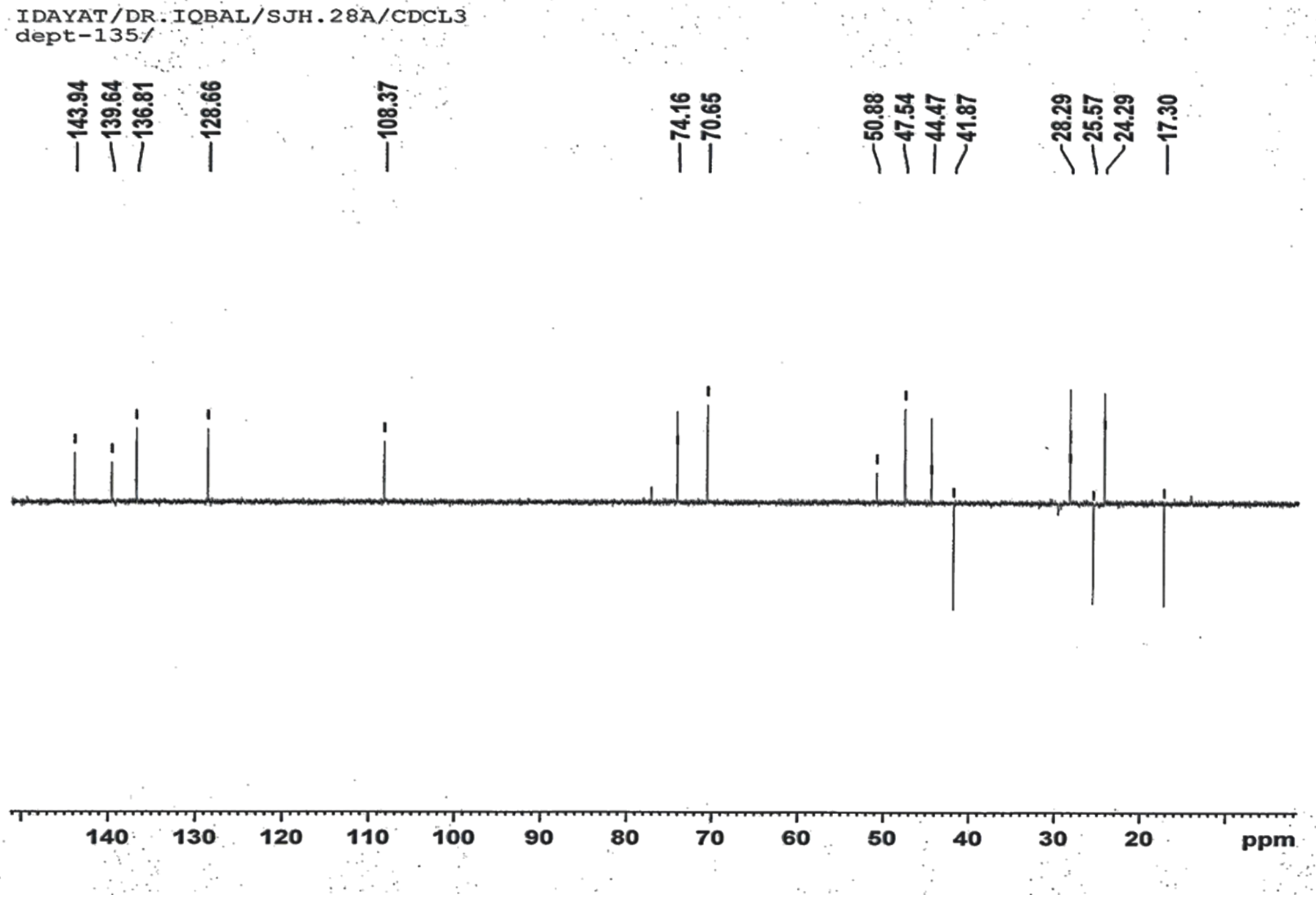

AVANCE NEO
400 MHz
LAB# 117

Current Data Parameters
NAME feb05-19
EXPNO 7
PROCNO 1

F2 - Acquisition Parameters
Date_ 20190207
Time 8.41 h
INSTRUM Avance NEO 400MHz
PROBHD Z114854_0013 (
PULPROG deptsp135
TD 32768
SOLVENT CDCl3
NS 5716
DS 8
SWH 20000.000 Hz
FIDRES 1.220703 Hz
AQ 0.8192000 sec
RG 27.0433
DW 25.000 usec
DE 6.50 usec
TE 300.0 K
CNST2 145.0000000
D1 1.50000000 sec
D2 0.00344828 sec
D12 0.00002000 sec
TD0 10
SFO1 100.6223267 MHz
NUC1 13C
P1 10.00 usec
P13 2000.00 usec
PLW0 0 W
PLW1 56.43000031 W
SPNAM[5] Crp60comp.4
SPOAL5 0.500
SPOFFS5 0 Hz
SPW5 8.62189960 W
SFO2 400.1316005 MHz
NUC2 1H
CPDPRG[2 waltz65
P3 14.00 usec
P4 28.00 usec
PCPD2 90.00 usec
PLW2 13.21300030 W
PLW12 0.31972000 W

F2 - Processing parameters
SI 32768
SF 100.6127695 MHz
WDW EM
SSB 0
LB 1.00 Hz
GB 0
PC 1.40

Appendix VI (g)

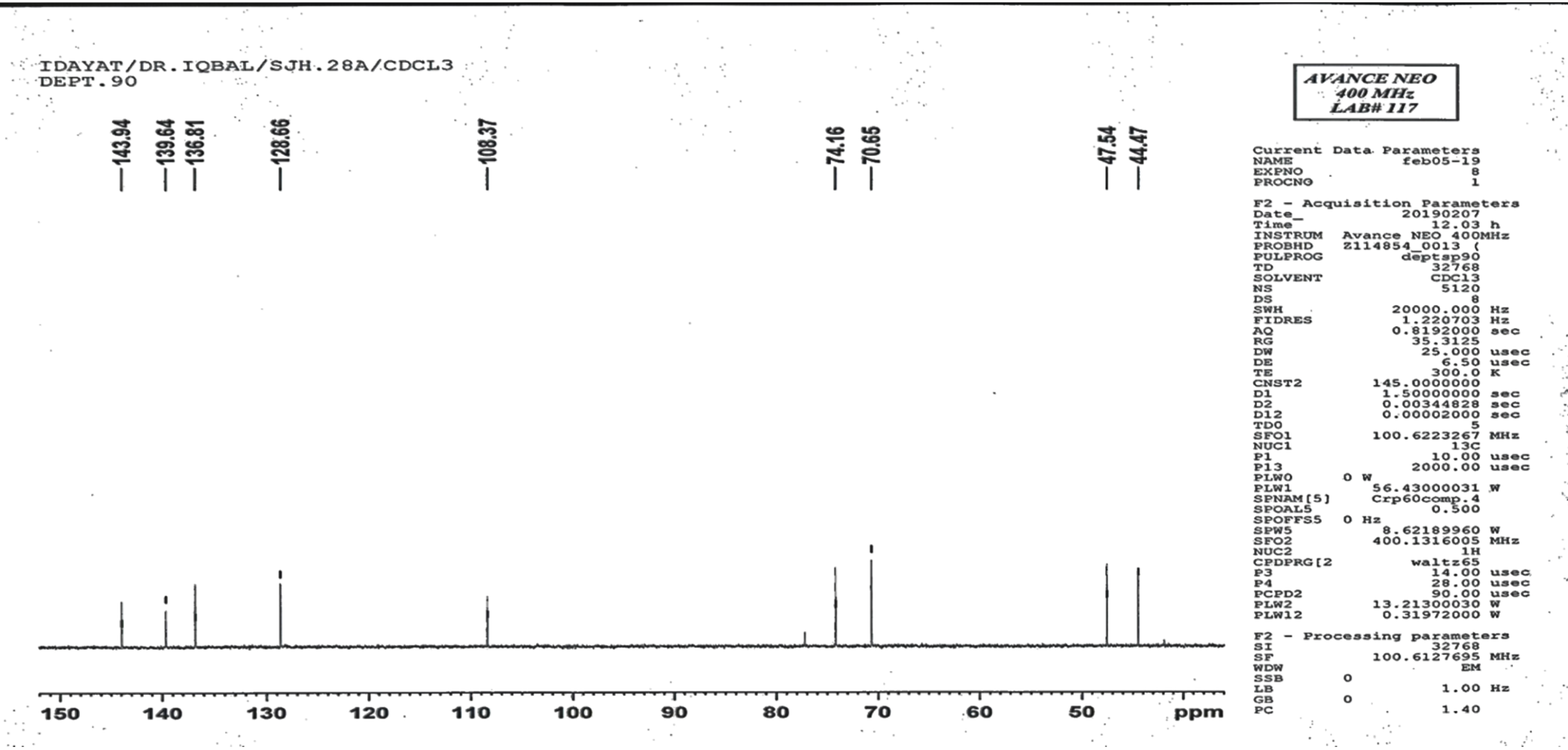

Appendix VI (h)

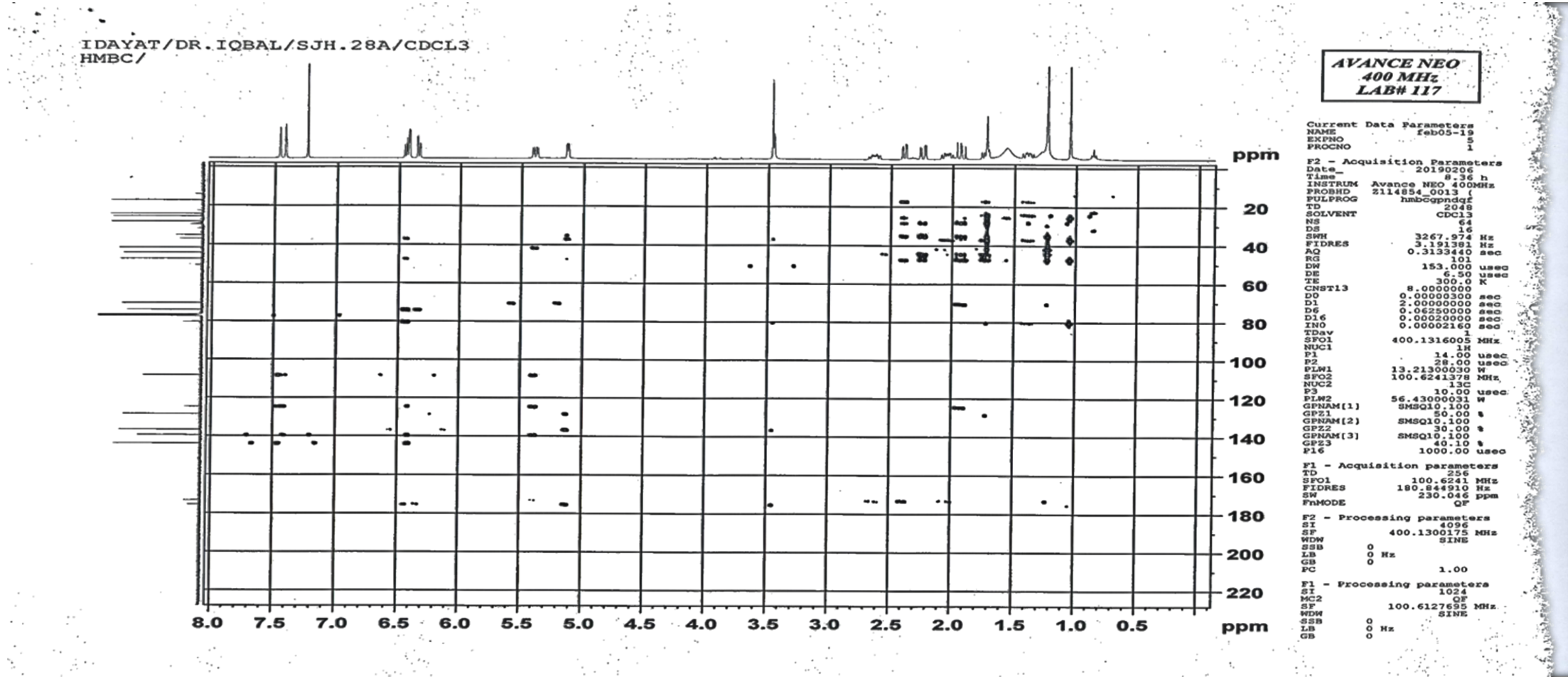

Appendix VI (i)

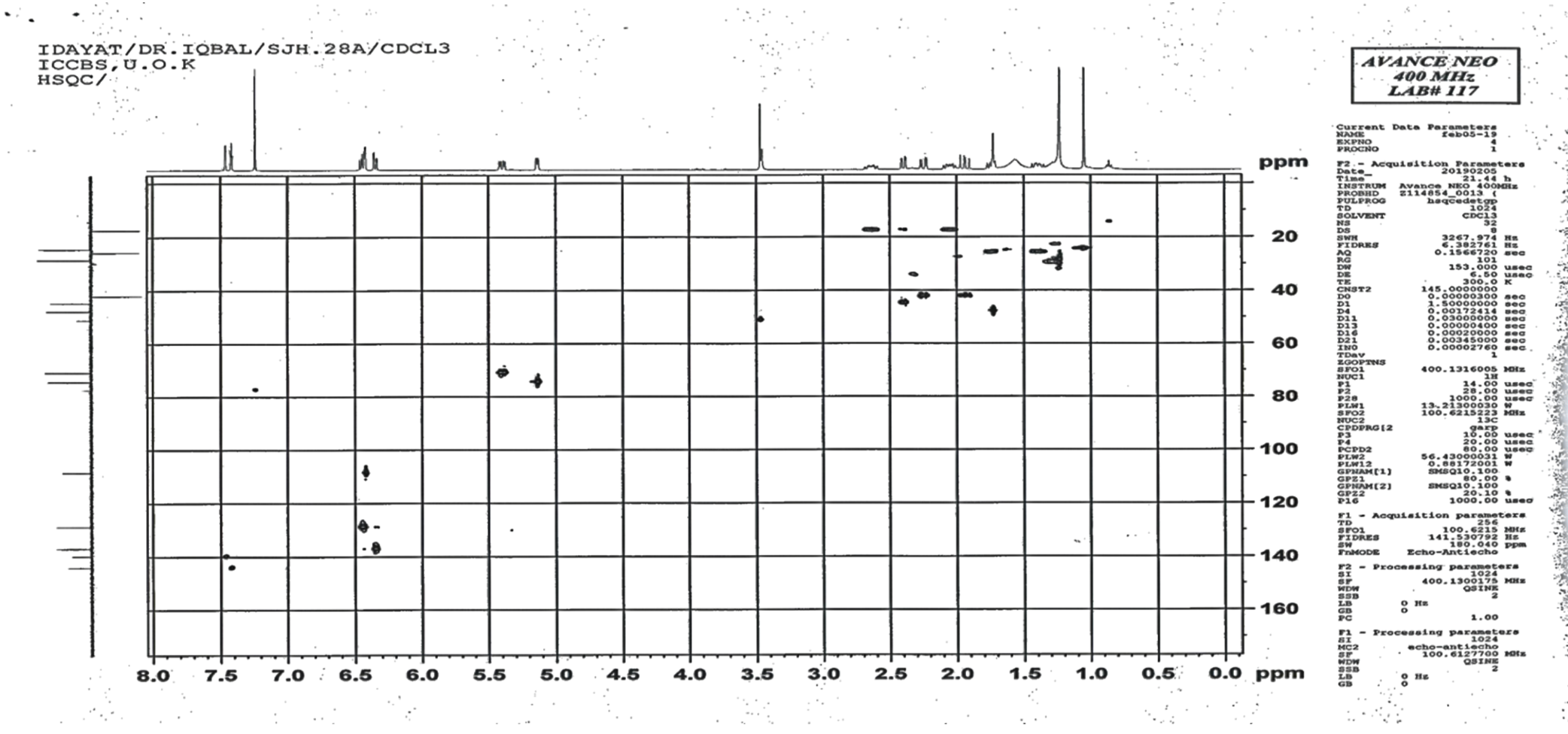

Appendix VI (j)

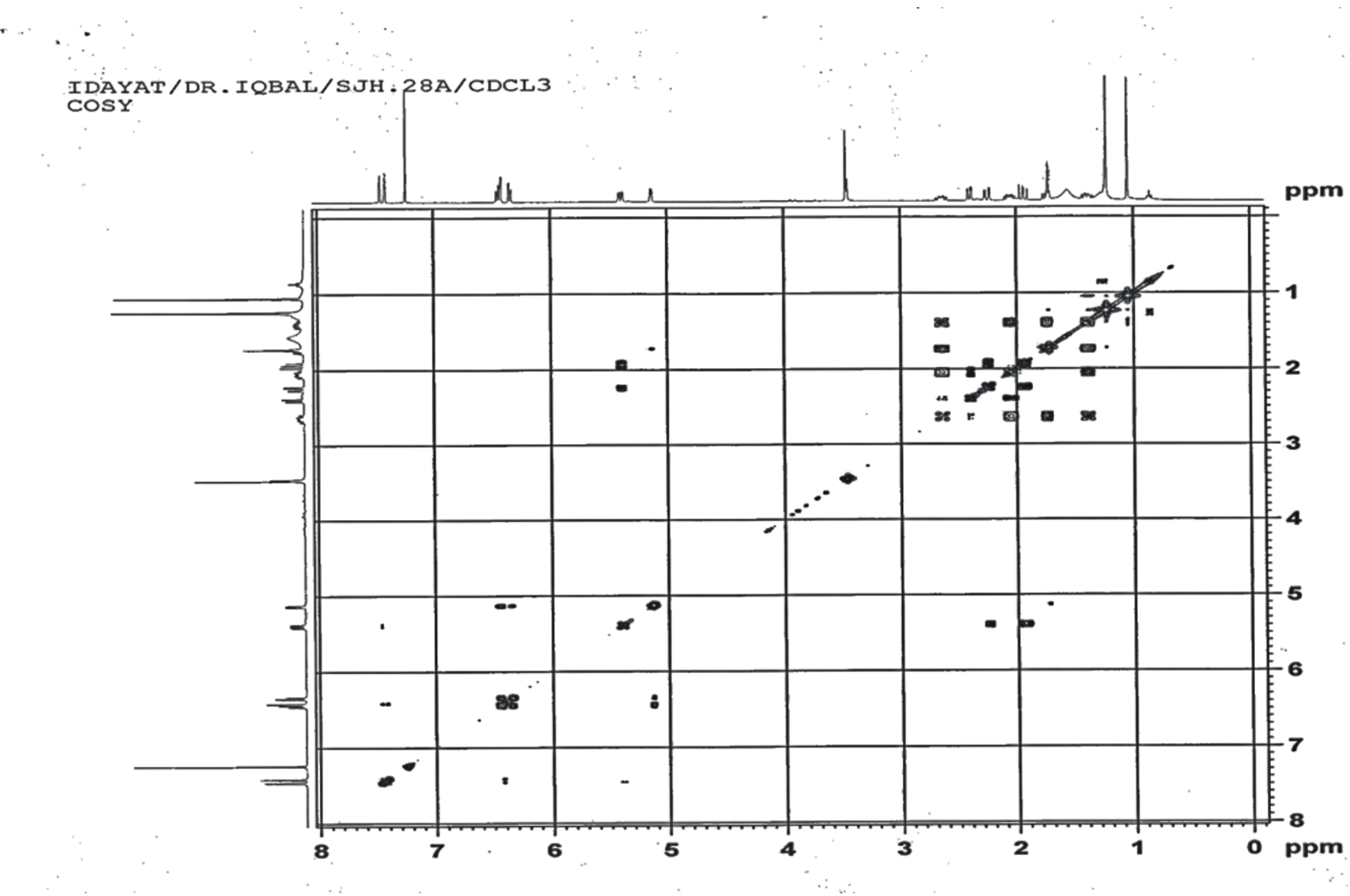

AVANCE NEO
400 MHz
LAB# 117

```
Current Data Parameters
NAME                  feb05-19
EXPNO                        2
PROCNO                       1

F2 - Acquisition Parameters
Date_                 20190205
Time                     14.20 h
INSTRUM   Avance NEO 400MHz
PROBHD    Z114854_0013 (
PULPROG              cosygpqf
TD                       2048
SOLVENT                 CDCl3
NS                           8
DS                           4
SWH                   3267.974 Hz
FIDRES                3.191381 Hz
AQ                    0.3133440 sec
RG                         101
DW                     153.000 usec
DE                       6.50 usec
TE                      300.0 K
D0                    0.00000300 sec
D1                    1.50000000 sec
D13                   0.00000400 sec
D16                   0.00020000 sec
IN0                   0.00030600 sec
TDav                         1
SFO1                400.1316005 MHz
NUC1                        1H
P0                       14.00 usec
P1                       14.00 usec
PLW1               13.21300030 W
GPNAM[1]            SMSQ10.100
GPZ1                    10.00 %
P16                   1000.00 usec

F1 - Acquisition parameters
TD                         256
SFO1                400.1316 MHz
FIDRES               25.531046 Hz
SW                       8.167 ppm
FnMODE                      QF

F2 - Processing parameters
SI                        1024
SF                  400.1300175 MHz
WDW                       SINE
SSB                          0
LB                        0 Hz
GB                           0
PC                        1.00

F1 - Processing parameters
SI                        1024
MC2                         QF
SF                  400.1300175 MHz
WDW                       SINE
SSB                          0
LB                        0 Hz
GB                           0
```

Appendix VI (k)

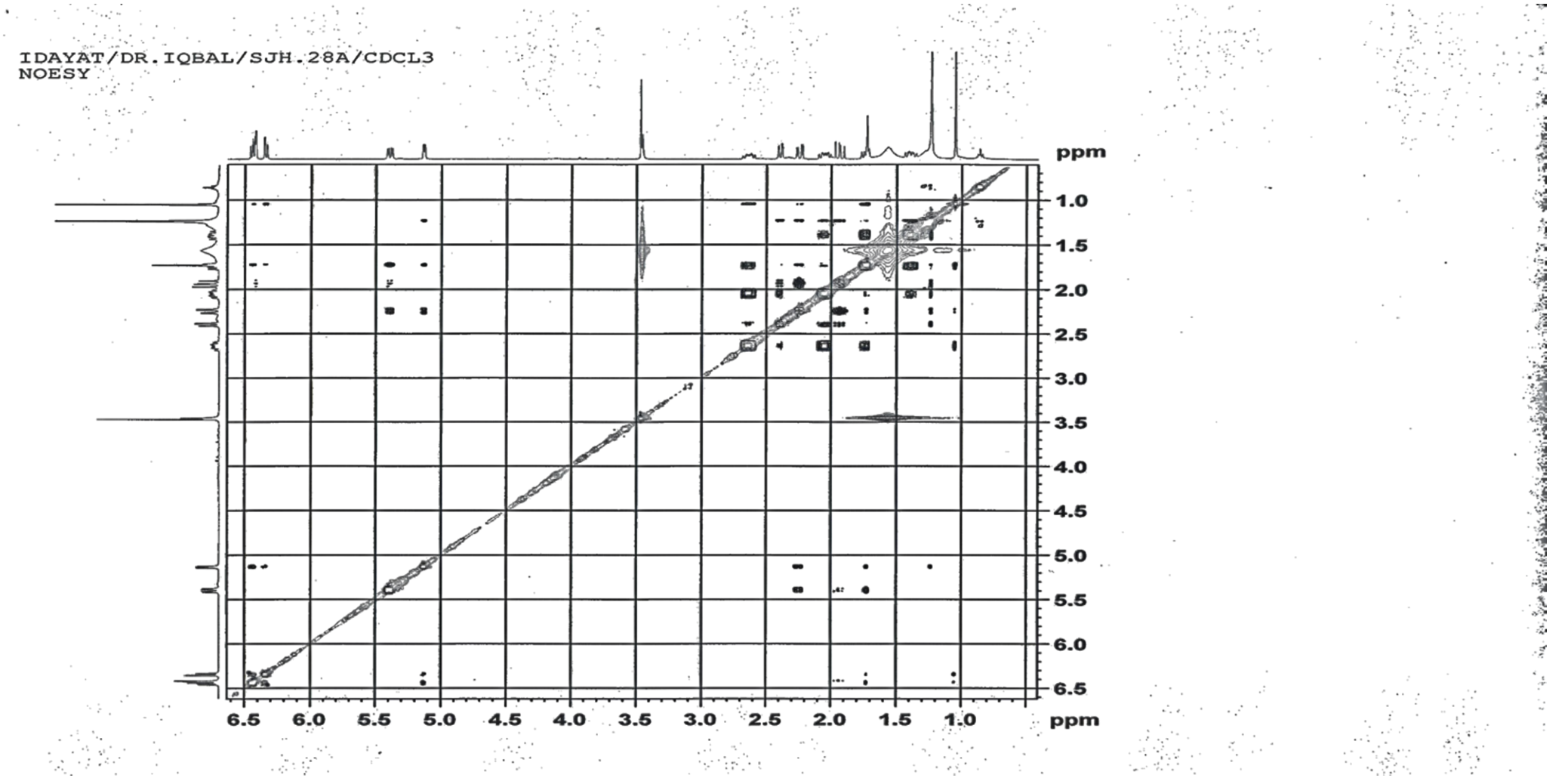

Appendix VII (a)

EI-MS, 1D and 2D NMR spectra of SJH-28B

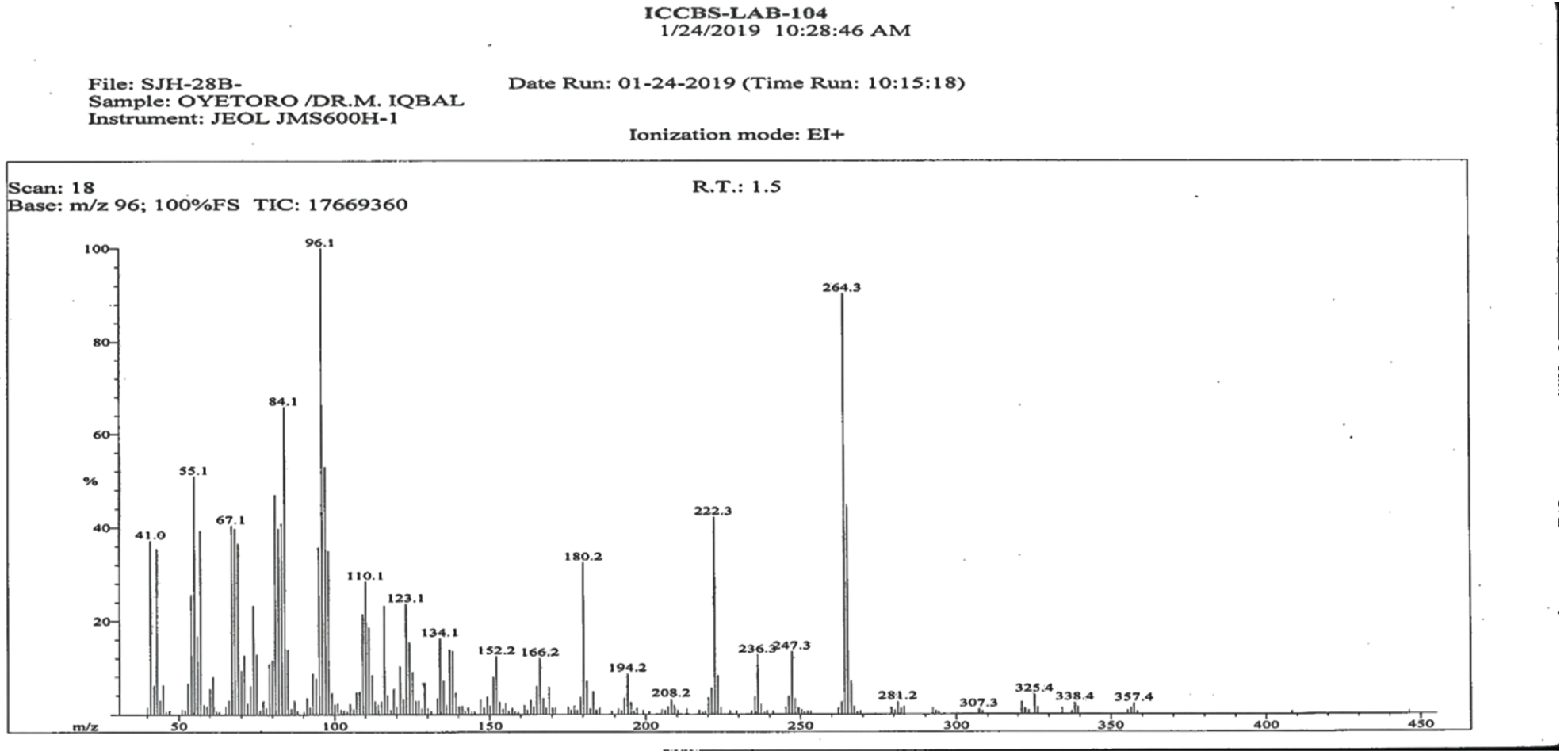

Appendix VII (b)

ICCBS-LAB-104
1/24/2019 10:29:10 AM

File: SJH-28B-
Sample: OYETORO /DR.M. IQBAL
Instrument: JEOL JMS600H-1

Date Run: 01-24-2019 (Time Run: 10:15:18)

Ionization mode: EI+

Scan: 18
Base: m/z 96; 100%FS TIC: 17669360

R.T.: 1.5

Threshold: 2% of Base

Displayed TIC: 17669360

Mass	%Base	Mass	%Base	Mass	%Base	Mass	%Base	Mass	%Base
41.0487	37.2	75.0586	12.8	108.1360	4.9	136.1569	2.1	208.2280	3.3
42.0466	6.2	77.0479	2.9	109.1118	21.5	137.1622	13.9	220.2582	3.7
43.0567	35.6	79.0629	10.9	110.1176	28.5	138.2000	13.5	221.2334	5.7
44.0294	3.1	80.0800	11.6	111.1280	18.7	139.1836	4.7	222.2836	42.2
45.0470	6.3	81.0812	47.0	112.1429	8.4	147.1408	3.1	223.3002	8.3
53.0564	6.7	82.0885	39.8	113.1099	2.9	149.1988	3.8	235.2734	3.9
54.0780	25.7	83.1020	40.9	114.0809	2.1	151.1795	8.0	236.2761	12.7
55.0902	51.0	84.0761	65.8	115.1089	2.8	152.2045	12.5	237.2807	2.2
56.0738	16.8	85.1015	13.9	116.0882	23.3	153.2024	2.7	246.2702	4.0
57.0844	39.4	87.0781	3.0	117.0983	4.1	155.1767	2.2	247.2968	13.5
58.0846	2.1	91.0744	3.5	119.1045	5.4	163.2242	3.0	248.2874	3.3
60.0518	5.5	93.0936	8.7	121.1275	10.3	165.1950	6.0	263.2428	2.7
61.0568	8.0	94.1233	7.7	122.1316	3.2	166.2315	12.0	264.3004	90.3
66.0620	3.0	95.1100	35.8	123.1399	23.7	167.2079	3.5	265.2817	44.9
67.0741	40.5	96.1016	100.0	124.1522	15.6	169.1999	5.8	266.3043	7.1
68.0938	39.8	97.1222	52.9	125.1411	9.1	179.2016	3.7	281.1811	2.7
69.1006	36.6	98.1231	35.1	126.1338	2.9	180.2467	32.5	321.1998	2.7
70.0940	9.3	99.1039	4.6	127.1027	2.9	181.2292	7.1	325.3538	4.2
71.0943	12.7	100.0888	2.2	129.1072	6.7	183.2020	4.8	338.3710	2.5
72.0807	2.3	101.0781	2.4	133.1622	3.5	193.1924	3.5	357.3961	2.3
73.0526	6.1	105.1081	2.2	134.0999	16.3	194.2433	8.7		
74.0522	23.3	107.1391	4.7	135.1551	7.2	195.2291	2.6		

Appendix VII (c)

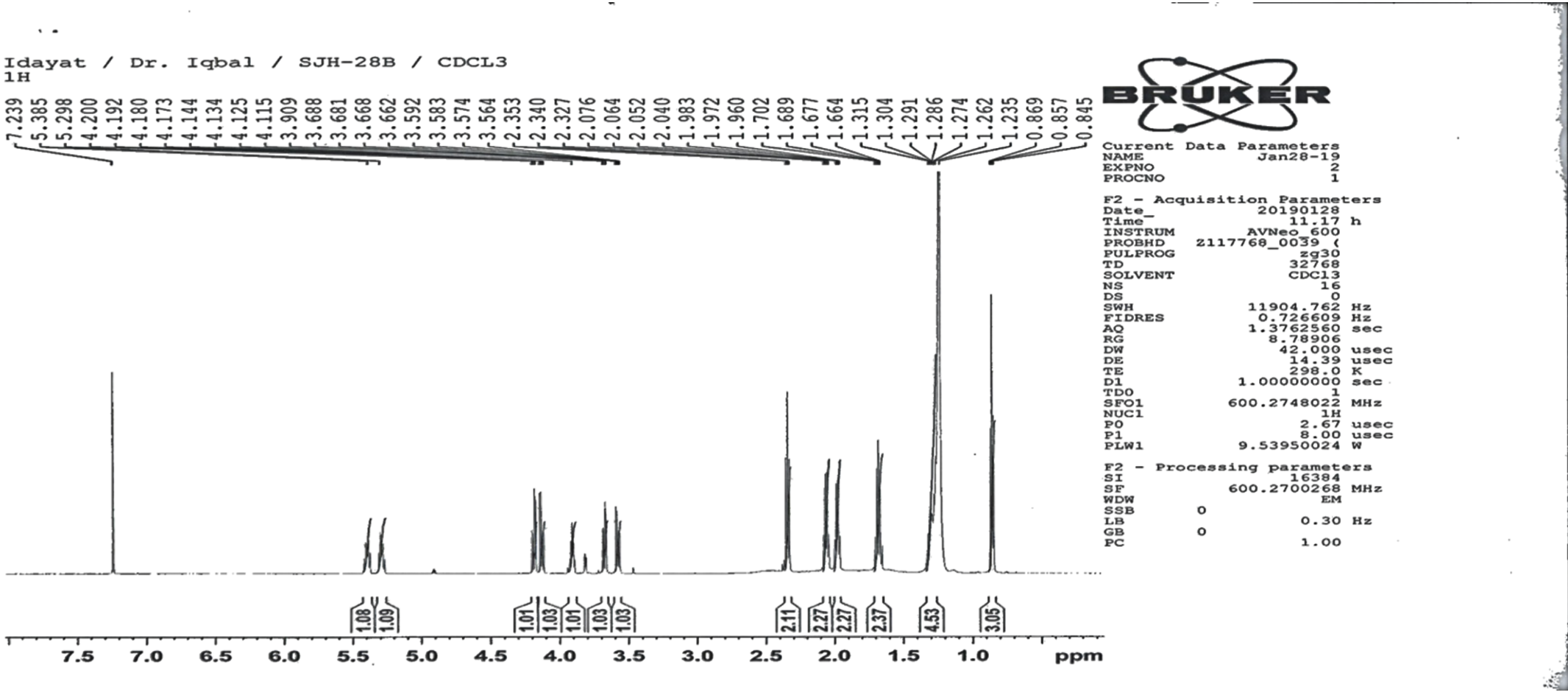

Appendix VII (d)

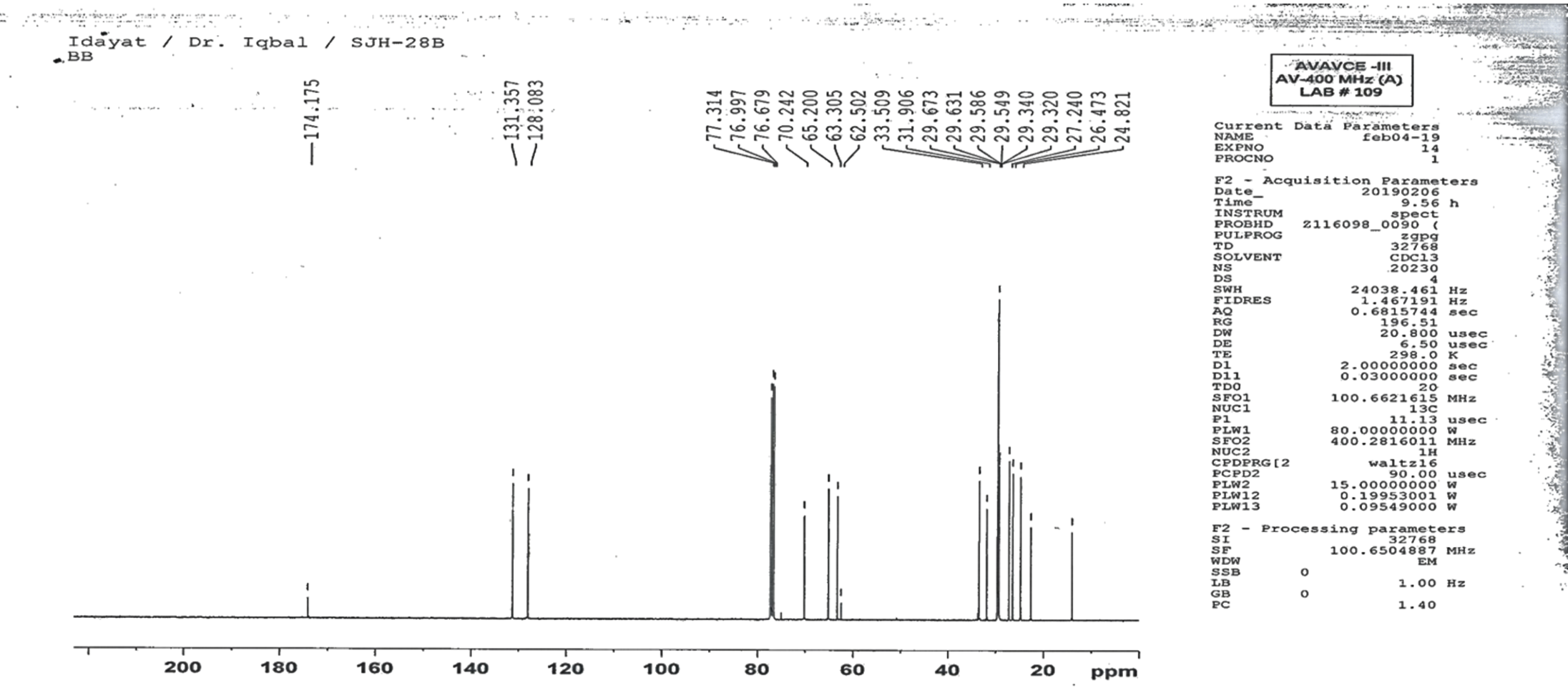

Appendix VII (e)

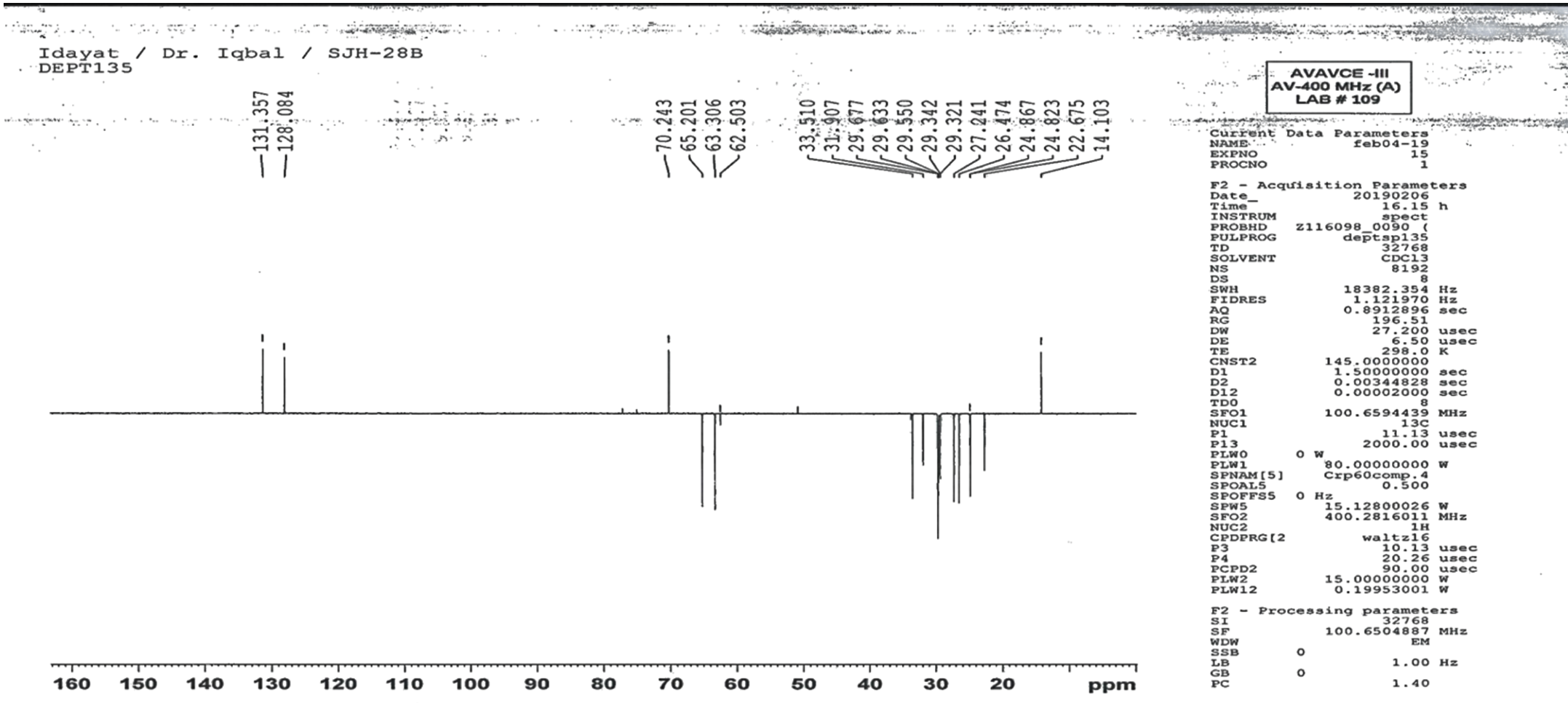

Appendix VII (f)

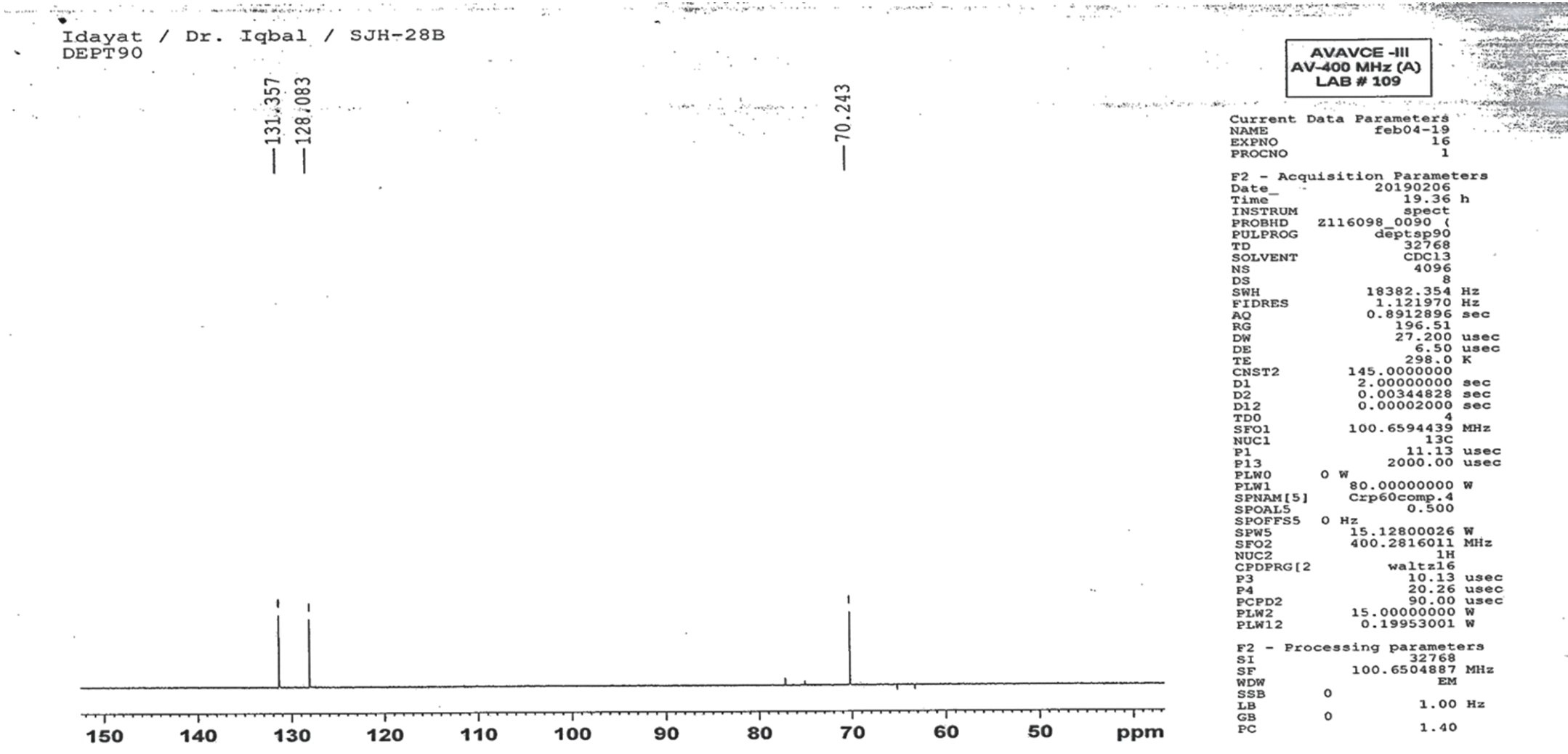

AVAVCE -III
AV-400 MHz (A)
LAB # 109

Current Data Parameters
NAME feb04-19
EXPNO 16
PROCNO 1

F2 - Acquisition Parameters
Date_ 20190206
Time 19.36 h
INSTRUM spect
PROBHD Z116098_0090 (
PULPROG deptsp90
TD 32768
SOLVENT CDCl3
NS 4096
DS 8
SWH 18382.354 Hz
FIDRES 1.121970 Hz
AQ 0.8912896 sec
RG 196.51
DW 27.200 usec
DE 6.50 usec
TE 298.0 K
CNST2 145.0000000
D1 2.00000000 sec
D2 0.00344828 sec
D12 0.00002000 sec
TD0 4
SFO1 100.6594439 MHz
NUC1 13C
P1 11.13 usec
P13 2000.00 usec
PLW0 0 W
PLW1 80.00000000 W
SPNAM[5] Crp60comp.4
SPOAL5 0.500
SPOFFS5 0 Hz
SPW5 15.12800026 W
SFO2 400.2816011 MHz
NUC2 1H
CPDPRG[2 waltz16
P3 10.13 usec
P4 20.26 usec
PCPD2 90.00 usec
PLW2 15.00000000 W
PLW12 0.19953001 W

F2 - Processing parameters
SI 32768
SF 100.6504887 MHz
WDW EM
SSB 0
LB 1.00 Hz
GB 0
PC 1.40

Appendix VII (g)

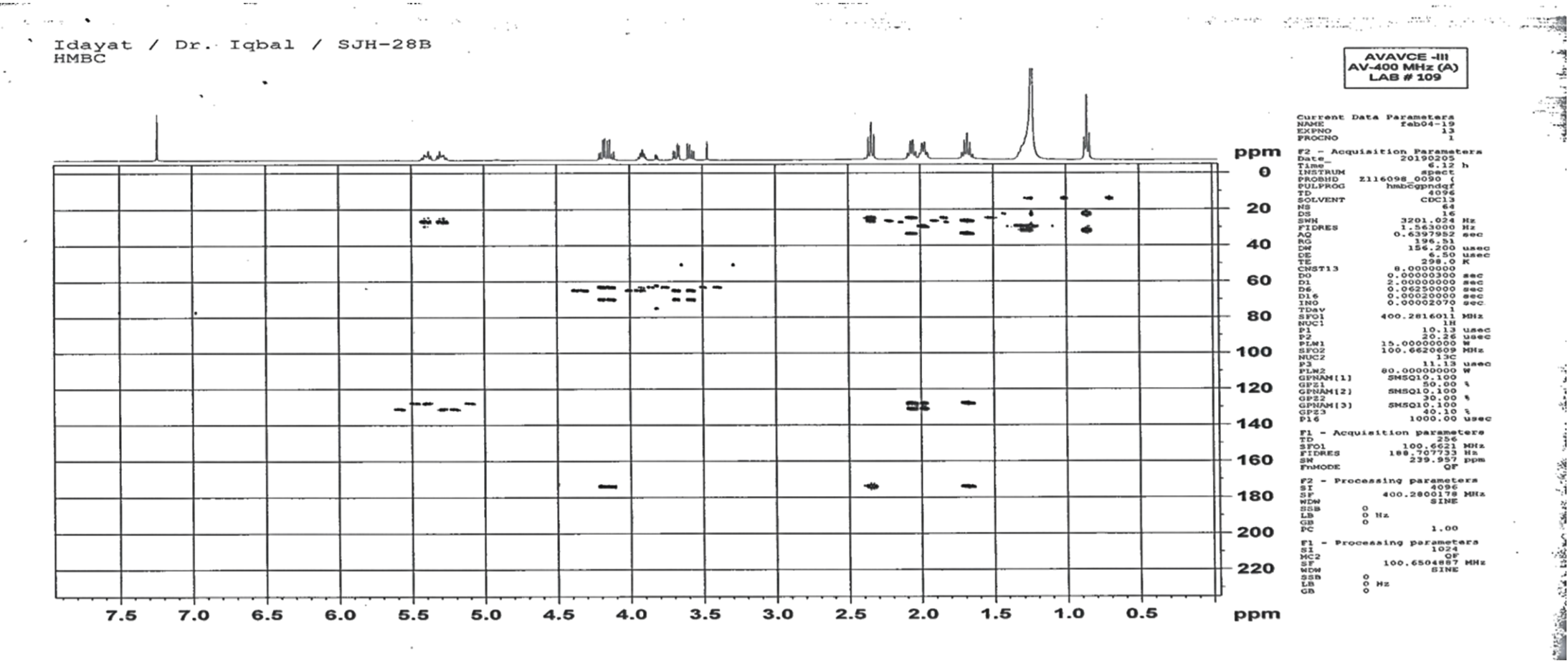

Appendix VII (h)

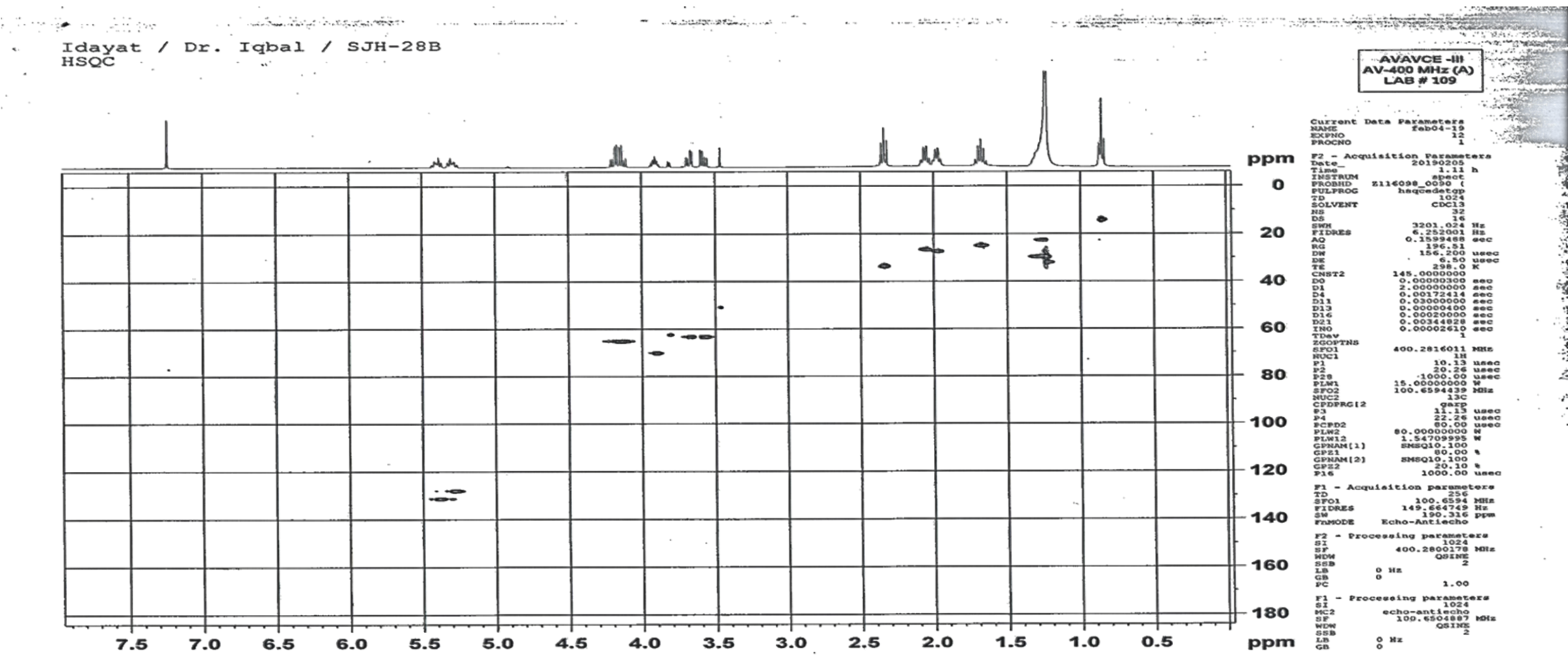

Appendix VII (i)

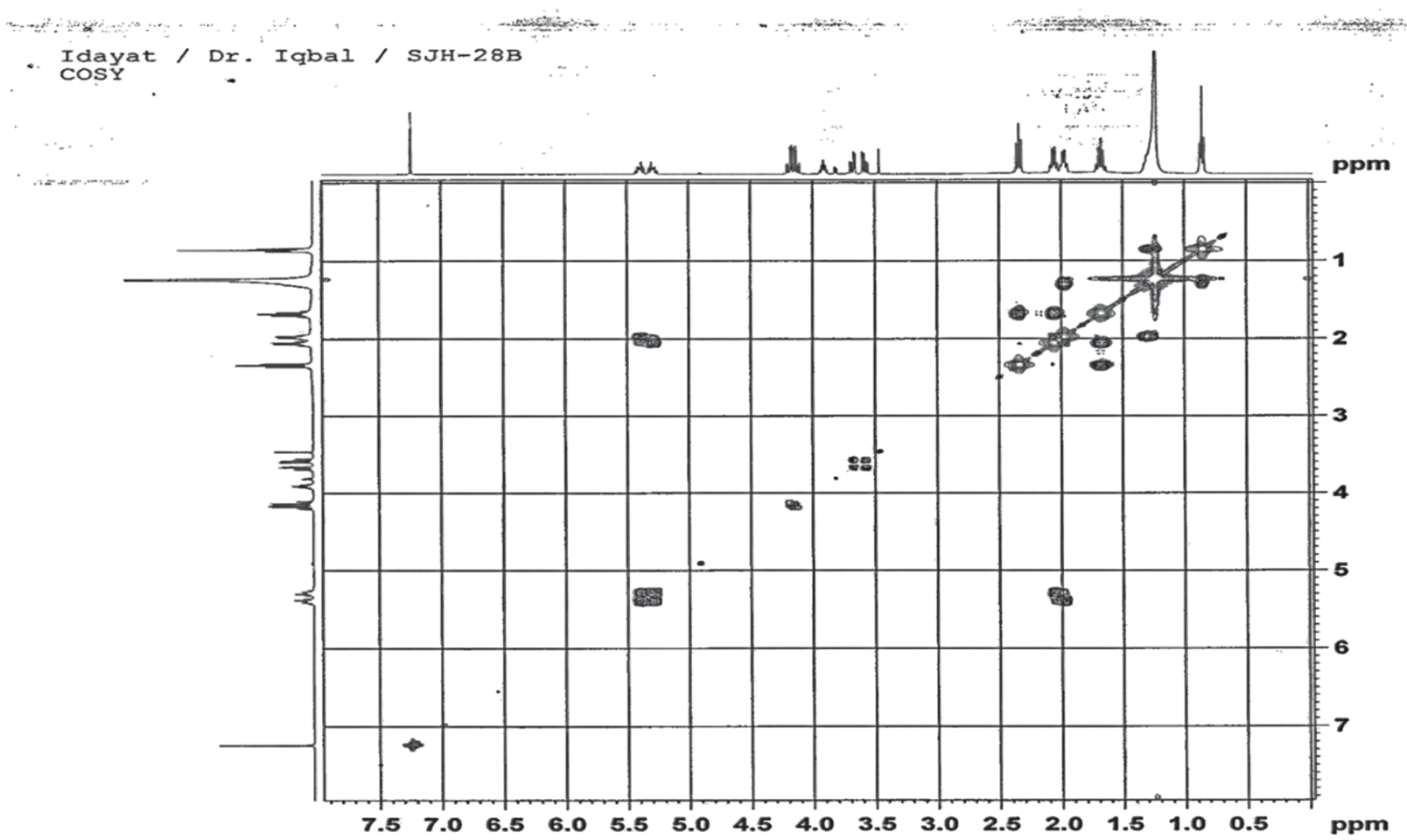

AVAVCE-III
AV-400 MHz (A)
LAB # 109

```
Current Data Parameters
NAME                  feb04-19
EXPNO                       10
PROCNO                       1

F2 - Acquisition Parameters
Date_                 20190204
Time                     17.01 h
INSTRUM                  spect
PROBHD     Z116098_0090 (
PULPROG               cosygpqf
TD                        2048
SOLVENT                  CDCl3
NS                          16
DS                           8
SWH                   3201.024 Hz
FIDRES                3.126000 Hz
AQ                    0.3198976 sec
RG                       196.51
DW                       156.200 usec
DE                         6.50 usec
TE                       298.0 K
D0                    0.00000300 sec
D1                    1.50000000 sec
D13                   0.00000400 sec
D16                   0.00020000 sec
IN0                   0.00031240 sec
TDav                         1
SFO1                400.2816011 MHz
NUC1                        1H
P0                       10.13 usec
P1                       10.13 usec
PLW1                15.00000000 W
GPNAM[1]             SMSQ10.100
GPZ1                     10.00 %
P16                    1000.00 usec

F1 - Acquisition parameters
TD                         256
SFO1                400.2816 MHz
FIDRES               25.008003 Hz
SW                        7.997 ppm
FnMODE                       QF

F2 - Processing parameters
SI                        1024
SF                  400.2800178 MHz
WDW                       SINE
SSB                  0
LB                   0 Hz
GB                   0
PC                        1.00

F1 - Processing parameters
SI                        1024
MC2                          QF
SF                  400.2800178 MHz
WDW                       SINE
SSB                  0
LB                   0 Hz
GB                   0
```

Appendix VII (j)

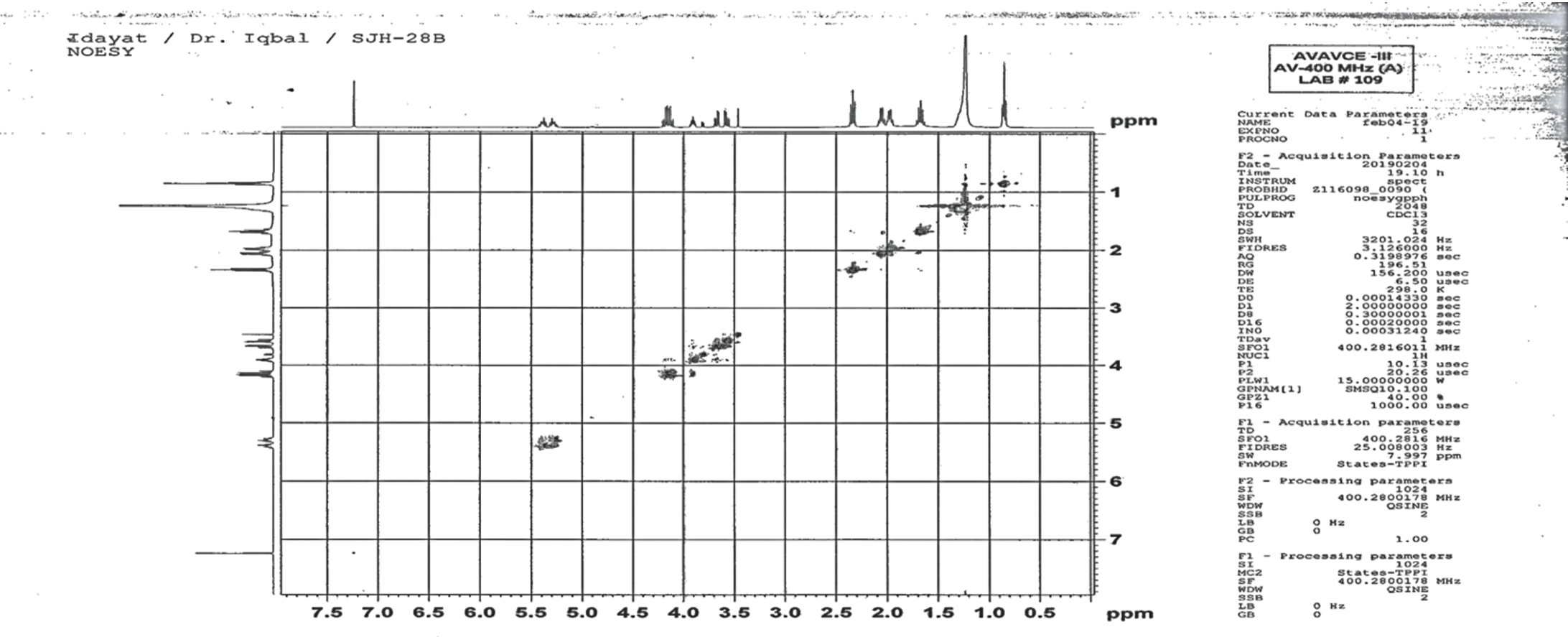

Appendix VIII (a)

EI-MS, 1D and 2D NMR spectra of SJH-34B

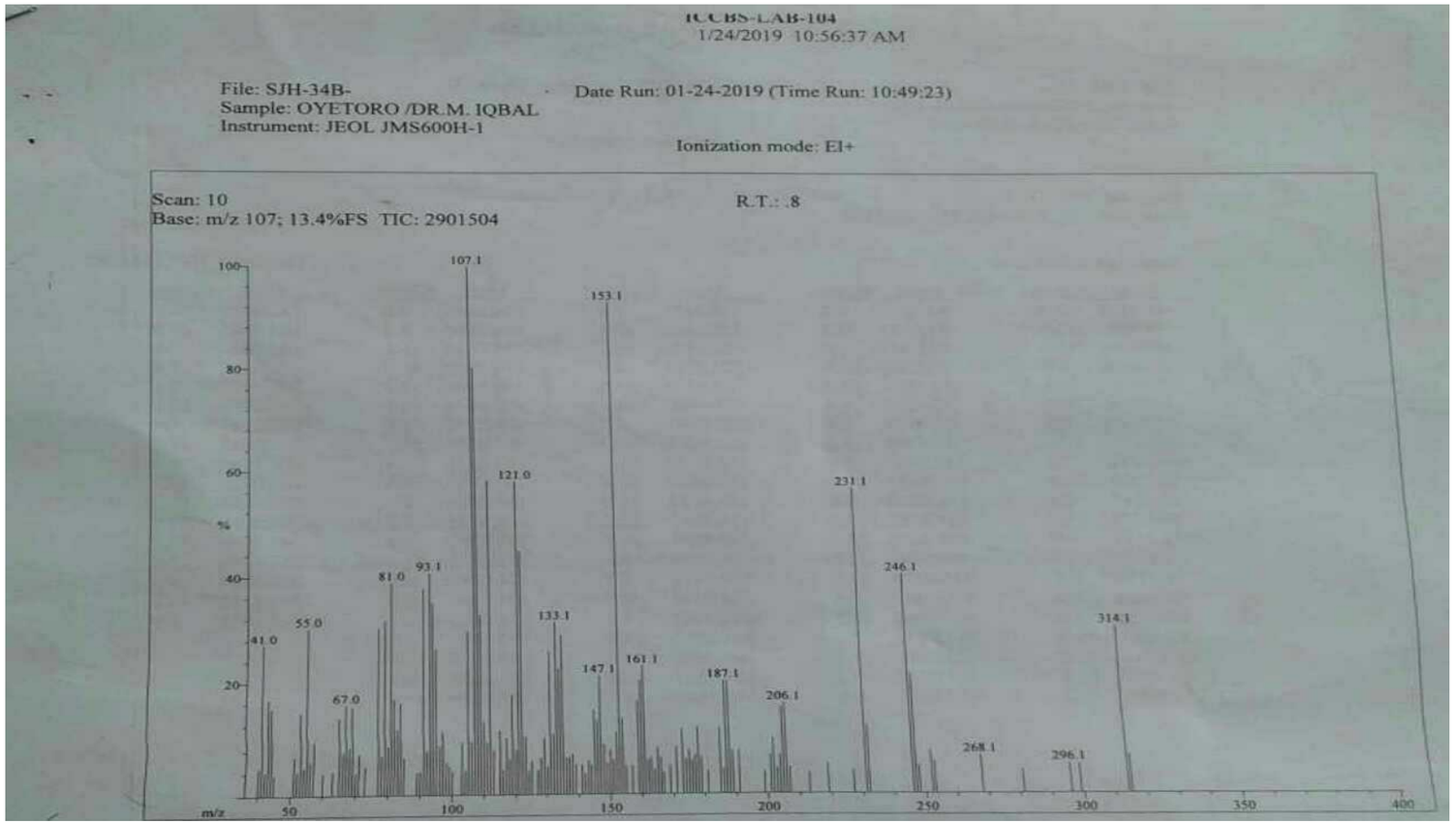

Appendix VIII (b)

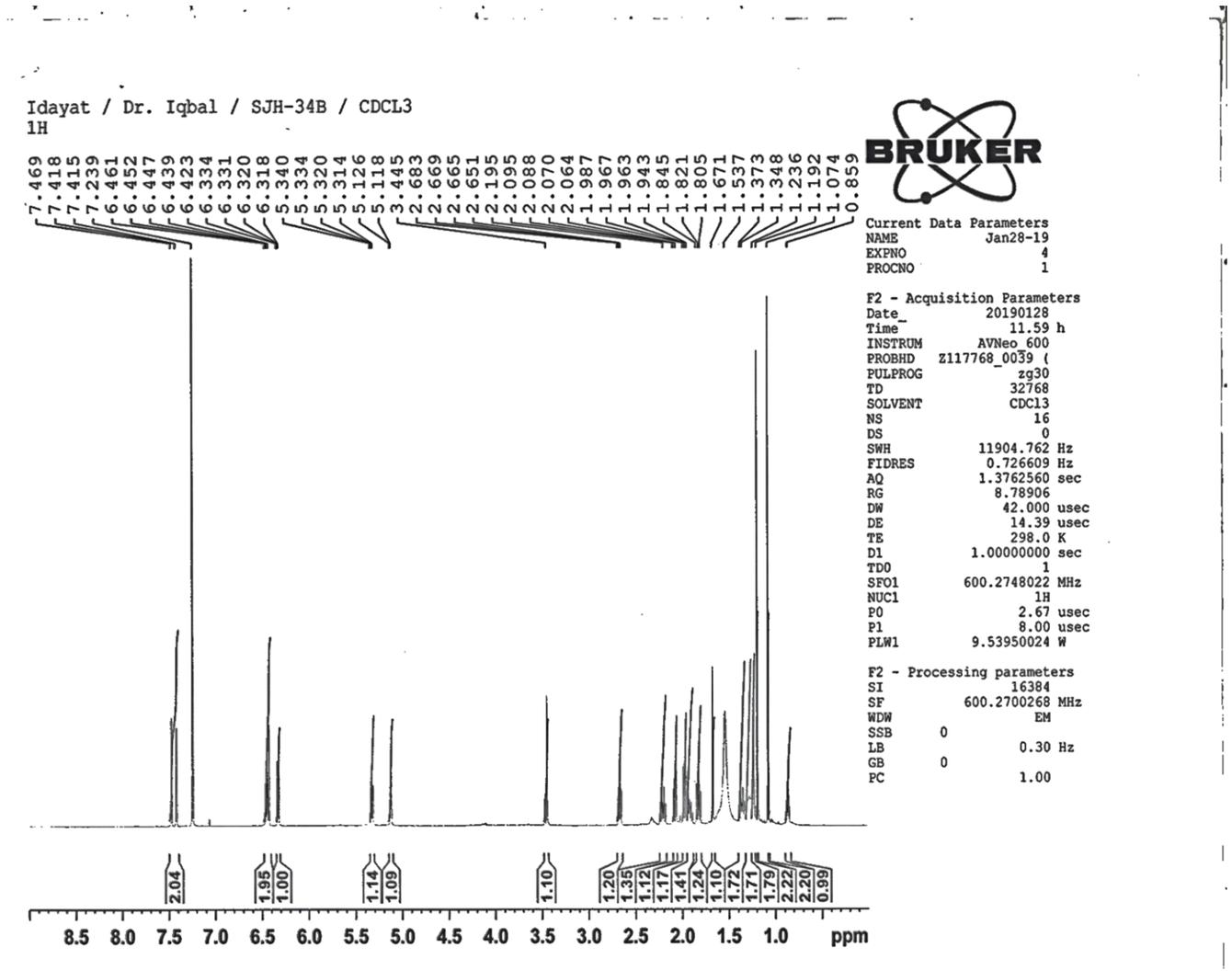

Appendix VIII (c)

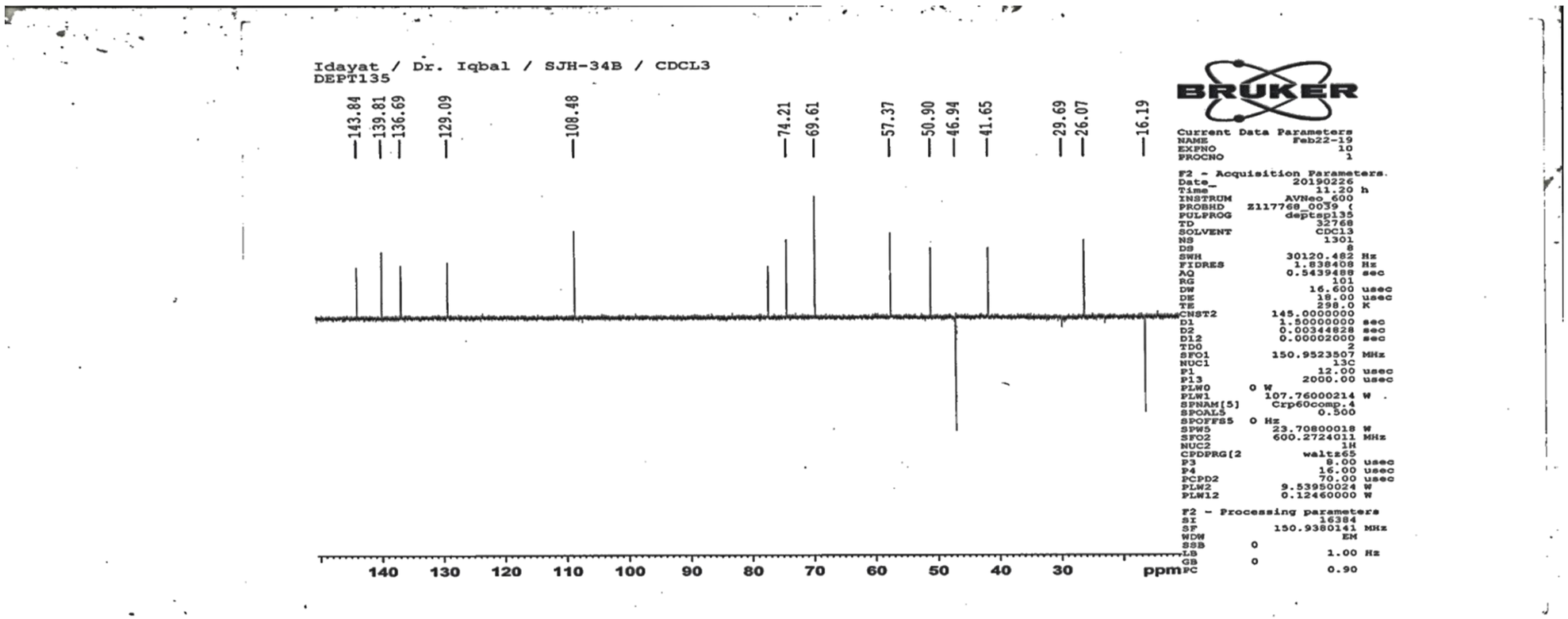

Appendix VIII (d)

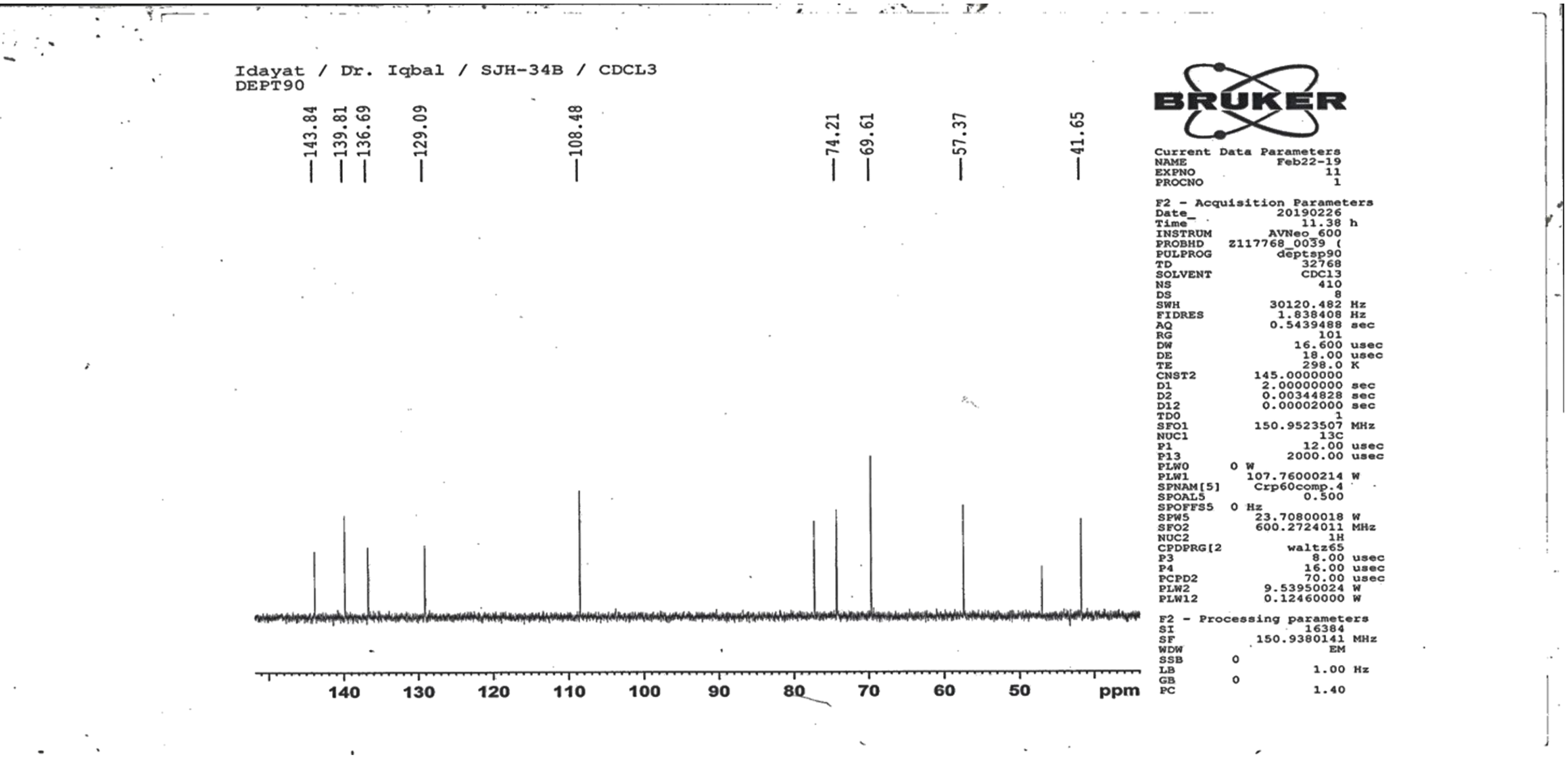

BRUKER

Current Data Parameters
NAME Feb22-19
EXPNO 11
PROCNO 1

F2 - Acquisition Parameters
Date_ 20190226
Time 11.38 h
INSTRUM AVNeo_600
PROBHD Z117768_0039 (
PULPROG deptsp90
TD 32768
SOLVENT CDCl3
NS 410
DS 8
SWH 30120.482 Hz
FIDRES 1.838408 Hz
AQ 0.5439488 sec
RG 101
DW 16.600 usec
DE 18.00 usec
TE 298.0 K
CNST2 145.0000000
D1 2.00000000 sec
D2 0.00344828 sec
D12 0.00002000 sec
TD0 1
SFO1 150.9523507 MHz
NUC1 13C
P1 12.00 usec
P13 2000.00 usec
PLW0 0 W
PLW1 107.76000214 W
SPNAM[5] Crp60comp.4
SPOAL5 0.500
SPOFFS5 0 Hz
SPW5 23.70800018 W
SFO2 600.2724011 MHz
NUC2 1H
CPDPRG[2 waltz65
P3 8.00 usec
P4 16.00 usec
PCPD2 70.00 usec
PLW2 9.53950024 W
PLW12 0.12460000 W

F2 - Processing parameters
SI 16384
SF 150.9380141 MHz
WDW EM
SSB 0
LB 1.00 Hz
GB 0
PC 1.40

Appendix VIII (e)

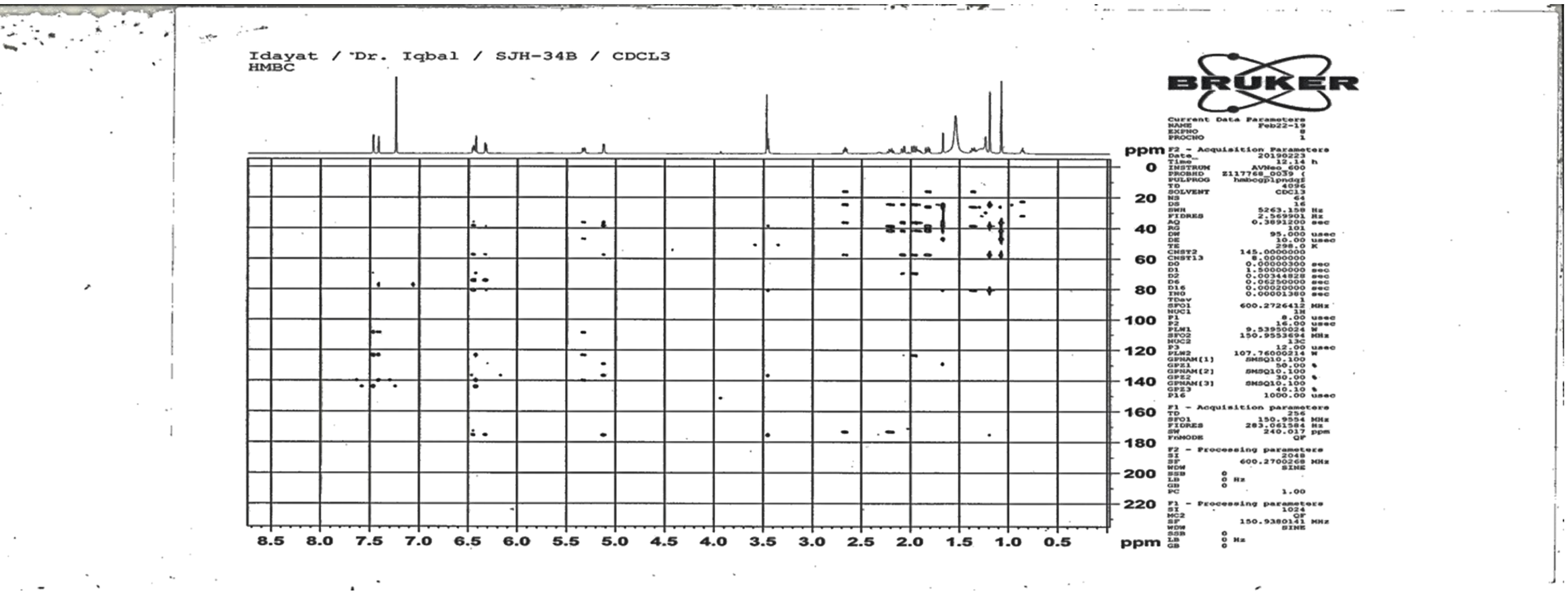

Appendix VIII (f)

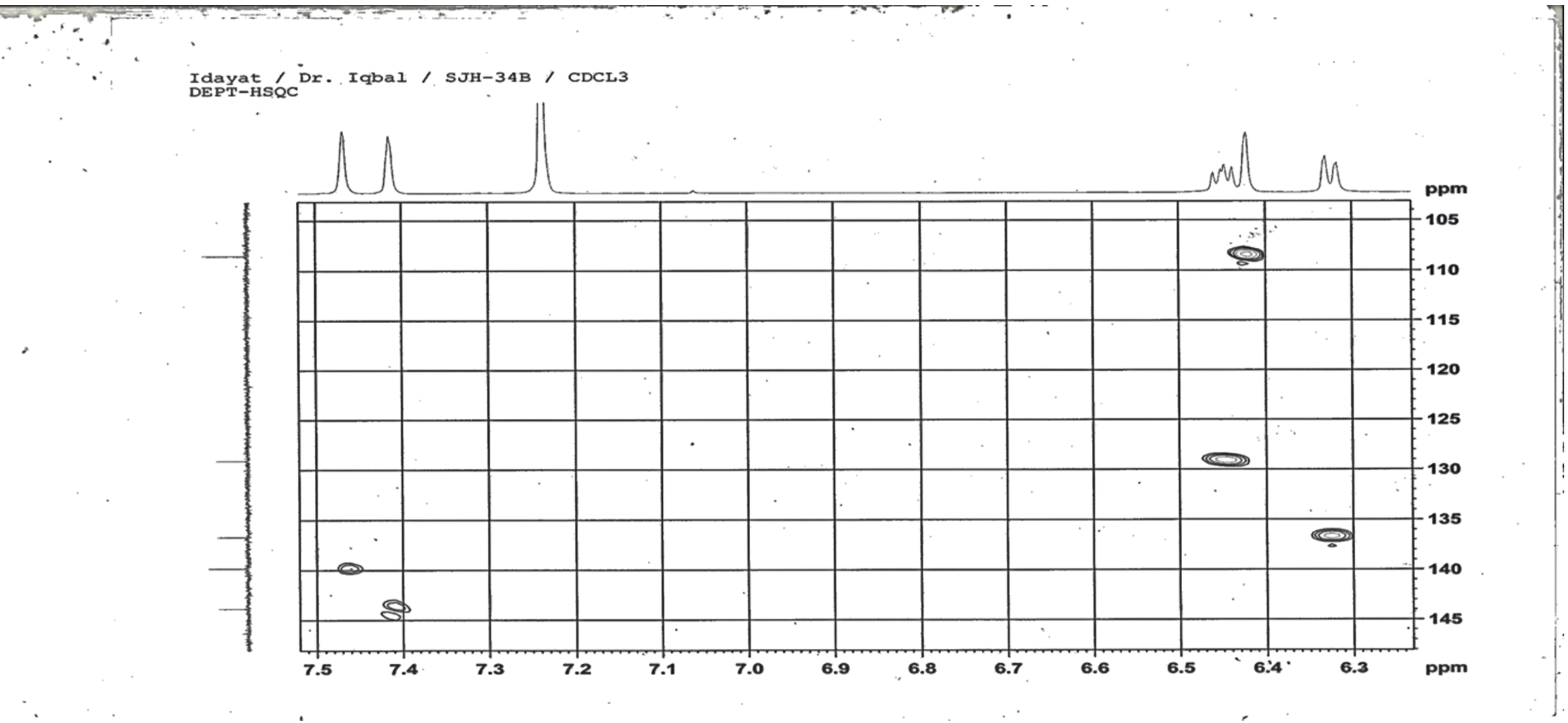

Appendix VIII (g)

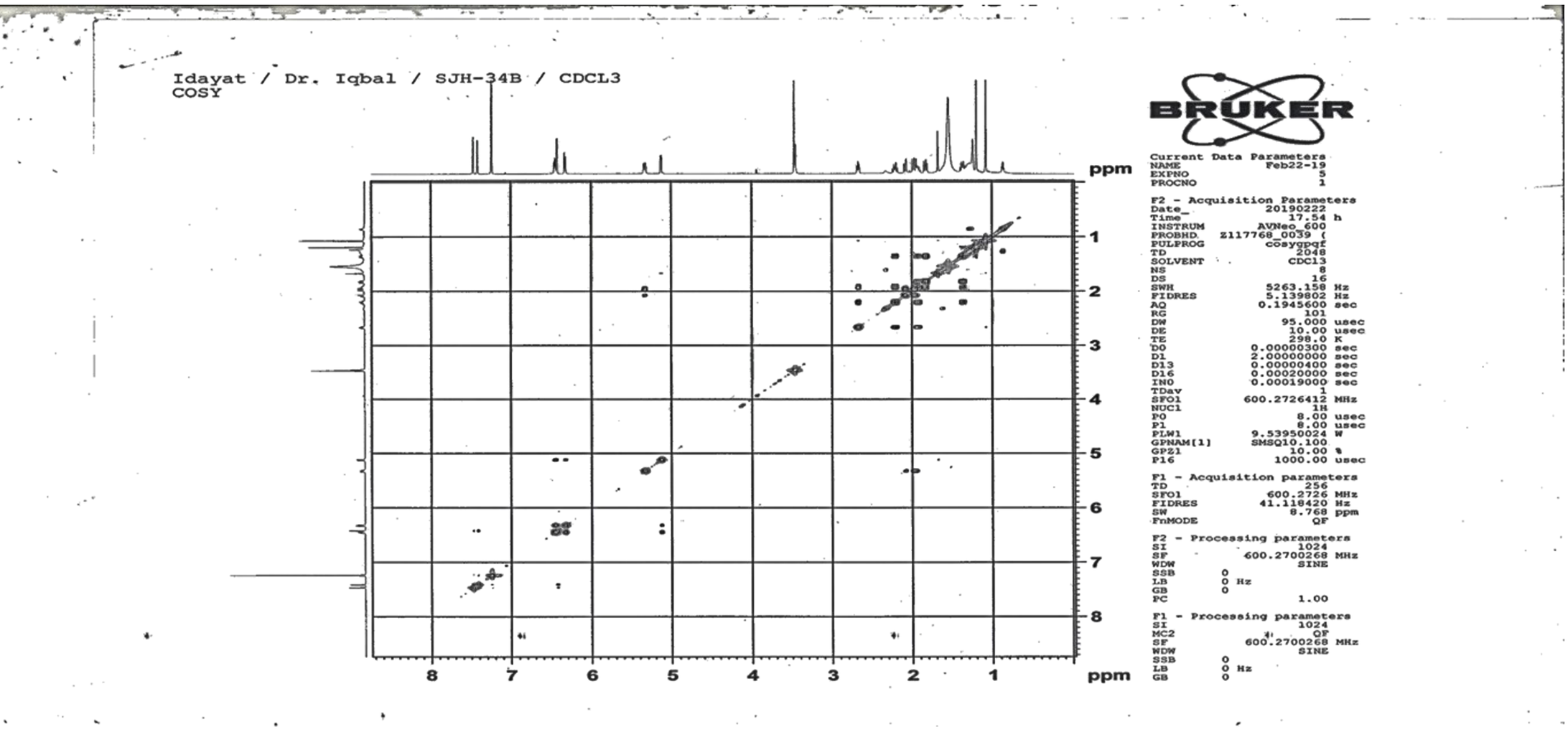

Appendix VIII (h)

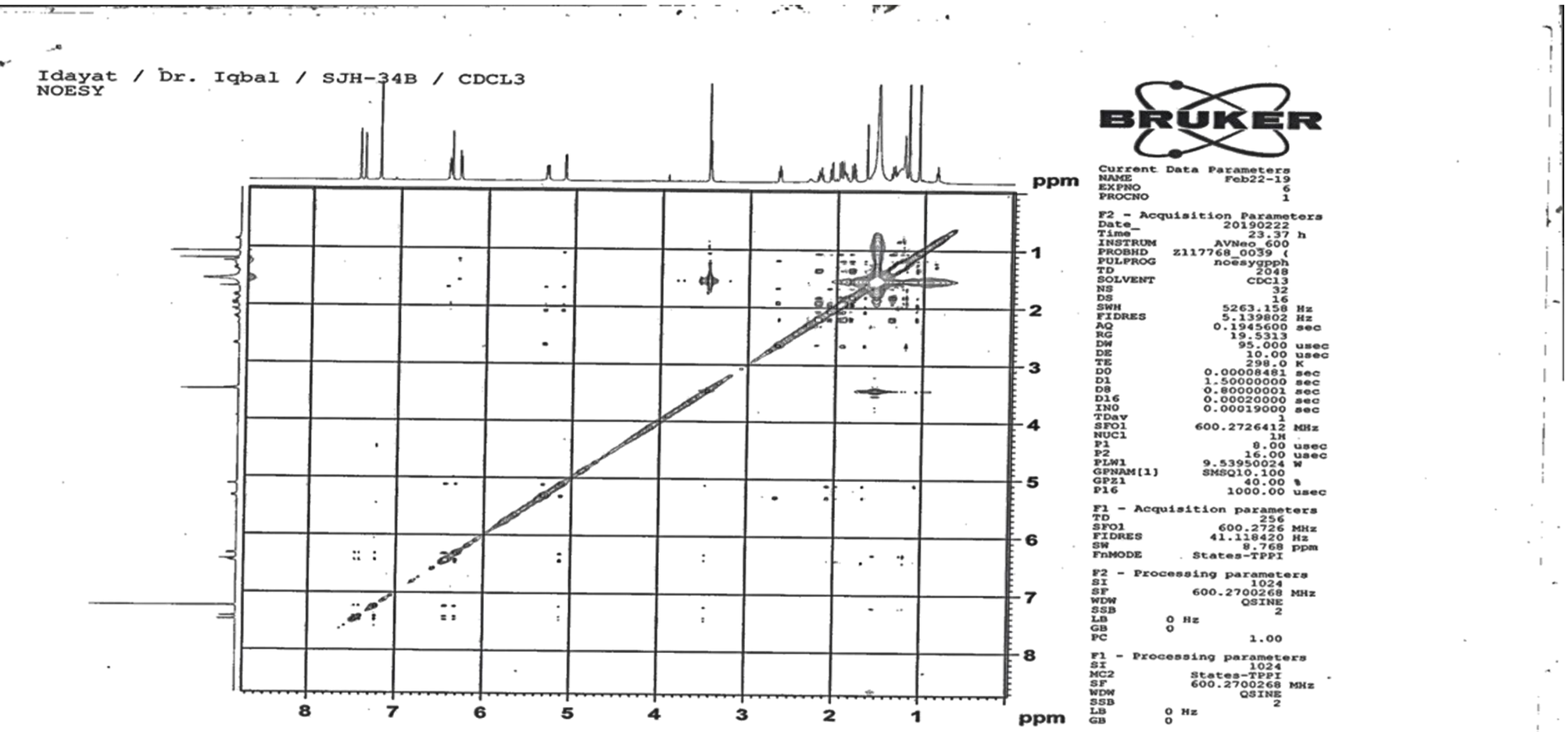

BRUKER

Current Data Parameters

NAME	Feb22-19	
EXPNO	6	
PROCNO	1	
F2 - Acquisition Parameters		
Date_	20190222	
Time	23.37	h
INSTRUM	AVNeo_600	
PROBHD	Z117768_0039 (	
PULPROG	noesygpph	
TD	2048	
SOLVENT	CDCl3	
NS	32	
DS	16	
SWH	5263.158	Hz
FIDRES	5.139802	Hz
AQ	0.1945600	sec
RG	19.5313	
DW	95.000	usec
DE	10.00	usec
TE	298.0	K
D0	0.00008481	sec
D1	1.50000000	sec
D8	0.80000001	sec
D16	0.00020000	sec
IN0	0.00019000	sec
TDav	1	
SFO1	600.2726412	MHz
NUC1	1H	
P1	8.00	usec
P2	16.00	usec
PLW1	9.53950024	W
GPNAM[1]	SMSQ10.100	
GPZ1	40.00	%
P16	1000.00	usec
F1 - Acquisition parameters		
TD	256	
SFO1	600.2726	MHz
FIDRES	41.118420	Hz
SW	8.768	ppm
FnMODE	States-TPPI	
F2 - Processing parameters		
SI	1024	
SF	600.2700268	MHz
WDW	QSINE	
SSB	2	
LB	0 Hz	
GB	0	
PC	1.00	
F1 - Processing parameters		
SI	1024	
MC2	States-TPPI	
SF	600.2700268	MHz
WDW	QSINE	
SSB	2	
LB	0 Hz	
GB	0	

Appendix VIII (i)

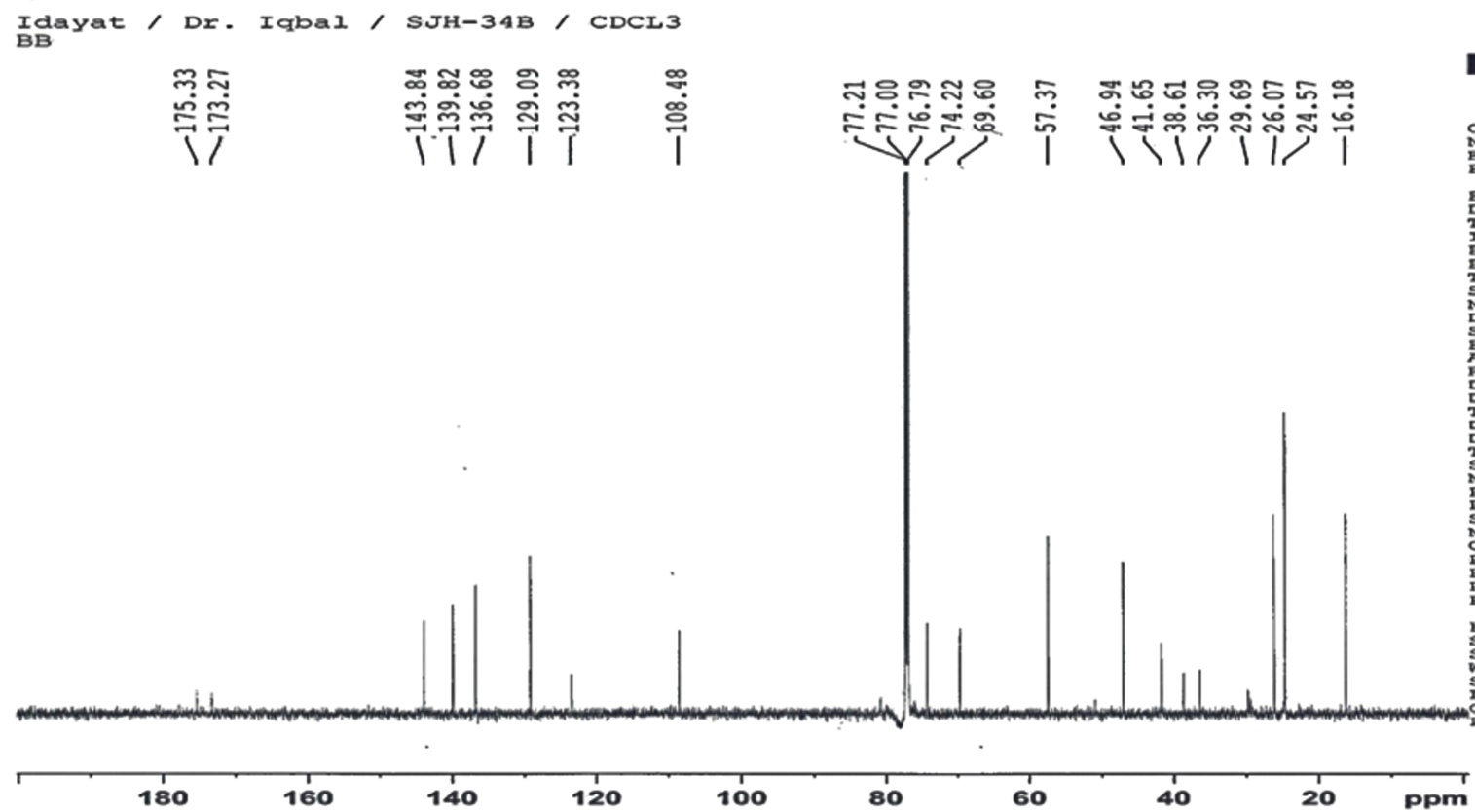


```
Current Data Parameters
NAME                  Feb22-19
EXPNO                        9
PROCNO                       1

F2 - Acquisition Parameters
Date_                 20190223
Time                     19.08 h
INSTRUM                AVNeo_600
PROBHD     Z117768_0039 (
PULPROG                   zgpg
TD                       32768
SOLVENT                  CDCl3
NS                       12288
DS                           4
SWH                  35714.285 Hz
FIDRES               2.179827 Hz
AQ                   0.4587520 sec
RG                         101
DW                    14.000 usec
DE                    18.00 usec
TE                       298.0 K
D1                 1.50000000 sec
D11                0.03000000 sec
TD0                         12
SFO1               150.9553694 MHz
NUC1                       13C
P1                    12.00 usec
PLW1              107.76000214 W
SFO2               600.2724011 MHz
NUC2                       1H
CPDPRG[2                waltz65
PCPD2                 70.00 usec
PLW2               9.53950024 W
PLW12              0.12460000 W
PLW13              0.06267200 W

F2 - Processing parameters
SI                       16384
SF                 150.9380141 MHz
WDW                         EM
SSB                  0
LB                        1.00 Hz
GB                   0
PC                        1.40
```

Appendix IX (a)

HR-MS and 1D NMR spectra of CPE-10A

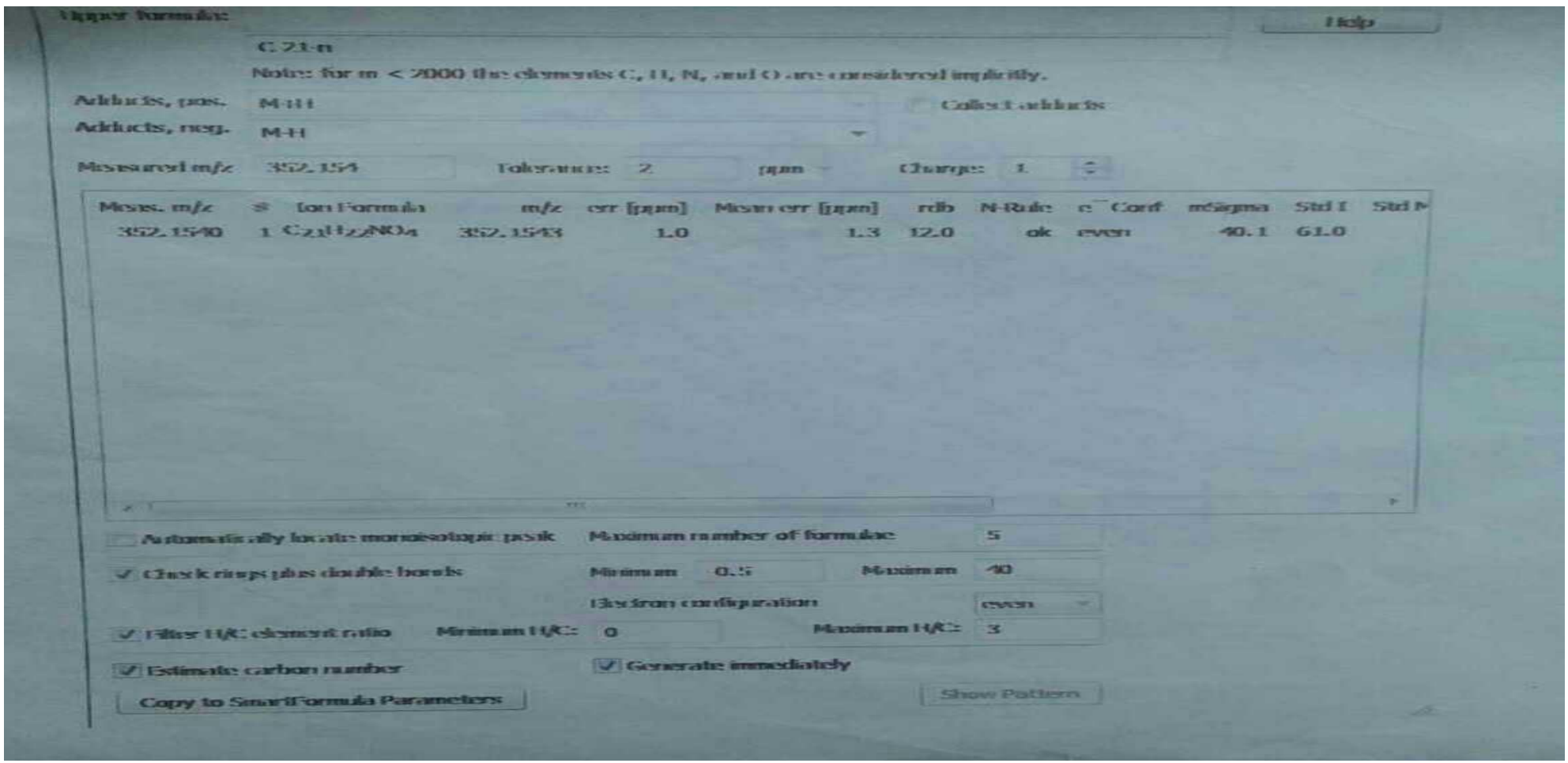

Appendix IX (b)

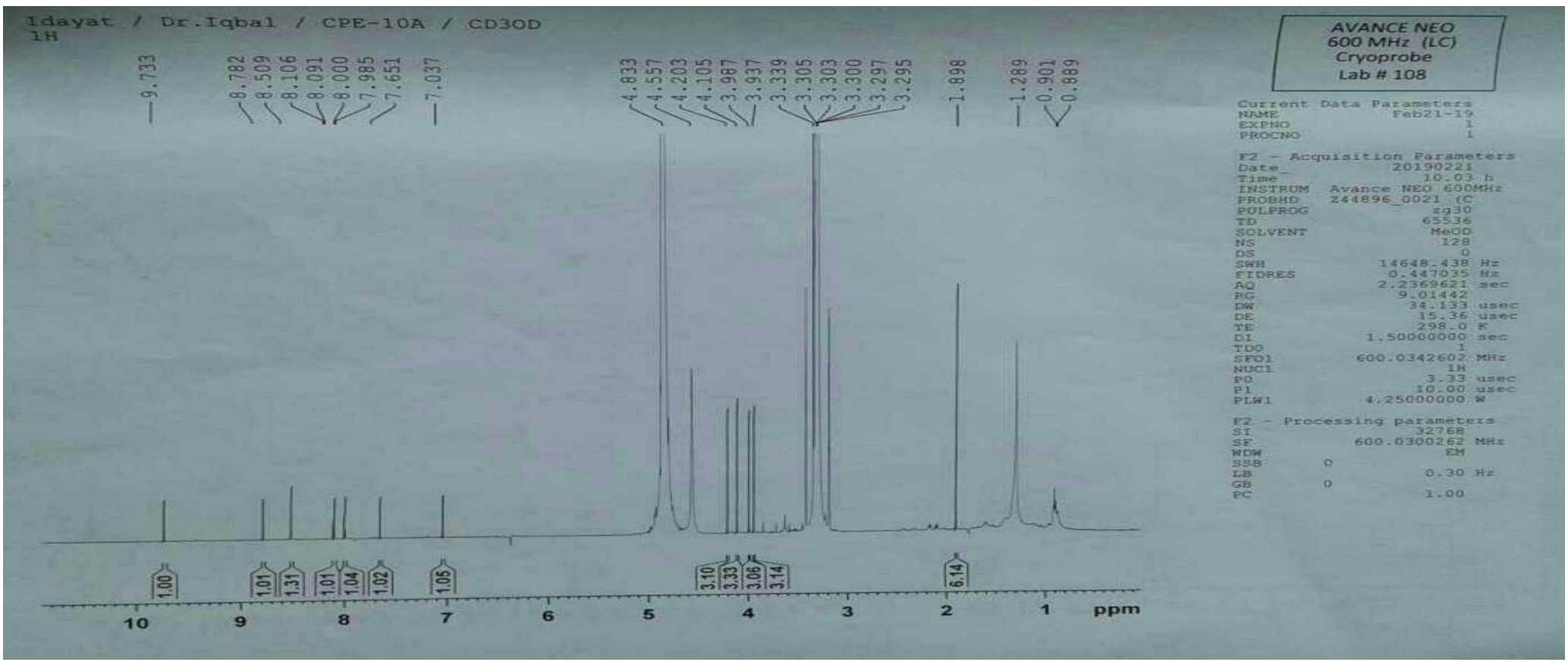

Appendix X (a)

EI-MS, 1D and 2D NMR spectra of SJE-10B

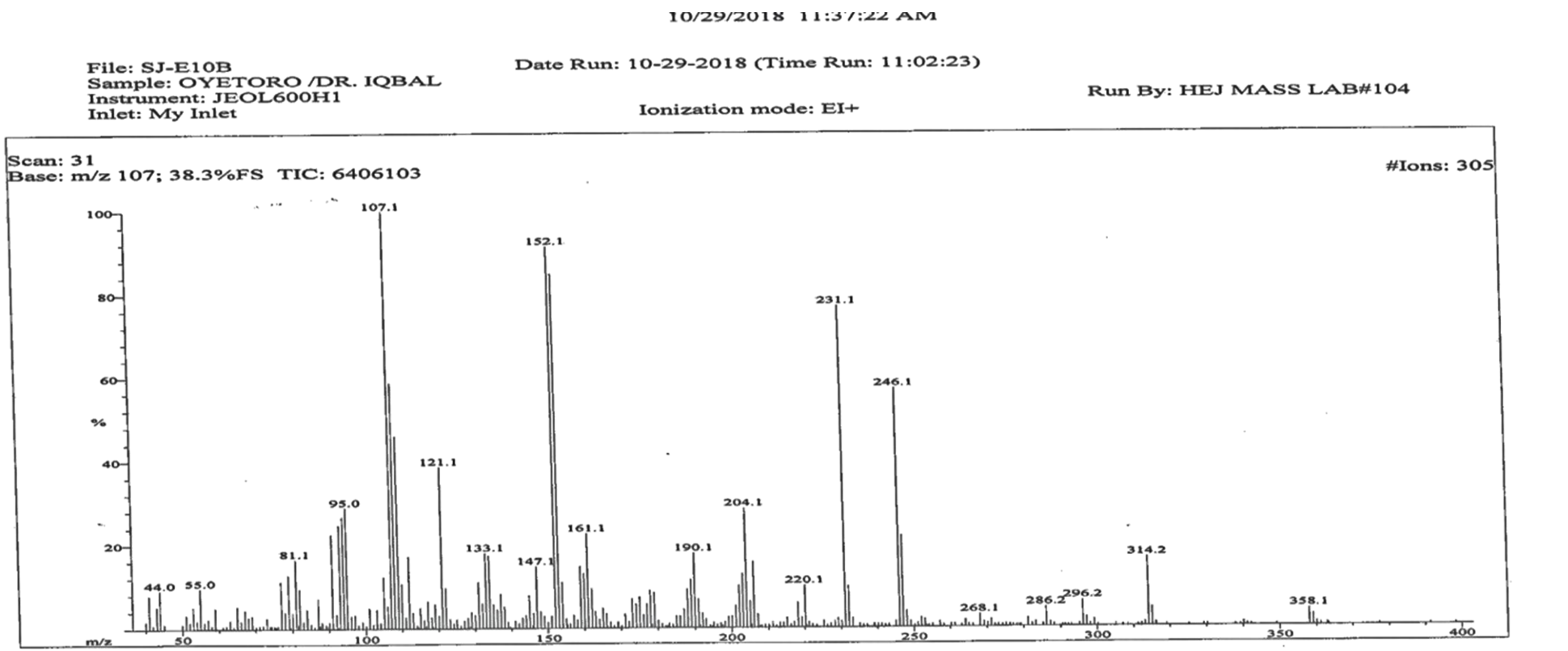

Appendix X (b)

ICCBS
10/29/2018 11:38:08 AM

File: SJ-E10B
Sample: OYETORO /DR. IQBAL
Instrument: JEOL600H1
Inlet: My Inlet

Date Run: 10-29-2018 (Time Run: 11:02:23)

Ionization mode: EI+

Run By: HEJ MASS LAB#104

Scan: 31
Base: m/z 107; 38.3%FS TIC: 6406103

#Ions: 305

Threshold: 2.5% of Base

Displayed TIC: 6406103

Mass	%Base	Mass	%Base	Mass	%Base	Mass	%Base	Mass	%Base
41.0319	8.0	94.0454	26.8	129.0666	3.9	160.0882	13.1	200.1530	2.8
43.0205	5.3	95.0285	29.0	130.0698	3.4	161.0797	22.7	201.1510	5.2
43.9904	9.1	96.0166	3.0	131.0769	11.1	162.0742	9.4	202.1512	10.1
51.0052	3.4	97.0340	3.3	132.0596	6.0	163.0716	4.0	203.1532	12.9
53.0141	5.2	101.0569	4.9	133.0743	18.1	165.0751	4.8	204.1226	28.6
55.0082	9.7	103.0487	4.6	134.0645	17.4	166.0812	3.5	205.1285	6.4
59.0324	4.9	105.0599	12.4	135.0583	5.8	171.0880	3.4	206.1365	15.8
65.0505	5.2	106.0726	5.4	136.0843	4.6	173.0986	6.9	207.1465	3.2
67.0708	4.4	107.0902	100.0	137.0855	8.3	174.0913	5.8	218.1626	5.9
68.0302	2.8	108.0612	58.8	138.0616	5.3	175.0864	7.4	220.1359	10.0
69.0577	3.2	109.0880	46.1	143.0513	2.6	176.0842	3.2	231.1334	77.1
73.0482	2.6	110.0678	10.8	144.0479	3.2	177.0525	5.7	232.1628	9.8
77.0567	11.3	111.0259	2.8	145.0479	7.9	178.0562	9.0	246.1204	57.1
78.0583	3.9	112.0140	17.3	146.0513	3.7	179.0631	8.5	247.1443	21.9
79.0660	12.8	113.0325	4.0	147.0878	14.8	185.1122	2.9	248.0943	3.9
80.0799	3.7	115.0824	5.0	148.0684	4.0	186.0758	2.9	268.1146	3.0
81.0555	16.6	117.0699	6.6	149.0522	2.9	187.1087	4.5	286.1627	4.6
82.0591	9.5	118.1096	2.8	151.0596	3.0	188.0775	9.2	296.1671	6.2
84.0390	4.6	119.1000	5.9	152.0533	91.6	189.0822	11.5	314.1729	16.5
87.0519	7.2	120.0671	3.2	153.0804	85.1	190.0894	17.9	315.1504	4.6
91.0557	22.6	121.0916	38.7	154.0807	10.9	191.0990	6.9	358.1409	4.1
92.0706	3.5	122.0927	9.7	157.0703	3.2	192.1109	3.5	359.1835	2.7
93.0673	24.8	128.0395	2.6	159.0688	14.8	199.1570	2.7		

Appendix X (c)

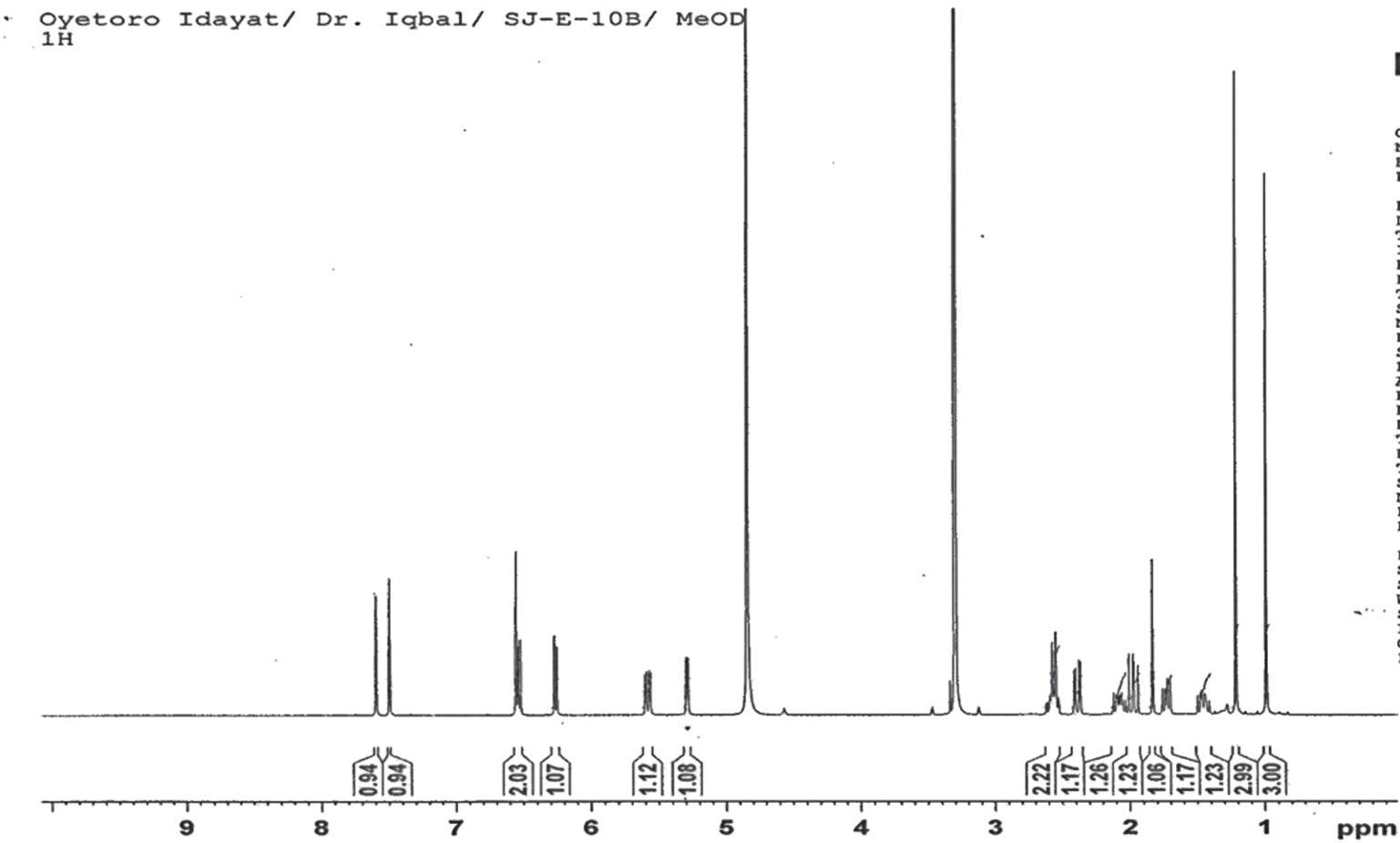

BRUKER

```
Current Data Parameters
NAME                  oct29-18
EXPNO                        1
PROCNO                       1

F2 - Acquisition Parameters
Date_                 20181029
Time                     15.08 h
INSTRUM                  spect
PROBHD    Z116098_0090 (
PULPROG                  zg30
TD                      32768
SOLVENT                  MeOD
NS                         64
DS                          0
SWH                   4807.692 Hz
FIDRES                0.293438 Hz
AQ                    3.4078720 sec
RG                       196.51
DW                      104.000 usec
DE                        6.50 usec
TE                       298.0 K
D1                    2.00000000 sec
TD0                          1
SFO1                400.2824017 MHz
NUC1                        1H
P1                       10.13 usec
PLW1                15.00000000 W

F2 - Processing parameters
SI                       16384
SF                  400.2800114 MHz
WDW                         EM
SSB                  0
LB                       0.30 Hz
GB                   0
PC                       1.00
```

Appendix X (d)

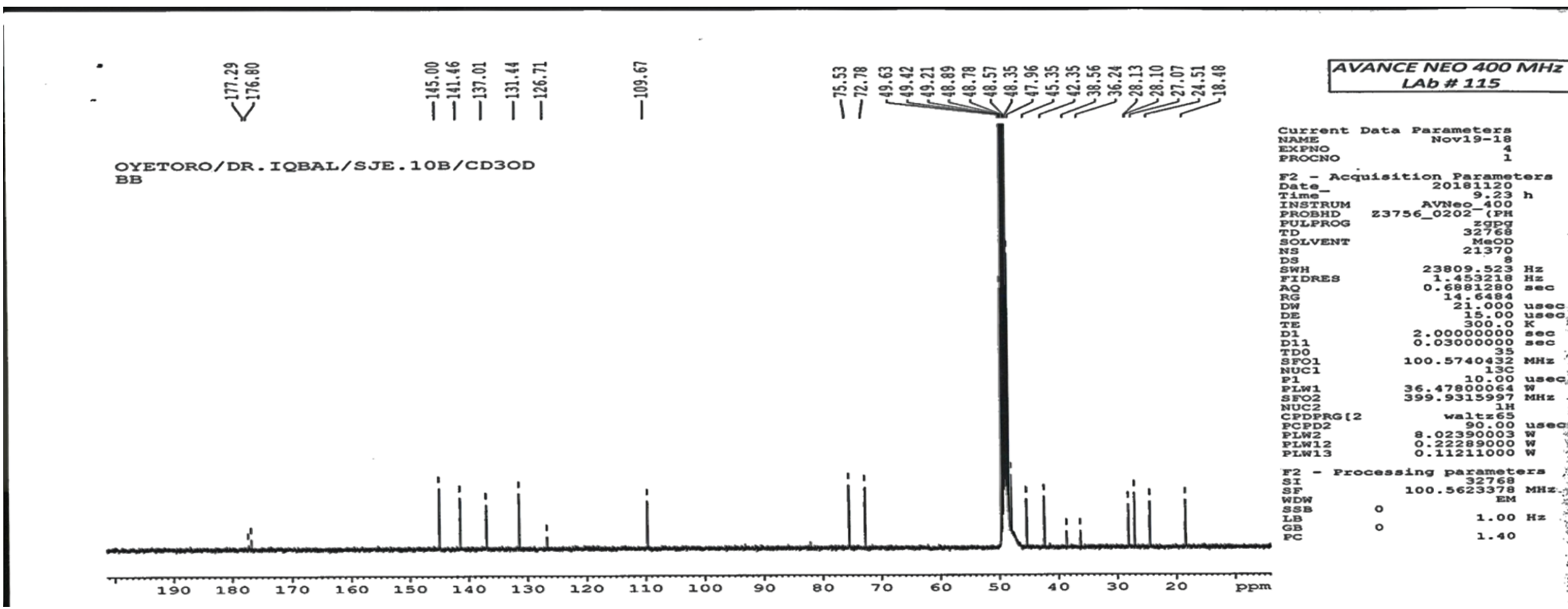
177.29
176.80
145.00
141.46
137.01
131.44
126.71
109.67
75.53
72.78
49.63
49.42
49.21
48.89
48.78
48.57
48.35
47.96
45.35
42.35
38.56
36.24
28.13
28.10
27.07
24.51
18.48
OYETORO/DR.IQBAL/SJE.10B/CD3OD
BB
AVANCE NEO 400 MHz
LAb # 115
Current Data Parameters
NAME Nov19-18
EXPNO 4
PROCNO 1
F2 - Acquisition Parameters
Date_ 20181120
Time 9.23 h
INSTRUM AVNeo_400
PROBHD Z3756_0202 (PH
PULPROG zgpg
TD 32768
SOLVENT MeOD
NS 21370
DS 8
SWH 23809.523 Hz
FIDRES 1.453218 Hz
AQ 0.6881280 sec
RG 14.6484
DW 21.000 usec
DE 15.00 usec
TE 300.0 K
D1 2.00000000 sec
D11 0.03000000 sec
TD0 35
SFO1 100.5740432 MHz
NUC1 13C
P1 10.00 usec
PLW1 36.47800064 W
SFO2 399.9315997 MHz
NUC2 1H
CPDPRG[2 waltz65
PCPD2 90.00 usec
PLW2 8.02390003 W
PLW12 0.22289000 W
PLW13 0.11211000 W
F2 - Processing parameters
SI 32768
SF 100.5623378 MHz
WDW EM
SSB 0
LB 1.00 Hz
GB 0
PC 1.40
190 180 170 160 150 140 130 120 110 100 90 80 70 60 50 40 30 20 ppm

Appendix X (e)

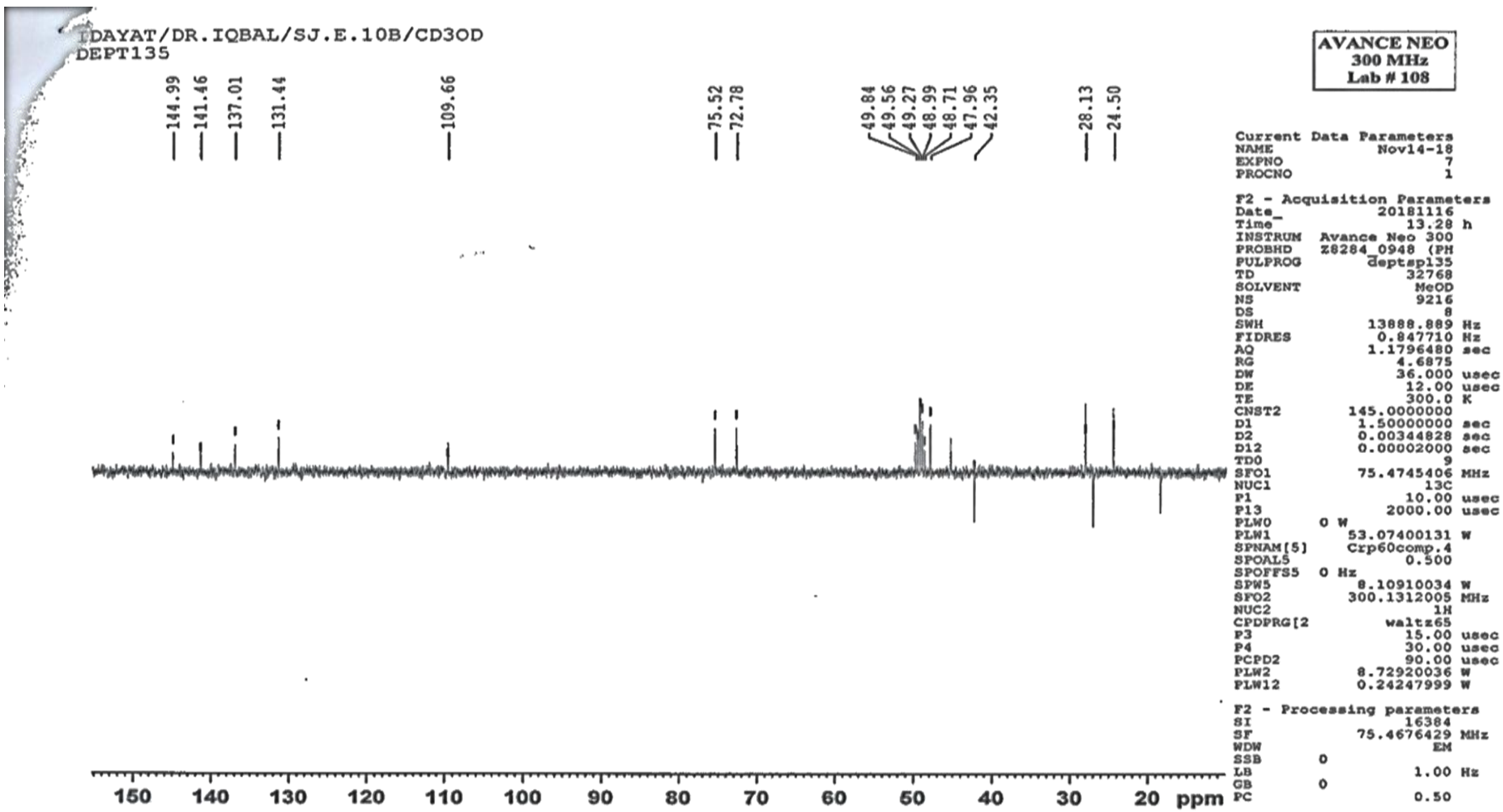
IDAYAT/DR.IQBAL/SJ.E.10B/CD3OD
DEPT135
144.99
141.46
137.01
131.44
109.66
75.52
72.78
49.84
49.56
49.27
48.99
48.71
47.96
42.35
28.13
24.50
150
140
130
120
110
100
90
80
70
60
50
40
30
20
ppm
AVANCE NEO
300 MHz
Lab # 108
Current Data Parameters
NAME Nov14-18
EXPNO 7
PROCNO 1
F2 - Acquisition Parameters
Date_ 20181116
Time 13.28 h
INSTRUM Avance Neo 300
PROBHD Z8284_0948 (PH
PULPROG deptsp135
TD 32768
SOLVENT MeOD
NS 9216
DS 8
SWH 13888.889 Hz
FIDRES 0.847710 Hz
AQ 1.1796480 sec
RG 4.6875
DW 36.000 usec
DE 12.00 usec
TE 300.0 K
CNST2 145.0000000
D1 1.50000000 sec
D2 0.00344828 sec
D12 0.00002000 sec
TD0 9
SFO1 75.4745406 MHz
NUC1 13C
P1 10.00 usec
P13 2000.00 usec
PLW0 0 W
PLW1 53.07400131 W
SPNAM[5] Crp60comp.4
SPOAL5 0.500
SPOFFS5 0 Hz
SPW5 8.10910034 W
SFO2 300.1312005 MHz
NUC2 1H
CPDPRG[2 waltz65
P3 15.00 usec
P4 30.00 usec
PCPD2 90.00 usec
PLW2 8.72920036 W
PLW12 0.24247999 W
F2 - Processing parameters
SI 16384
SF 75.4676429 MHz
WDW EM
SSB 0
LB 1.00 Hz
GB 0
PC 0.50

Appendix X (f)

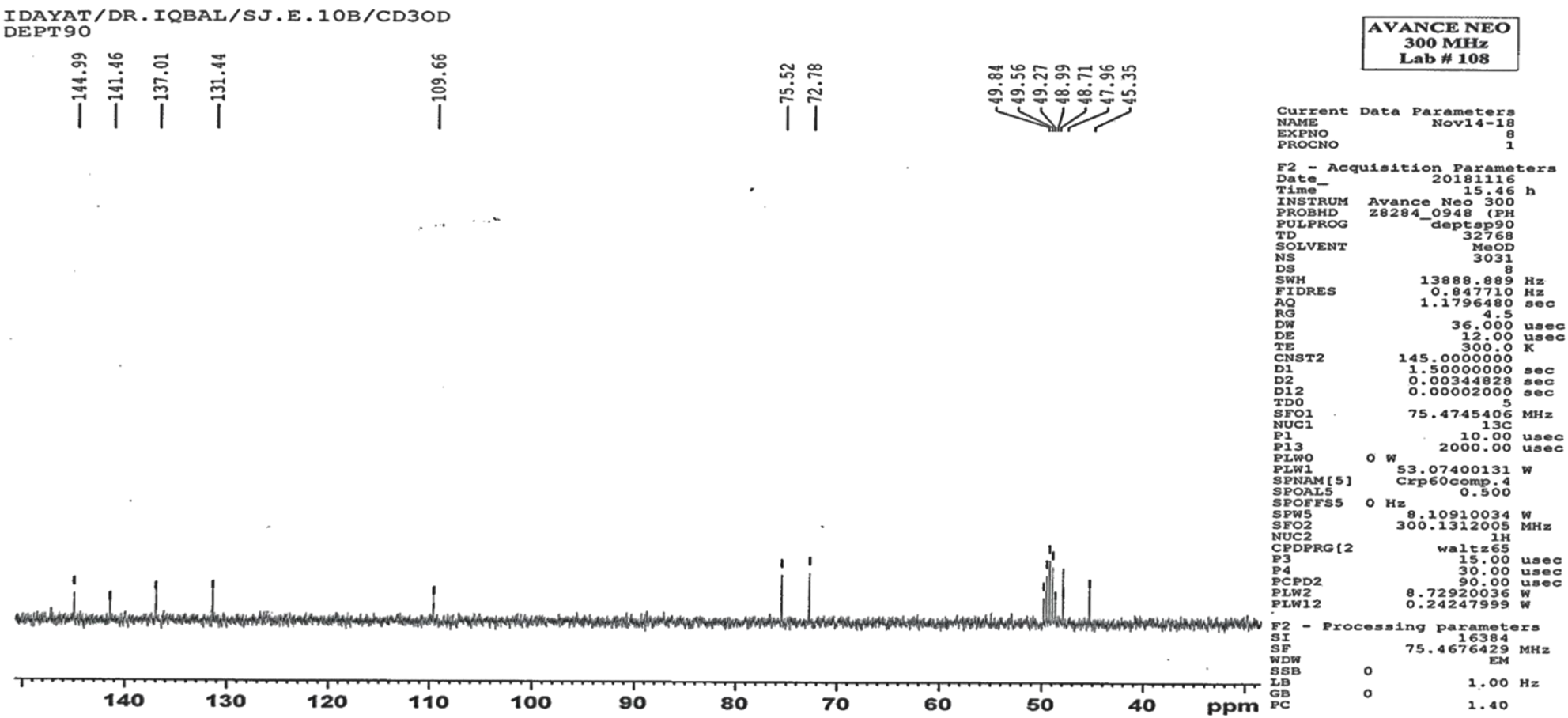
IDAYAT/DR.IQBAL/SJ.E.10B/CD3OD
DEPT90
144.99
141.46
137.01
131.44
109.66
75.52
72.78
49.84
49.56
49.27
48.99
48.71
47.96
45.35
140
130
120
110
100
90
80
70
60
50
40
ppm
AVANCE NEO
300 MHz
Lab # 108
Current Data Parameters
NAME Nov14-18
EXPNO 8
PROCNO 1
F2 - Acquisition Parameters
Date_ 20181116
Time_ 15.46 h
INSTRUM Avance Neo 300
PROBHD Z8284_0948 (PH
PULPROG deptsp90
TD 32768
SOLVENT MeOD
NS 3031
DS 8
SWH 13888.889 Hz
FIDRES 0.847710 Hz
AQ 1.1796480 sec
RG 4.5
DW 36.000 usec
DE 12.00 usec
TE 300.0 K
CNST2 145.0000000
D1 1.50000000 sec
D2 0.00344828 sec
D12 0.00002000 sec
TD0 5
SFO1 75.4745406 MHz
NUC1 13C
P1 10.00 usec
P13 2000.00 usec
PLW0 0 W
PLW1 53.07400131 W
SPNAM[5] Crp60comp.4
SPOAL5 0.500
SPOFFS5 0 Hz
SPW5 8.10910034 W
SFO2 300.1312005 MHz
NUC2 1H
CPDPRG[2 waltz65
P3 15.00 usec
P4 30.00 usec
PCPD2 90.00 usec
PLW2 8.72920036 W
PLW12 0.24247999 W
F2 - Processing parameters
SI 16384
SF 75.4676429 MHz
WDW EM
SSB 0
LB 1.00 Hz
GB 0
PC 1.40

Appendix X (g)

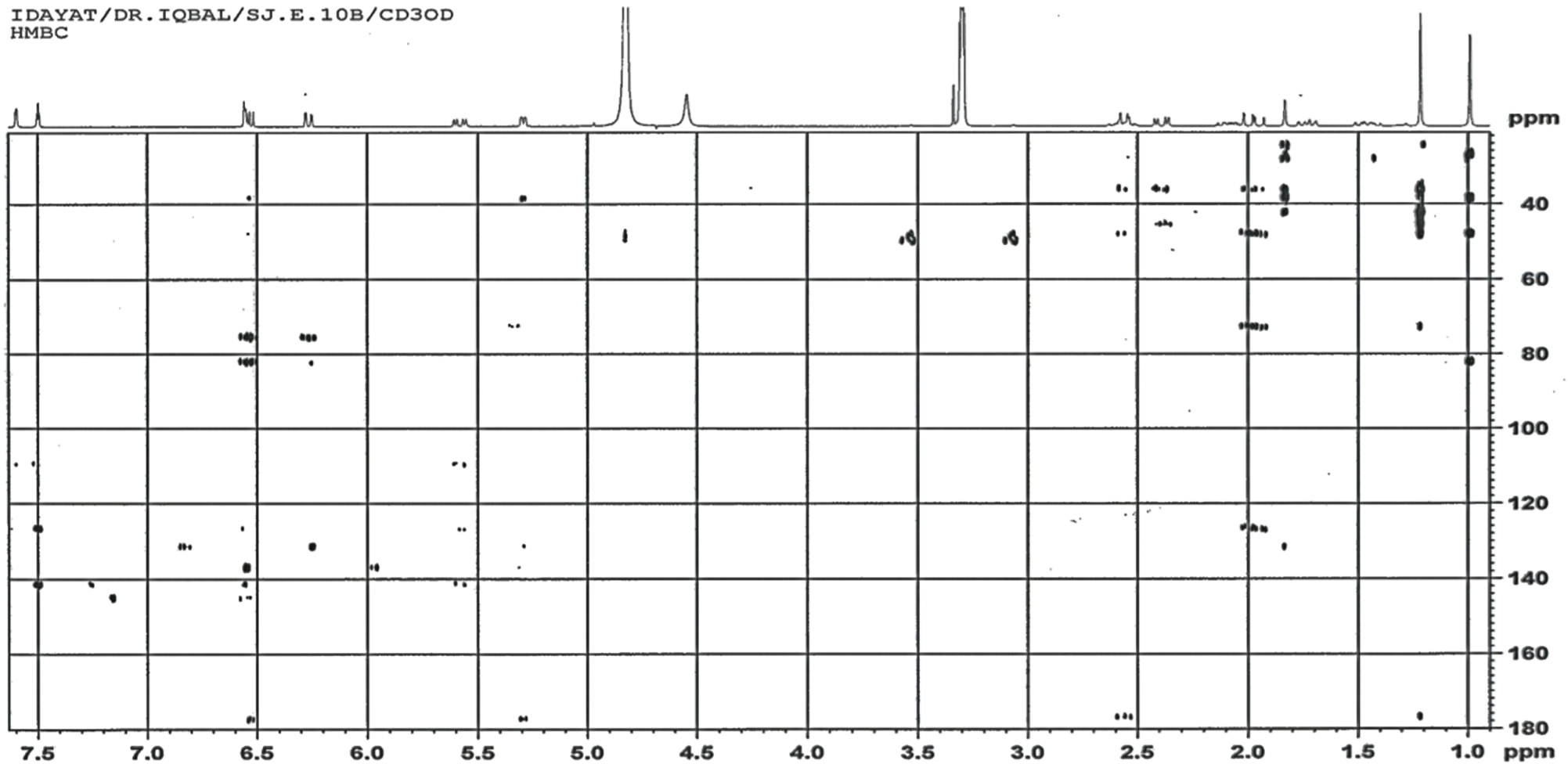
IDAYAT/DR.IQBAL/SJ.E.10B/CD3OD
HMBC
ppm
40
60
80
100
120
140
160
180
7.5
7.0
6.5
6.0
5.5
5.0
4.5
4.0
3.5
3.0
2.5
2.0
1.5
1.0
ppm

Appendix X (h)

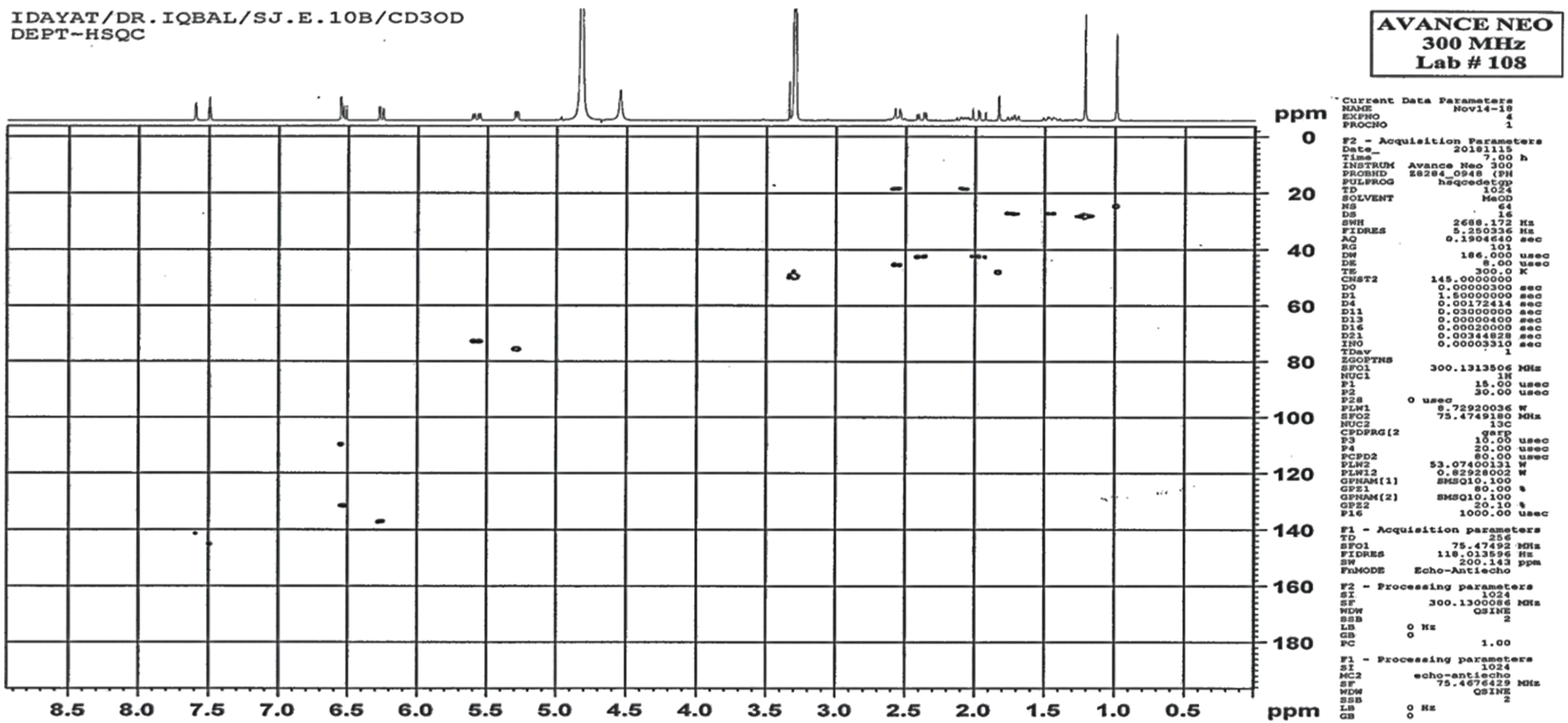
IDAYAT/DR.IQBAL/SJ.E.10B/CD3OD
DEPT-HSQC
AVANCE NEO
300 MHz
Lab # 108
ppm
0
20
40
60
80
100
120
140
160
180
8.5
8.0
7.5
7.0
6.5
6.0
5.5
5.0
4.5
4.0
3.5
3.0
2.5
2.0
1.5
1.0
0.5
ppm
Current Data Parameters
NAME Nov14-18
EXPNO 4
PROCNO 1
F2 - Acquisition Parameters
Date_ 20181115
Time 7.00 h
INSTRUM Avance Neo 300
PROBHD Z8264_0948 (PH
PULPROG hsqcedetgp
TD 1024
SOLVENT MeOD
NS 64
DS 16
SWH 2688.172 Hz
FIDRES 5.250336 Hz
AQ 0.1904640 sec
RG 101
DW 186.000 usec
DE 8.00 usec
TE 300.0 K
CNST2 145.0000000
D0 0.00000300 sec
D1 1.50000000 sec
D4 0.00172414 sec
D11 0.03000000 sec
D13 0.00000400 sec
D16 0.00020000 sec
D21 0.00344828 sec
IN0 0.00003310 sec
TDav 1
ZGOPTNS
SFO1 300.1313506 MHz
NUC1 1H
P1 15.00 usec
P2 30.00 usec
P28 0 usec
PLW1 8.72920036 W
SFO2 75.4749180 MHz
NUC2 13C
CPDPRG[2 garp
P3 10.00 usec
P4 20.00 usec
PCPD2 80.00 usec
PLW2 53.07400131 W
PLW12 0.82928002 W
GPNAM[1] SMSQ10.100
GPZ1 80.00 %
GPNAM[2] SMSQ10.100
GPZ2 20.10 %
P16 1000.00 usec
F1 - Acquisition parameters
TD 256
SFO1 75.47492 MHz
FIDRES 118.013596 Hz
SW 200.143 ppm
FnMODE Echo-Antiecho
F2 - Processing parameters
SI 1024
SF 300.1300086 MHz
WDW QSINE
SSB 2
LB 0 Hz
GB 0
PC 1.00
F1 - Processing parameters
SI 1024
MC2 echo-antiecho
SF 75.4676429 MHz
WDW QSINE
SSB 2
LB 0 Hz
GB 0

Appendix XI (a)

EI-MS, 1D and 2D NMR spectra of SJE-10C

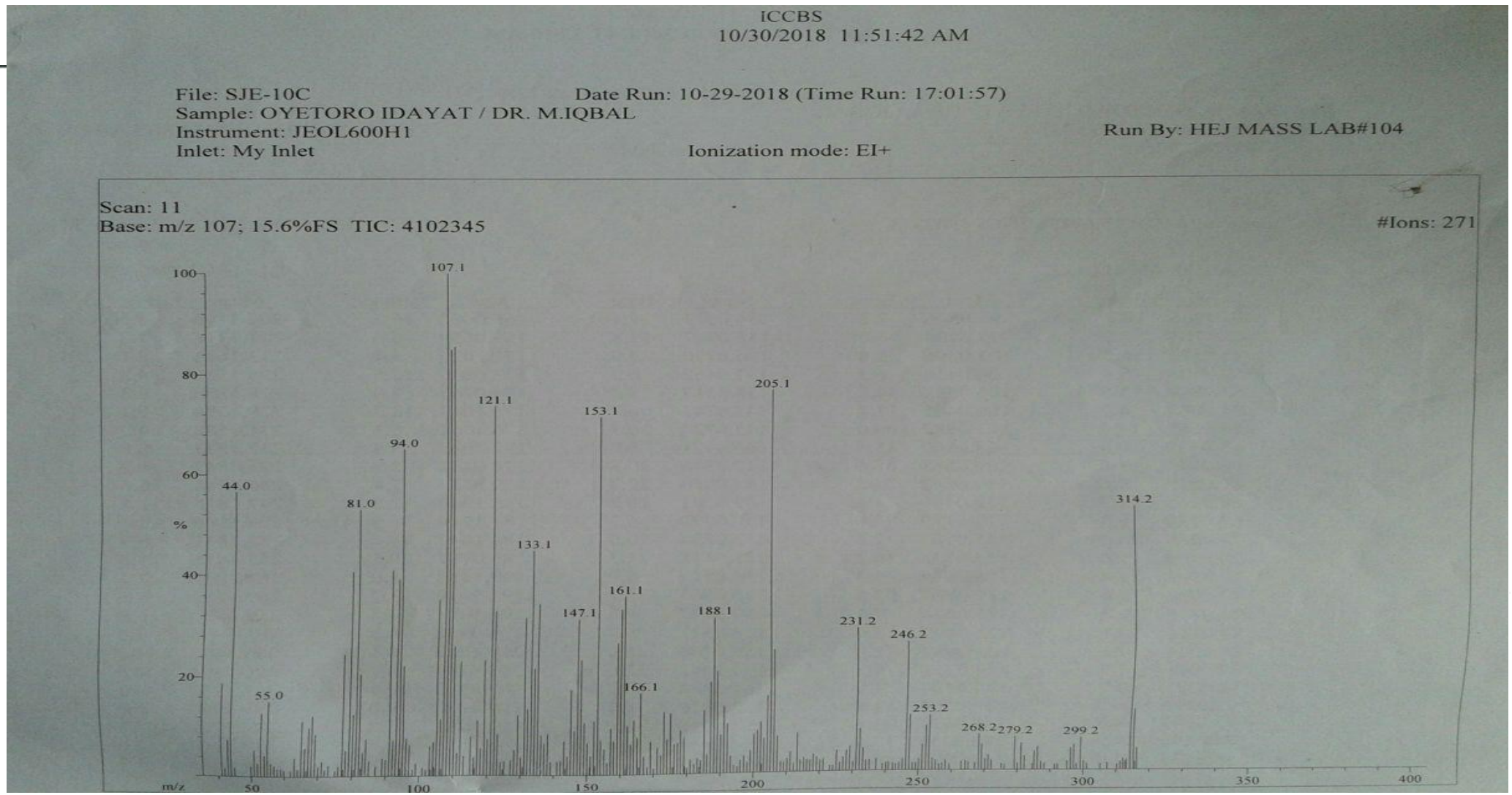

Appendix XI (b)

ICCBS
10/30/2018 11:52:10 AM

File: SJE-10C Date Run: 10-29-2018 (Time Run: 17:01:57)
Sample: OYETORO IDAYAT / DR. M.IQBAL
Instrument: JEOL600H1 Run By: HEJ MASS LAB#104
Inlet: My Inlet Ionization mode: EI+

Scan: 11
Base: m/z 107; 15.6%FS TIC: 4102345 #Ions: 271

Threshold: 4% of Base Displayed TIC: 4102345

Mass	%Base	Mass	%Base	Mass	%Base	Mass	%Base	Mass	%Base
40.9966	18.7	96.0506	7.2	134.0517	21.1	166.0602	16.2	207.1196	7.5
42.9704	7.5	97.0204	6.0	135.0747	33.8	169.0659	6.6	211.1146	4.1
43.9573	56.5	103.0396	5.8	136.0730	7.9	171.1026	5.4	213.1611	8.1
50.9598	5.4	104.0436	6.5	137.0462	6.2	173.0829	12.5	225.1530	4.3
52.9880	12.5	105.0523	34.8	138.0517	8.0	174.0763	7.0	228.1859	4.3
54.0085	4.2	106.0405	11.1	143.0742	6.7	175.1043	12.2	229.1390	5.1
54.9651	14.9	107.0587	100.0	145.0724	16.9	176.1351	6.1	231.1588	29.2
65.0339	10.9	108.0560	85.1	146.0471	8.7	177.1042	6.4	232.1523	8.8
66.0211	5.6	109.0578	85.6	147.0546	30.8	178.0438	8.9	233.1843	4.8
67.0559	9.6	110.0642	25.5	148.0656	22.8	179.0513	7.4	246.1568	26.6
68.0161	11.7	111.0489	4.4	149.0501	10.2	185.1040	12.8	247.1815	11.6
69.0238	8.3	112.0119	22.6	150.0379	6.3	187.1018	18.5	251.1100	5.4
77.0286	24.0	115.0563	7.6	152.0534	10.6	188.1047	31.1	252.1831	9.3
78.0309	5.0	117.0718	10.8	153.0813	71.3	189.0767	20.6	253.1815	11.5
79.0393	40.4	118.0856	5.3	154.0519	6.9	190.1182	8.0	268.2072	7.4
80.0539	12.0	119.0767	22.8	155.0865	5.1	191.0949	13.7	269.1953	5.3
81.0302	52.8	120.0444	7.1	157.1047	9.1	192.1075	10.2	279.1891	6.8
82.0346	20.1	121.0697	73.6	158.0571	6.7	199.0901	4.6	281.1674	5.5
83.0224	4.6	122.0987	32.5	159.0740	26.0	200.1555	8.1	286.1898	4.7
83.9933	7.2	123.0771	8.1	160.0942	32.6	201.1544	8.7	296.1998	4.5
91.0377	40.7	128.0503	4.9	161.0864	35.2	202.1552	10.4	297.1977	5.1
92.0296	6.9	129.0504	11.8	162.0816	9.7	203.1235	7.0	299.1993	6.6
93.0507	38.9	131.0621	31.1	163.0798	6.0	204.1283	15.8	314.2200	53.3
94.0296	64.9	132.0455	13.0	164.0495	10.8	205.1349	76.8	315.2407	12.5
95.0134	21.7	133.0609	44.4	165.0848	7.4	206.1436	24.9	316.2635	4.4

Appendix XI (c)

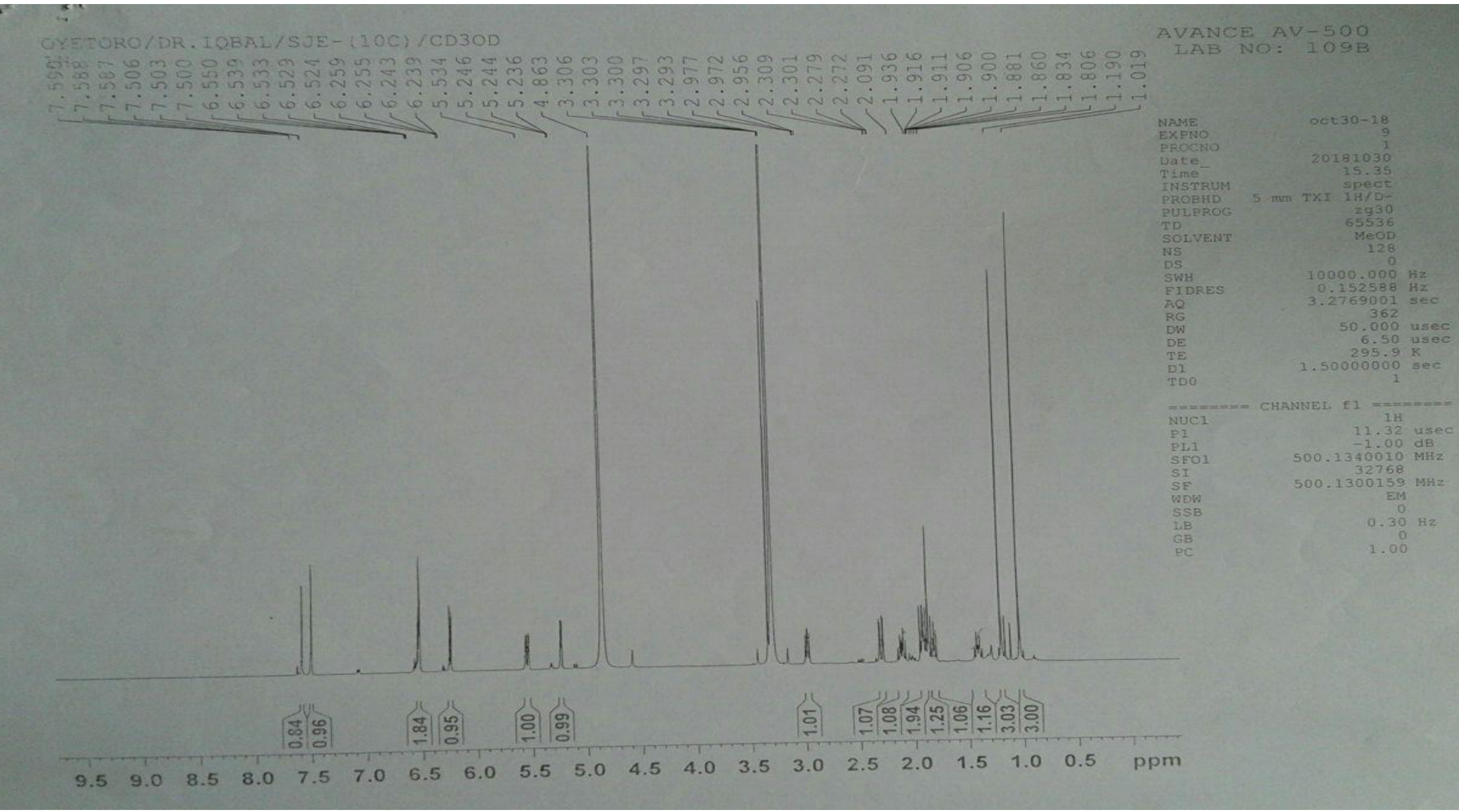

Appendix XI (d)

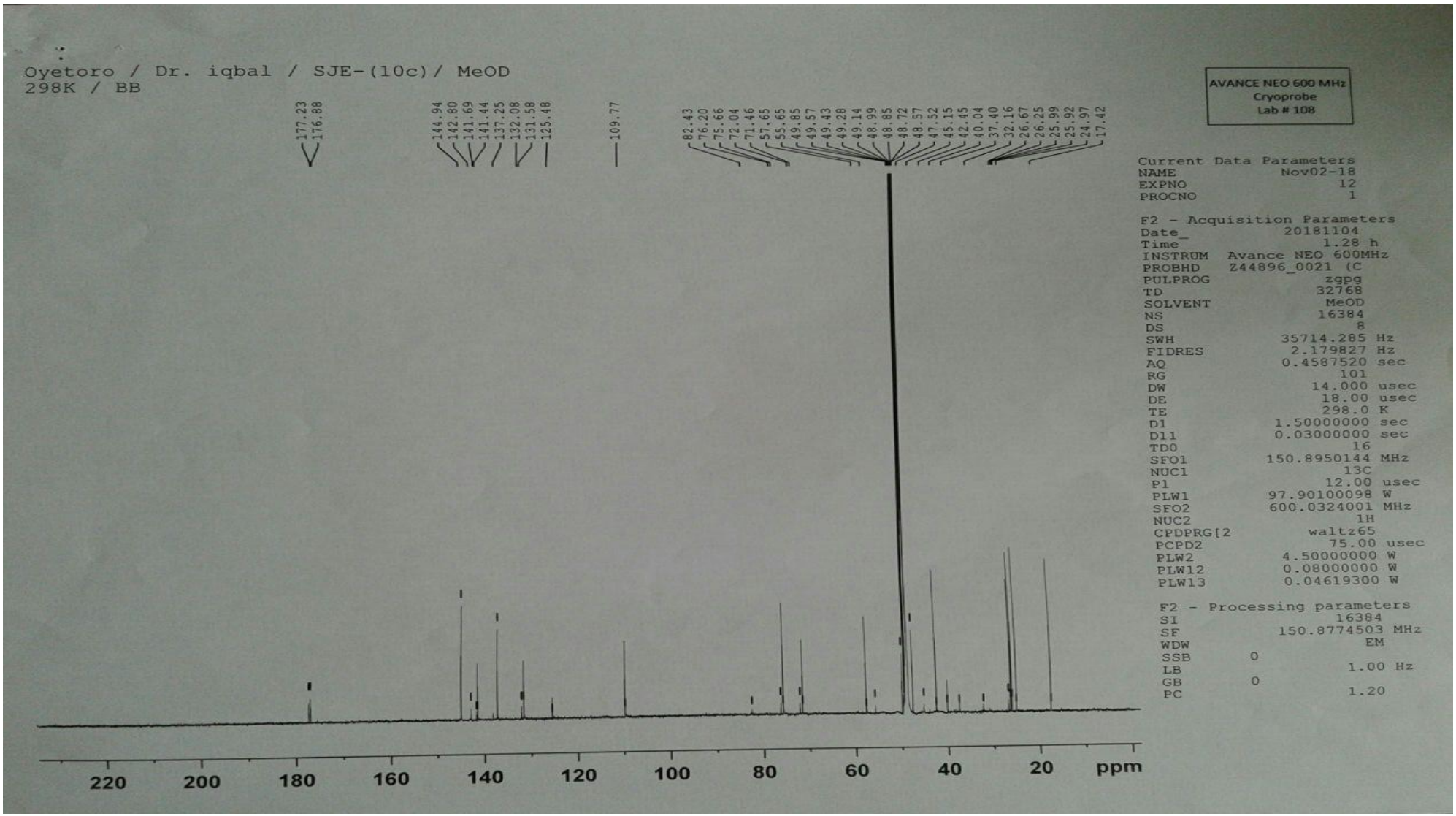

Appendix XI (e)

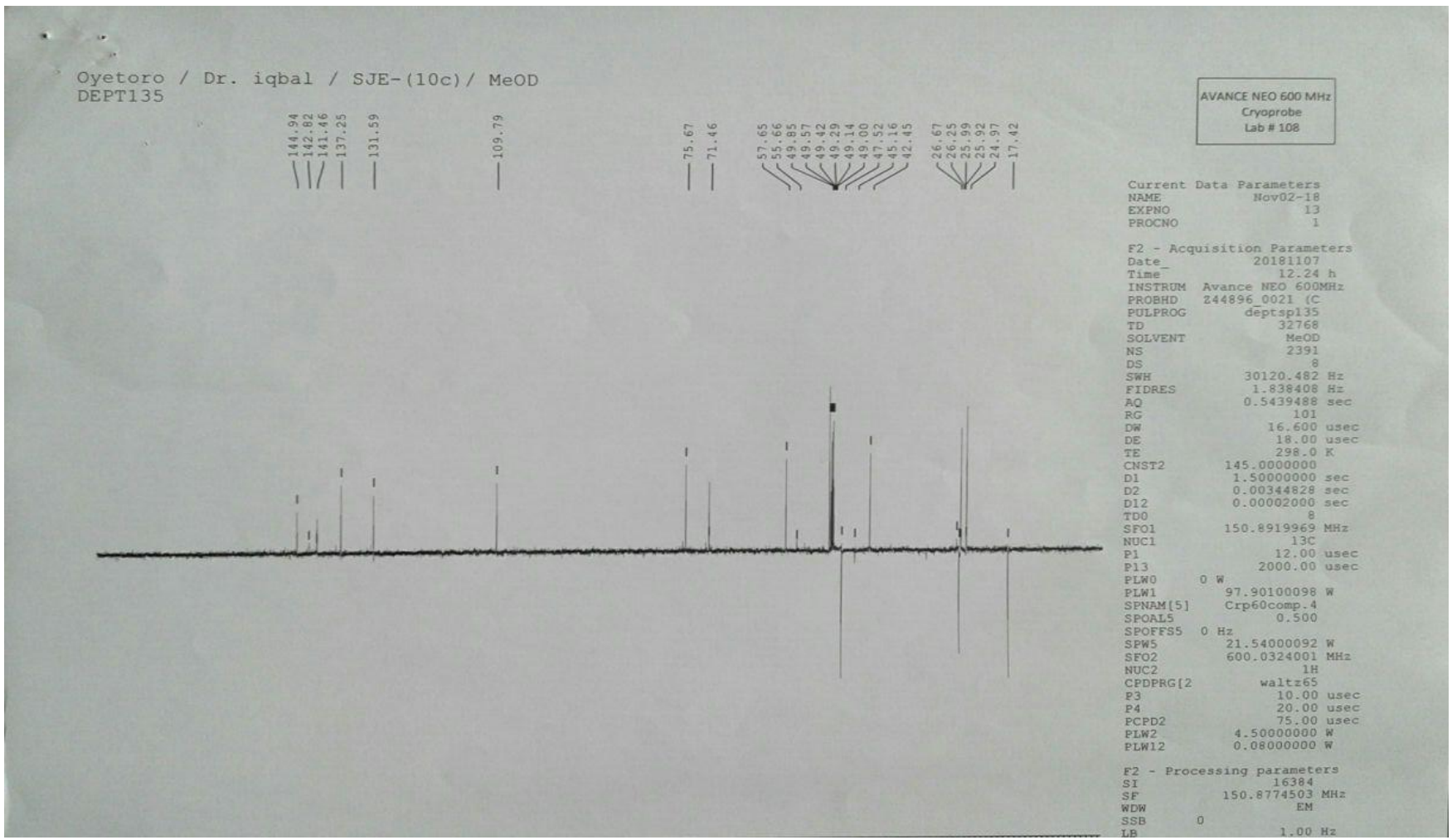

Appendix XI (f)

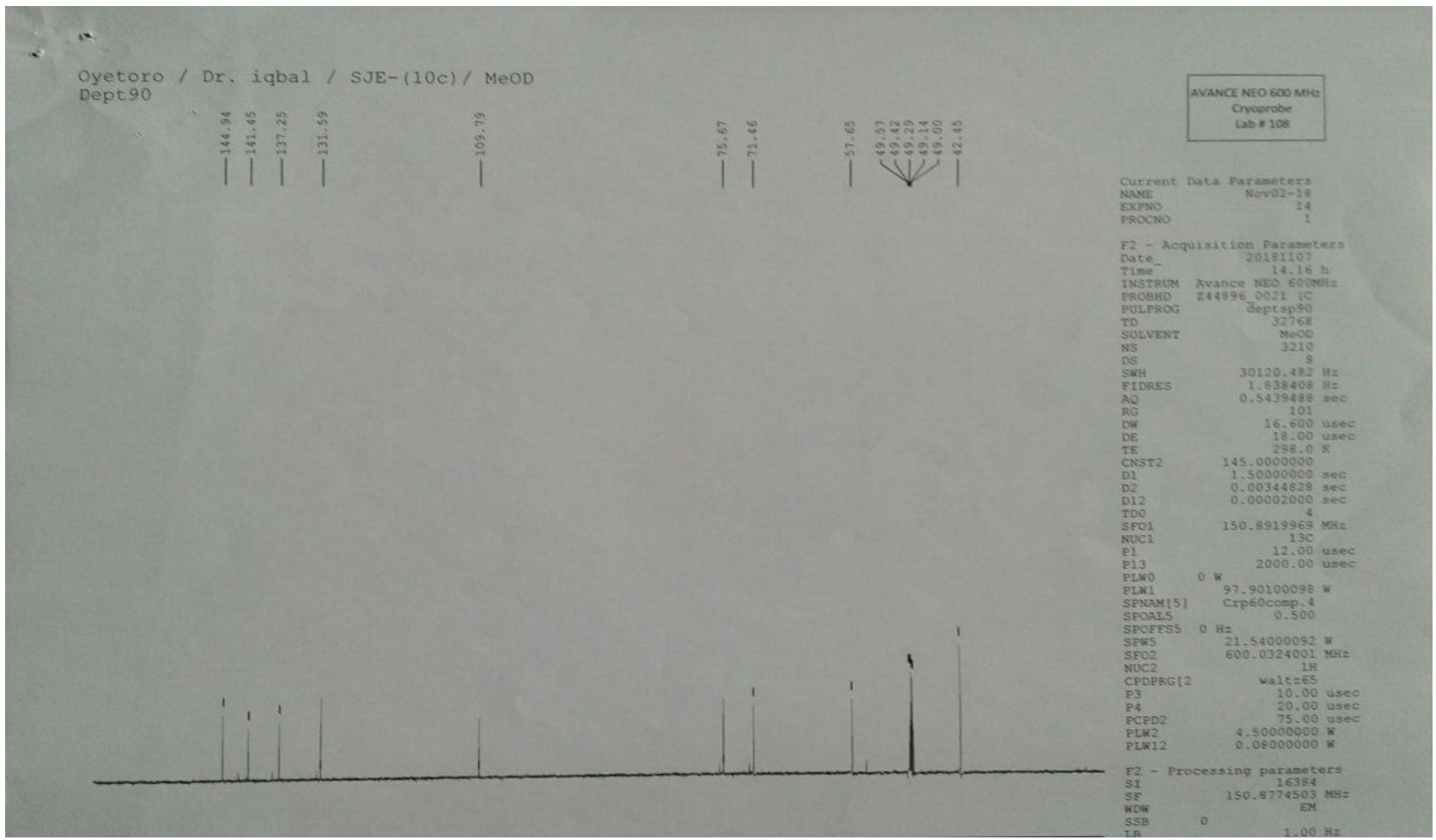

Appendix XI (g)

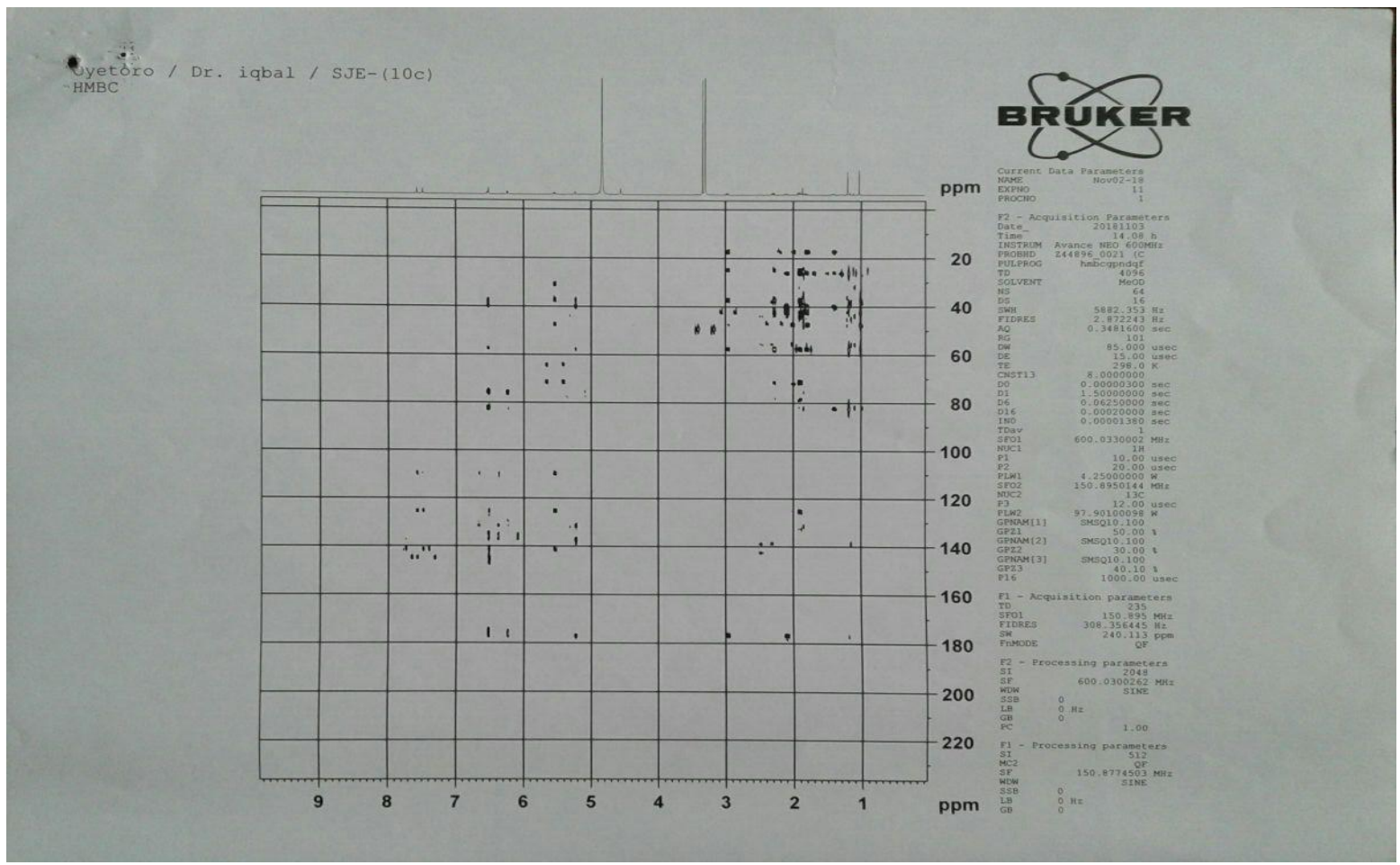

Appendix XI (h)

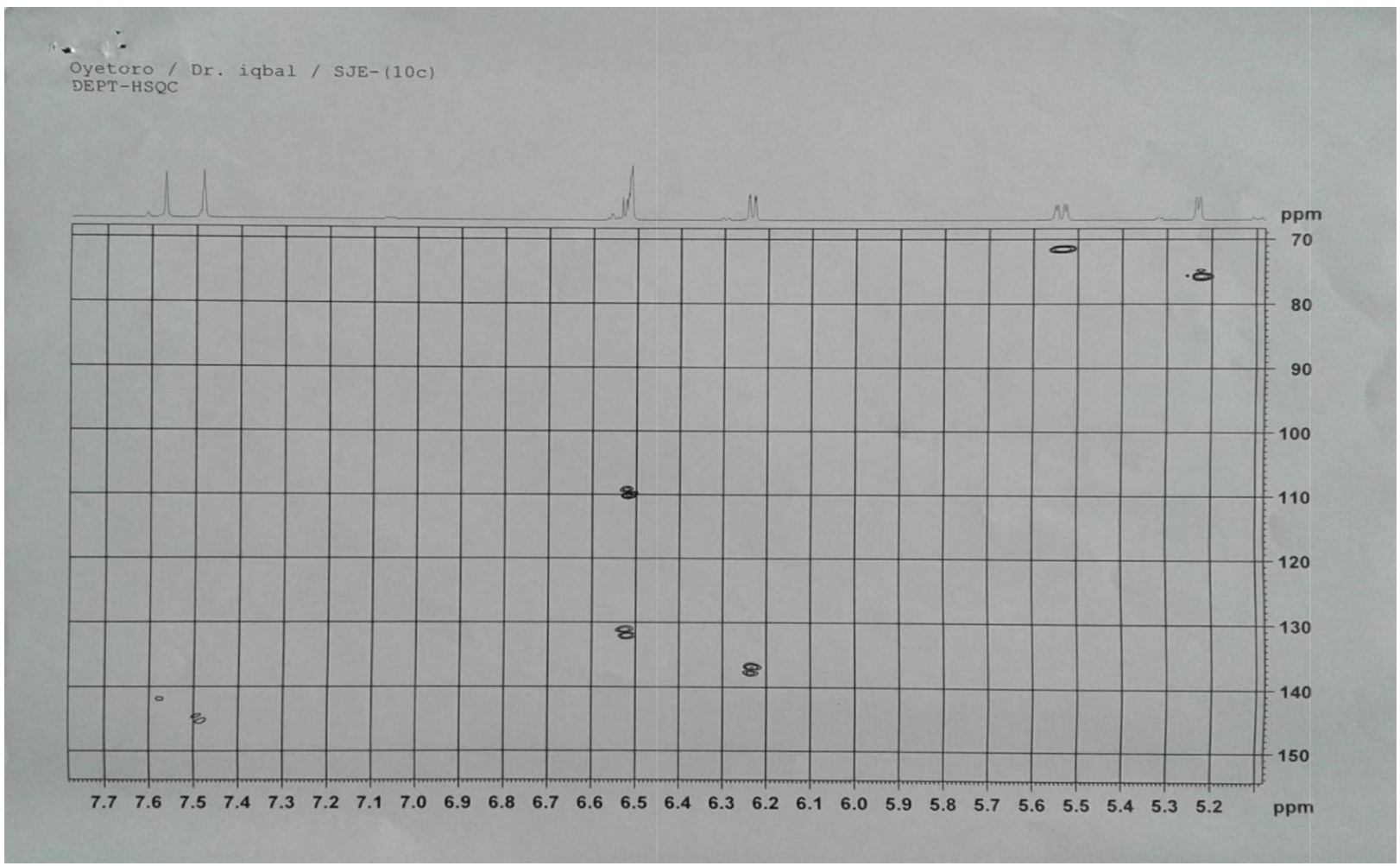

Appendix XI (i)

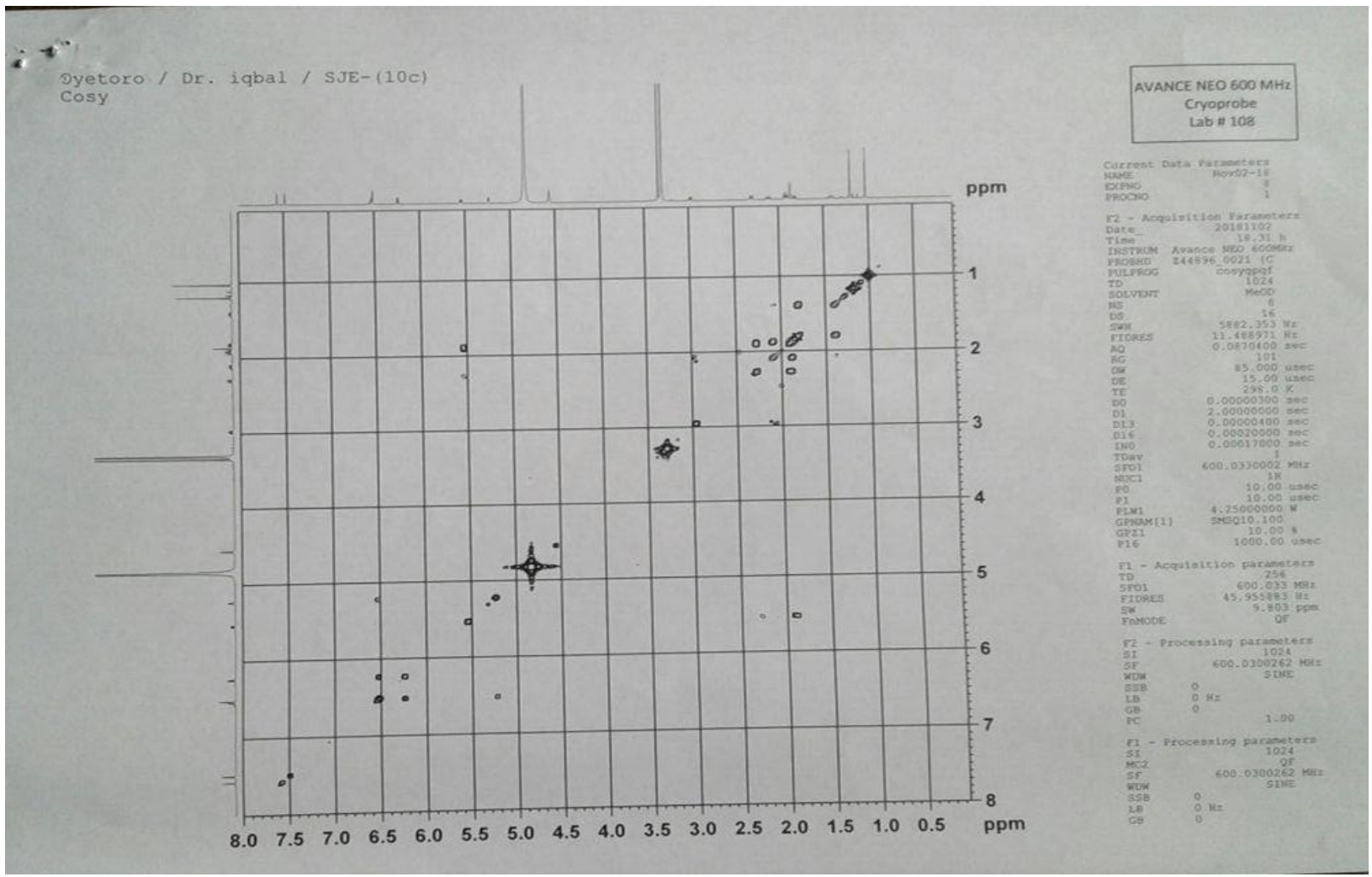

Appendix XII (a)

EI-MS, 1D and 2D NMR spectra of SJE 23D

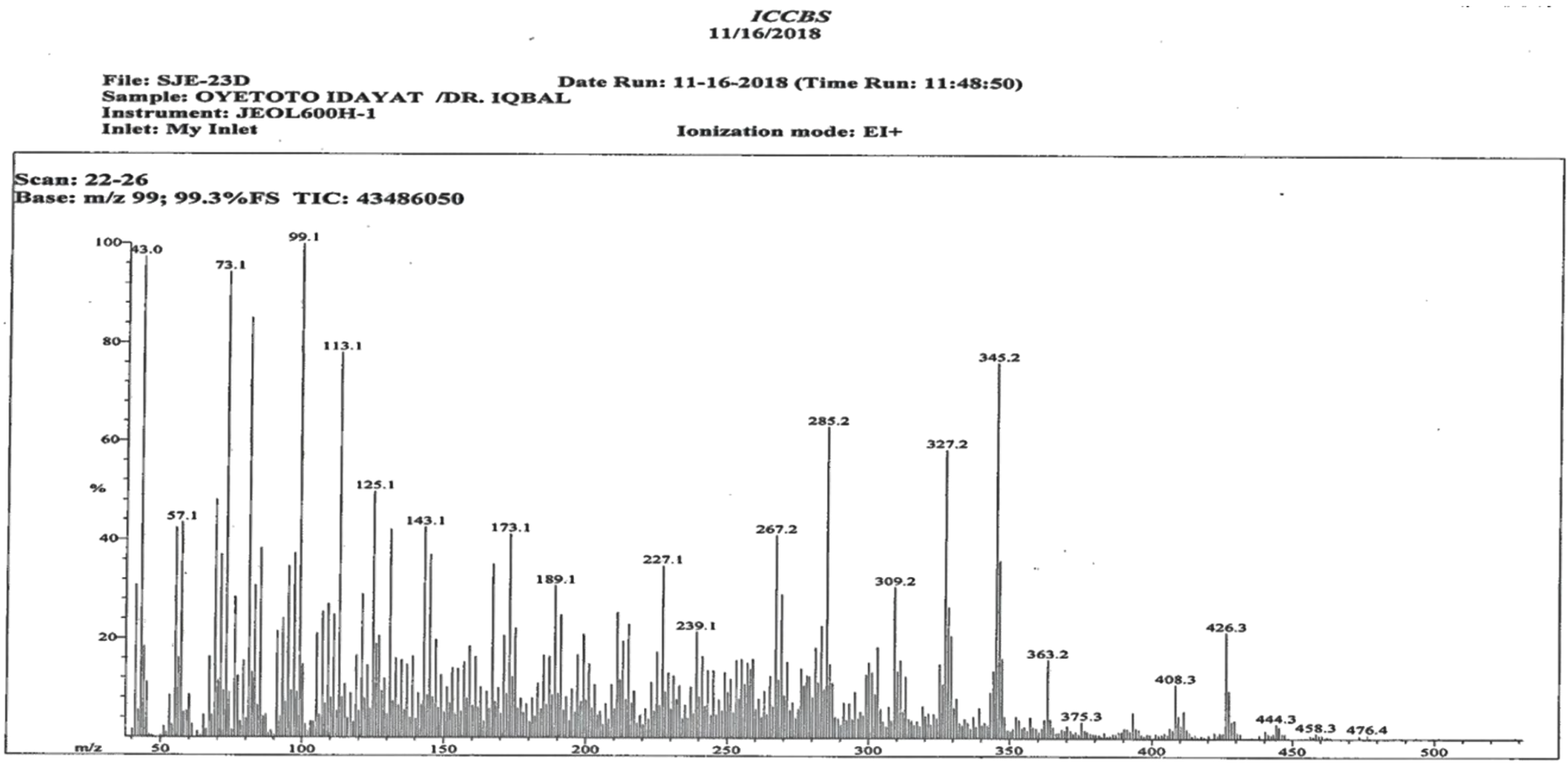

Appendix XII (b)

ICCBS
11/16/2018

File: SJE-23D **Date Run: 11-16-2018 (Time Run: 11:48:50)**
Sample: OYETOTO IDAYAT /DR. IQBAL
Instrument: JEOL600H-1
Inlet: My Inlet **Ionization mode: EI+**

Scan: 22-26
Base: m/z 99; 99.3%FS TIC: 43486050

Threshold: 6% of Base **Displayed TIC: 43486050**

Mass	%Base	Mass	%Base	Mass	%Base	Mass	%Base	Mass	%Base	Mass	%Base
41.0	30.9	95.1	34.7	133.1	16.1	169.1	10.0	211.1	25.4	251.2	11.9
43.0	97.4	96.1	9.5	134.1	6.5	171.1	20.7	212.1	11.7	253.2	15.7
44.0	18.4	97.1	37.3	135.1	15.7	172.1	8.8	213.1	19.6	254.2	7.9
45.0	11.2	98.1	9.1	137.1	14.7	173.1	41.2	214.1	7.7	255.2	16.0
53.1	8.6	99.1	100.0	139.1	16.5	174.1	12.3	215.1	23.0	256.2	10.9
55.1	42.4	100.1	14.8	141.1	9.0	175.1	22.2	216.1	7.0	257.2	15.2
56.1	16.1	105.1	21.1	142.1	6.6	177.1	7.9	217.1	9.5	258.2	13.9
57.1	43.4	107.1	25.5	143.1	42.6	179.1	6.8	223.1	11.2	259.2	16.0
60.0	8.6	108.1	6.9	144.1	8.6	181.1	8.0	225.1	17.4	261.2	8.0
67.1	16.3	109.1	27.1	145.1	37.1	183.1	11.1	226.1	6.5	263.2	9.5
69.1	48.0	110.1	8.1	146.1	8.2	185.1	16.7	227.1	34.9	265.2	12.6
70.1	11.4	111.1	24.9	147.1	19.8	186.1	6.7	228.1	9.3	266.2	6.3
71.1	37.0	113.1	78.1	149.1	12.6	187.1	16.5	229.1	13.2	267.2	41.1
72.1	9.5	114.1	8.3	151.1	10.2	188.1	8.7	231.1	12.6	268.2	11.8
73.1	94.3	115.1	10.8	152.1	6.8	189.1	30.8	232.1	7.8	269.2	29.1
74.0	9.1	117.1	8.9	153.1	14.1	190.1	8.9	233.1	10.6	270.2	8.5
76.0	28.5	119.1	16.7	155.1	13.9	191.1	24.9	235.1	6.7	271.2	15.5
77.0	12.5	121.1	29.0	157.1	15.3	193.1	8.2	237.1	10.3	273.2	7.2
79.1	15.6	122.1	7.8	158.1	7.9	195.1	9.7	239.1	21.5	276.1	14.1
81.1	85.1	123.1	14.7	159.1	18.5	197.1	16.8	240.1	8.3	277.2	10.5
82.1	13.2	125.1	49.7	160.1	6.4	198.1	7.3	241.1	16.5	278.1	12.7
83.1	30.8	126.1	18.9	161.1	16.4	199.2	21.0	242.1	6.4	279.1	12.5
84.1	6.5	127.1	20.7	162.1	6.1	200.2	7.6	243.1	13.7	280.1	8.3
85.1	38.3	128.1	9.4	163.1	10.2	201.1	14.9	245.1	13.7	281.1	18.3
91.1	21.5	129.1	12.0	165.1	9.3	203.1	10.8	247.1	7.7	282.2	11.2
93.1	24.2	131.1	42.1	167.2	35.1	207.1	6.8	249.2	13.2	283.1	22.7
94.1	7.2	132.1	7.3	168.1	7.3	209.1	10.8	250.2	9.3	284.2	9.9

Appendix XII (c)

11/16/2018

File: SJE-23D Date Run: 11-16-2018 (Time Run: 11:48:50)
Sample: OYETOTO IDAYAT /DR. IQBAL
Instrument: JEOL600H-1
Inlet: My Inlet Ionization mode: EI+

Scan: 22-26
Base: m/z 99; 99.3%FS TIC: 43486050

Threshold: 1% of Base

Displayed TIC: 43486050

Mass	%Base	Mass	%Base	Mass	%Base	Mass	%Base	Mass	%Base	Mass	%Base
280.1	8.3	302.2	9.0	324.2	4.0	346.2	36.0	368.3	1.8	410.3	2.6
281.1	18.3	303.2	18.4	325.2	15.0	347.2	16.1	369.3	1.6	411.3	5.5
282.2	11.2	304.2	6.0	326.2	10.9	348.2	4.3	370.3	2.5	412.3	1.9
283.1	22.7	305.2	3.3	327.2	58.4	349.2	1.6	371.3	1.6	413.2	1.3
284.2	9.9	306.2	2.4	328.2	26.6	350.3	1.4	373.3	1.3	422.3	1.2
285.2	63.0	307.1	6.4	329.2	20.8	351.2	2.0	375.3	3.3	424.3	1.2
286.2	15.0	308.1	3.6	330.2	6.1	352.2	4.3	376.3	1.7	425.3	1.1
287.2	11.2	309.2	30.7	331.2	8.0	353.3	3.7	377.3	1.3	426.3	21.5
288.2	4.3	310.2	13.5	332.2	3.1	354.3	2.1	383.2	1.2	427.3	9.6
289.2	3.9	311.2	15.9	333.2	2.5	355.2	2.3	388.3	1.3	428.3	3.4
290.2	2.6	312.2	5.3	334.2	3.9	356.2	1.6	389.3	1.4	429.3	3.7
291.2	7.2	313.2	12.5	335.2	3.1	357.2	4.3	390.3	2.1	430.3	1.3
292.2	3.6	314.2	3.9	336.2	1.9	358.3	2.2	391.3	2.0	431.4	1.0
293.2	7.0	315.2	3.6	337.2	4.3	359.2	2.0	392.3	1.5	440.3	1.6
294.2	3.8	316.2	2.7	338.2	2.4	360.3	1.3	393.3	5.3	443.3	1.0
295.2	9.4	317.2	3.5	339.2	6.2	361.2	2.0	394.3	2.0	444.3	3.0
296.2	4.0	318.2	2.5	340.2	2.7	362.2	3.8	395.3	1.8	445.3	2.4
297.2	5.4	319.2	6.5	341.2	3.1	363.2	15.9	404.3	1.2	446.3	1.1
298.2	4.6	320.2	4.5	342.2	2.5	364.2	3.8	406.3	2.1	447.3	1.0
299.2	12.8	321.2	5.0	343.2	9.2	365.3	2.3	407.3	1.7	458.3	1.2
300.2	15.3	322.2	2.8	344.2	13.6	366.3	1.0	408.3	10.9		
301.2	13.3	323.2	4.9	345.2	76.2	367.3	1.1	409.3	4.5		

Appendix XII (d)

ICCBS
11/16/2018

File: SJE-23D **Date Run: 11-16-2018 (Time Run: 11:48:50)**
Sample: OYETOTO IDAYAT /DR. IQBAL
Instrument: JEOL600H-1
Inlet: My Inlet **Ionization mode: EI+**

Scan: 22-26
Base: m/z 99; 99.3%FS TIC: 43486050

(Continued)

Threshold: 6% of Base **Displayed TIC: 43486050**

Mass	%Base	Mass	%Base	Mass	%Base	Mass	%Base	Mass	%Base	Mass	%Base
285.2	63.0	286.2	15.0	287.2	11.2						

Appendix XII (e)

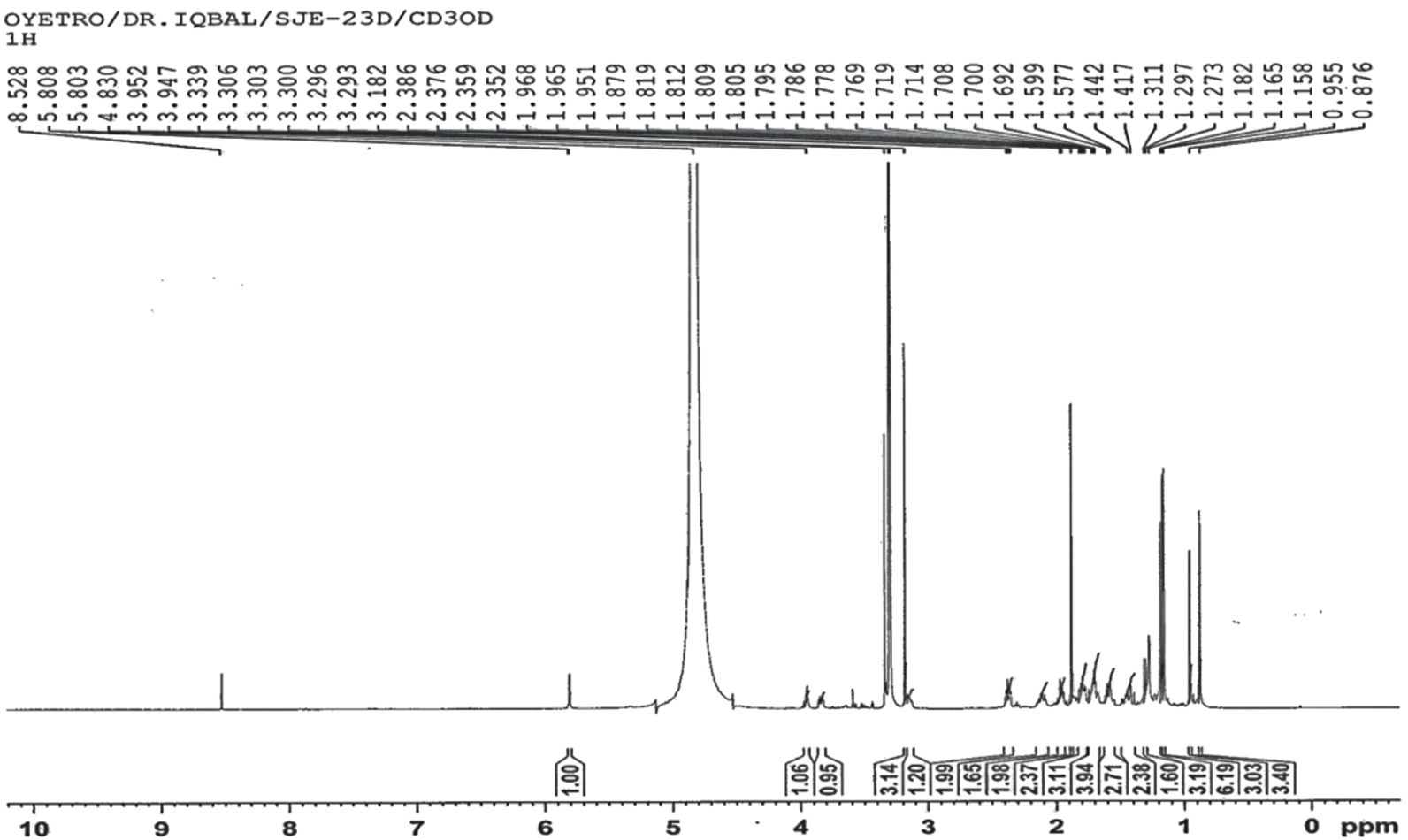

AVANCE NEO 500 MHz
Cryoprobe
Lab # 108

Current Data Parameters	
NAME	Nov20-18
EXPNO	1
PROCNO	1
F2 - Acquisition Parameters	
Date_	20181120
Time	15.57 h
INSTRUM	Avance Neo 500
PROBHD	Z44862_0021 (C
PULPROG	zg30
TD	32768
SOLVENT	MeOD
NS	128
DS	0
SWH	10000.000 Hz
FIDRES	0.610352 Hz
AQ	1.6384000 sec
RG	62.779
DW	50.000 usec
DE	25.00 usec
TE	298.0 K
D1	1.50000000 sec
TD0	1
SFO1	500.3340026 MHz
NUC1	1H
P0	5.00 usec
P1	15.00 usec
PLW1	9.74149990 W
F2 - Processing parameters	
SI	32768
SF	500.3300145 MHz
WDW	EM
SSB	0
LB	0.30 Hz
GB	0
PC	1.00

Appendix XII (f)

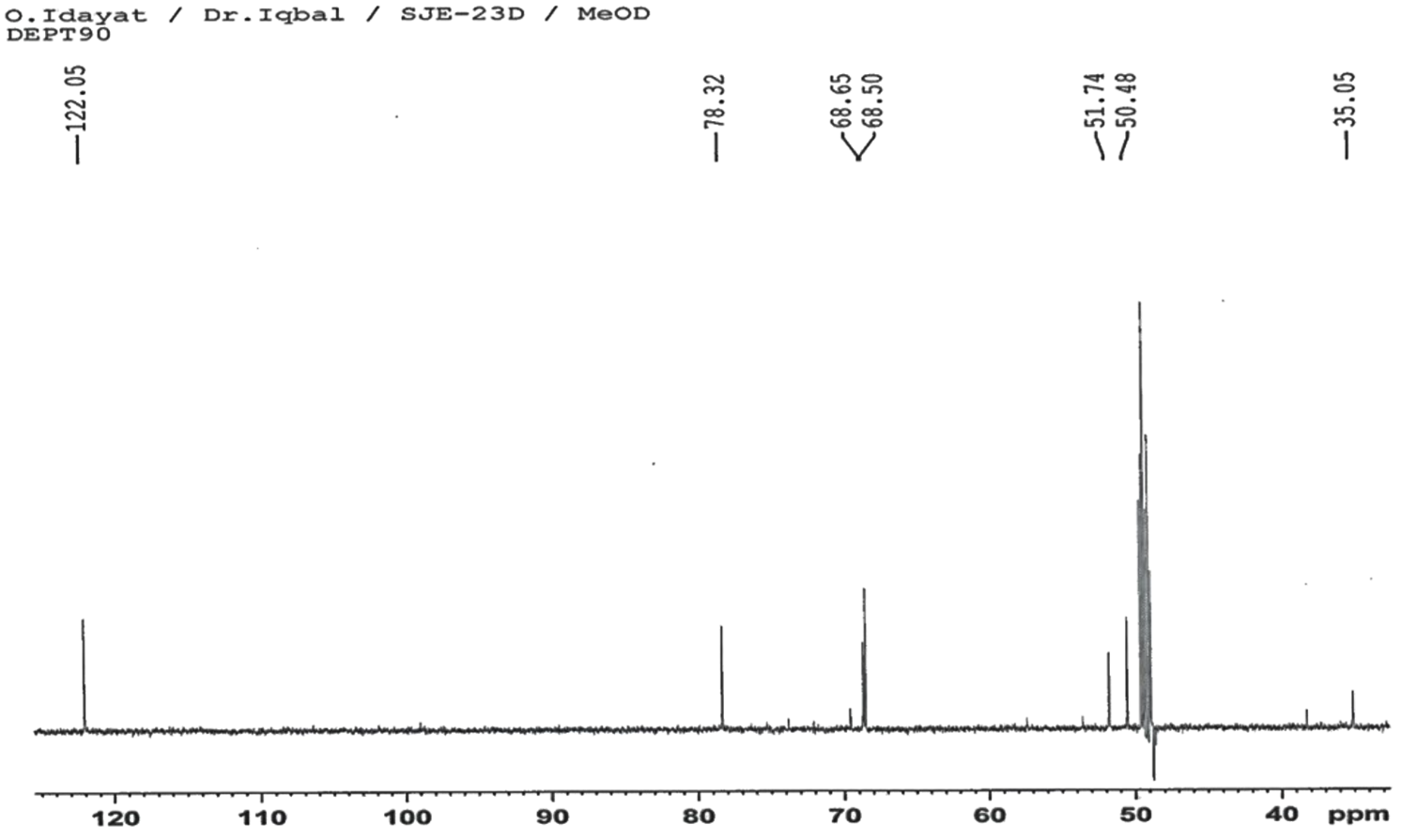

BRUKER

Current Data Parameters
NAME Nov28-18
EXPNO 8
PROCNO 1

F2 - Acquisition Parameters
Date_ 20181129
Time 10.46 h
INSTRUM AVNeo_600
PROBHD Z117768_0039 (
PULPROG deptsp90
TD 32768
SOLVENT MeOD
NS 1066
DS 8
SWH 30120.482 Hz
FIDRES 1.838408 Hz
AQ 0.5439488 sec
RG 101
DW 16.600 usec
DE 18.00 usec
TE 298.0 K
CNST2 145.0000000
D1 2.00000000 sec
D2 0.00344828 sec
D12 0.00002000 sec
TD0 2
SFO1 150.9523507 MHz
NUC1 13C
P1 12.00 usec
P13 2000.00 usec
PLW0 0 W
PLW1 107.76000214 W
SPNAM[5] Crp60comp.4
SPOAL5 0.500
SPOFFS5 0 Hz
SPW5 23.70800018 W
SFO2 600.2724011 MHz
NUC2 1H
CPDPRG[2 waltz65
P3 8.00 usec
P4 16.00 usec
PCPD2 70.00 usec
PLW2 9.53950024 W
PLW12 0.12460000 W

F2 - Processing parameters
SI 16384
SF 150.9378068 MHz
WDW EM
SSB 0
LB 1.00 Hz
GB 0
PC 1.40

Appendix XII (g)

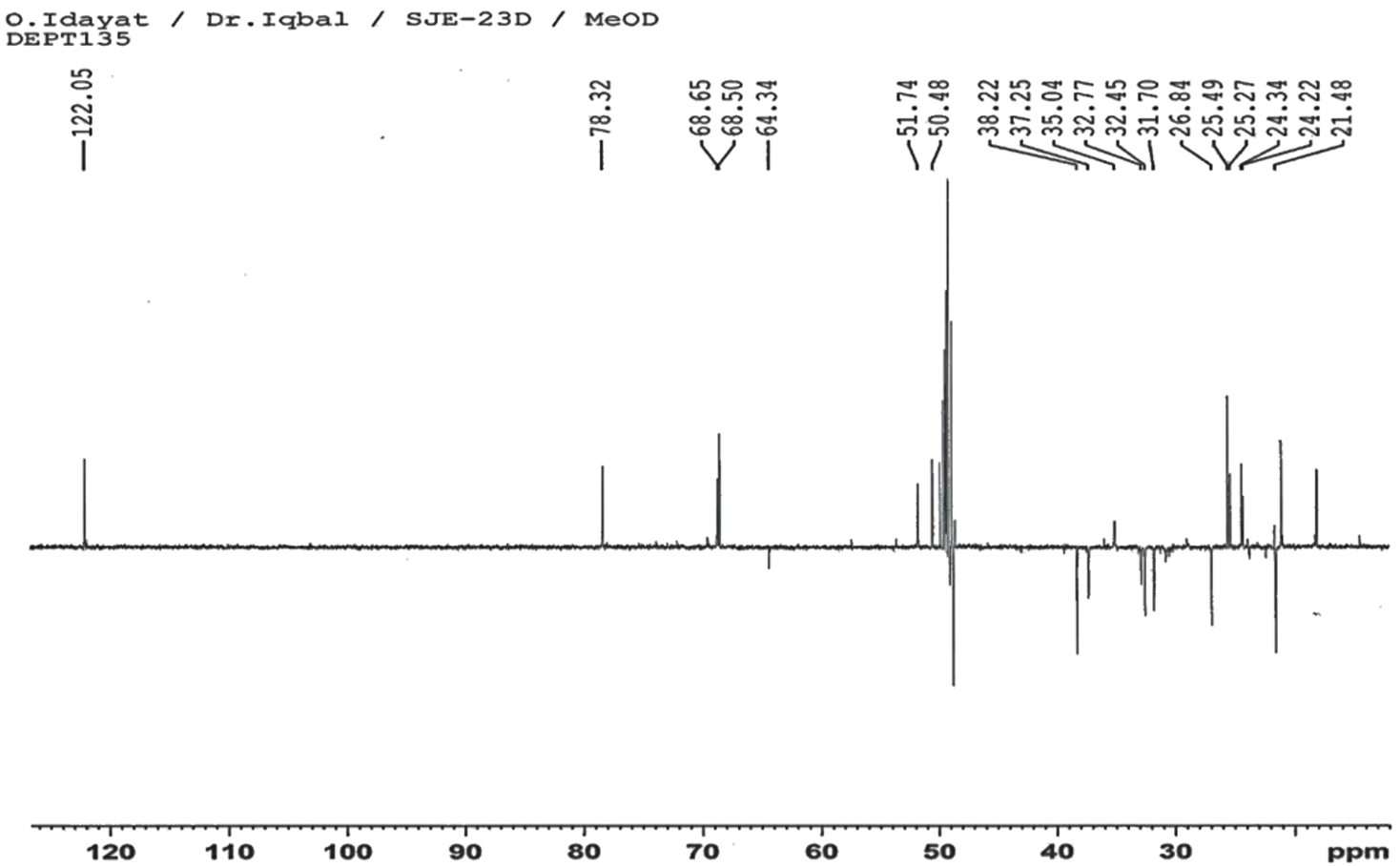

BRUKER

Current Data Parameters
NAME Nov28-18
EXPNO 7
PROCNO 1

F2 - Acquisition Parameters
Date_ 20181129
Time 10.00 h
INSTRUM AVNeo_600
PROBHD Z117768_0039 (
PULPROG deptsp135
TD 32768
SOLVENT MeOD
NS 2788
DS 8
SWH 30120.482 Hz
FIDRES 1.838408 Hz
AQ 0.5439488 sec
RG 101
DW 16.600 usec
DE 18.00 usec
TE 298.0 K
CNST2 145.0000000
D1 1.50000000 sec
D2 0.00344828 sec
D12 0.00002000 sec
TD0 5
SFO1 150.9523507 MHz
NUC1 13C
P1 12.00 usec
P13 2000.00 usec
PLW0 0 W
PLW1 107.76000214 W
SPNAM[5] Crp60comp.4
SPOAL5 0.500
SPOFFS5 0 Hz
SPW5 23.70800018 W
SFO2 600.2724011 MHz
NUC2 1H
CPDPRG[2 waltz65
P3 8.00 usec
P4 16.00 usec
PCPD2 70.00 usec
PLW2 9.53950024 W
PLW12 0.12460000 W

F2 - Processing parameters
SI 16384
SF 150.9378068 MHz
WDW EM
SSB 0
LB 1.00 Hz
GB 0
PC 1.40

Appendix XII (i)

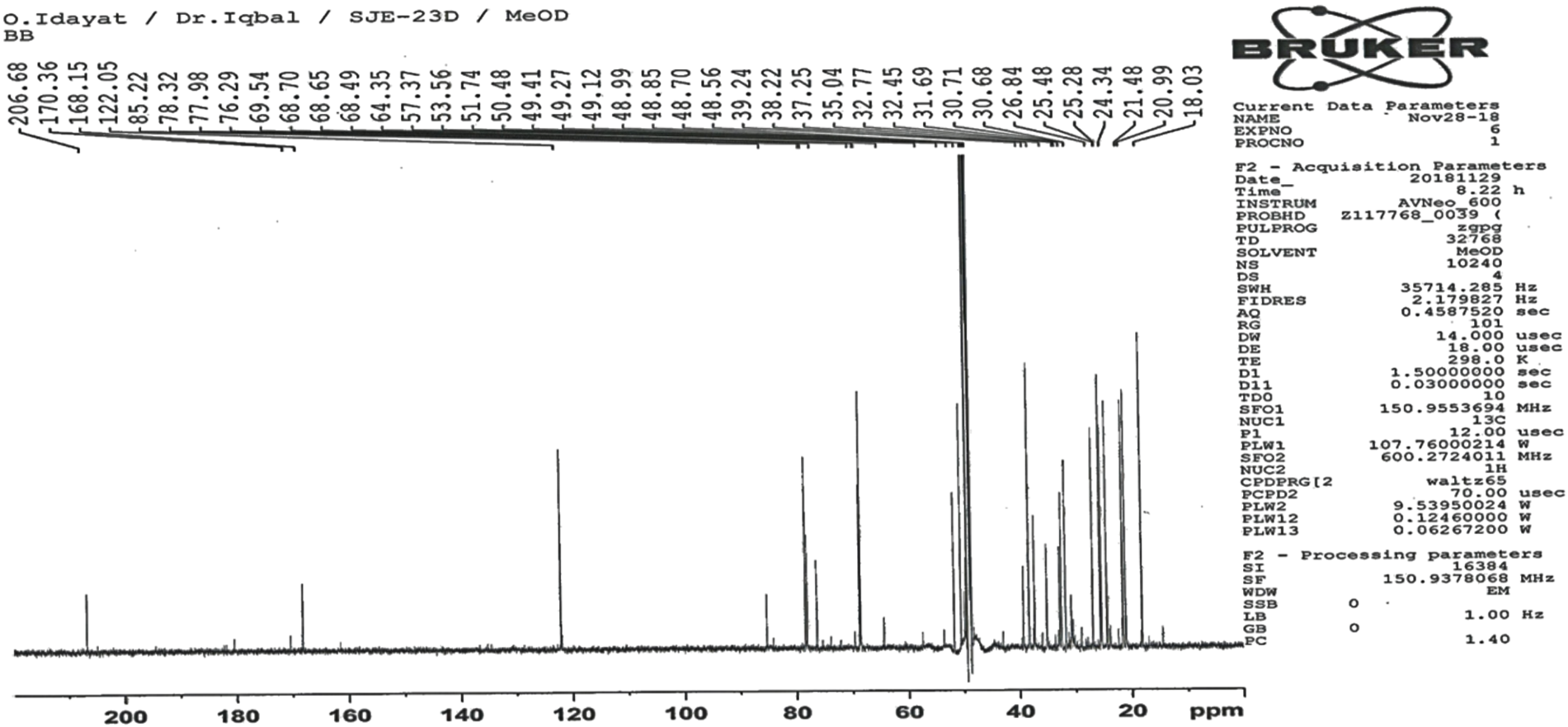

Appendix XII (i)

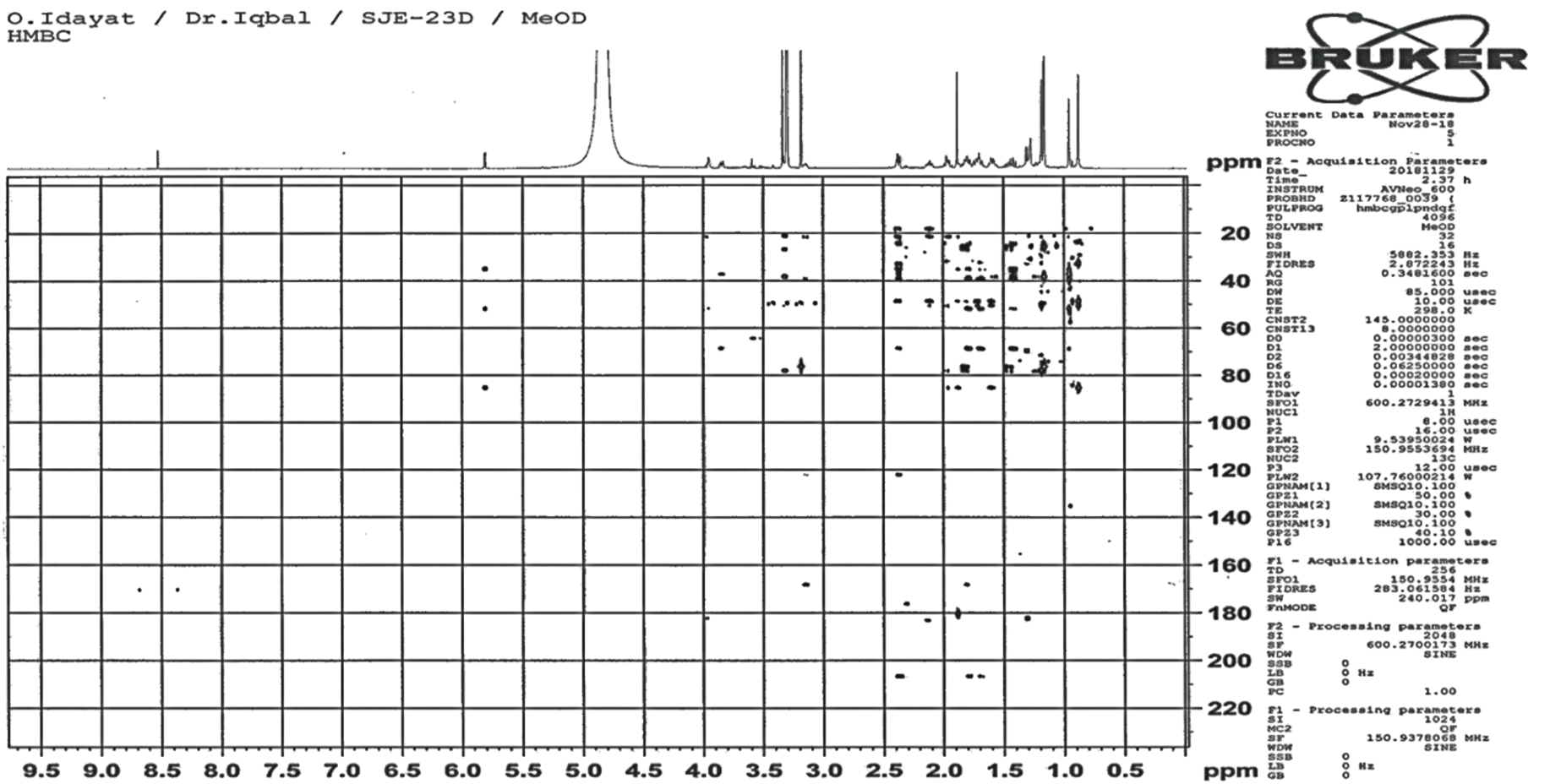

Appendix XIII (a)

EI-MS, 1D and 2D NMR spectra of SJE-28B

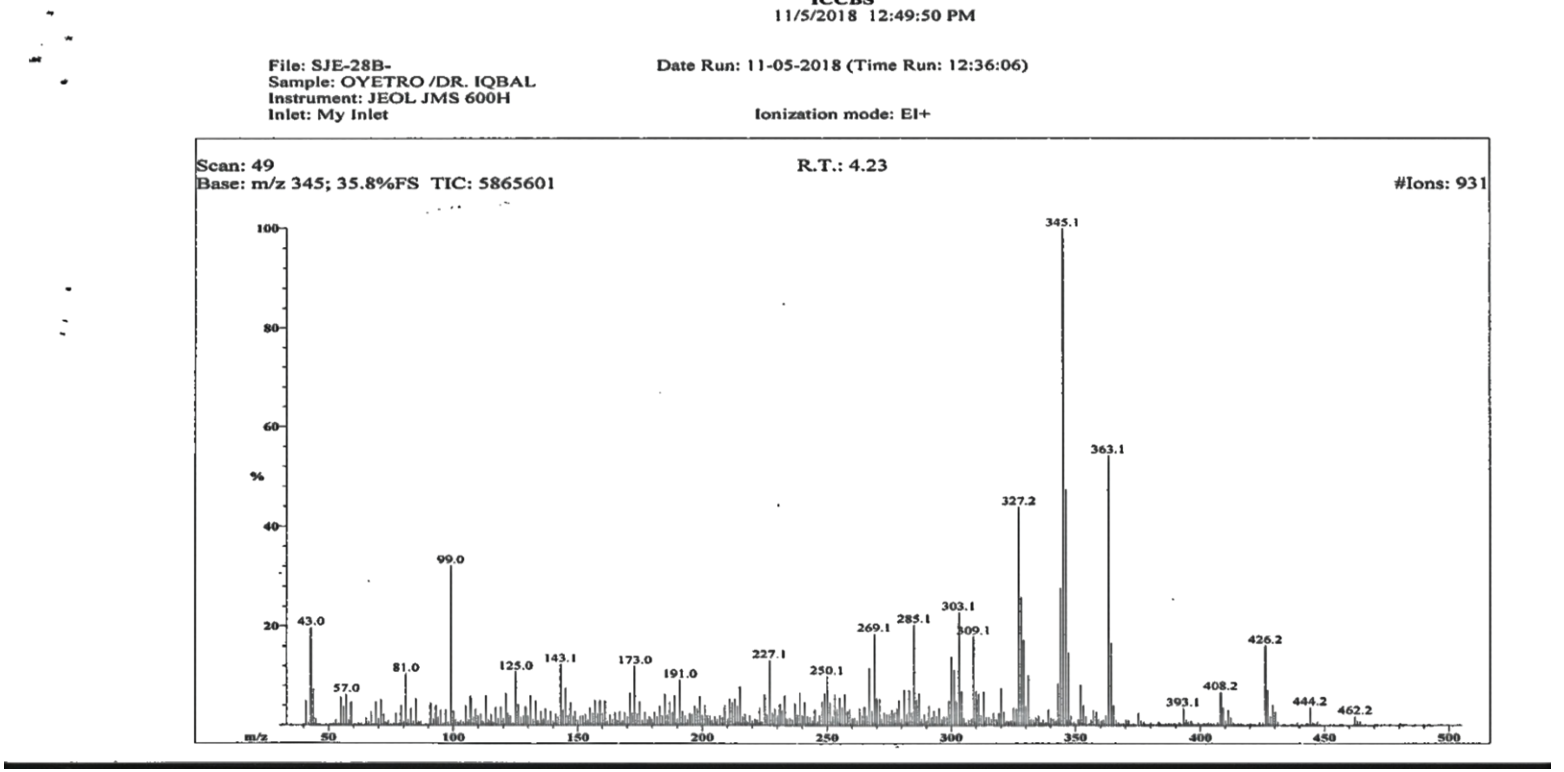

Appendix XIII (b)

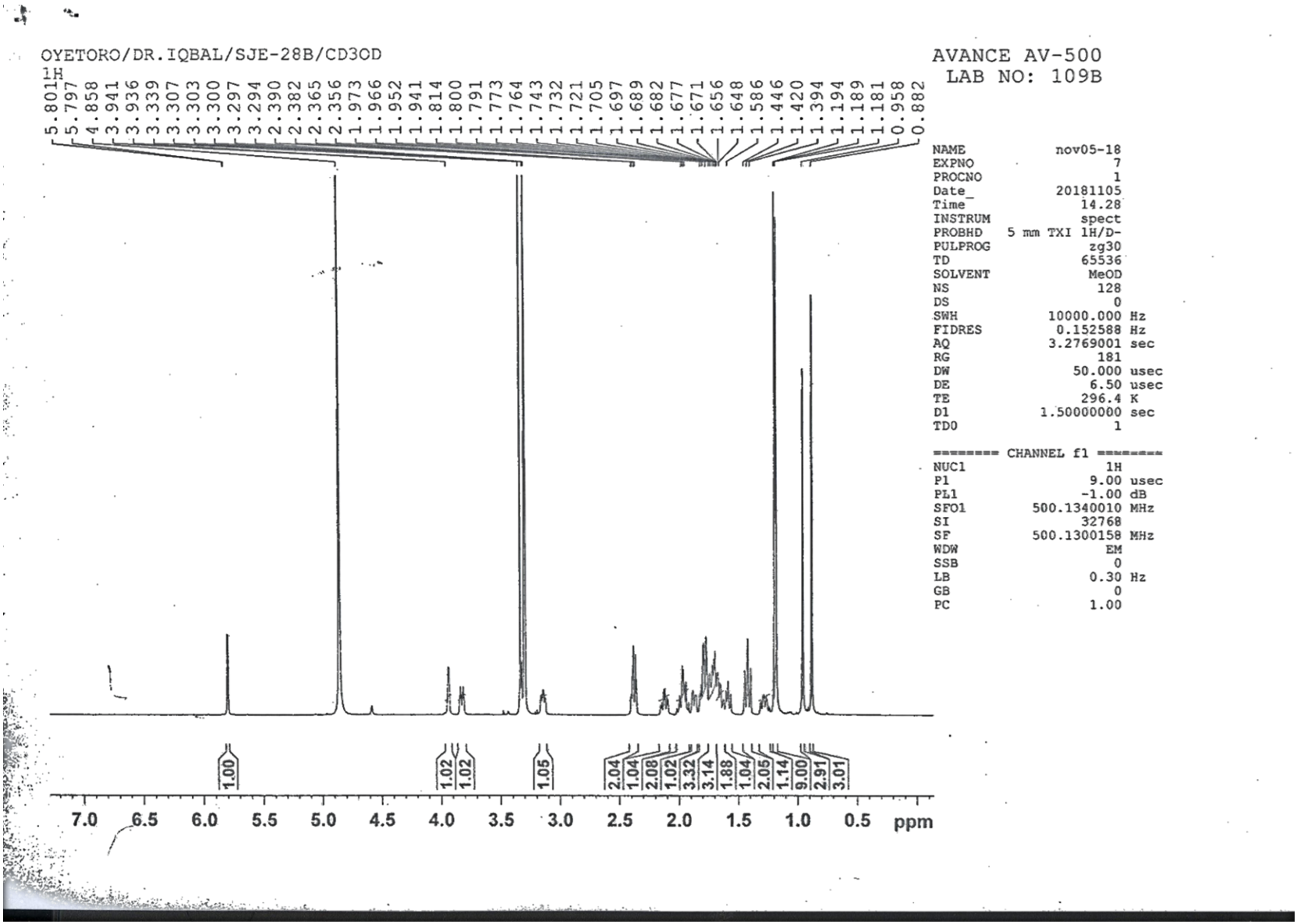

Appendix XIII (c)

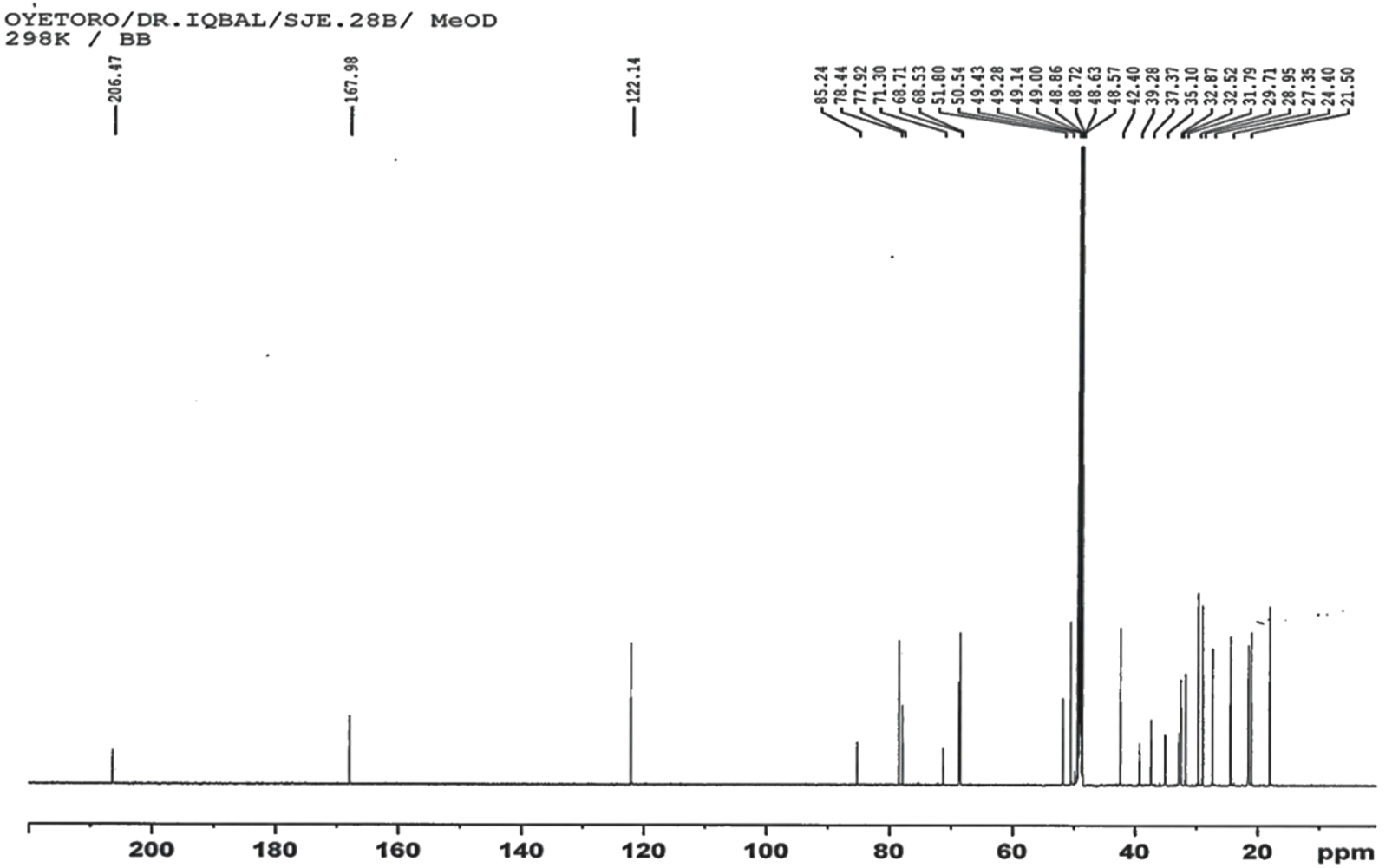

AVANCE NEO 600 MHz
Cryoprobe
Lab # 108

Current Data Parameters	
NAME	Nov12-18
EXPNO	6
PROCNO	1
F2 - Acquisition Parameters	
Date_	20181113
Time	10.14 h
INSTRUM	Avance NEO 600MHz
PROBHD	Z44896_0021 (C
PULPROG	zgpg
TD	32768
SOLVENT	MeOD
NS	3250
DS	8
SWH	35714.285 Hz
FIDRES	2.179827 Hz
AQ	0.4587520 sec
RG	101
DW	14.000 usec
DE	18.00 usec
TE	298.0 K
D1	1.50000000 sec
D11	0.03000000 sec
TD0	16
SFO1	150.8950144 MHz
NUC1	13C
P1	12.00 usec
PLW1	97.90100098 W
SFO2	600.0324001 MHz
NUC2	1H
CPDPRG[2	waltz65
PCPD2	75.00 usec
PLW2	4.50000000 W
PLW12	0.08000000 W
PLW13	0.04619300 W
F2 - Processing parameters	
SI	16384
SF	150.8774503 MHz
WDW	EM
SSB	0
LB	1.00 Hz
GB	0
PC	1.20

Appendix XIII (d)

OYETORO/DR.IQBAL/SJE.28B/ MeOD
Cosy

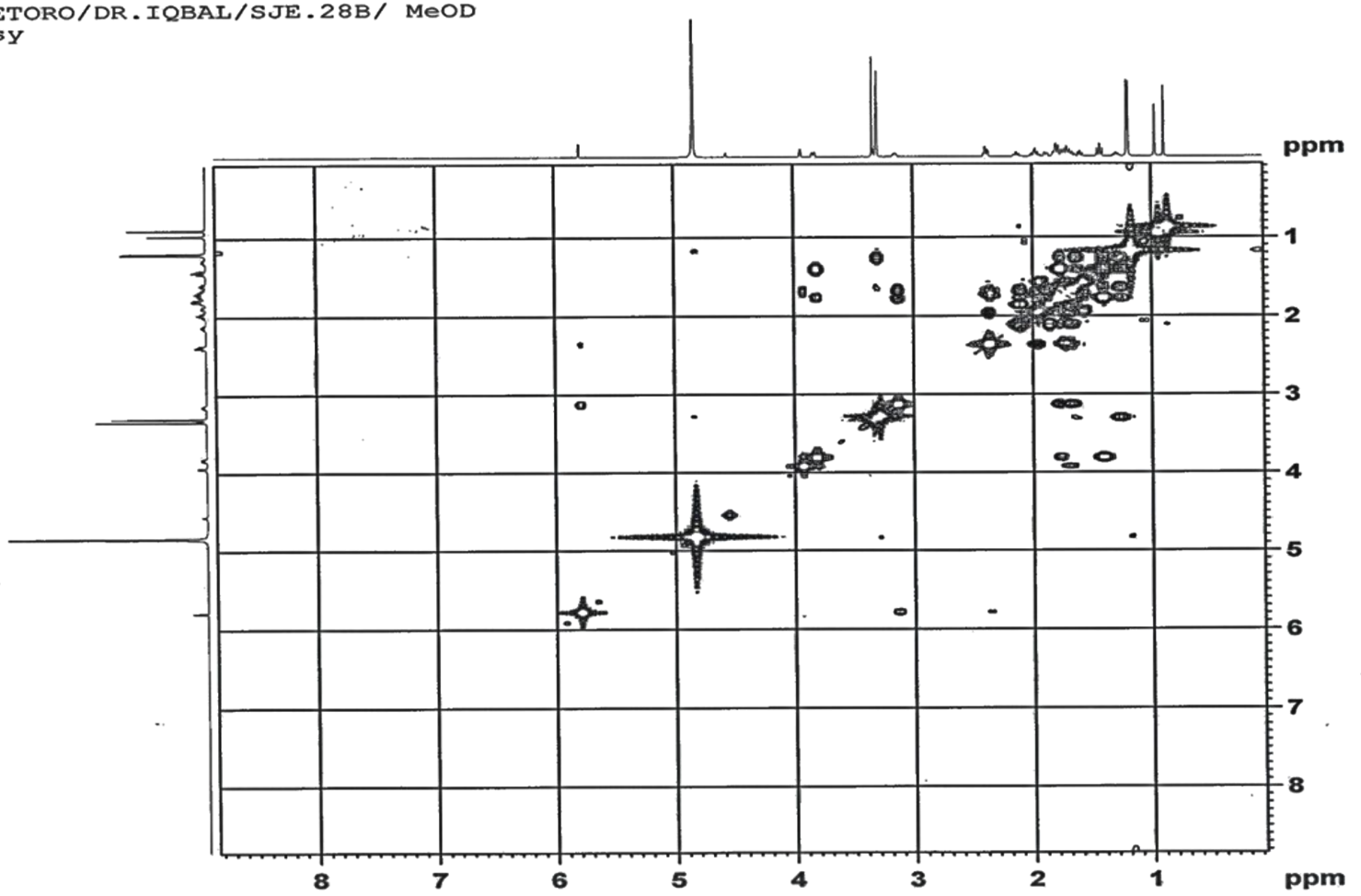

AVANCE NEO 600 MHz
Cryoprobe
Lab # 108

```
Current Data Parameters
NAME                  Nov12-18
EXPNO                        2
PROCNO                       1

F2 - Acquisition Parameters
Date_                 20181112
Time                     11.48 h
INSTRUM  Avance NEO 600MHz
PROBHD   Z44896_0021 (C
PULPROG              cosygpqf
TD                       1024
SOLVENT                  MeOD
NS                          8
DS                         16
SWH                  5263.158 Hz
FIDRES              10.279605 Hz
AQ                   0.0972800 sec
RG                     73.2422
DW                     95.000 usec
DE                     15.00 usec
TE                     298.0 K
D0                0.00000300 sec
D1                2.00000000 sec
D13               0.00000400 sec
D16               0.00020000 sec
IN0               0.00019000 sec
TDav                         1
SFO1             600.0327001 MHz
NUC1                      1H
P0                     10.00 usec
P1                     10.00 usec
PLW1              4.25000000 W
GPNAM[1]          SMSQ10.100
GPZ1                   10.00 %
P16                  1000.00 usec

F1 - Acquisition parameters
TD                         256
SFO1                600.0327 MHz
FIDRES             41.118420 Hz
SW                     8.771 ppm
FnMODE                    QF

F2 - Processing parameters
SI                       1024
SF                600.0300262 MHz
WDW                      SINE
SSB                         0
LB                        0 Hz
GB                          0
PC                       1.00

F1 - Processing parameters
SI                       1024
MC2                        QF
SF                600.0300262 MHz
WDW                      SINE
SSB                         0
LB                        0 Hz
GB                          0
```

Appendix XIII (e)

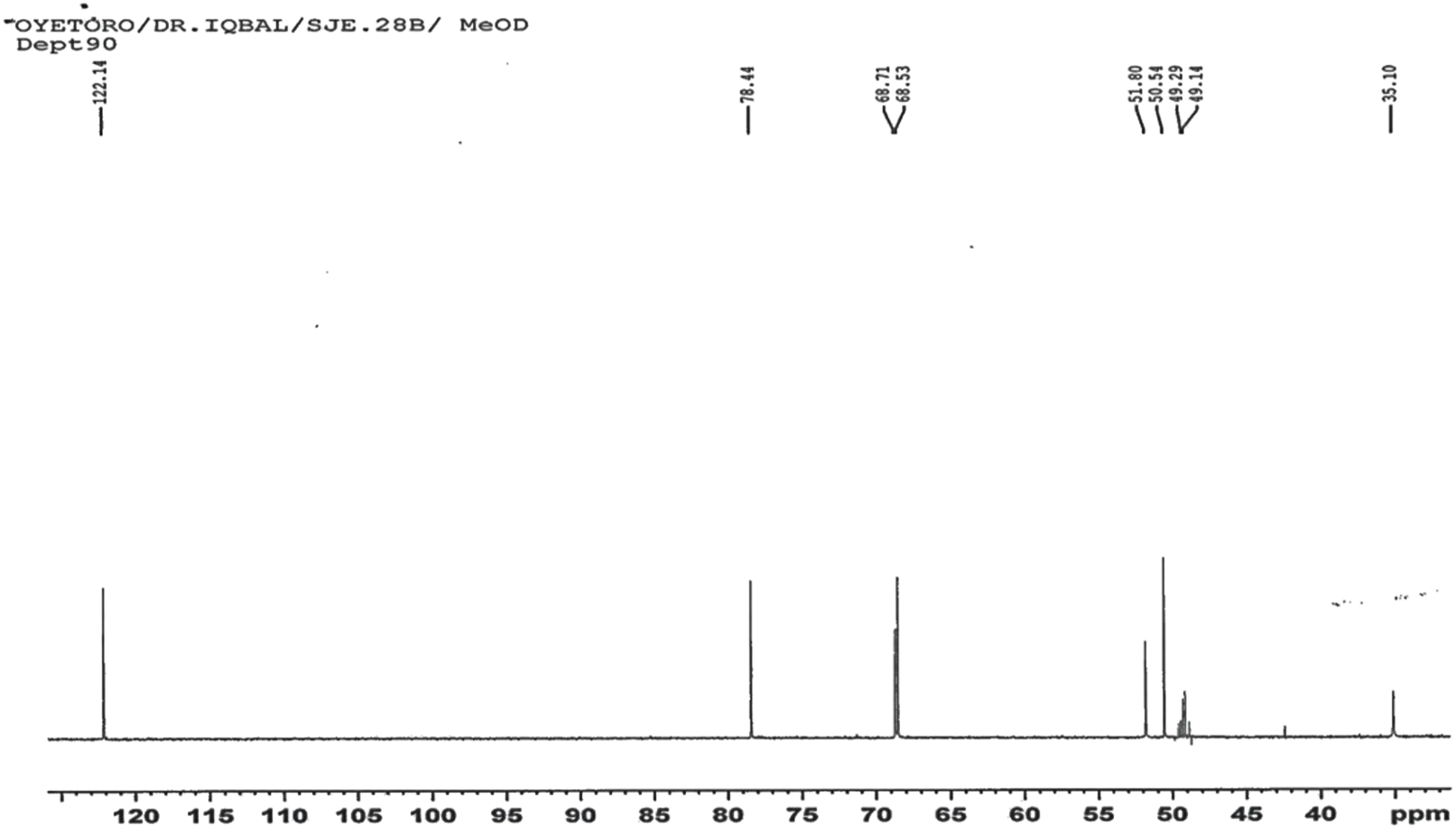

AVANCE NEO 600 MHz
Cryoprobe
Lab # 108

Current Data Parameters		
NAME	Nov12-18	
EXPNO	8	
PROCNO	1	
F2 - Acquisition Parameters		
Date_	20181113	
Time	11.55 h	
INSTRUM	Avance NEO 600MHz	
PROBHD	Z44896_0021 (C	
PULPROG	deptsp90	
TD	32768	
SOLVENT	MeOD	
NS	1509	
DS	8	
SWH	30120.482	Hz
FIDRES	1.838408	Hz
AQ	0.5439488	sec
RG	101	
DW	16.600	usec
DE	18.00	usec
TE	298.0	K
CNST2	145.0000000	
D1	1.50000000	sec
D2	0.00344828	sec
D12	0.00002000	sec
TD0	4	
SFO1	150.8919969	MHz
NUC1	13C	
P1	12.00	usec
P13	2000.00	usec
PLW0	0 W	
PLW1	97.90100098	W
SPNAM[5]	Crp60comp.4	
SPOAL5	0.500	
SPOFFS5	0 Hz	
SPW5	21.54000092	W
SFO2	600.0324001	MHz
NUC2	1H	
CPDPRG[2	waltz65	
P3	10.00	usec
P4	20.00	usec
PCPD2	75.00	usec
PLW2	4.50000000	W
PLW12	0.08000000	W
F2 - Processing parameters		
SI	16384	
SF	150.8774503	MHz
WDW	EM	
SSB	0	
LB	1.00	Hz
GB	0	
PC	1.40	

Appendix XIII (f)

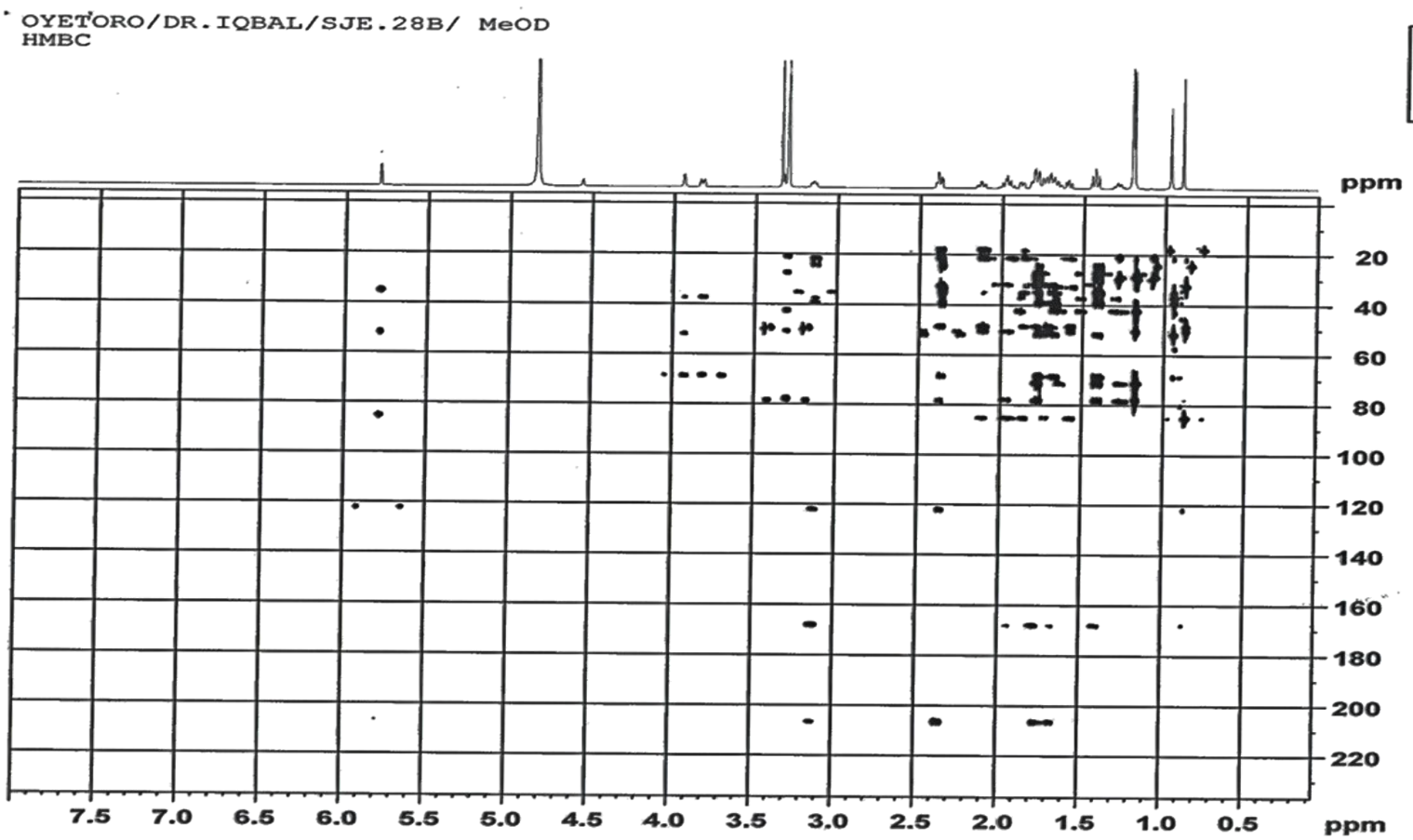

AVANCE NEO 600 MHz
Cryoprobe
Lab # 108

```
Current Data Parameters
NAME                  Nov12-18
EXPNO                        5
PROCNO                       1

F2 - Acquisition Parameters
Date_                 20181113
Time                      8.24 h
INSTRUM   Avance NEO 600MHz
PROBHD    244896_0021 (C
PULPROG         hmbcgpndqf
TD                        4096
SOLVENT                   MeOD
NS                          64
DS                          16
SWH                   5263.158 Hz
FIDRES                2.569901 Hz
AQ                    0.3891200 sec
RG                          101
DW                       95.000 usec
DE                       15.00 usec
TE                       298.0 K
CNST13                8.00000000
D0                    0.00000300 sec
D1                    1.50000000 sec
D6                    0.06250000 sec
D16                   0.00020000 sec
IN0                   0.00001380 sec
TDav                         1
SFO1                600.0327001 MHz
NUC1                        1H
P1                       10.00 usec
P2                       20.00 usec
PLW1                  4.25000000 W
SFO2                150.8950144 MHz
NUC2                        13C
P3                       12.00 usec
PLW2                 97.90100098 W
GPNAM[1]              SMSQ10.100
GPZ1                     50.00 %
GPNAM[2]              SMSQ10.100
GPZ2                     30.00 %
GPNAM[3]              SMSQ10.100
GPZ3                     40.10 %
P16                    1000.00 usec

F1 - Acquisition parameters
TD                          256
SFO1                150.895 MHz
FIDRES               283.061584 Hz
SW                   240.113 ppm
FnMODE                      QF

F2 - Processing parameters
SI                         2048
SF                600.0300262 MHz
WDW                       SINE
SSB                  0
LB                   0 Hz
GB                   0
PC                        1.00

F1 - Processing parameters
SI                          512
MC2                         QF
SF                150.8774503 MHz
WDW                       SINE
SSB                  0
LB                   0 Hz
GB                   0
```

Appendix XIII (g)

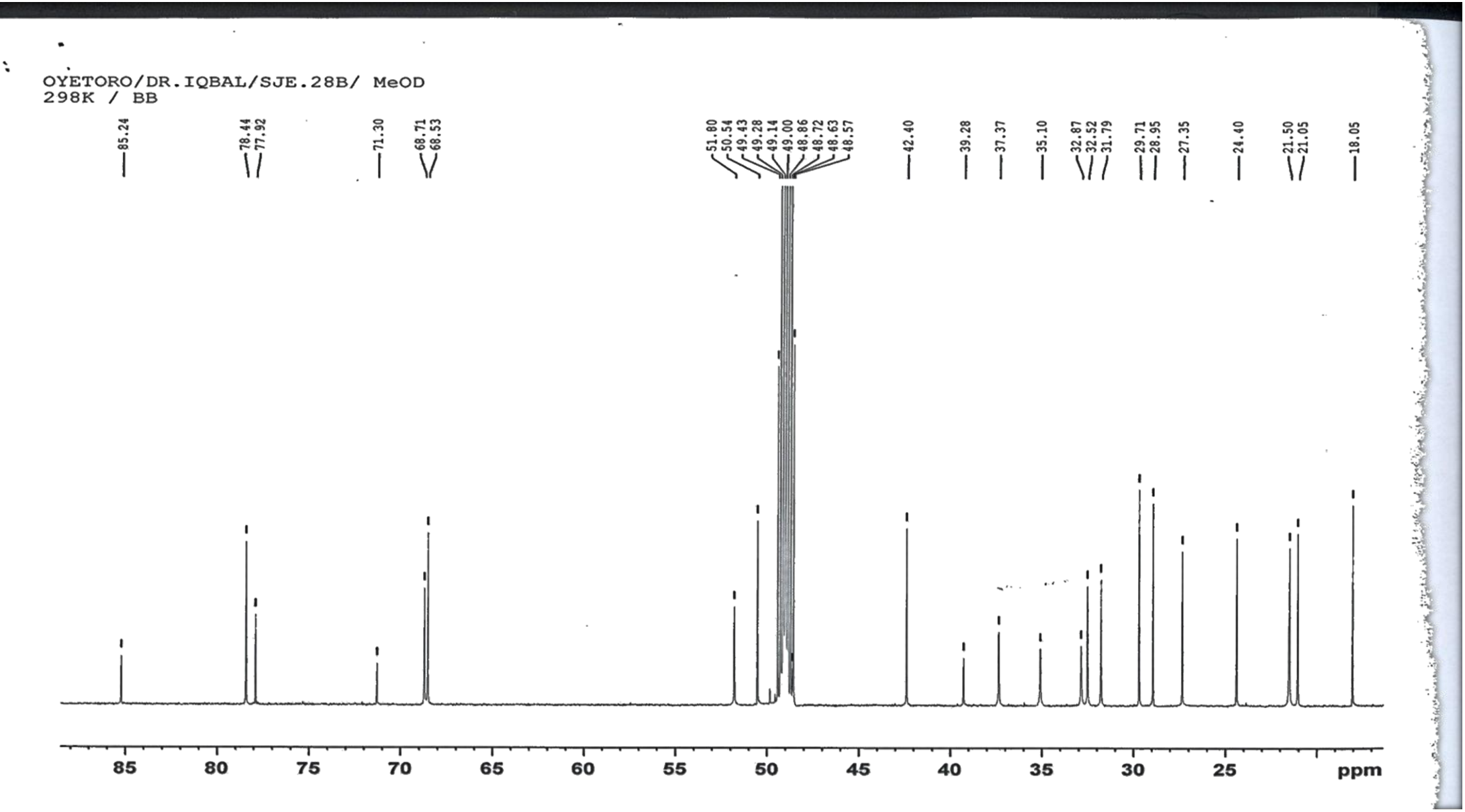

Appendix XIII (h)

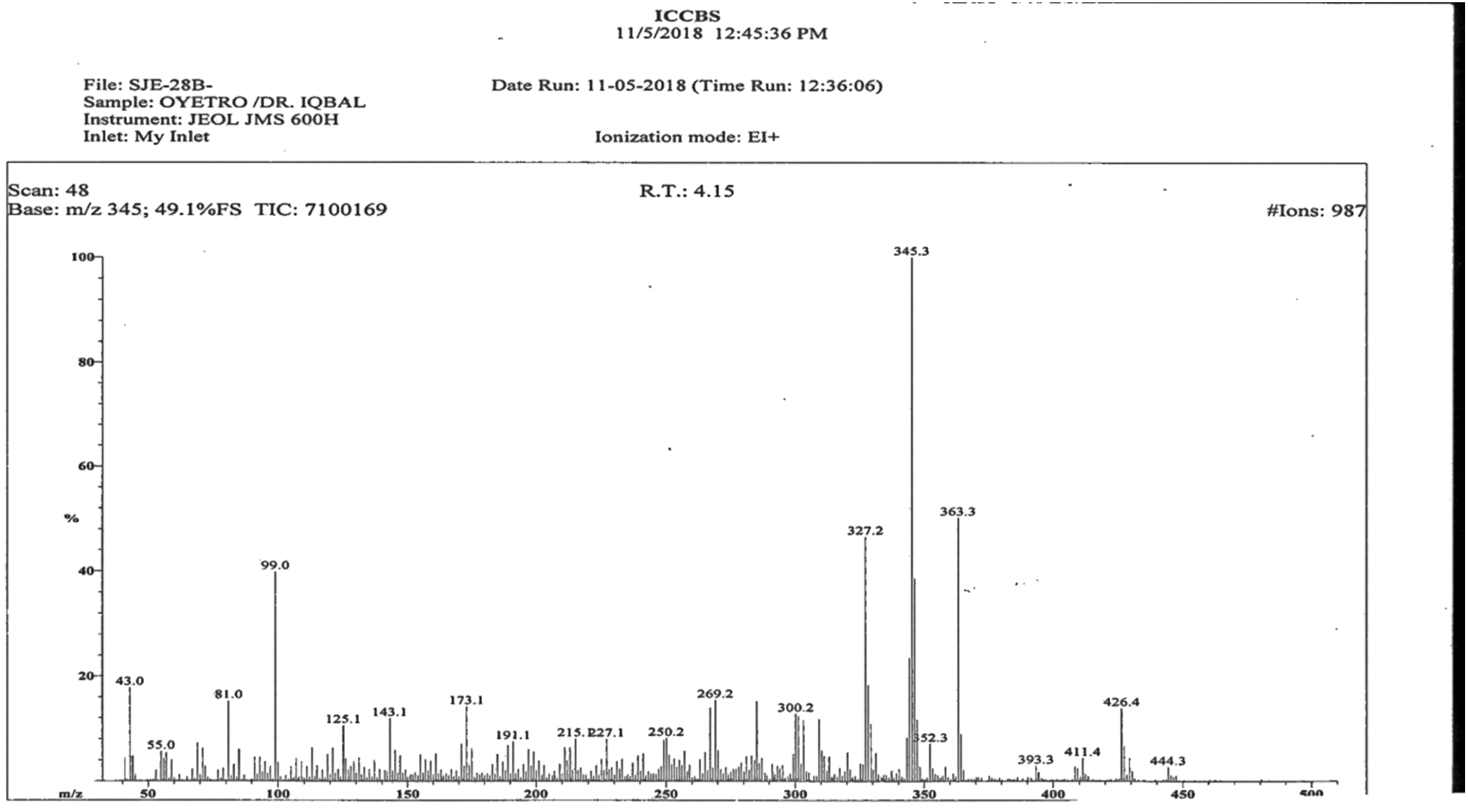

Appendix XIII (i)

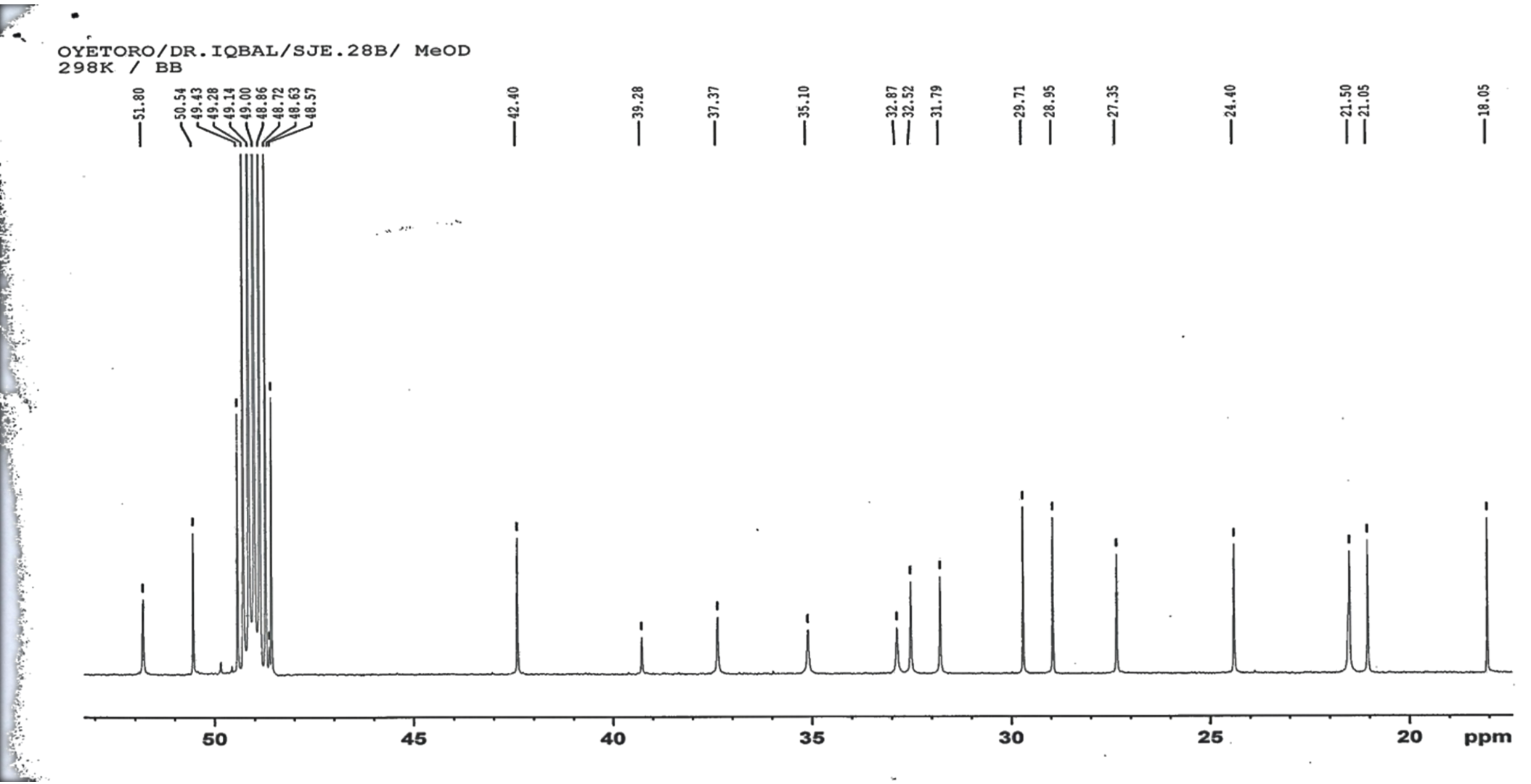

Appendix XIII (j)

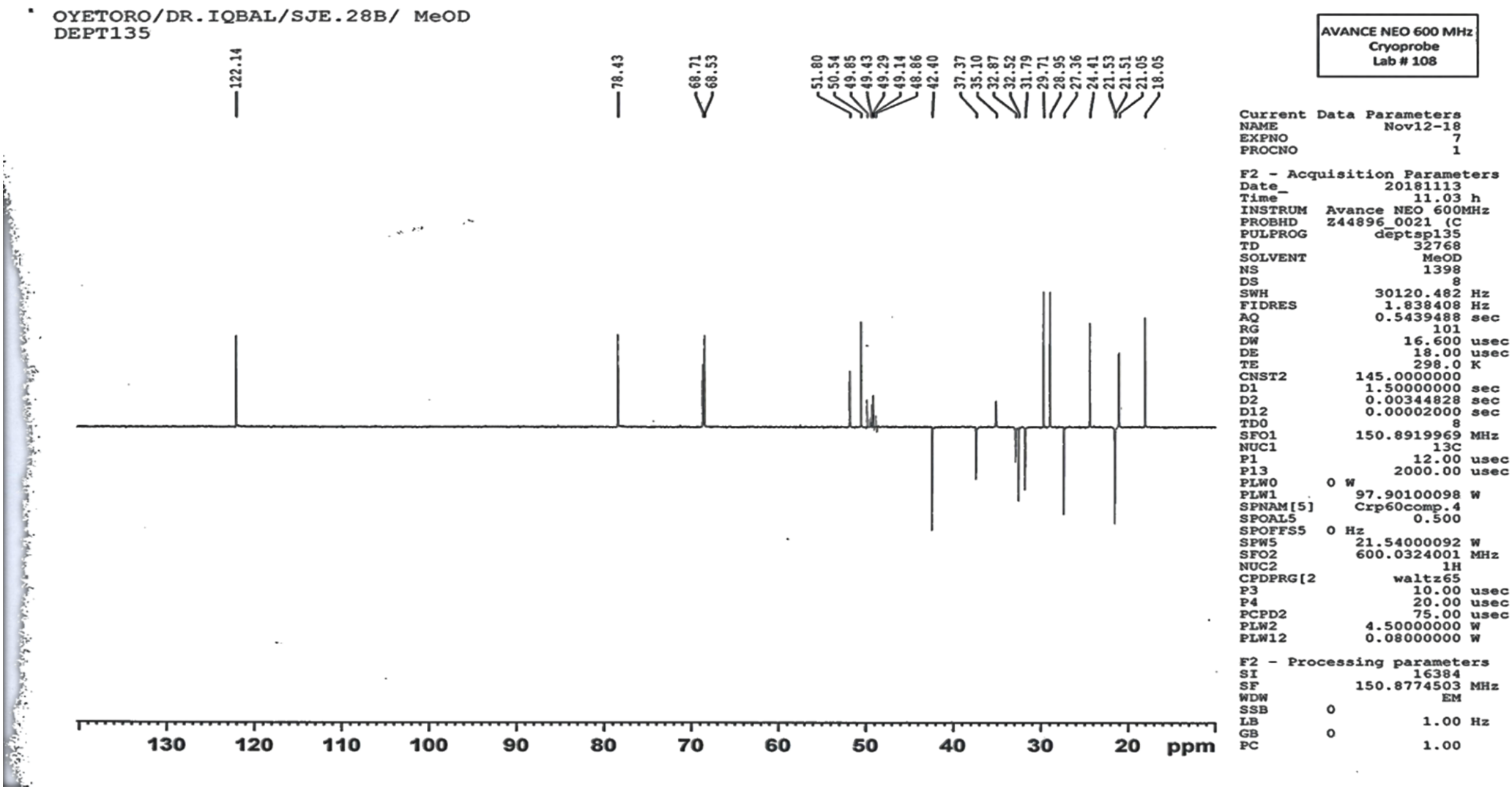

Appendix XIII (k)

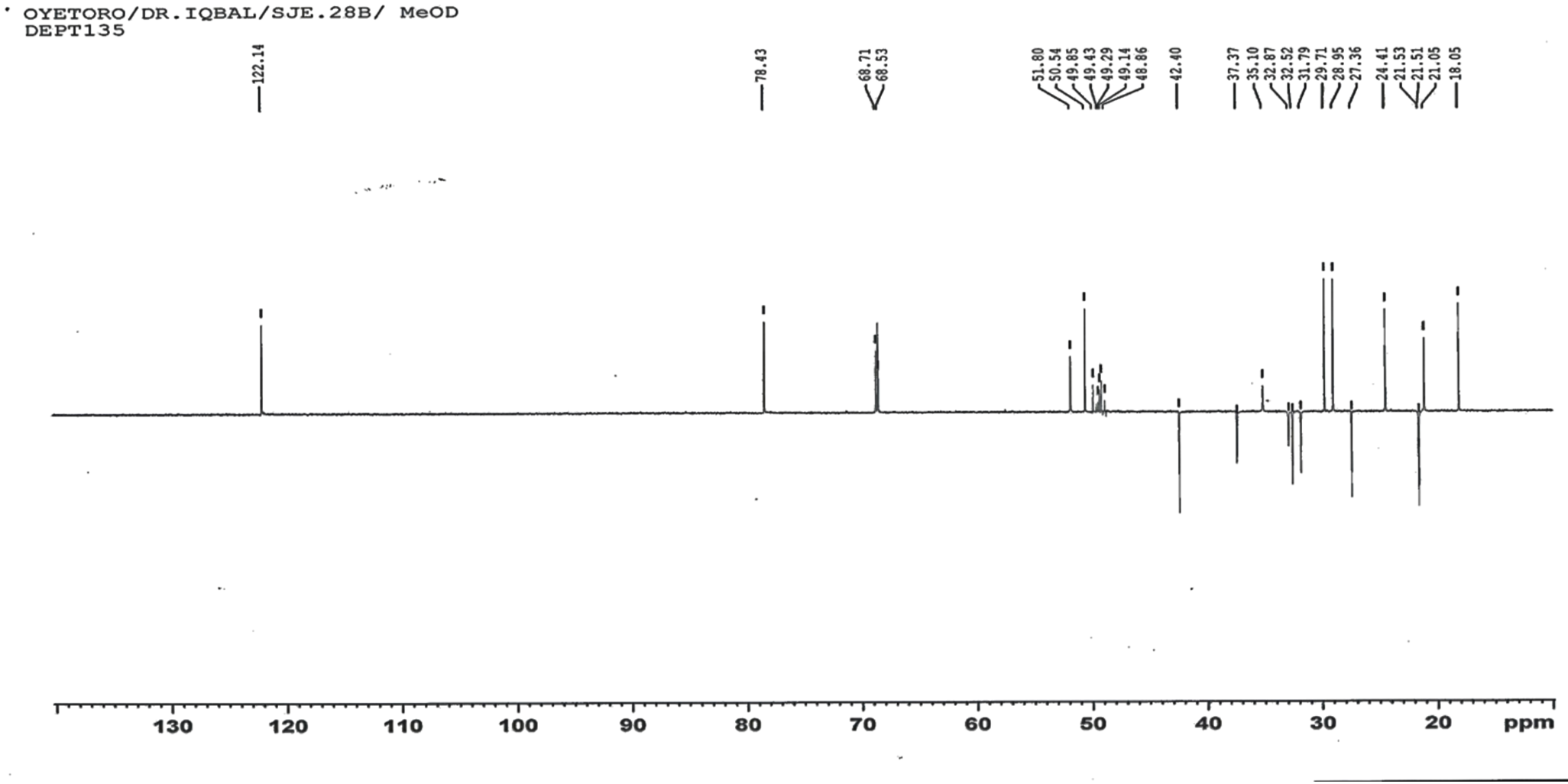

Appendix XIV

IR spectra of SJB-12B

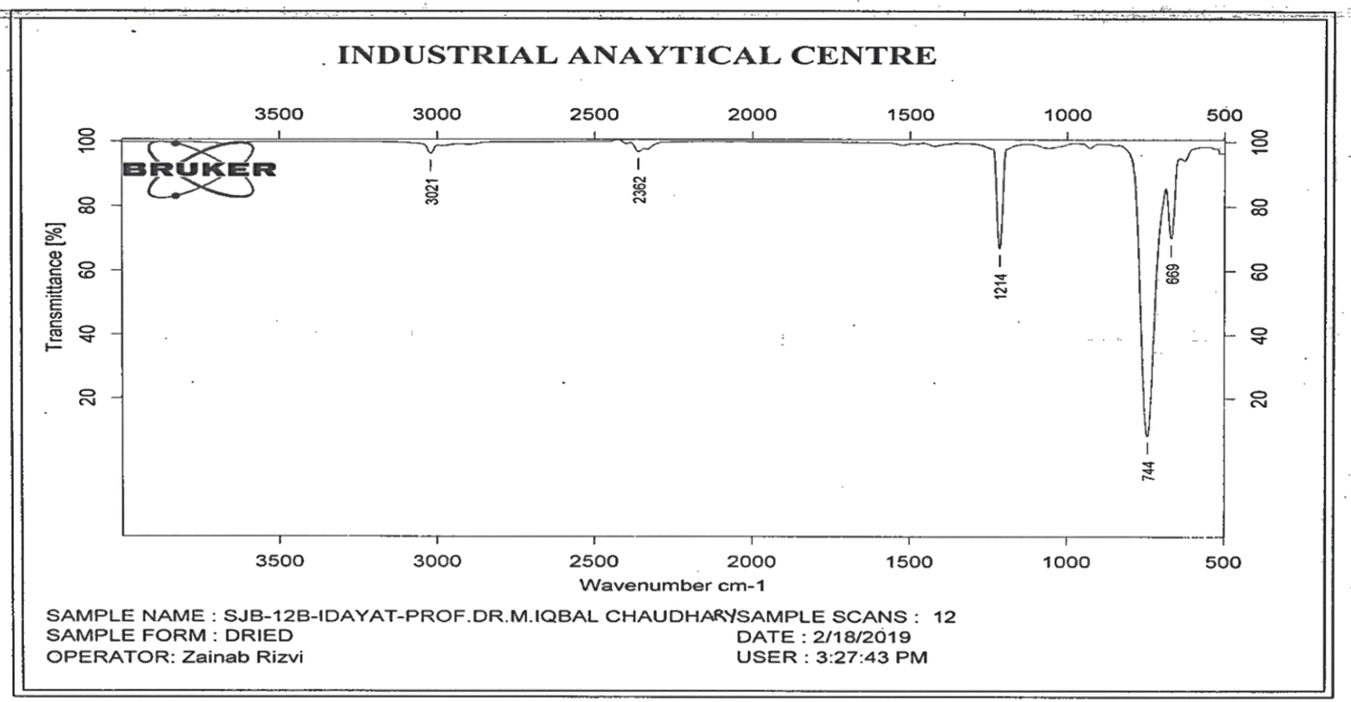

Appendix XV

IR spectra of SJB-26A

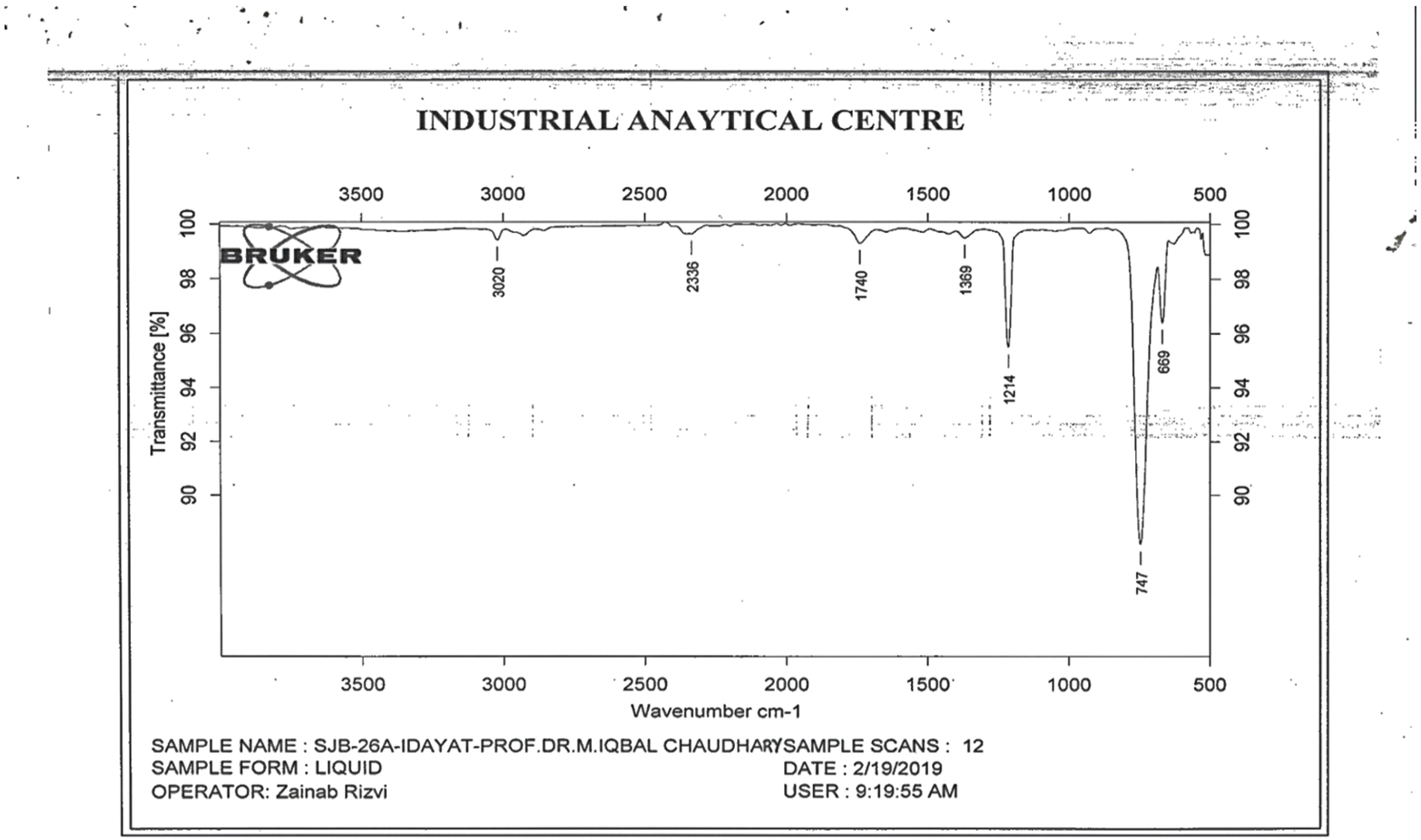

Appendix XVI

IR spectra of SJH-28A

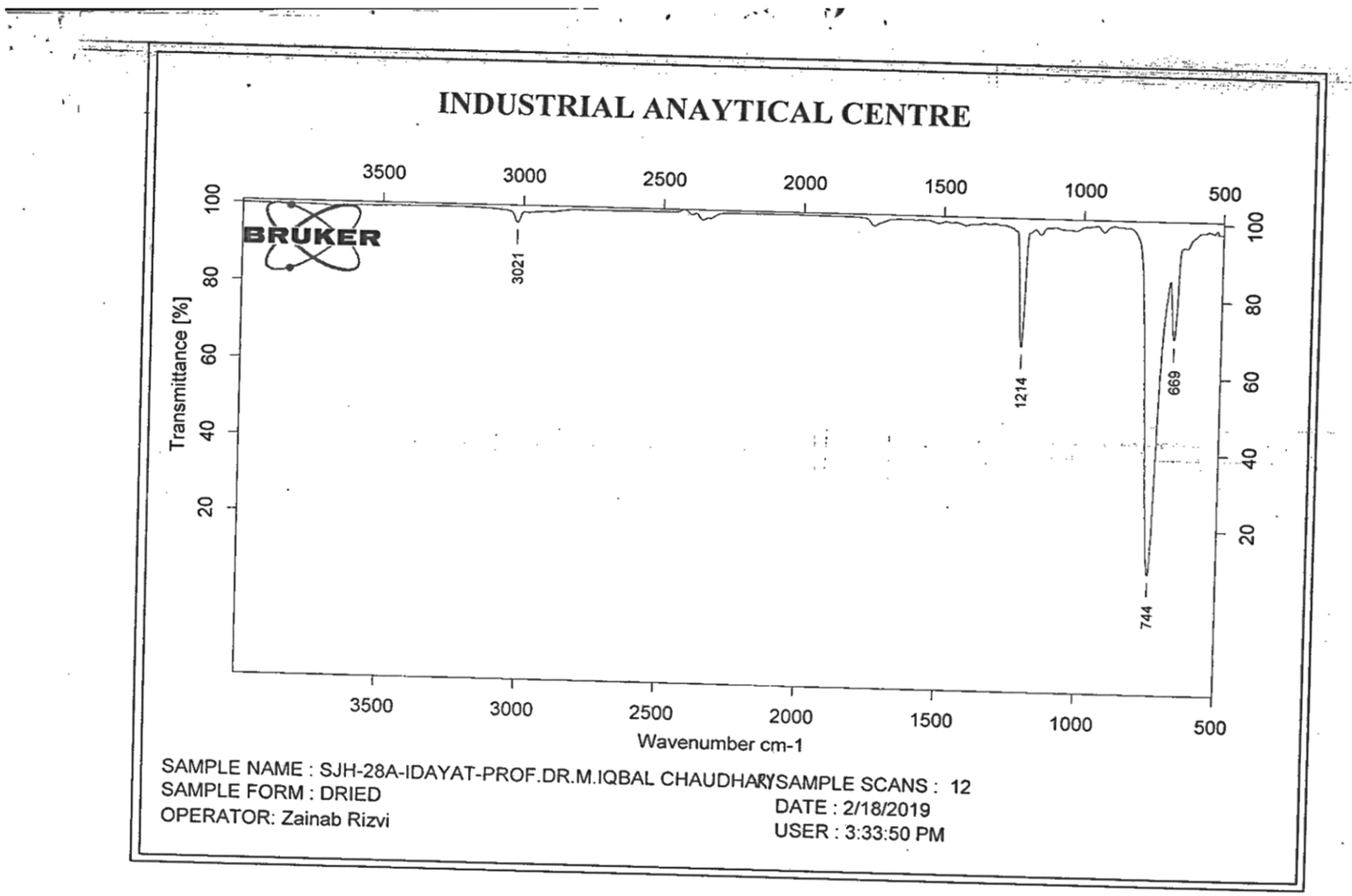

Appendix XVII

IR spectra of SJH-28B

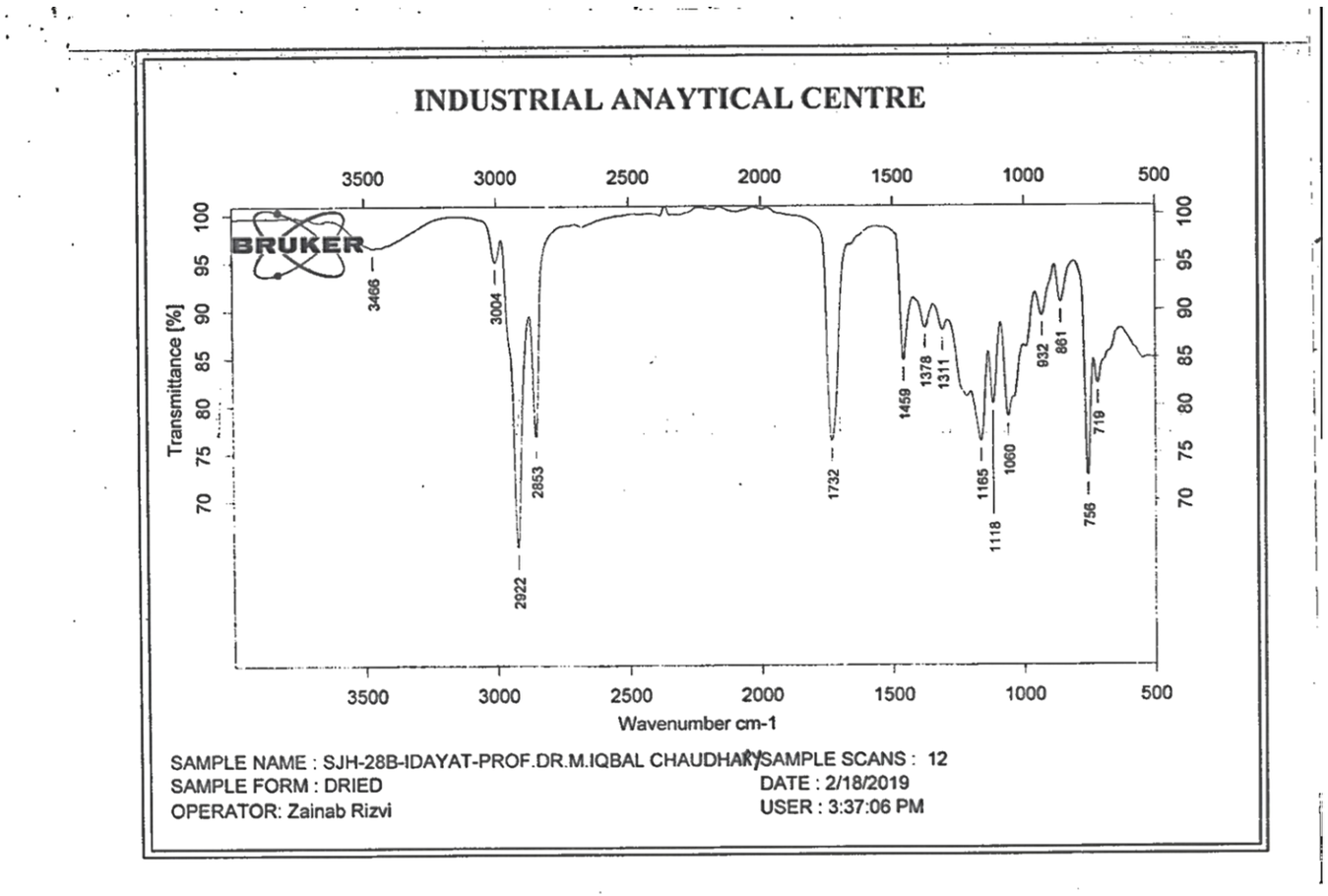

Appendix XVIII

FAB-MS of SJB-12

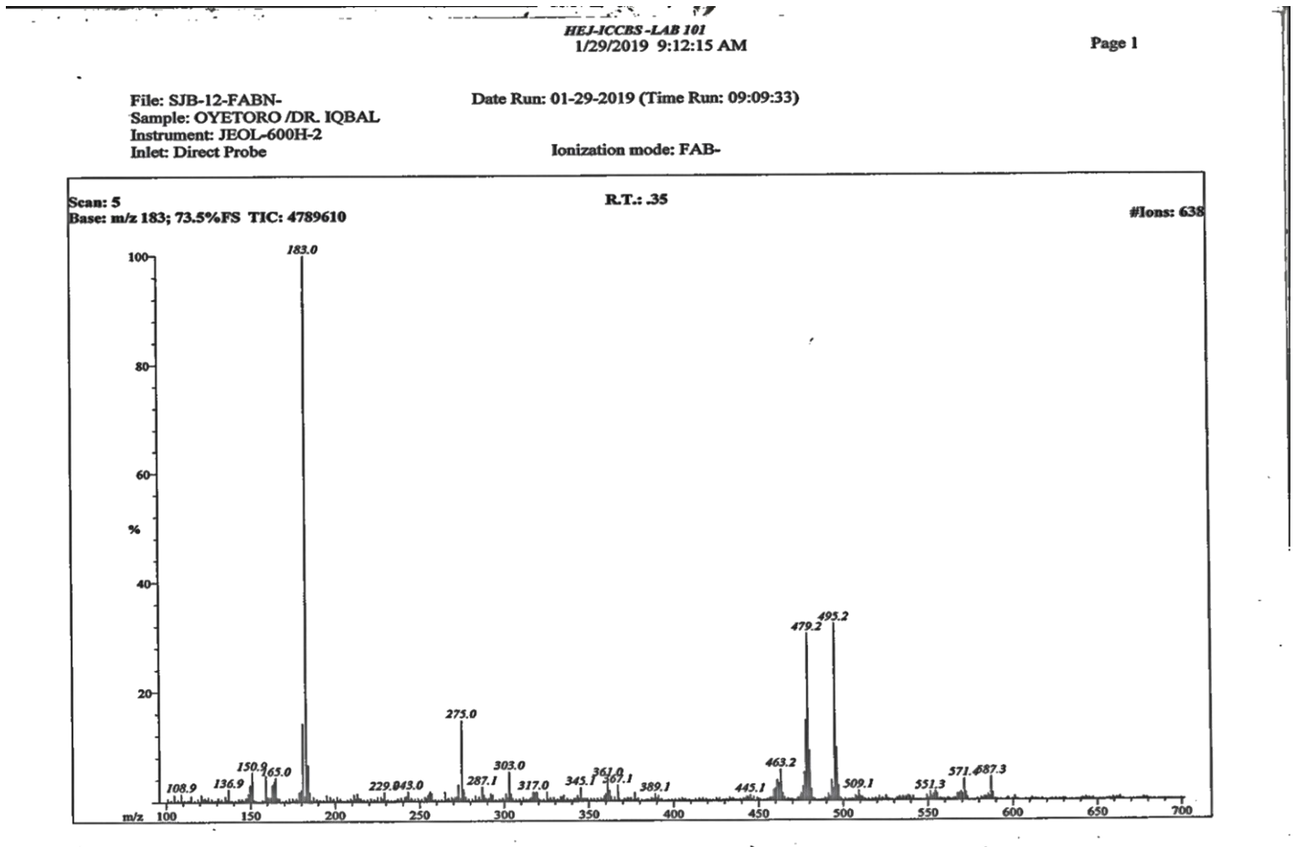

Appendix XIX

FAB-MS of SJB-12B

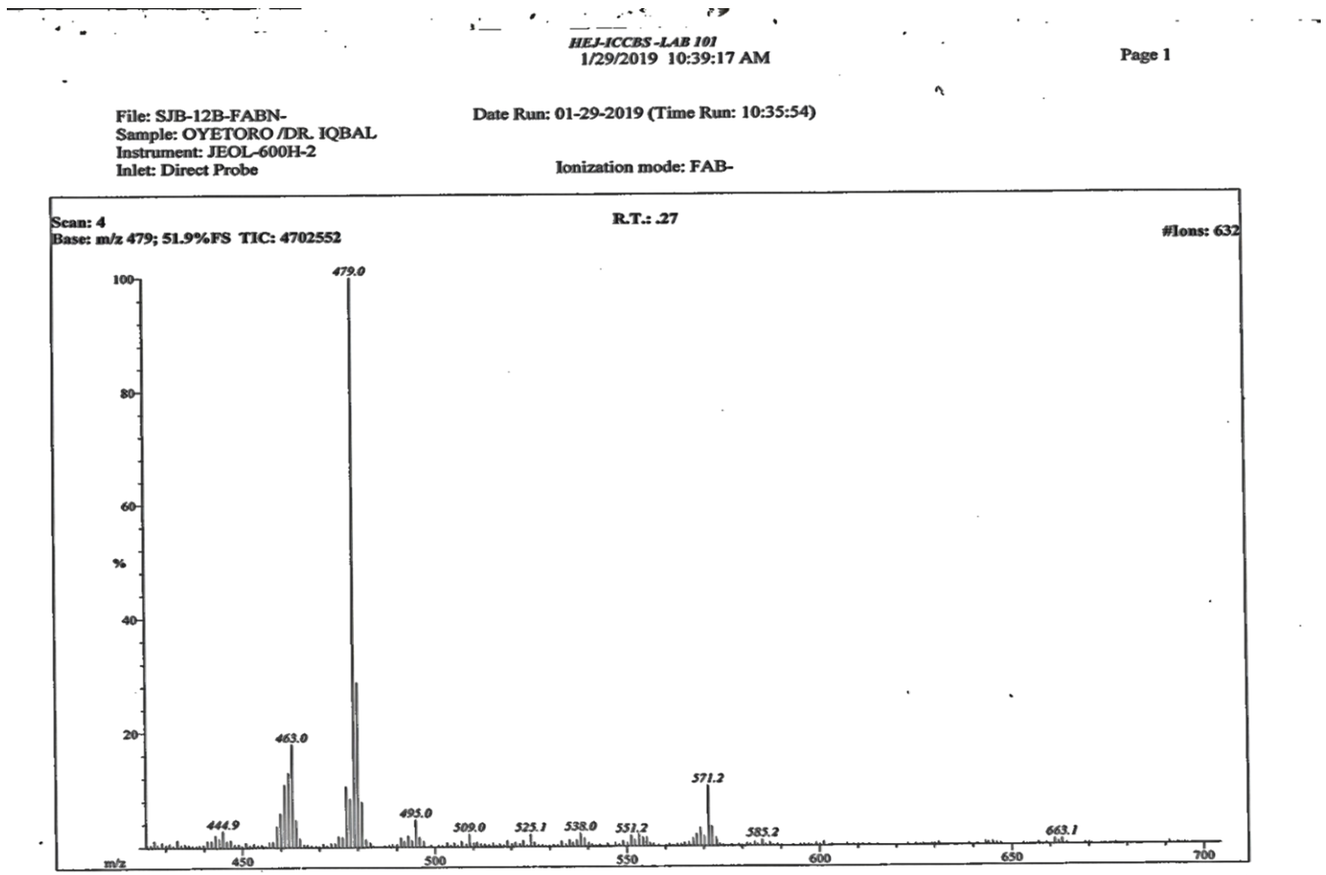

Appendix XX

FAB-MS of SJB-26A

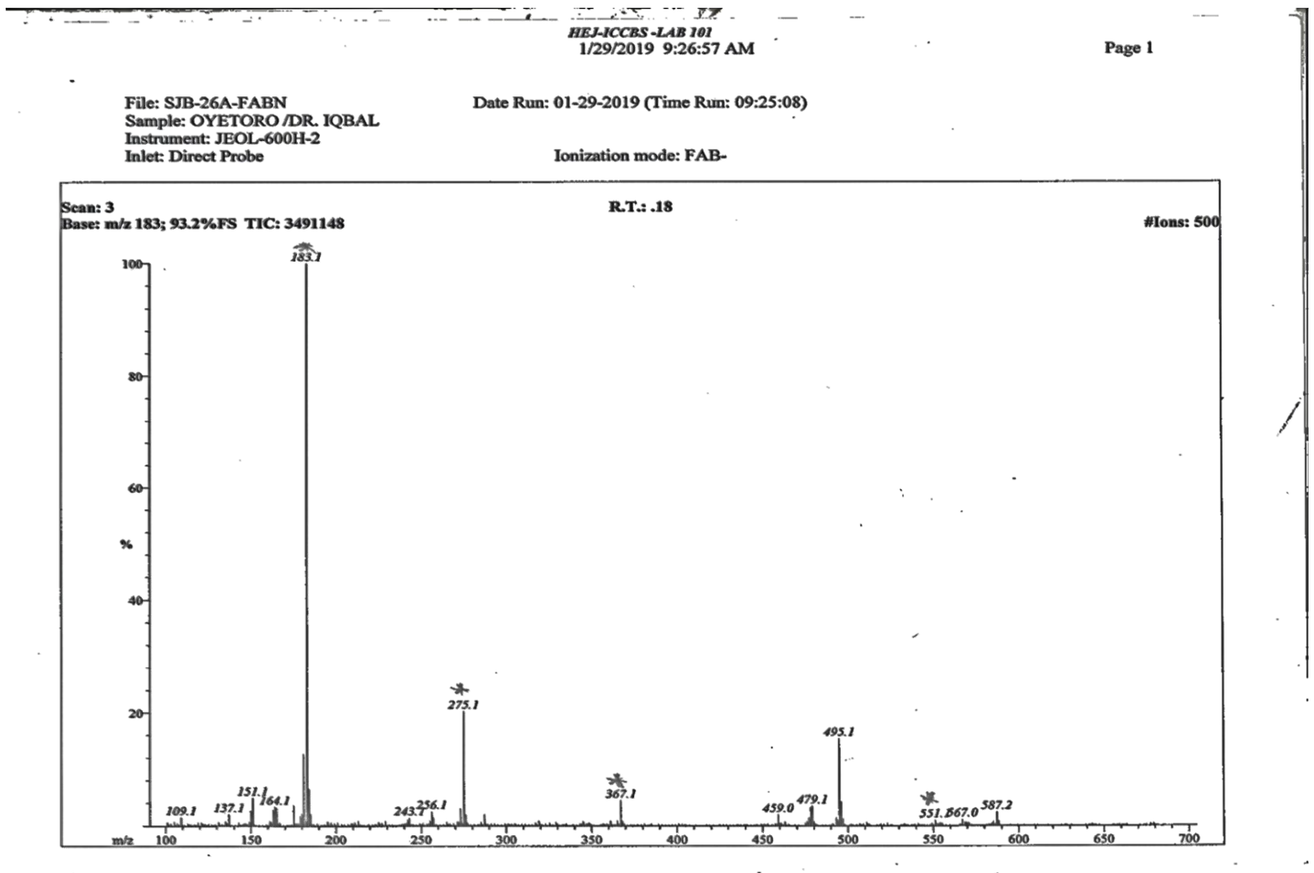

Appendix XXI

FAB-MS of SJE-23D